The Magnetic Microstructure of Nanostructered Materials

Magnetic Microstructure: Magnetic Domains

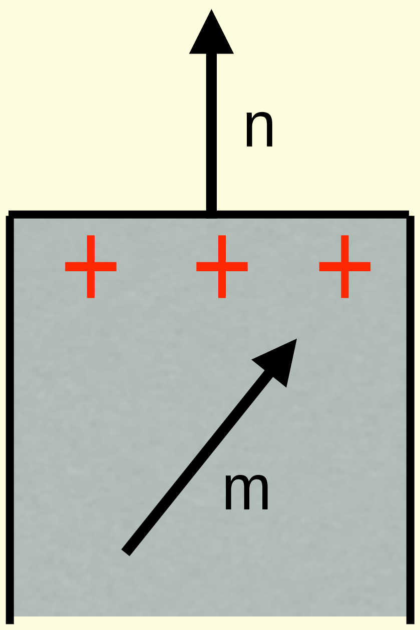

Magnetic surface
charge = m•n

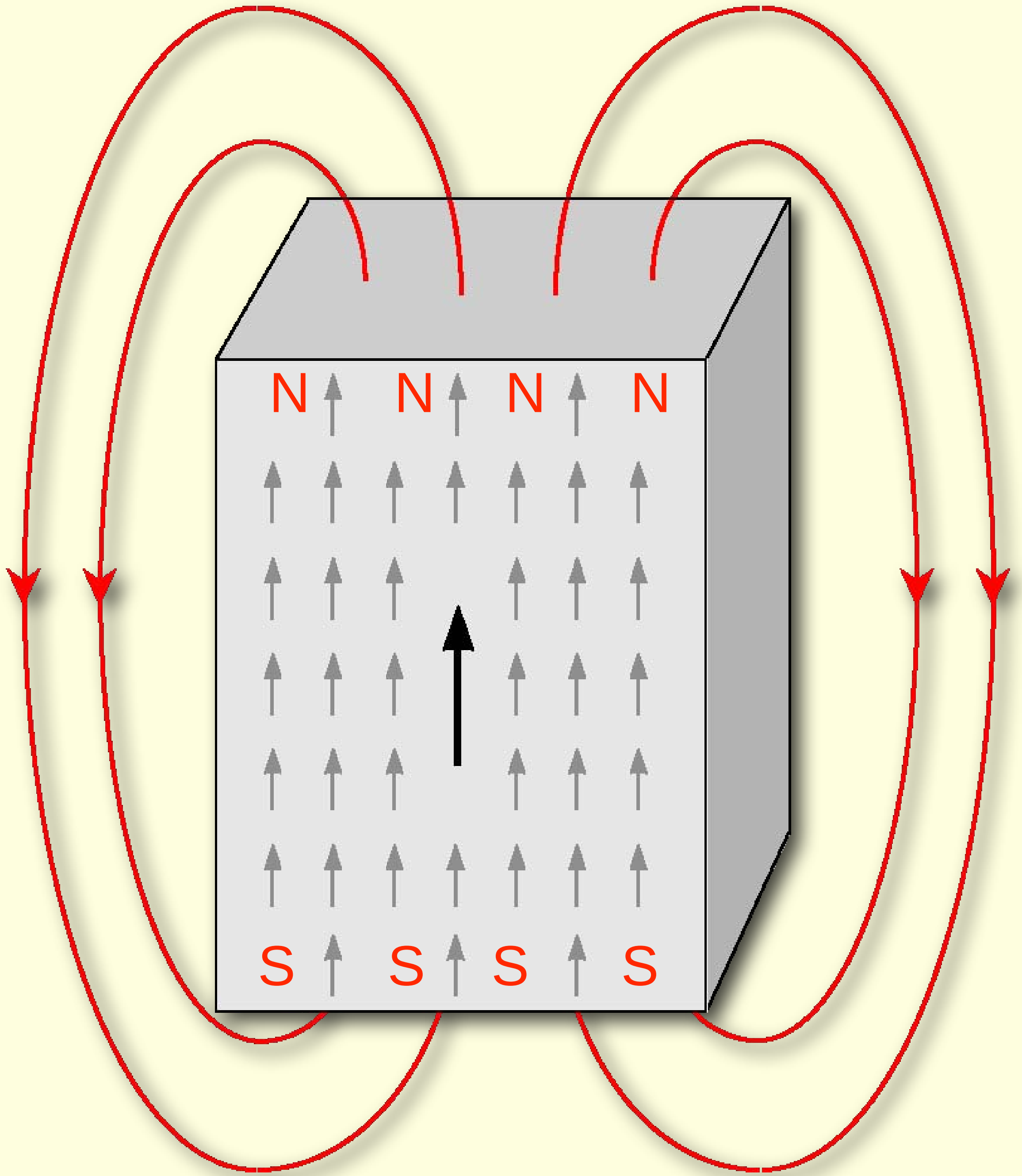

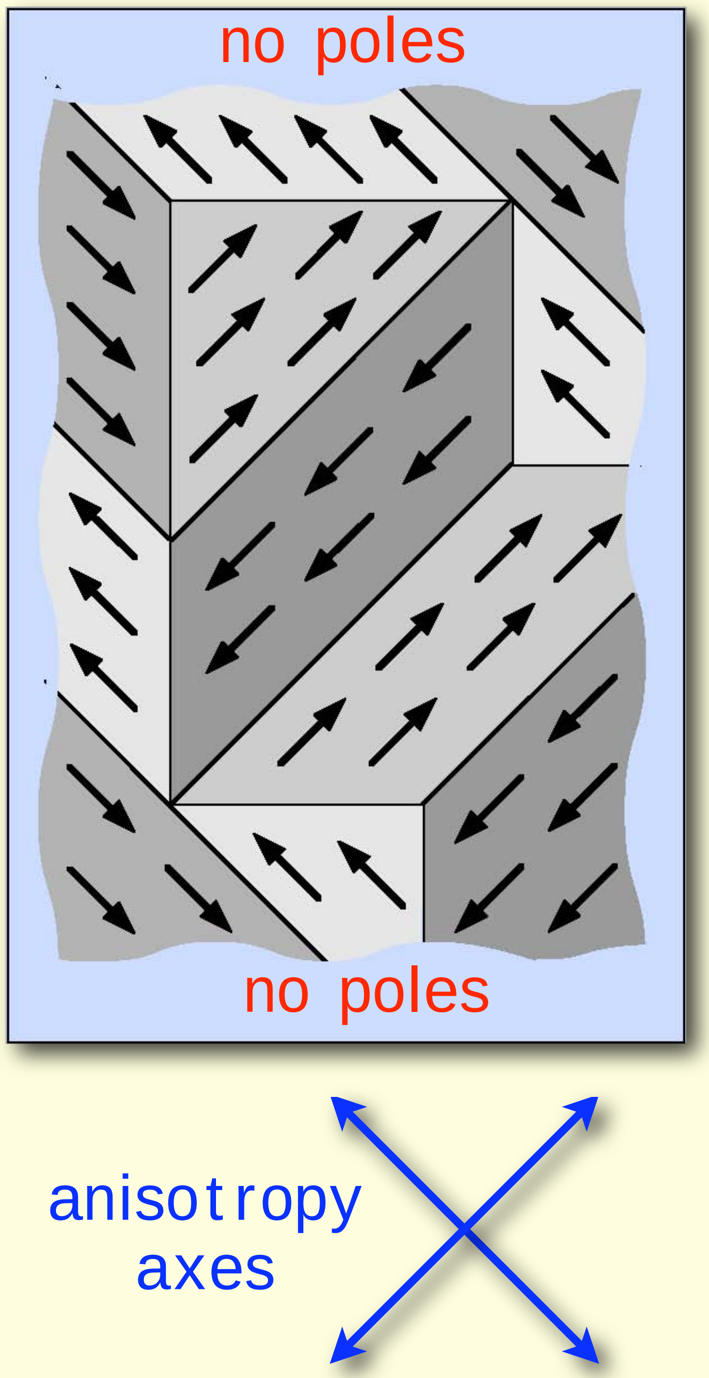

Magnetic Domains:
Areas of different magnetization direction,
but equal magnetization strength (M_s)

Quality factor Q

Character of magnetic domains is determined by quality factor Q (= material parameter)

$$Q = \frac{\text{Anisotropy constant } K}{\text{Stray-field energy coefficient } (K_d = \mu_0 M_s^2/2)}$$

NiFe film element

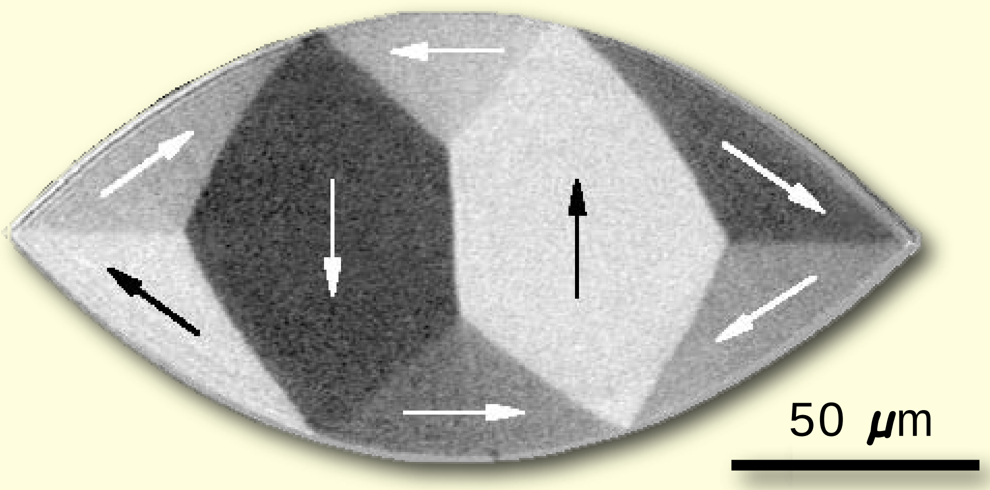

anisotropy axis

Q < 1:
→ stray field energy dominates
→ flux-closed magnetization
→ soft magnets

Garnet film

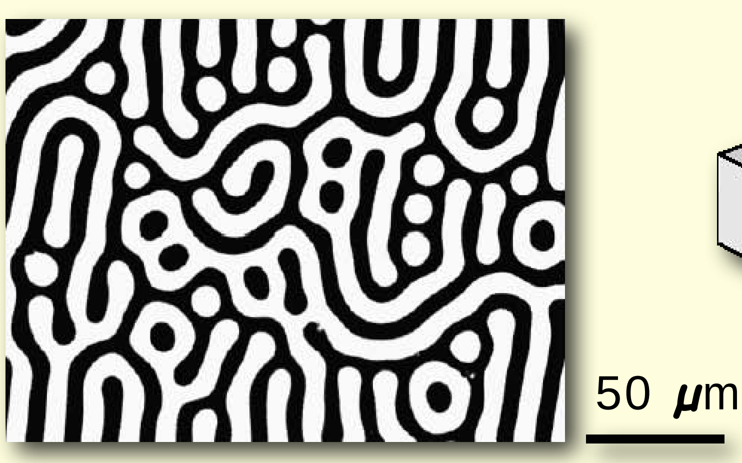

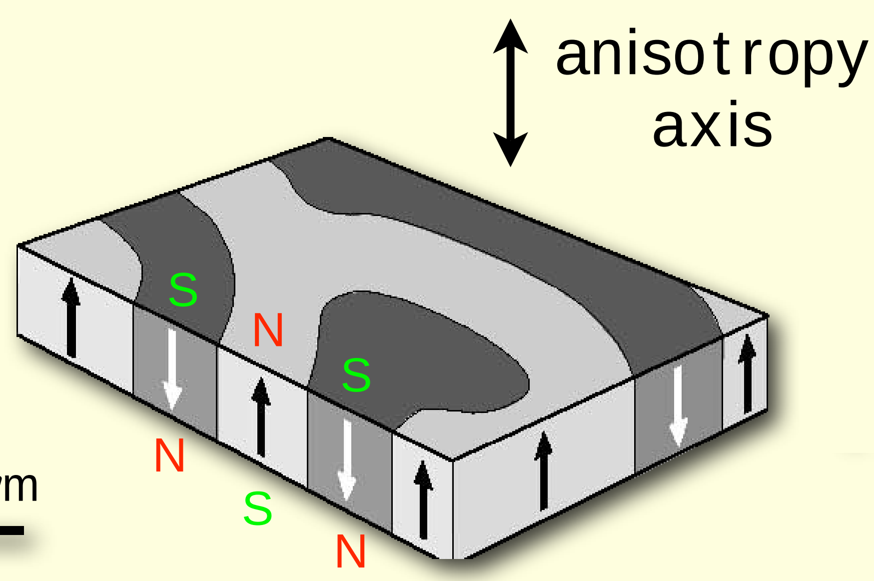

Q > 1:
→ anisotropy energy dominates
→ „open“ magnetization
→ hard magnets

Domain wall

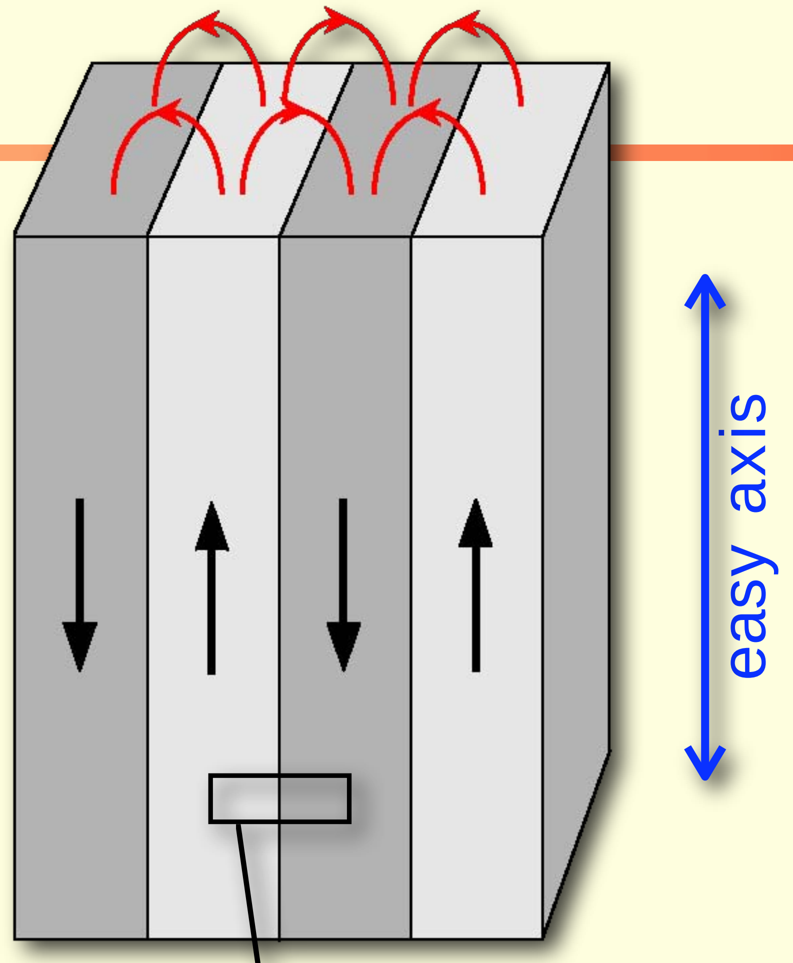

Bloch wall width:

$$\sim \sqrt{A/K}$$

A: exchange constant

K: anisotropy constant

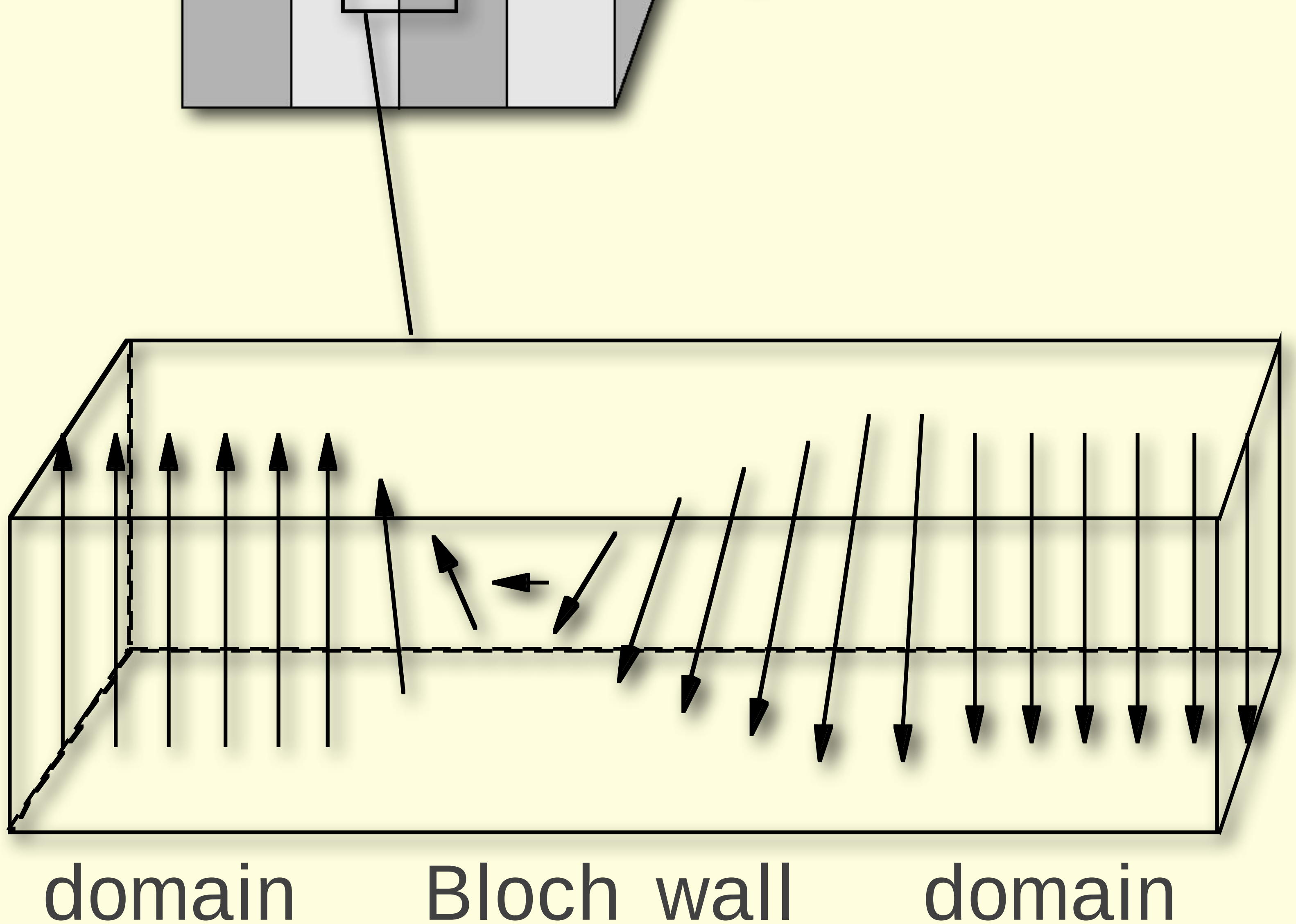

Single domain particle

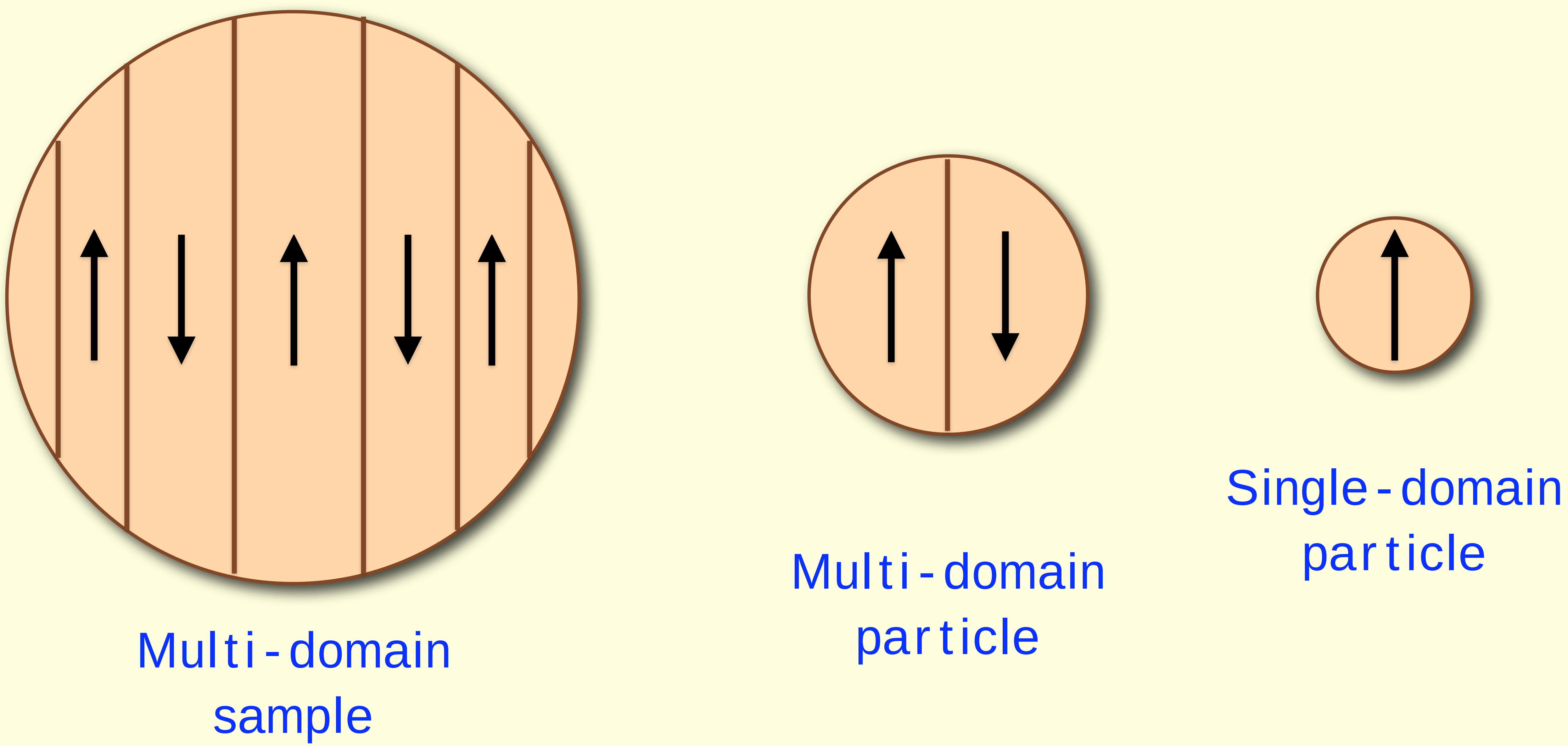

Coercivity and grain size

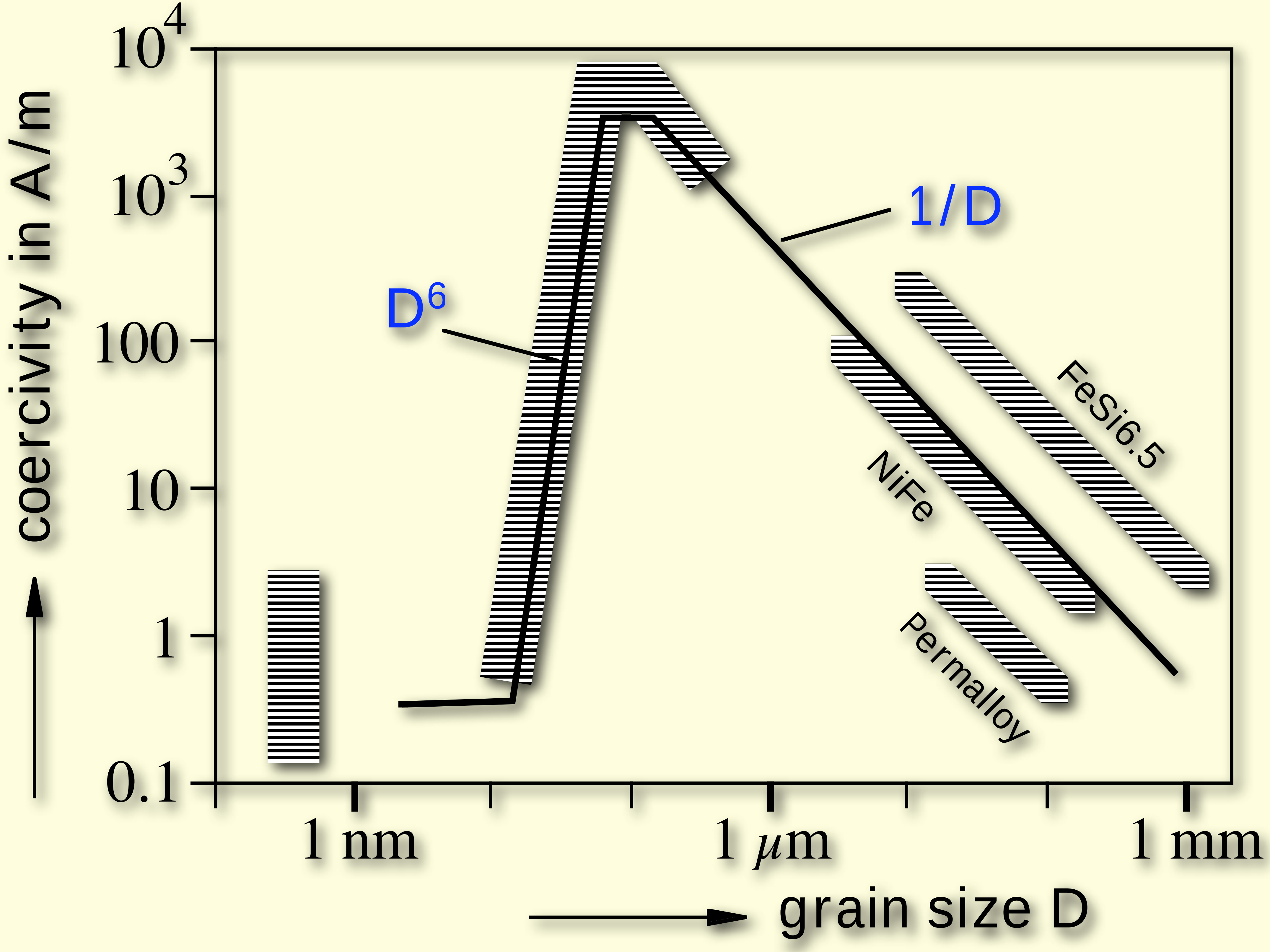

G. Herzer, Nanocrystalline soft magnetic alloys. In: Buschow KHJ, editor. Handbook of Magnetic Materials, vol. 10. Elsevier Science B.V., p.415 (1997)

Coercivity and grain size

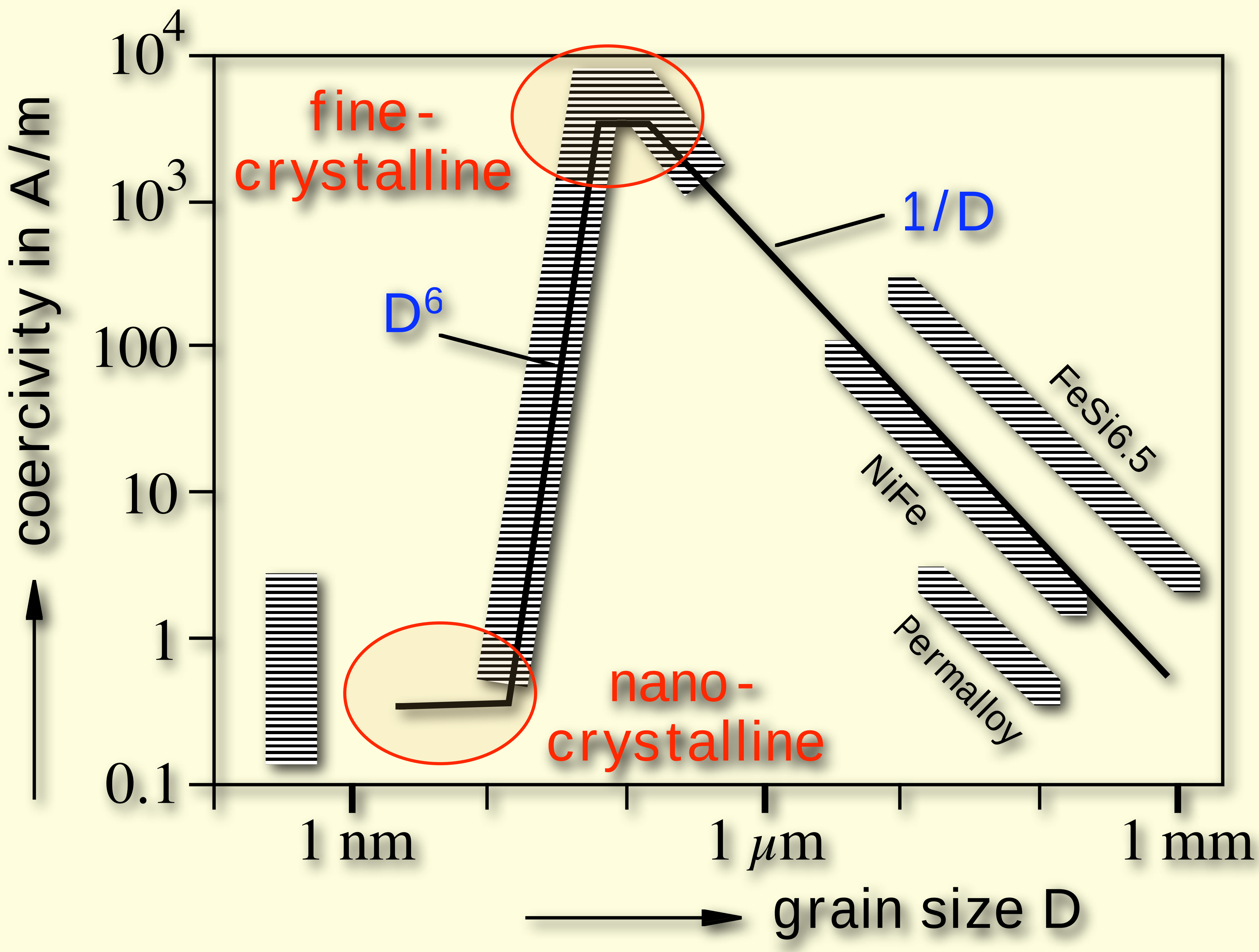

G. Herzer, Nanocrystalline soft magnetic alloys. In: Buschow KHJ, editor. Handbook of Magnetic Materials, vol. 10. Elsevier Science B.V., p.415 (1997)

Coercivity and grain size

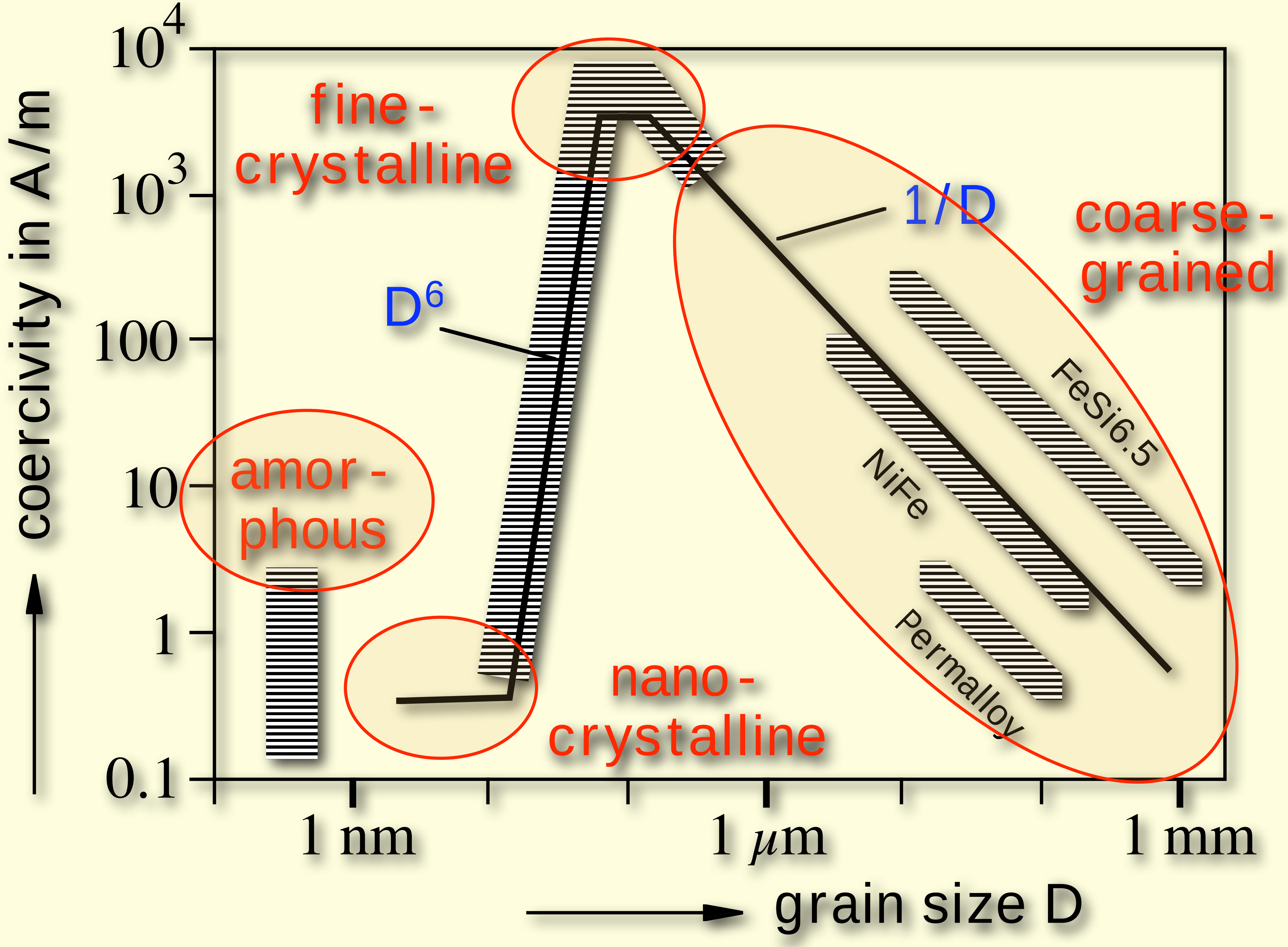

G. Herzer, Nanocrystalline soft magnetic alloys. In: Buschow KHJ, editor. Handbook of Magnetic Materials, vol. 10. Elsevier Science B.V., p.415 (1997)

Overview

1. Domains in coarse-grained material

2. Domains in amorphous material

3. Domains in nanocrystalline, soft magnetic ($Q \ll 1$) materials

4. Domains in fine- and nanostructured, permanent magnetic ($Q > 1$) materials

Overview

1. Domains in coarse-grained material

2. Domains in amorphous material

3. Domains in nanocrystalline, soft magnetic ($Q<<1$) materials

4. Domains in fine- and nanostructured, permanent magnetic ($Q>1$) materials

Non-oriented electrical steel

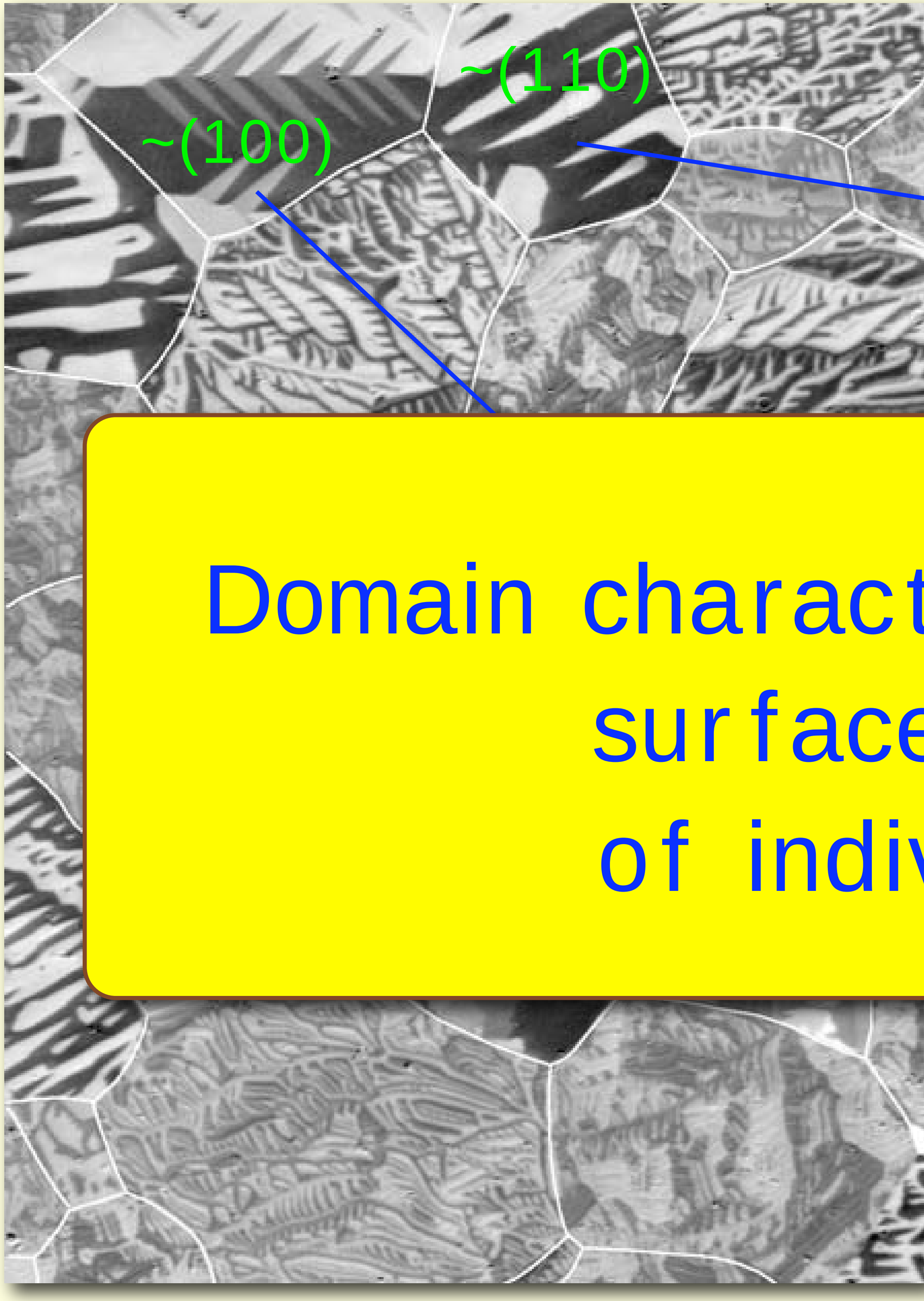

0.5 mm

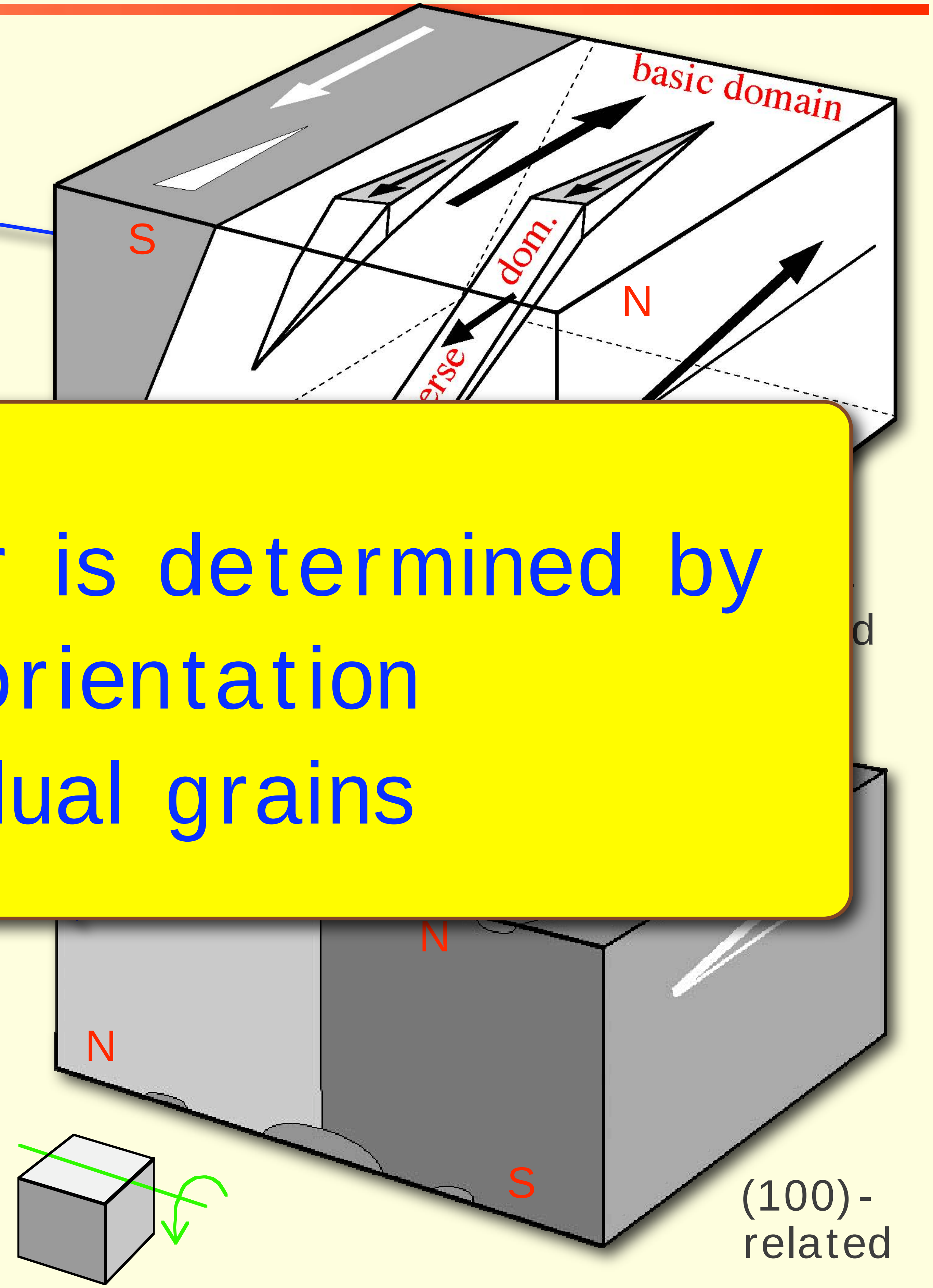

Domain character is determined by surface orientation of individual grains

Coarse-grained materials

Non-oriented electrical steel

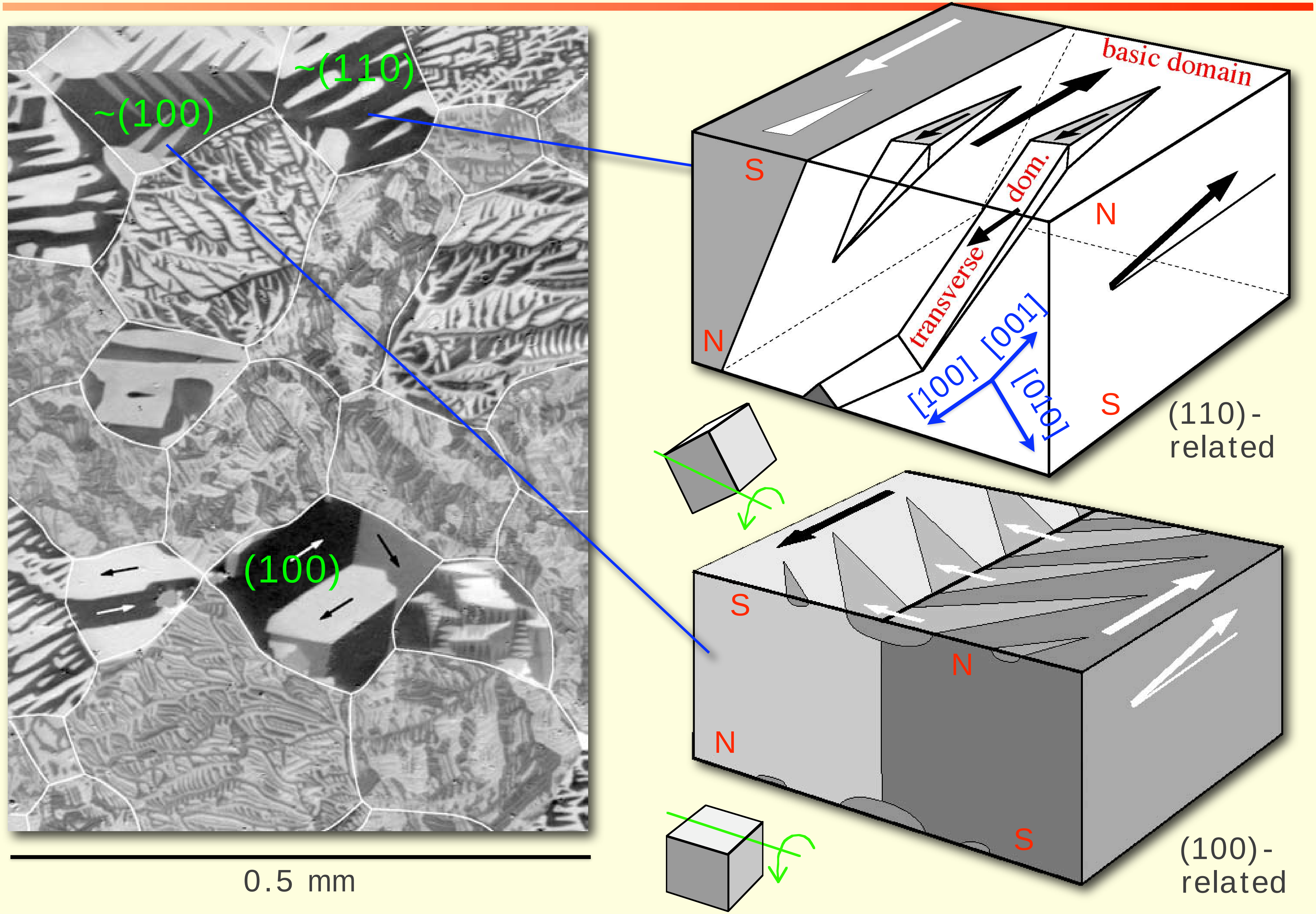

Coarse-grained materials

Non-oriented electrical steel

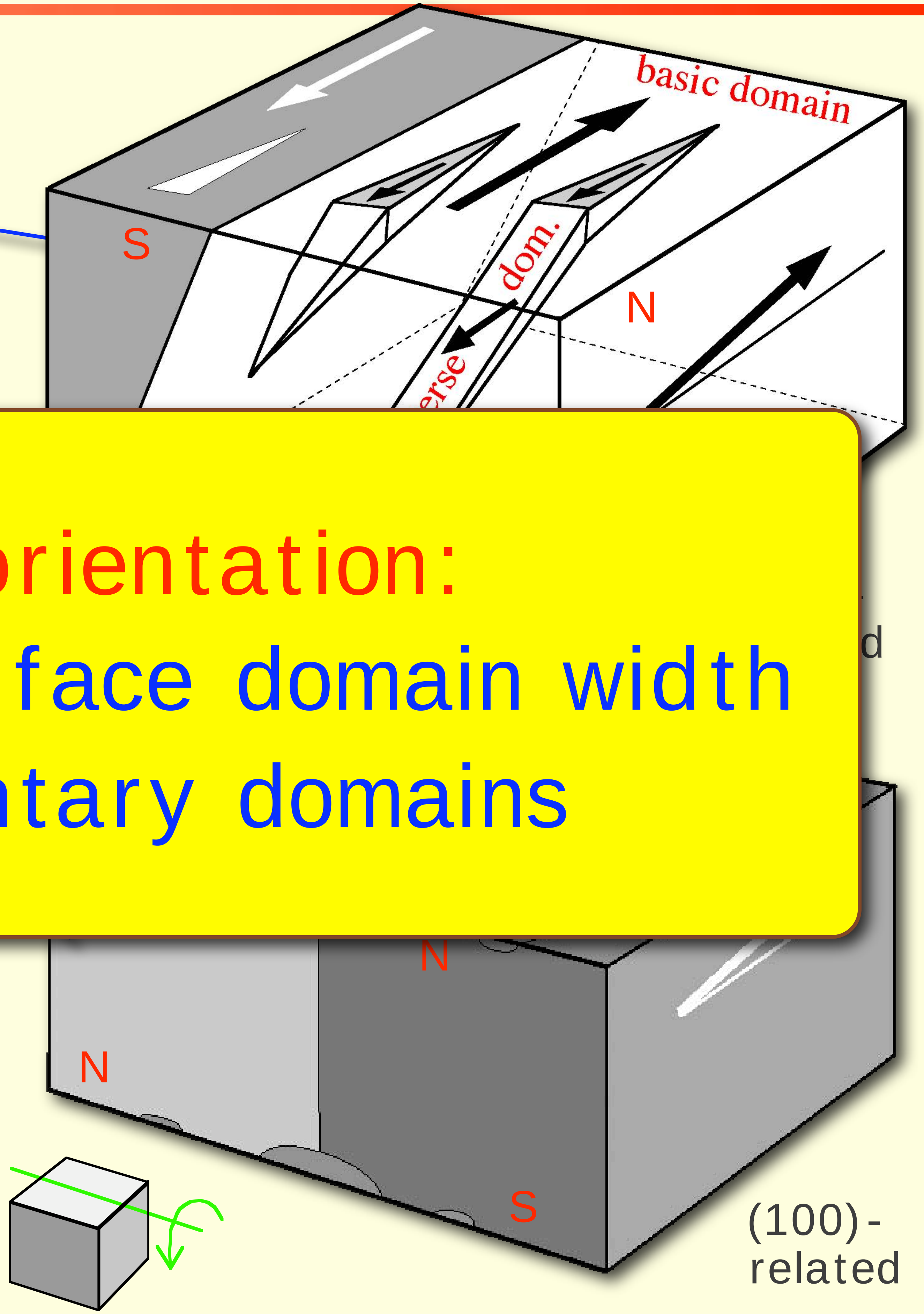

Weak misorientation:

Refinement of surface domain width by supplementary domains

Non-oriented electrical steel

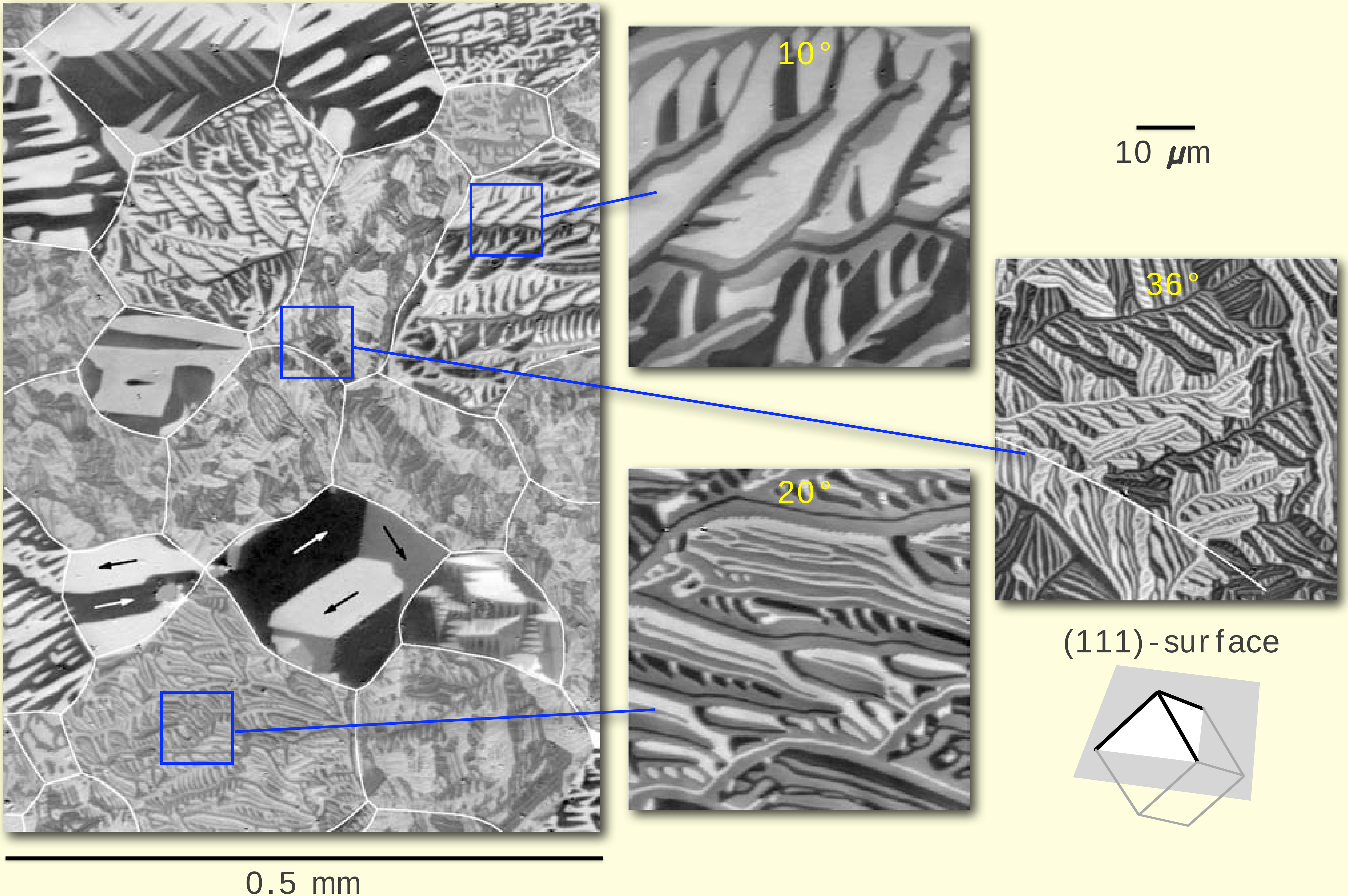

Non-oriented electrical steel

0.5 mm

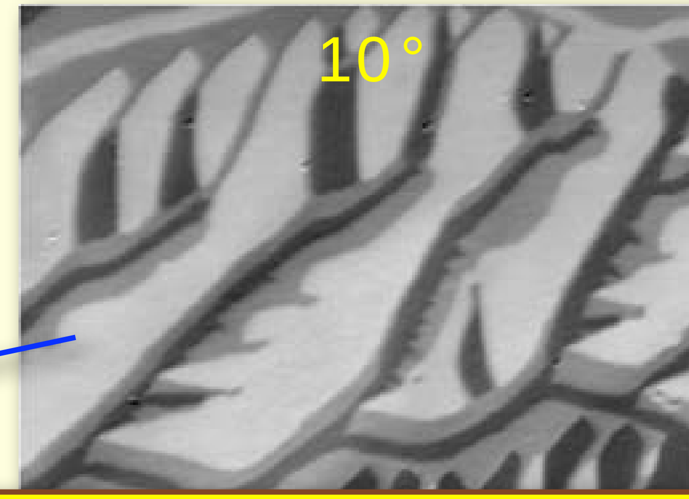

10 μm

Increasing misorientation:
Domain complexity increases

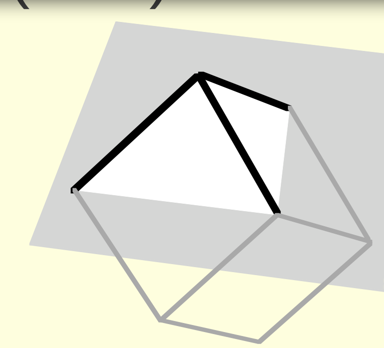

Extreme misorientation: FeSi (111) surface

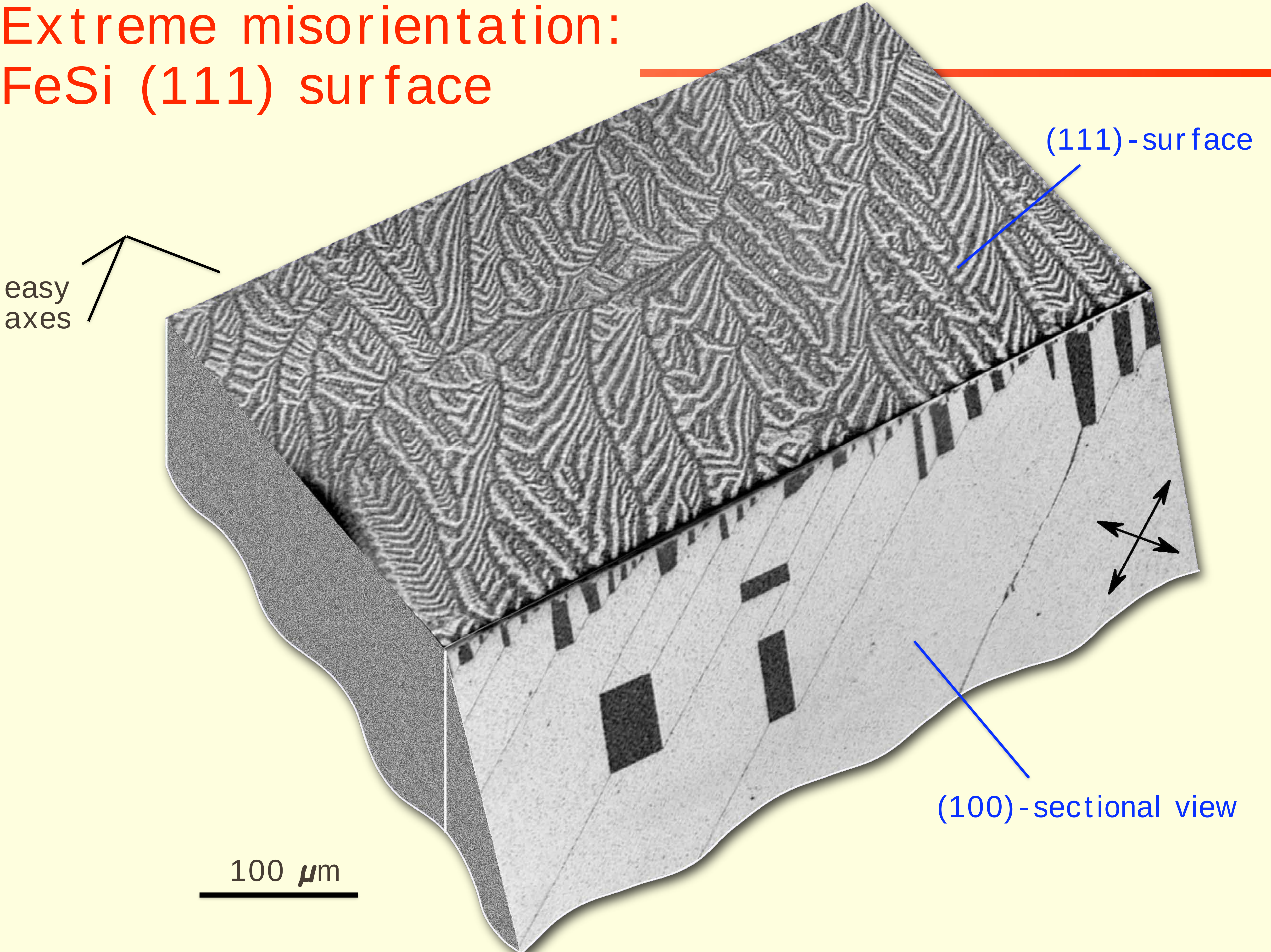

Extreme misorientation: FeSi (111) surface

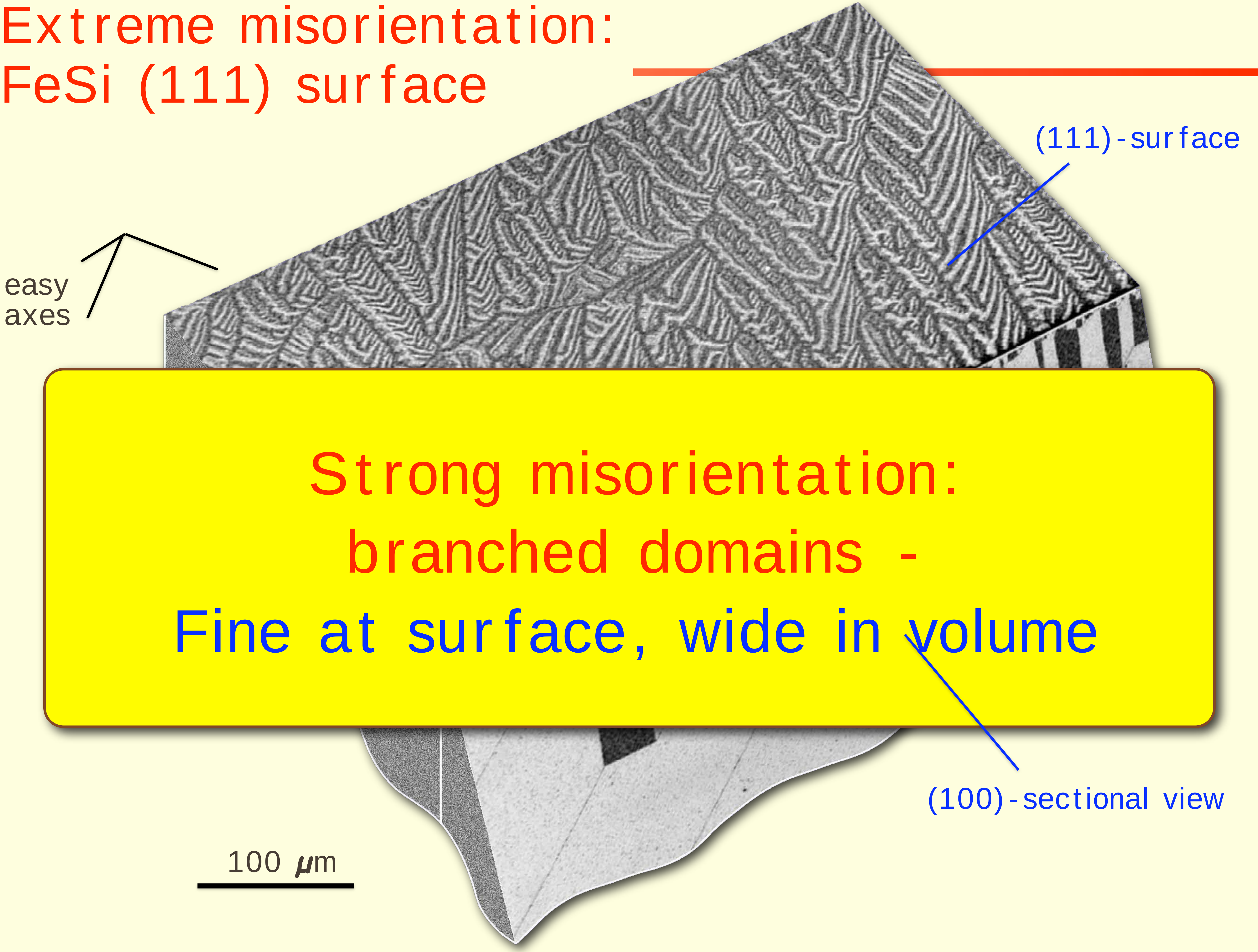

Strong misorientation:
branched domains -
Fine at surface, wide in volume

Extreme misorientation: 2-dim. model

Four-phase branching: the echelon pattern

Fe plate

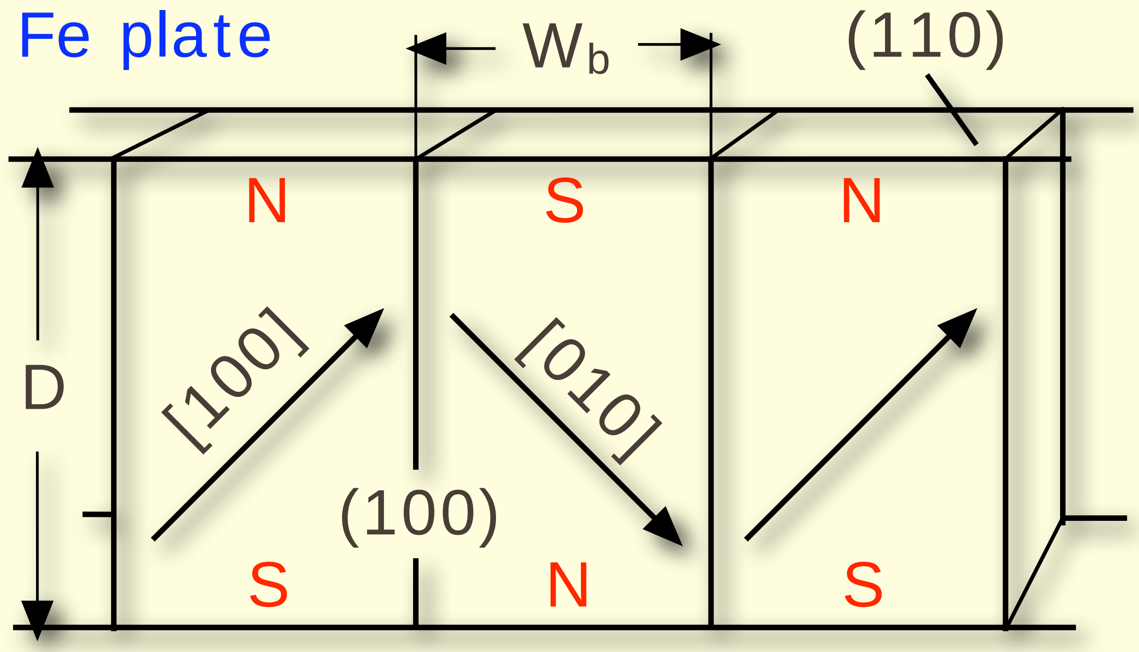

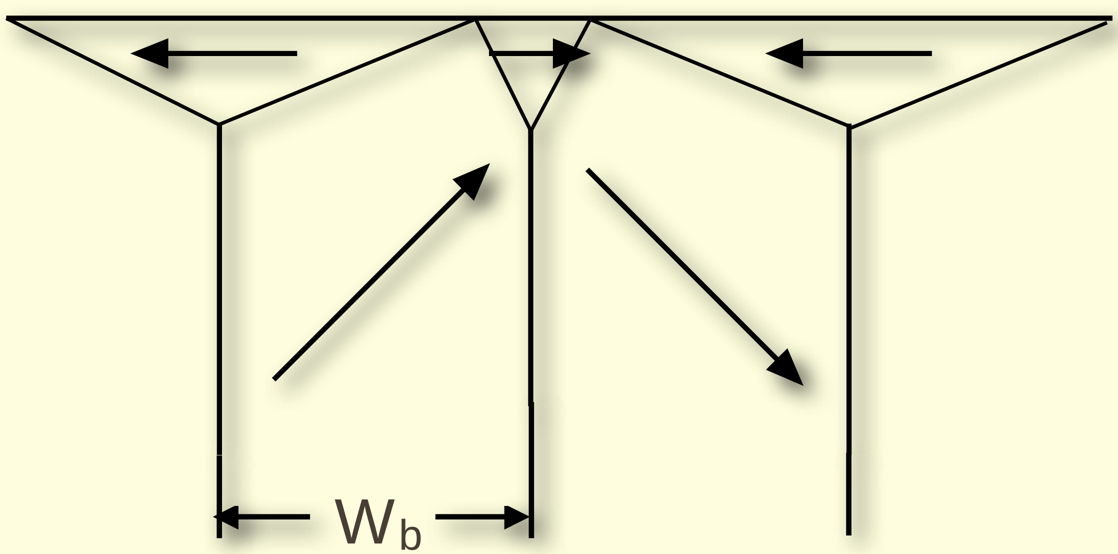

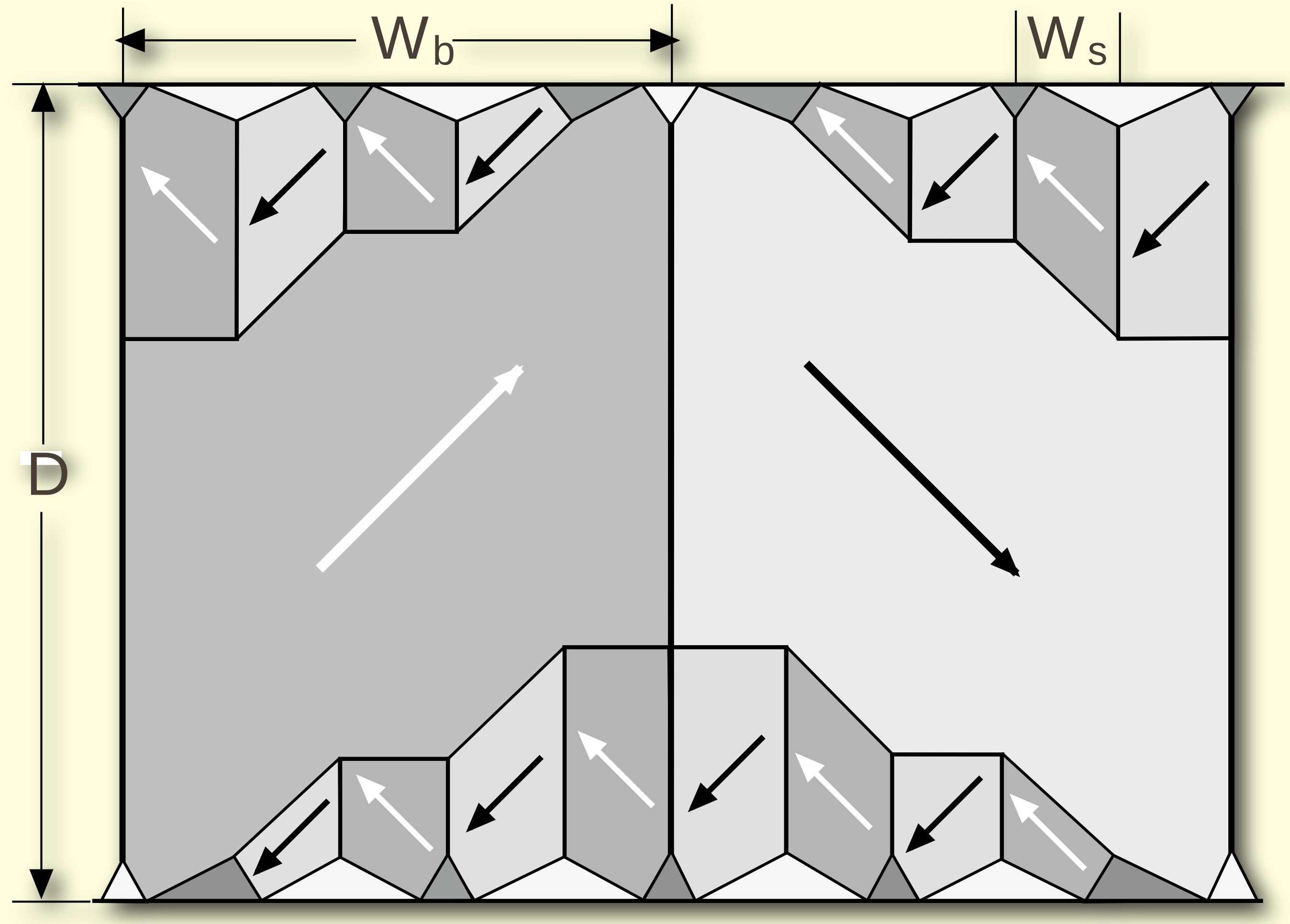

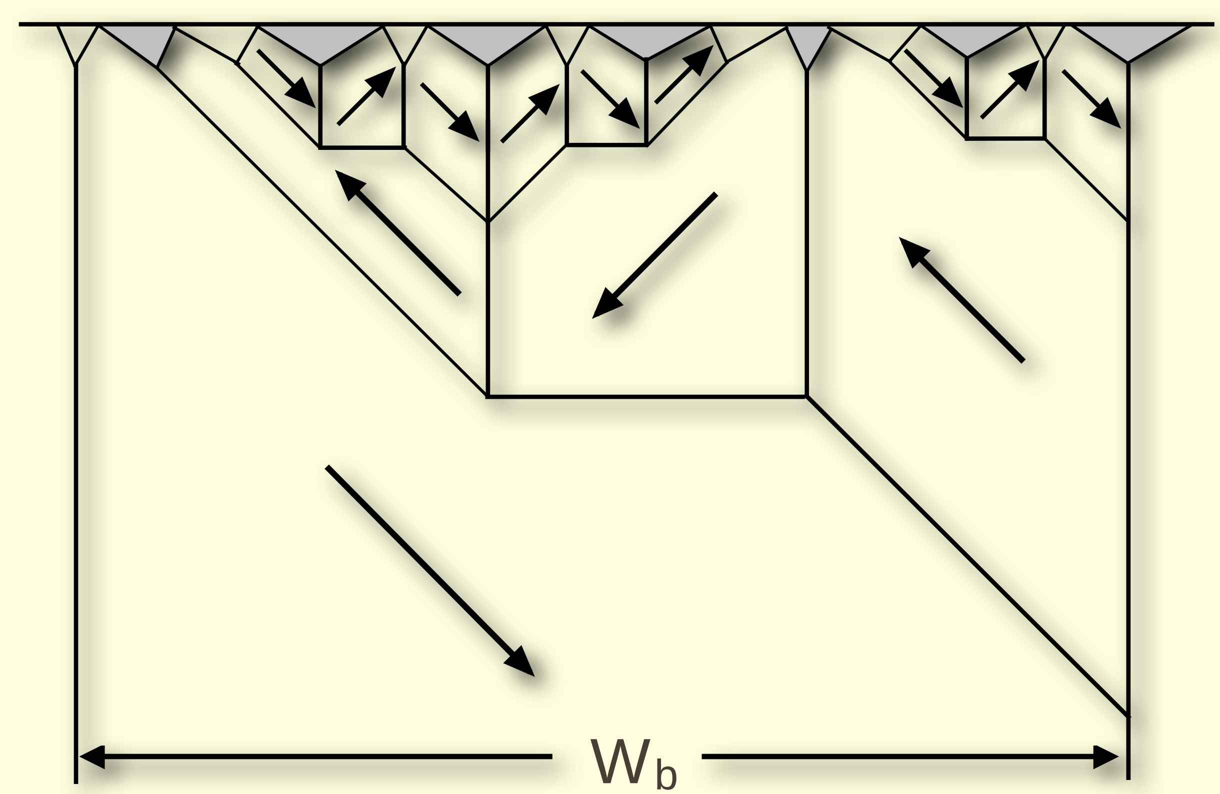

$$W_b \sim \sqrt{D}$$

Extreme misorientation: 2-dim. model

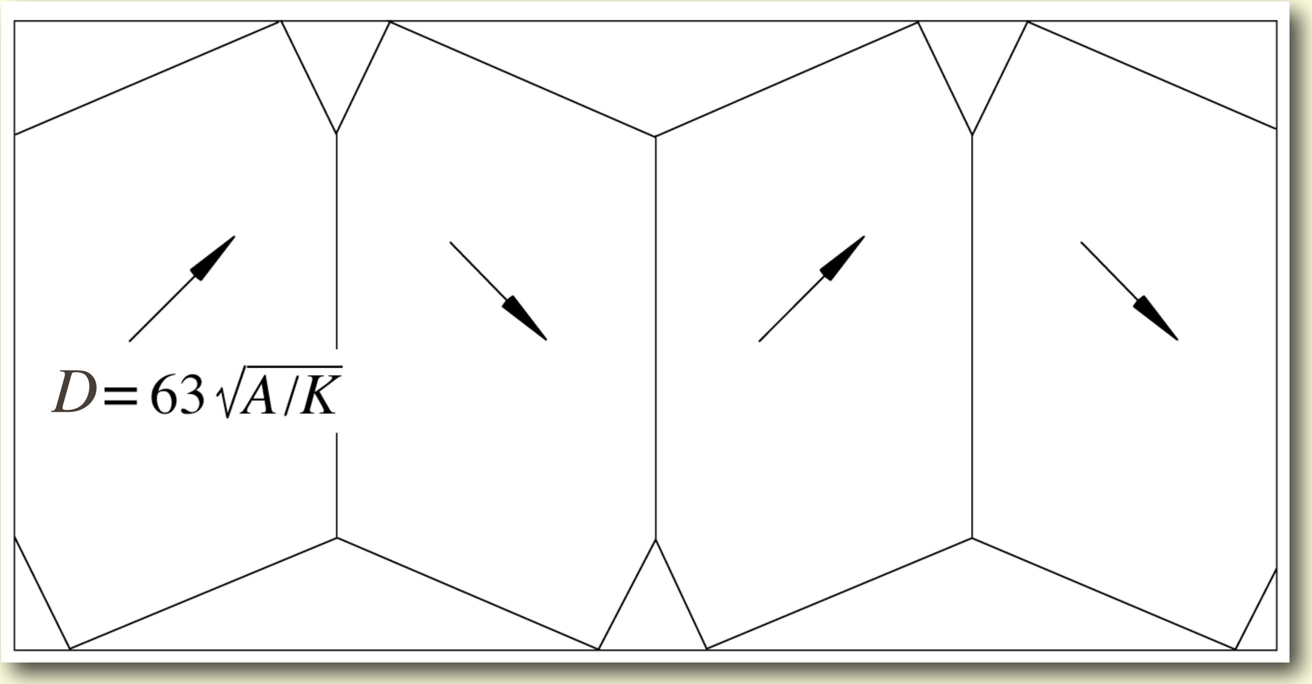

no branching

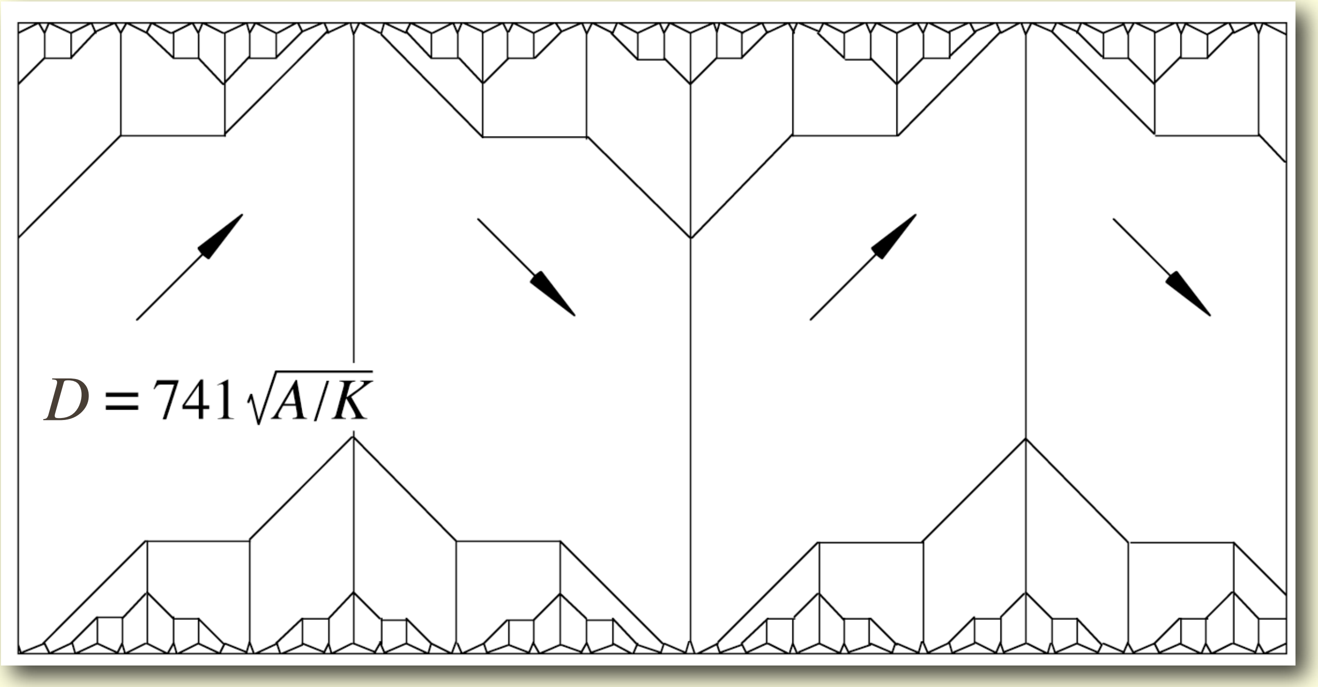

two generations

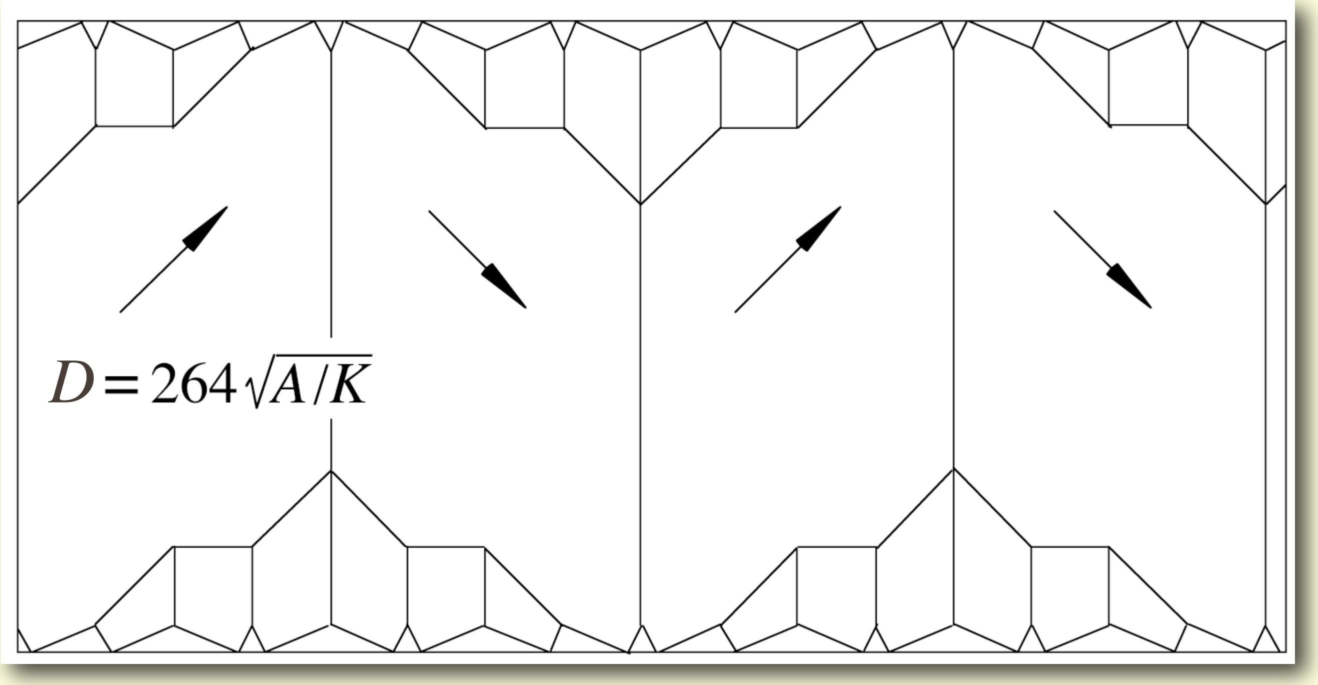

one generation

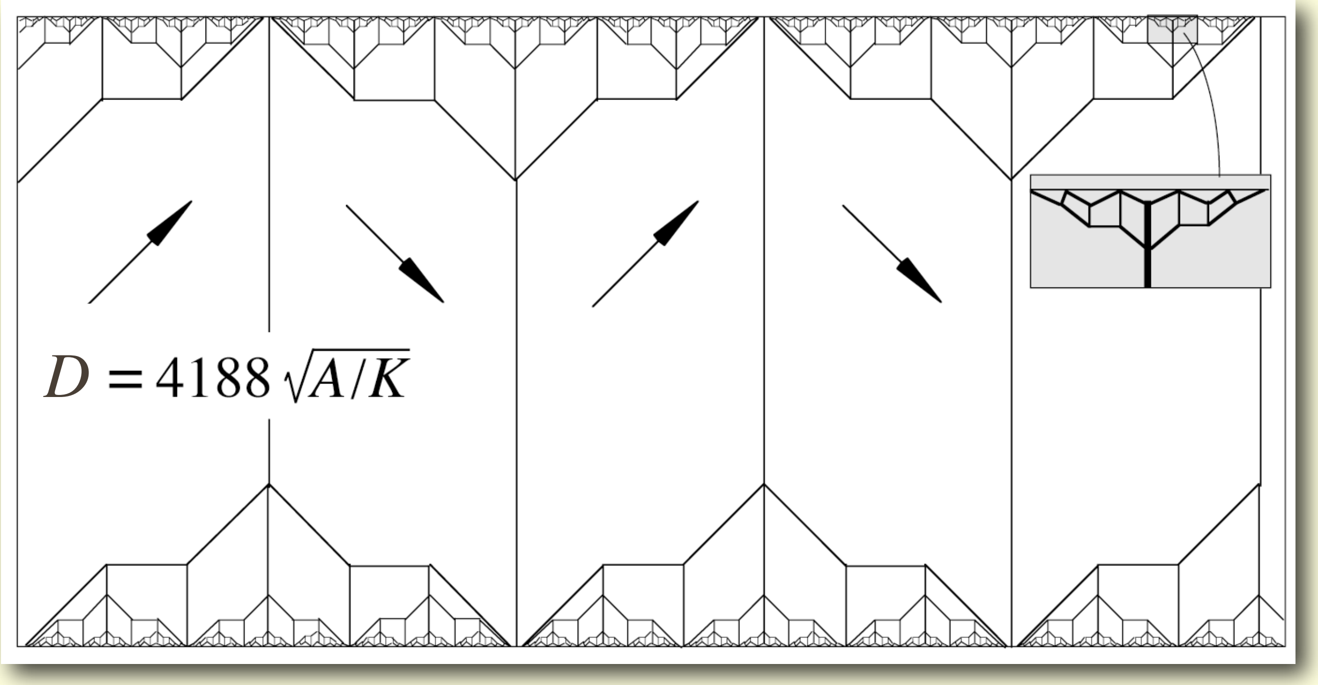

three generations

Multi-phase branching

Experiment: Fe 12.8at%Si

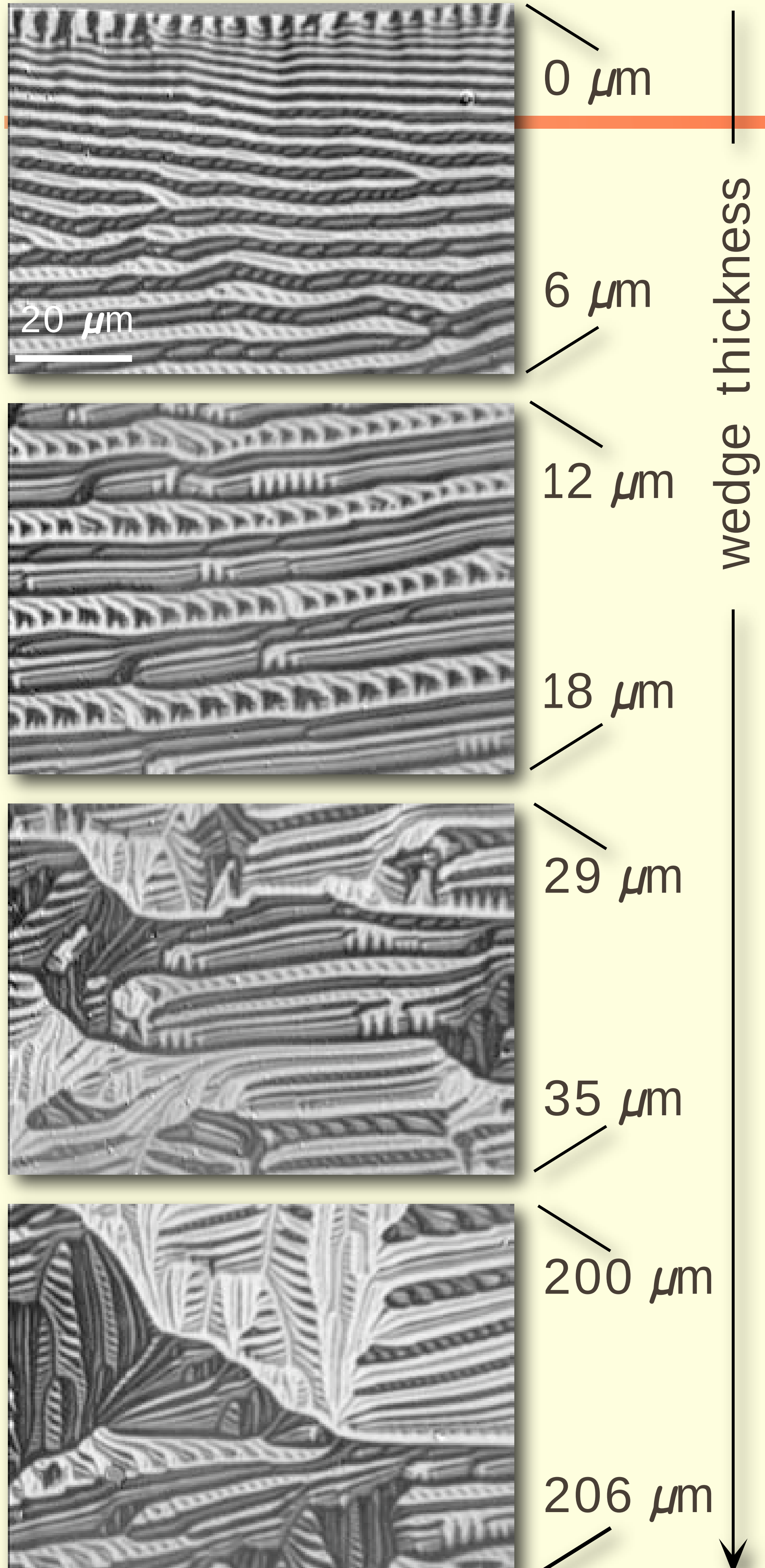

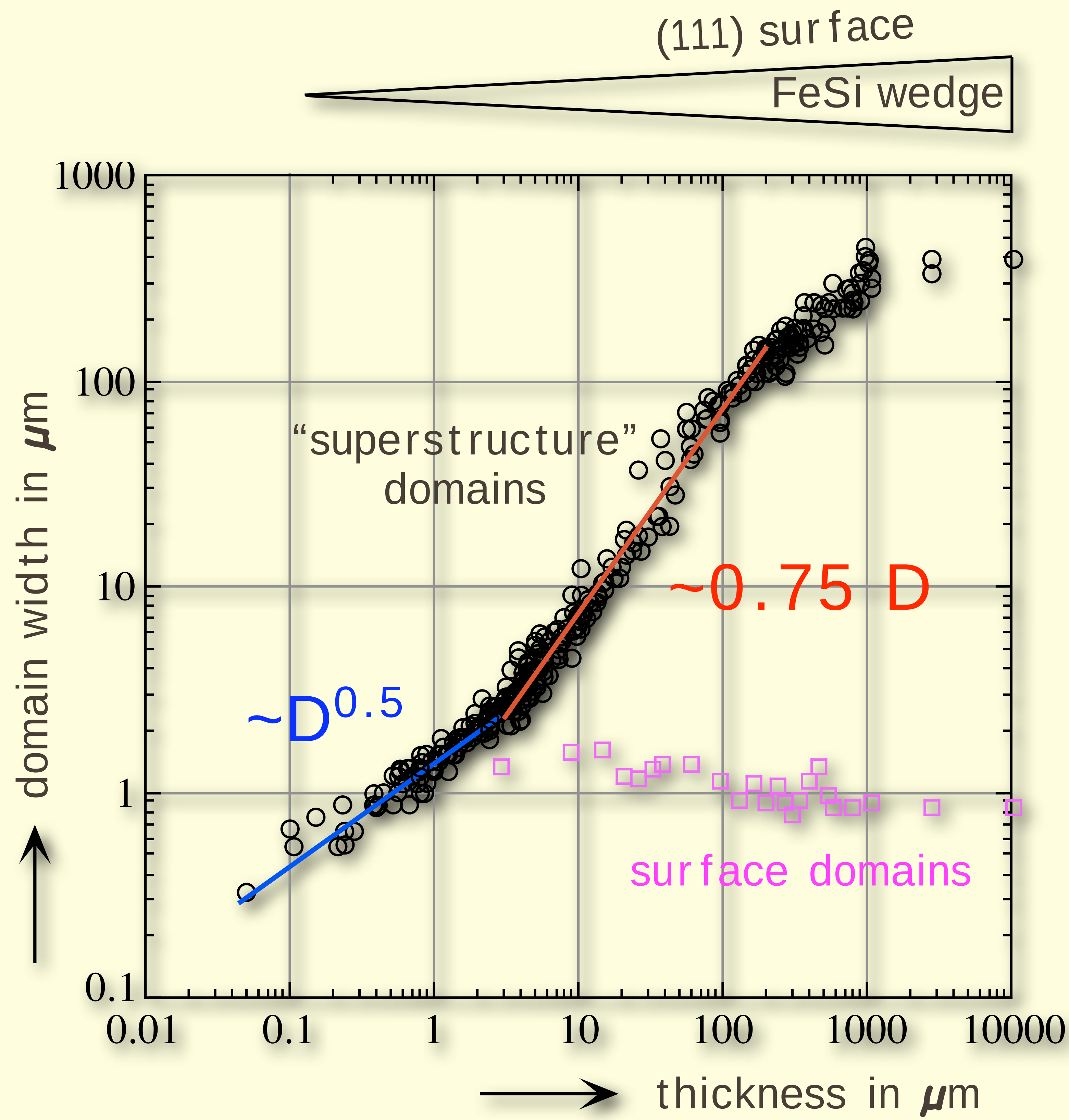

Multi-phase branching

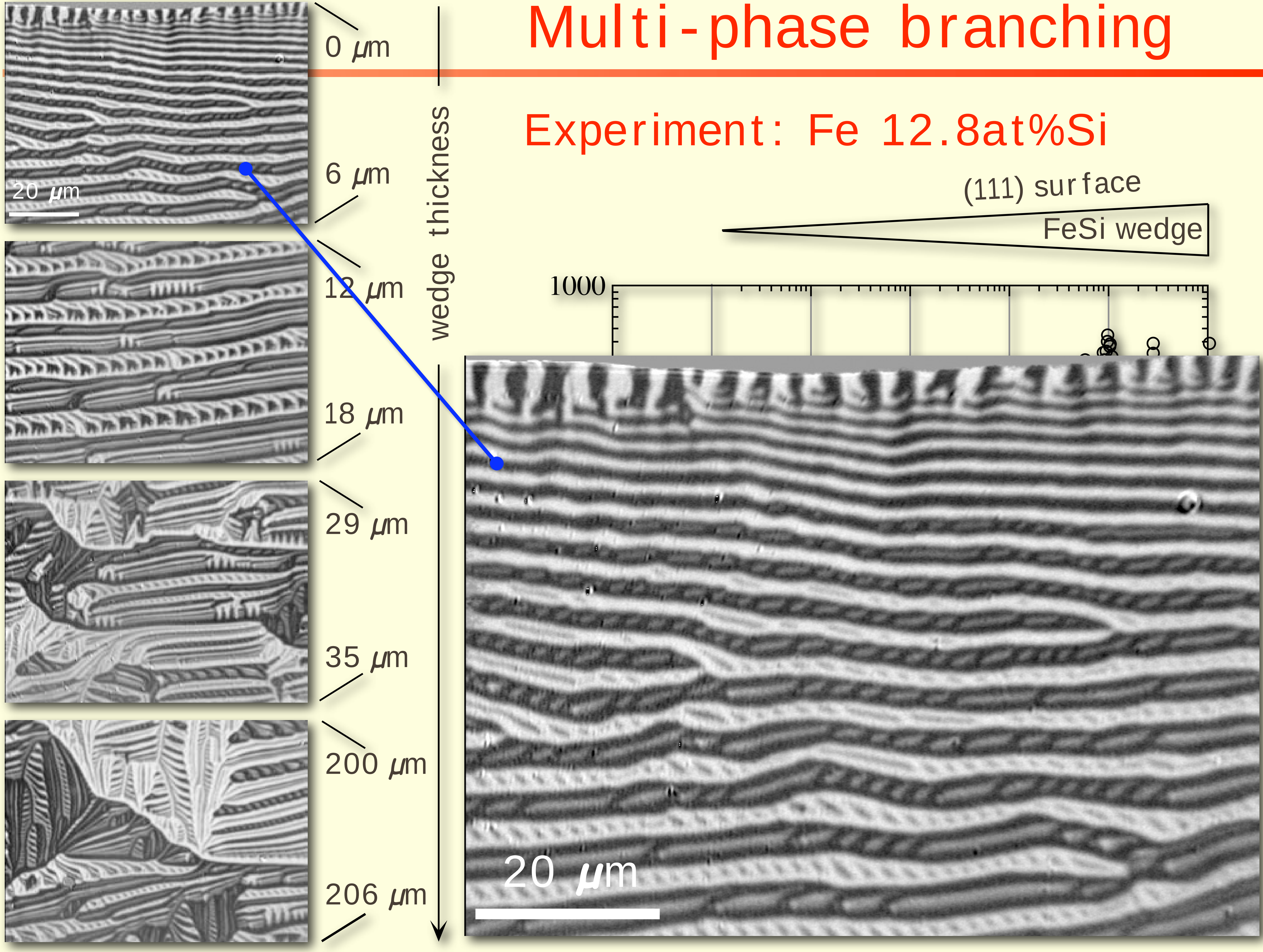

Multi-phase branching

Experiment: Fe 12.8at%Si

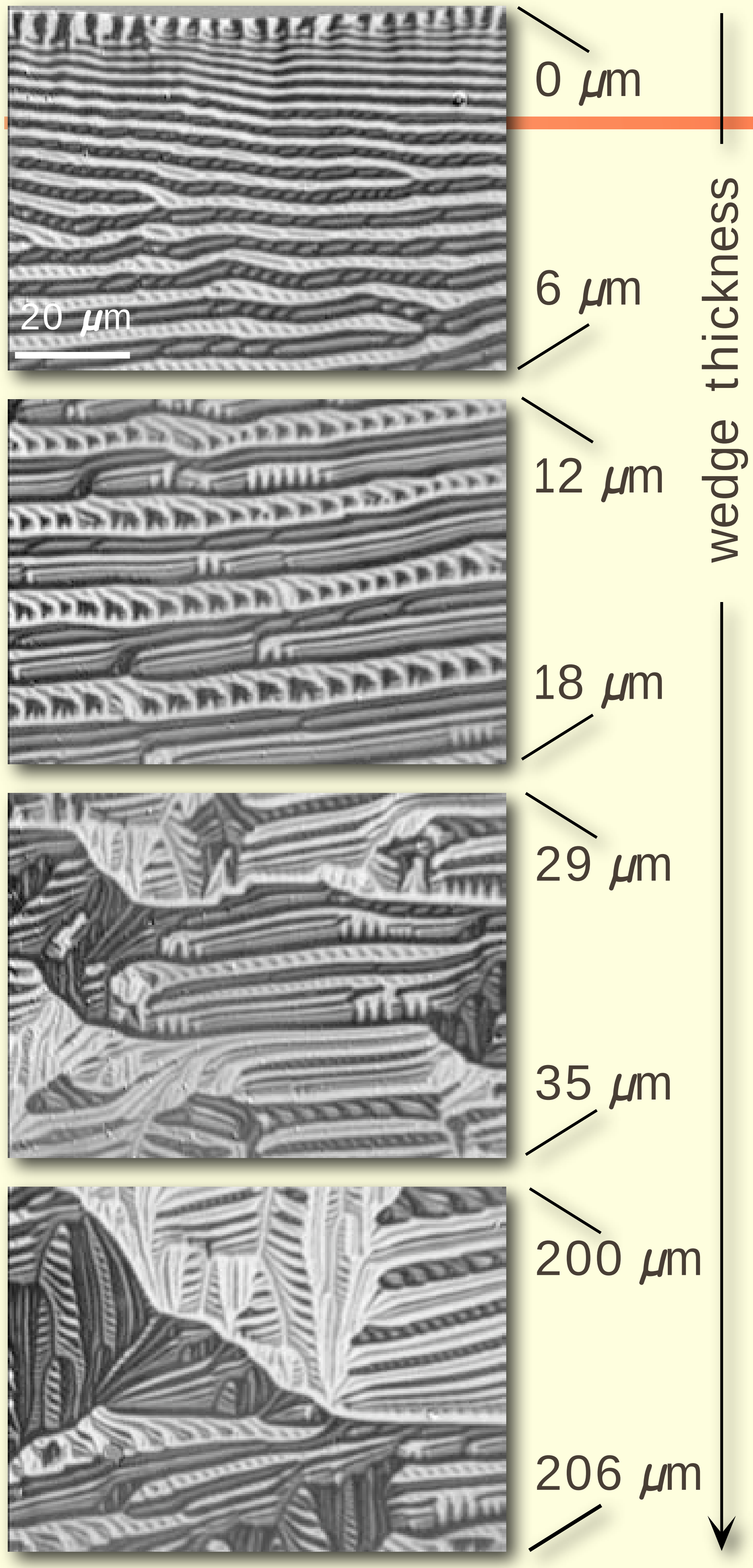

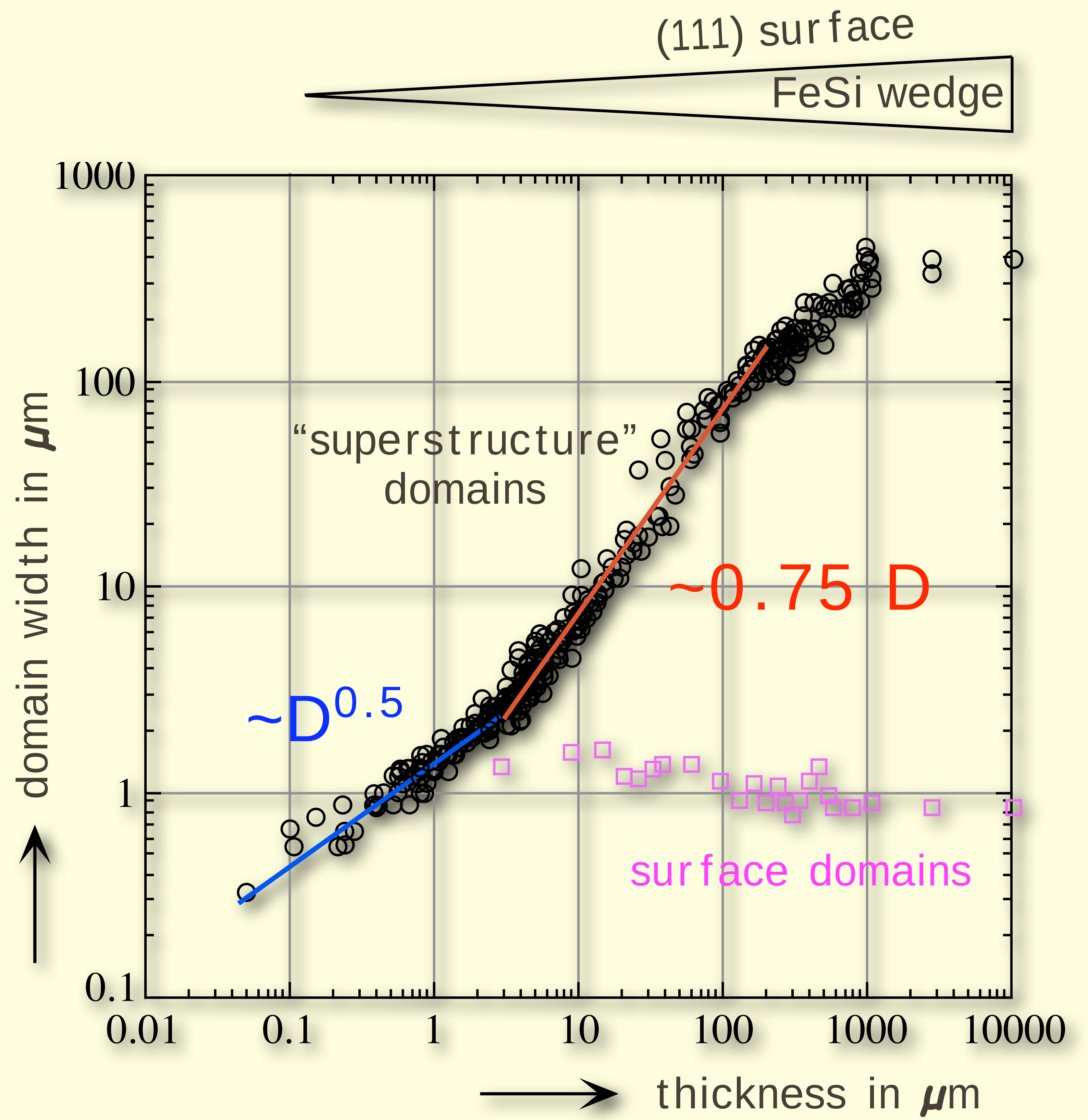

Multi-phase branching

Experiment: Fe 12.8at%Si

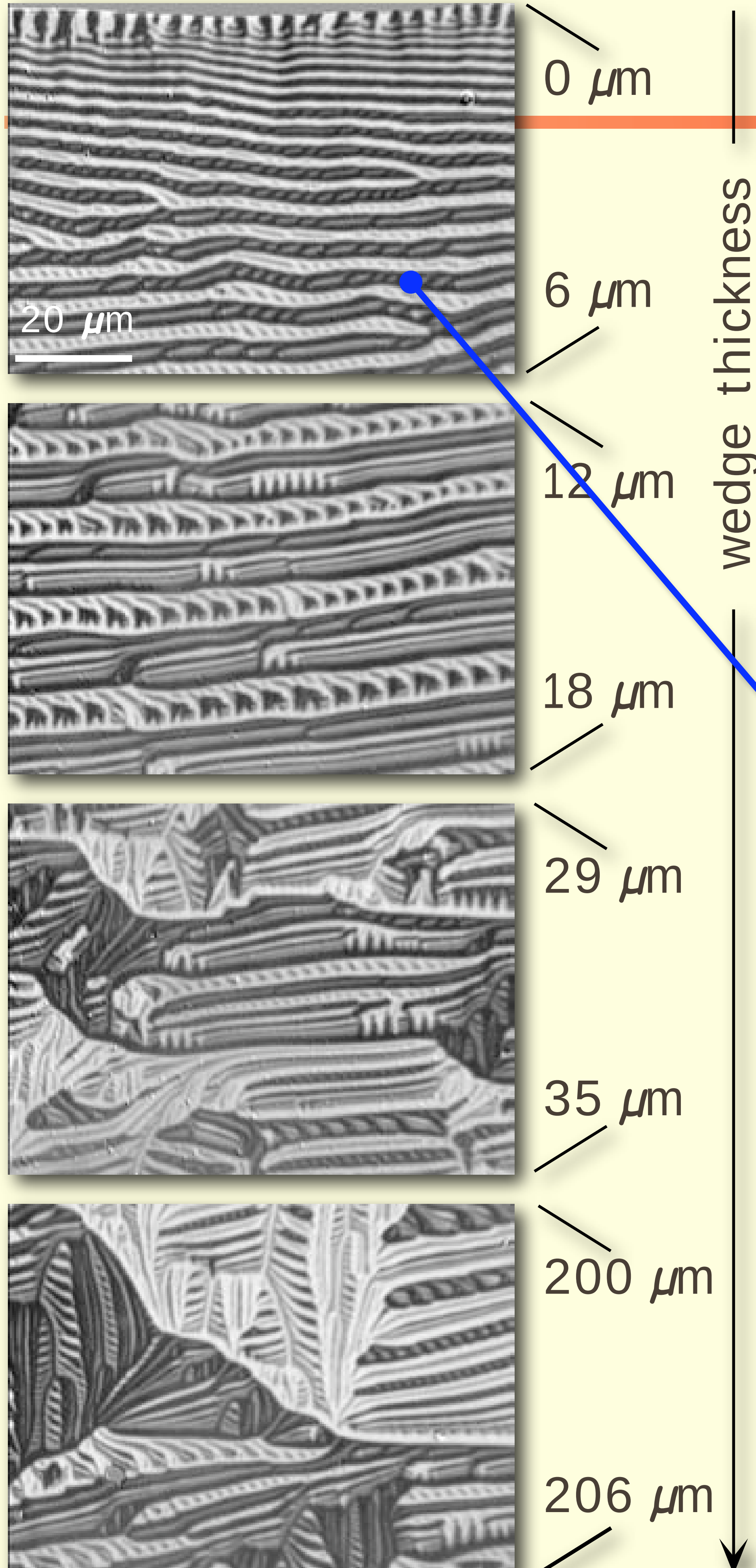

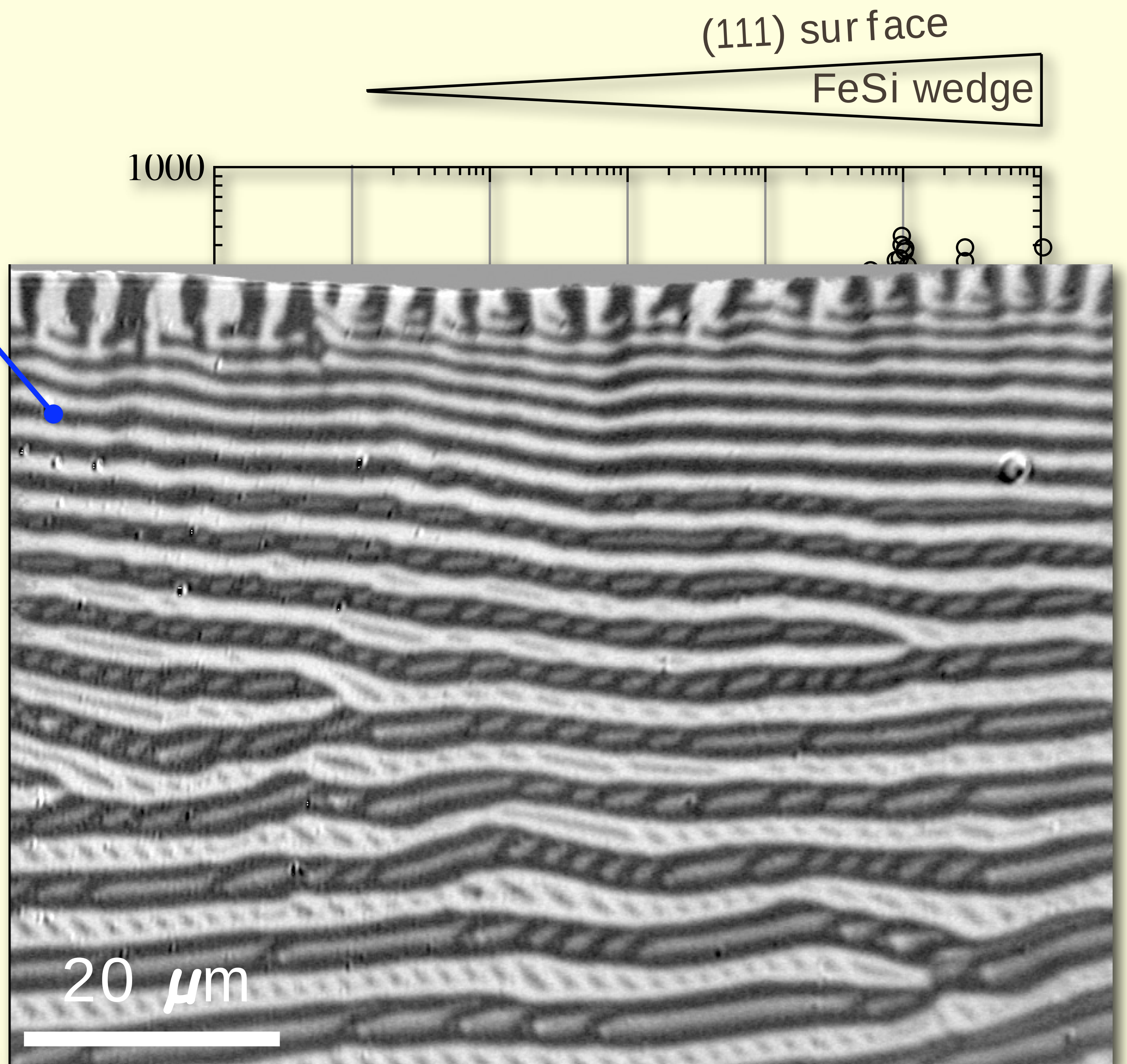

Multi-phase branching

Experiment: Fe 12.8at%Si

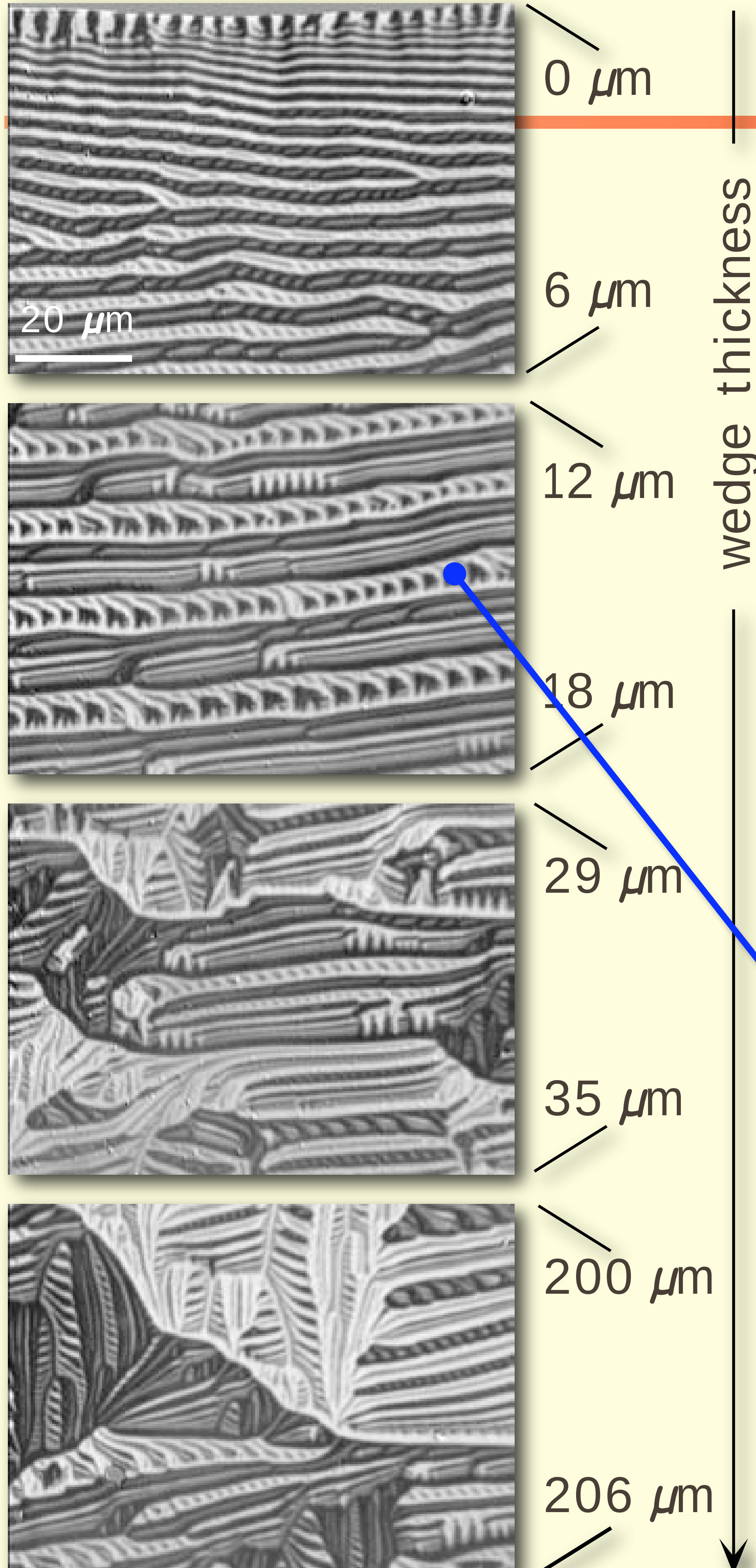

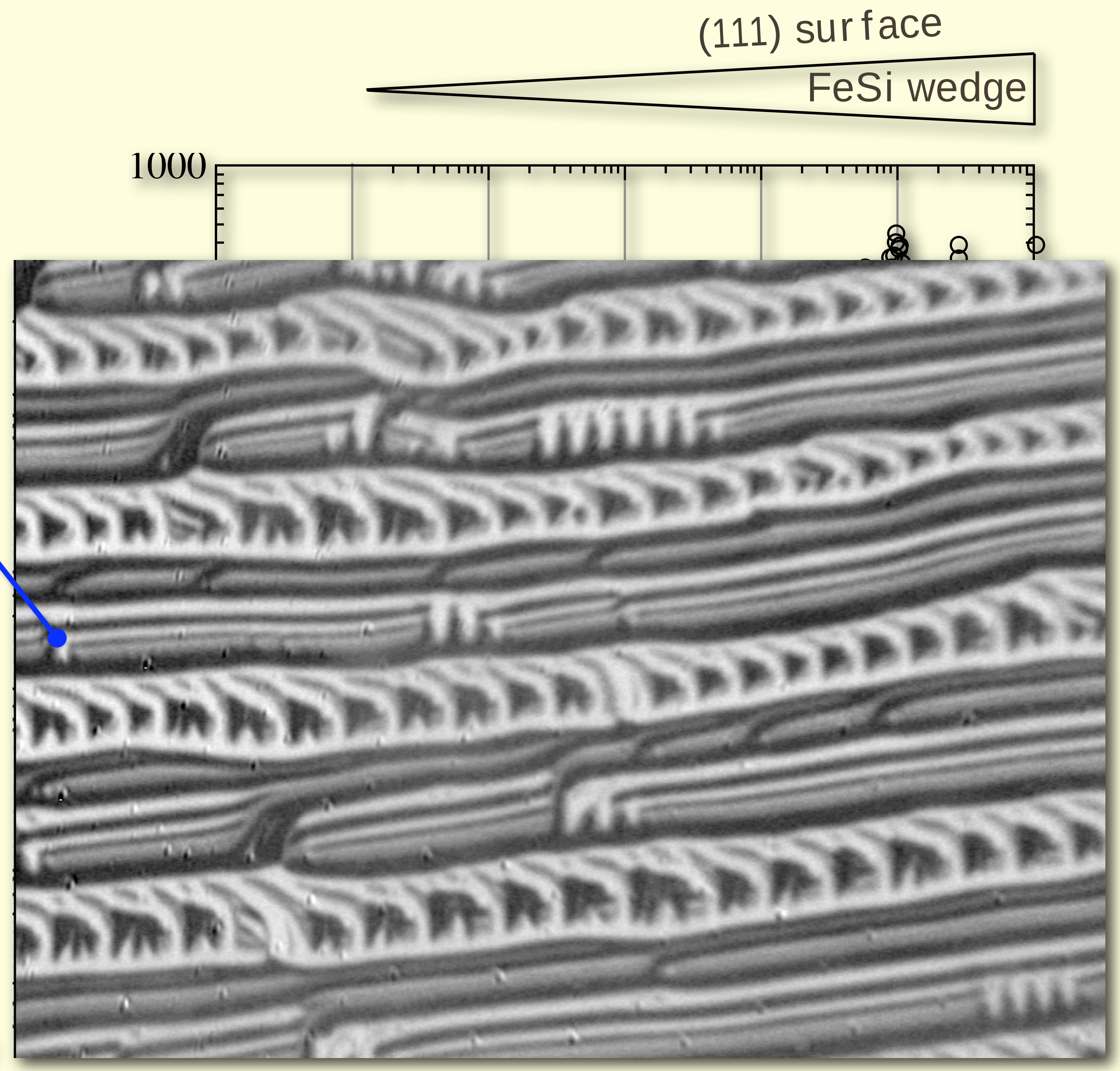

Multi-phase branching

Experiment: Fe 12.8at%Si

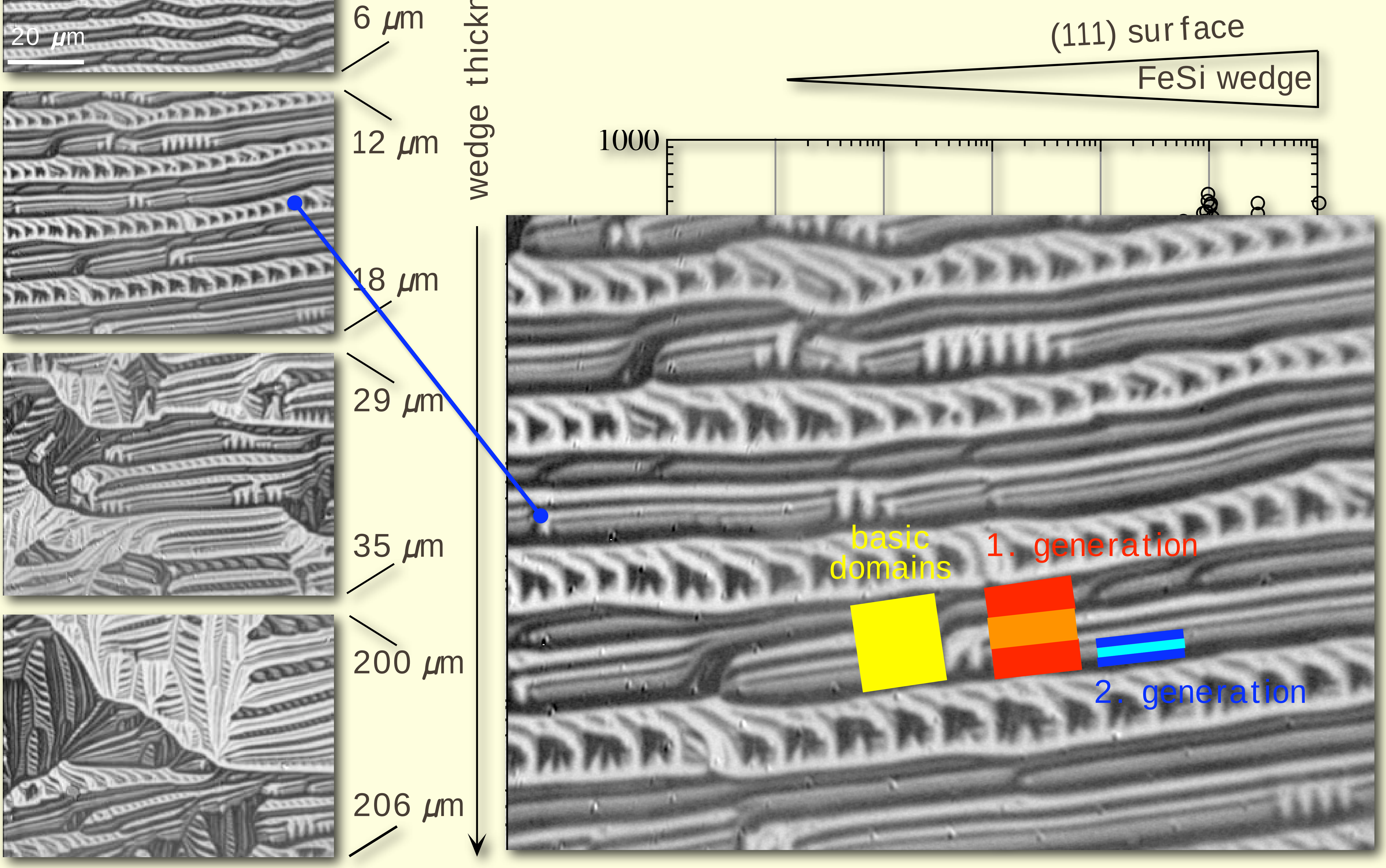

Multi-phase branching

Experiment: Fe 12.8at%Si

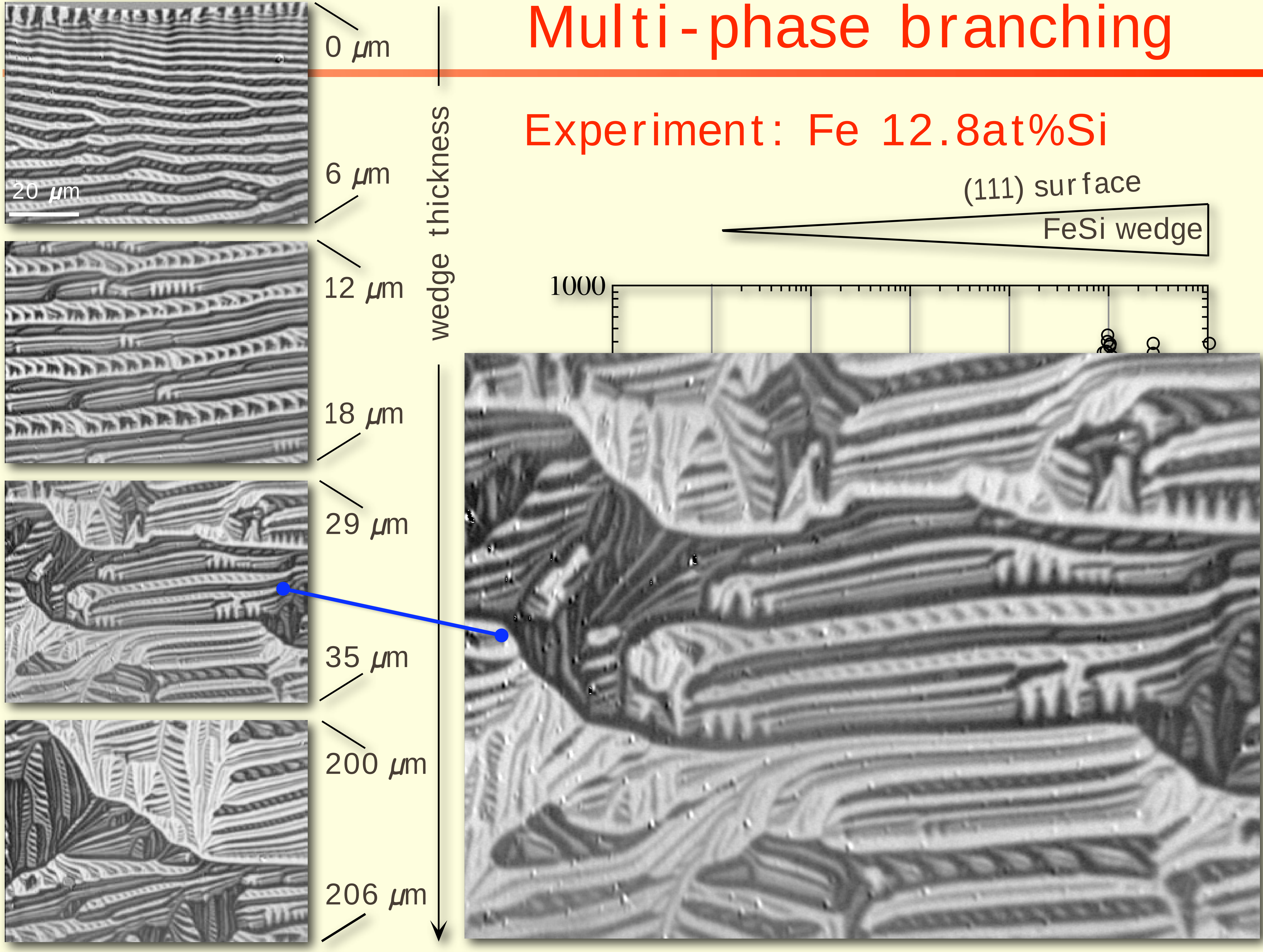

Multi-phase branching

Experiment: Fe 12.8at%Si

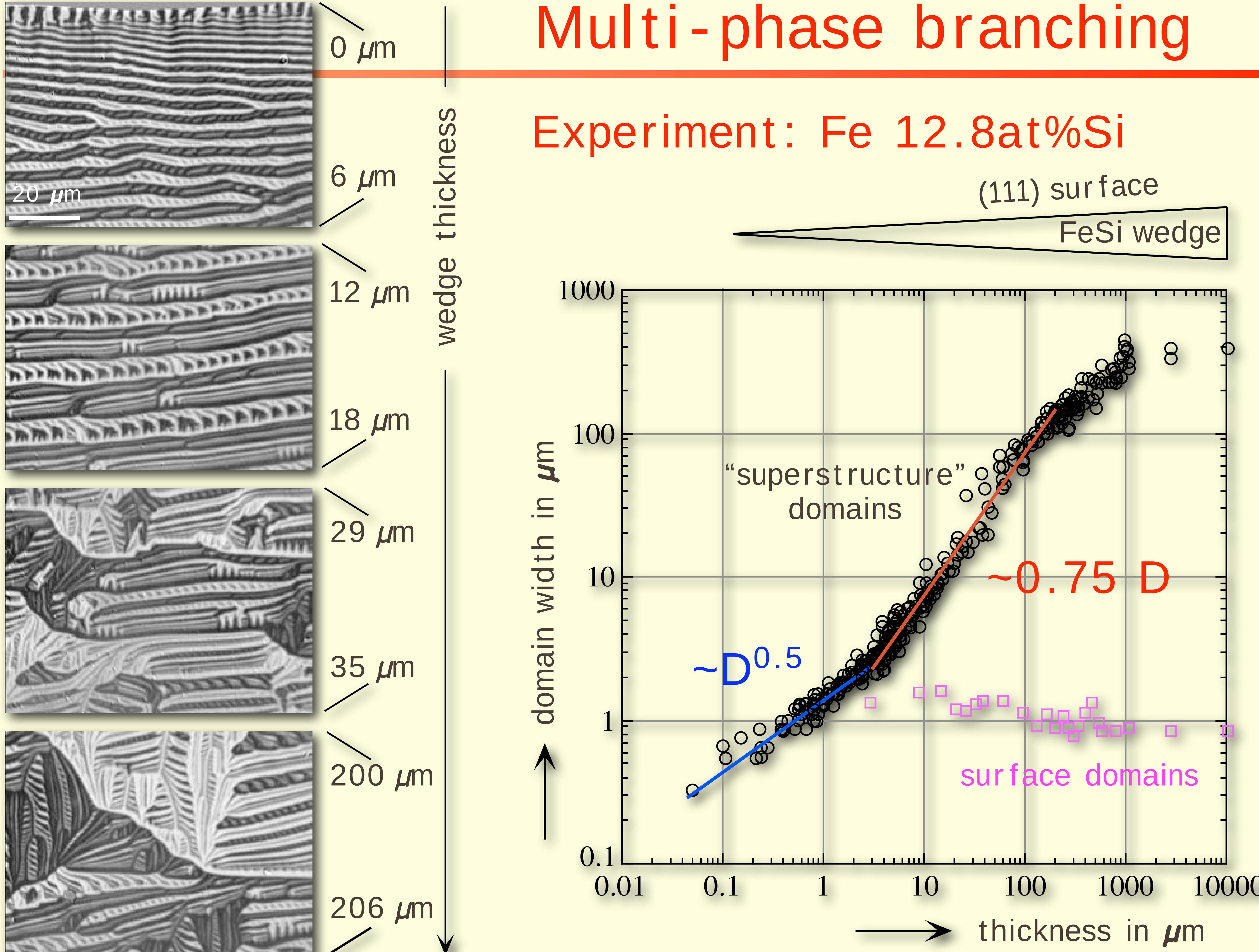

Multi-phase branching

Experiment: Fe 12.8at%Si

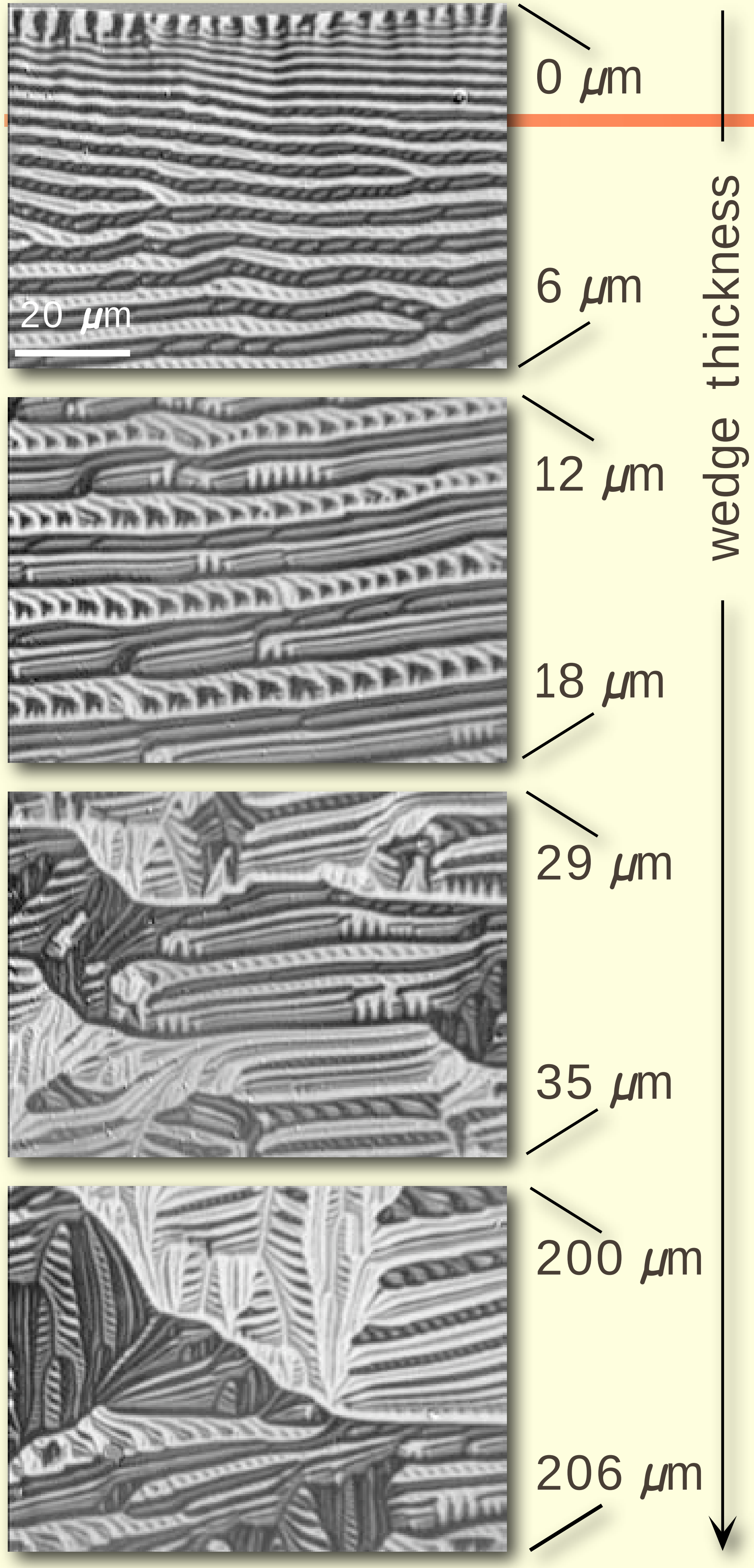

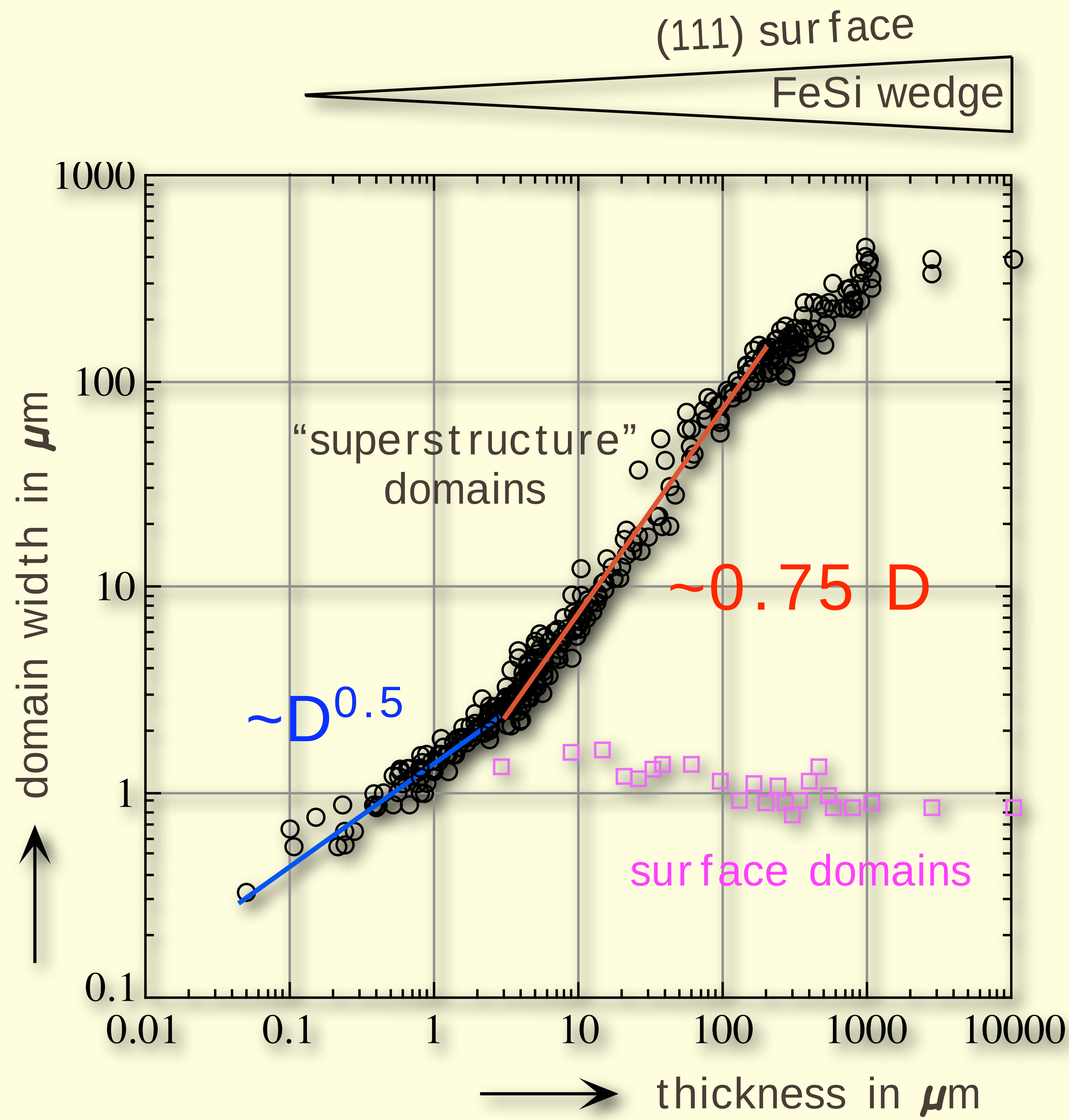

Multi-phase branching

Experiment: Fe 12.8at%Si

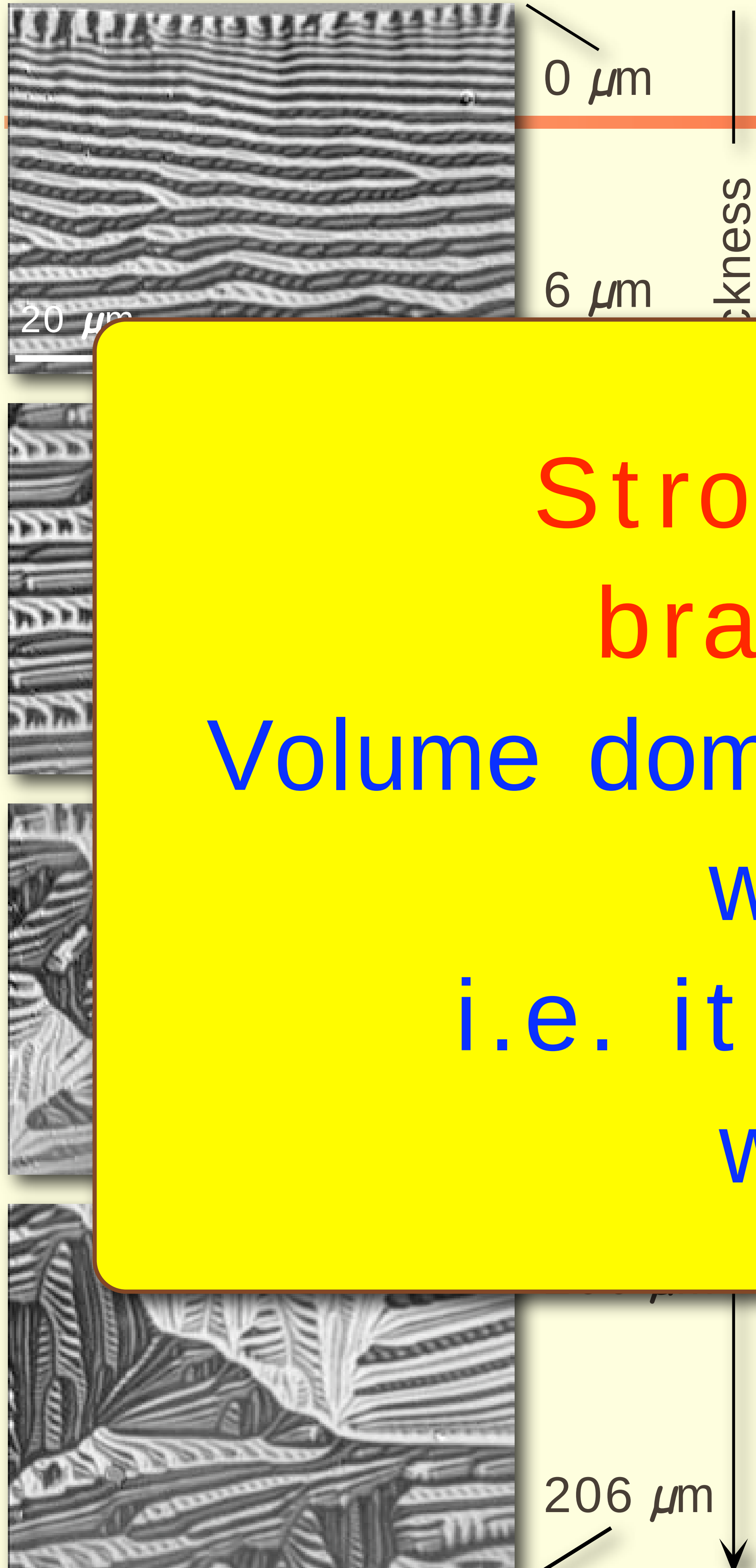

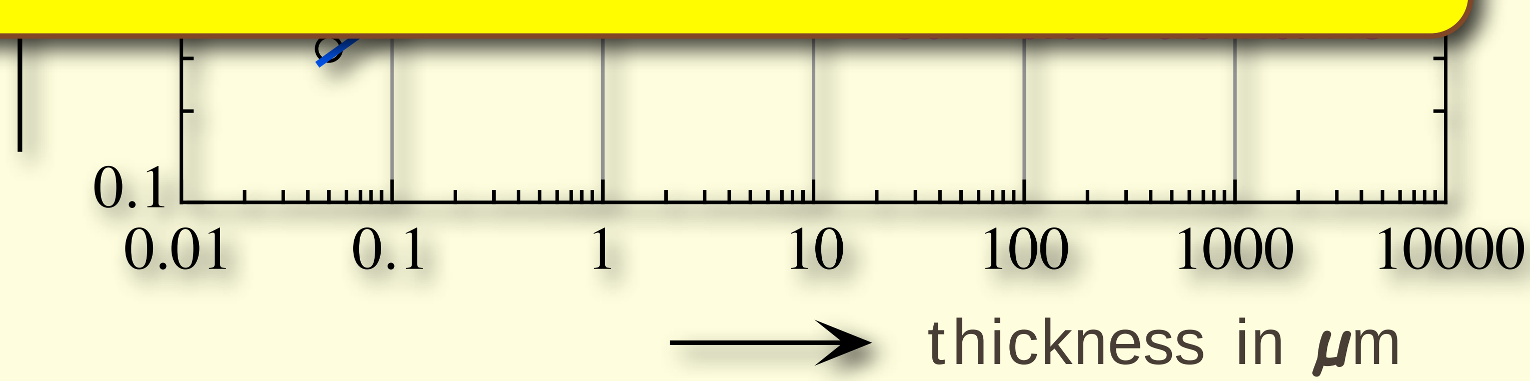

Strong misorientation:
branched domains -
Volume domain width scales linearly
with thickness,
i.e. it also scales linearly
with grain size

With decreasing grain size the domains get finer.

With decreasing grain size
the domains get finer.

How is coercivity related
to grain size?

Grain boundary domains

Goss sheets

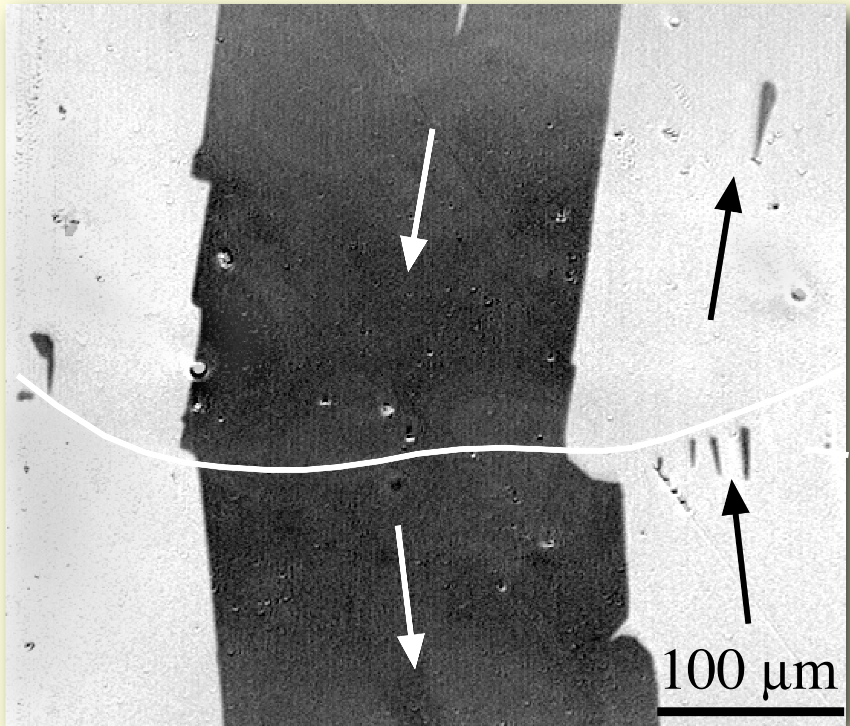

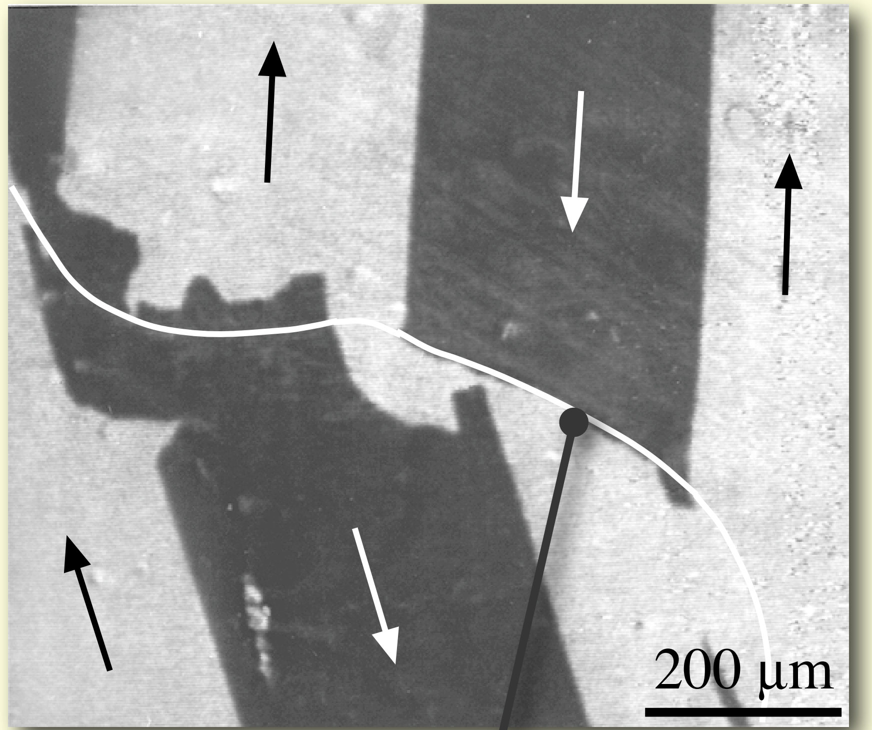

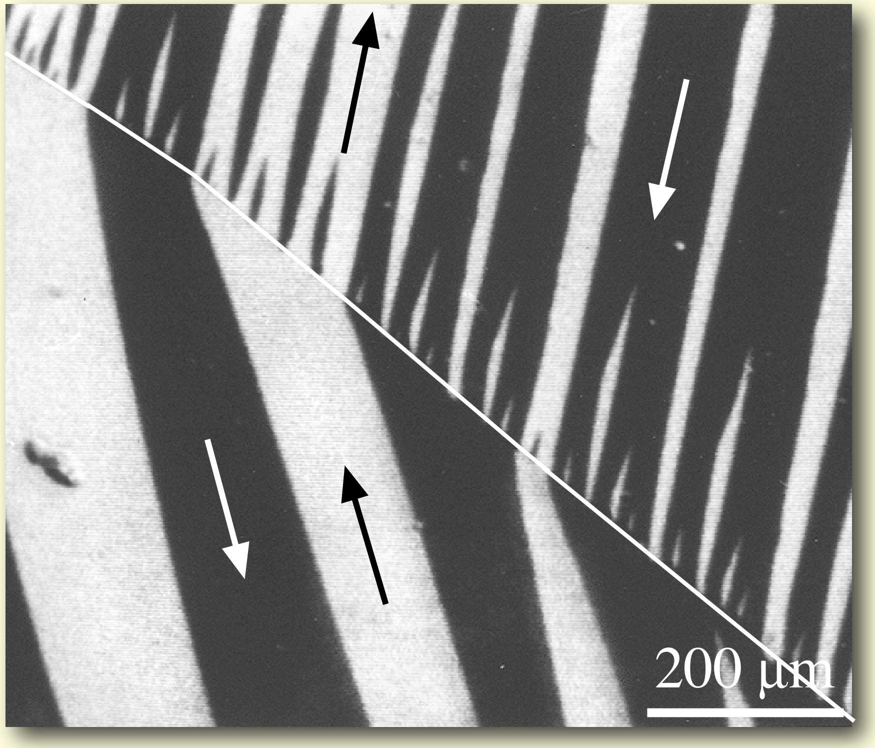

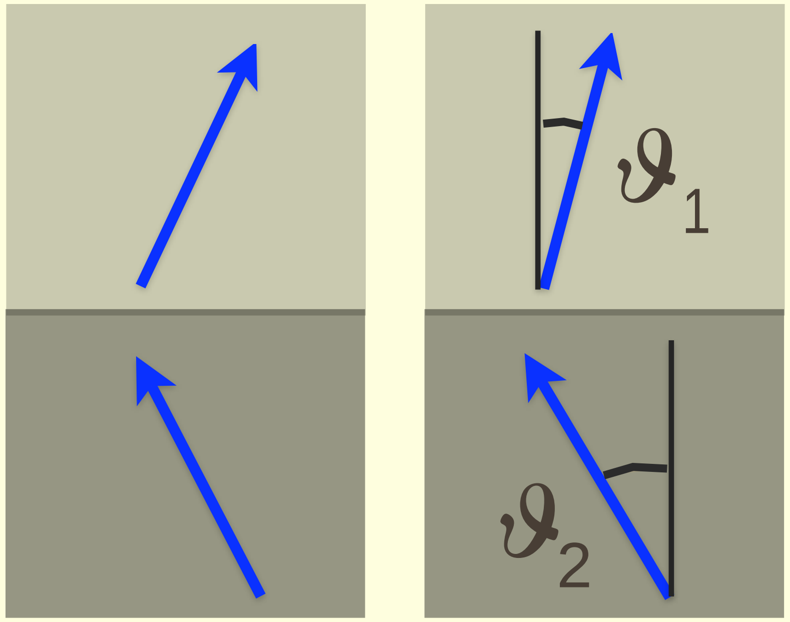

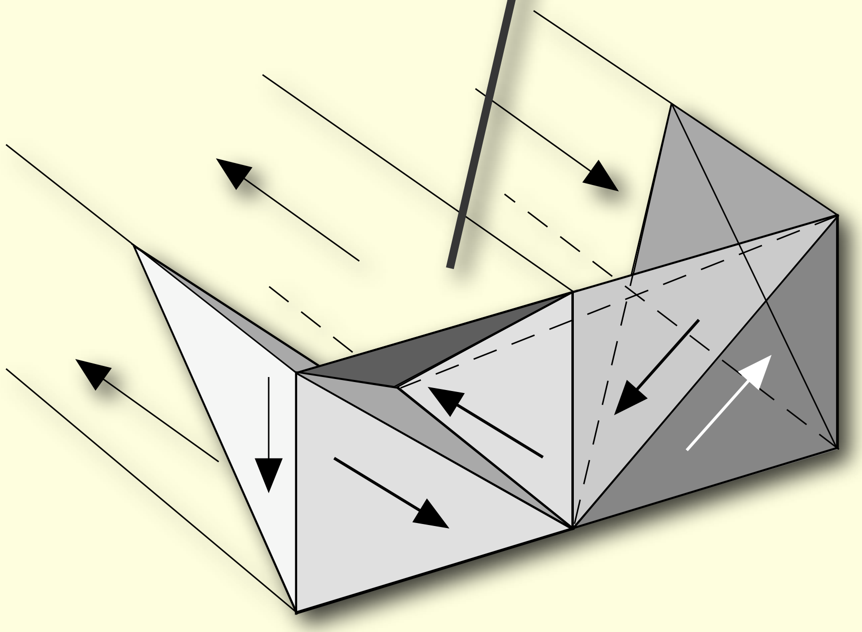

interface charge
$= \cos\vartheta_1 - \cos\vartheta_2$

Ni(55%)Fe

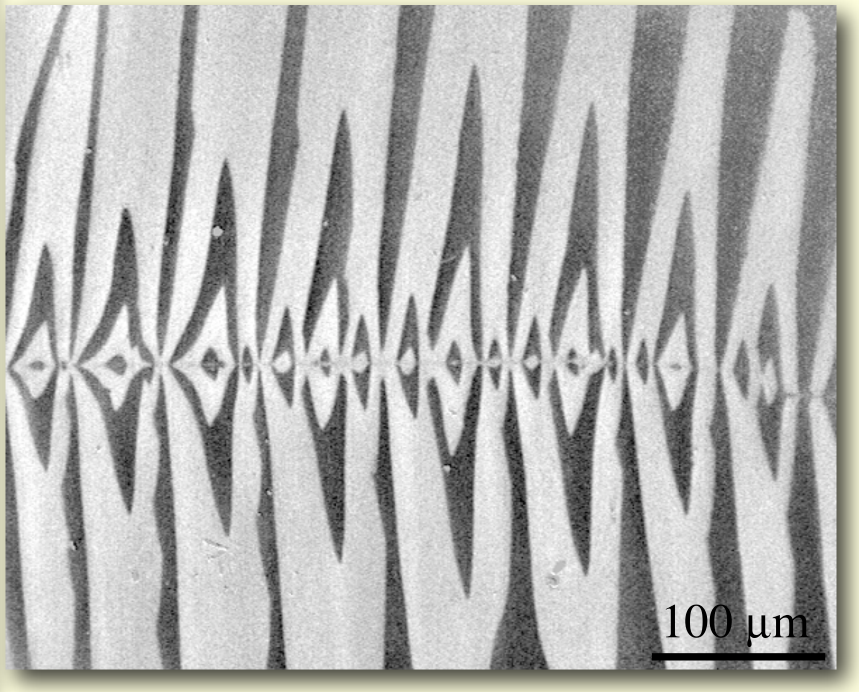

Grain boundary domains

Goss sheets

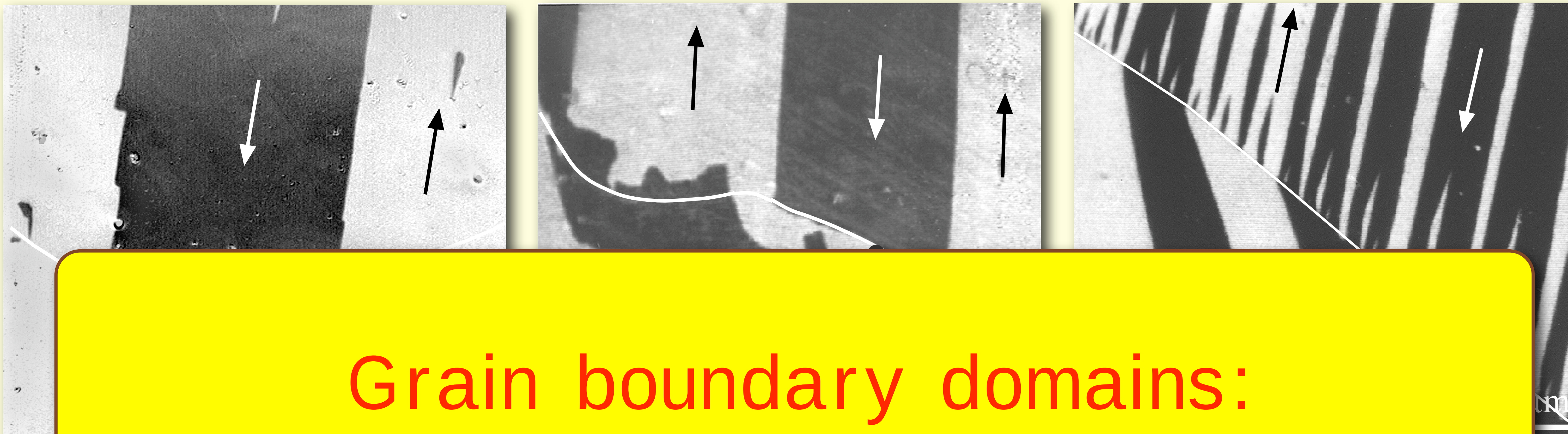

Grain boundary domains:

avoid (reduce) magnetic charges

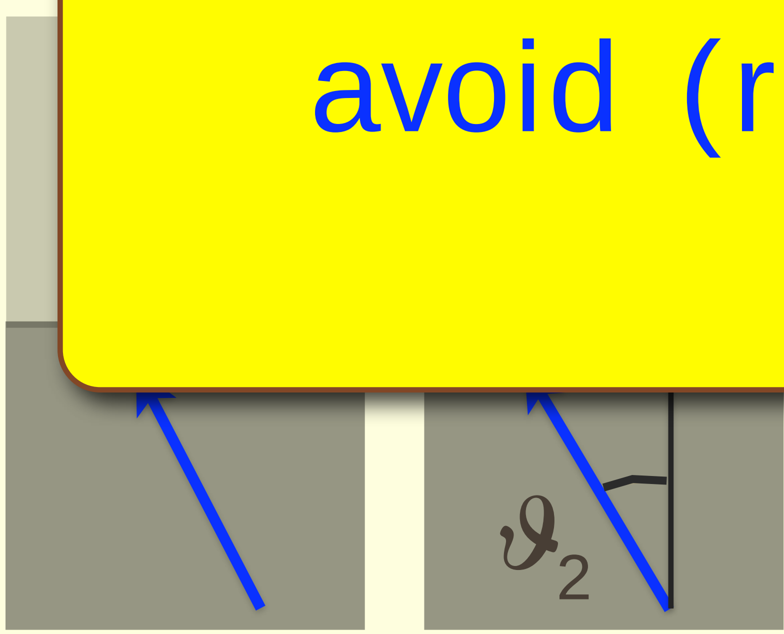

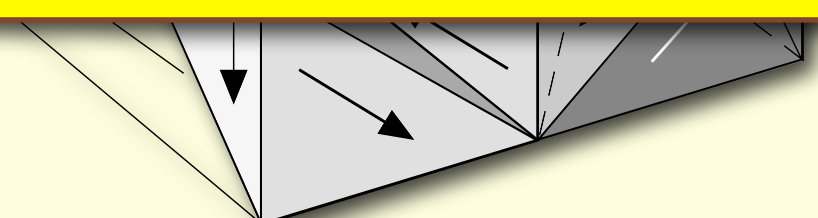

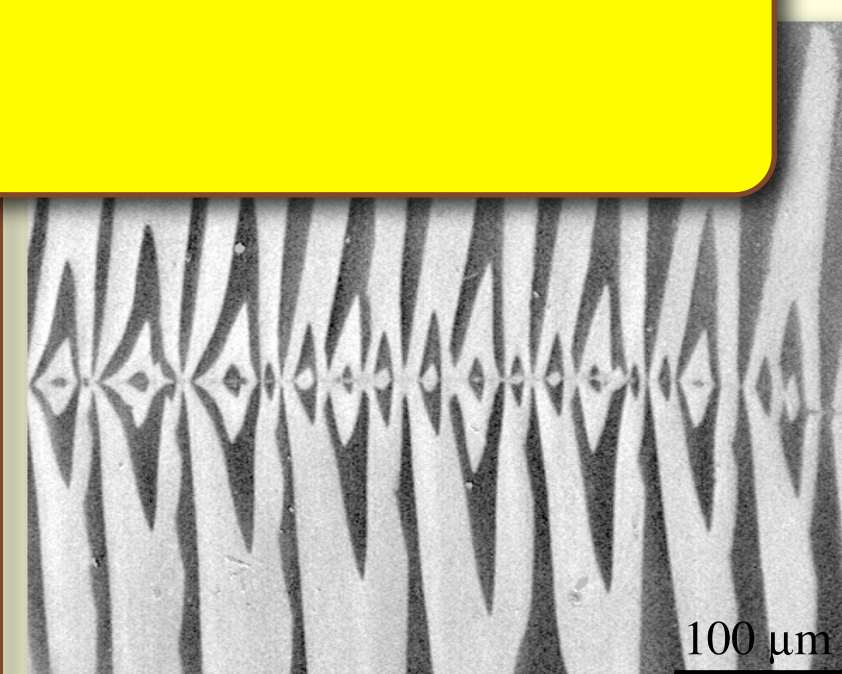

interface charge

$= \cos\vartheta_1 - \cos\vartheta_2$

Grain boundary domains

FeSi non-oriented sheet

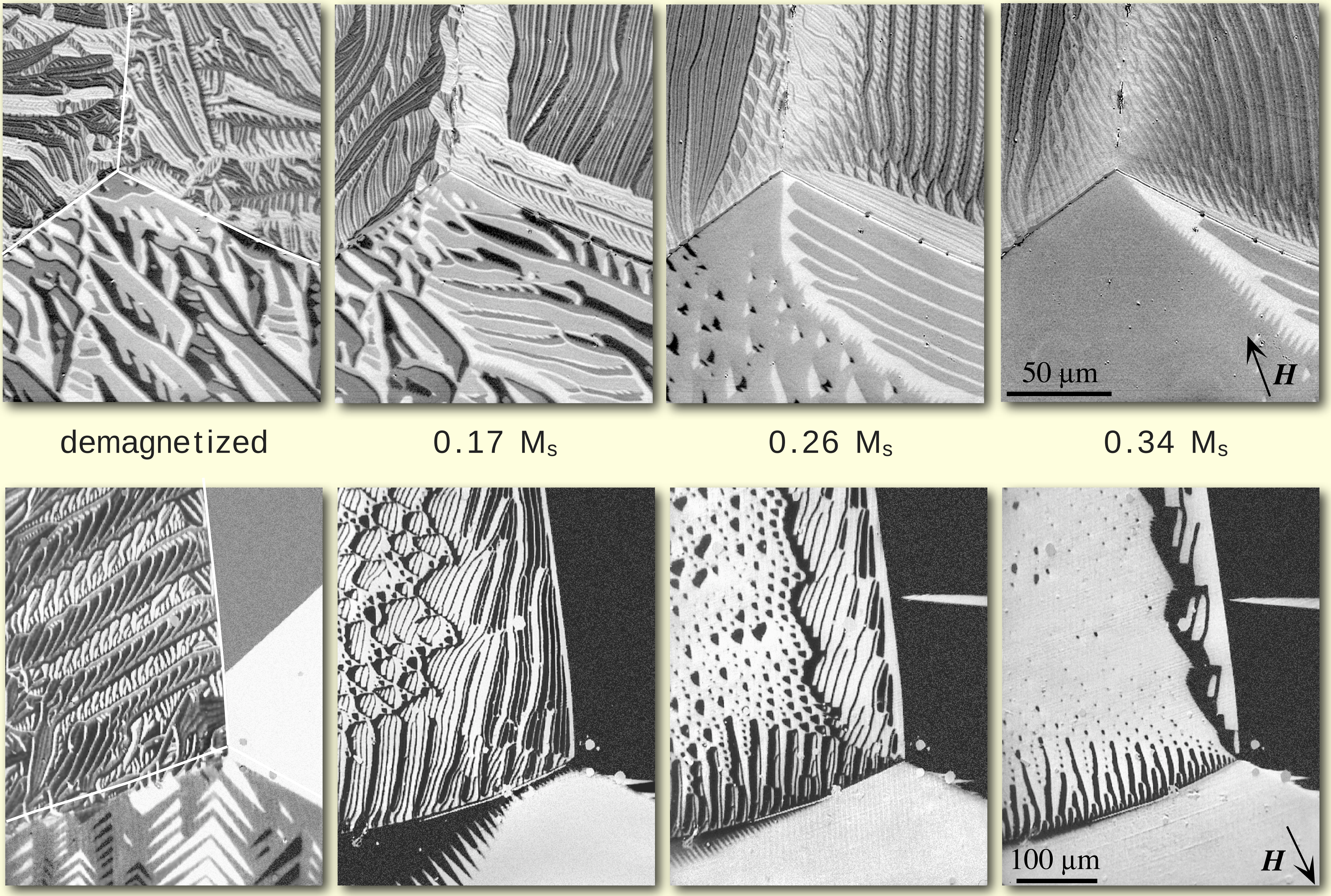

Grain boundary domains

FeSi non-oriented sheet

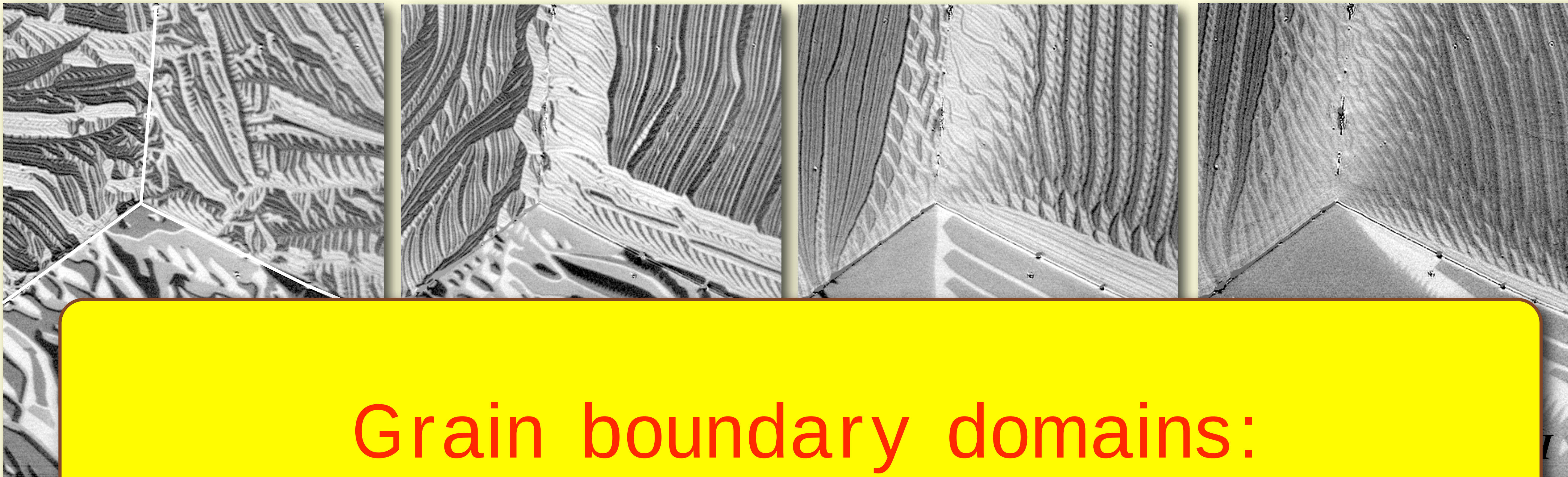

Grain boundary domains:

extend 50 - 100 μm into grains

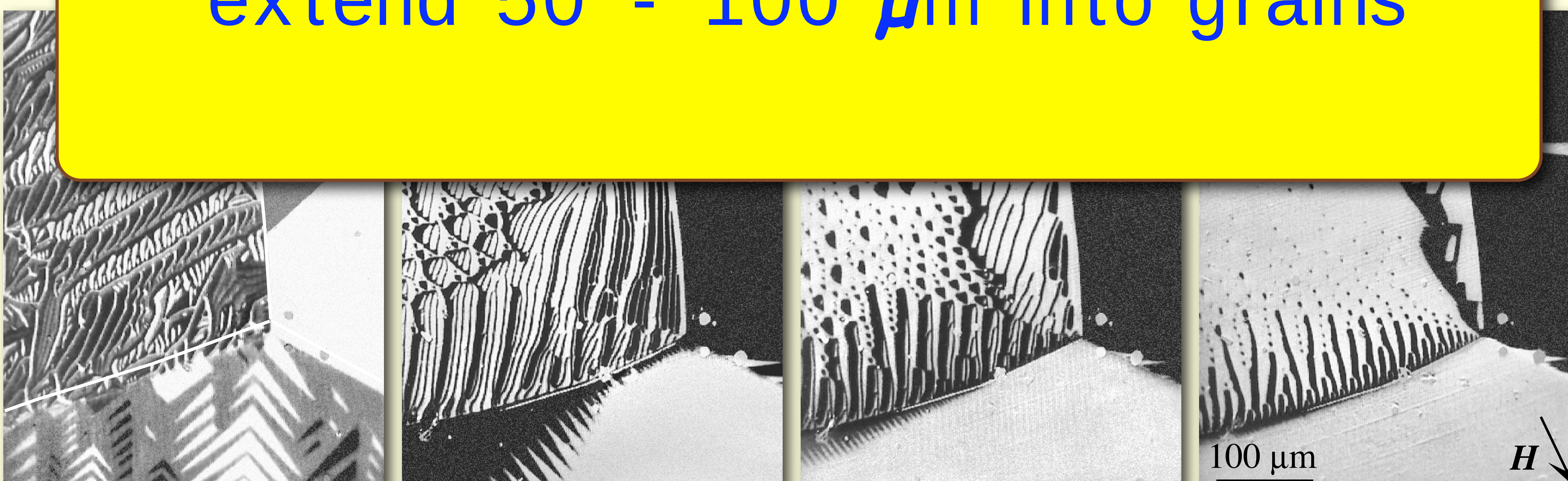

Coarse-grained materials

Grain boundary domains

FeSi non-oriented sheet

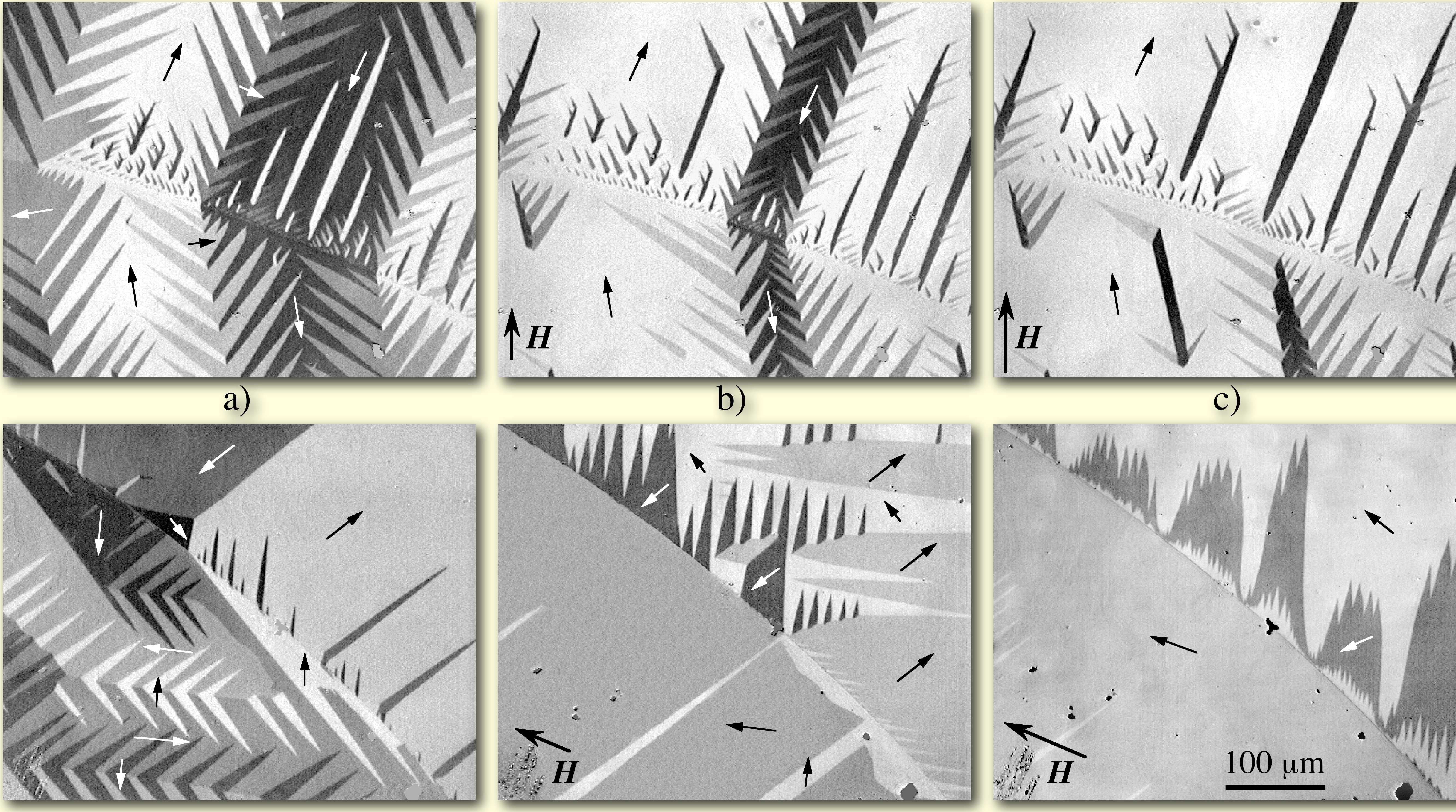

Coarse-grained materials

Grain boundary domains

FeSi non-oriented sheet

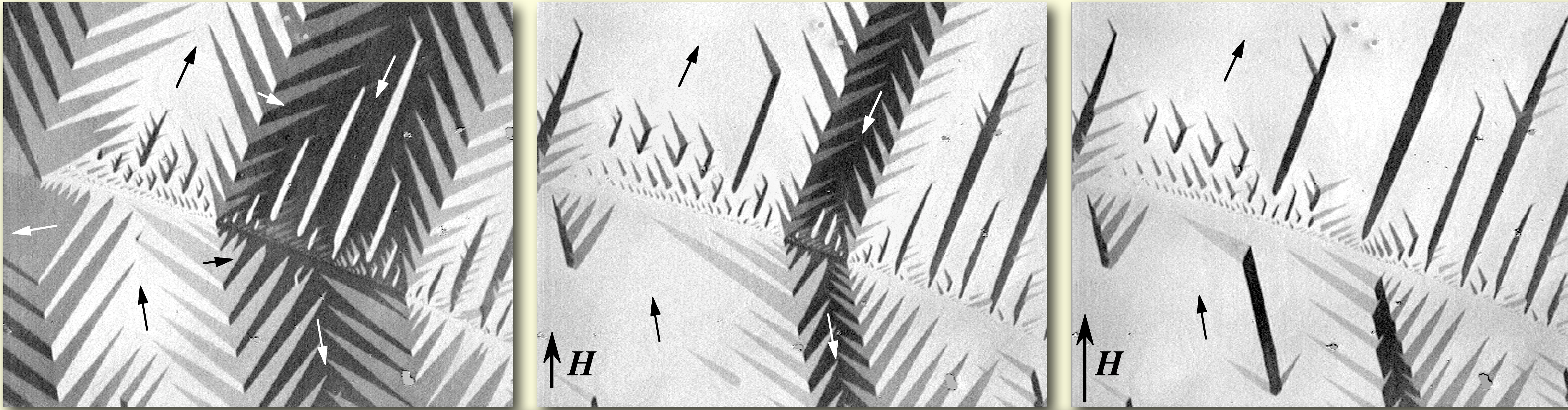

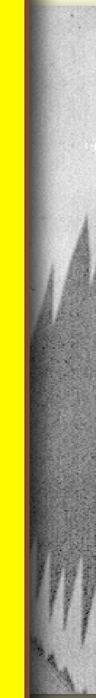

Grain boundary domains:

Their reorganization in magnetic field costs energy

↓

They are responsible for coercivity.

Grain boundary domains

Their relative volume increases with decreasing grain size

↓

Coercivity increases with decreasing grain size

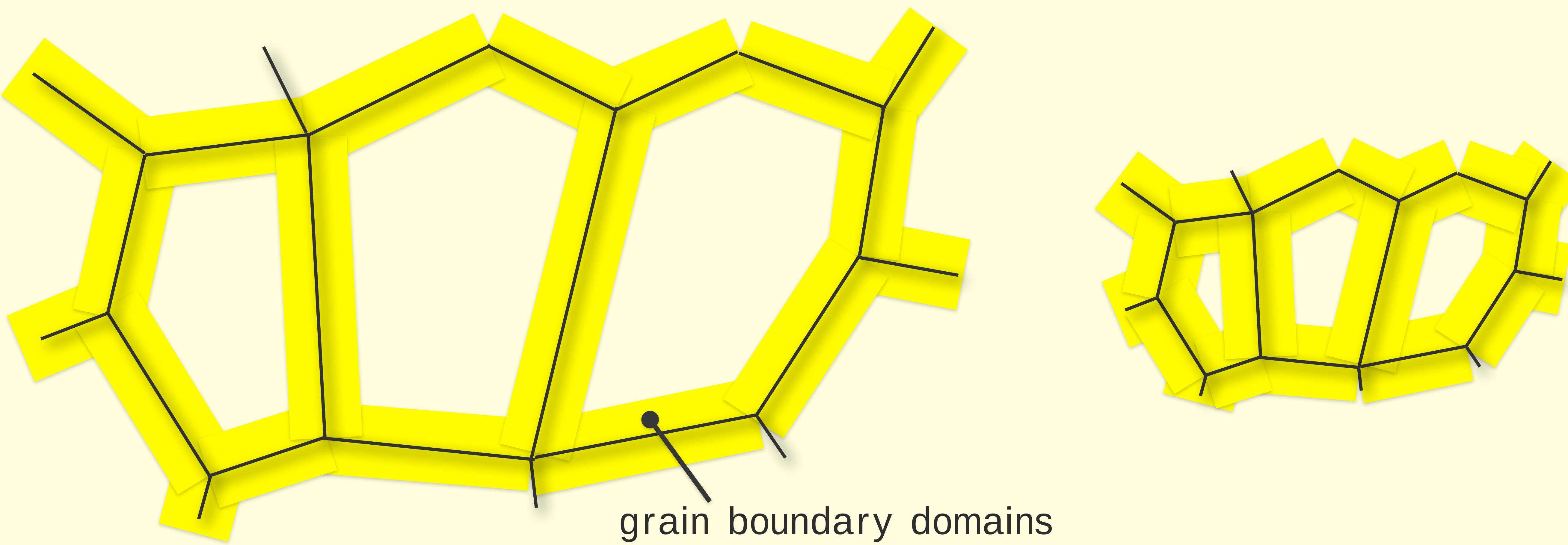

Coercivity and grain size

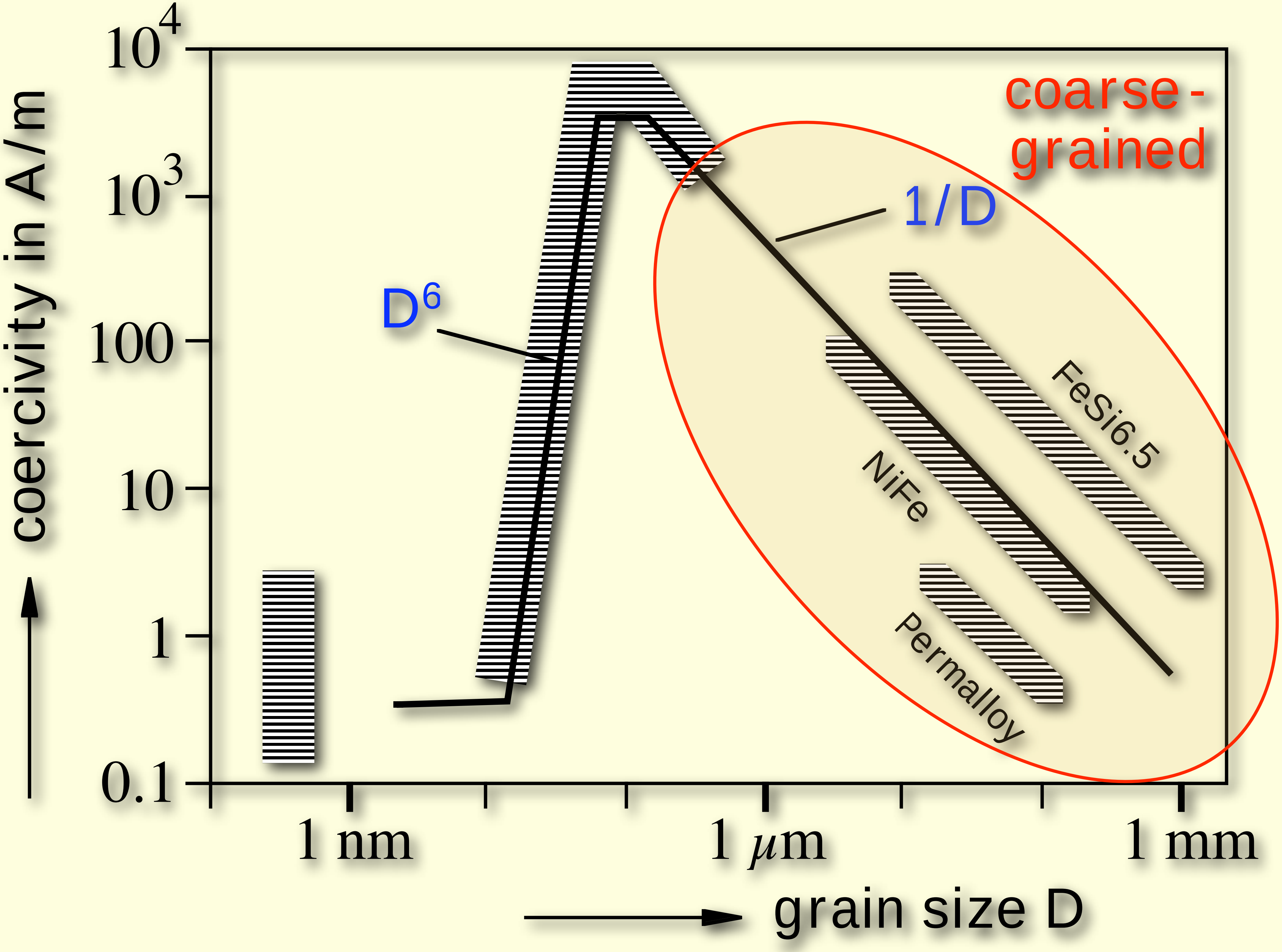

G. Herzer, Nanocrystalline soft magnetic alloys. In: Buschow KHJ, editor. Handbook of Magnetic Materials, vol. 10. Elsevier Science B.V., p.415 (1997)

Coercivity and grain size

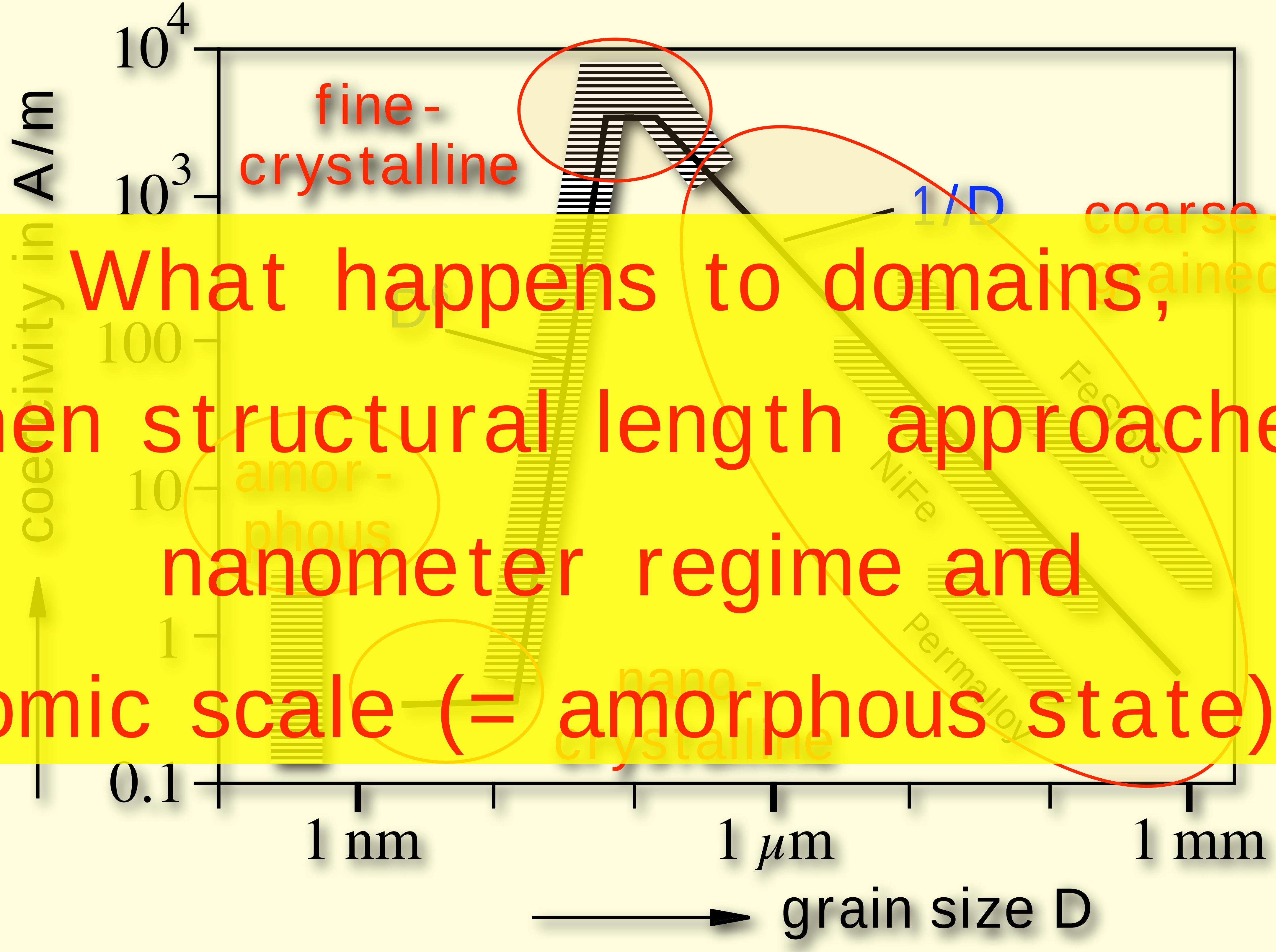

What happens to domains, when structural length approaches nanometer regime and atomic scale (= amorphous state) ?

G. Herzer, Nanocrystalline soft magnetic alloys. In: Buschow KHJ, editor. Handbook of Magnetic Materials, vol. 10. Elsevier Science B.V., p.415 (1997)

Coercivity and grain size

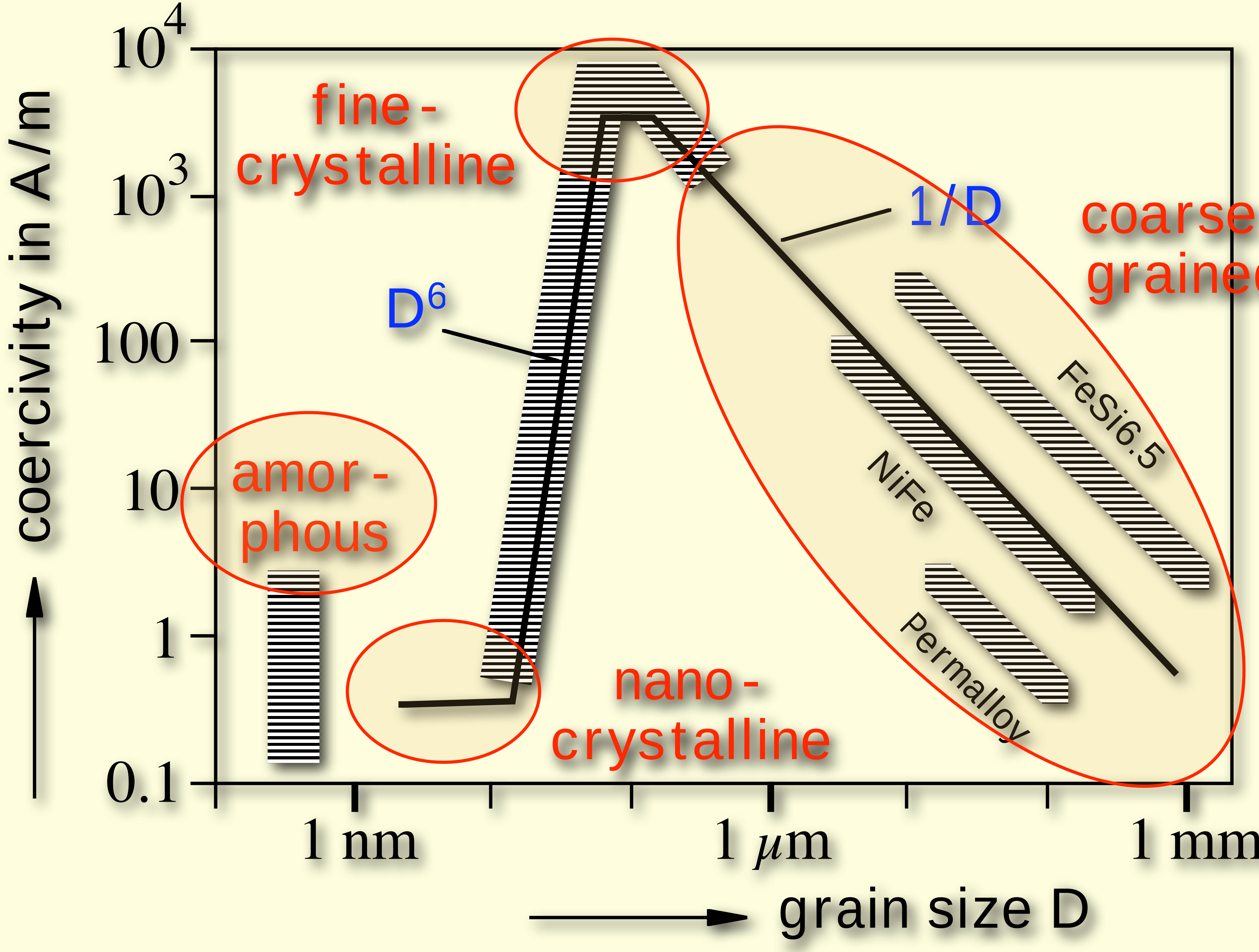

G. Herzer, Nanocrystalline soft magnetic alloys. In: Buschow KHJ, editor. Handbook of Magnetic Materials, vol. 10. Elsevier Science B.V., p.415 (1997)

Overview

1. Domains in coarse-grained material

2. Domains in amorphous material

3. Domains in nanocrystalline, soft magnetic ($Q<<1$) materials

4. Domains in fine- and nanostructured, permanent magnetic ($Q>1$) materials

Rapidly quenched amorphous ribbons

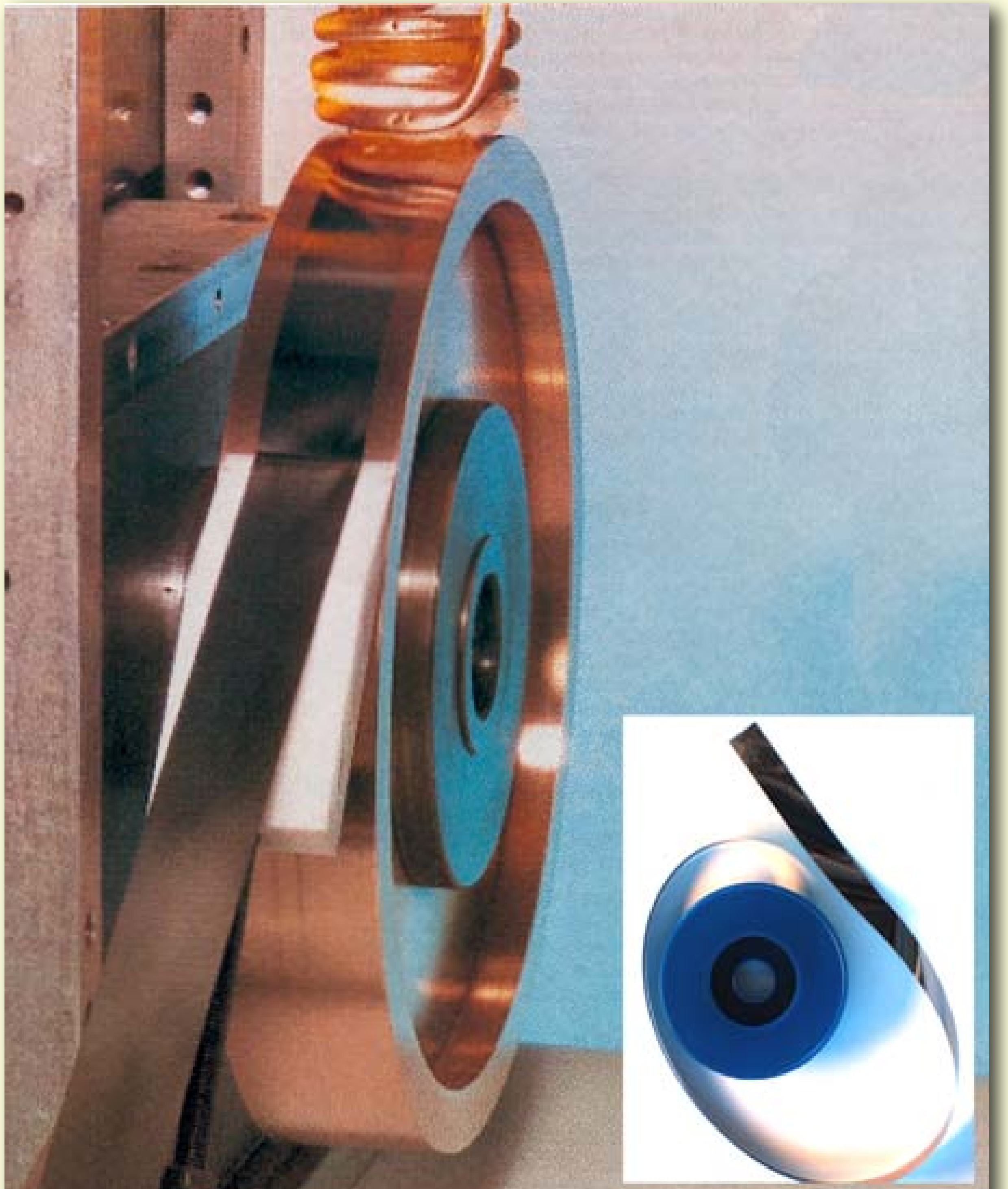

- thickness 20 μm
- ferromagnetic (with Fe, Ni, Co)
- $T_{75-83}\ M_{25-17}$

  T = Fe, Co, Ni
  M = P, C, B, Si, Al....

- no magnetocrystalline anisotropy

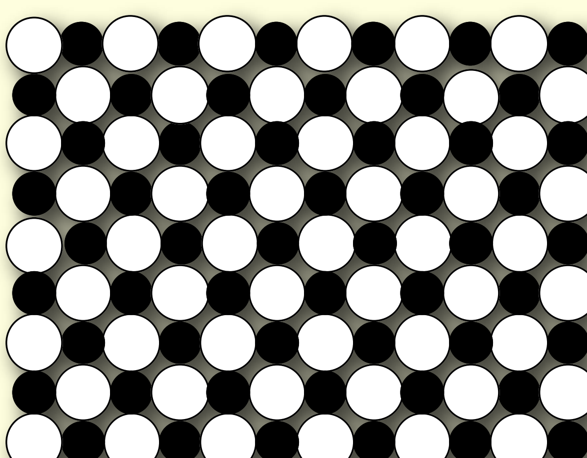

crystalline

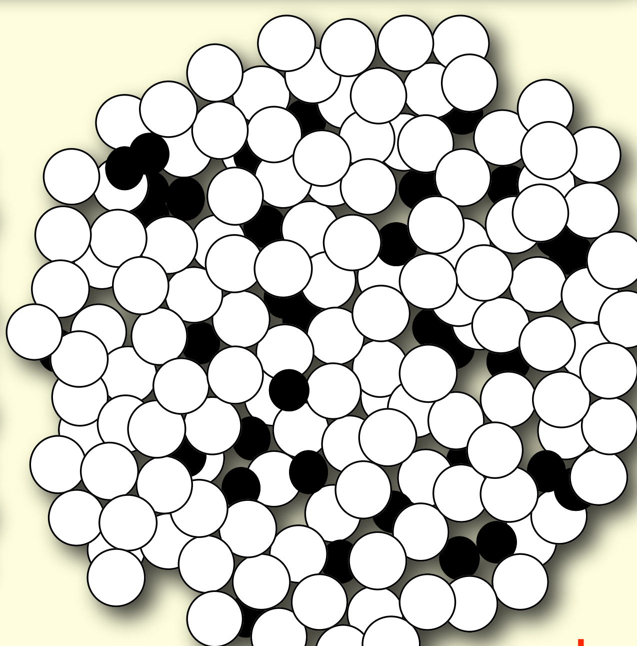

amorphous

Magnetic microstructure of amorphous ribbons

m(r) continuously flowing ?

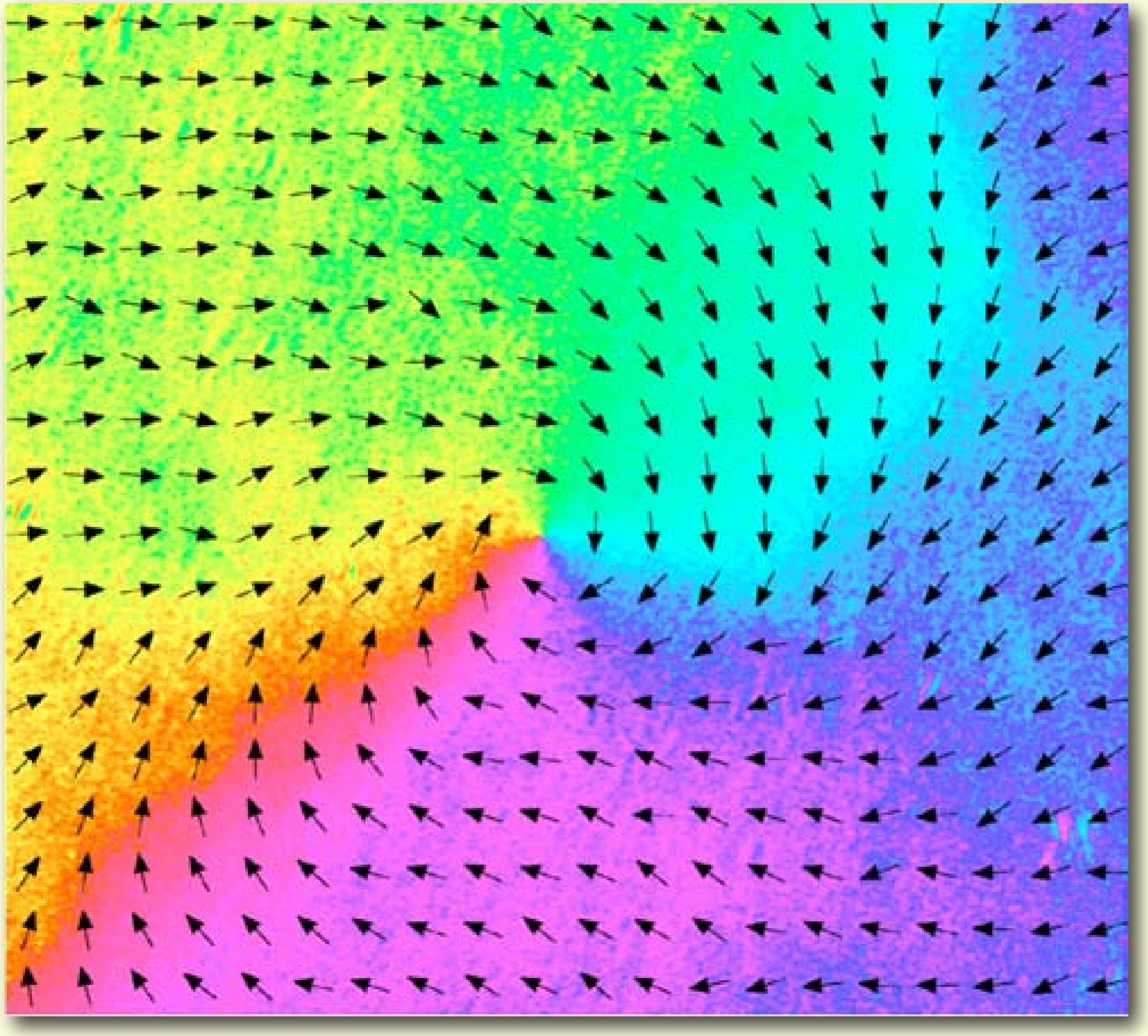

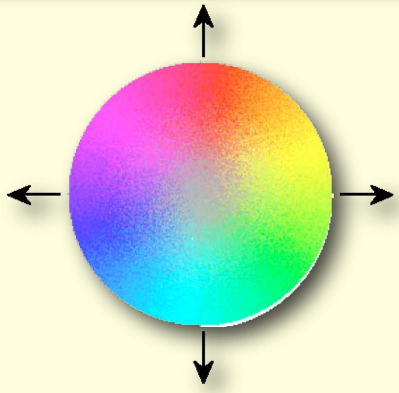

or regular domains ?

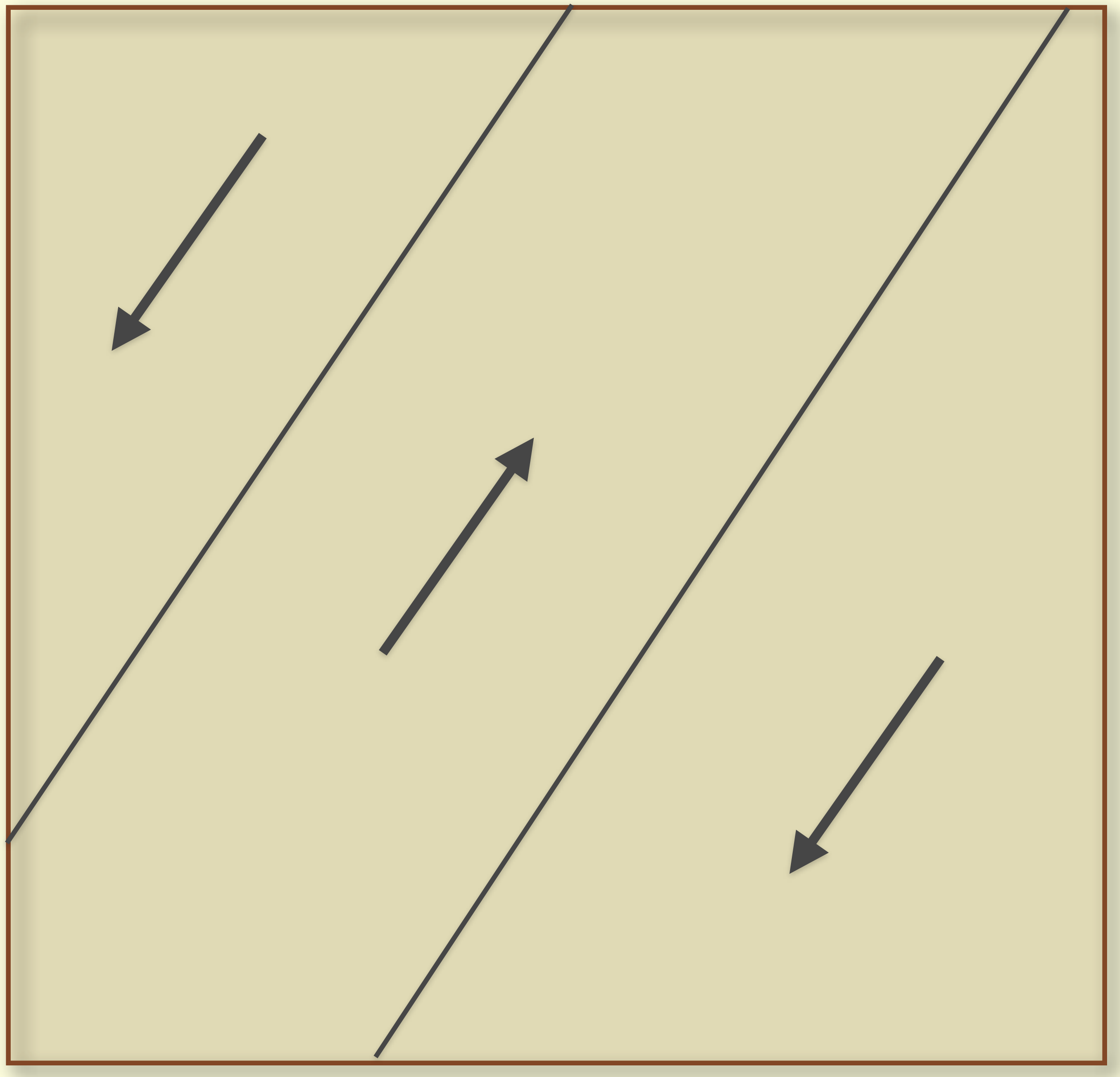

Excursion:

Some general considerations on anisotropy and domains

Van den Berg Concept

[H.A.M. van den Berg, 1986]

- Assumption: anisotropy-free film element

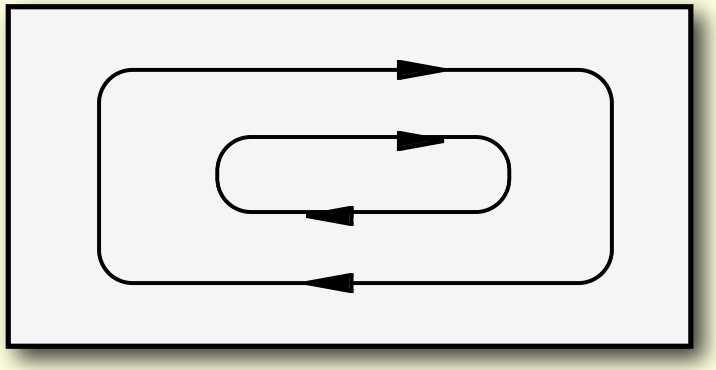

expect: continuously flowing m(r)

Van den Berg Concept

[H.A.M. van den Berg, 1986]

- Assumption: anisotropy-free film element
- Stray-field freedom requires:

  - div m = 0
  - m(x,y) || sample edge
  - m(x,y) || film plane
  - |m| = 1

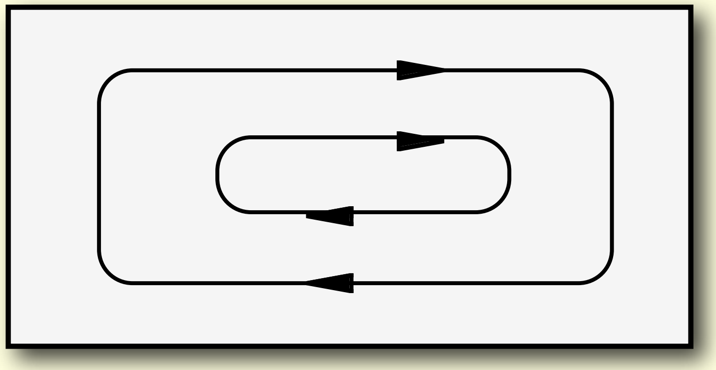

expect: continuously flowing m(r)

Conditions cannot be met by continuous pattern (exception: circular element)

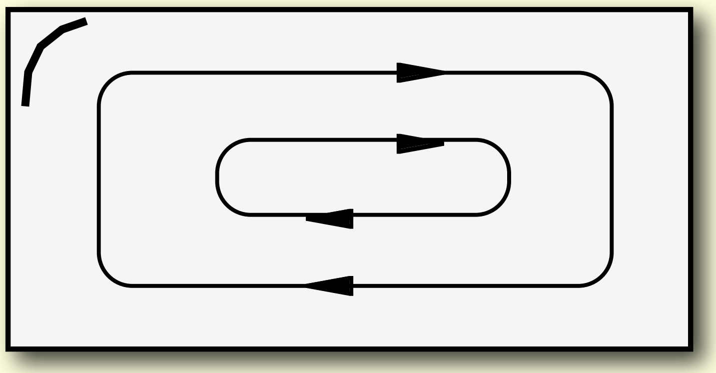

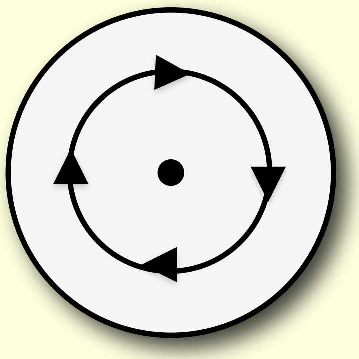

Consequence:

Regular domain pattern with discontinuities (domain walls), enforced by element shape to avoid magnetic poles

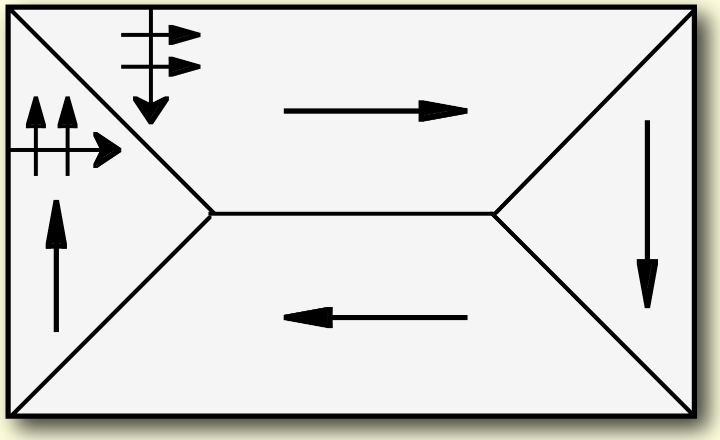

Van den Berg Construction

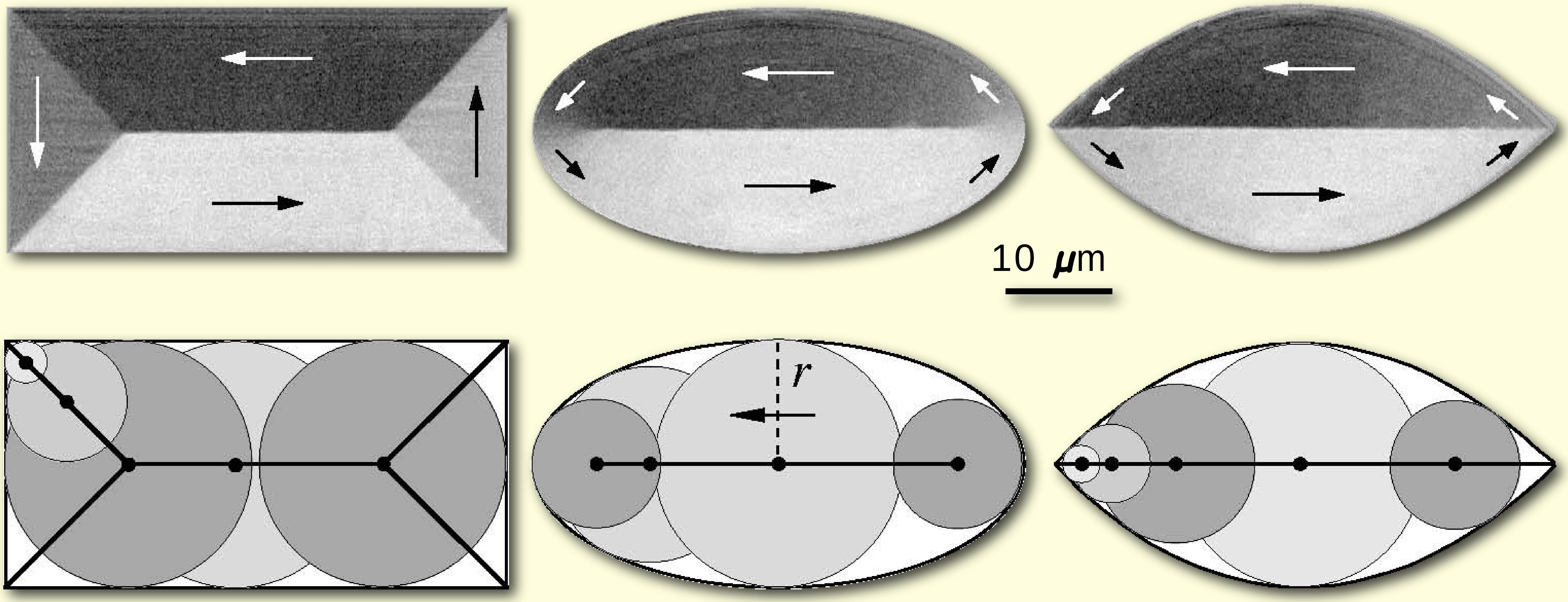

- Take circles that touch edge at two or more points. Centers of circles form walls
- In every circle the magnetization direction must be perpendicular to each touching radius
- If a circle touches edge in more than 2 points: its center forms wall junction
- If touching points fall together: wall ends at center of circle = zone of concentric rotation
- Acute corner: boundary runs into corner

Van den Berg Construction

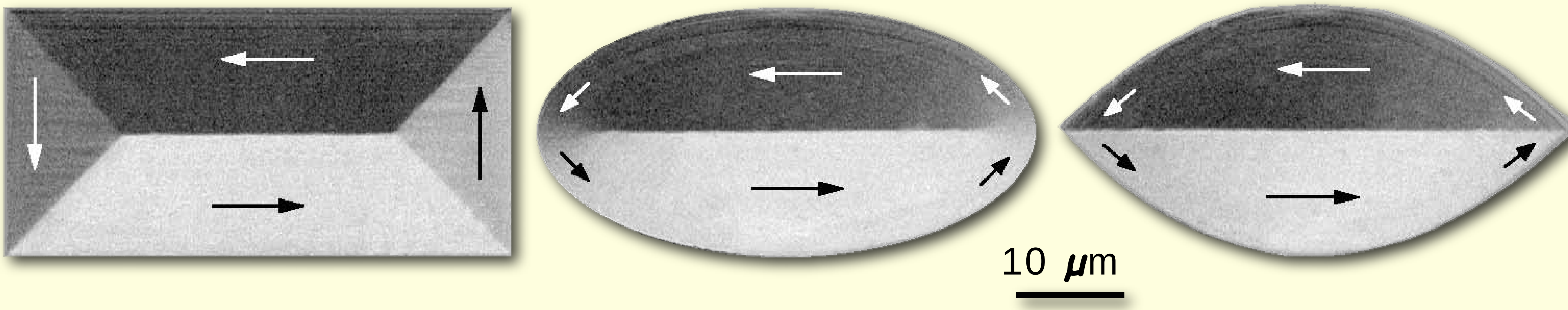

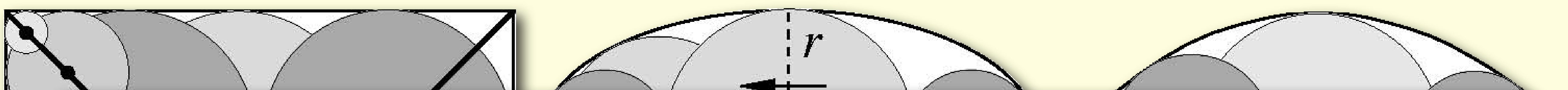

Anisotropy-free film element:

Domain walls and rotation areas, formed by requirement of stray-field freedom

- Acute corner: boundary runs into corner

Van den Berg Construction

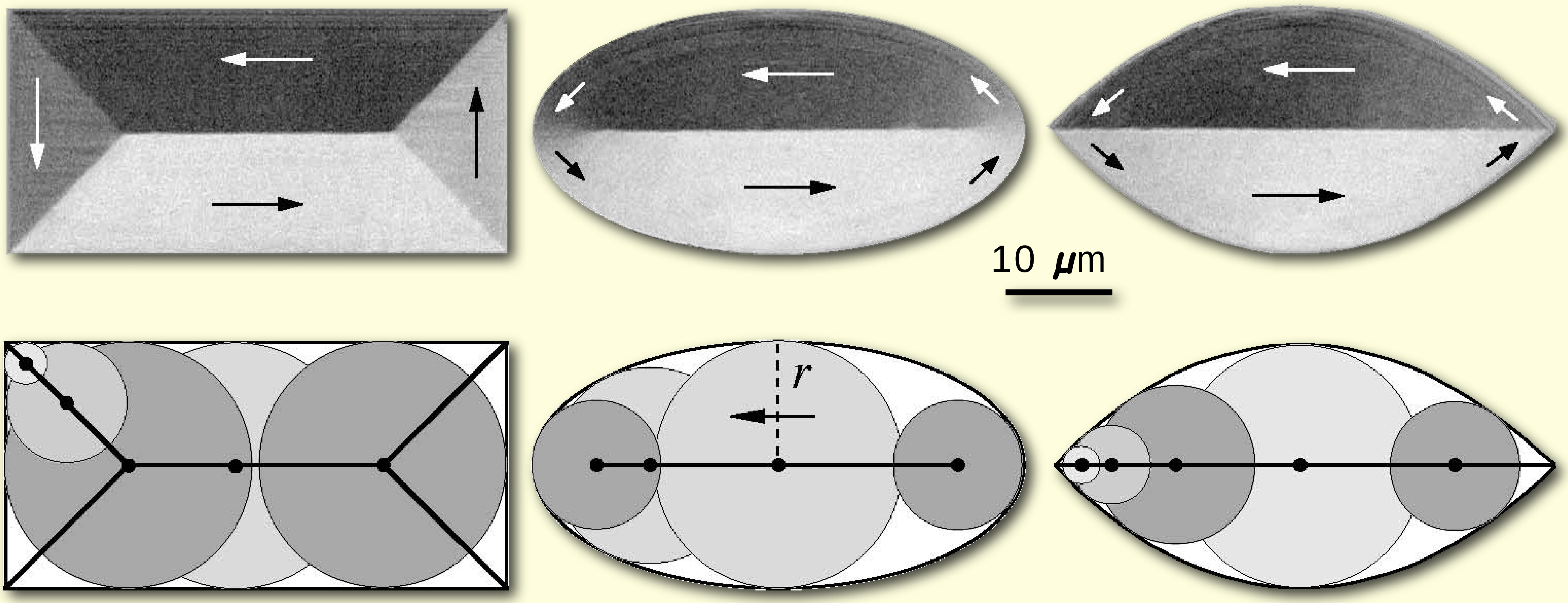

- Take circles that touch edge at two or more points. Centers of circles form walls
- In every circle the magnetization direction must be perpendicular to each touching radius
- If a circle touches edge in more than 2 points: its center forms wall junction
- If touching points fall together: wall ends at center of circle = zone of concentric rotation
- Acute corner: boundary runs into corner

Van den Berg Construction

van den Berg discontinuities are in reality domain walls

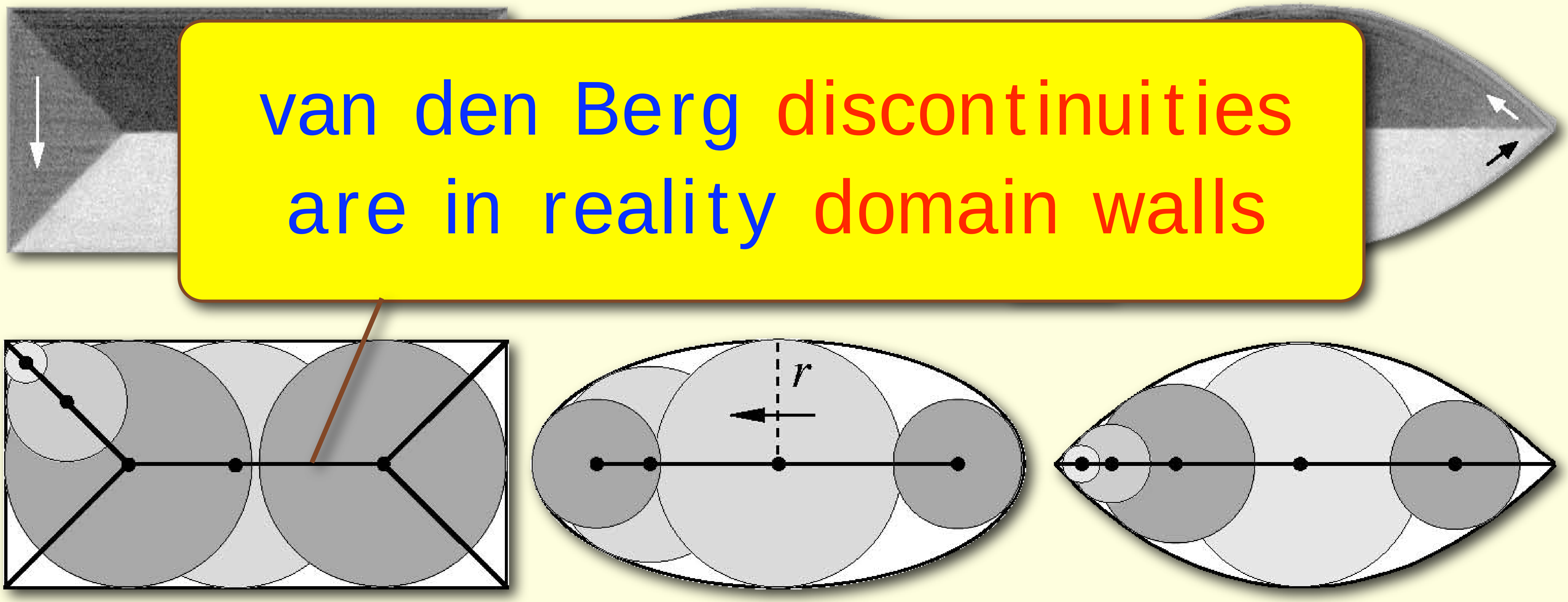

- Take circles that touch edge at two or more points. Centers of circles form walls
- In every circle the magnetization direction must be perpendicular to each touching radius
- If a circle touches edge in more than 2 points: its center forms wall junction
- If touching points fall together: wall ends at center of circle = zone of concentric rotation
- Acute corner: boundary runs into corner

180° wall types in soft magnetic films

Néel wall

film thickness
< 100 nm

scales with $\sqrt{A/K_d}$

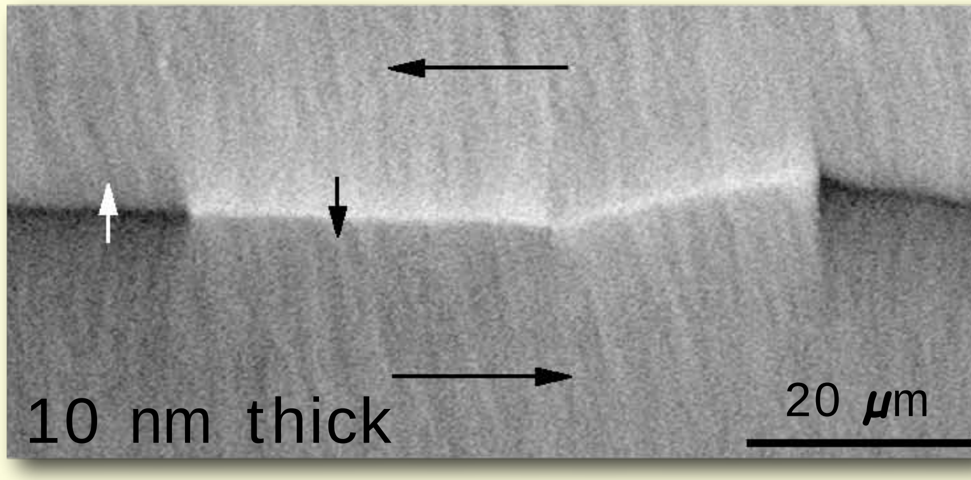

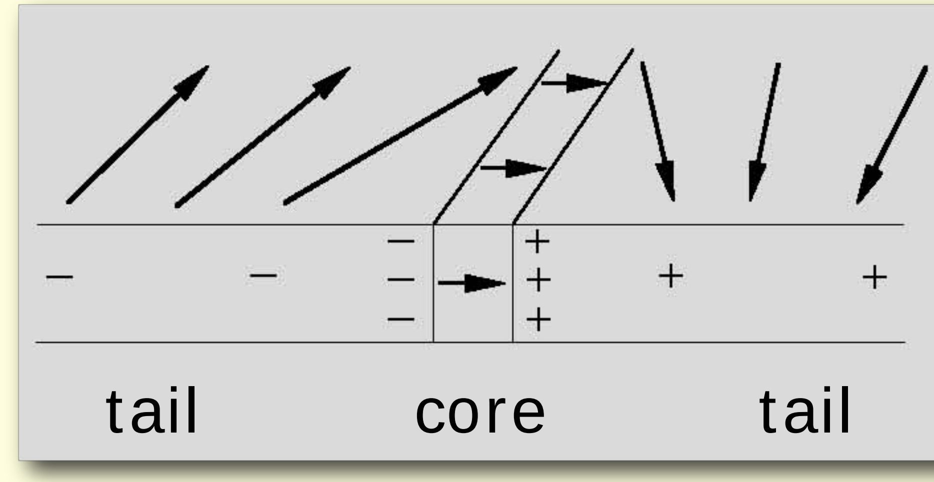

Asymmetric
Bloch wall

film thickness
> 100 nm

scales with
thickness

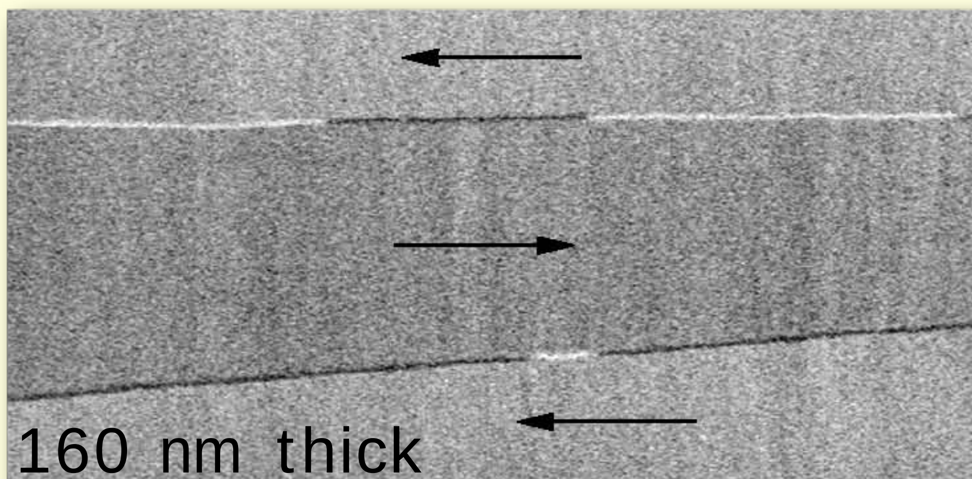

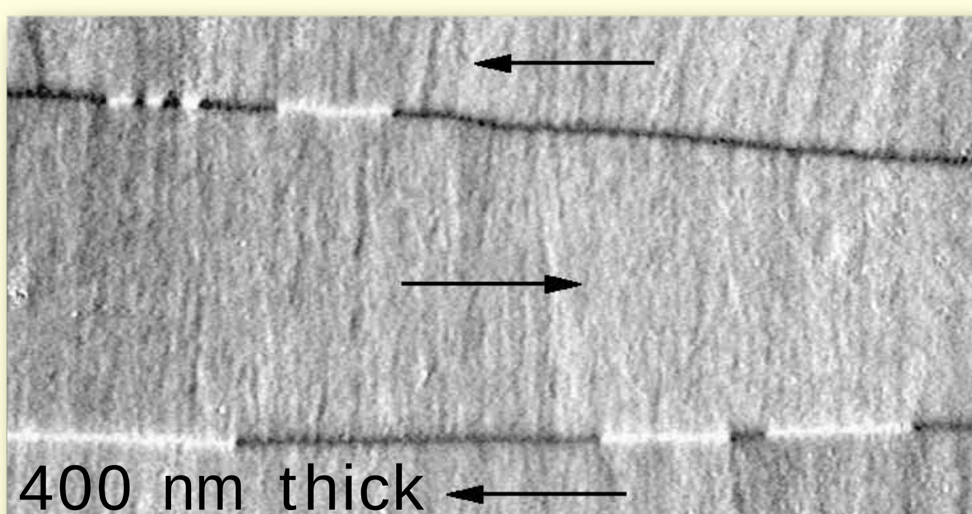

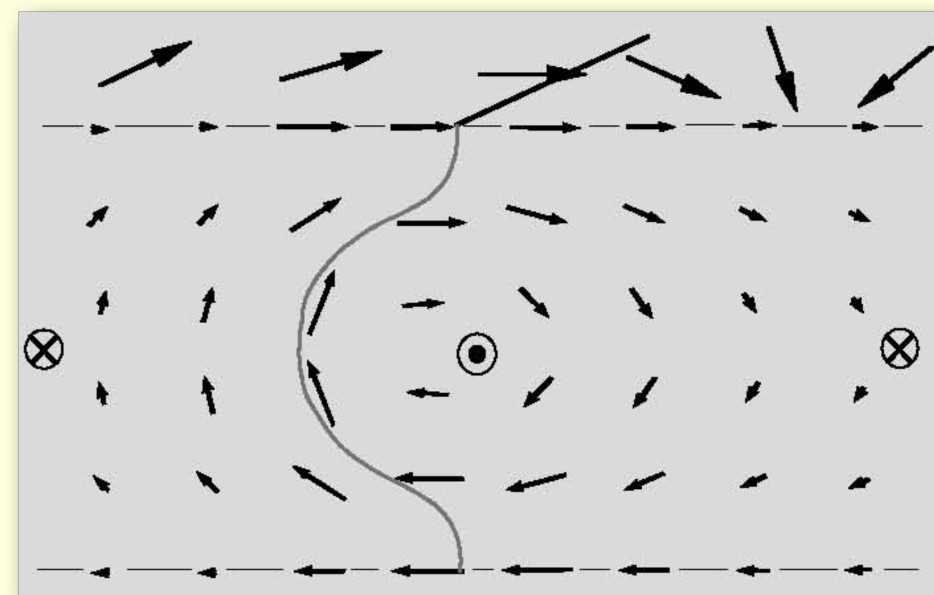

Permalloy
(NiFe)

180° wall types in soft magnetic films

Néel wall

film thickness
< 100 nm

scales with $\sqrt{A/K_d}$

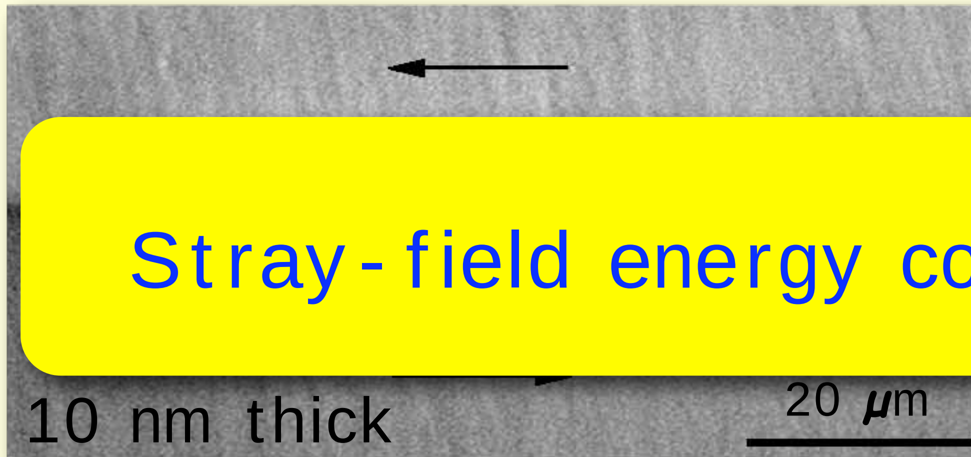

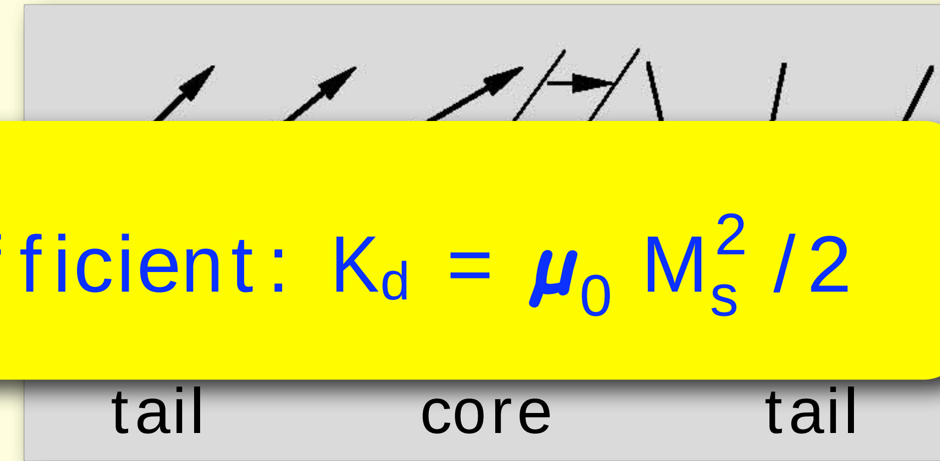

Stray-field energy coefficient: $K_d = \mu_0 M_s^2/2$

Asymmetric
Bloch wall

film thickness
> 100 nm

scales with
thickness

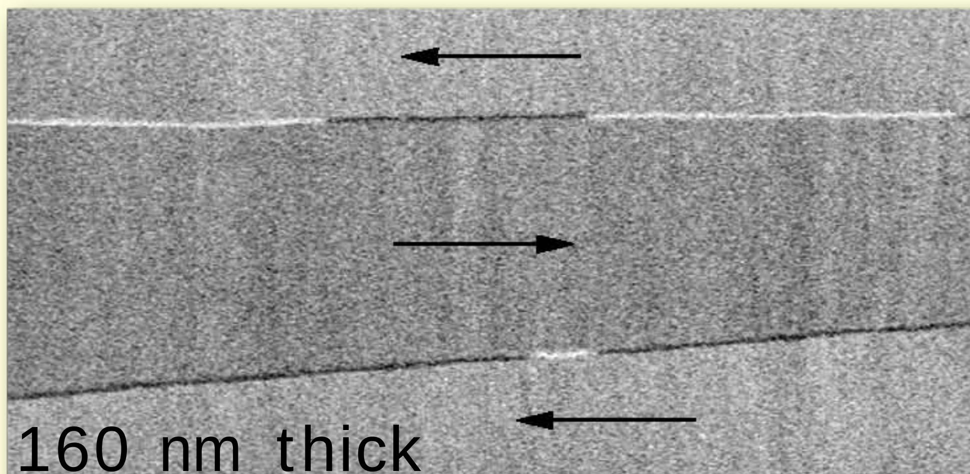

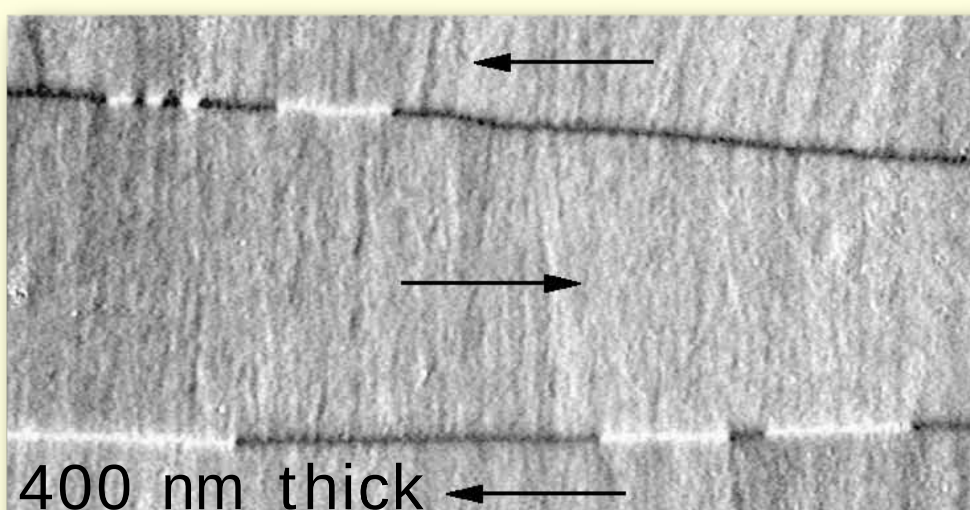

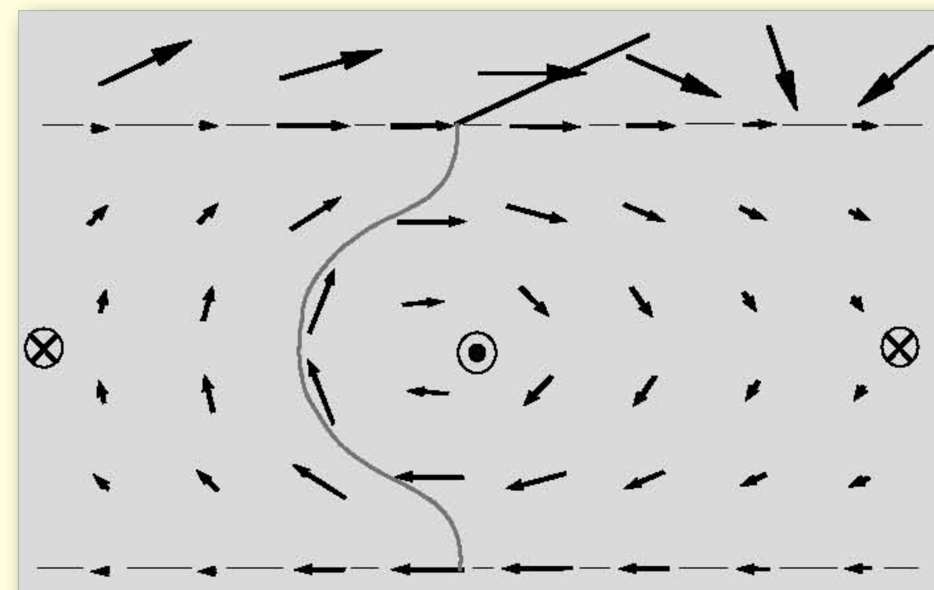

Permalloy
(NiFe)

180° wall types in soft magnetic films

Néel wall

film thickness
< 100 nm

scales with $\sqrt{A/K_d}$

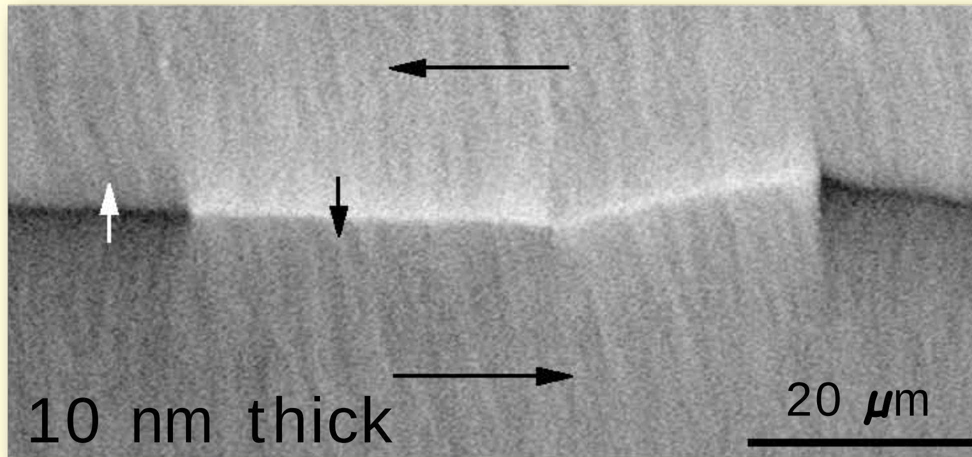

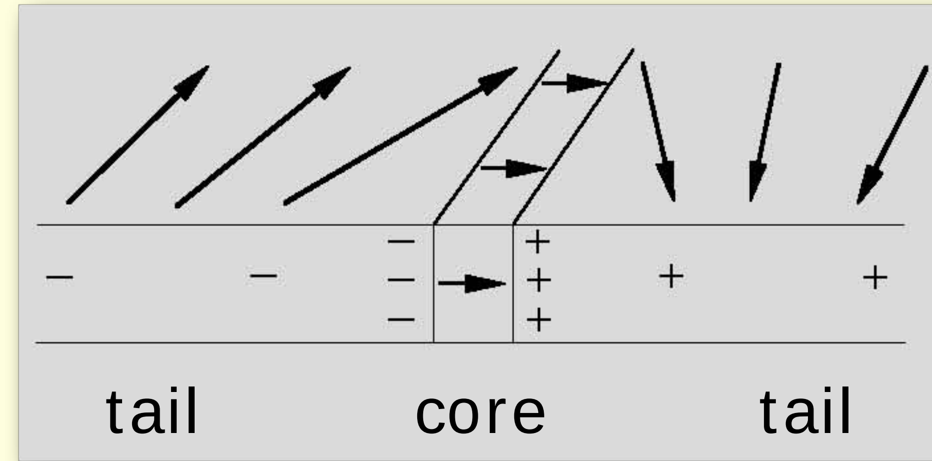

Asymmetric Bloch wall

film thickness
> 100 nm

scales with thickness

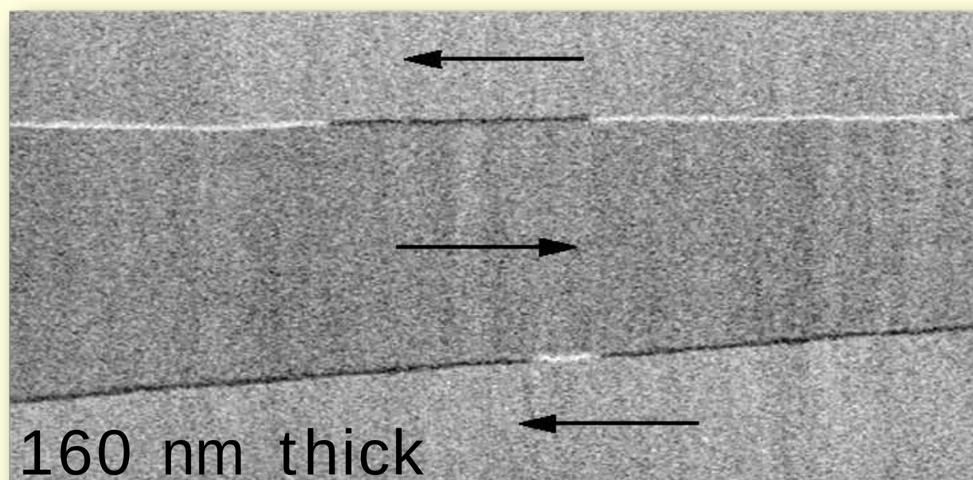

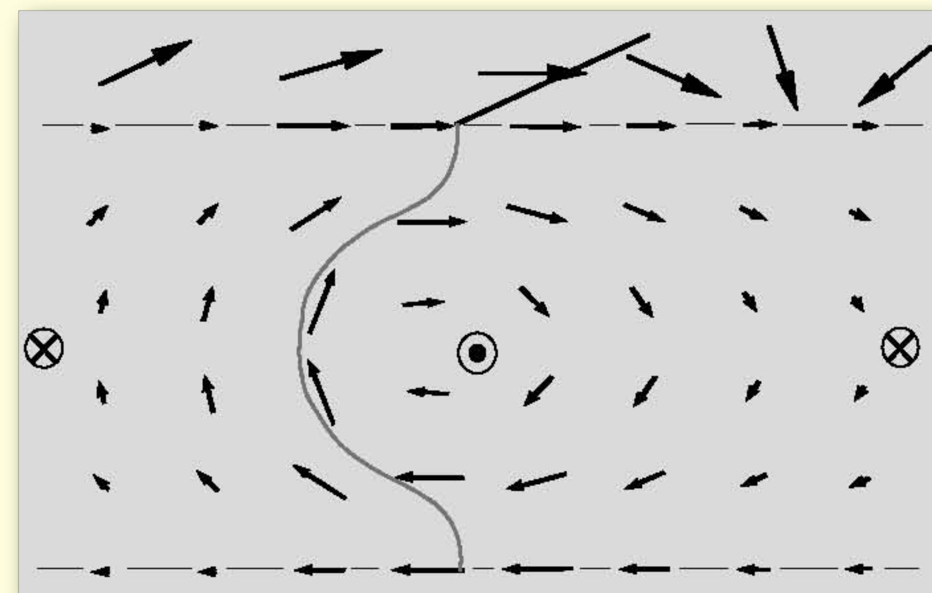

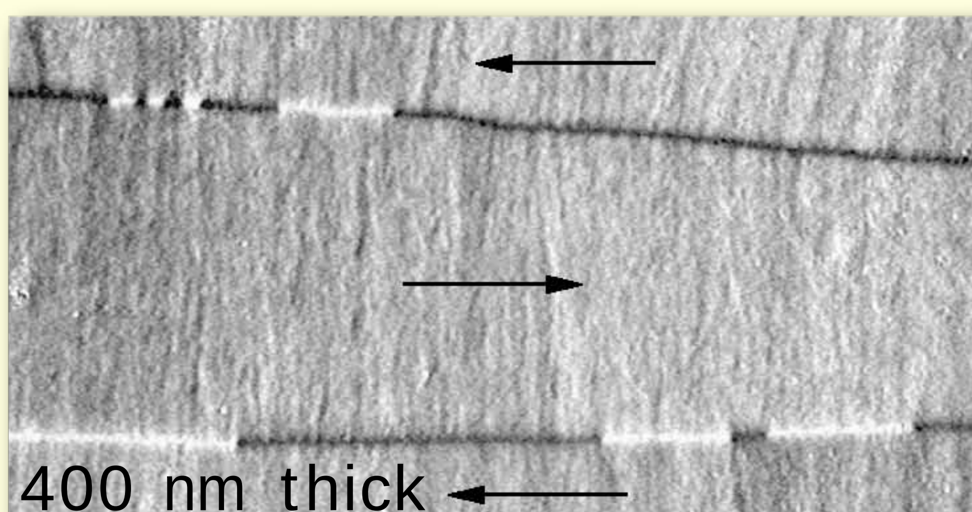

Permalloy
(NiFe)

180° wall types in soft magnetic films

Néel wall

film thickness
< 100 nm

scales with $\sqrt{A/K_d}$

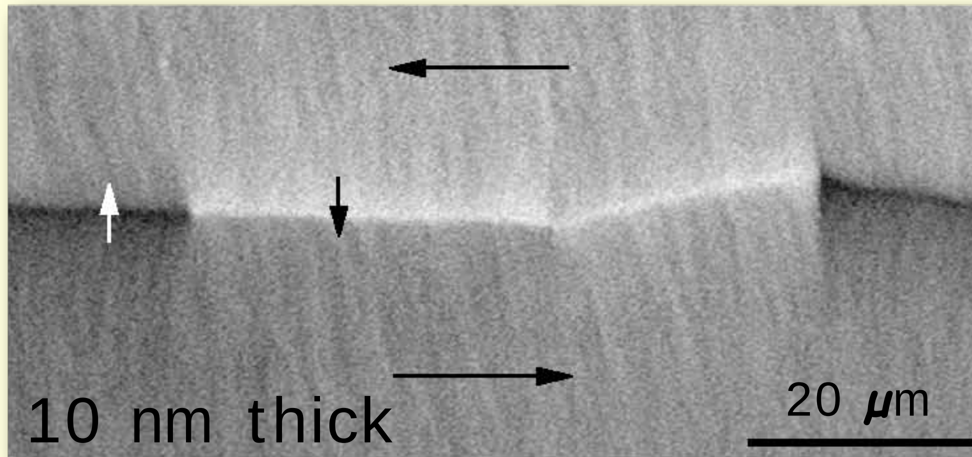

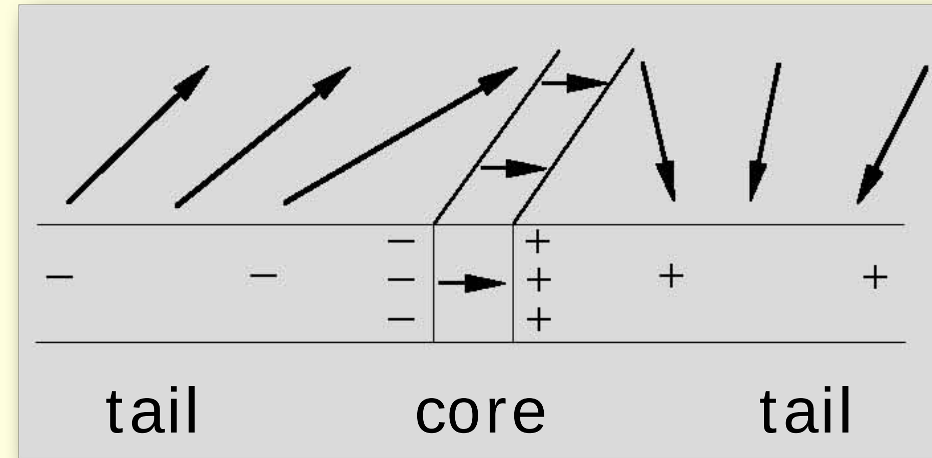

(NiFe)

Anisotropy-free film element:

Existence of real domain walls does not change van den Berg theory

Van den Berg Construction

Transition to three-dimensional bodies (i.e. bulk materials):

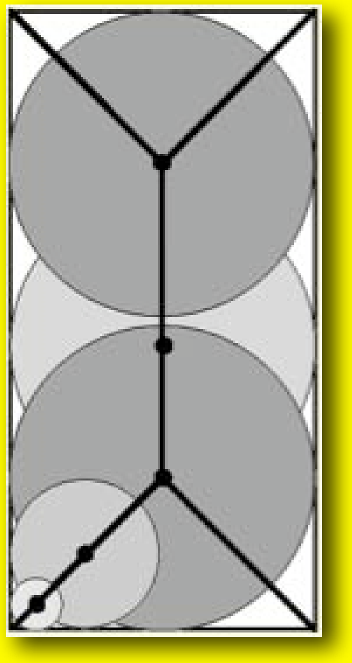

Replace touching circles by touching spheres

↓

Centers of spheres define position of domain walls

↓

Expect regular domains with defined walls also in anisotropy-free bulk materials

180° wall types in soft magnetic films

Thickness > 5 $\sqrt{A/K_d}$: vortex restricted to surface, Bloch-character in volume

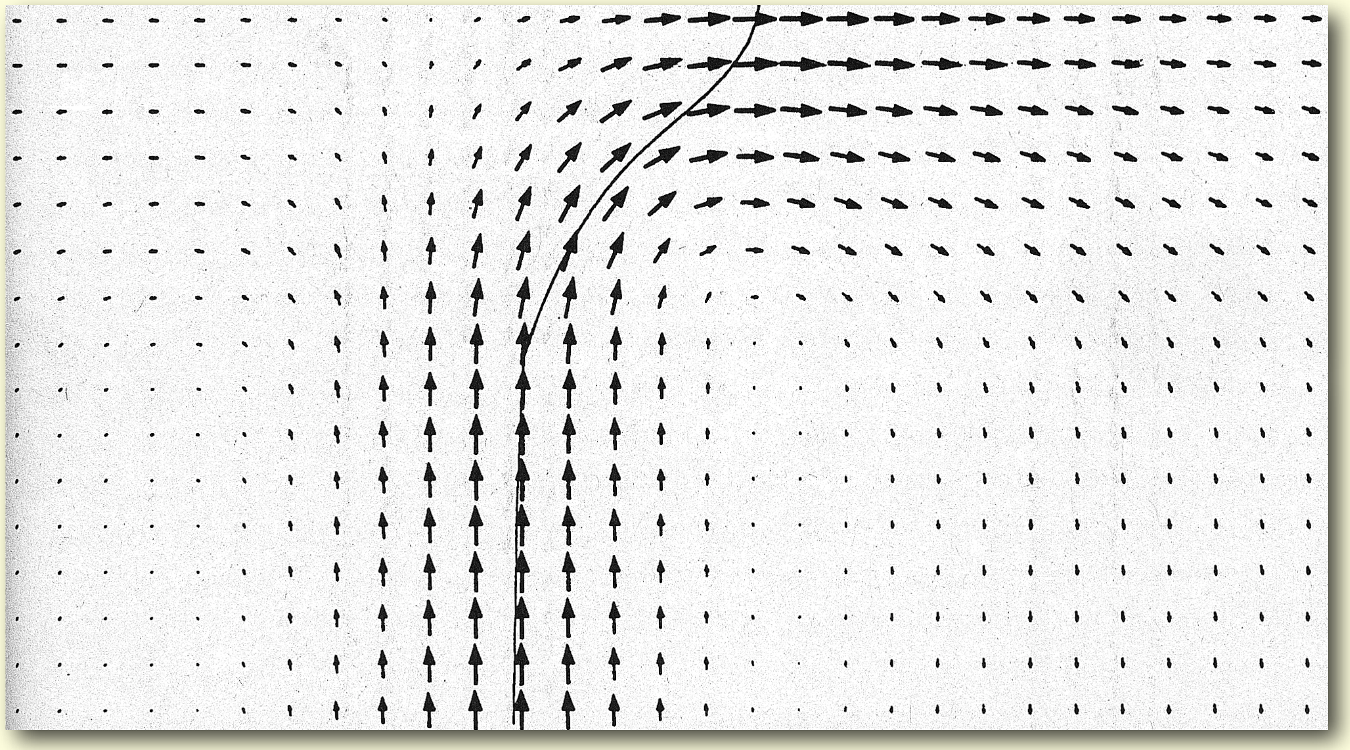

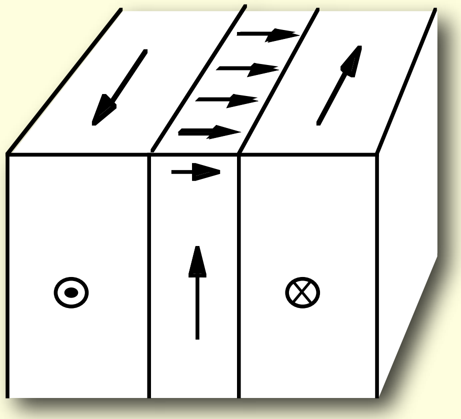

Fe (100) wall,
thickness 200 nm

A. Aharoni, J. P. Jakubovocs
Phys. Rev. B 43 (1991) 1290

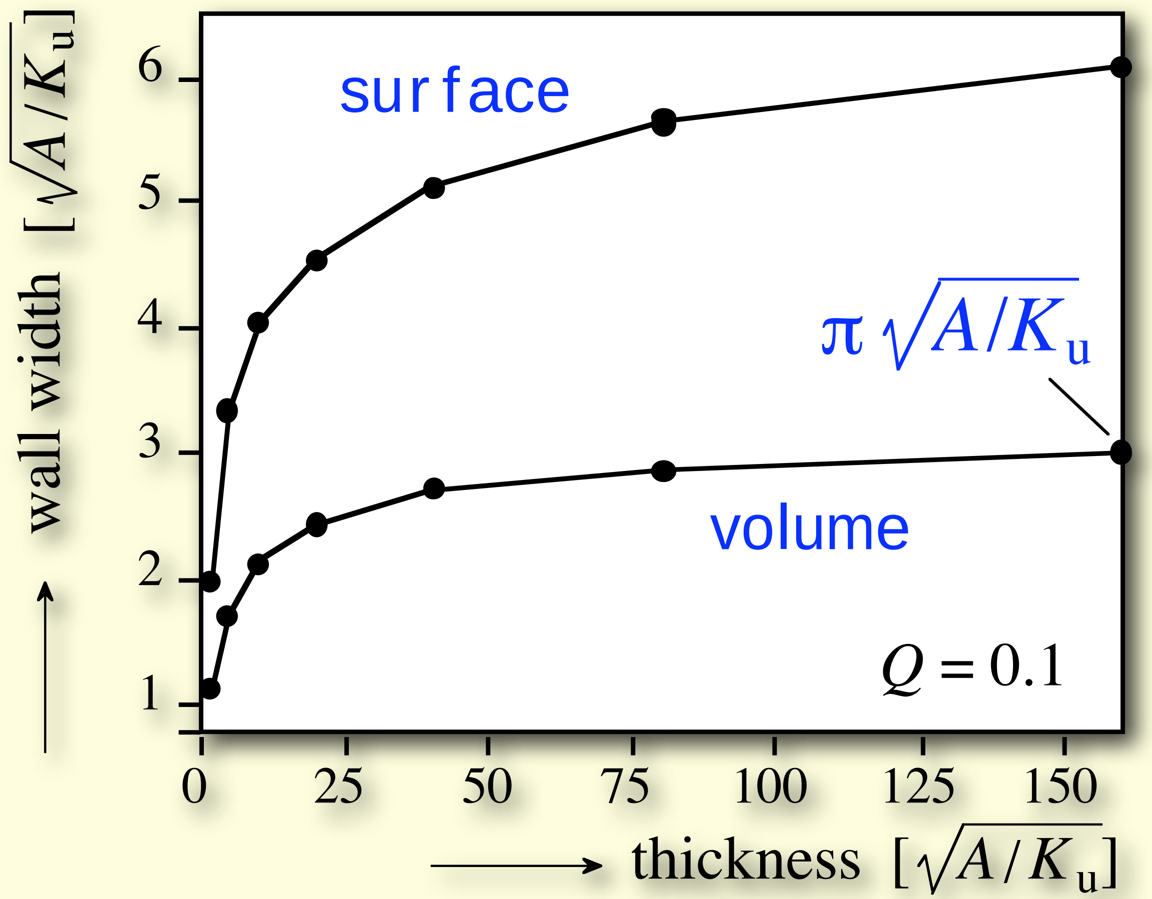

Wall width at surface increases steadily with thickness

Wall width in volume approaches classical value

W. Rave and A. Hubert
JMMM 184 (1998) 179

180° wall types in soft magnetic films

Thickness > 5 $\sqrt{A/K_d}$: vortex restricted to surface, Bloch-character in volume

Bulk low-anisotropy materials:

Domain walls required (van den Berg),
Wall width scales with $\sqrt{A/K}$

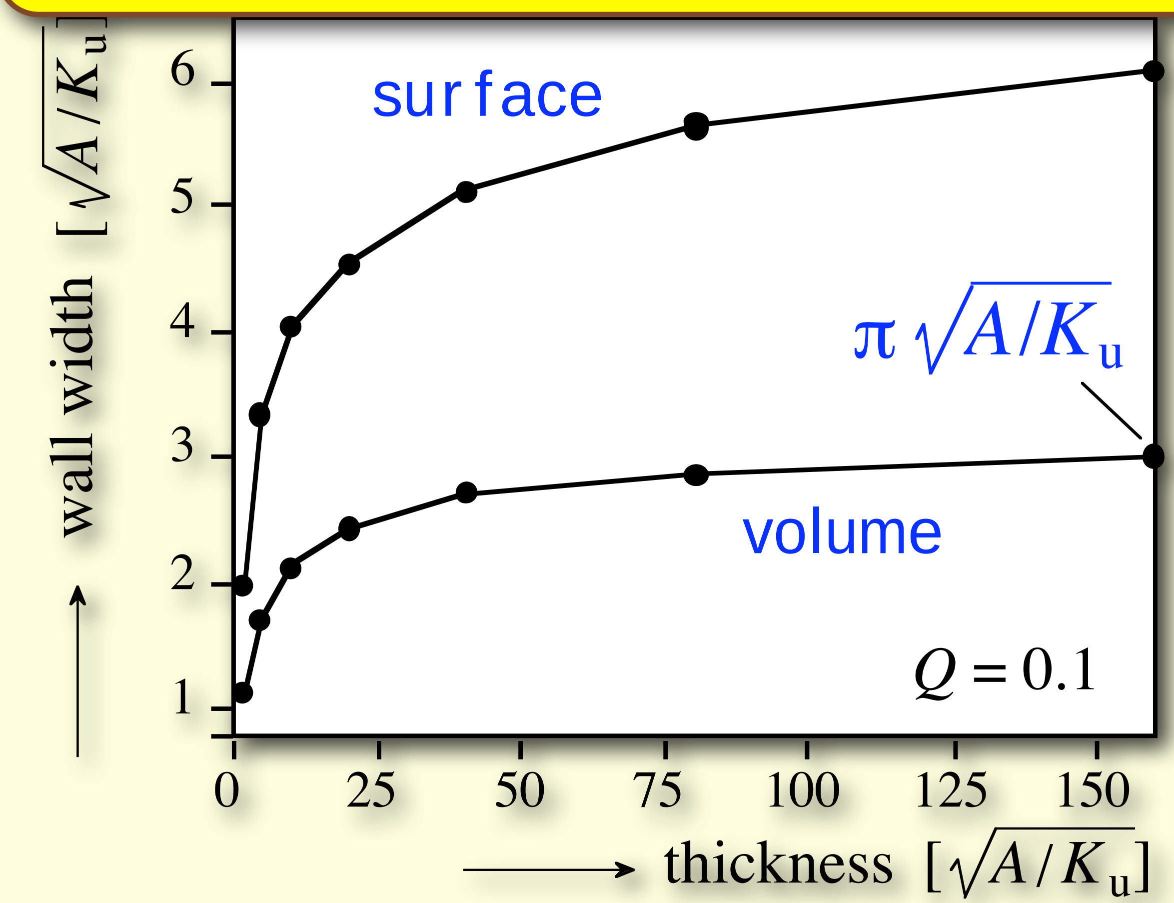

Wall width at surface increases steadily with thickness

Wall width in volume approaches classical value

W. Rave and A. Hubert
JMMM 184 (1998) 179

180° wall types in soft magnetic films

Thickness > 5 $\sqrt{A/K_d}$: vortex restricted to surface, Bloch-character in volume

Bulk low-anisotropy materials:

Domain walls required (van den Berg),
Wall width scales with $\sqrt{A/K}$

↓

Bulk anisotropy-free materials:

Domain walls are not defined anymore

Consequence

In bulk materials with
vanishing anisotropy
we do no expect regular,
homogeneously magnetized domains with
well defined walls,
but continuous patterns

Magnetic microstructure of amorphous ribbons

m(r) continuously flowing ?

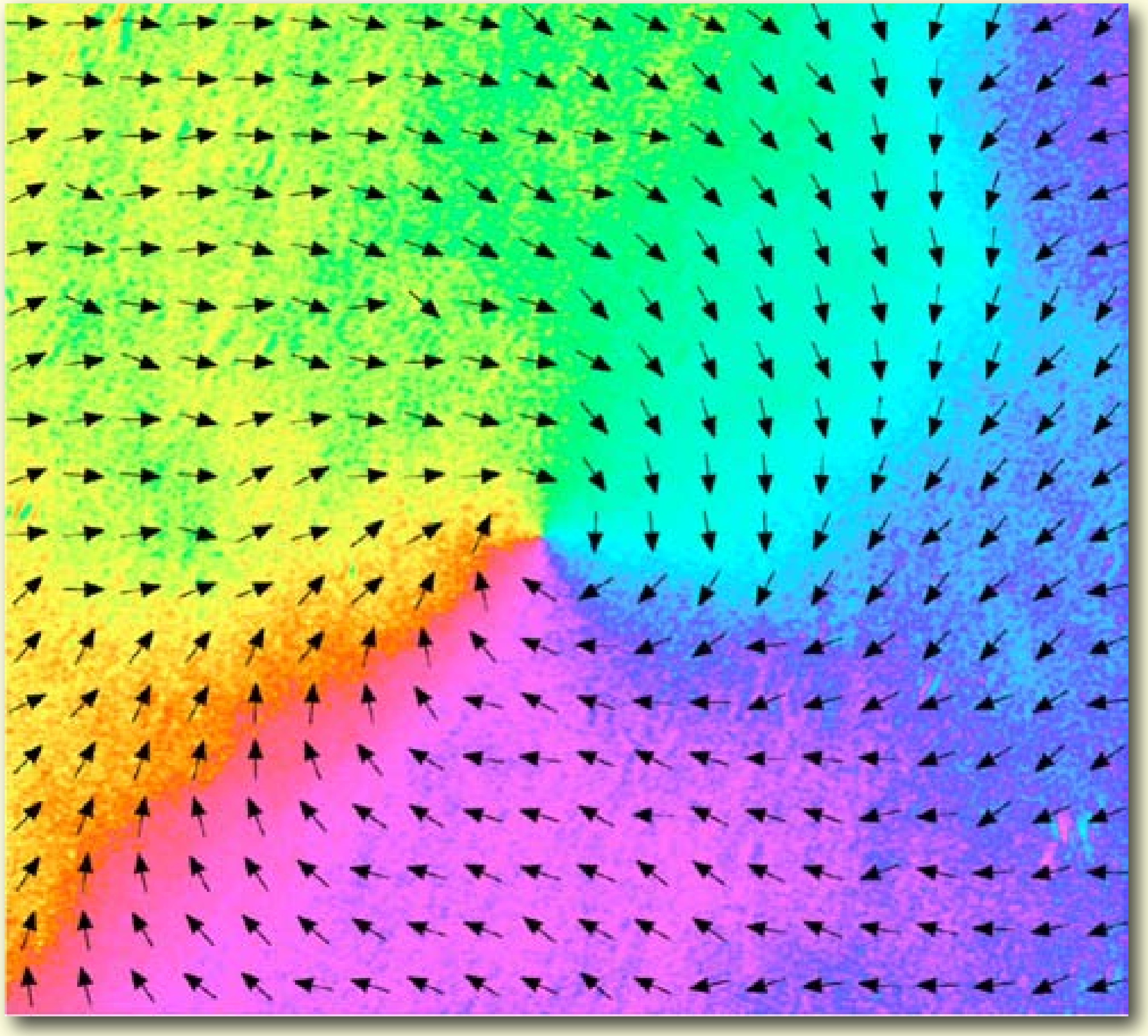

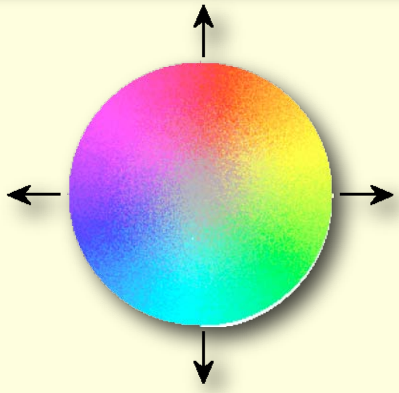

or regular domains ?

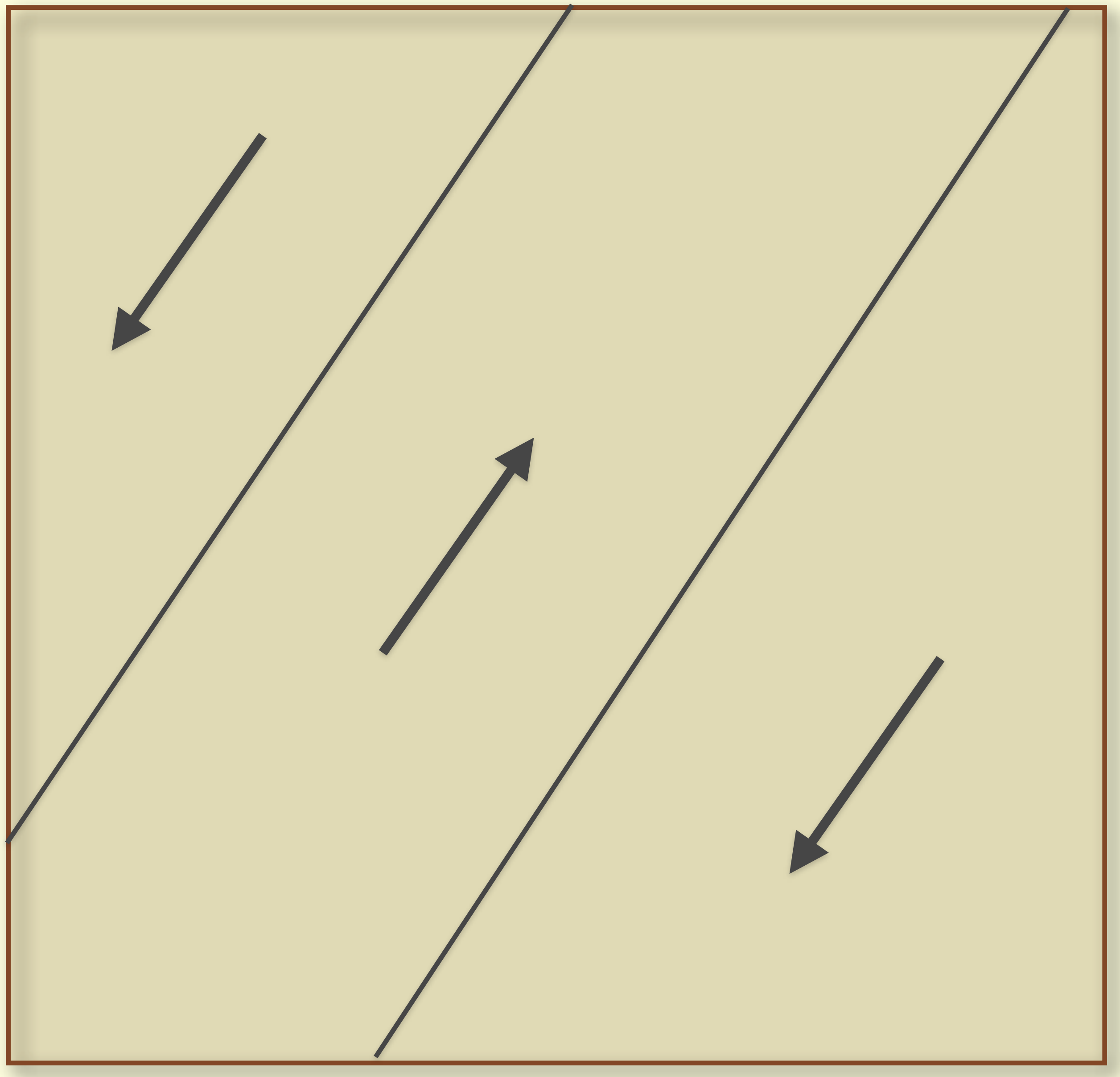

Magnetic microstructure of amorphous ribbons

m(r) continuously flowing ?

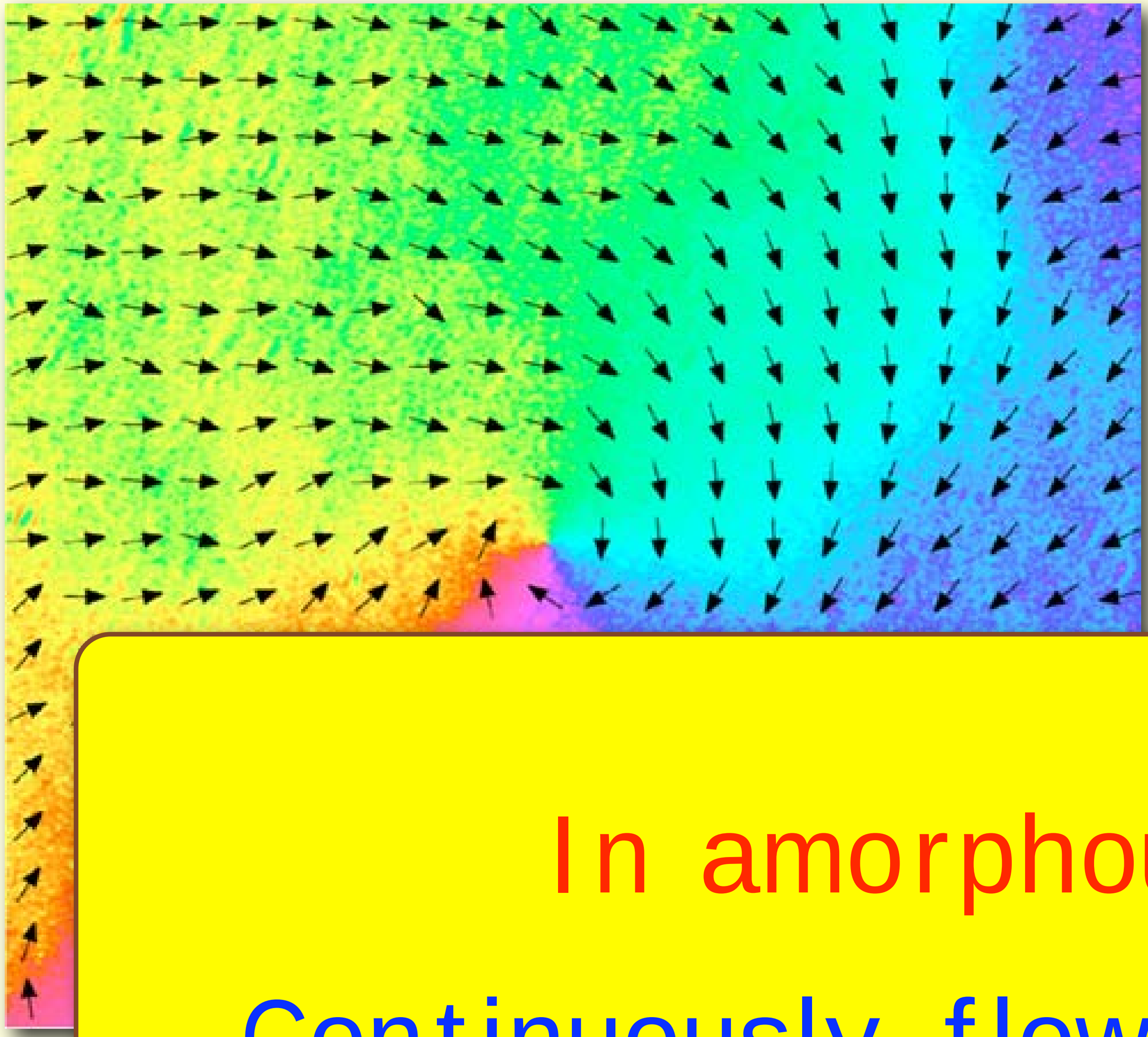

or regular domains ?

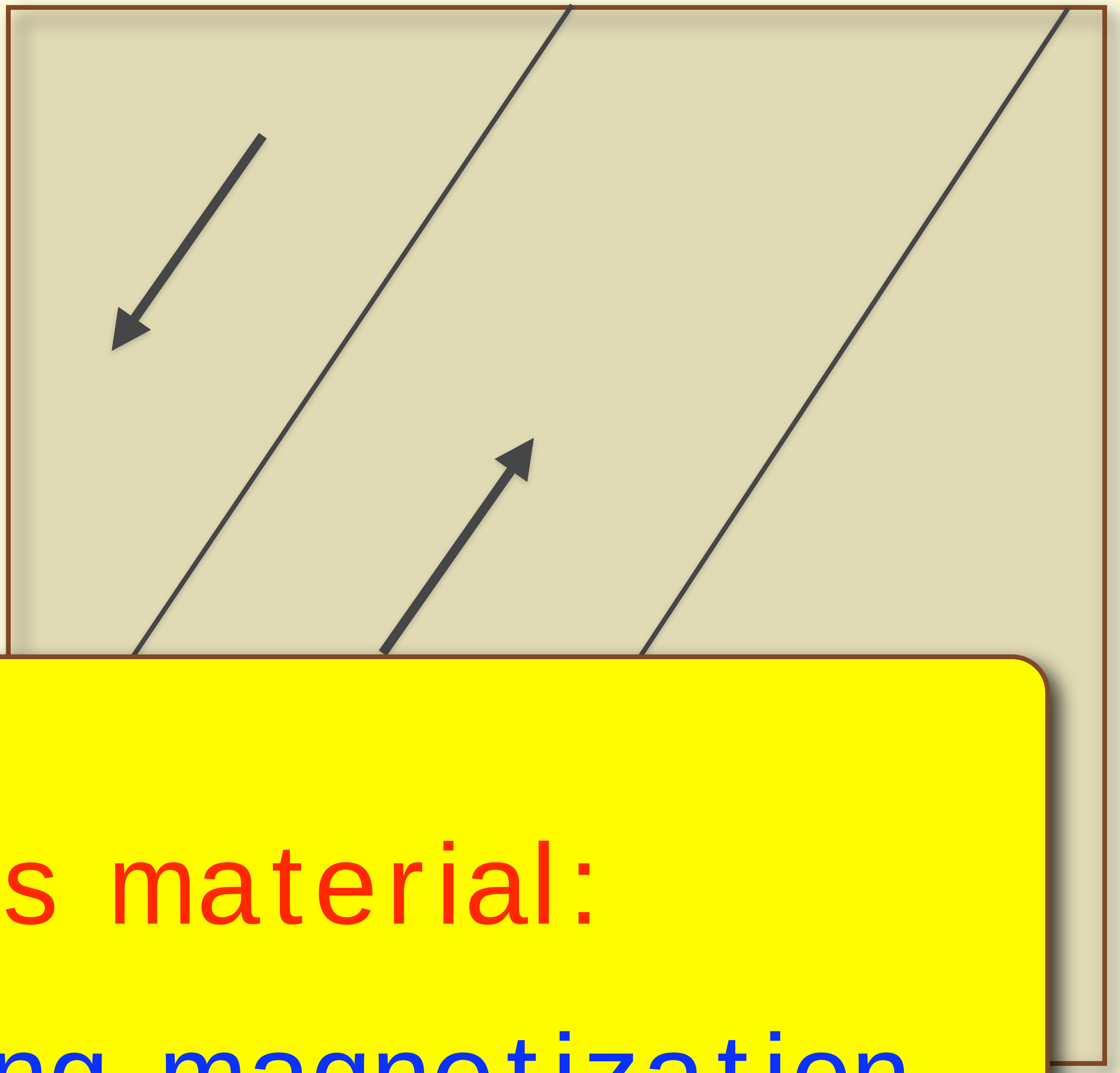

In amorphous material:

Continuously flowing magnetization expected rather than regular domains

Amorphous ribbon (as-quenched): hysteresis loop

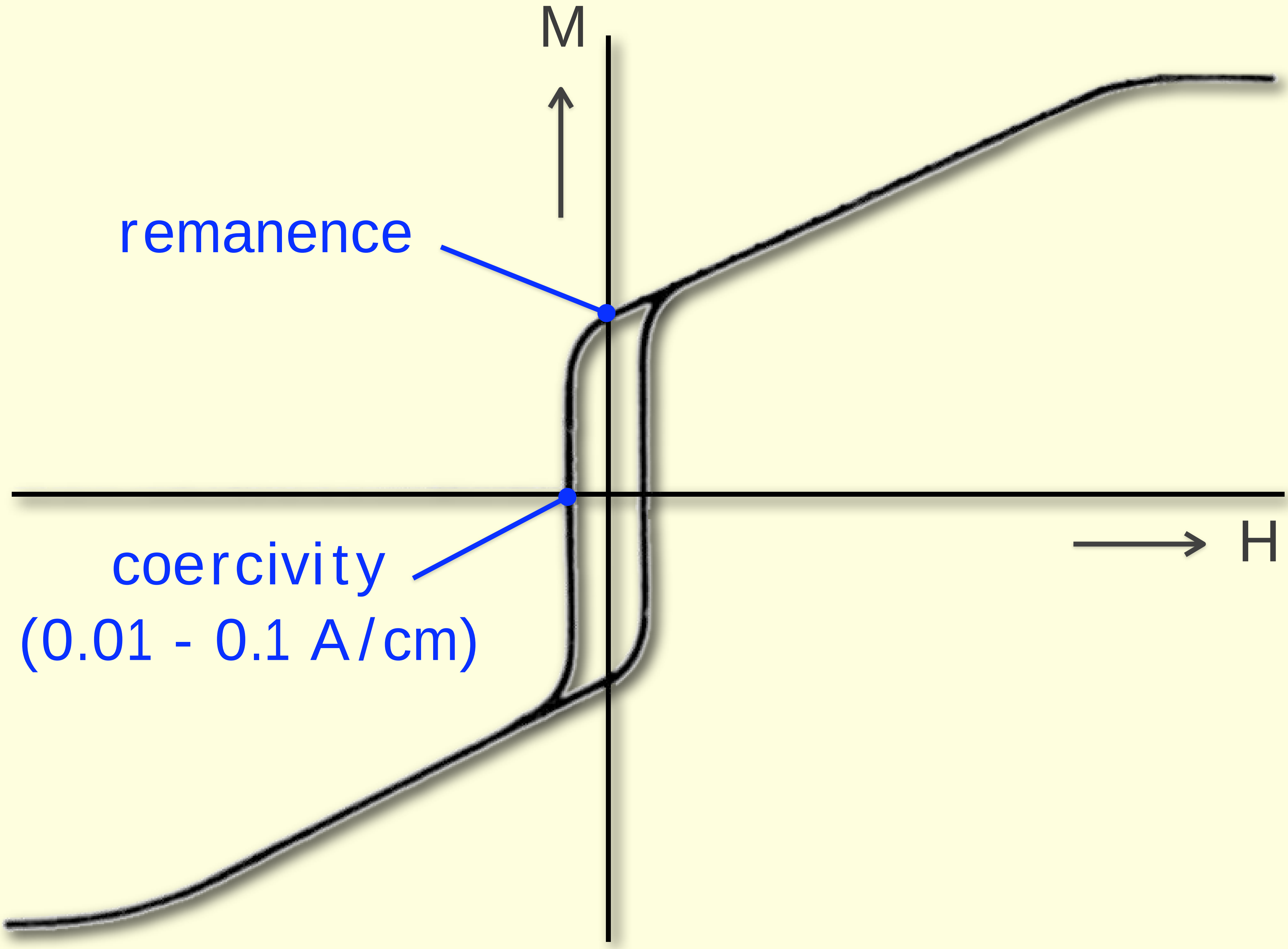

Amorphous ribbon (as-quenched): hysteresis loop

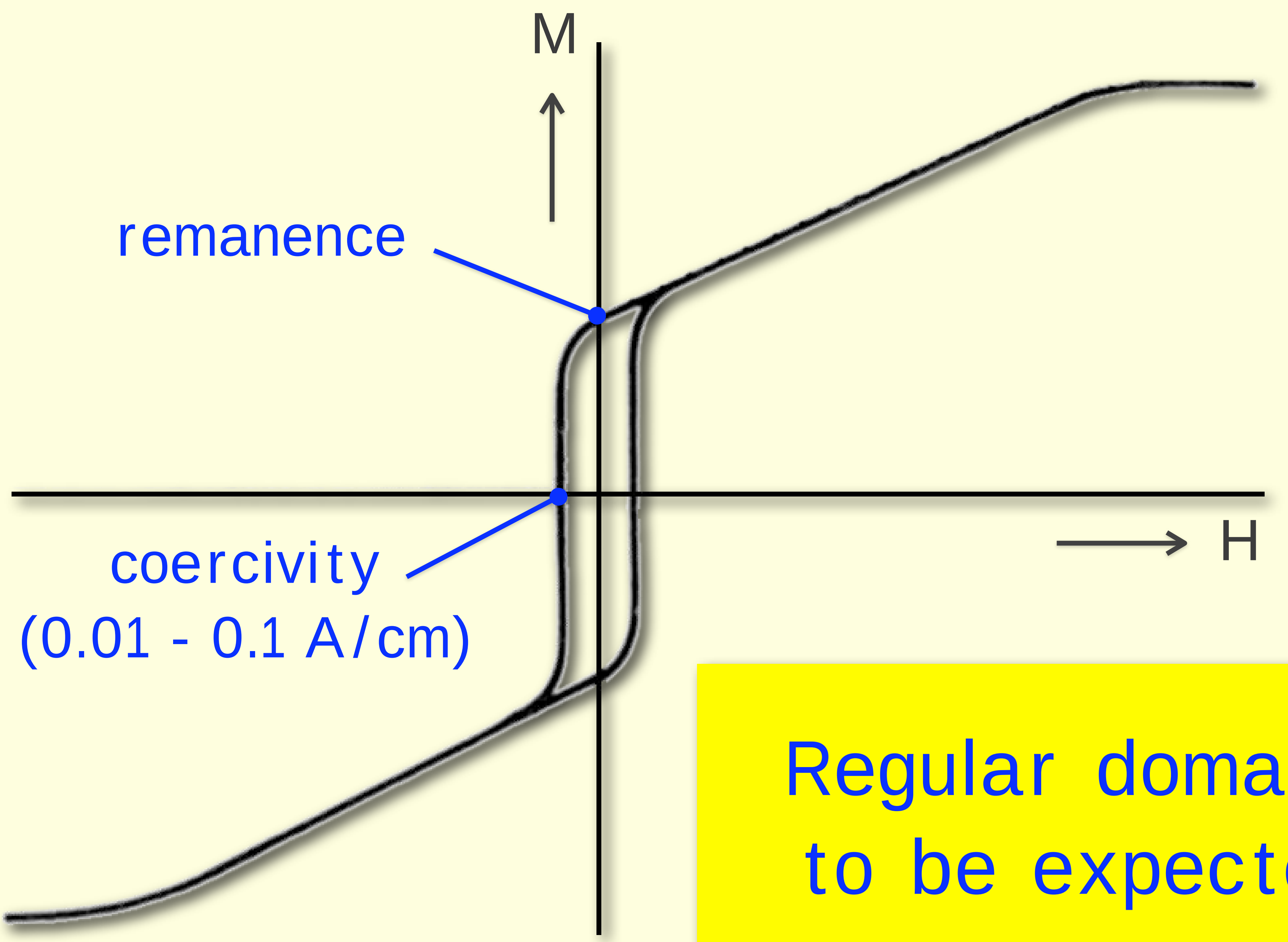

Regular domains to be expected

“Regular domains” in amorphous ribbons

“Regular domains” in amorphous ribbons

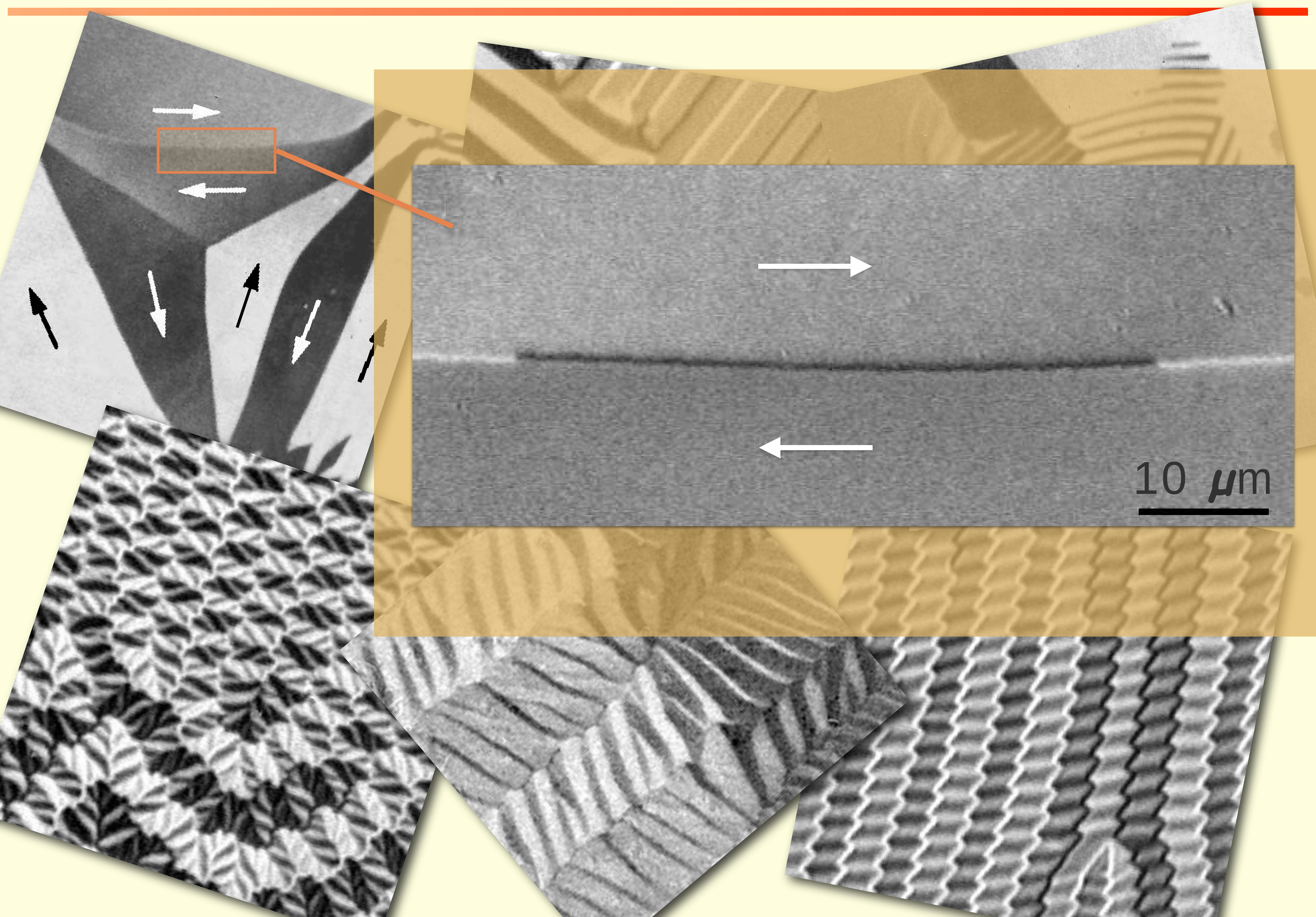

“Regular domains” in amorphous ribbons

Amorphous ribbons show

regular domains and walls

(rather than „flowing“ patterns)

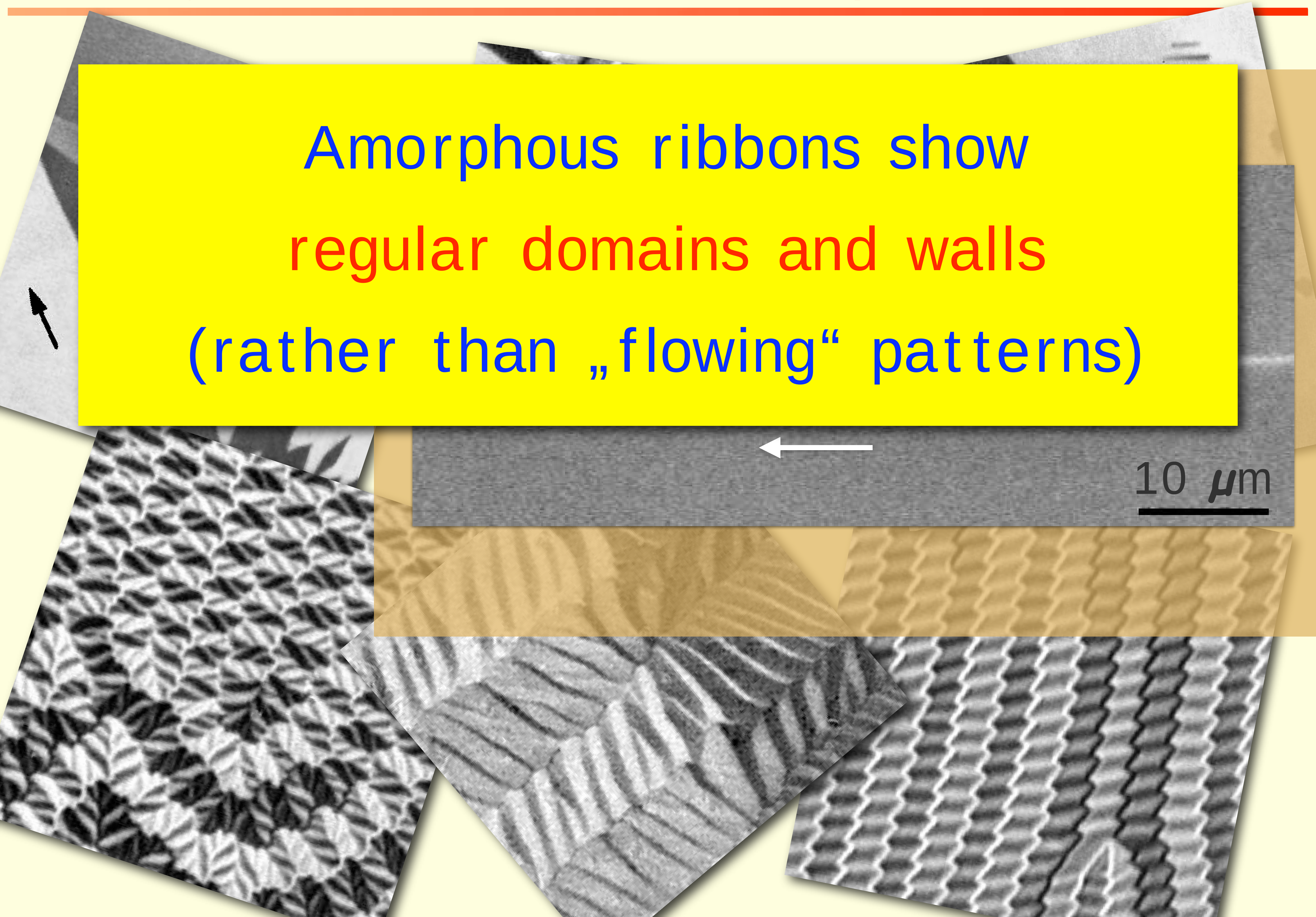

Walls in high-permeable Permalloy cores

(sheets: 50 μm thick)

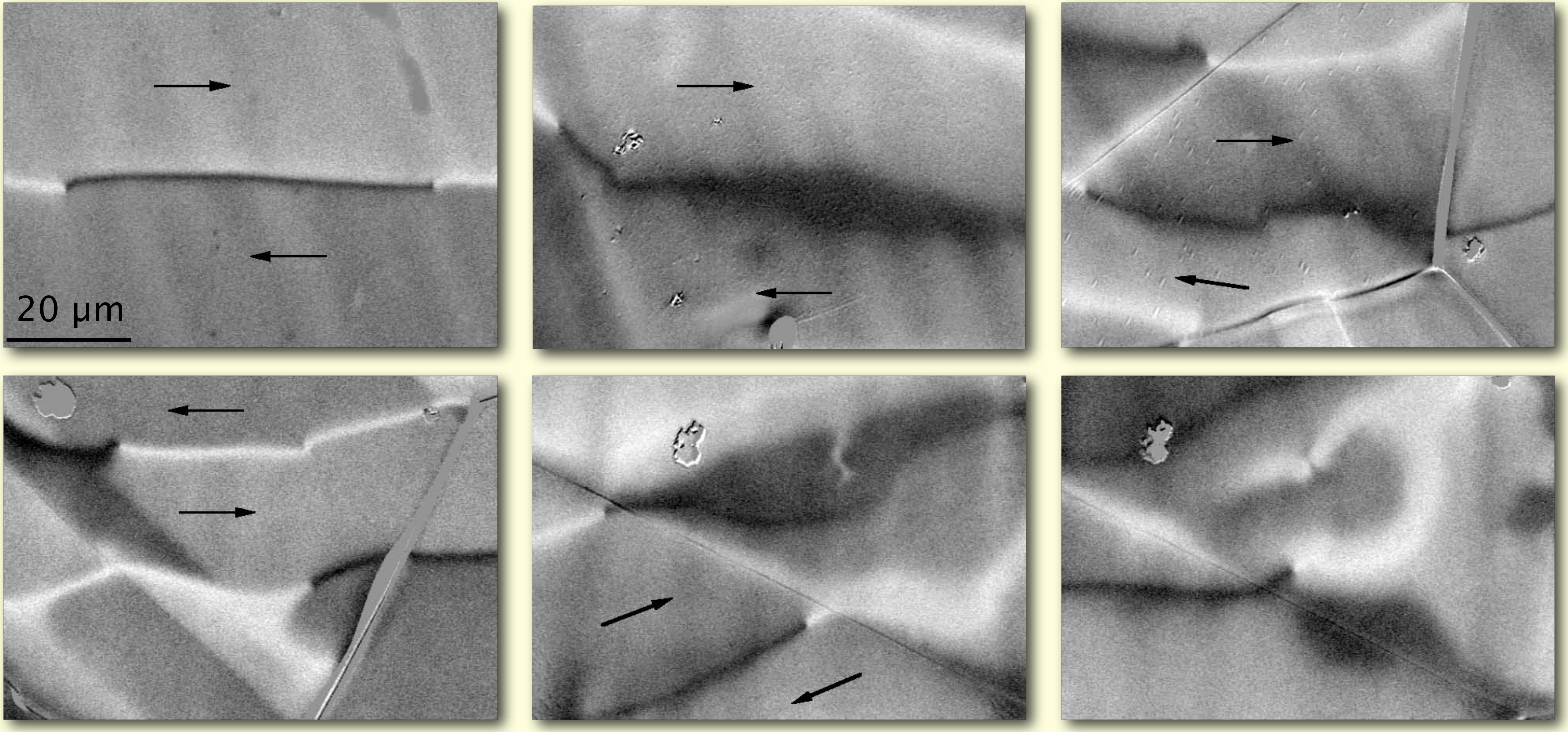

Also Permalloy shows (more or less) regular domains walls

“Regular domains” in amorphous ribbons

Amorphous ribbons show

regular domains

(rather than „flowing“ patterns)




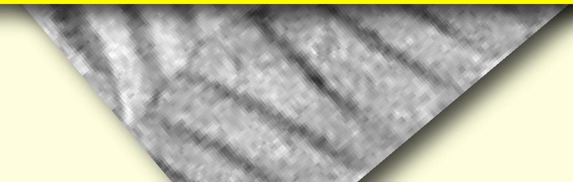
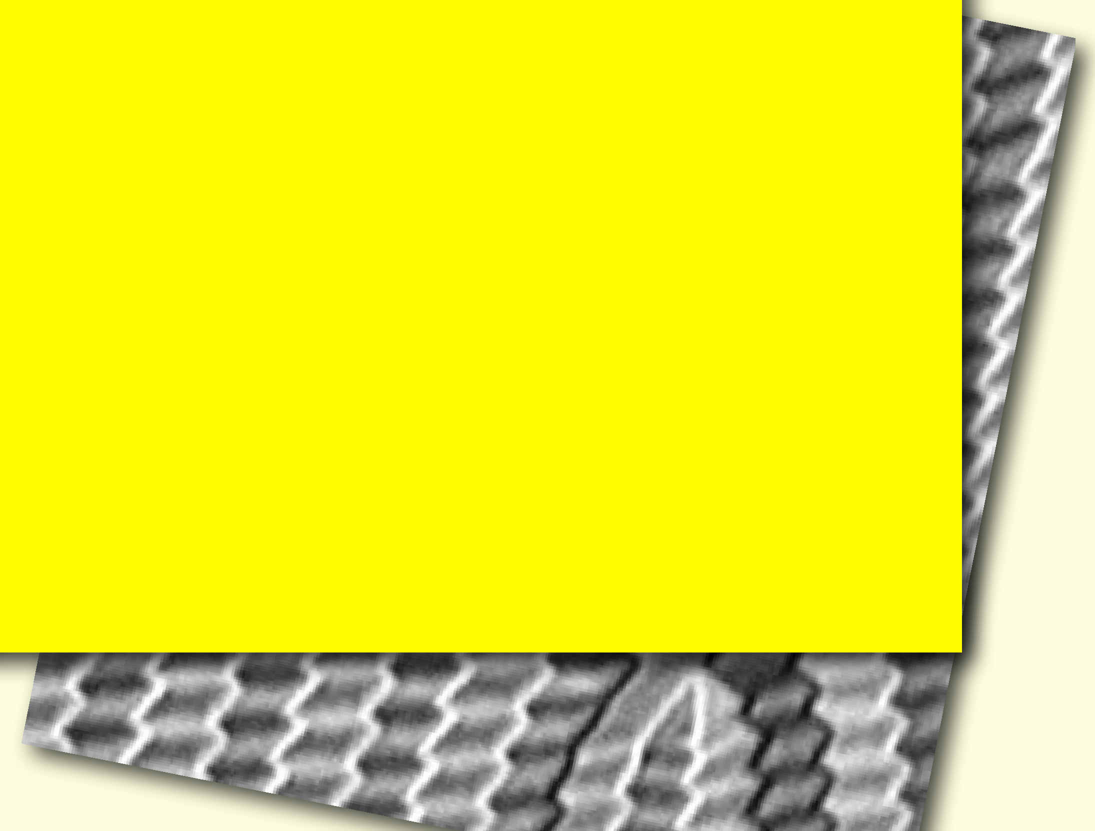

“Regular domains” in amorphous ribbons

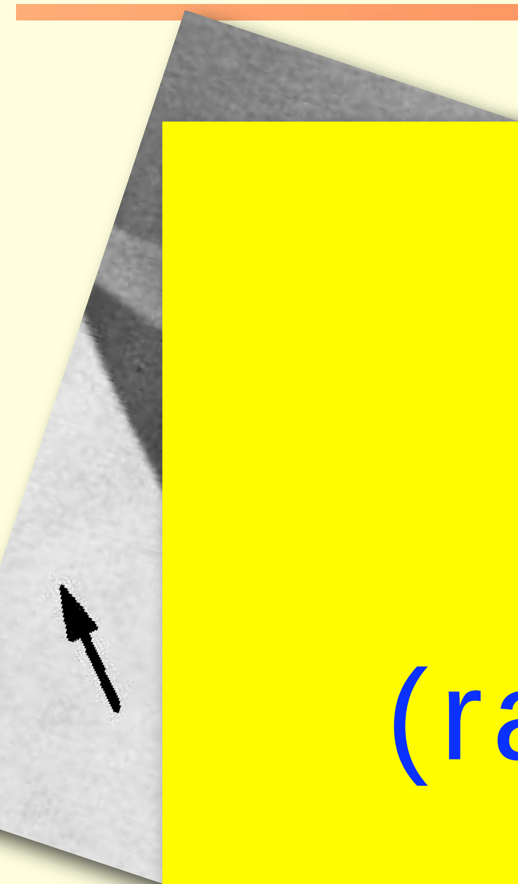

Amorphous ribbons show

regular domains

(rather than „flowing“ patterns)

Reason:

Residual anisotropies

Residual anisotropies in amorphous ribbons

- magnetization-induced

  minute deviations from random pair ordering

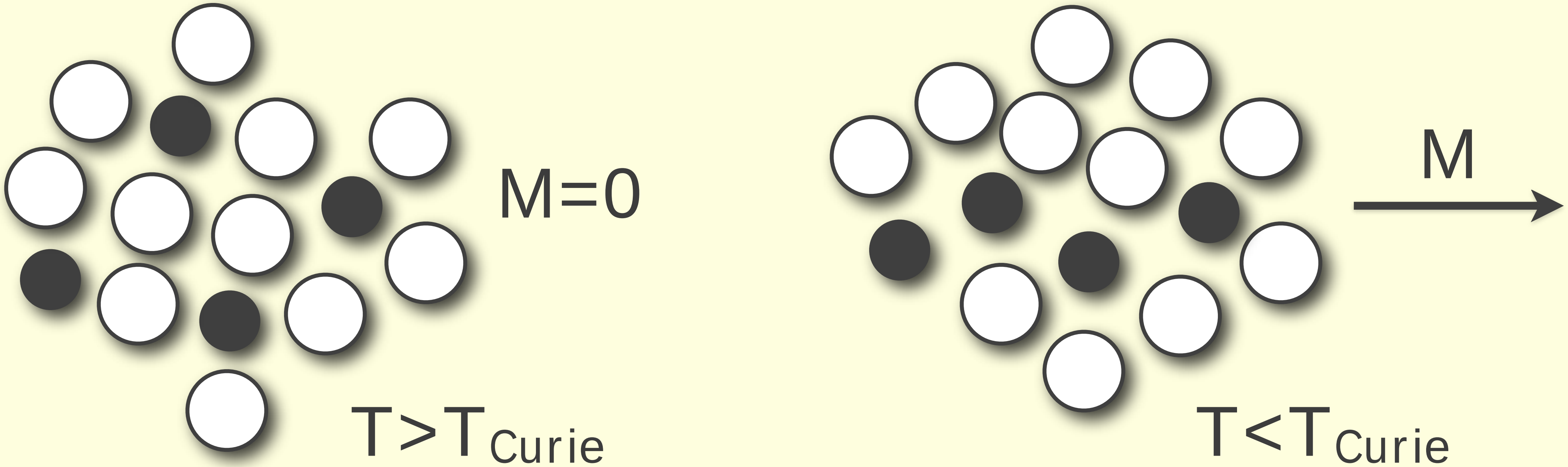

- stress-induced

  internal mechanical stress,
  e.g. due to differences in quenching speed

Stress-induced anisotropy

magnetoelastic coupling energy

$$e_{me} = \frac{3}{2} \lambda_s \, \sigma \sin^2\theta$$

magnetostriction constant

mechanical stress

angle between M and stress σ

$\lambda_s > 0, \sigma > 0$:

$\sigma < 0$:

$\sigma < 0$:
(planar)

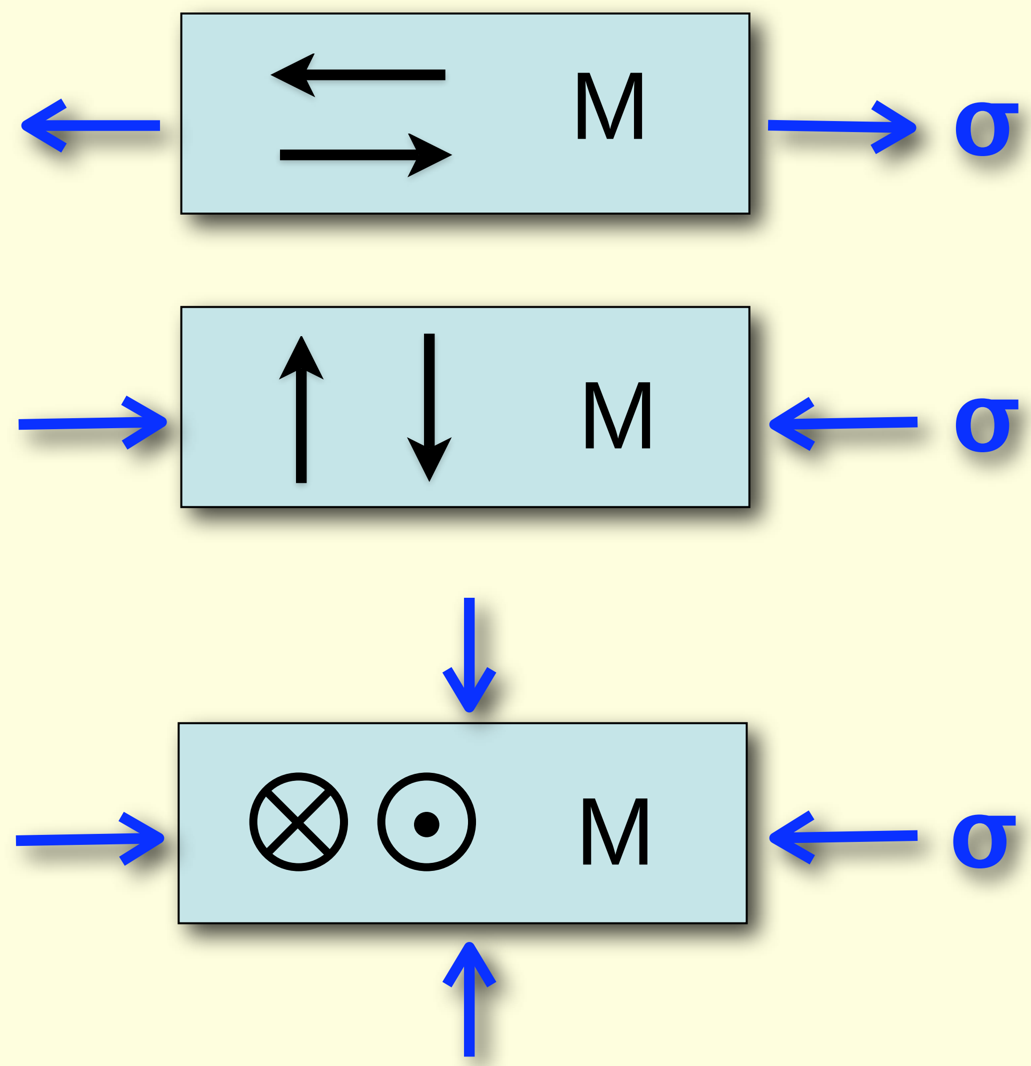

As-quenched $Fe_{78}Si_{13}B_9$ amorphous ribbon

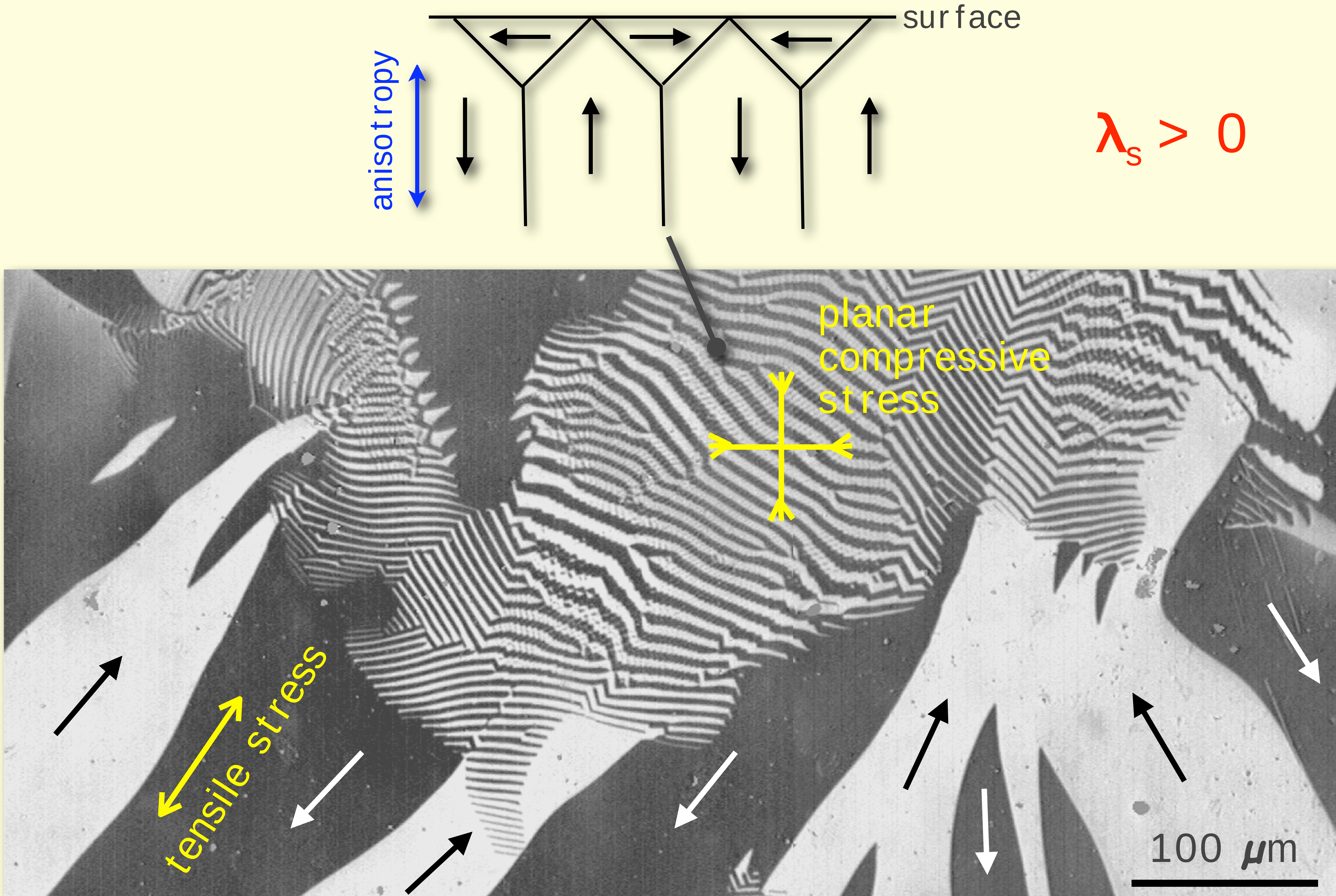

Amorphous ribbons: Magnetostriction & domains

$$e_{me} = \frac{3}{2}\lambda_s \, \sigma \sin^2\theta$$

magnetostriction constant

mechanical stress

angle between M and stress σ

same location, independently demagnetized ⟶ local anisotropy

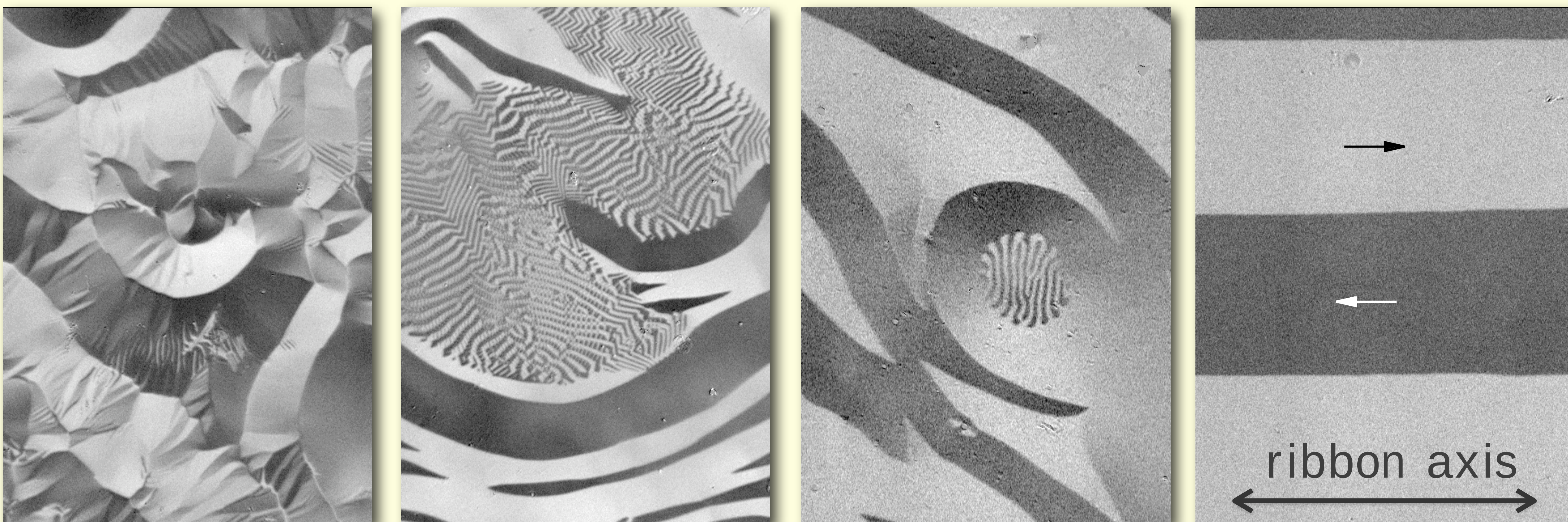

$\lambda_s = +35 \cdot 10^{-6}$
$(FeCo)_{83}(Si,B)_{17}$

$\lambda_s = +24 \cdot 10^{-6}$
$Fe_{76}(Si,B)_{24}$

$\lambda_s = +8 \cdot 10^{-6}$
$Ni_{39}Fe_{39}(Si,B,C)_{22}$

$\lambda_s < 0.2 \cdot 10^{-6}$
$(Co,Fe,Mn,Mo)_{77}(Si,B)_{23}$

As-quenched $Fe_{78}Si_{13}B_9$ amorphous ribbon

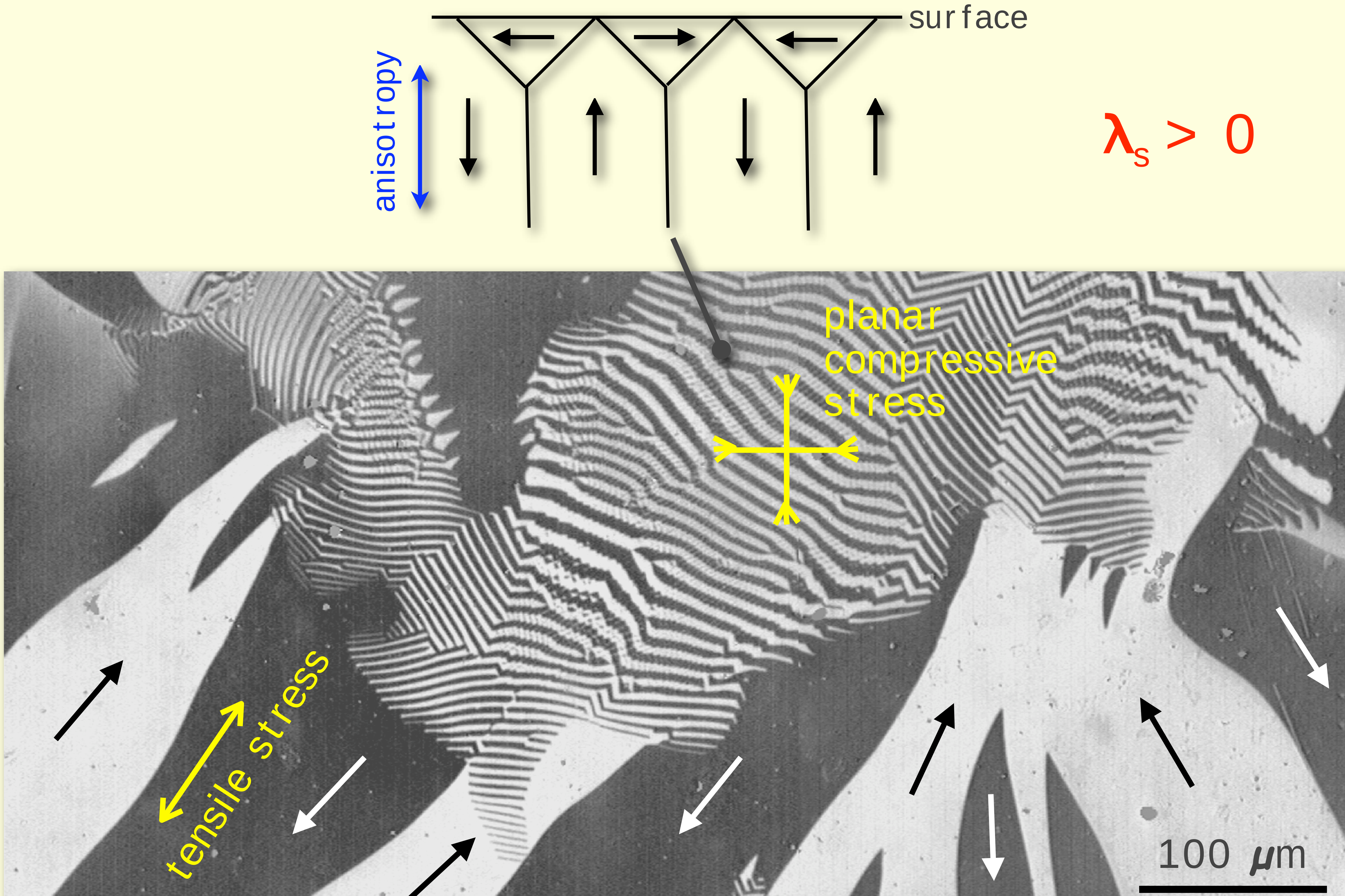

Compare: stripe domains in magnetic films

FeSiBCuNb amorphous film (2 μm thick)

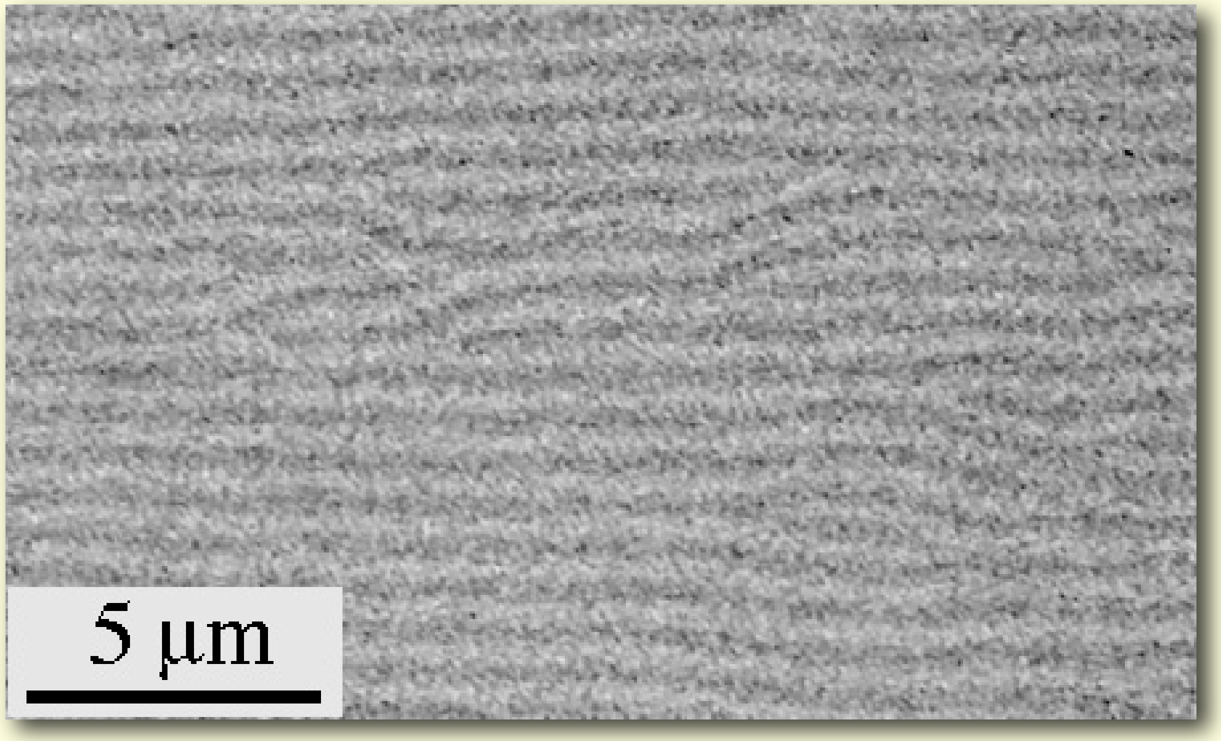

← H

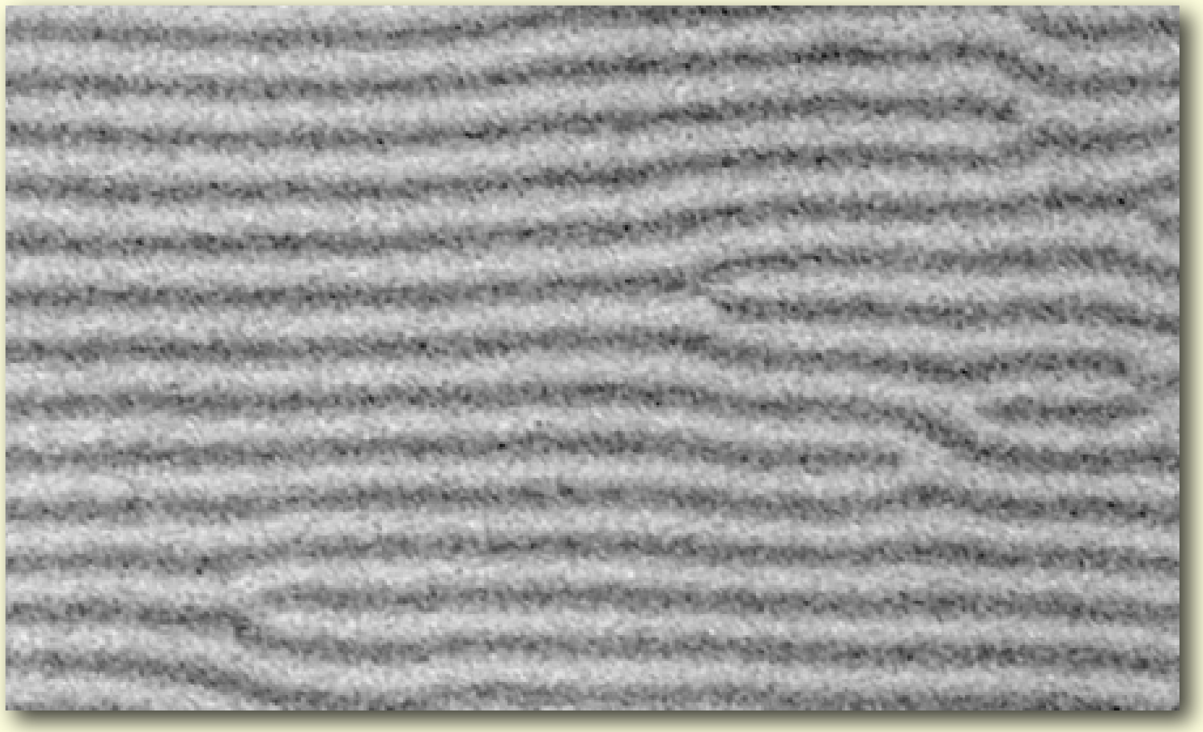

H = 0

reason: planar compressive stress $\boldsymbol{\sigma}_p$

$$\boxed{e_{me} = \frac{3}{2}\lambda_s \sigma_p \sin^2\theta}$$

$\boldsymbol{\lambda}_s > 0$, $\boldsymbol{\sigma}_p < 0$:

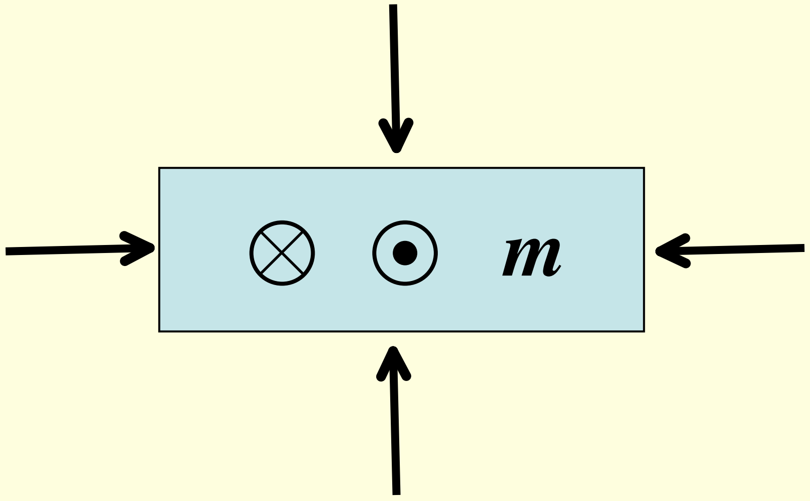

$\boldsymbol{\theta}$: angle between m and $\boldsymbol{\sigma}_p$

→ perpendicular anisotropy

Compare: stripe domains in magnetic films

low anisotropy
(i.e. Q<<1) film
→ dense stripe domains

for comparison:
high anisotropy film
(garnet, Q>1)

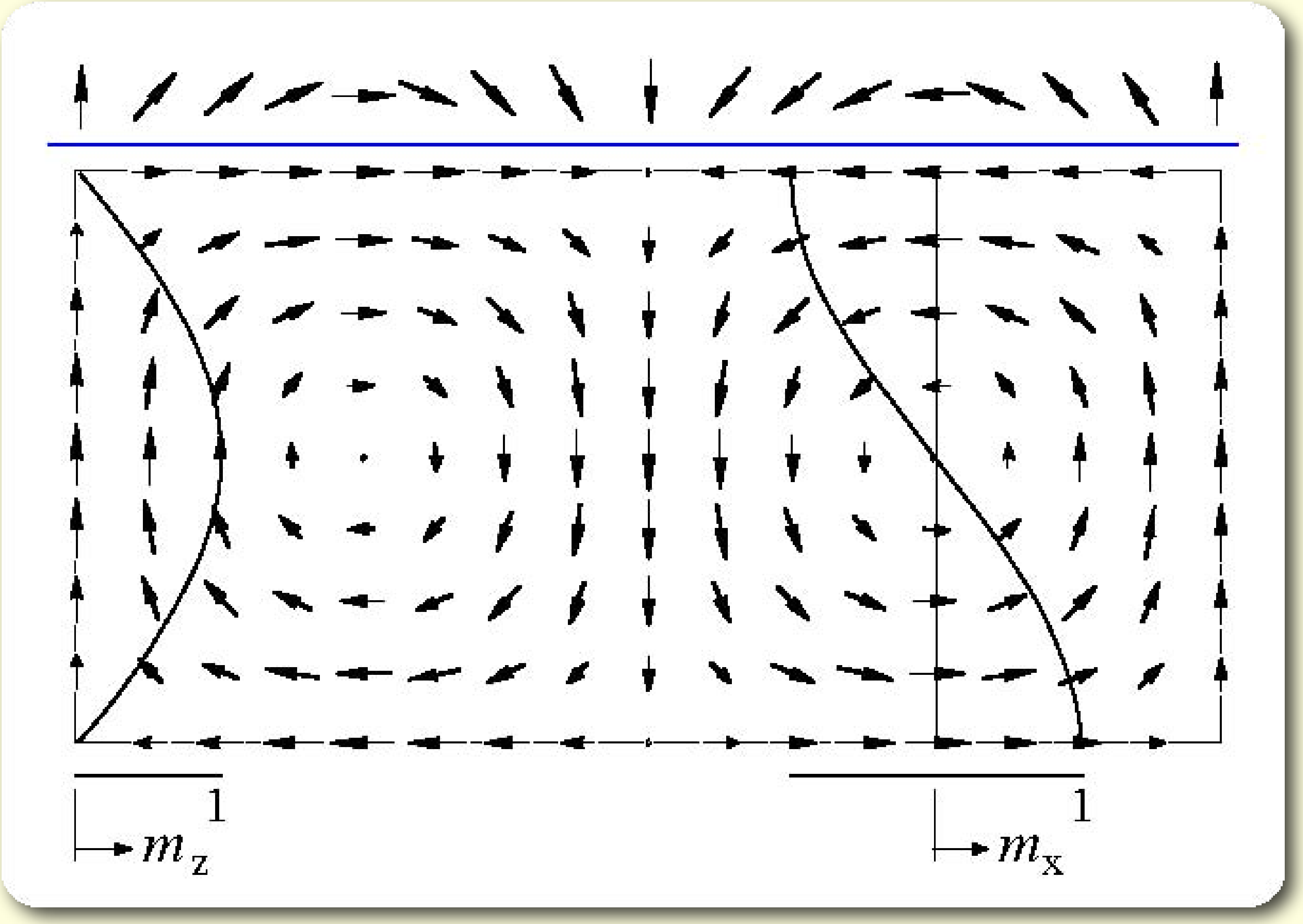

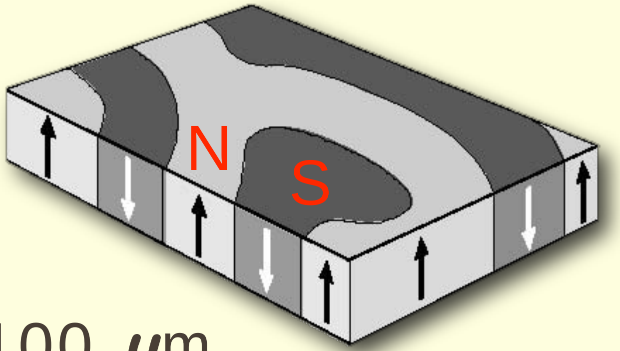

Compare: stripe domains in magnetic films

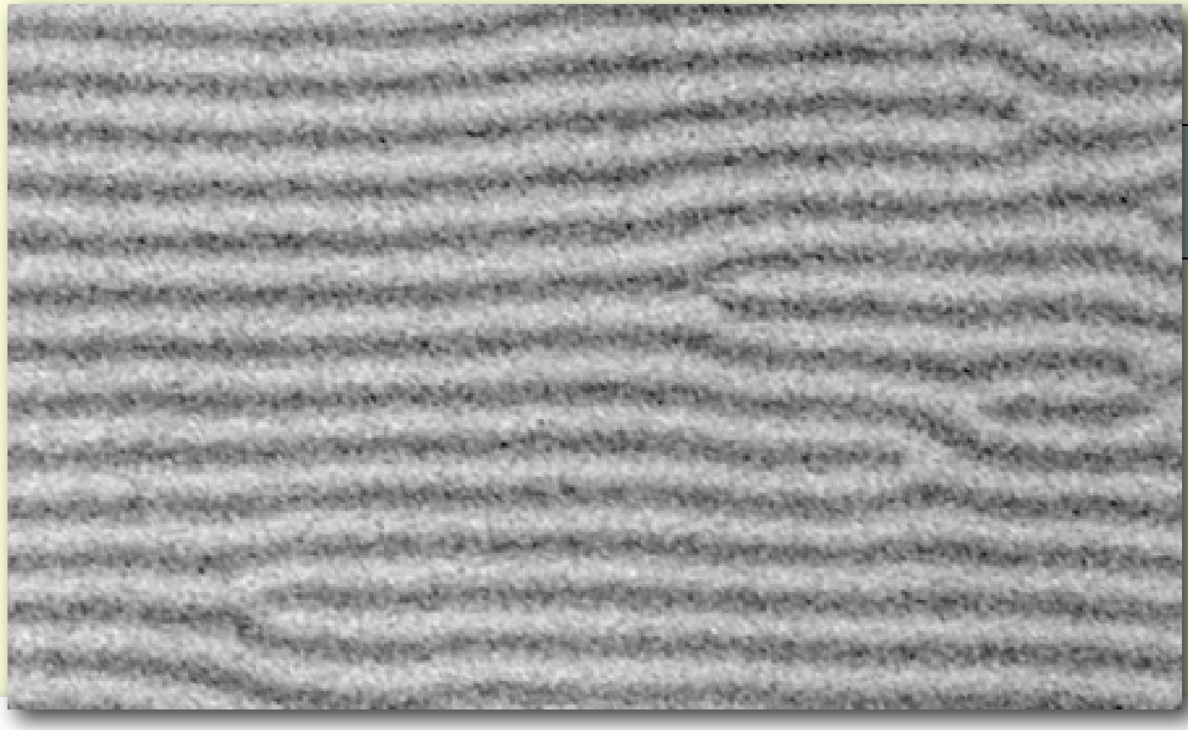

opy

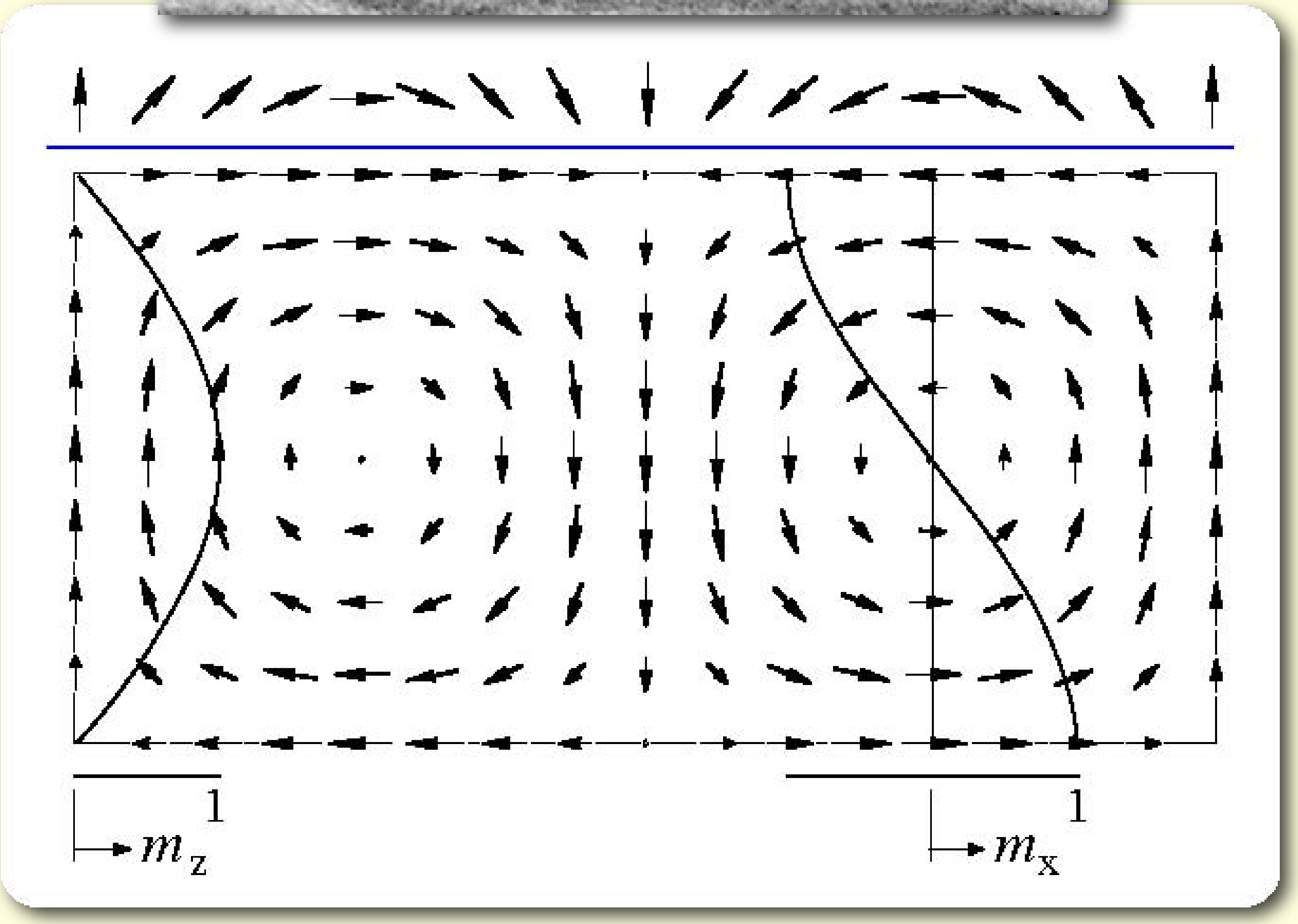

for comparison:
high anisotropy film
(garnet, Q>1)

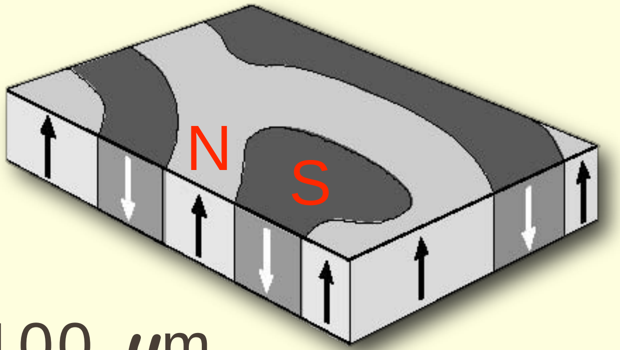

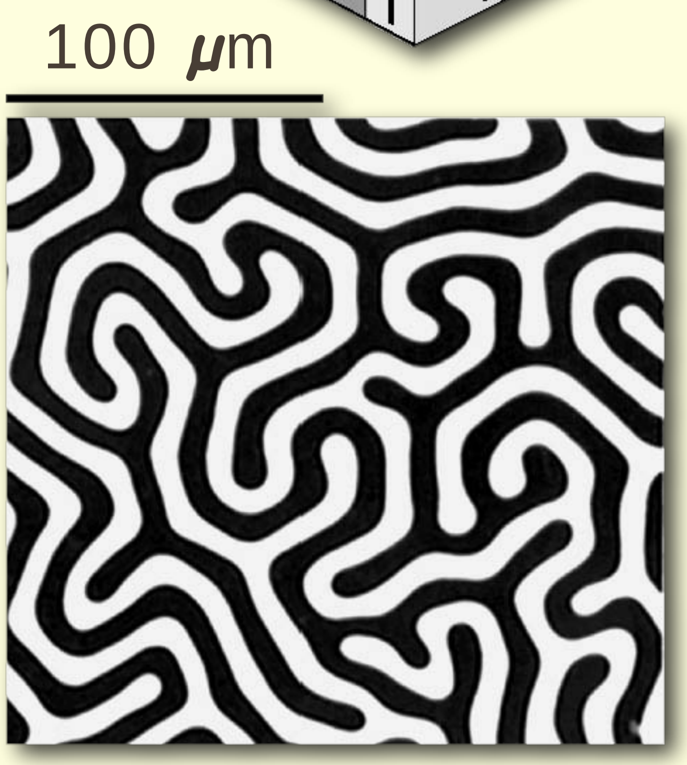

Compare: stripe domains in magnetic films

amorphous thin film
(2 μm thick)

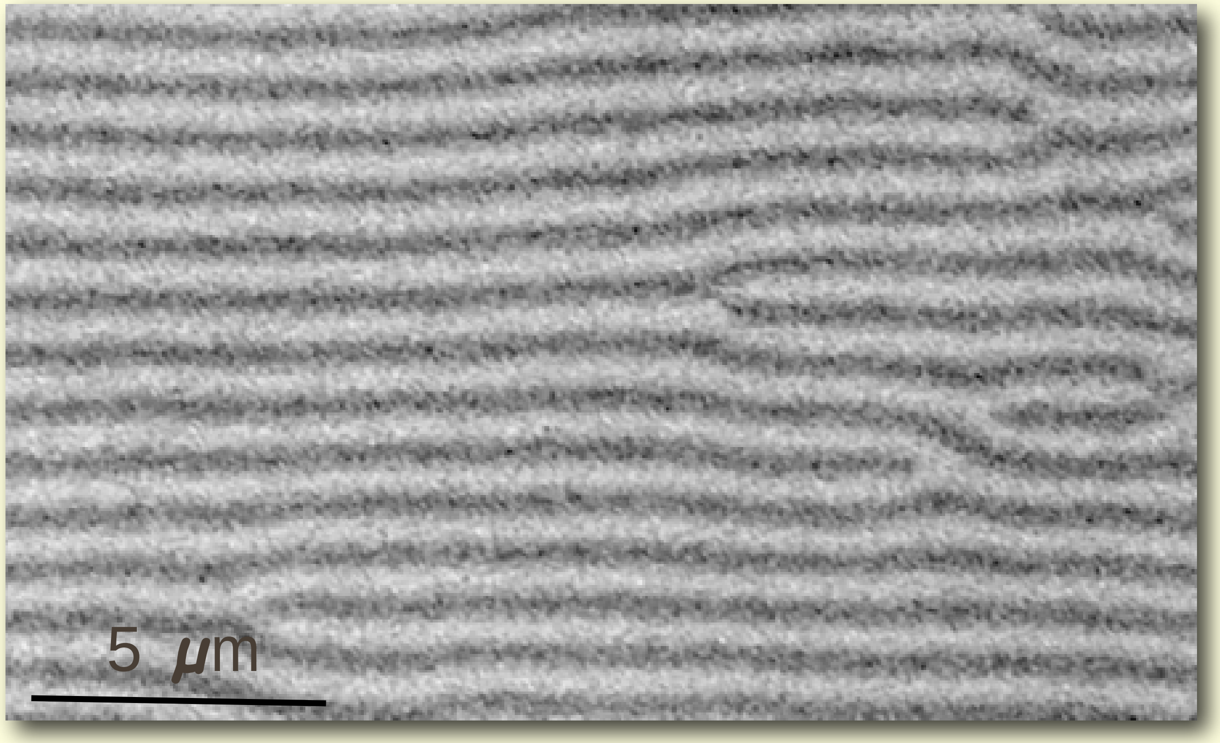

amorphous ribbon
(20 μm thick)

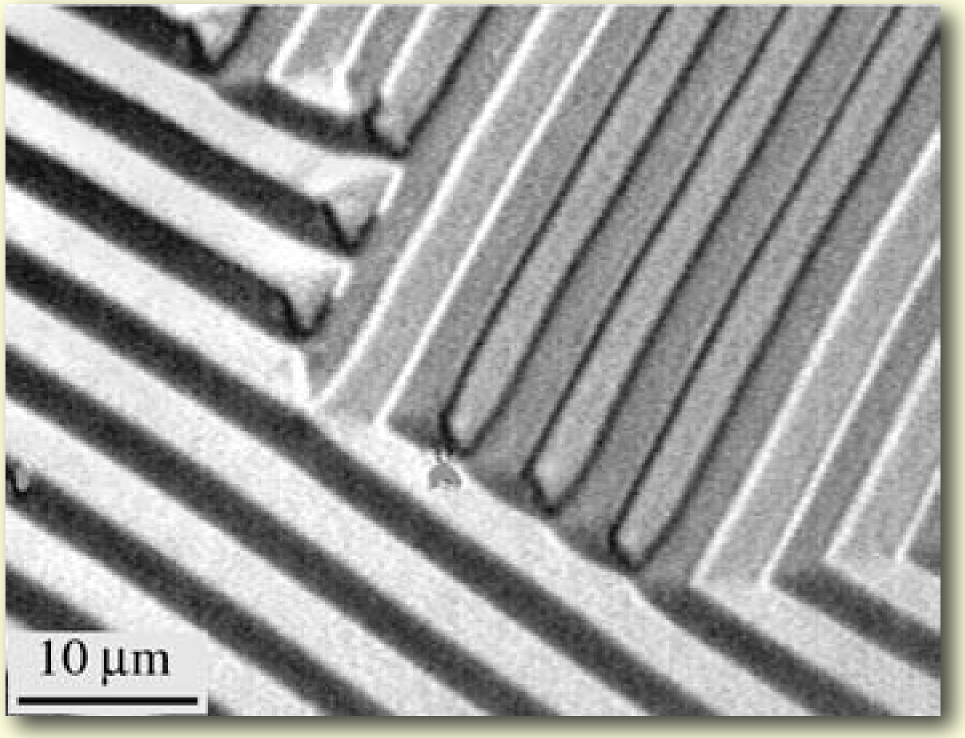

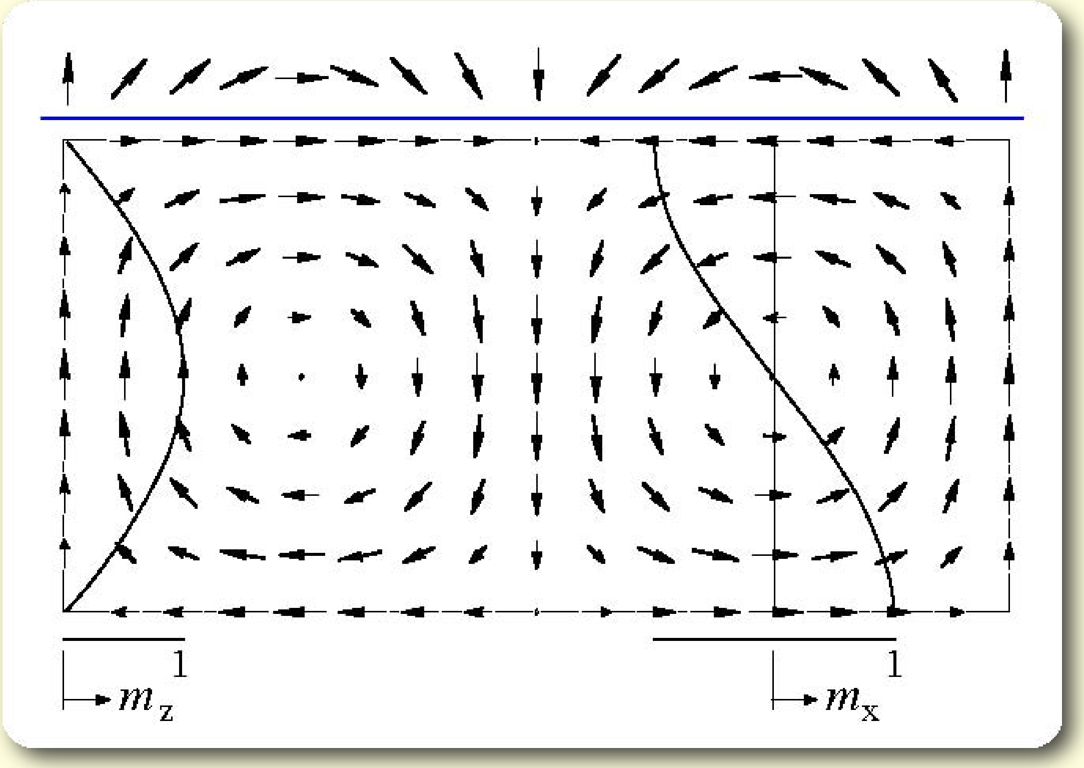

anisotropy

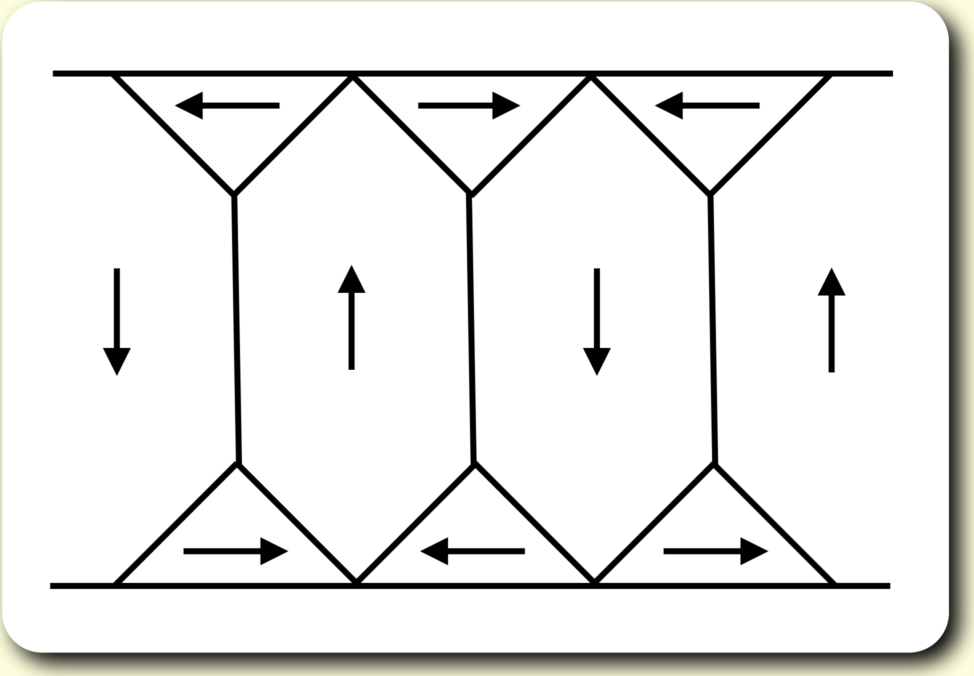

Branched domains in amorphous ribbons

amorphous ribbon (20 μm thick)
increasing perpendicular anisotropy (stress)

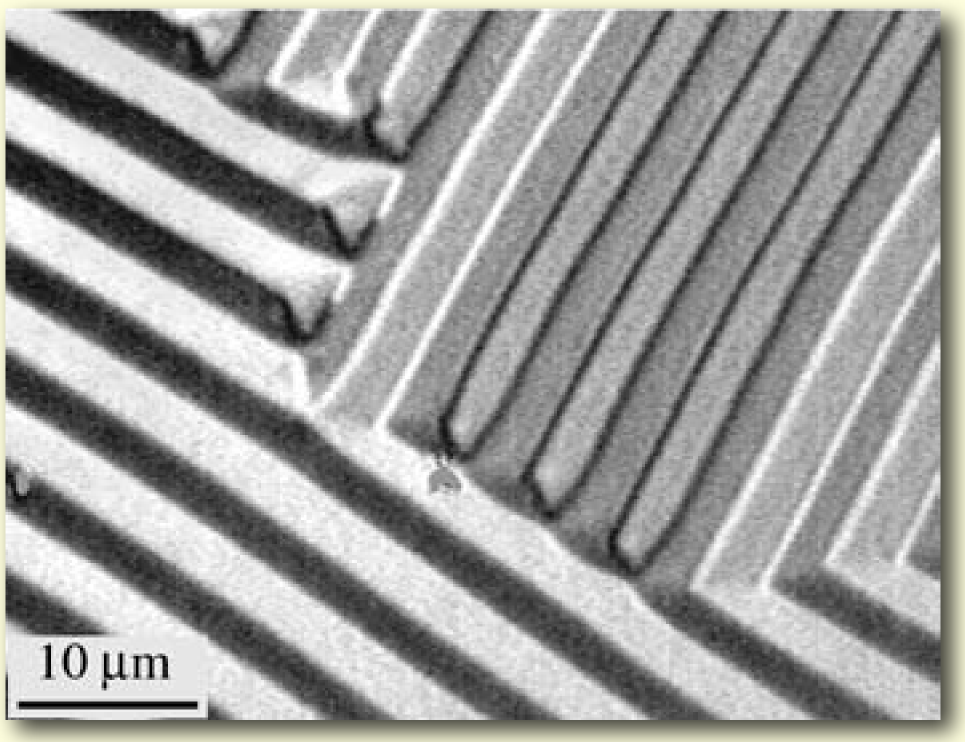

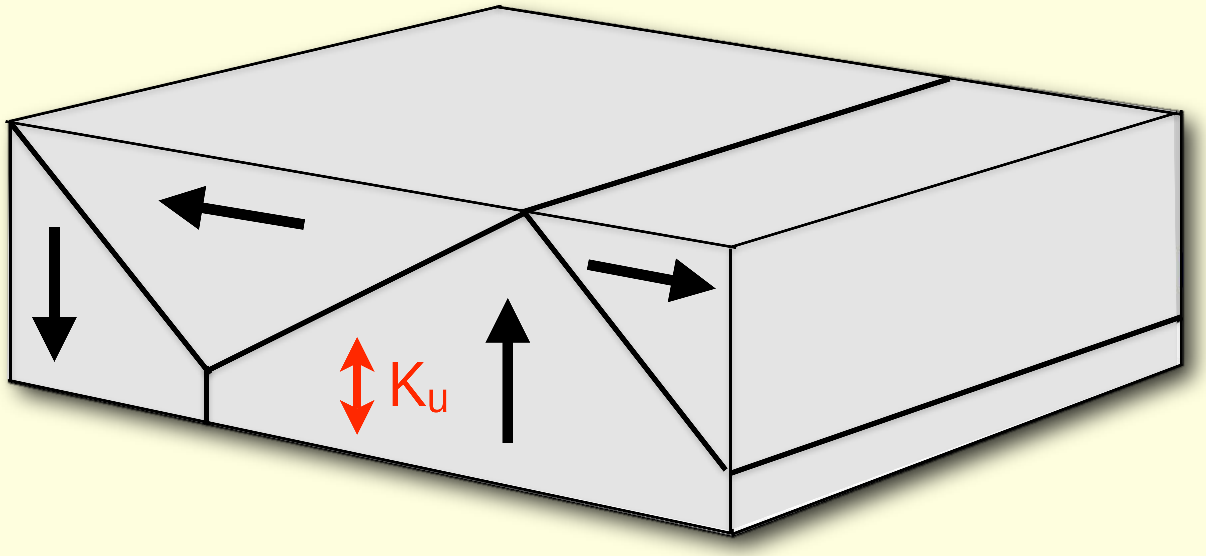

(FeSiB)

Branched domains in amorphous ribbons

amorphous ribbon (20 μm thick)

increasing perpendicular anisotropy (stress)

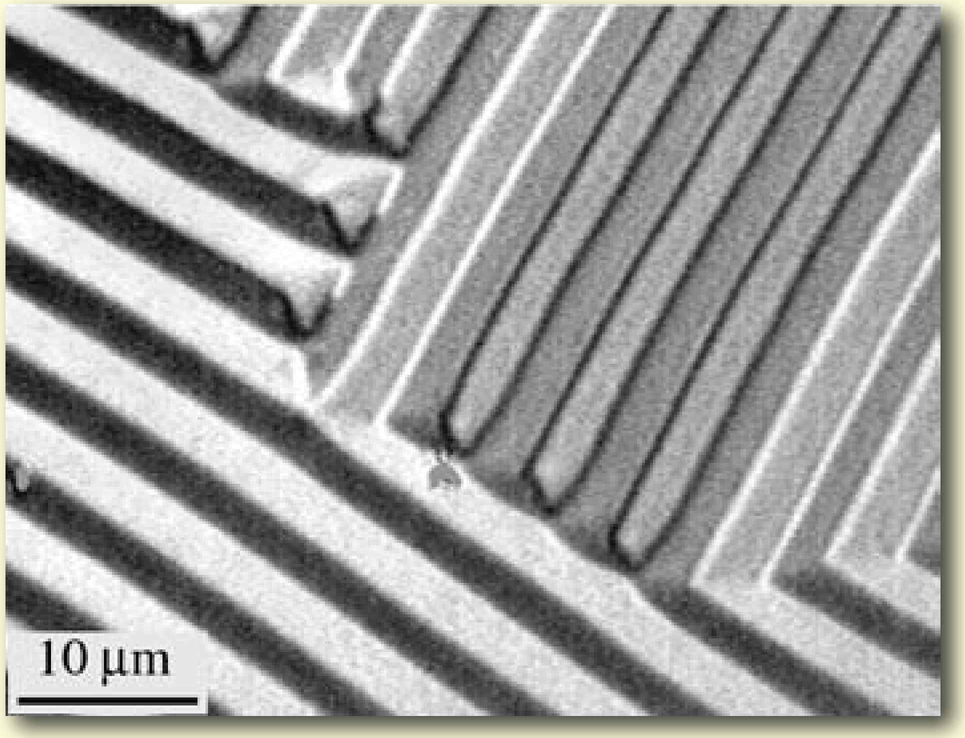

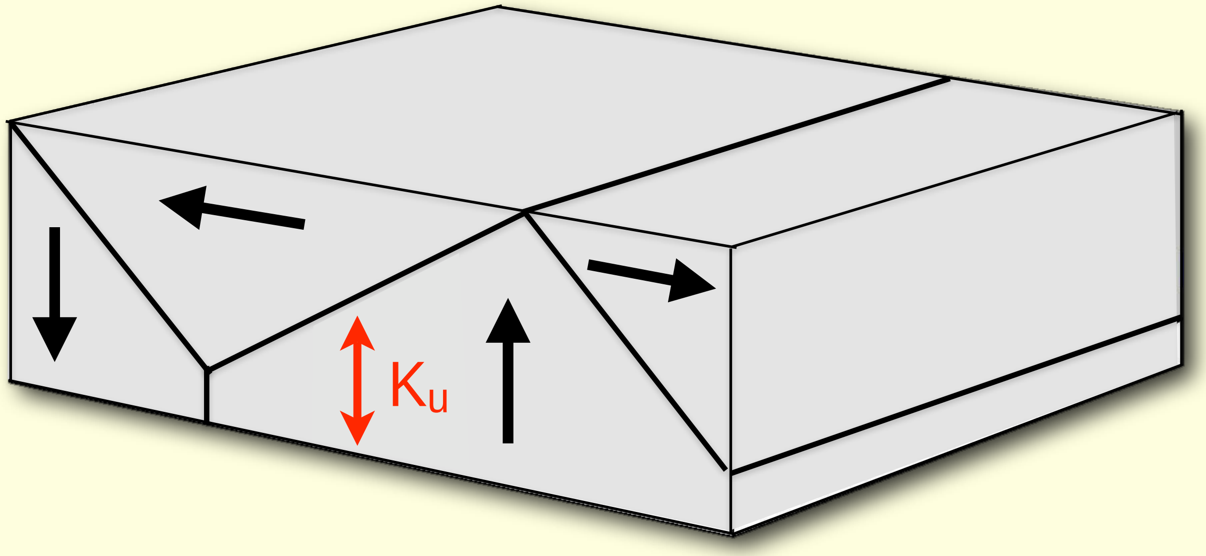

(FeSiB)

Branched domains in amorphous ribbons

amorphous ribbon (20 μm thick)
increasing perpendicular anisotropy (stress)

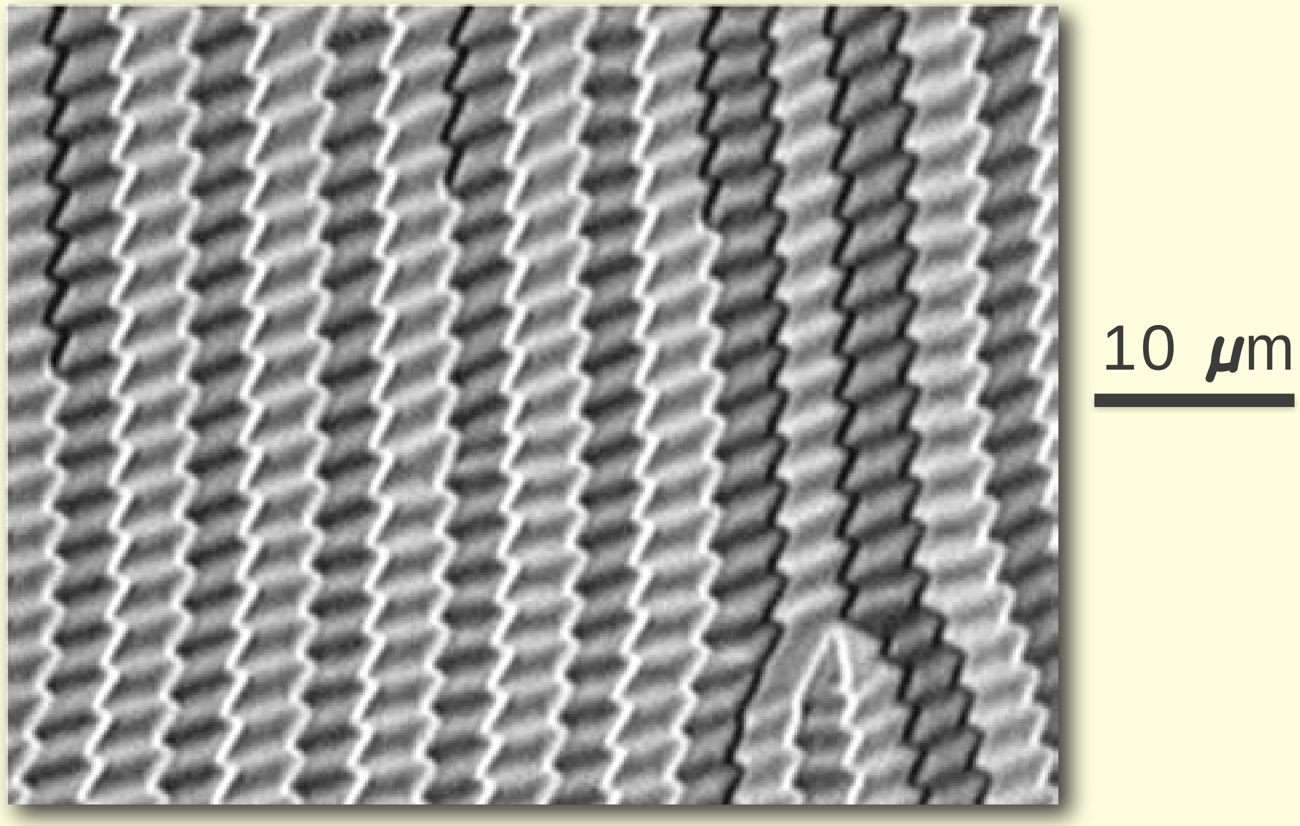

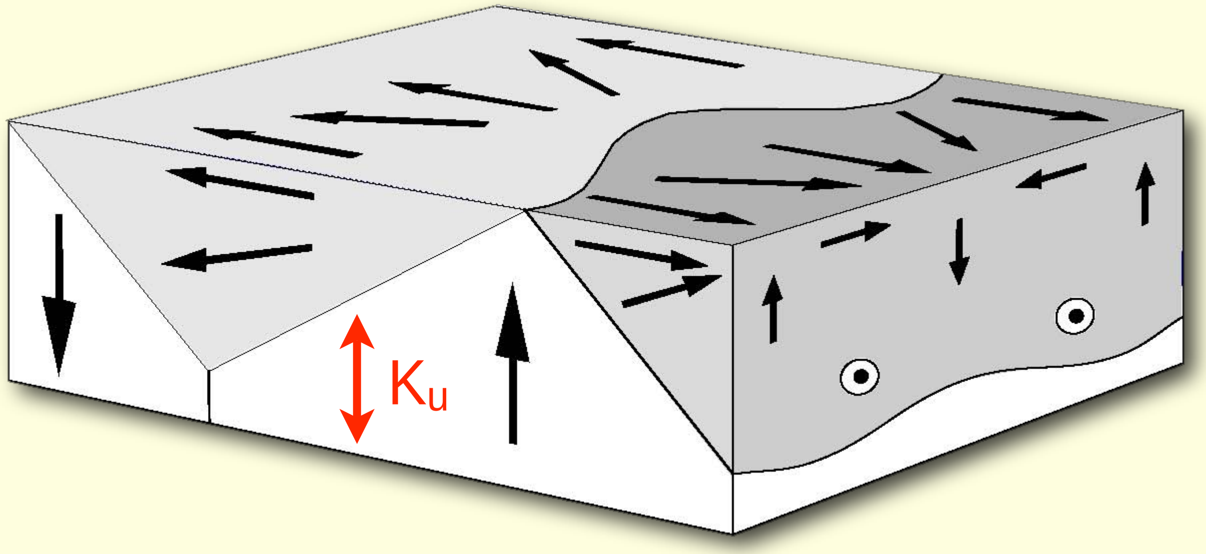

(FeSiB)

Branched domains in amorphous ribbons

amorphous ribbon (20 μm thick)
increasing perpendicular anisotropy (stress)

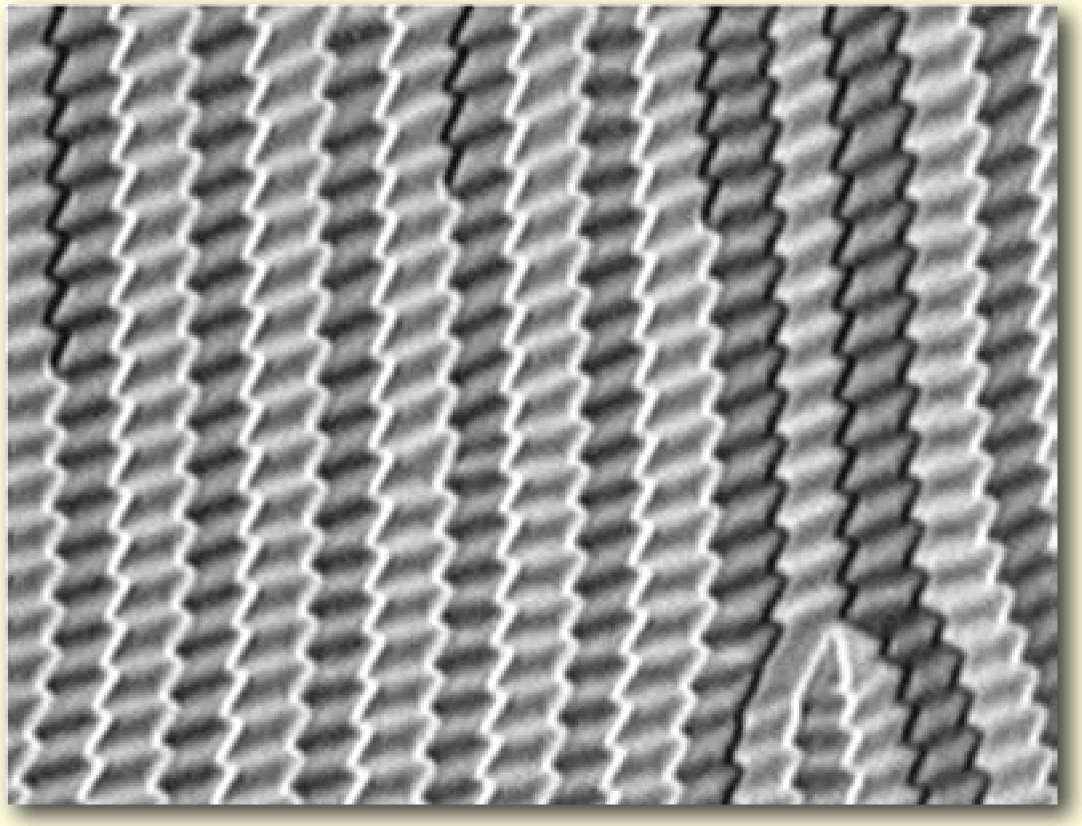

10 μm

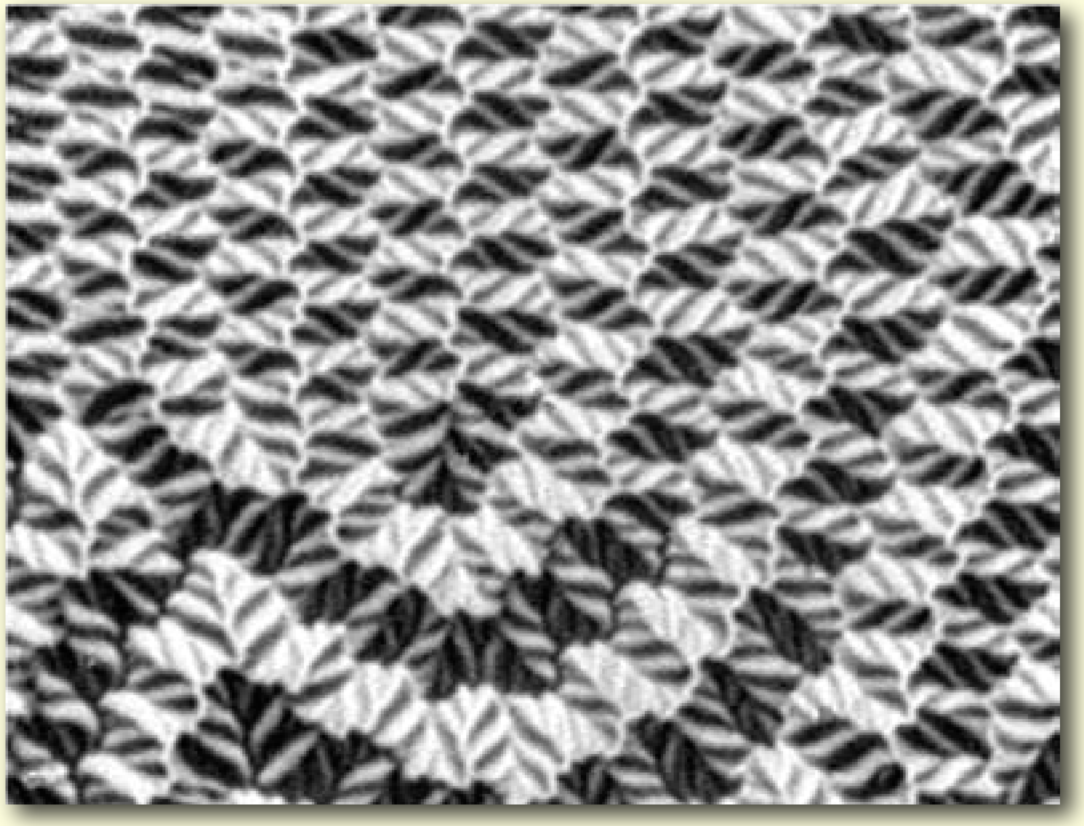

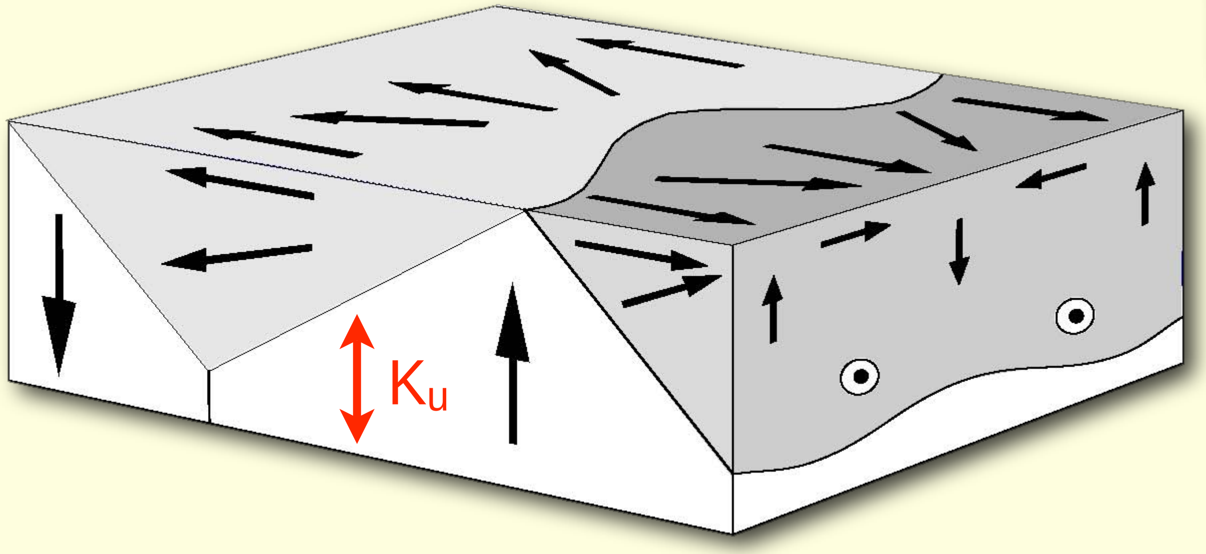

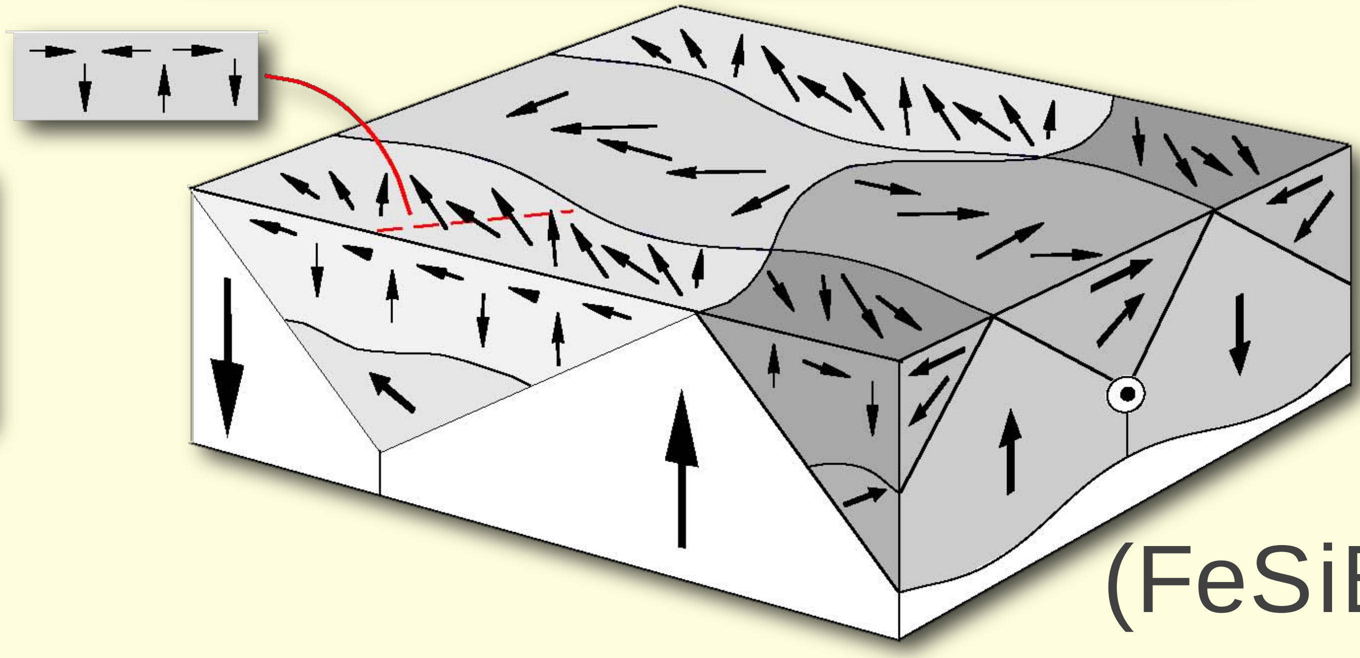

(FeSiB)

Domain control by field annealing

CoFeSiB-alloy with $\lambda_s \sim 0$
→ no stress effects
→ controlled anisotropy by field-annealing

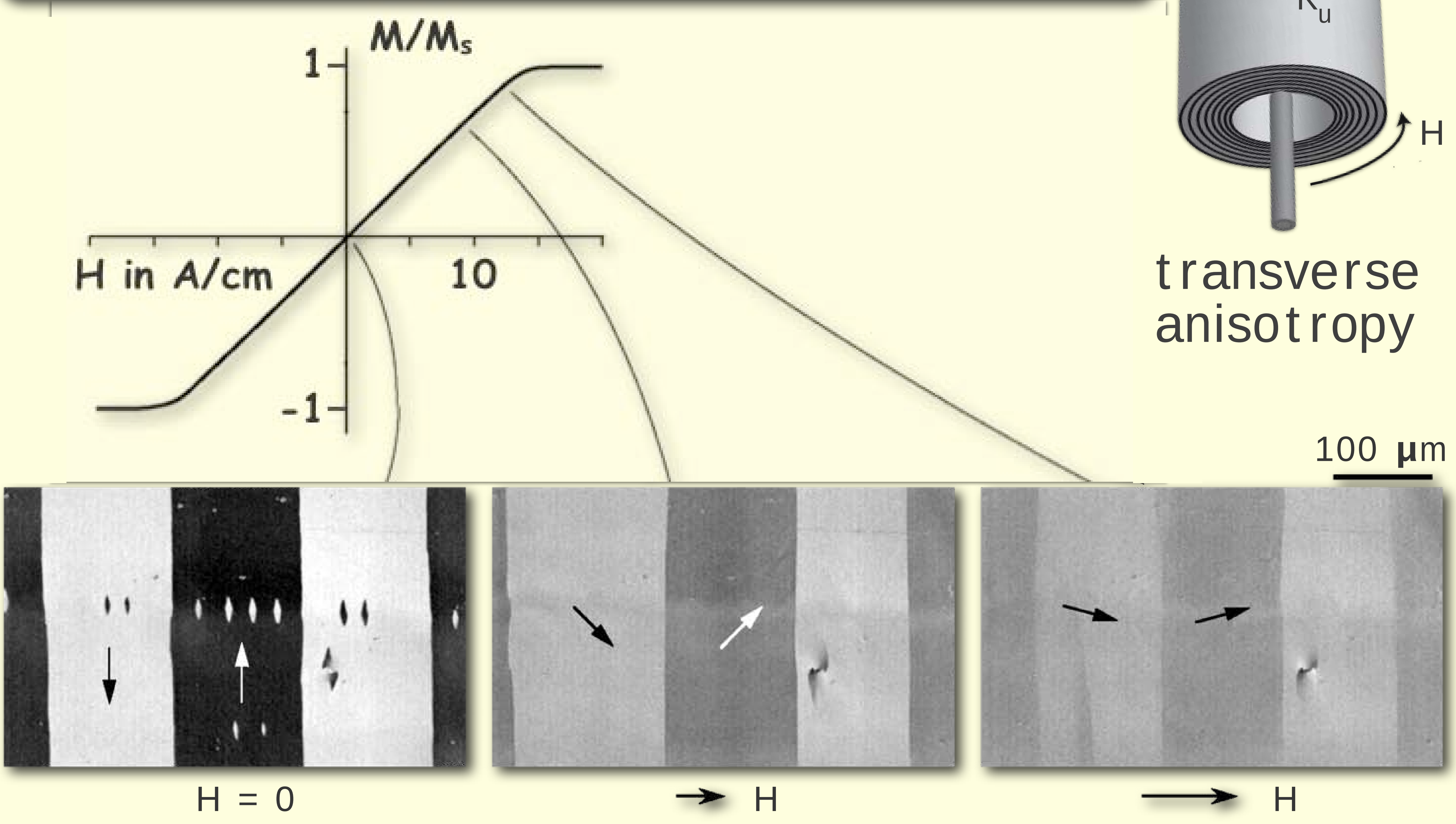

Generation of anisotropy-free amorphous ribbons:

- magnetostriction-free ribbon (Co-based alloy) (T_{Curie} = 220°C, T_{cryst} = 540°C)
- polished on both sides
- stress relieve annealed just below T_{cryst} (at 430°C)
- cooled in rotating field

Continuous magnetization-patterns

in magnetostriction-free metallic glass
after annealing in rotating field

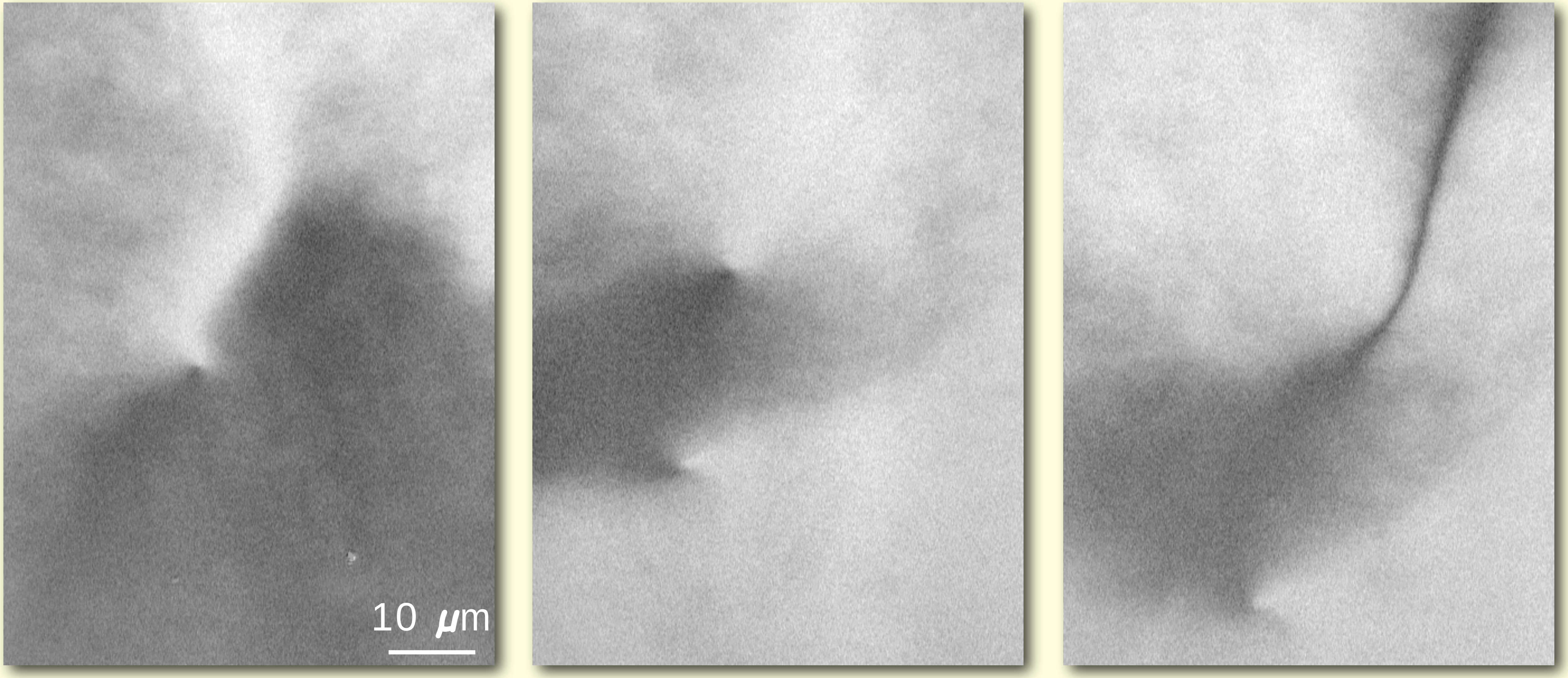

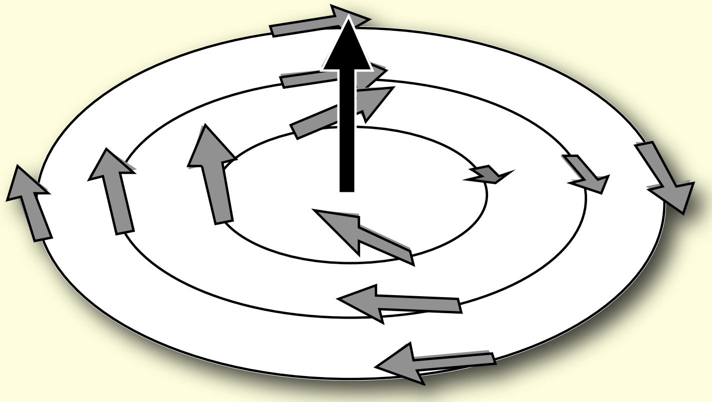

Continuous magnetization-patterns

in magnetostriction-free metallic glass
after annealing in rotating field

Continuously „flowing“ patterns are
possible in specially treated
amorphous ribbons
(suppression of residual anisotropies)

Branched domains in amorphous ribbons

amorphous ribbon (20 μm thick)
increasing perpendicular anisotropy (stress)

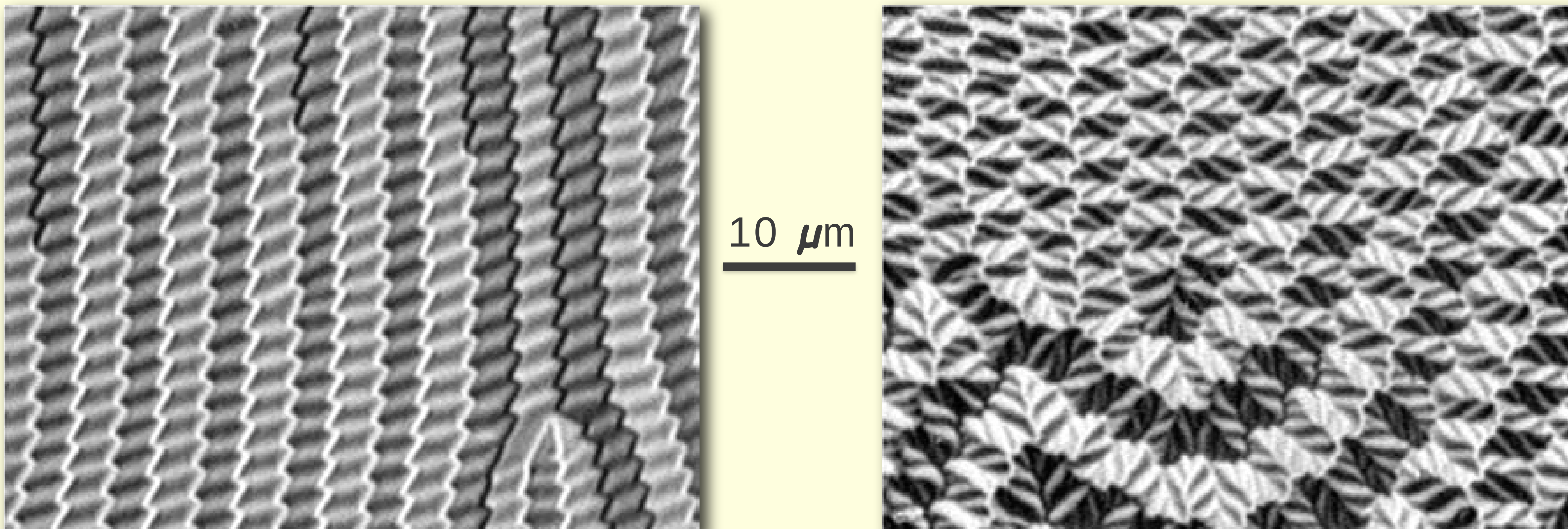

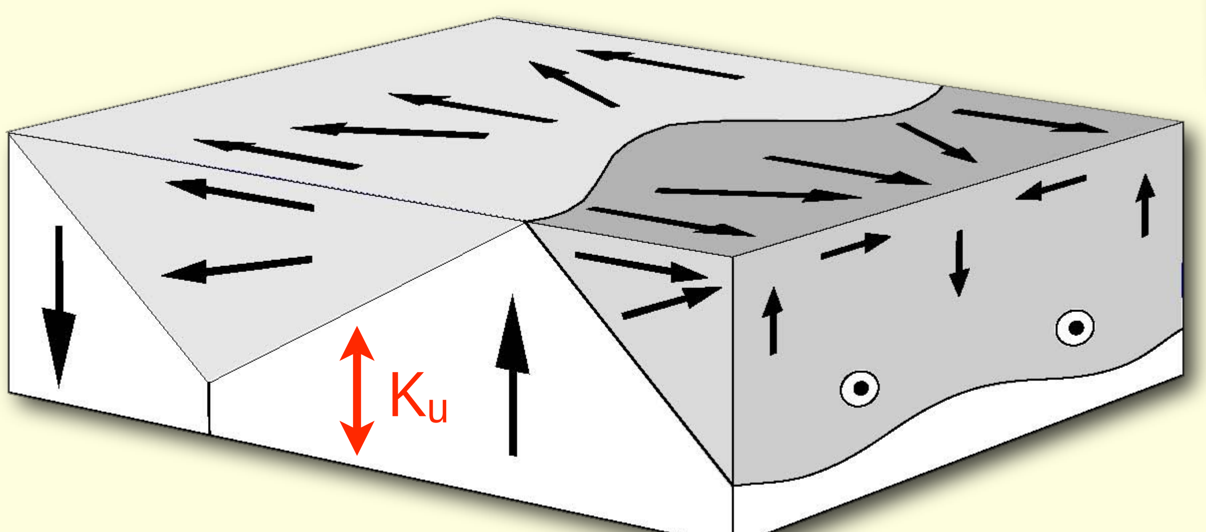

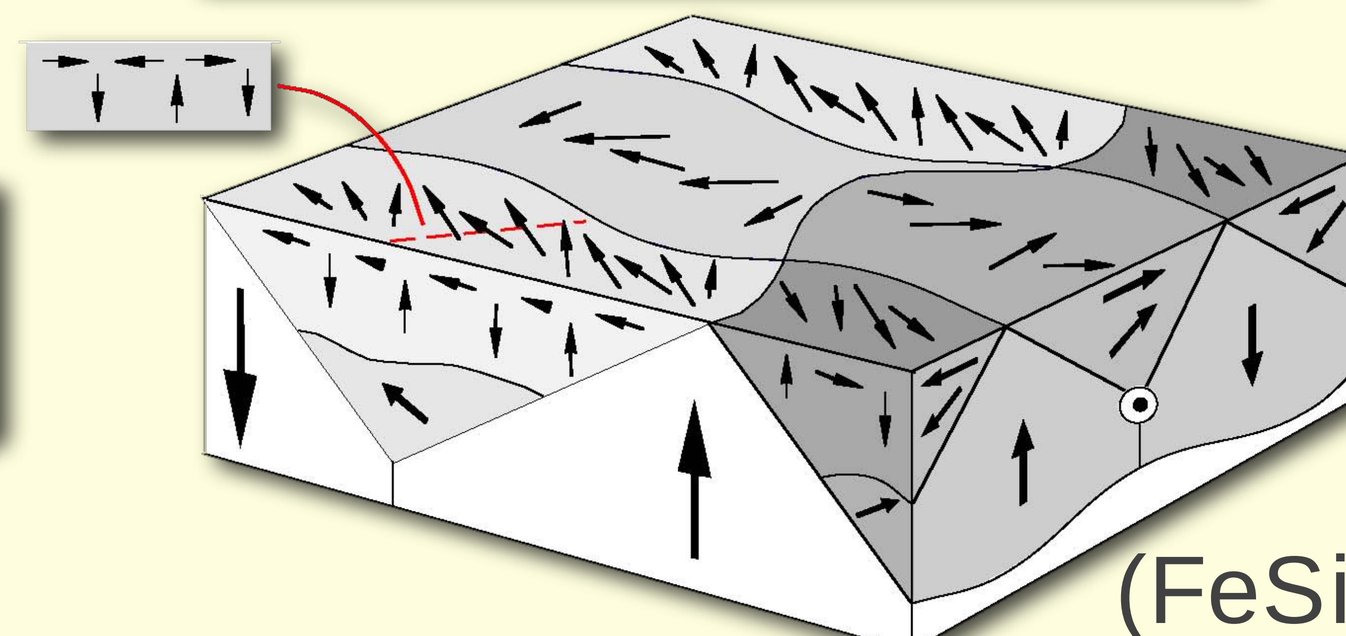

(FeSiB)

Branched domains in amorphous ribbons

amorphous ribbon (20 μm thick)
increasing perpendicular anisotropy (stress)

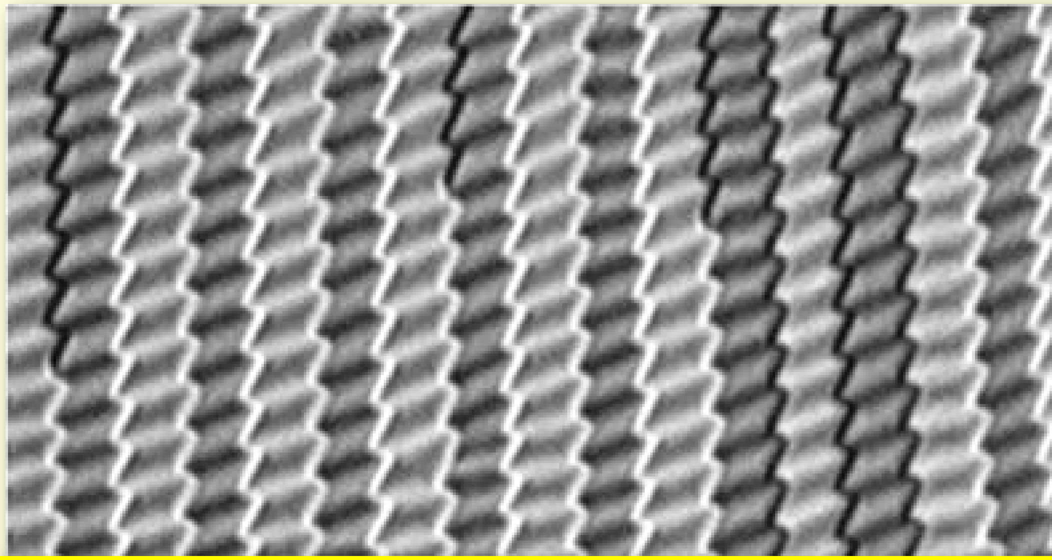

10 μm

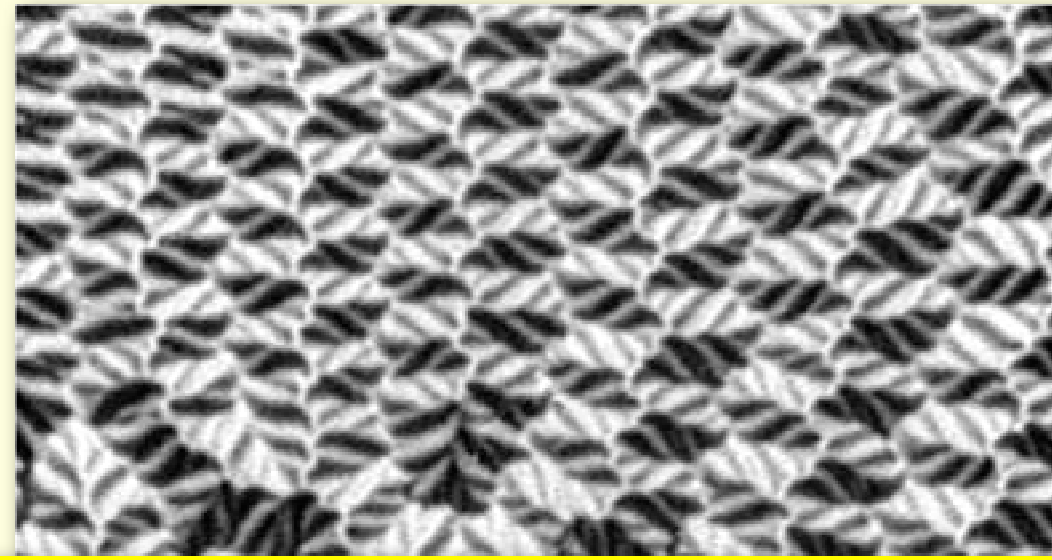

Continuously „flowing“ patterns also occur in case of conflicting influences (anisotropy plays role)

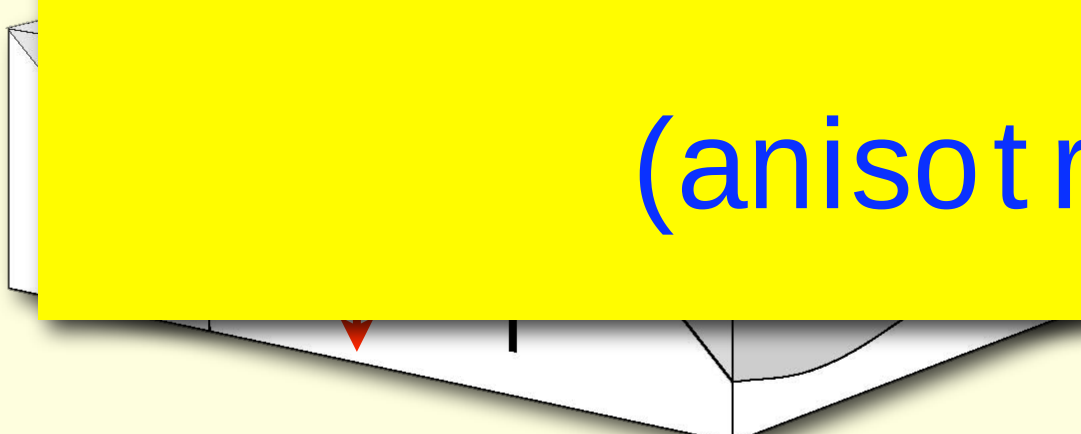

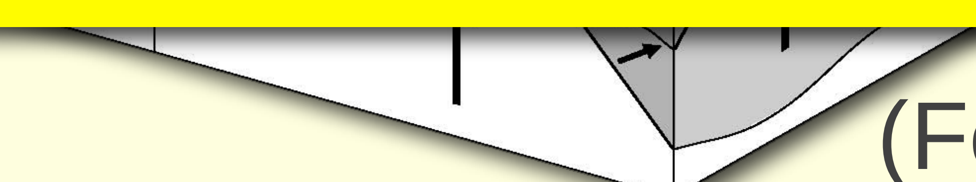

(FeSiB)

Summary: Coercivity and domains

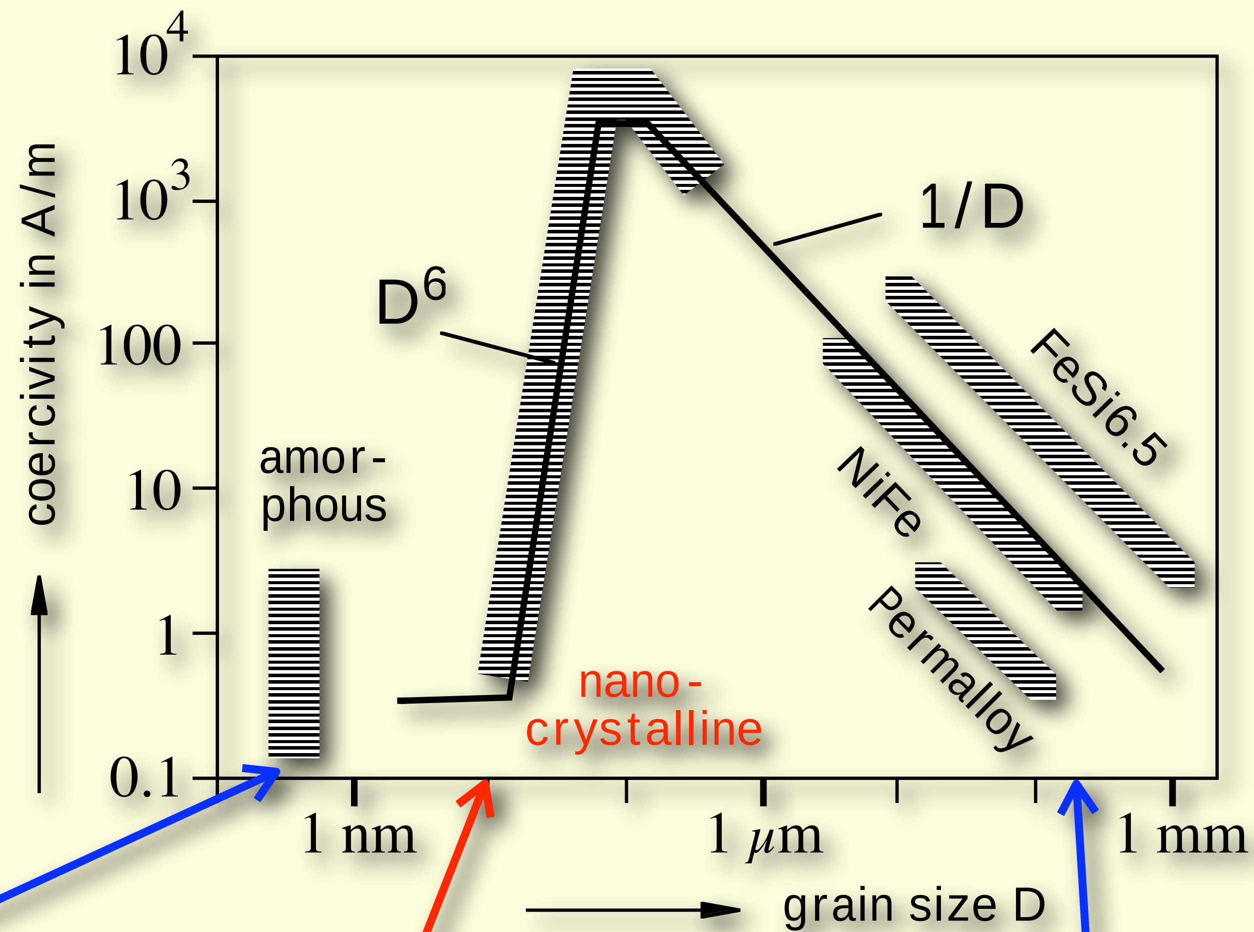

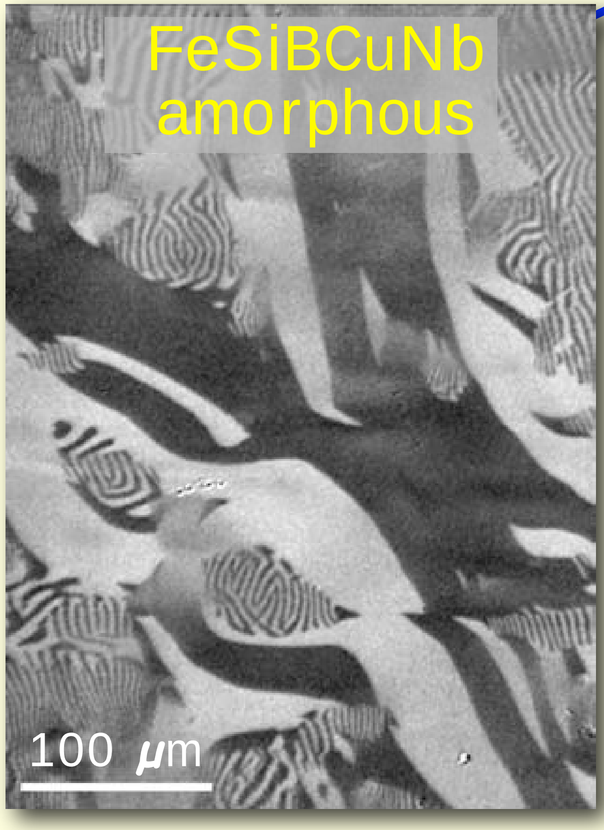

?

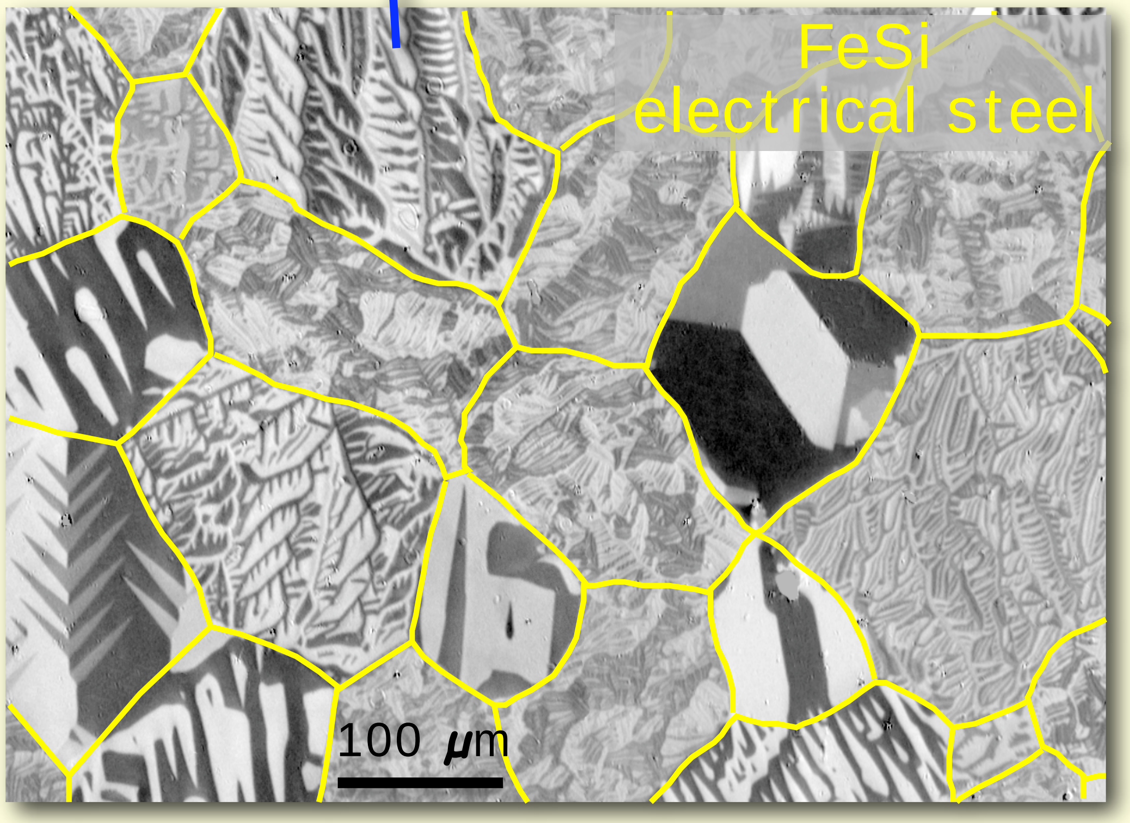

Overview

1. Domains in coarse-grained material

2. Domains in amorphous material

3. Domains in nanocrystalline, soft magnetic ($Q \ll 1$) materials

4. Domains in fine- and nanostructured, permanent magnetic ($Q > 1$) materials

Nanocrystalline soft magnets

Nanocrystalline ribbon $Fe_{73}Si_{16}B_7Cu_1Nb_3$
(Finemet, Vitroperm)

rapid quenching

↓

amorphous ribbon

↓ 550°C

nanocrystalline ribbon

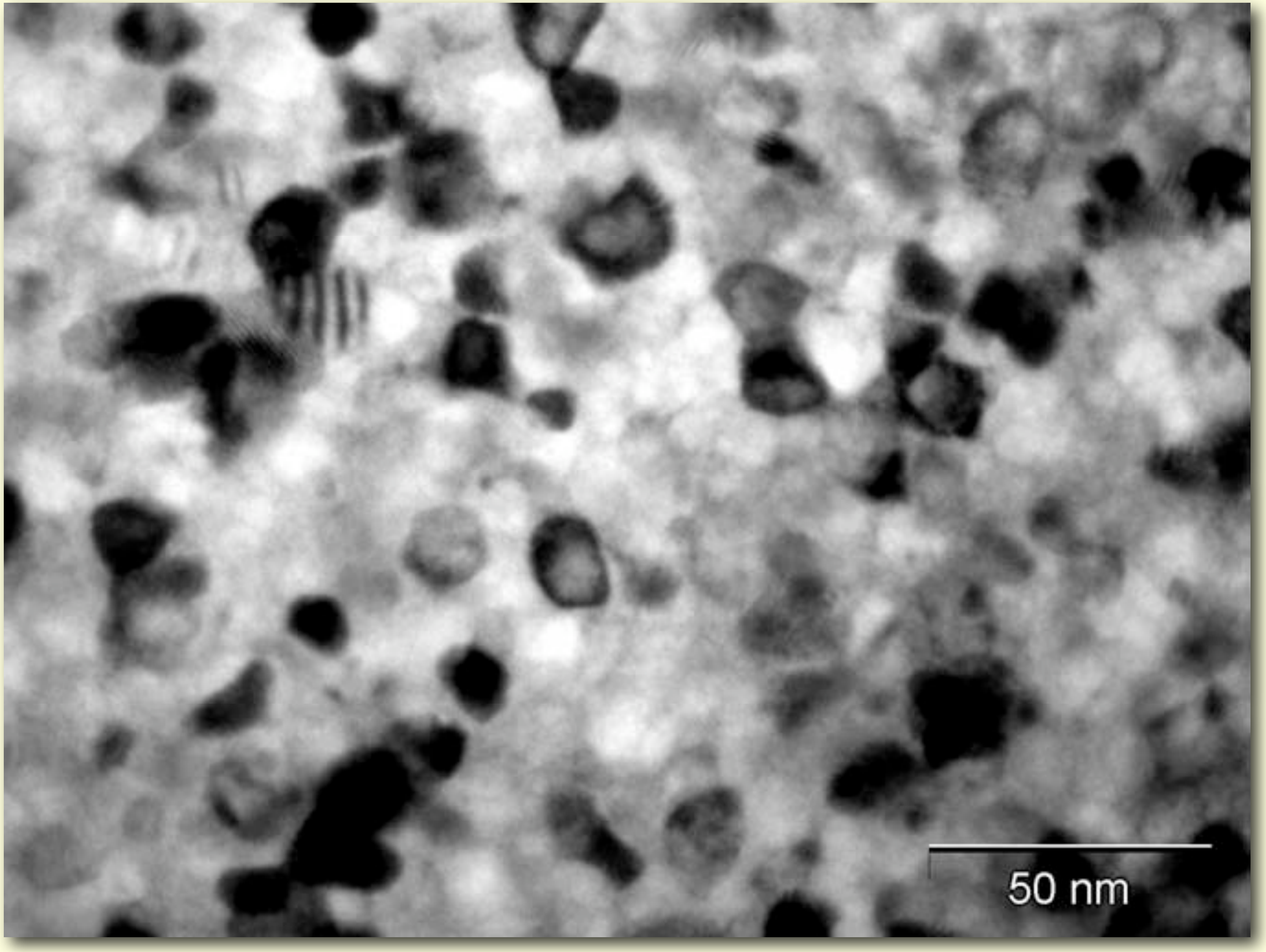

Nanocrystalline soft magnets

Nanocrystalline ribbon $Fe_{73}Si_{16}B_7Cu_1Nb_3$
(Finemet, Vitroperm)

rapid quenching

↓

amorphous ribbon

↓ 550°C

nanocrystalline ribbon

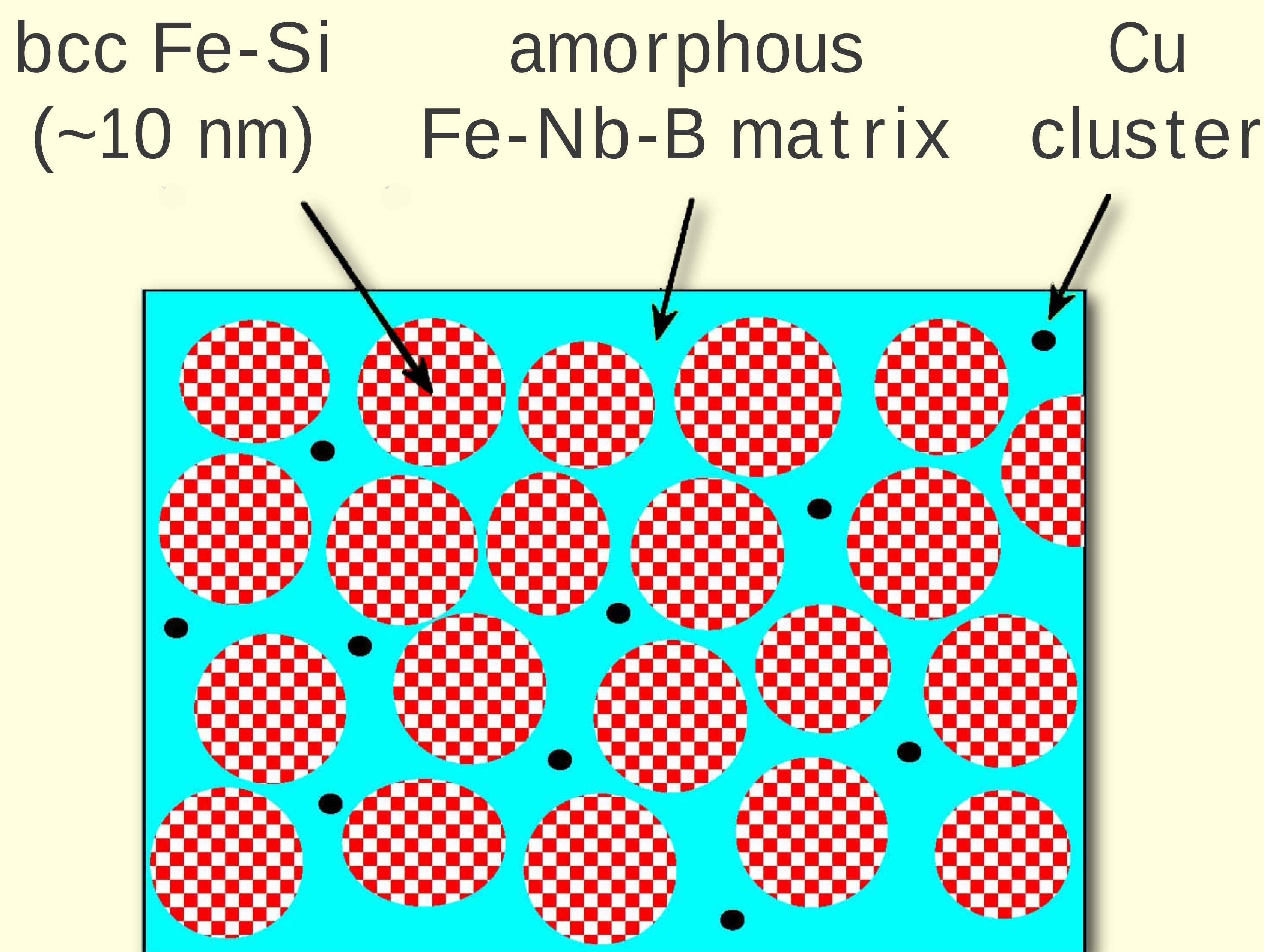

Coercivity and grain size

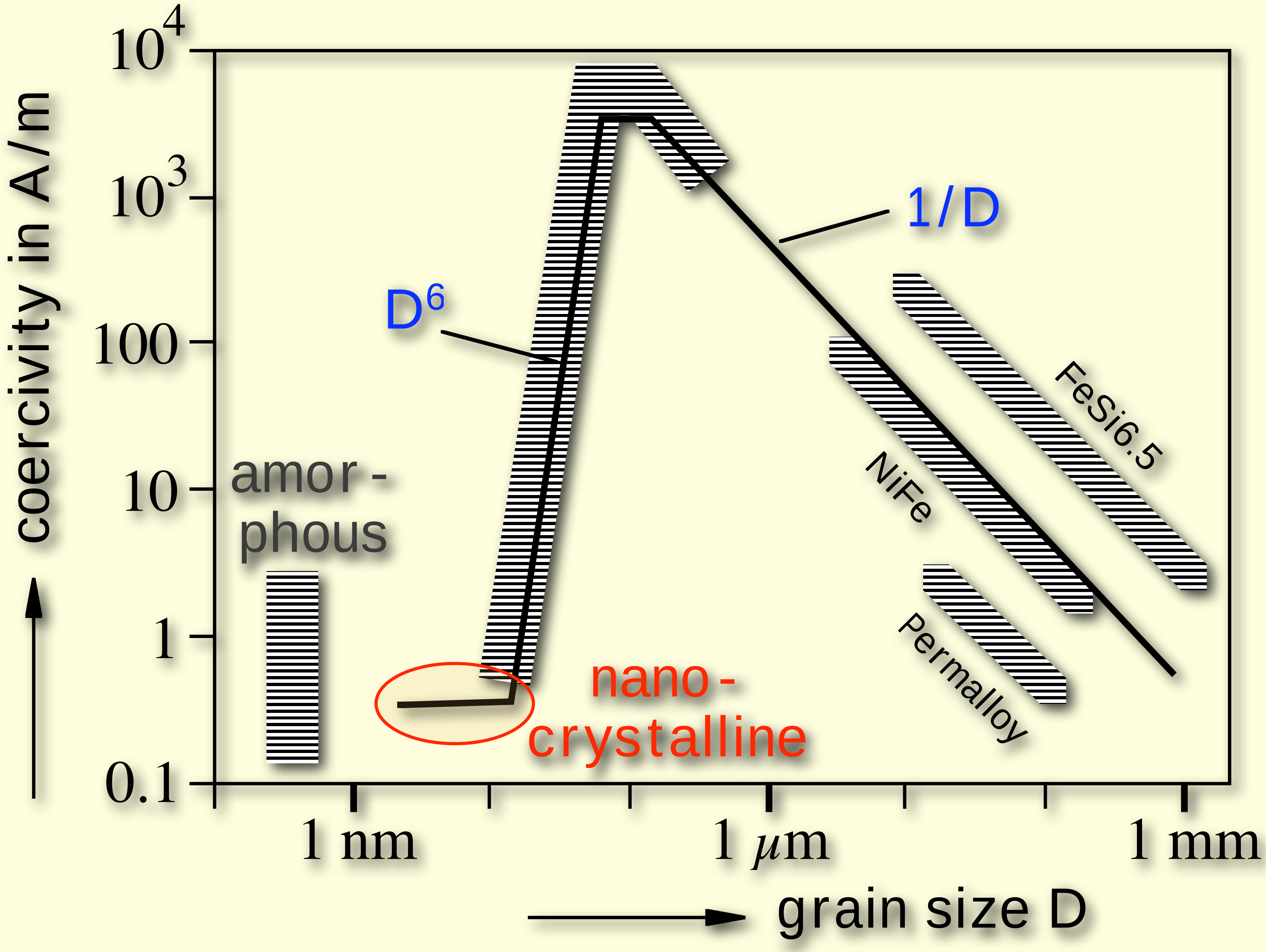

Nanocrystalline soft magnets: Principle

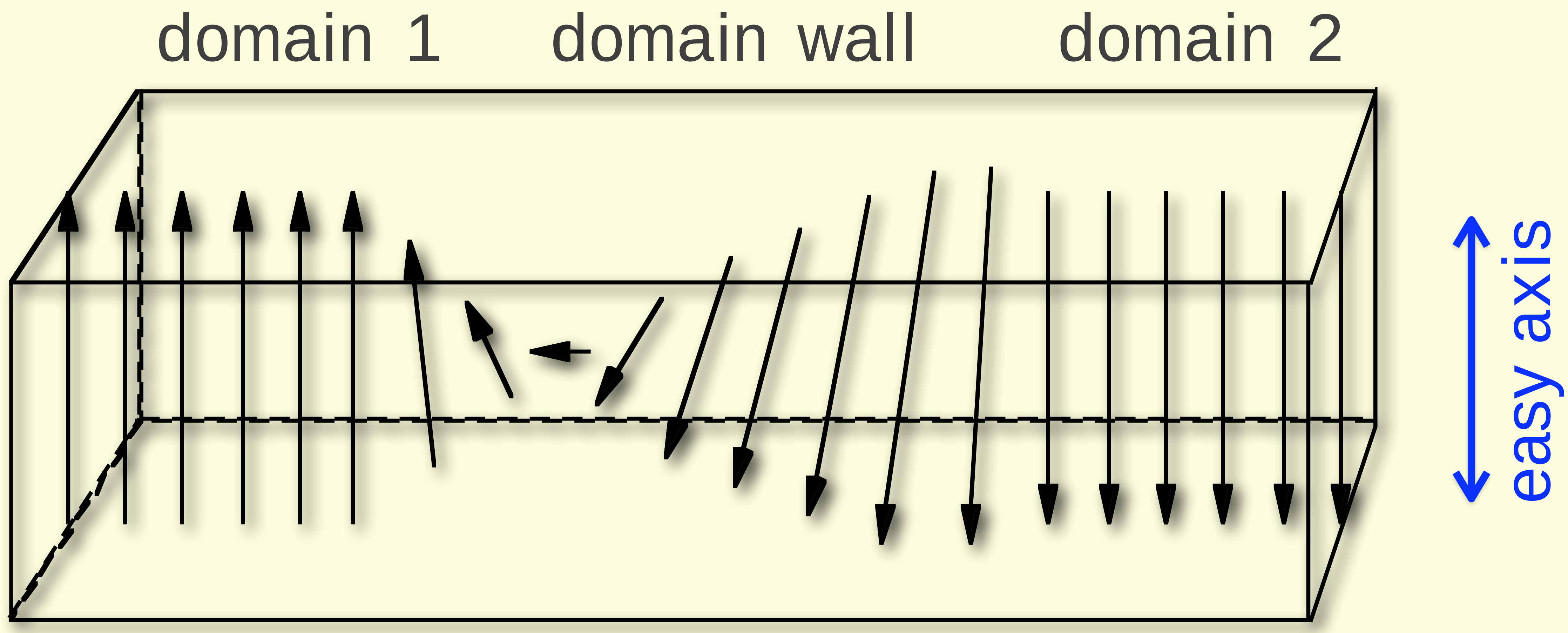

Nanocrystalline soft magnets: Principle

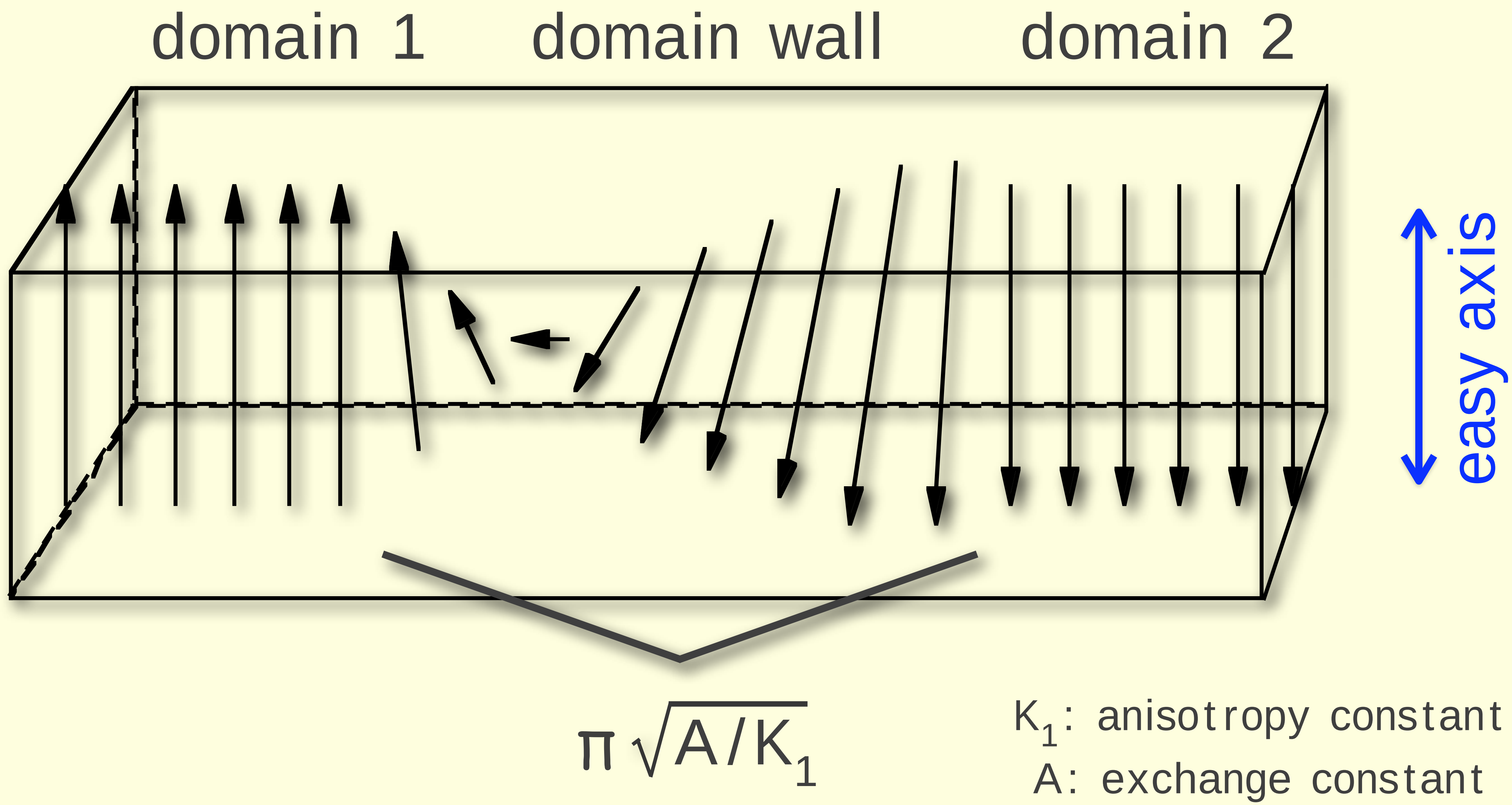

K_1: anisotropy constant

A: exchange constant

Nanocrystalline soft magnets: Principle

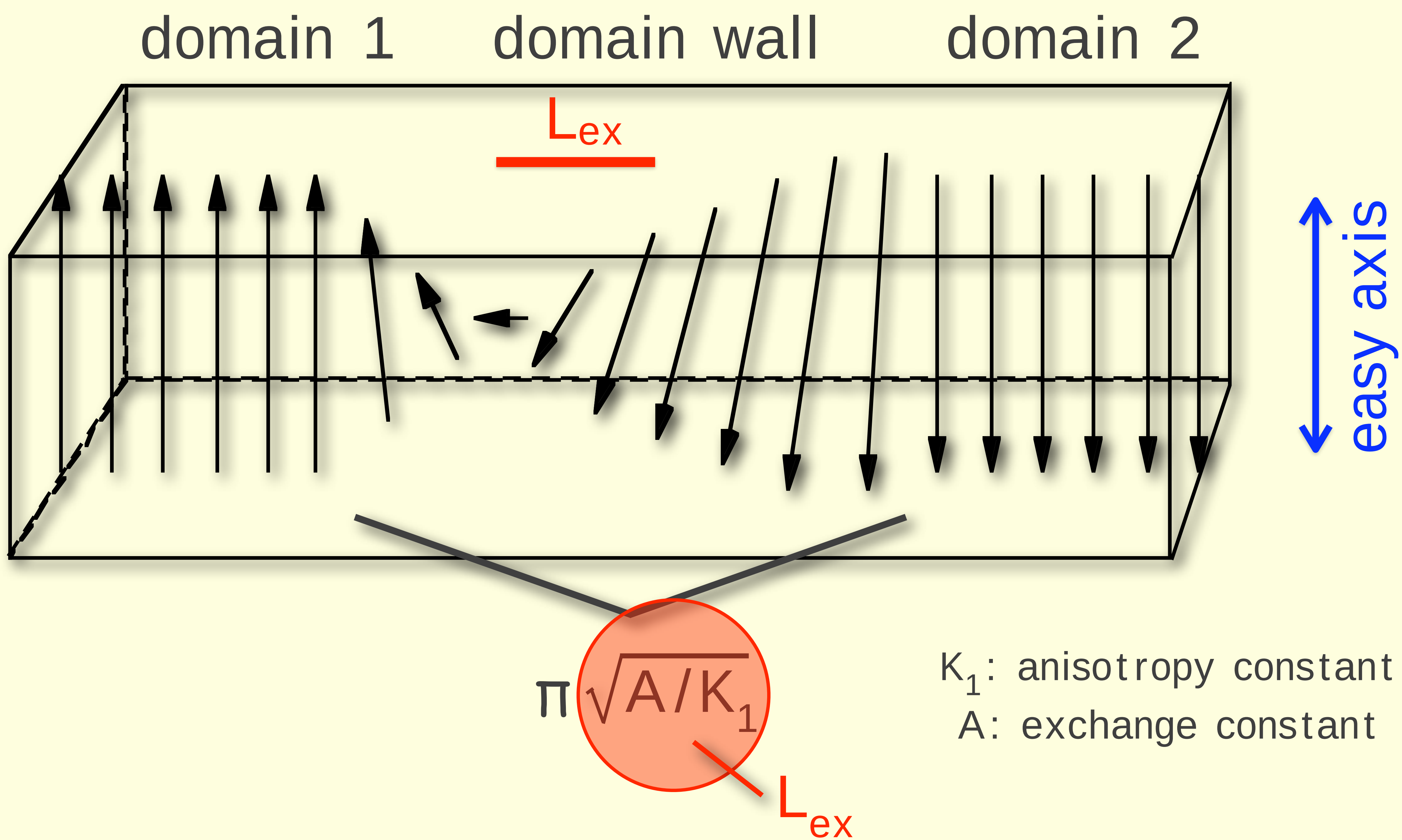

K_1: anisotropy constant
A: exchange constant

ferromagnetic correlation length (exchange length):

minimum scale for appreciable variation of magnetization
(parallel moments for $L<L_{ex}$)

Nanocrystalline soft magnets: Principle

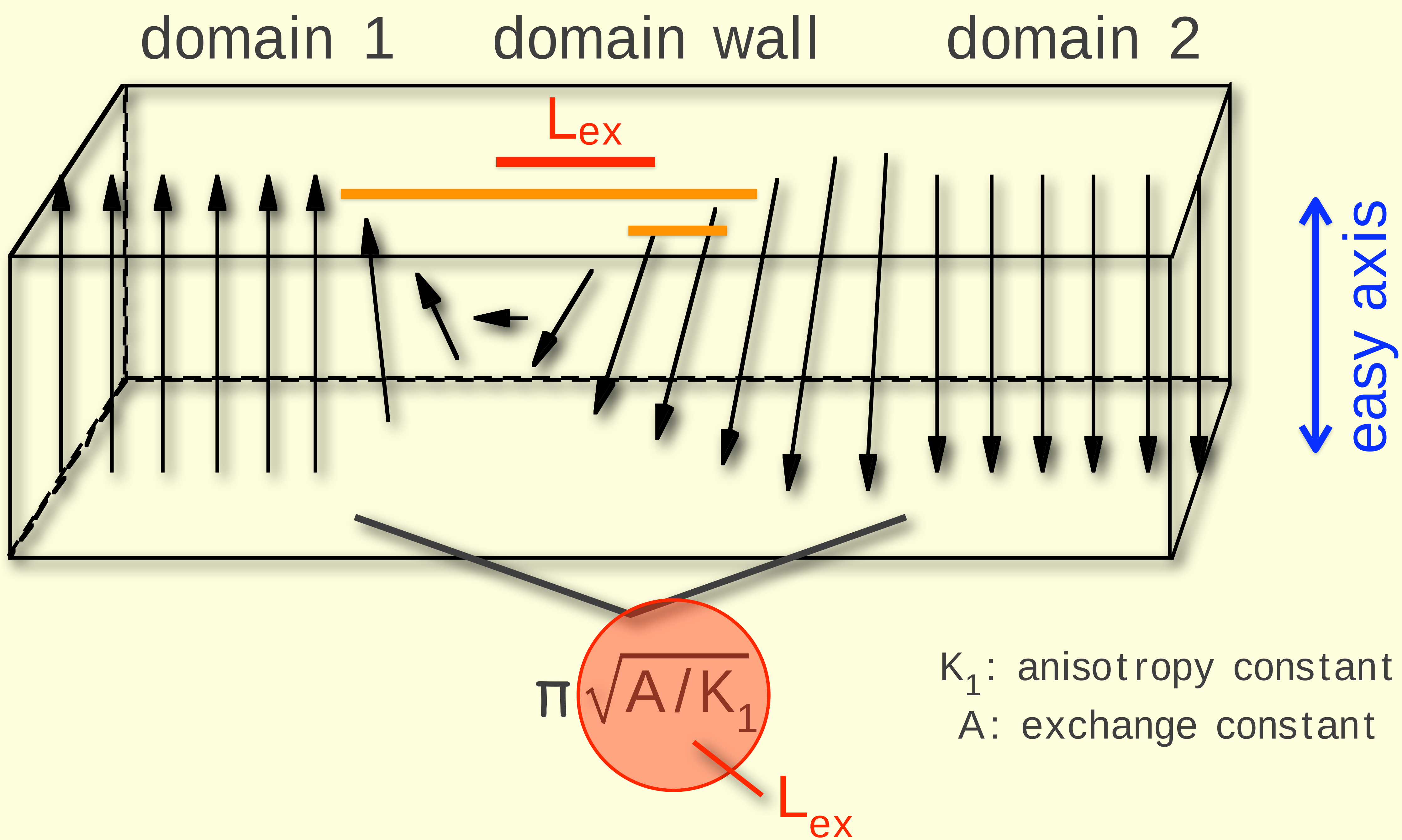

ferromagnetic correlation length (exchange length):

minimum scale for appreciable variation of magnetization (parallel moments for $L<L_{ex}$)

Nanocrystalline soft magnets: Principle

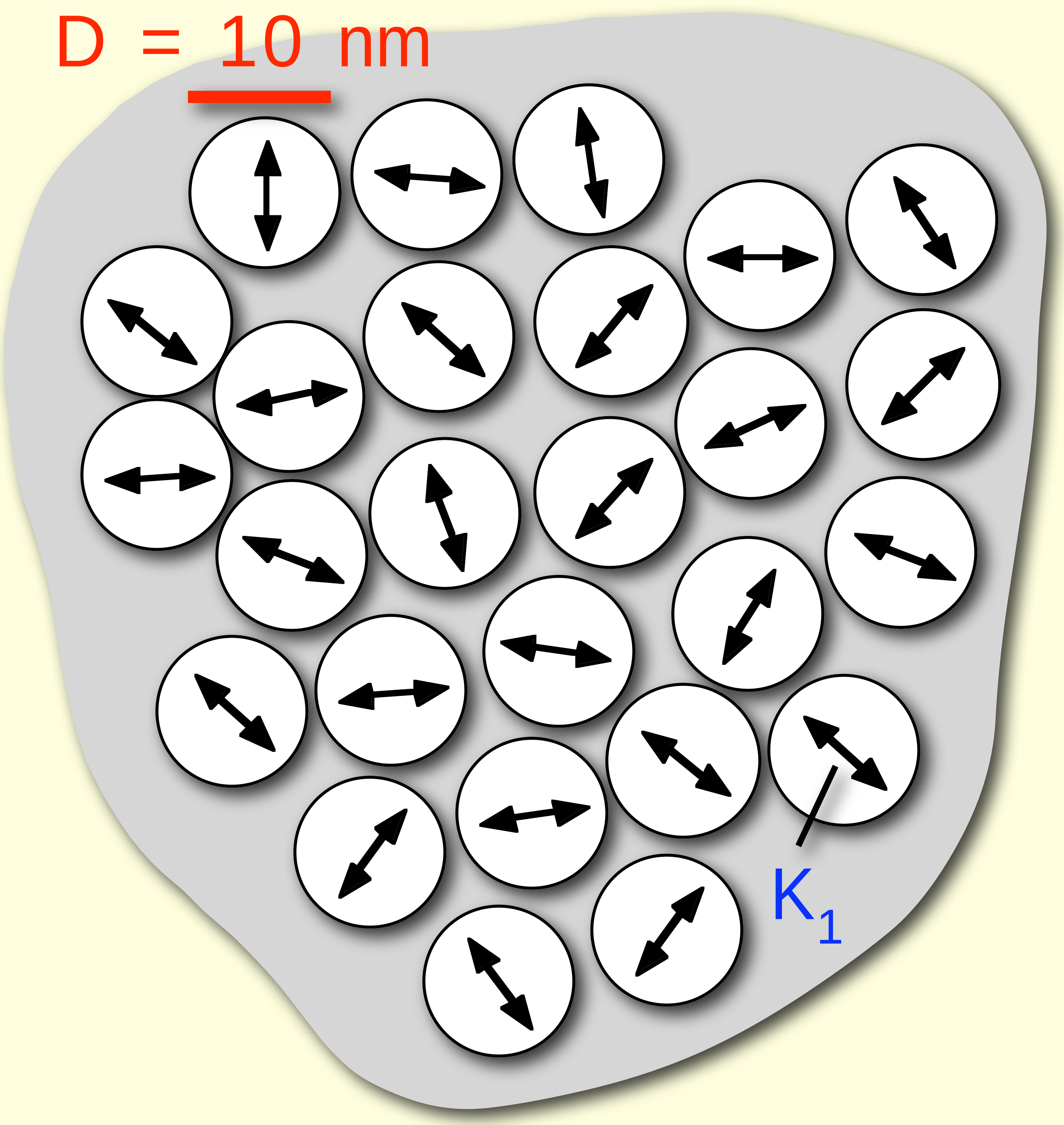

Nanocrystalline soft magnets: Principle

$Fe_{80}Si_{20}$:
$K_1 = 8\ kJ/m^3$
$A = 10^{-11}\ J/m$

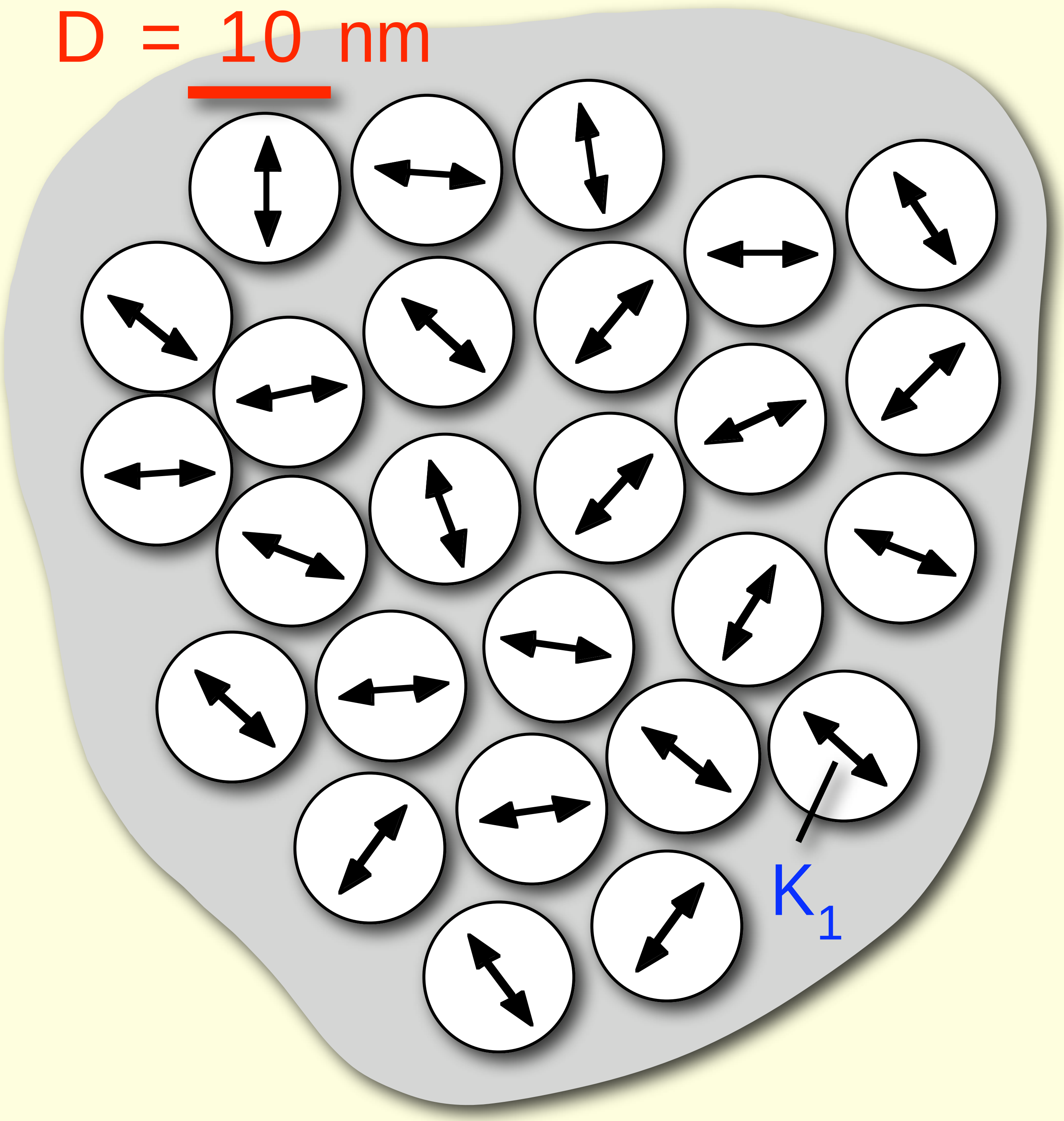

Nanocrystalline soft magnets: Principle

$Fe_{80}Si_{20}$:

$K_1 = 8\ kJ/m^3$

$A = 10^{-11}\ J/m$

➡ $L_{ex} = \sqrt{A/K_1} = 35\ nm$

➡ $D < L_{ex}$

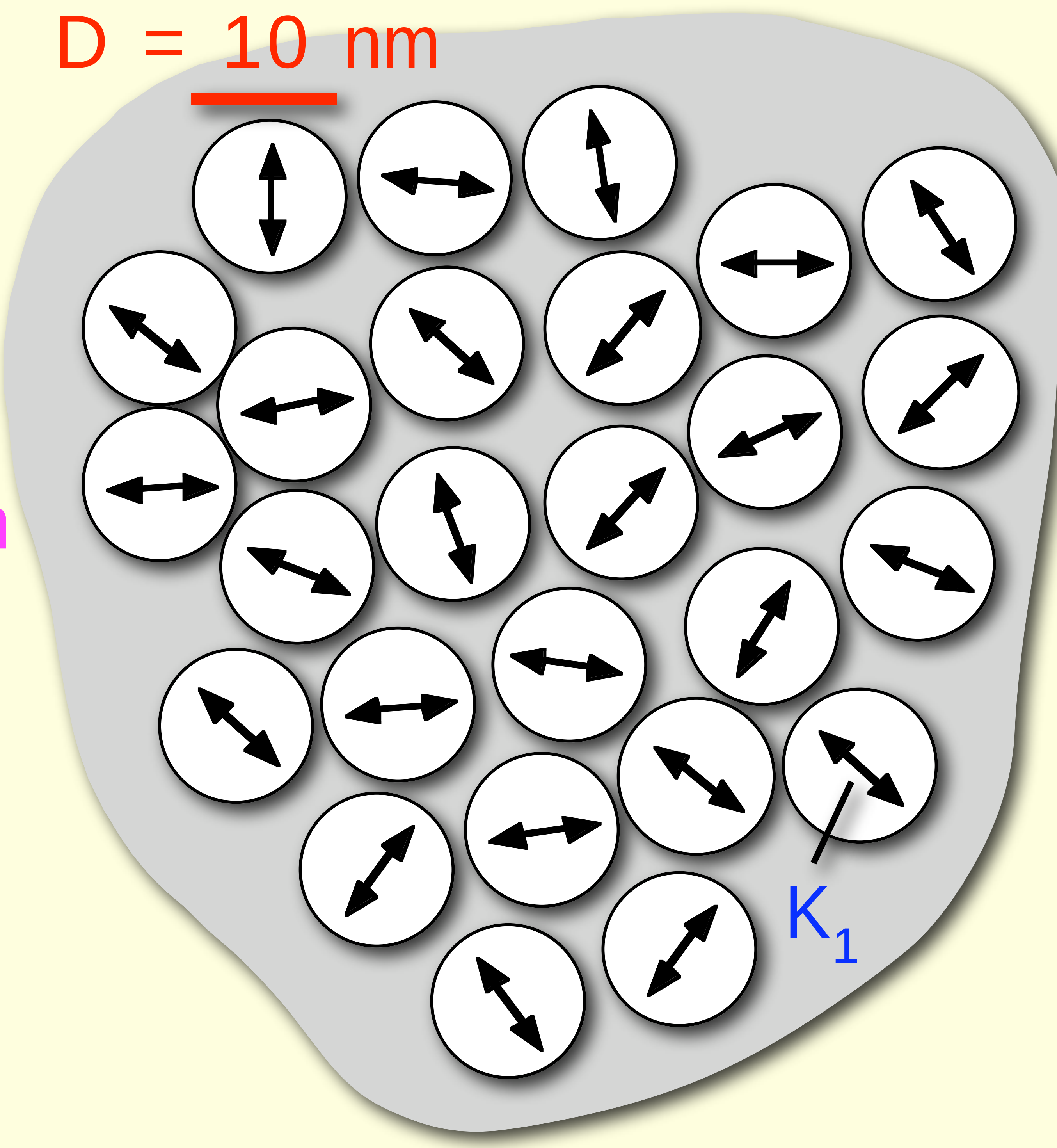

Nanocrystalline soft magnets: Principle

$Fe_{80}Si_{20}$:
$K_1 = 8\ kJ/m^3$
$A = 10^{-11}\ J/m$

➡ $L_{ex} = \sqrt{A/K_1} = 35\ nm$

➡ $D < L_{ex}$

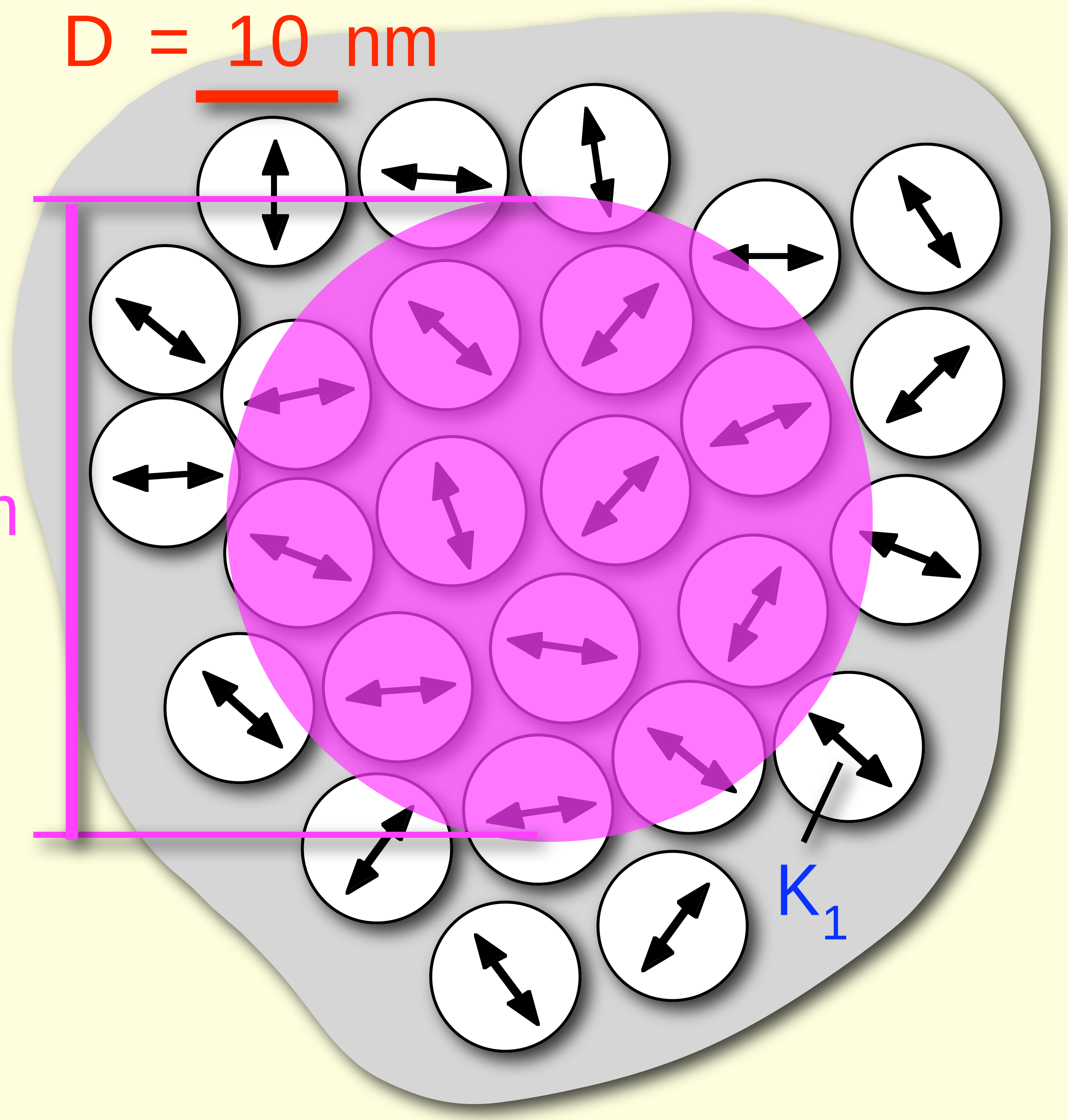

Nanocrystalline soft magnets: Principle

$Fe_{80}Si_{20}$:

$K_1 = 8\ kJ/m^3$

$A = 10^{-11}\ J/m$

➡ $L_{ex} = \sqrt{A/K_1} = 35\ nm$

➡ $D < L_{ex}$

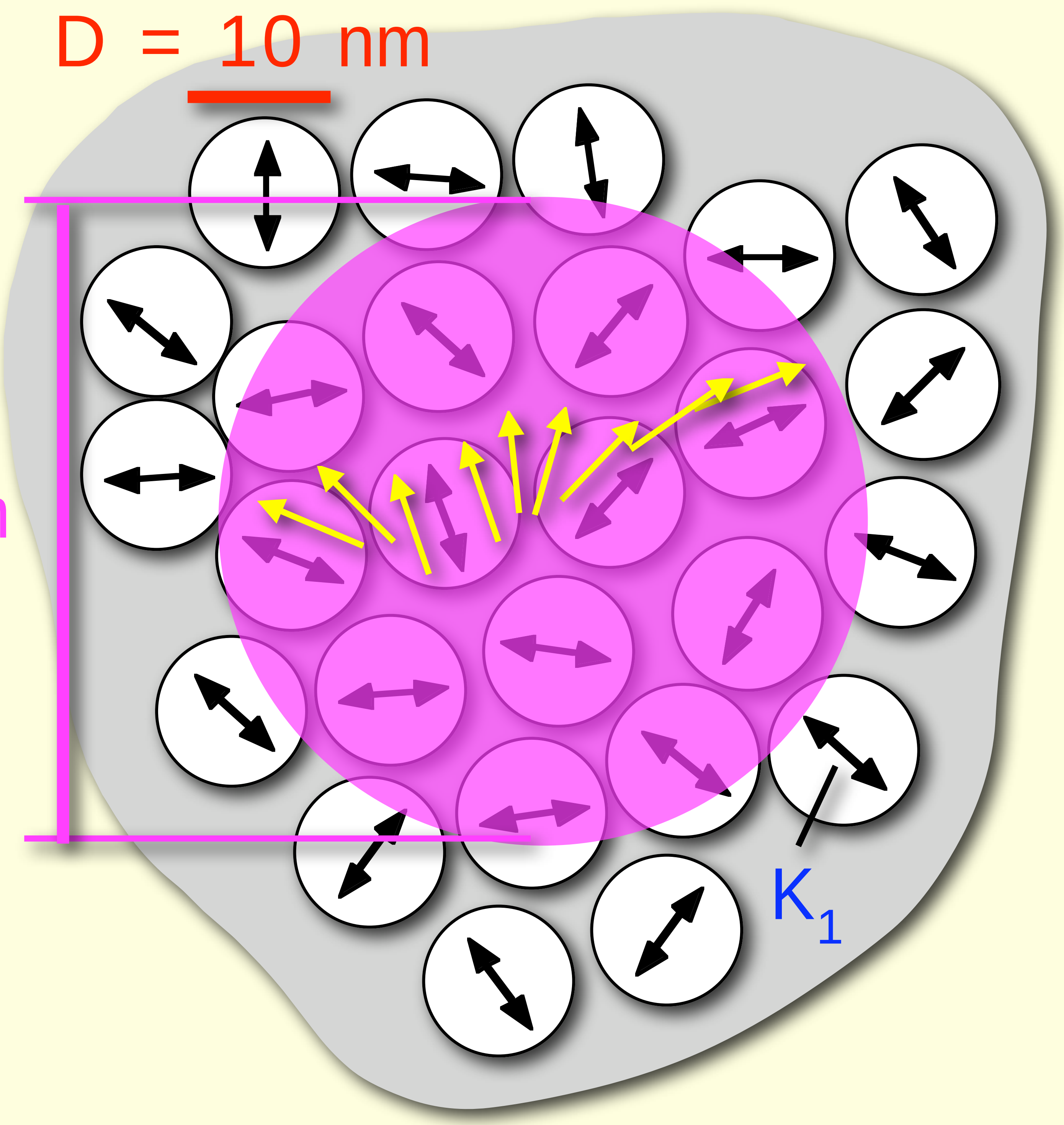

Nanocrystalline soft magnets: Principle

$Fe_{80}Si_{20}$:
$K_1 = 8\ kJ/m^3$
$A = 10^{-11}\ J/m$

➡ $L_{ex} = \sqrt{A/K_1} = 35\ nm$

➡ $D < L_{ex}$

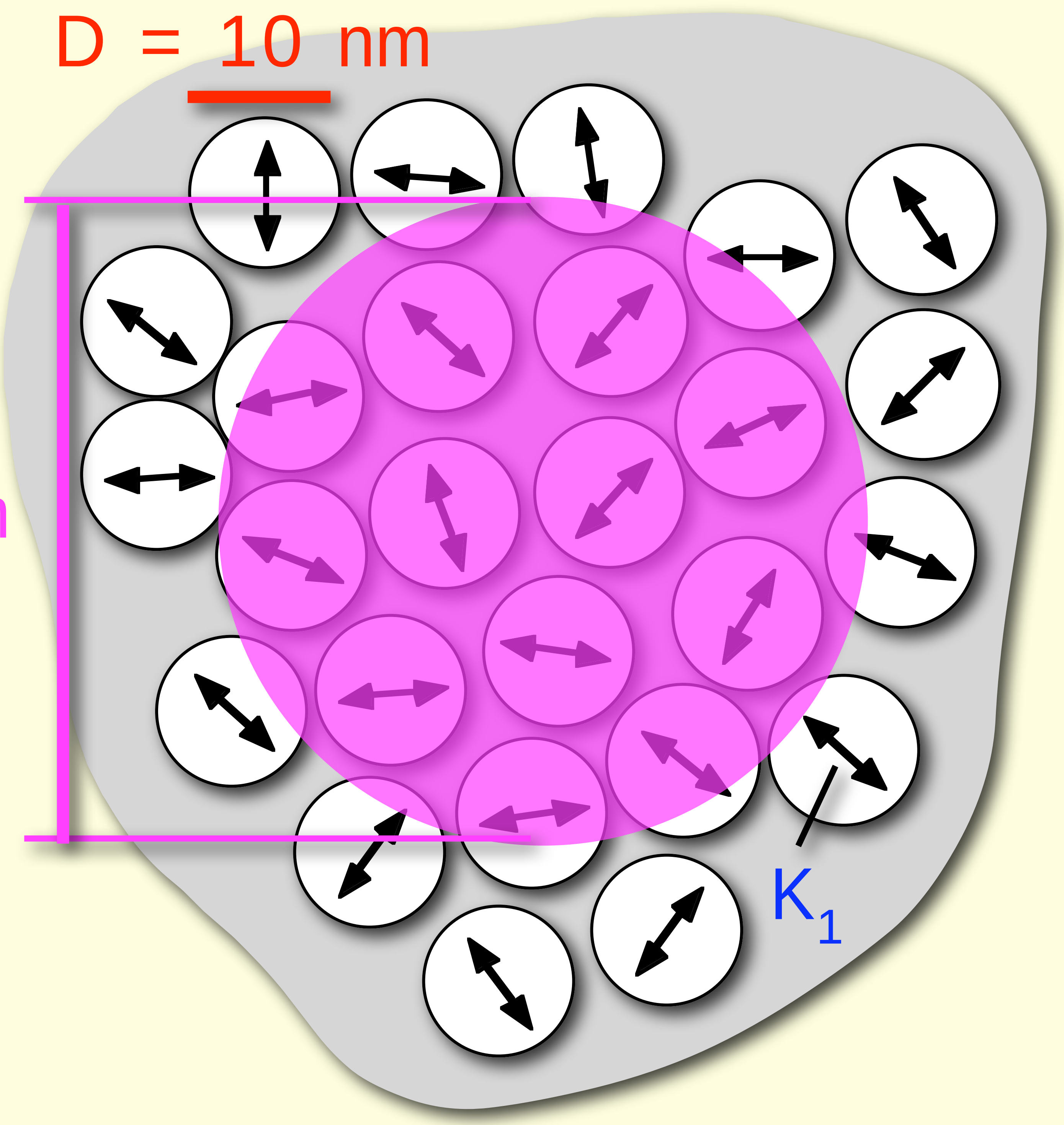

Nanocrystalline soft magnets: Principle

$Fe_{80}Si_{20}$:

$K_1 = 8\ kJ/m^3$

$A = 10^{-11}\ J/m$

➡ $L_{ex} = \sqrt{A/K_1} = 35\ nm$

➡ $D < L_{ex}$

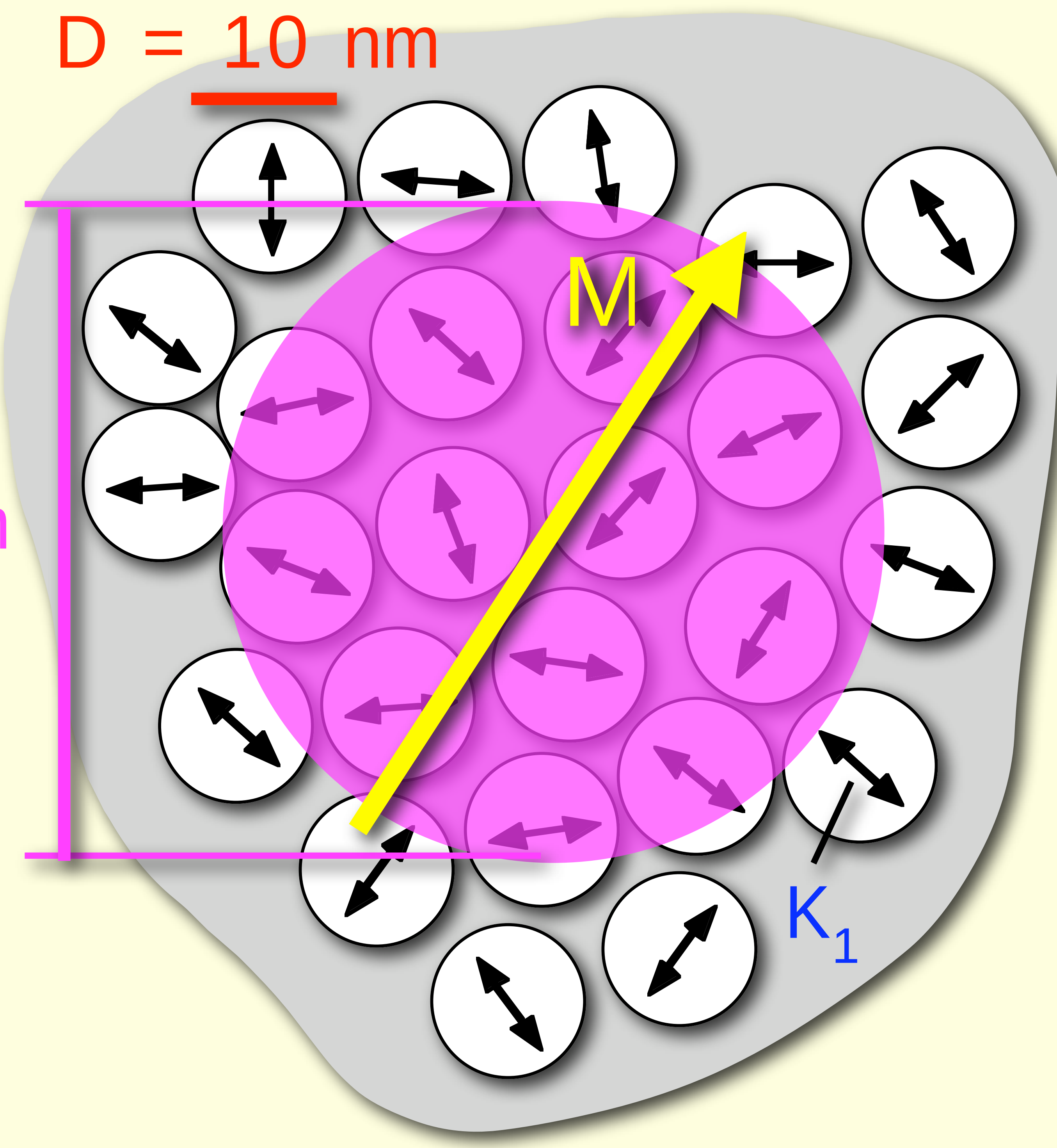

Nanocrystalline soft magnets: Principle

$Fe_{80}Si_{20}$:

$K_1 = 8\ kJ/m^3$

$A = 10^{-11}\ J/m$

➡ $L_{ex} = \sqrt{A/K_1} = 35\ nm$

➡ $D < L_{ex}$

random anisotropy model [Herzer 1989]:

exchange interaction averages over anisotropy of individual grains

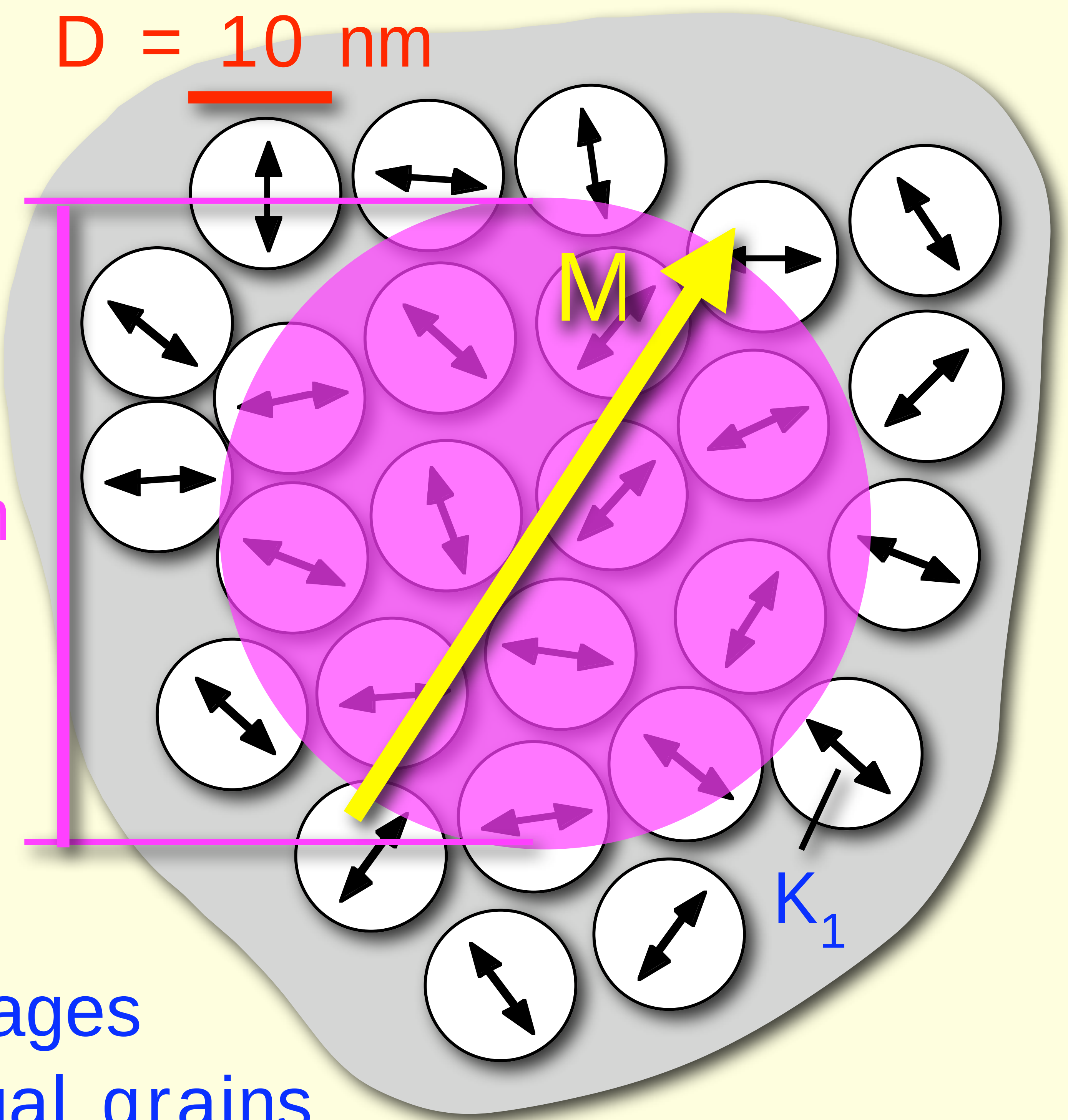

Nanocrystalline soft magnets: Principle

$Fe_{80}Si_{20}$:
$K_1 = 8\ kJ/m^3$
$A = 10^{-11}\ J/m$

→ $L_{ex} = \sqrt{A/K_1} = 35\ nm$

→ $D < L_{ex}$

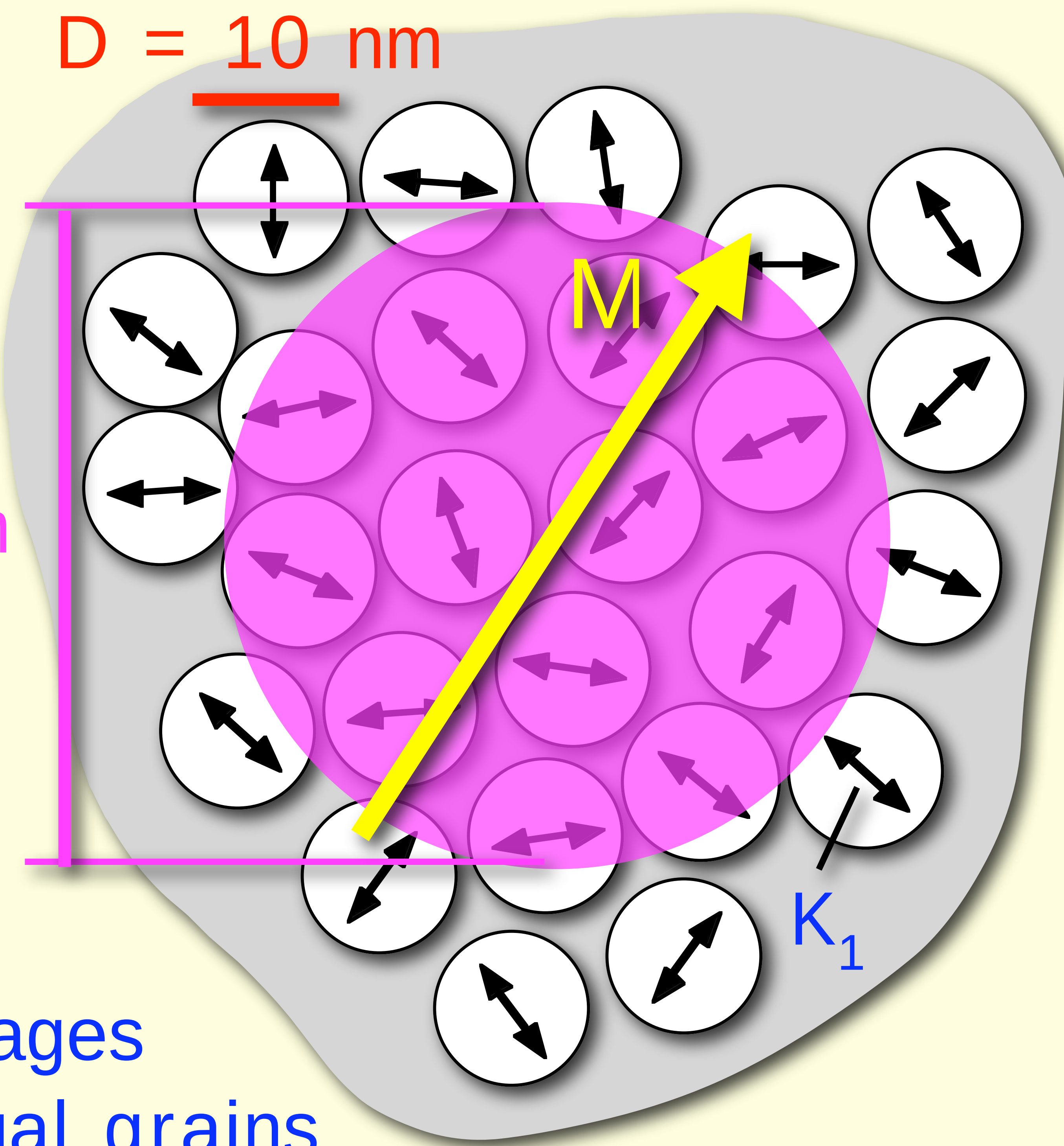

random anisotropy model
[Herzer 1989]:
exchange interaction averages
over anisotropy of individual grains

→ $\langle K_1 \rangle \approx |K_1|\ (D/L_{ex})^6 = 3\ J/m^3$ → very weak eff. anisotropy

Nanocrystalline soft magnets: Principle

$Fe_{80}Si_{20}$:

$K_1 = 8\ kJ/m^3$

$A = 10^{-11}\ J/m$

➡ $L_{ex} = \sqrt{A/K_1} = 35\ nm$

➡ $D < L_{ex}$

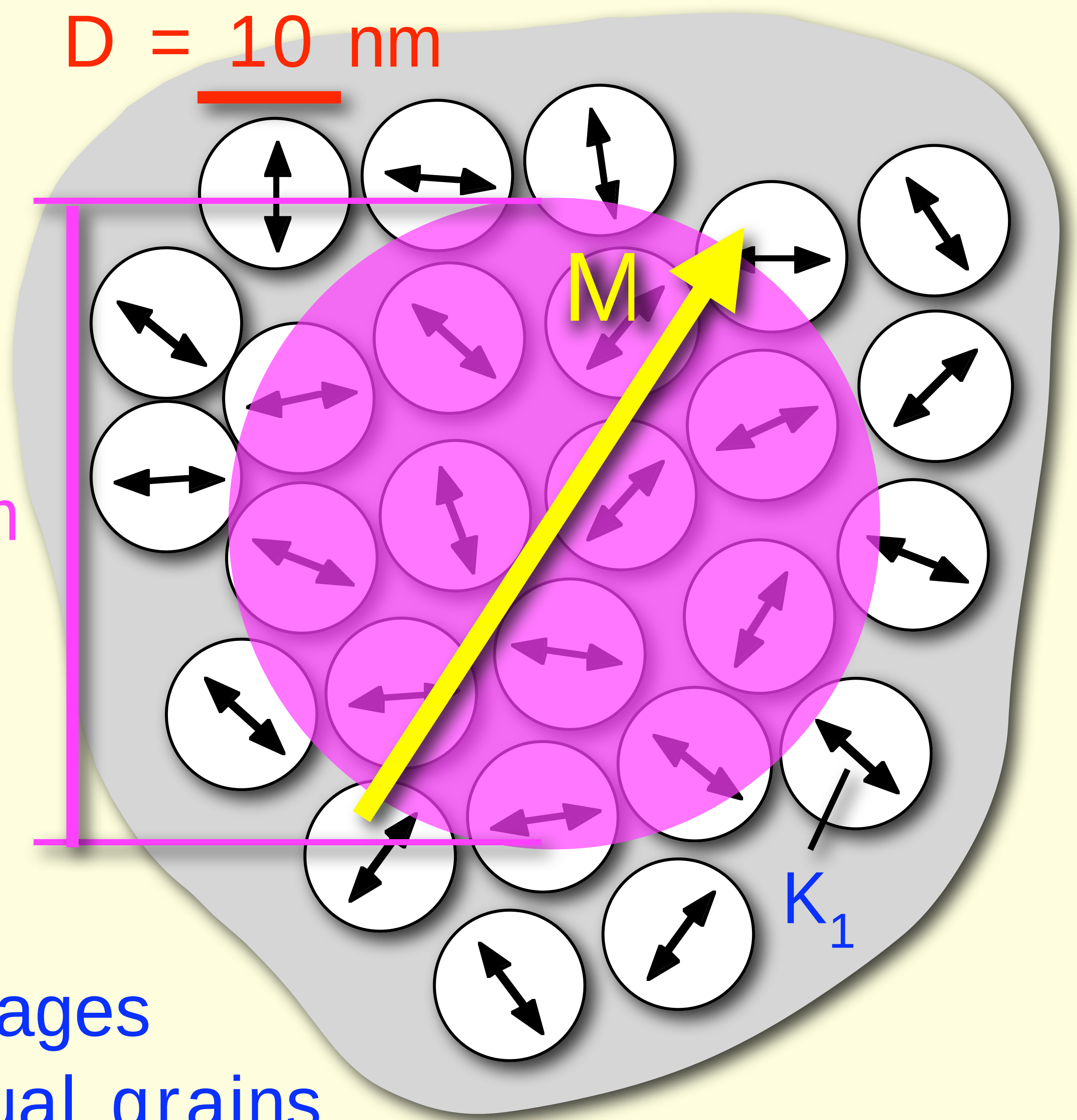

random anisotropy model [Herzer 1989]:

exchange interaction averages over anisotropy of individual grains

➡ $\langle K_1 \rangle \approx |K_1|\ (D/L_{ex})^6 = 3\ J/m^3$ ➡ very weak eff. anisotropy

FeSiBCuNb: domain state

amorphous (as-quenched)

nanocrystalline

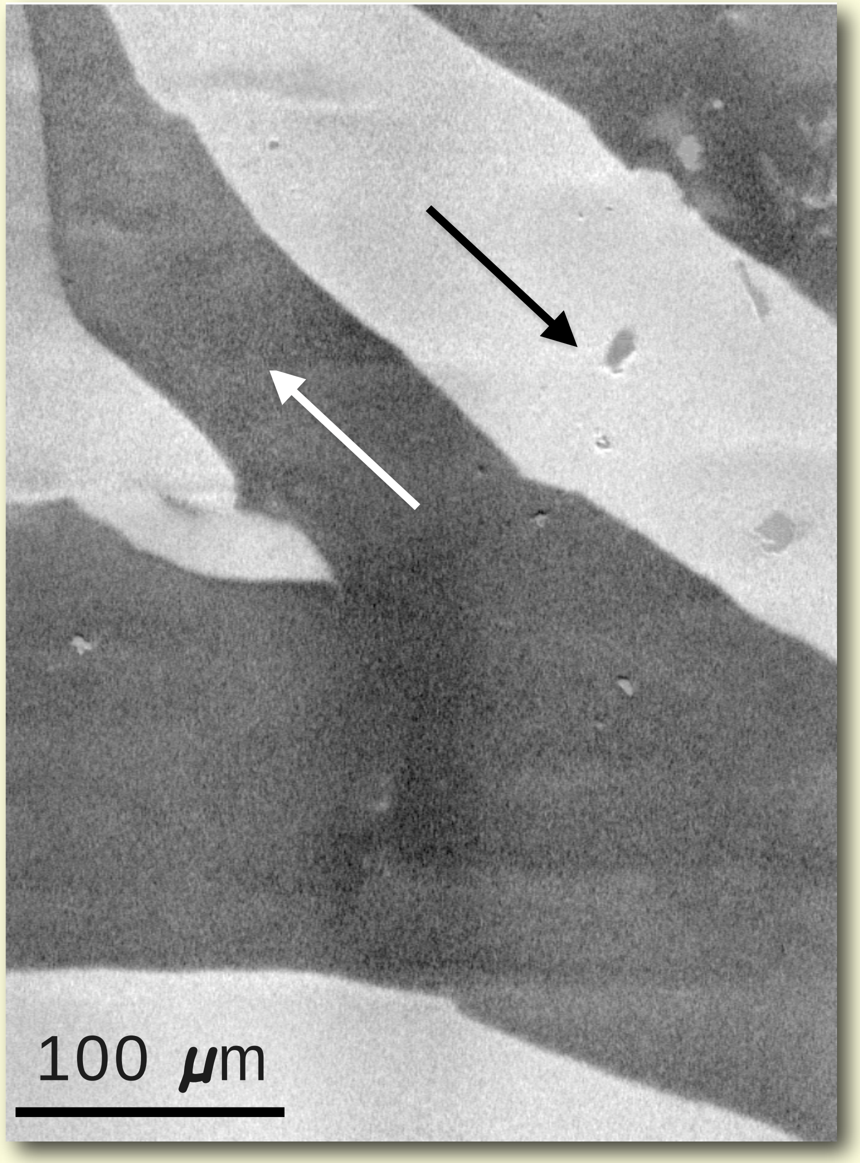

nanocrystalline

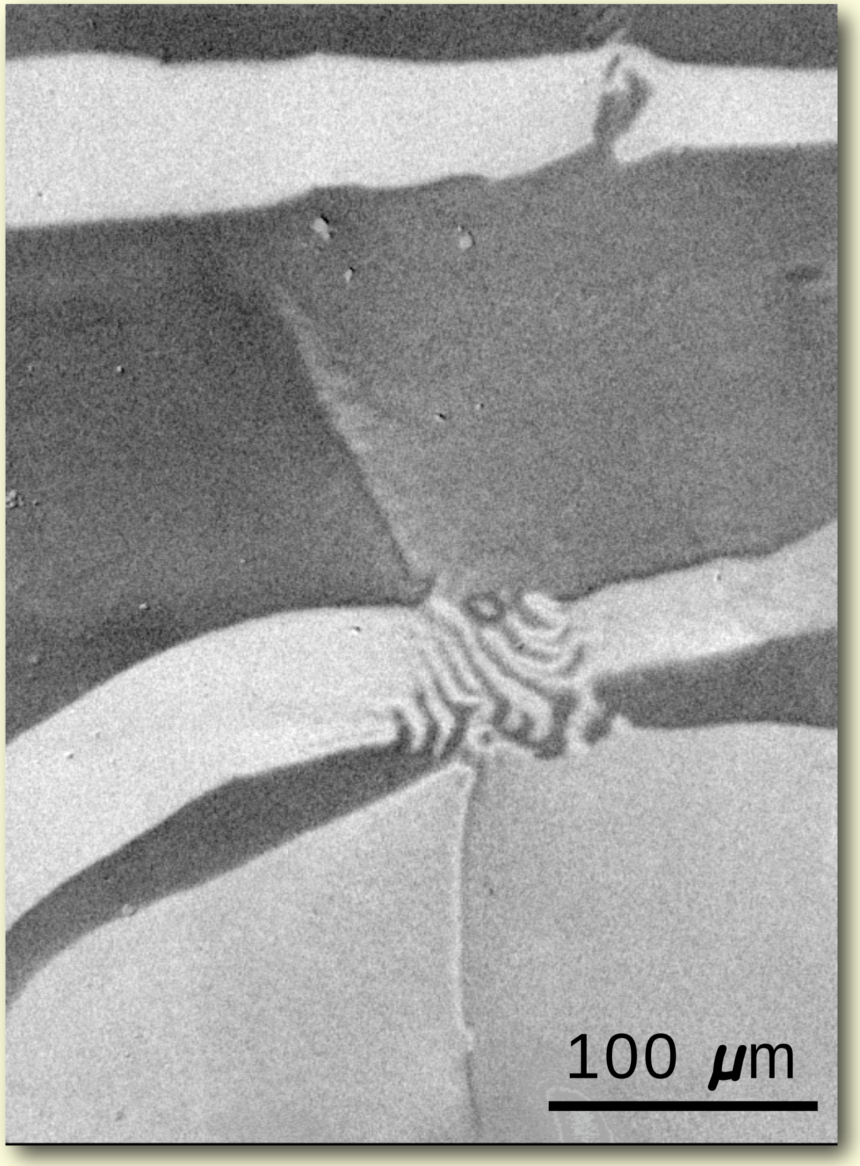

homogeneous domains on macroscopic scale, direction determined by induced anisotropy

Nanocrystalline soft magnets: Principle

$Fe_{80}Si_{20}$:

$K_1 = 8\ kJ/m^3$

$A = 10^{-11}\ J/m$

$\rightarrow L_{ex} = \sqrt{A/K_1} = 35\ nm$

exchange length

random anisotropy model

$\rightarrow \langle K_1 \rangle = 3\ J/m^3$

average anisotropy

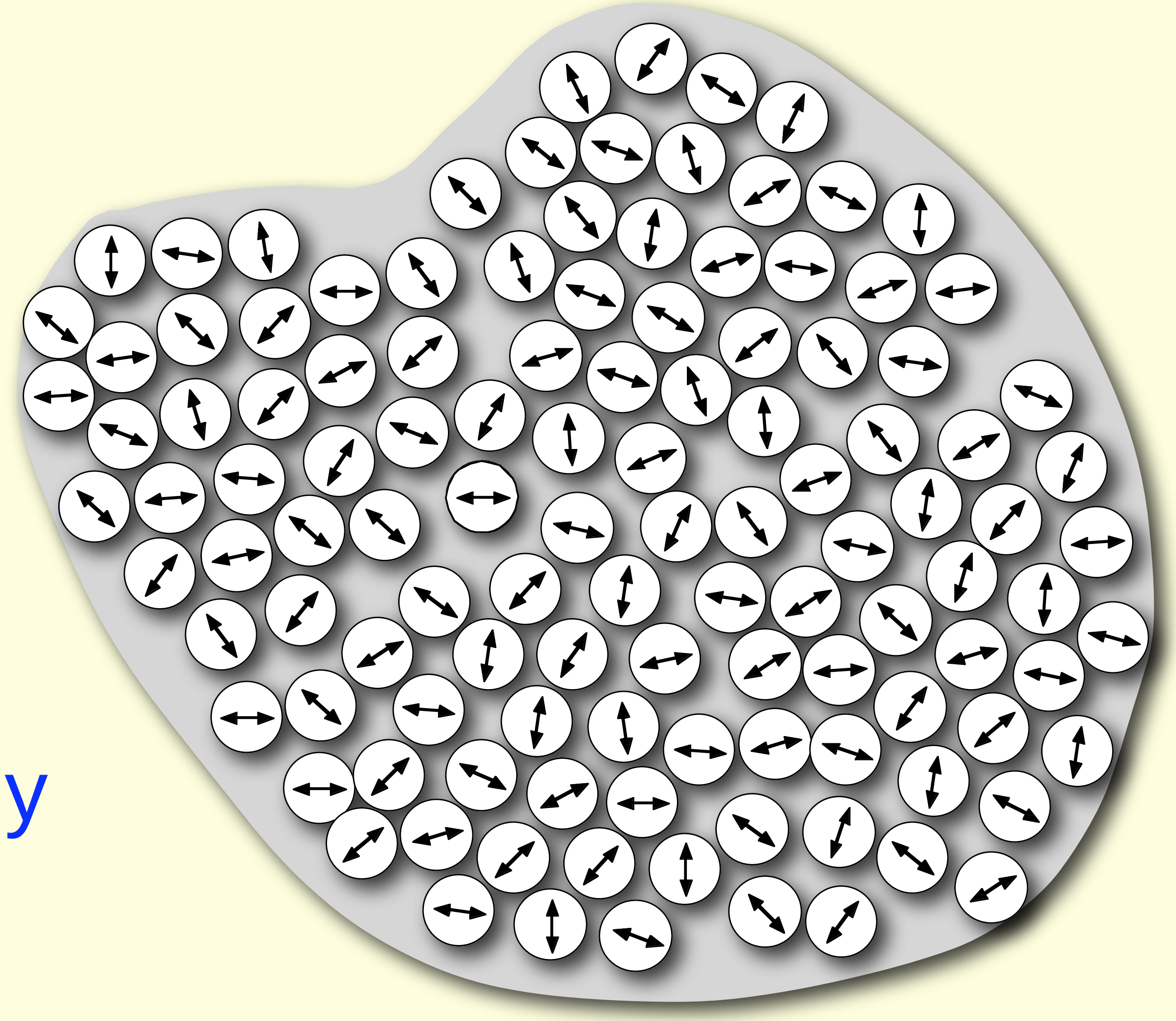

Nanocrystalline soft magnets: Principle

$Fe_{80}Si_{20}$:

$K_1 = 8\ \mathrm{kJ/m^3}$

$A = 10^{-11}\ \mathrm{J/m}$

→ $L_{ex} = \sqrt{A/K_1} = 35\ \mathrm{nm}$

exchange length

random anisotropy model

→ $\langle K_1 \rangle = 3\ \mathrm{J/m^3}$

average anisotropy

→ $L_{ex} = \sqrt{A/\langle K_1 \rangle} = 2\ \mu\mathrm{m}$

renormalized exchange length

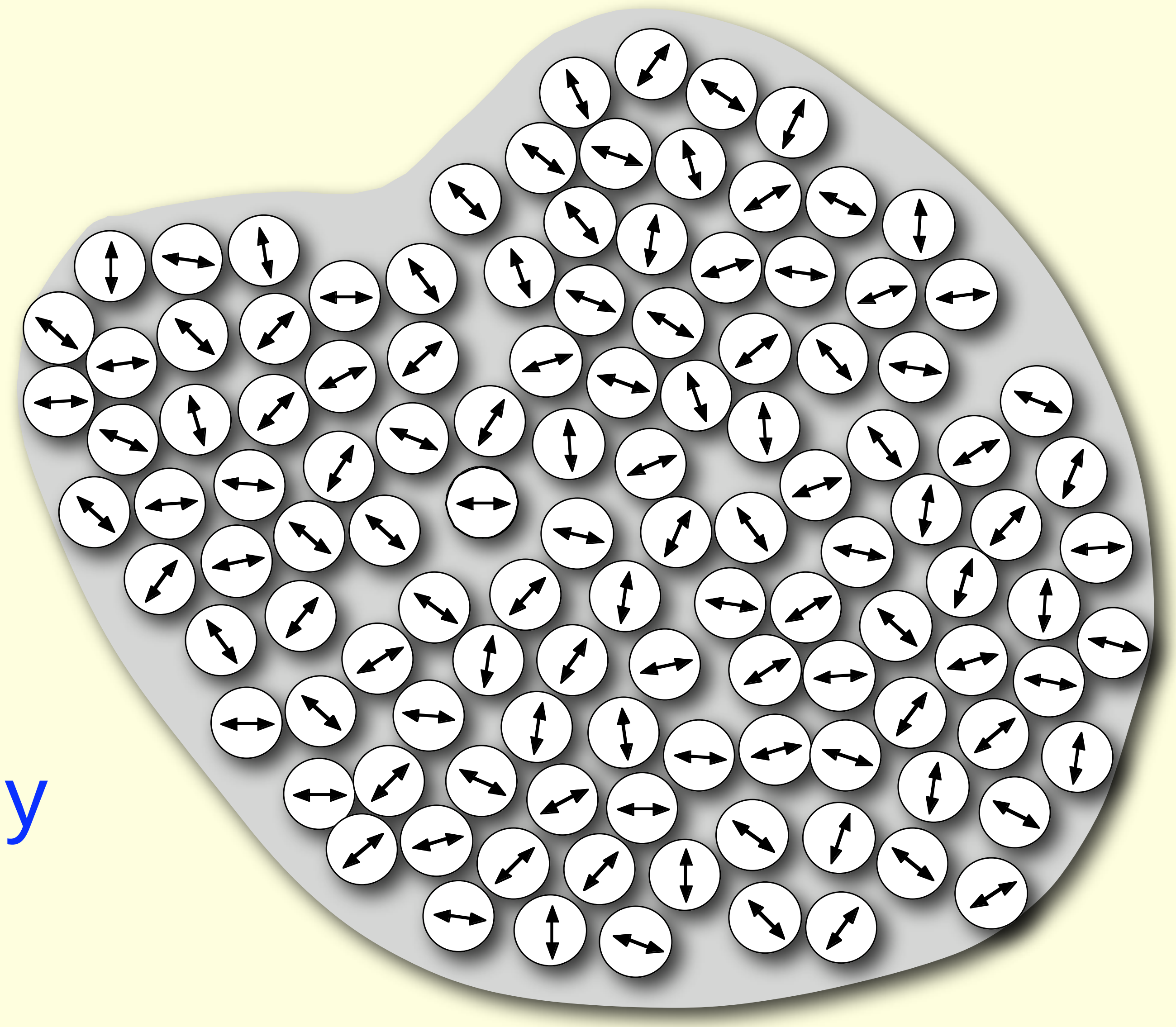

Comparison of domain walls

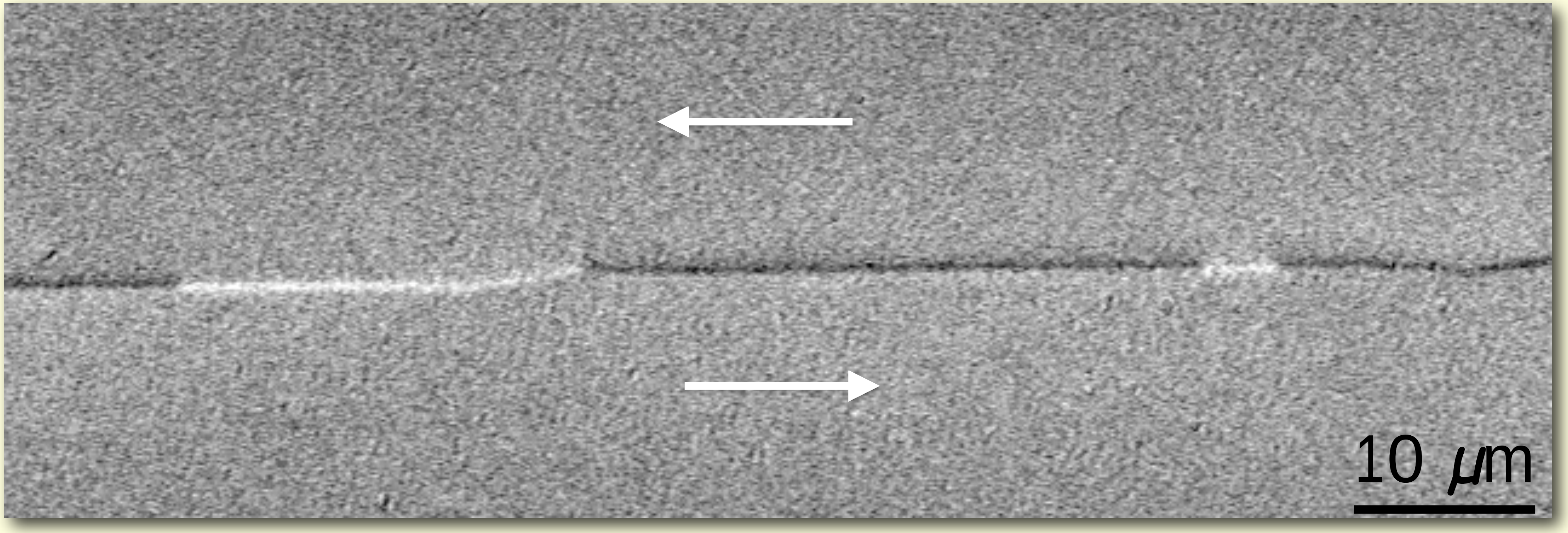

Fe-Si Goss sheet, surface wall width: 150 nm

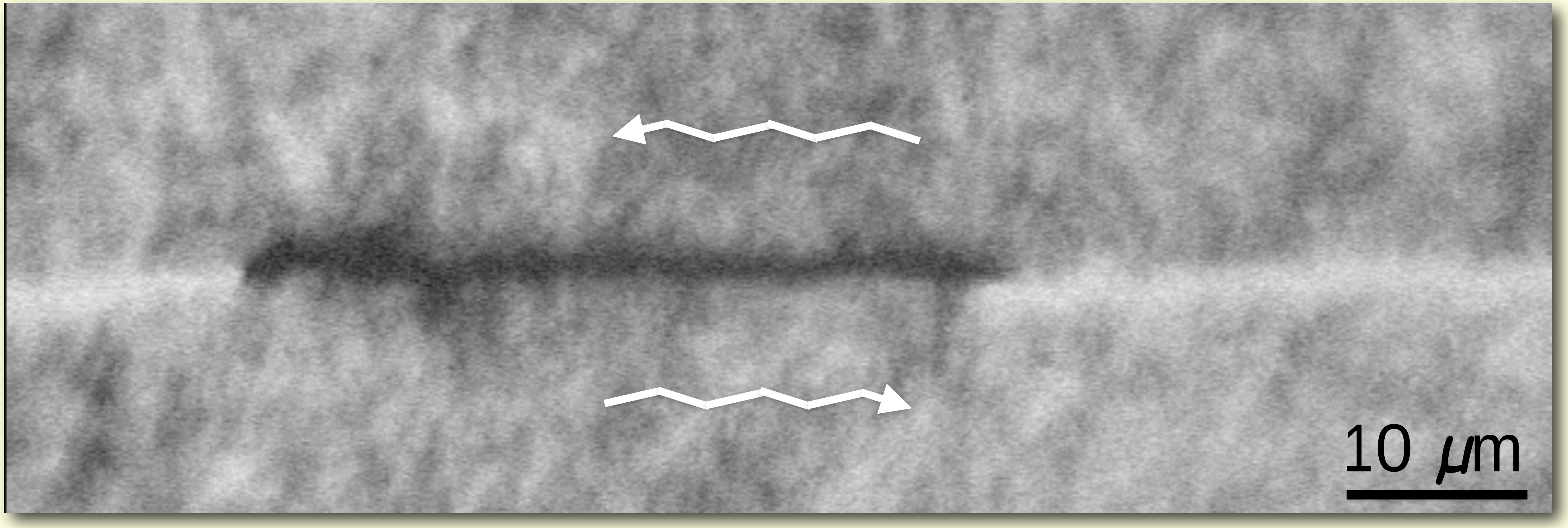

nanocrystalline ribbon, surface wall width: several μm

Nanocrystalline soft magnets: Principle

$Fe_{80}Si_{20}$:

$K_1 = 8 \text{ kJ/m}^3$

$A = 10^{-11} \text{ J/m}$

→ $L_{ex} = \sqrt{A/K_1} = 35 \text{ nm}$

exchange length

random anisotropy model

→ $\langle K_1 \rangle = 2.3 \text{ J/m}^3$

average anisotropy

→ $L_{ex} = \sqrt{A/\langle K_1 \rangle} = 2\ \mu\text{m}$

renormalized exchange length

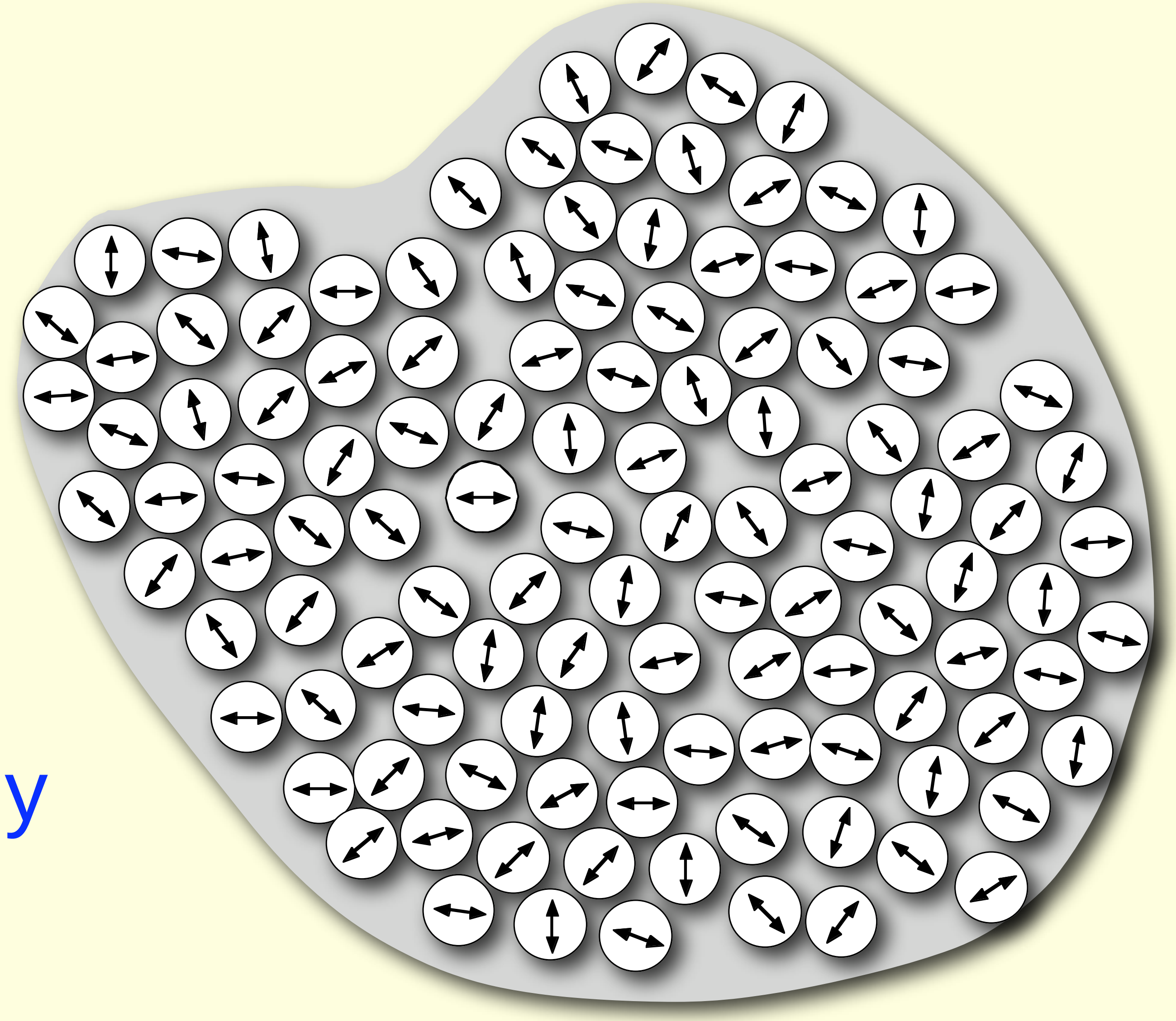

Nanocrystalline soft magnets: Principle

$Fe_{80}Si_{20}$:
$K_1 = 8\ kJ/m^3$
$A = 10^{-11}\ J/m$

$\rightarrow L_{ex} = \sqrt{A/K_1} = 35\ nm$
exchange length

random anisotropy model

$\rightarrow \langle K_1 \rangle = 2.3\ J/m^3$
average anisotropy

$\rightarrow L_{ex} = \sqrt{A/\langle K_1 \rangle} = 2\ \mu m$
renormalized exchange length

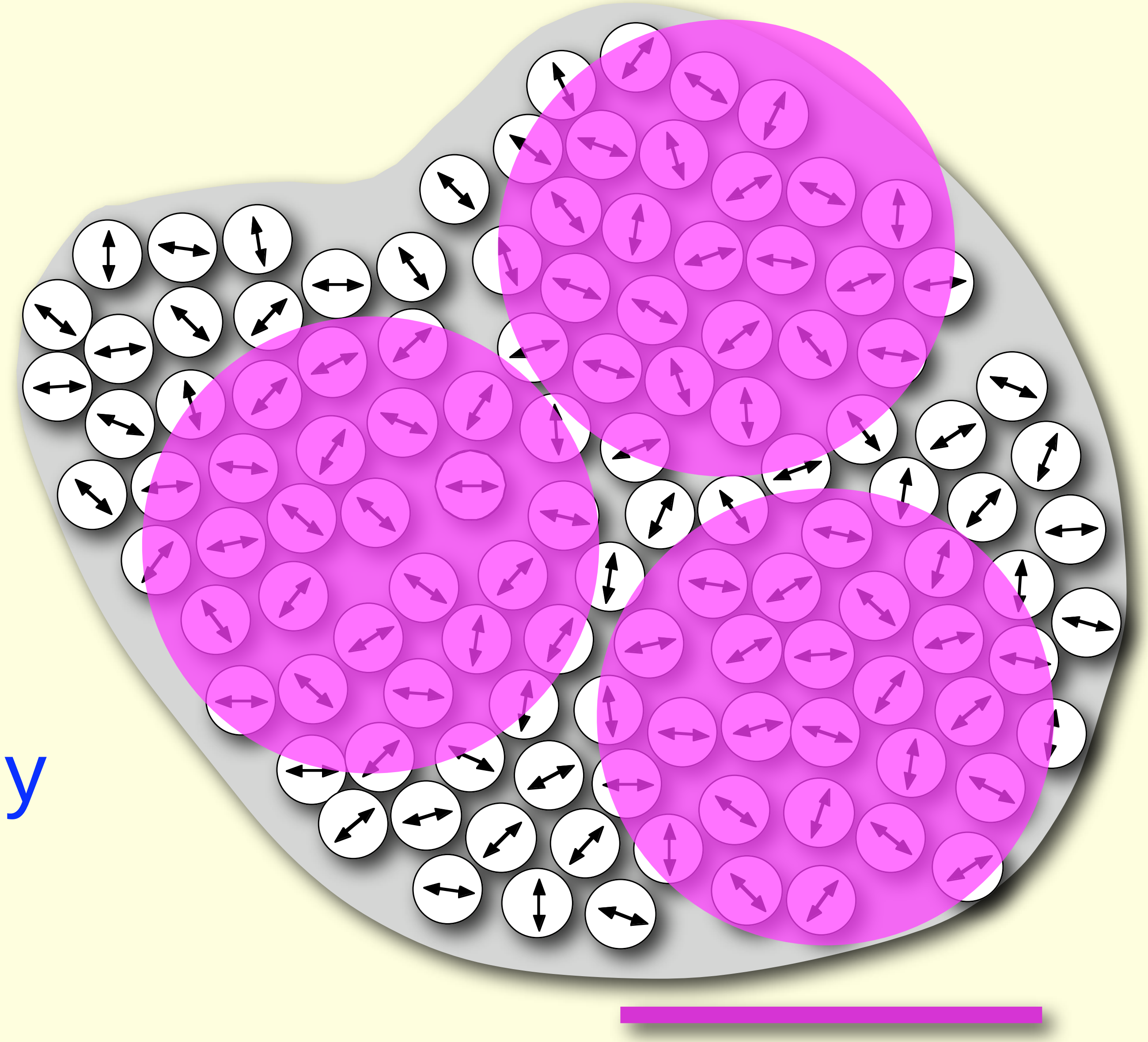

$L_{ex} = 2\ \mu m$

Nanocrystalline soft magnets: Principle

$Fe_{80}Si_{20}$:
$K_1 = 8\ kJ/m^3$
$A = 10^{-11}\ J/m$

→ $L_{ex} = \sqrt{A/K_1} = 35\ nm$
exchange length

random anisotropy model

→ $\langle K_1 \rangle = 2.3\ J/m^3$
average anisotropy

→ $L_{ex} = \sqrt{A/\langle K_1 \rangle} = 2\ \mu m$
renormalized exchange length

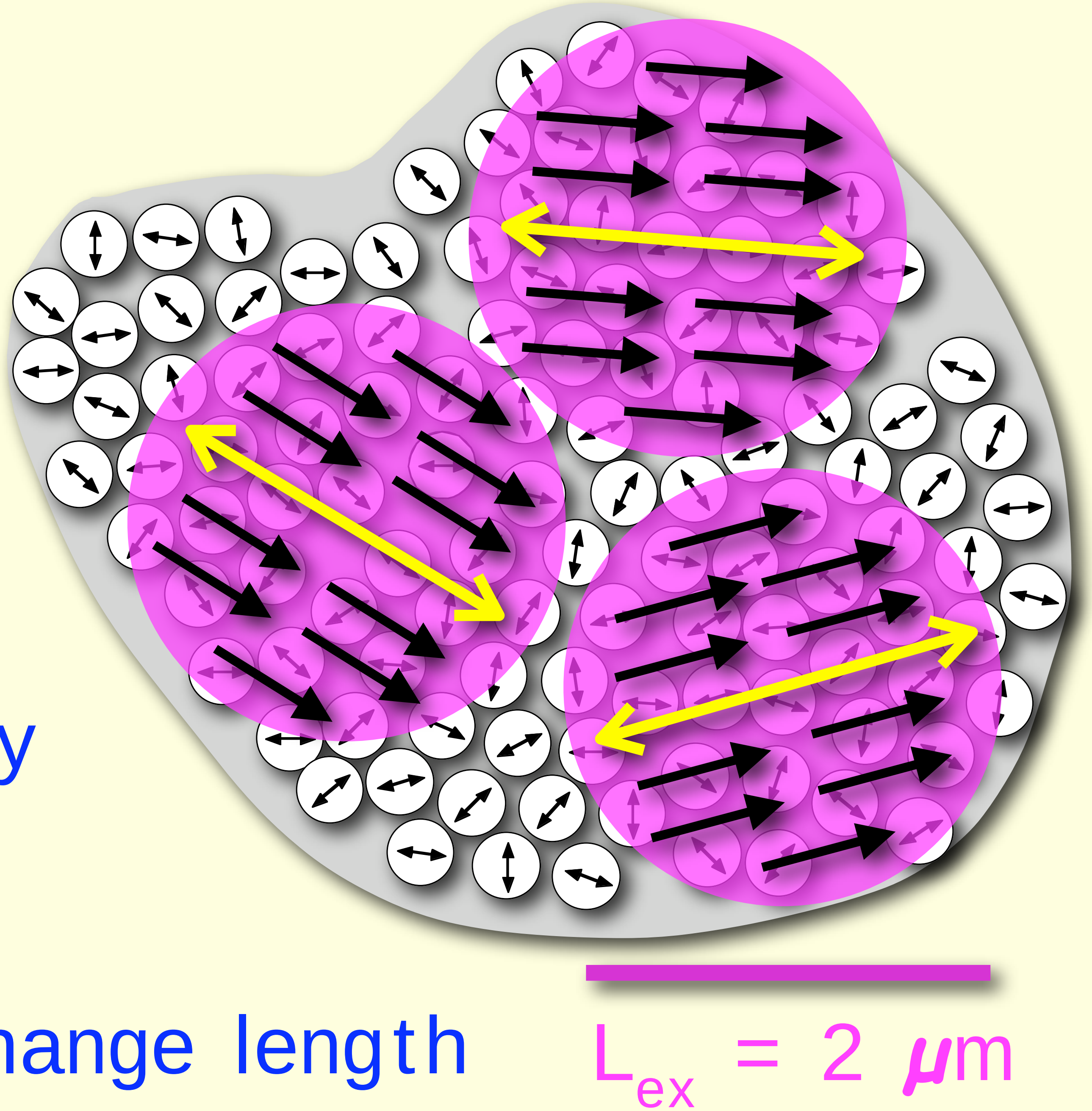

Nanocrystalline soft magnets: Principle

$Fe_{80}Si_{20}$:

$K_1 = 8\ kJ/m^3$

$A = 10^{-11}\ J/m$

→ $L_{ex} = \sqrt{A/K_1} = 35\ nm$

exchange length

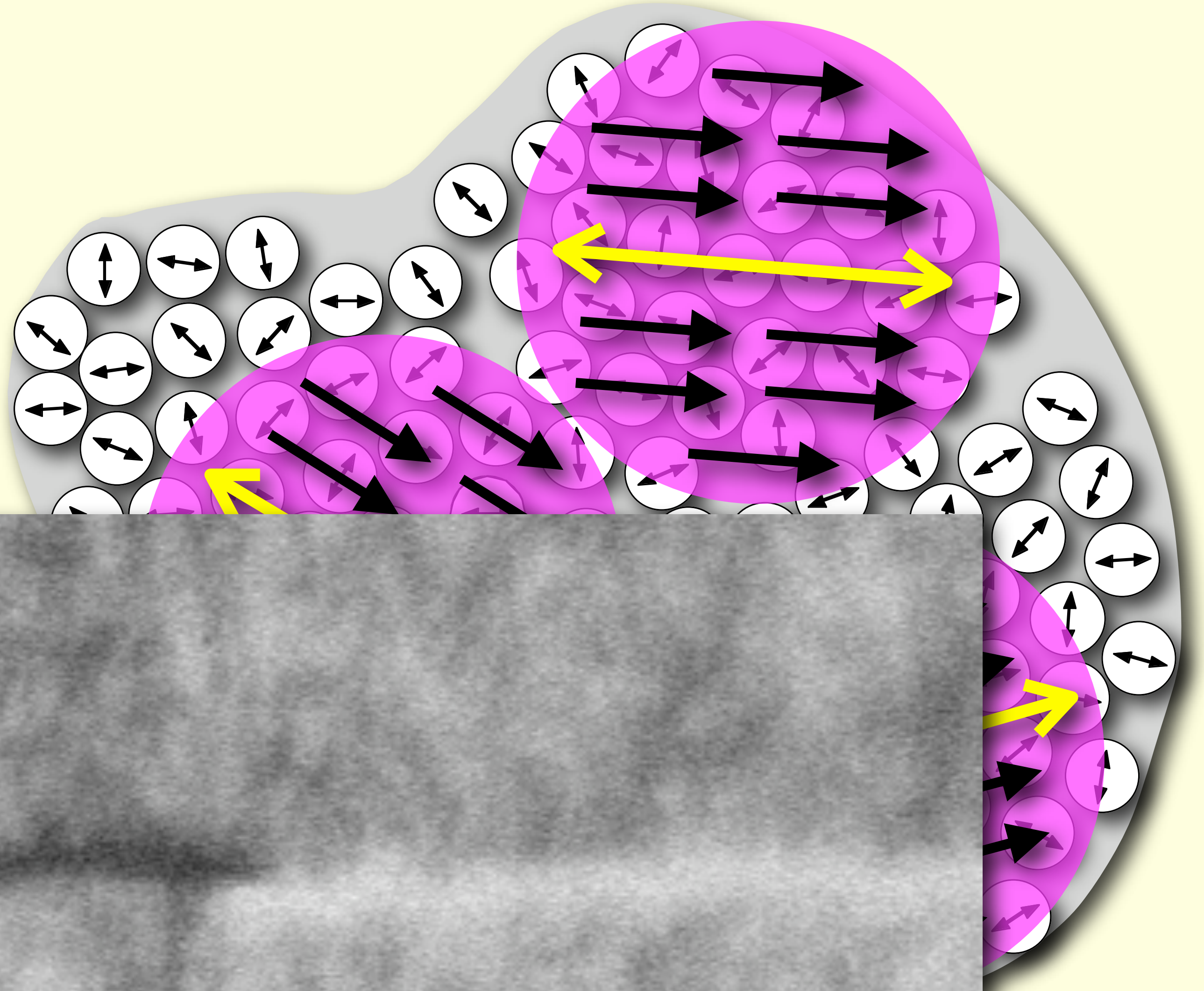

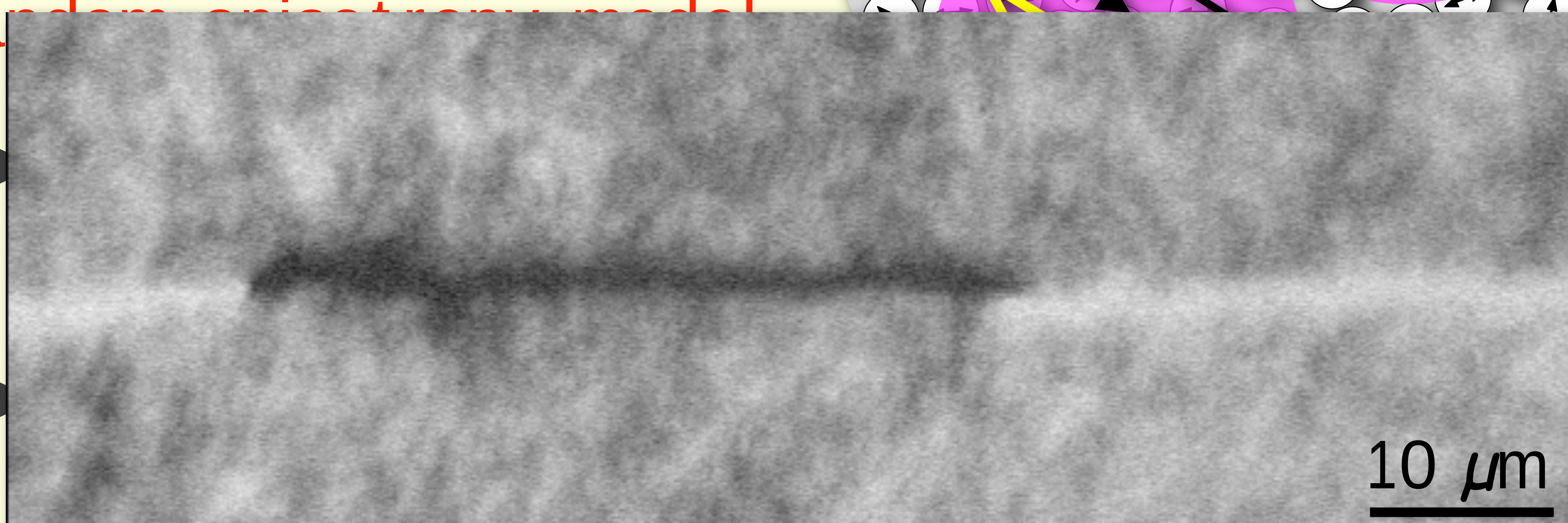

Random anisotropy effect in Permalloy

coarse-grained material
(grain size: 30 μm)

fine-grained material
(grain size: 13 μm)

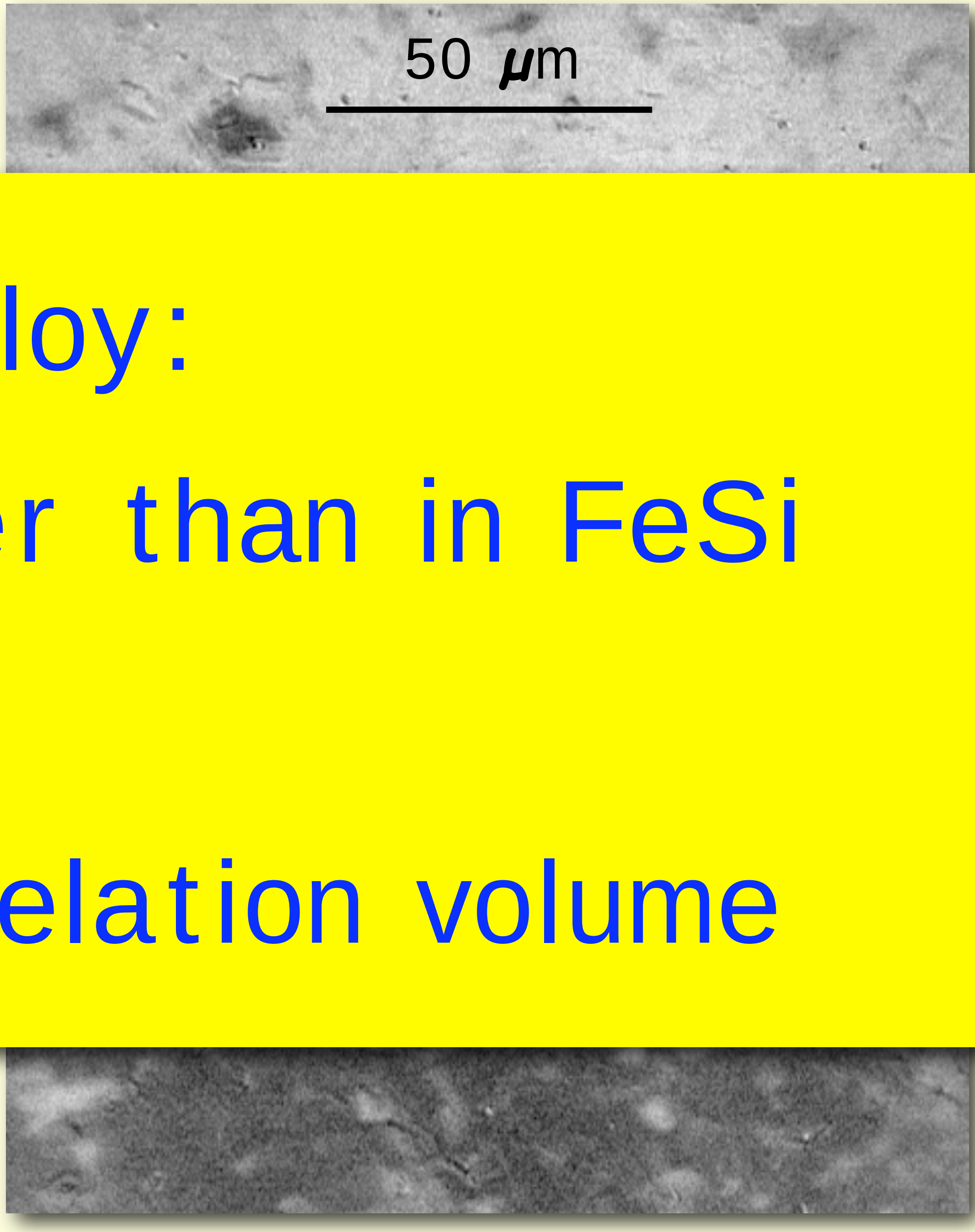

Permalloy:

K_{cryst} much smaller than in FeSi

$\downarrow$

much larger correlation volume

Random anisotropy effect in Permalloy

coarse-grained material
(grain size: 30 μm)

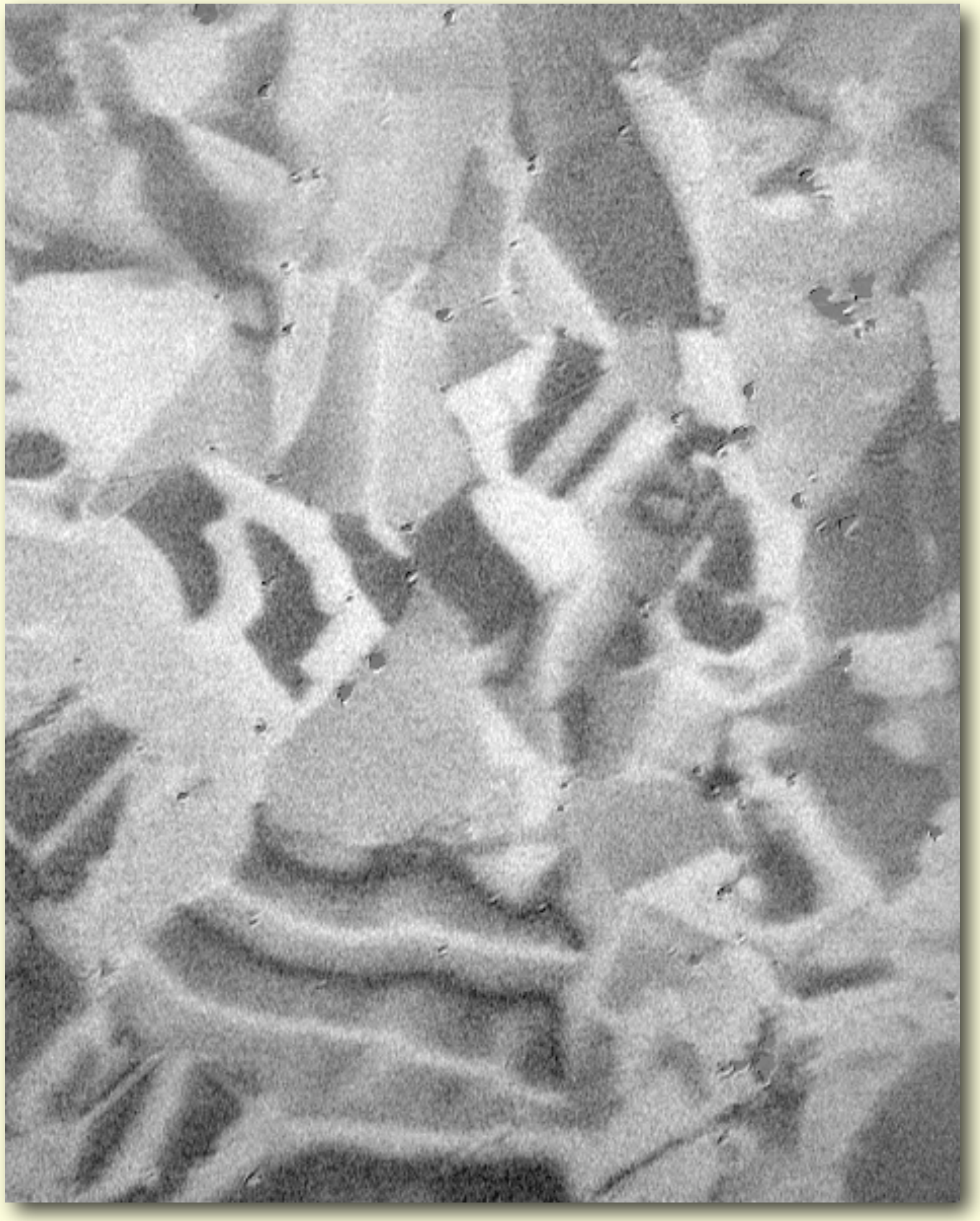

fine-grained material
(grain size: 13 μm)

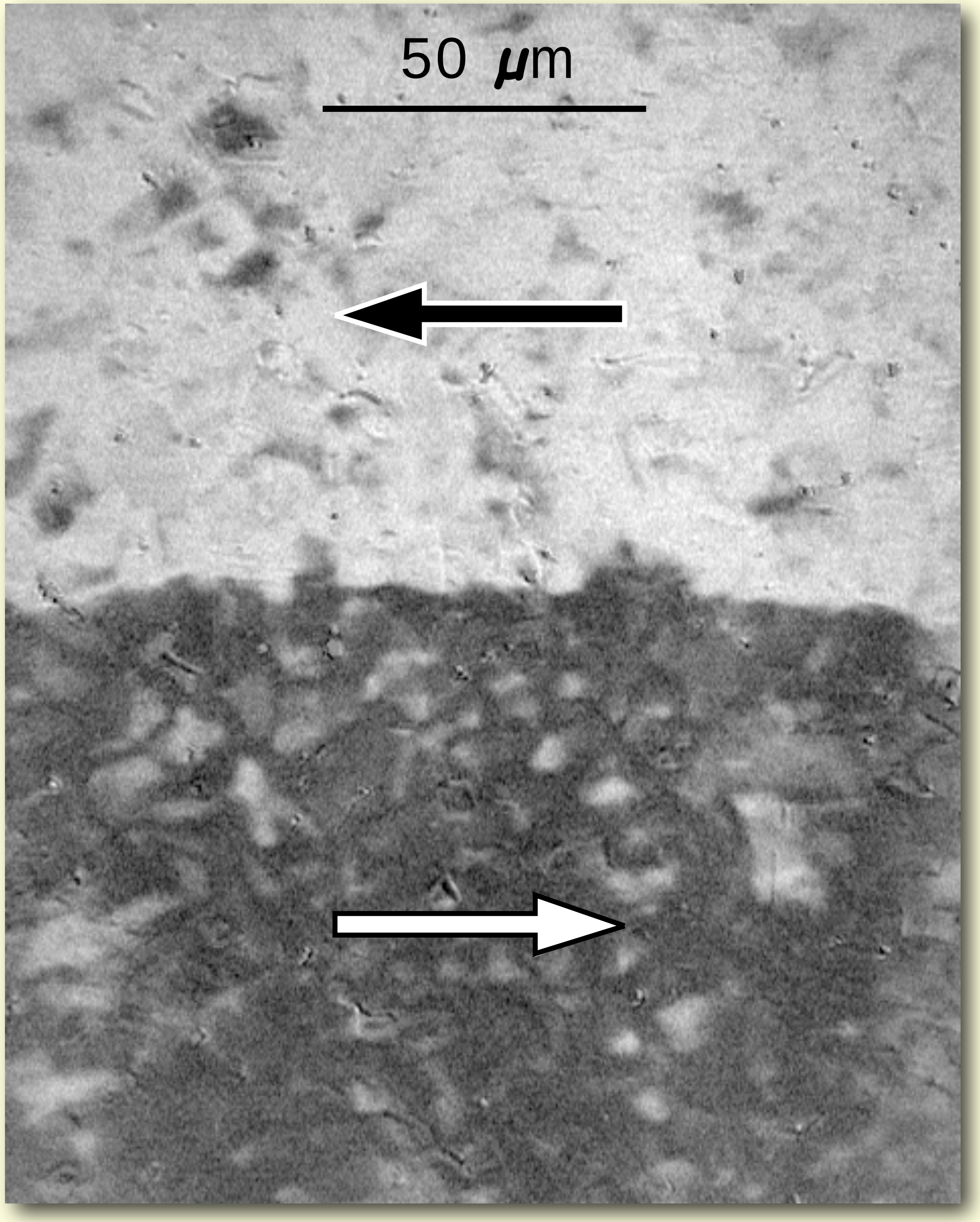

Interplay random/induced anisotropy

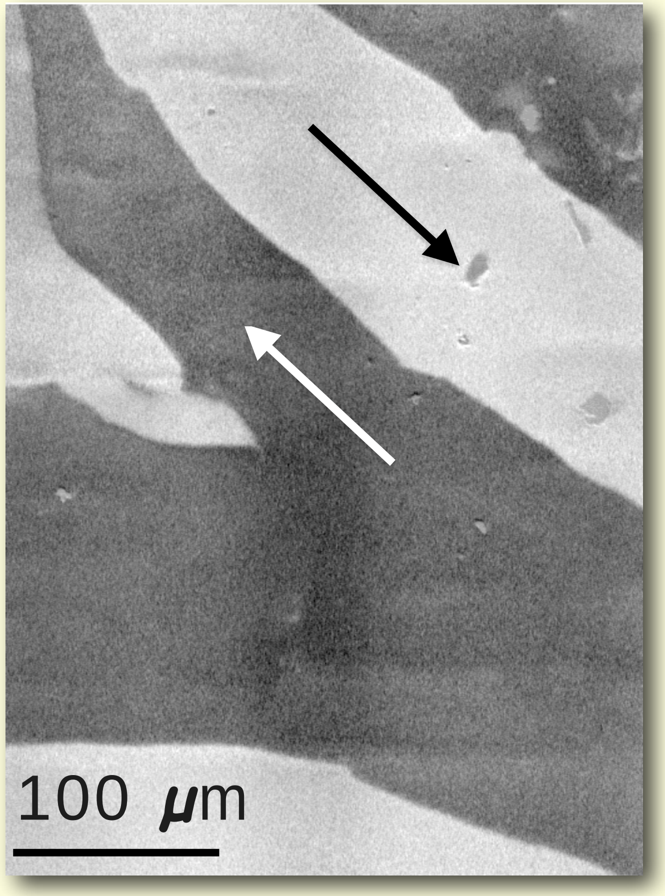

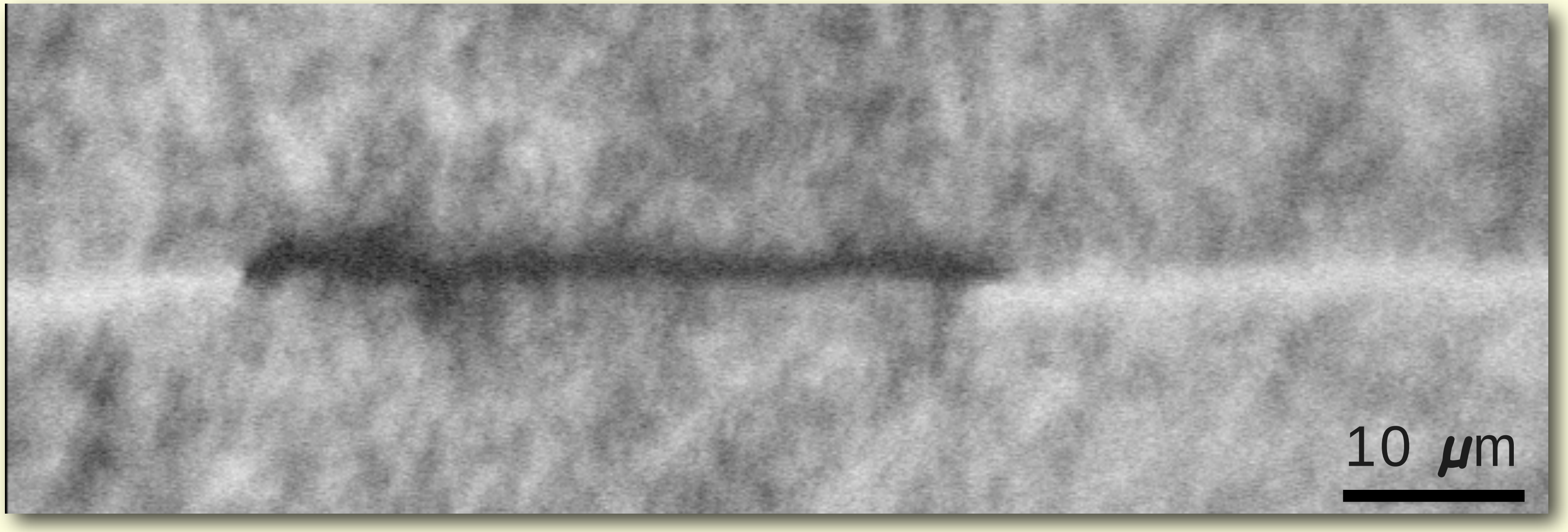

- random anisotropy $\langle K_1 \rangle$: modulated on scale of renormalized exchange length, $\langle K_1 \rangle \approx 3\ \mathrm{J/m^3}$
- induced anisotropy K_u: uniform on large scale, $K_u \approx 3 - 30\ \mathrm{J/m^3}$

interplay

Interplay random/induced anisotropy

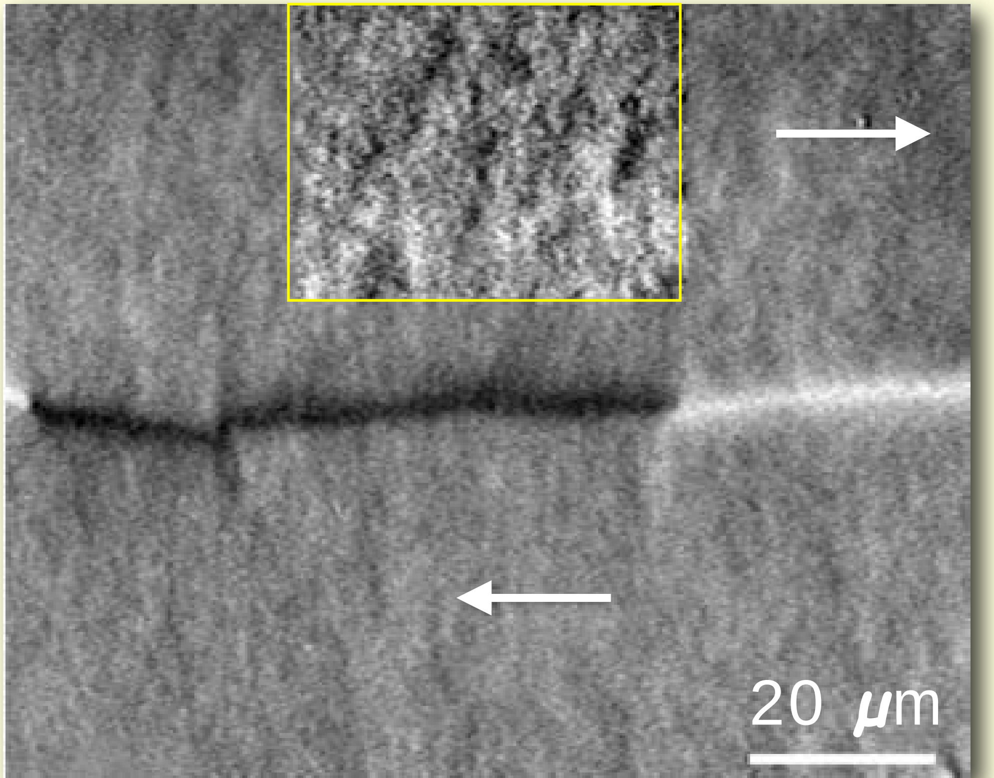

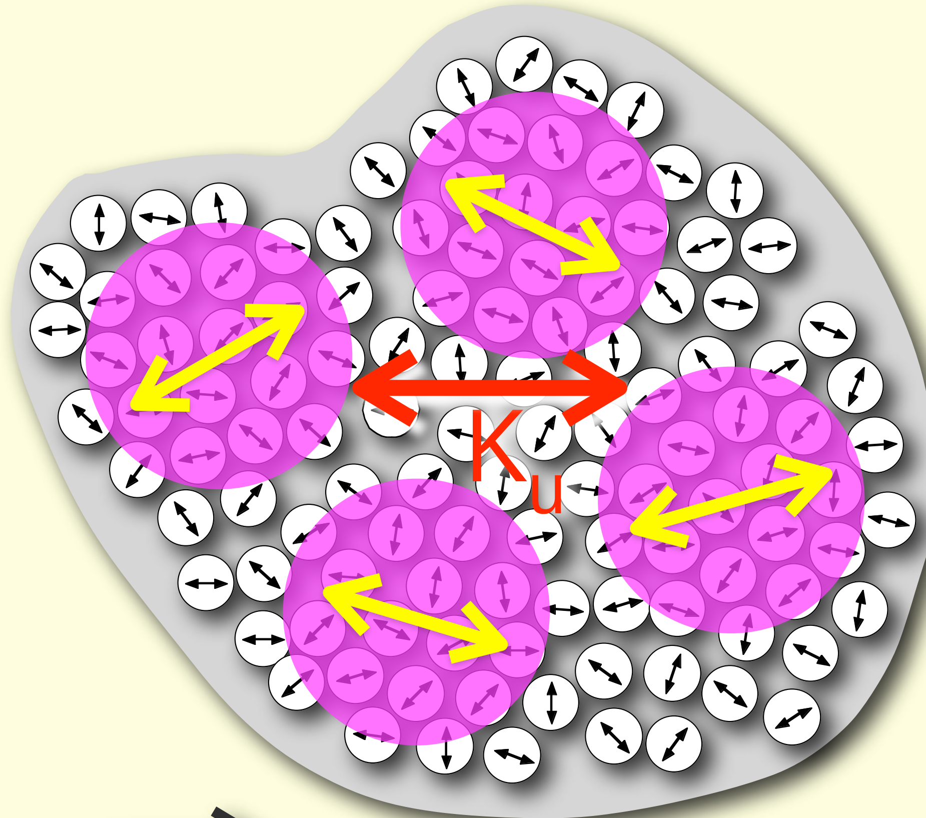

low induced anisotropy

(K_u = 3 J/m^3)

H_{anneal}

$$L_{ex} = \sqrt{A/\langle K \rangle}$$

$$\langle K \rangle = \sqrt{\langle K_1^2 \rangle + K_u^2}$$

3 J/m^3

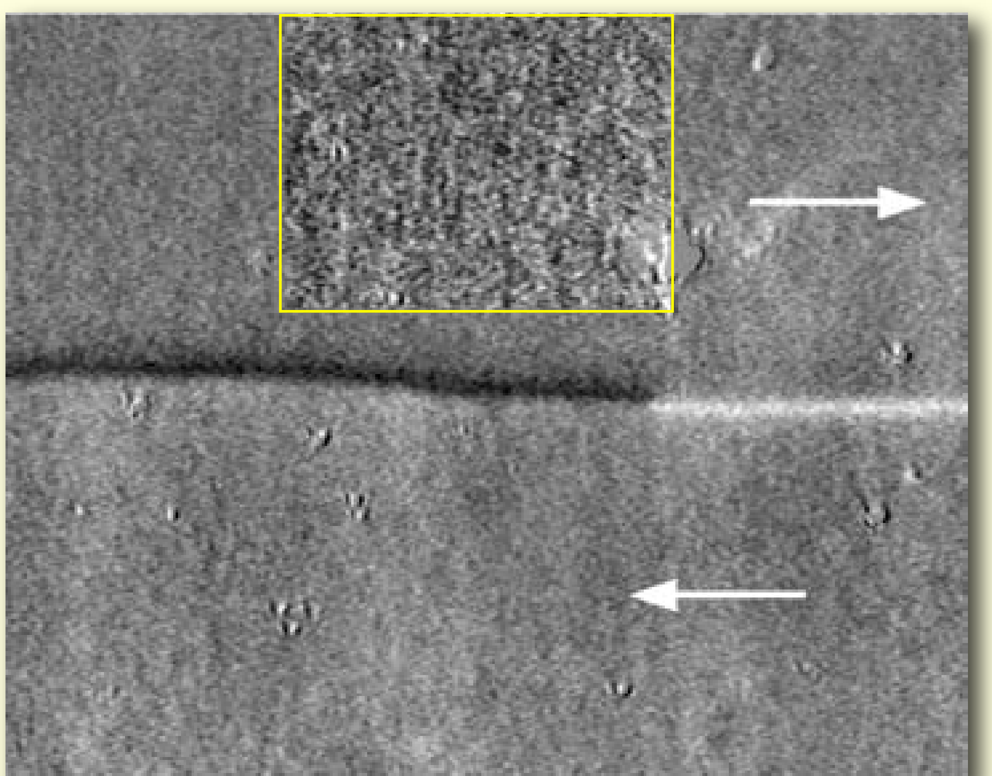

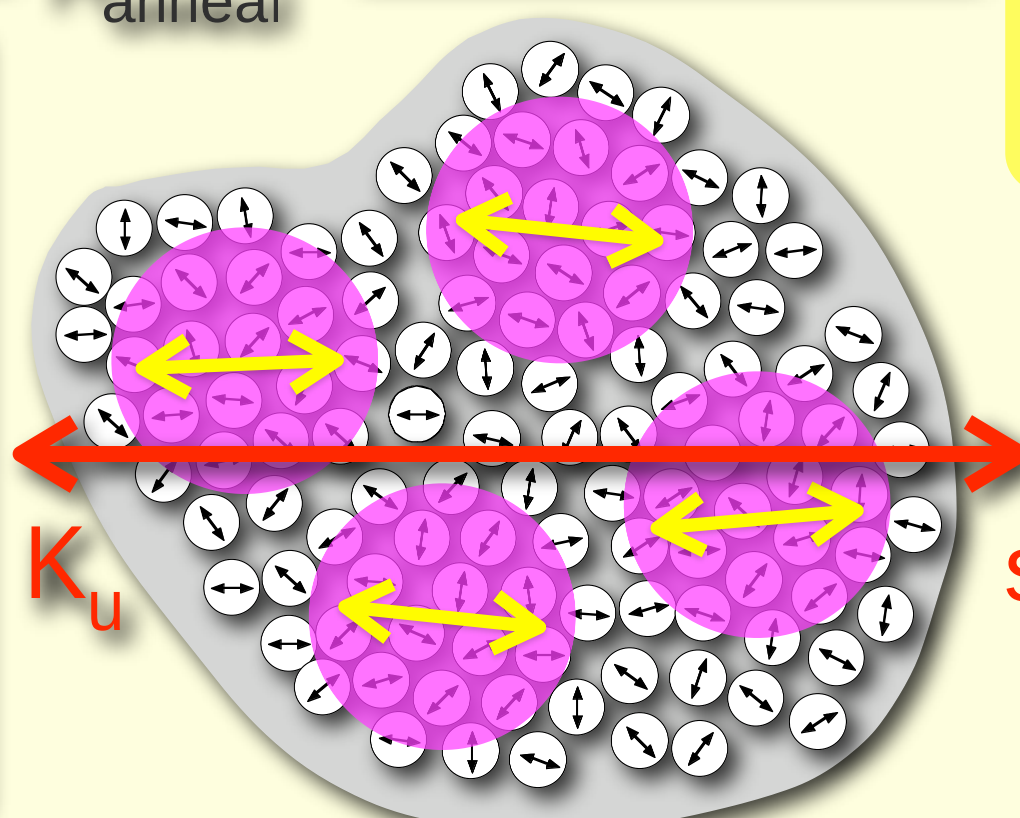

strong induced anisotropy

(K_u = 30 J/m^3)

Interplay random/induced anisotropy

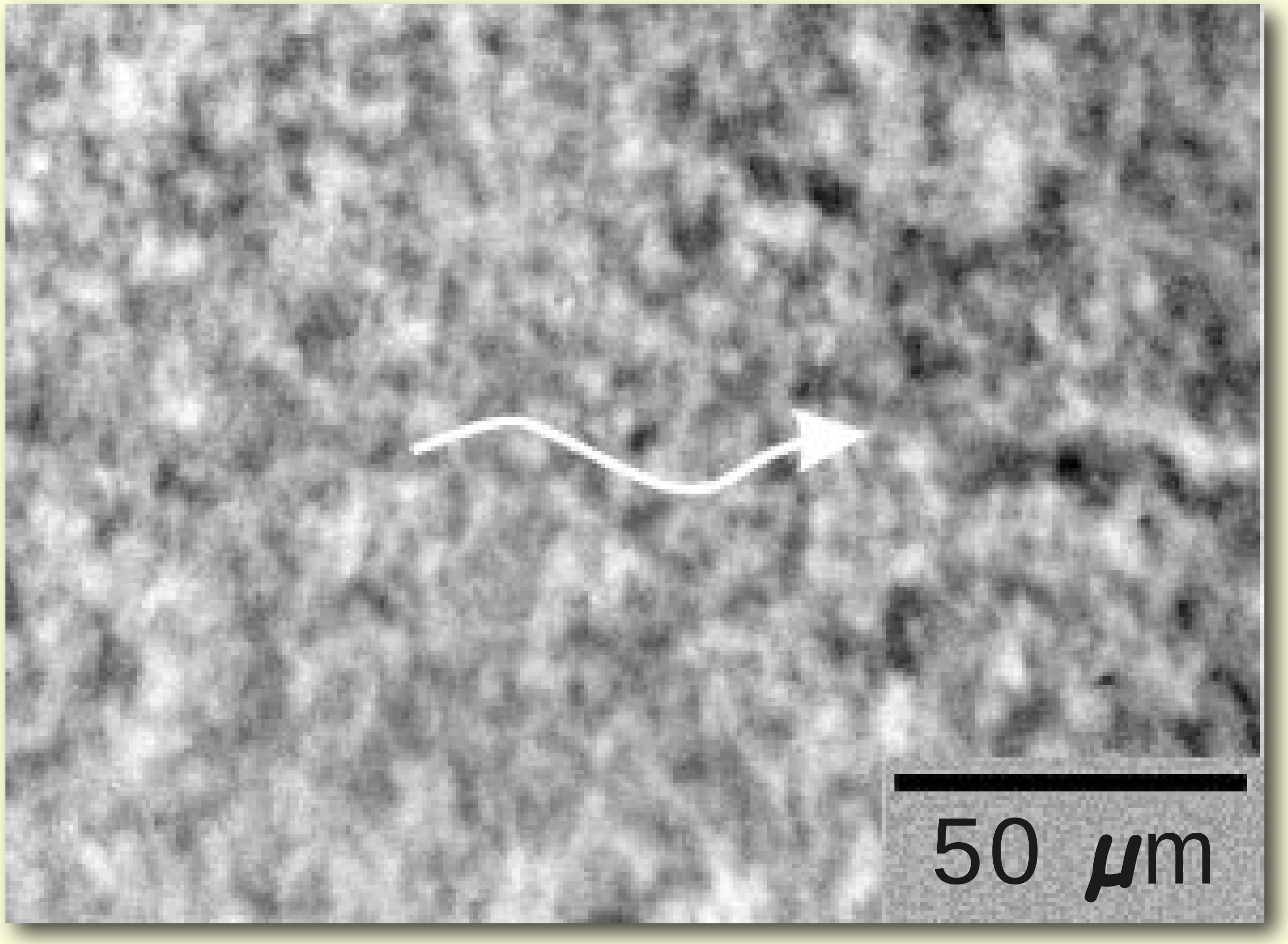

low induced anisotropy

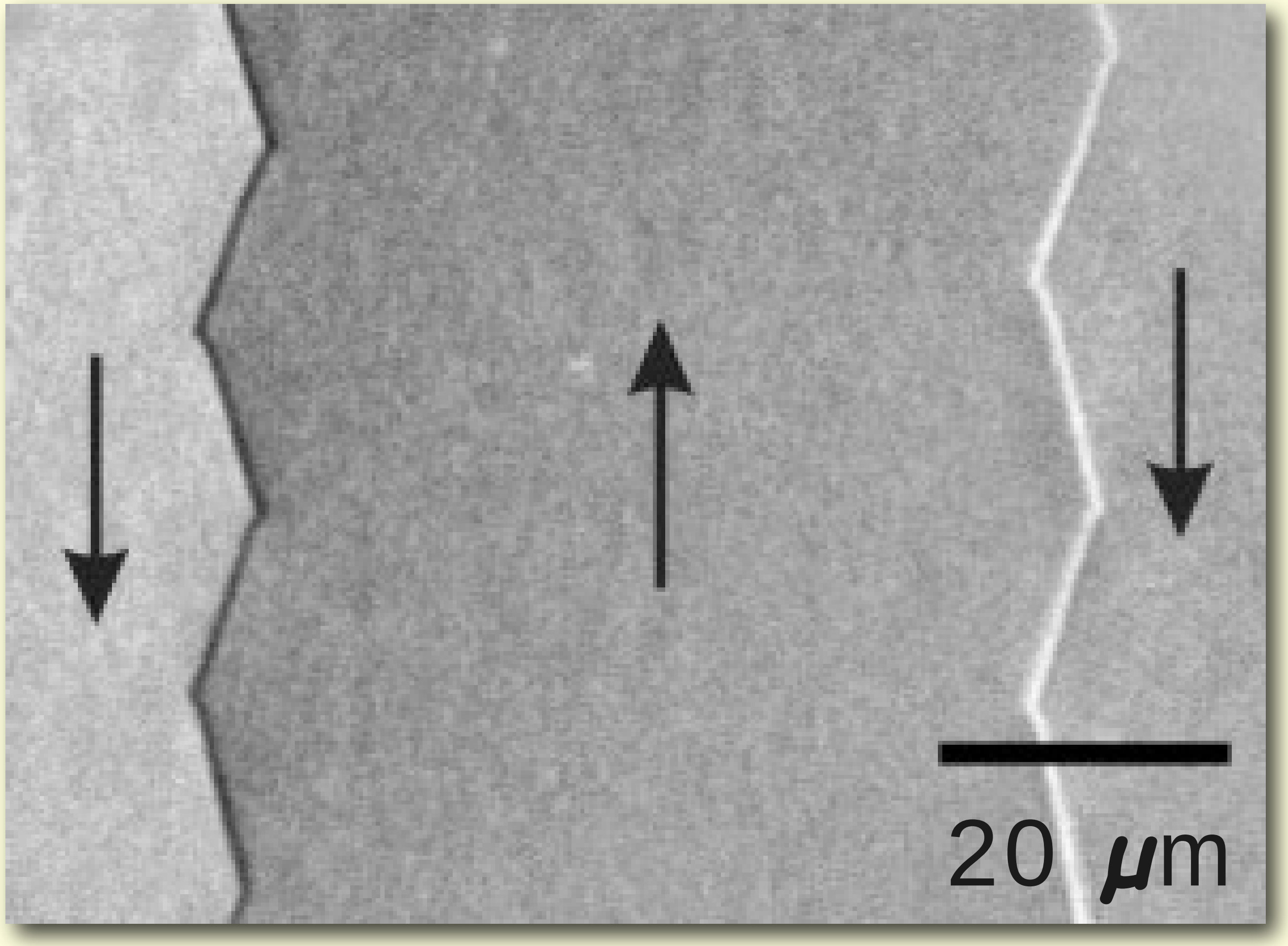

strong creep-induced anisotropy

Interplay random/induced anisotropy

Nanocryst. core with longitudinal anisotropy

$K_u = 5$ J/m^3 (weak)

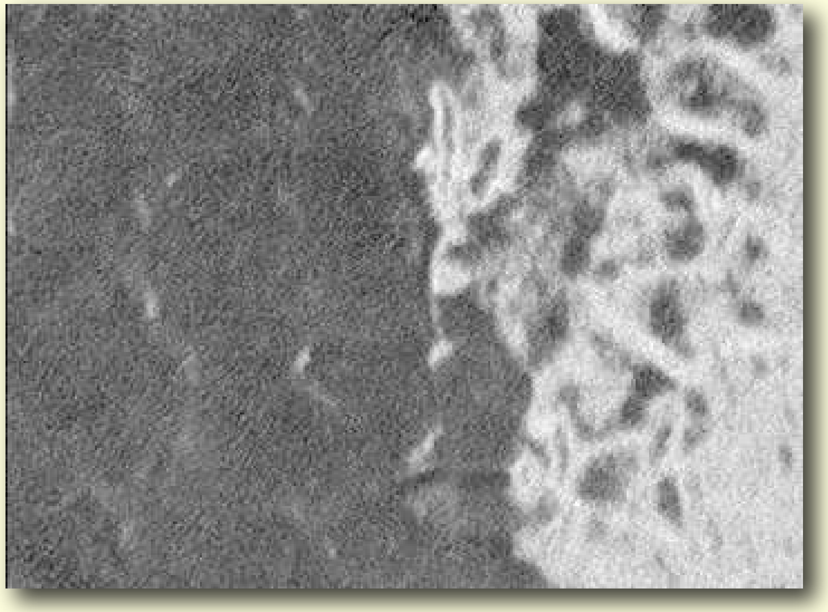

$K_u = 10$ J/m^3 (moderate)

$K_u = 29$ J/m^3 (strong)

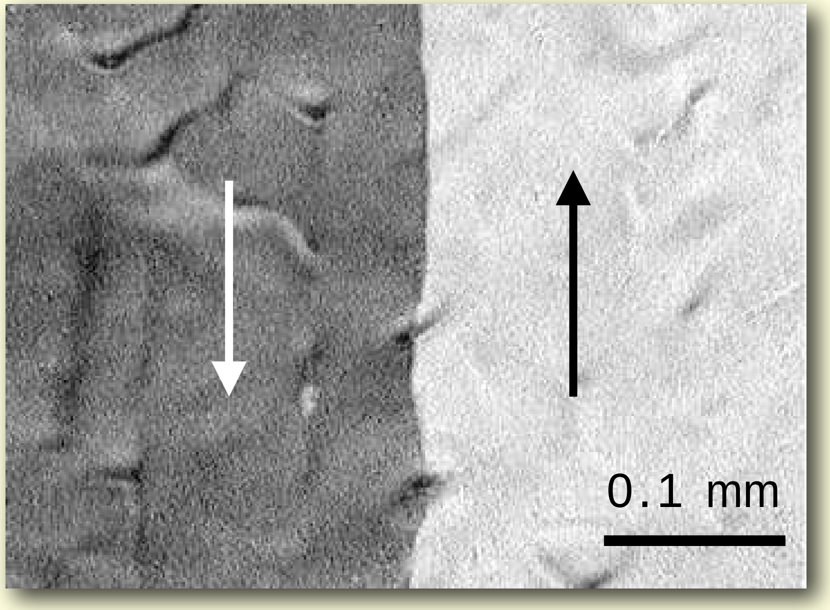

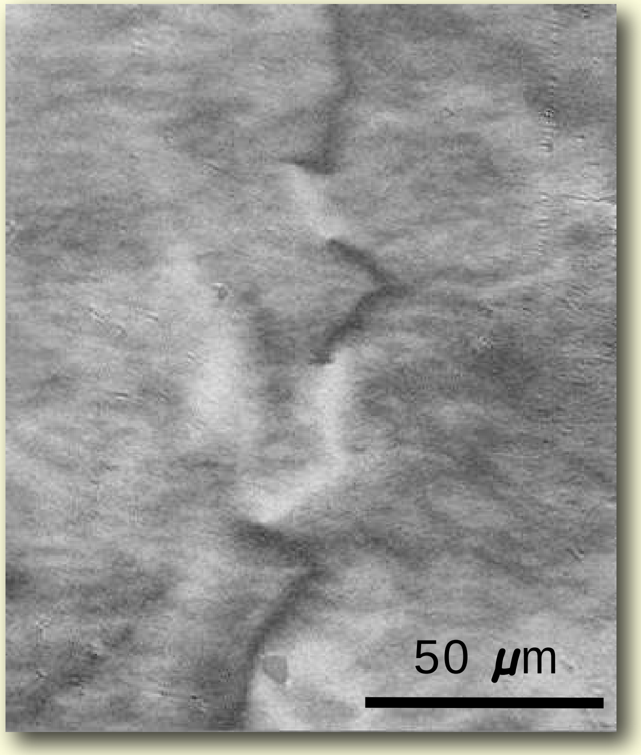

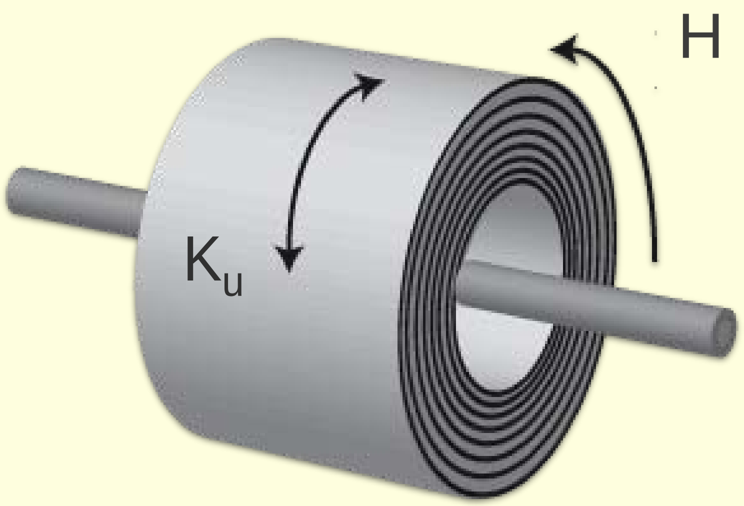

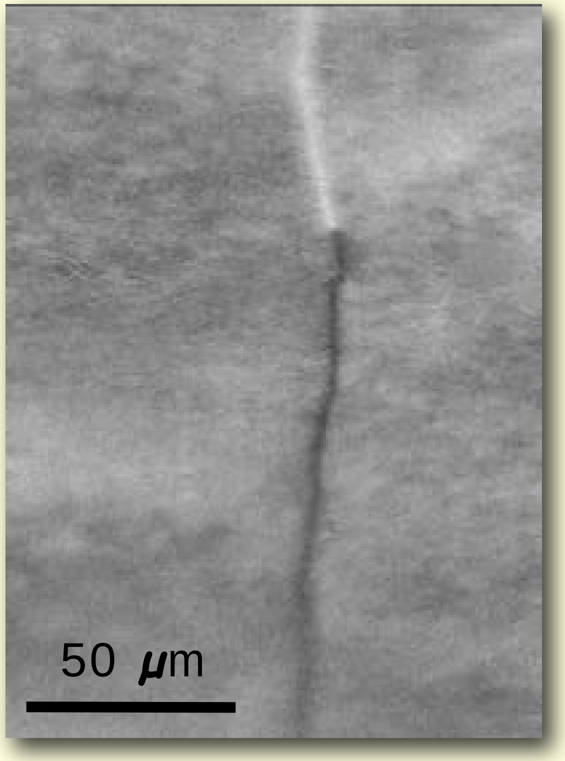

Nanocryst. core with transverse anis.

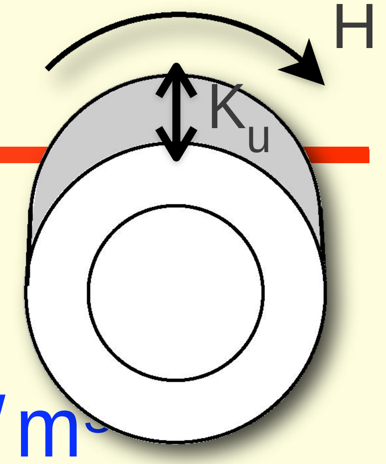

— decreasing induced transverse anisotropy →

K_u = 33 J/m³	7.7 J/m³	2.3 J/m³	0.6 J/m³
μ_{15} = 22.000	86.200	274.500	559.900

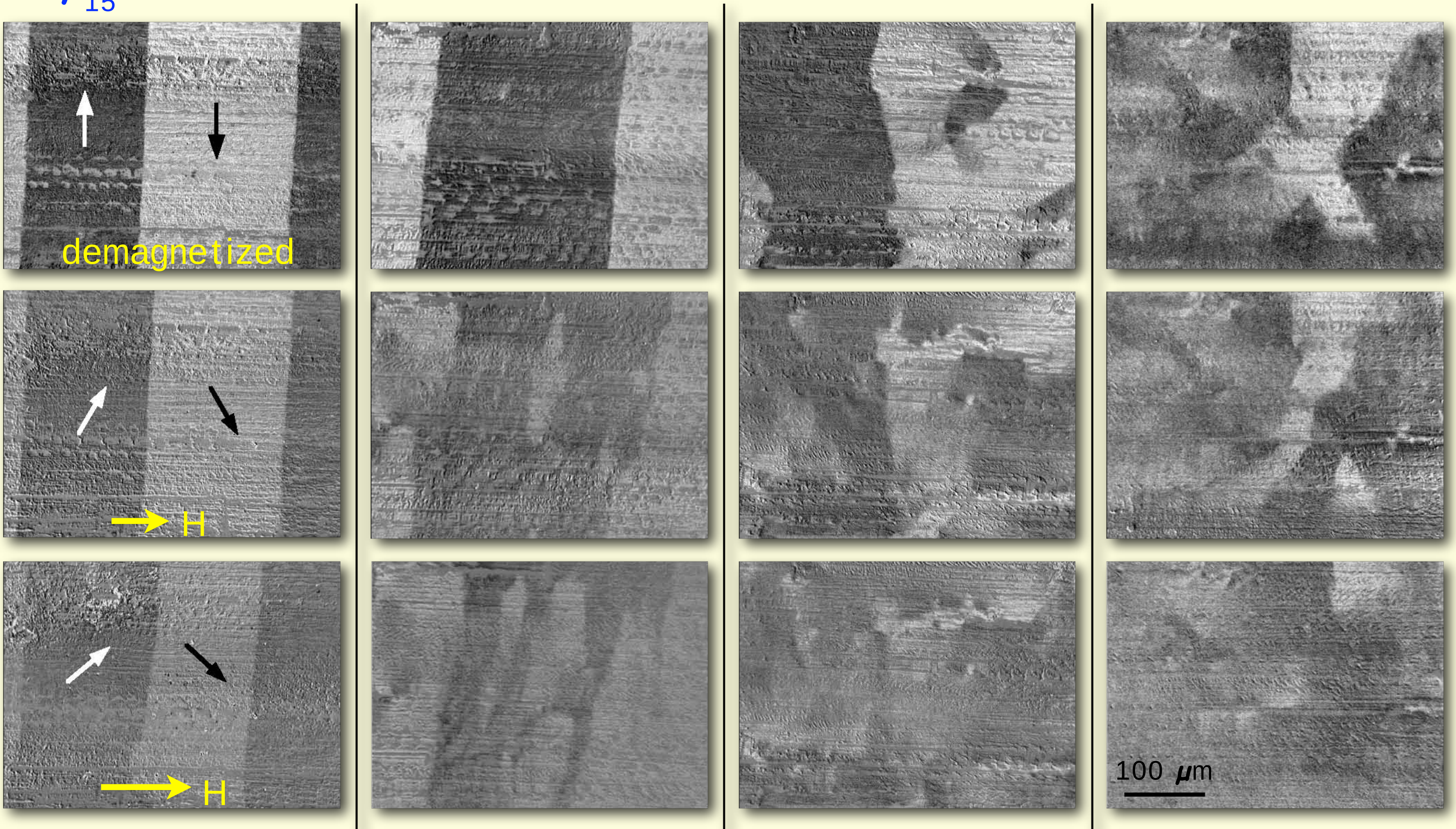

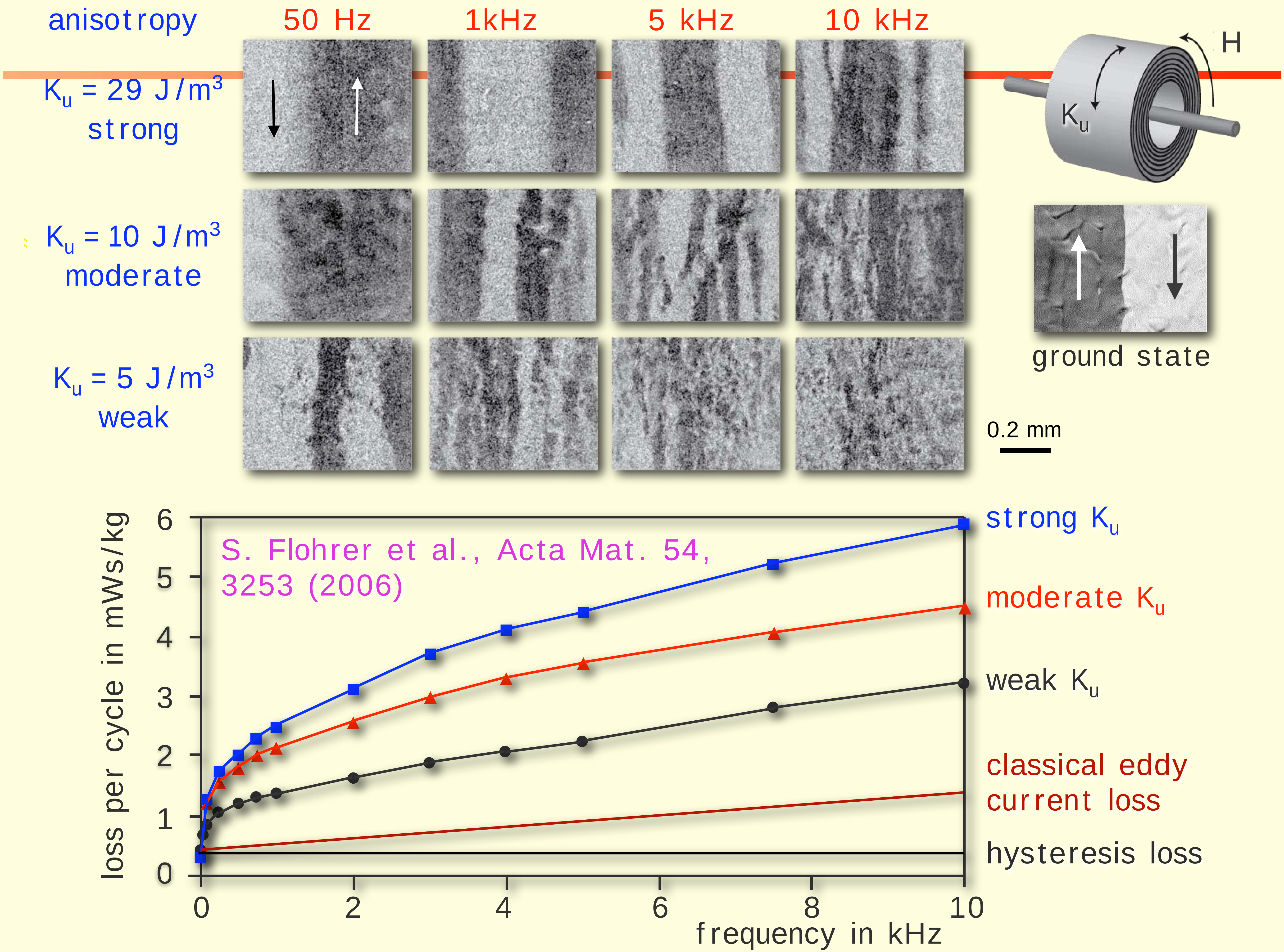

anisotropy
50 Hz
1kHz
5 kHz
10 kHz
H
K_u = 29 J/m^3
strong
K_u
K_u = 10 J/m^3
moderate
ground state
K_u = 5 J/m^3
weak
0.2 mm
S. Flohrer et al., Acta Mat. 54, 3253 (2006)
loss per cycle in mWs/kg
frequency in kHz
strong K_u
moderate K_u
weak K_u
classical eddy current loss
hysteresis loss
0
1
2
3
4
5
6
0
2
4
6
8
10

Heating above T_{Curie} of amorphous phase

$$\langle K_1 \rangle \sim \frac{K_1}{\sqrt{N}}$$

N: number of grains within correlation volume

low induced anisotropy
(K_u = 3 J/m^3)

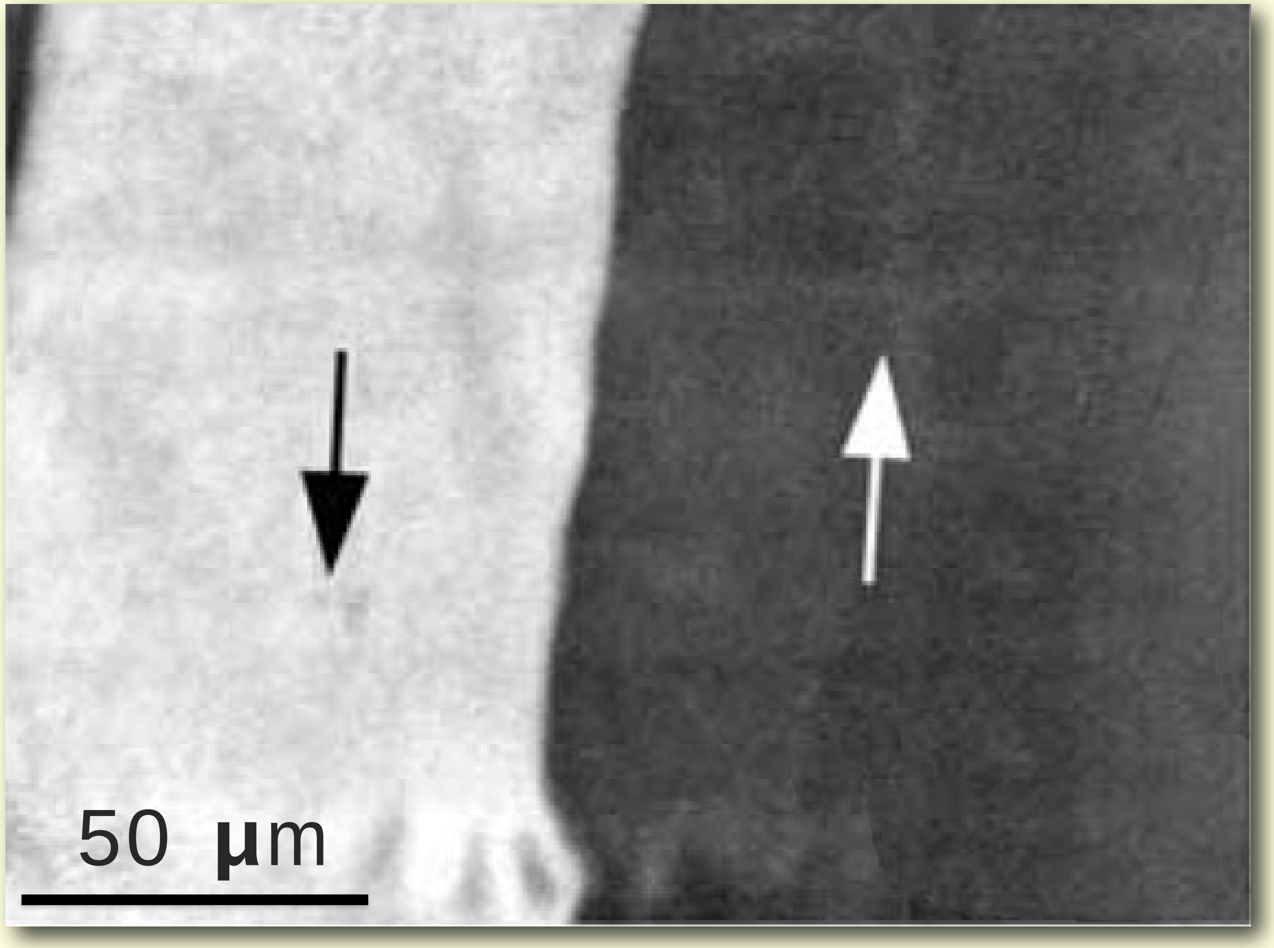

strong induced anisotropy
(K_u = 30 J/m^3)

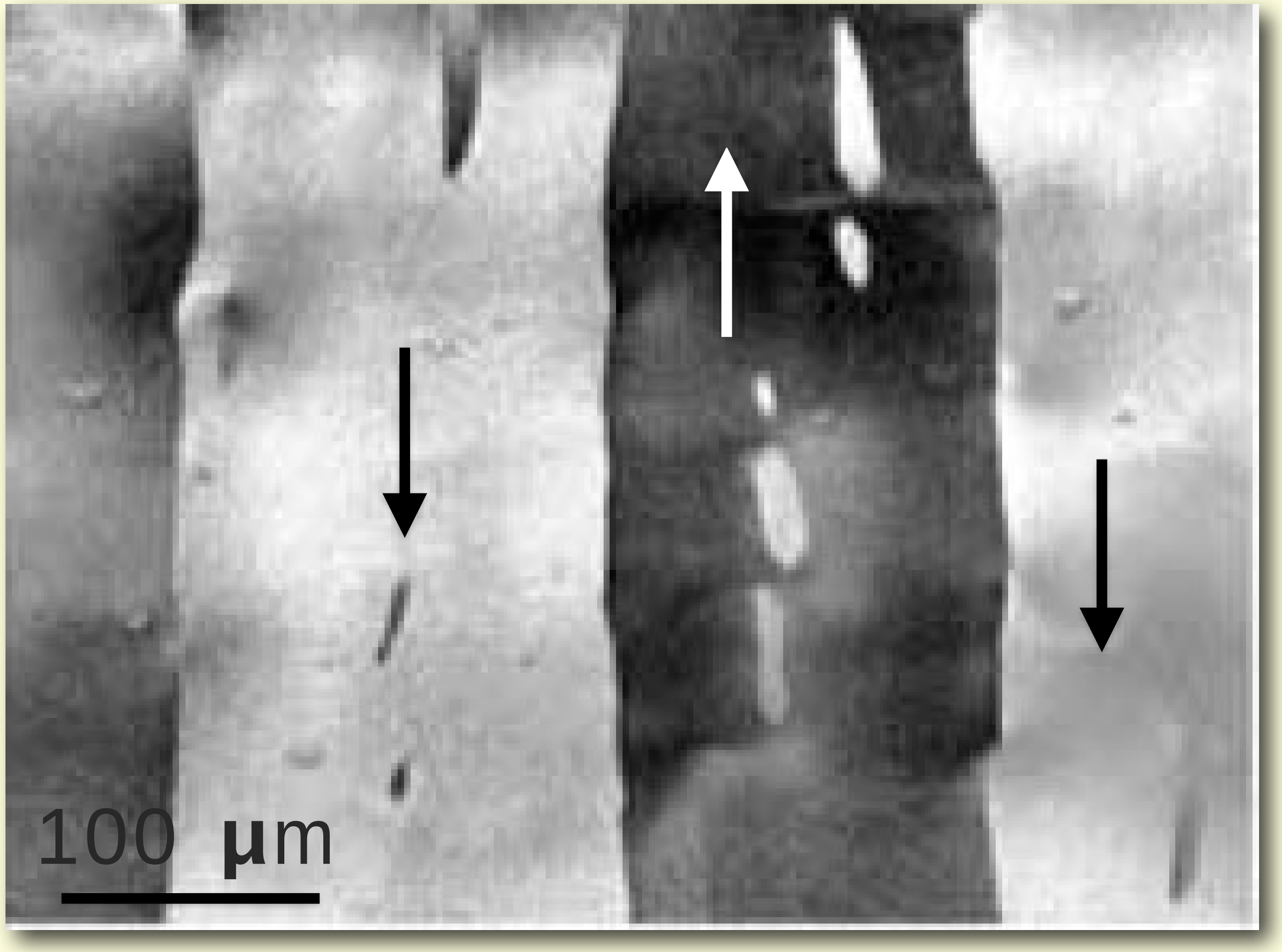

room temperature

Heating above T_{Curie} of amorphous phase

$$\langle K_1 \rangle \sim \frac{K_1}{\sqrt{N}}$$

N: number of grains within correlation volume

low induced anisotropy
(K_u = 3 J/m^3)

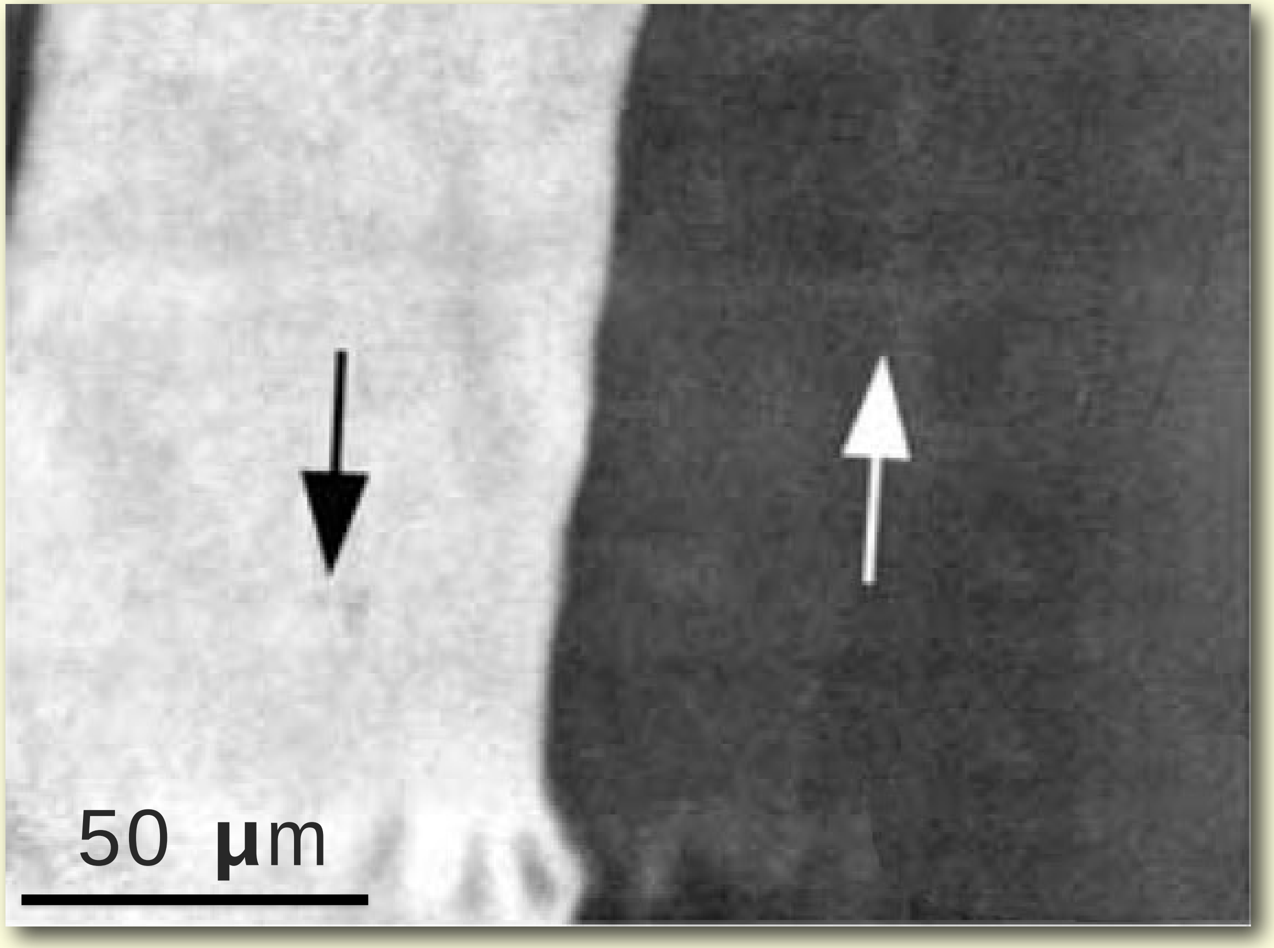

strong induced anisotropy
(K_u = 30 J/m^3)

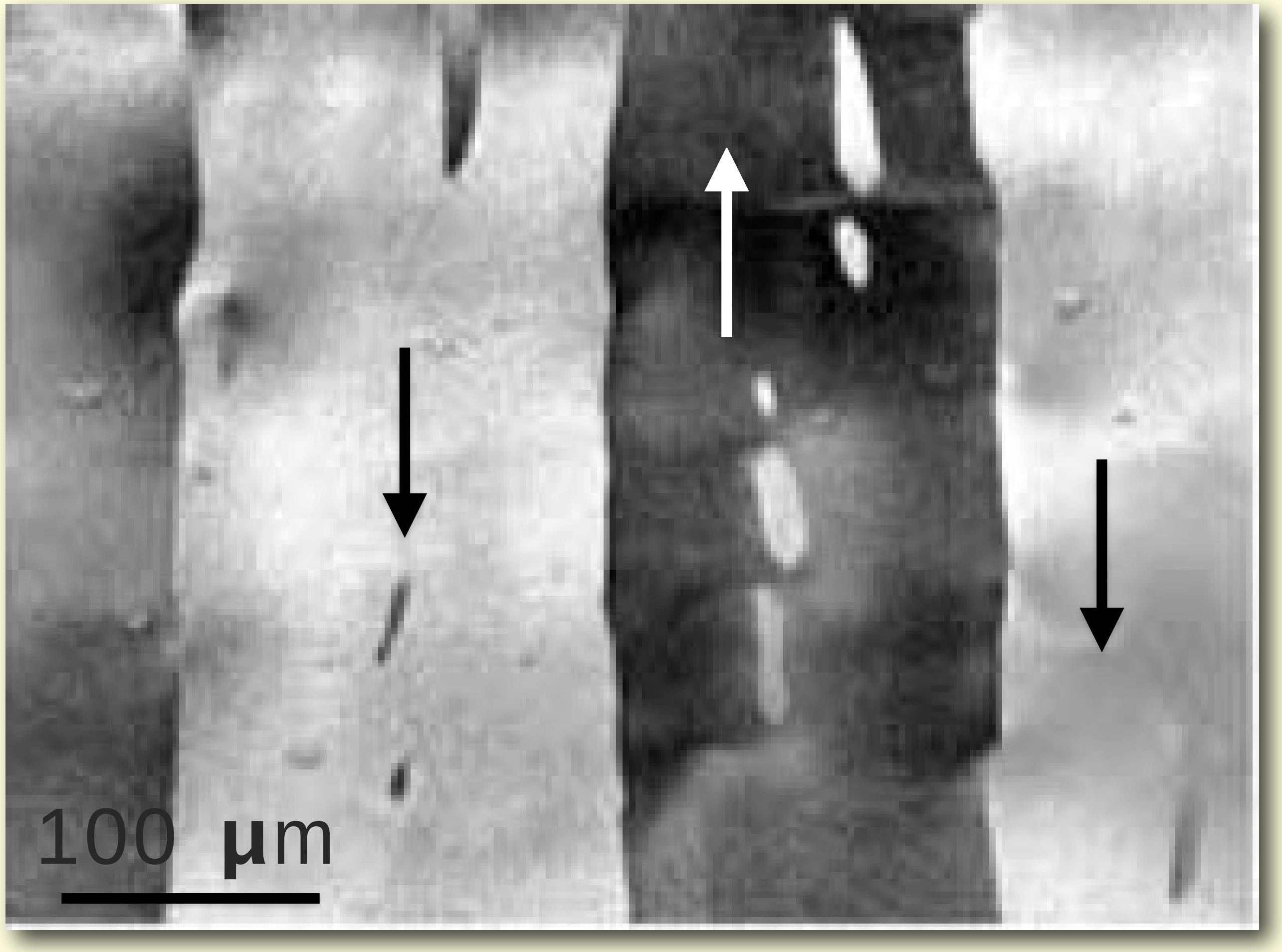

Heating above T_{Curie} of amorphous phase

$$\langle K_1 \rangle \sim \frac{K_1}{\sqrt{N}}$$

N: number of grains within correlation volume

low induced anisotropy
(K_u = 3 J/m^3)

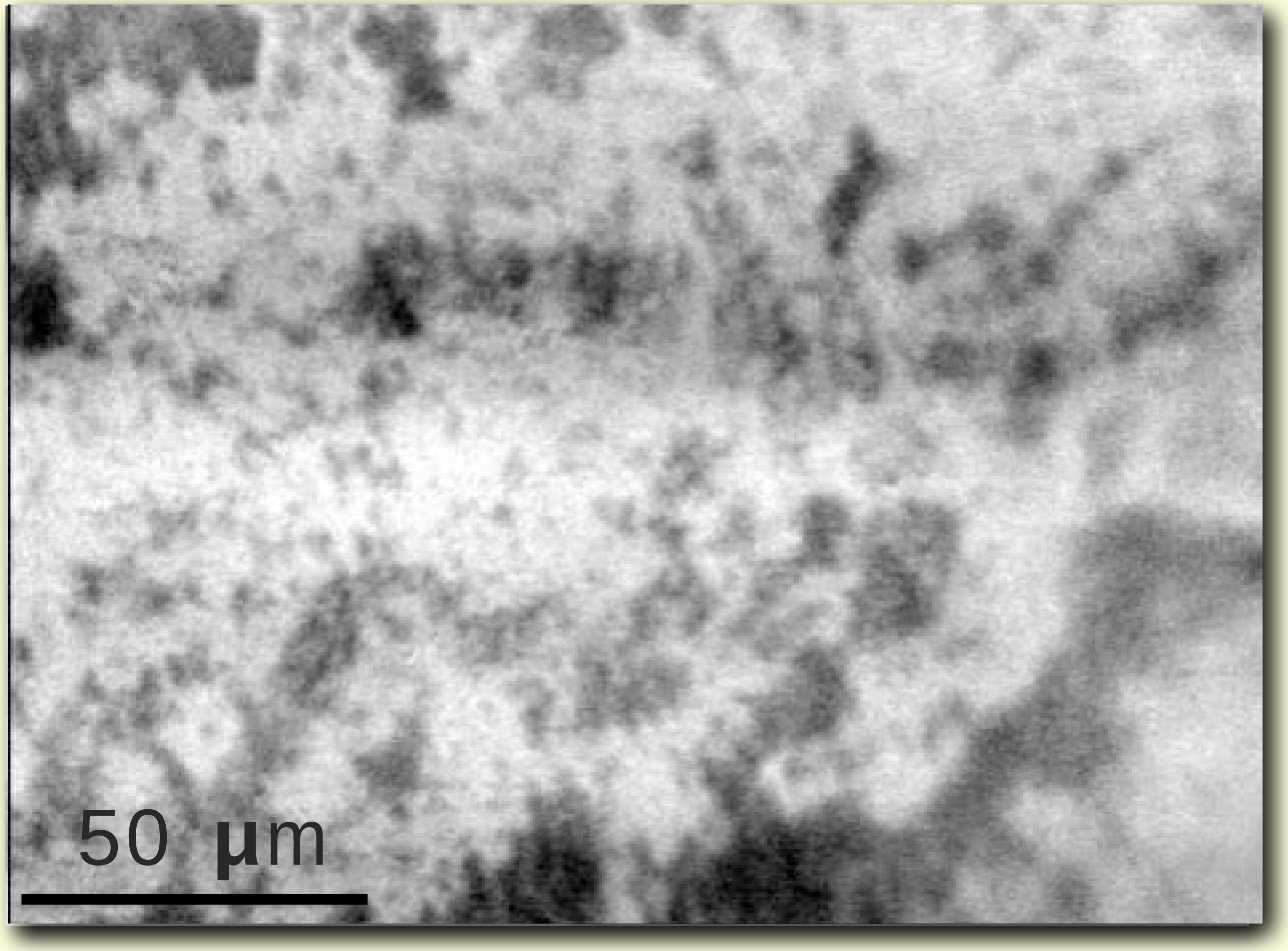

strong induced anisotropy
(K_u = 30 J/m^3)

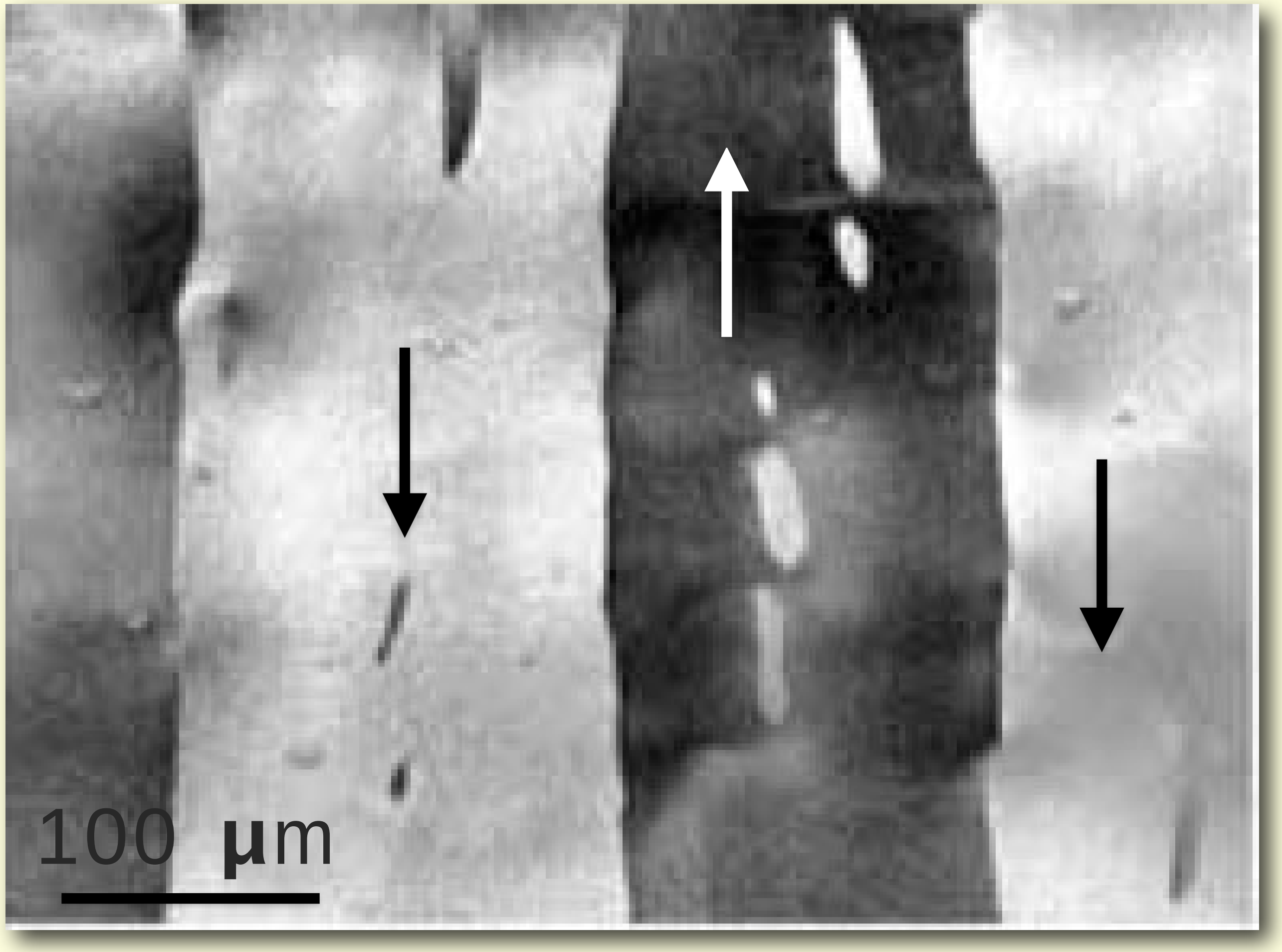

350°C

Heating above T_{Curie} of amorphous phase

$$\langle K_1 \rangle \sim \frac{K_1}{\sqrt{N}}$$

N: number of grains within correlation volume

low induced anisotropy (K_u = 3 J/m^3)

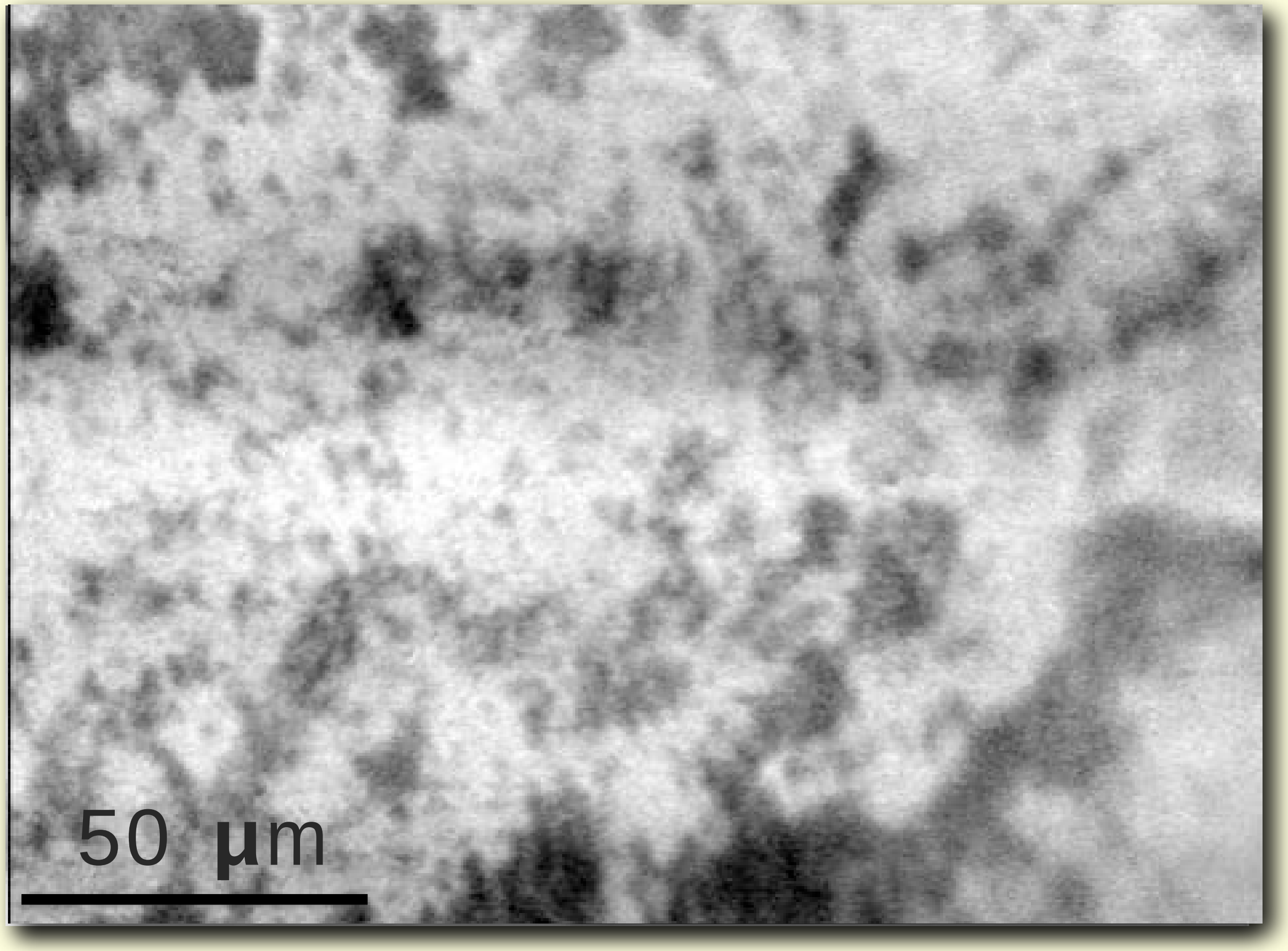

350°C

strong induced anisotropy (K_u = 30 J/m^3)

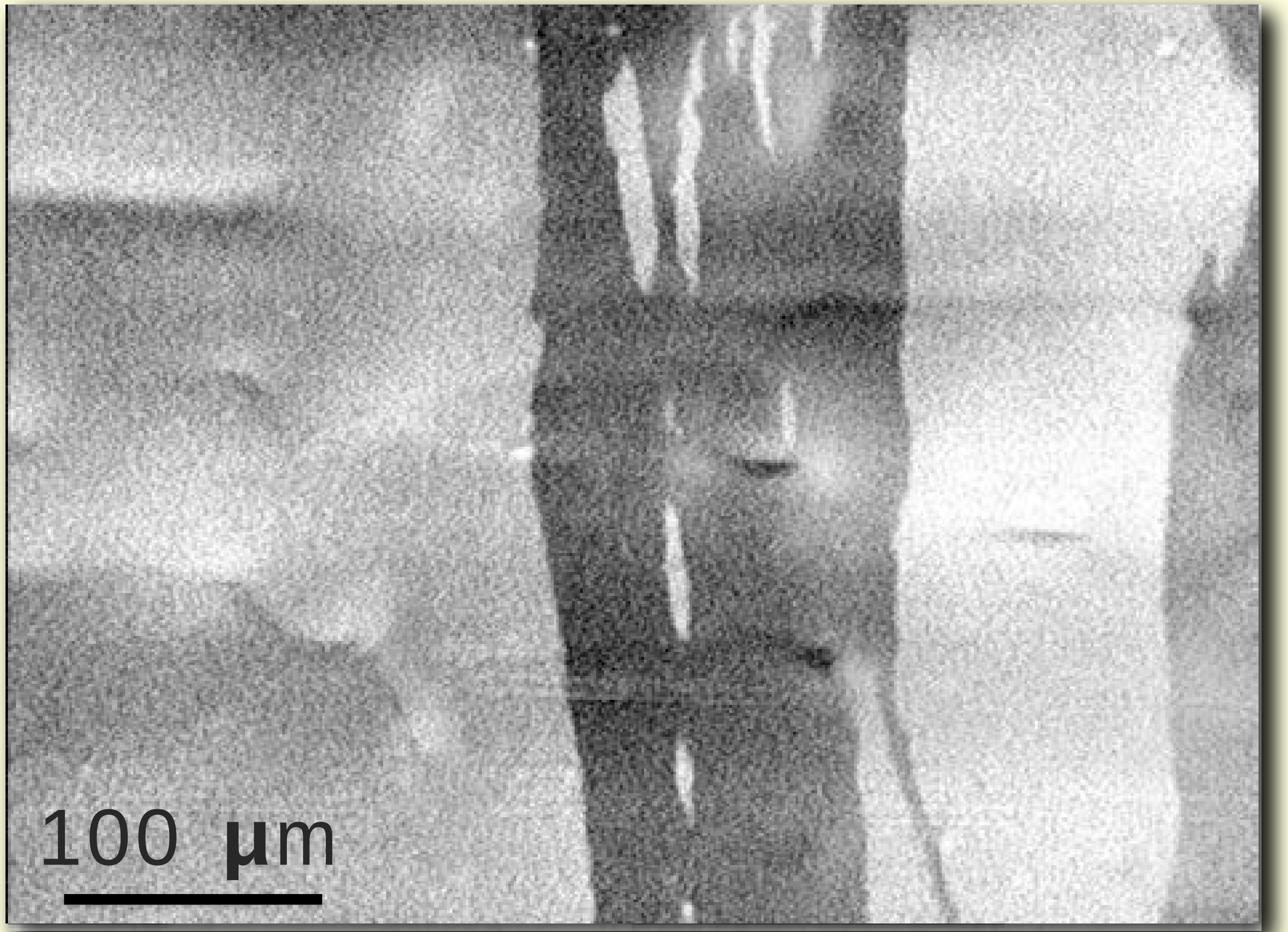

550°C

$Co_{45}Fe_{28.5}Si_{13.5}B_9Cu_1Nb_3$

$$\langle K_1 \rangle \sim \frac{K_1}{\sqrt{N}}$$

increases anisotropy of grains

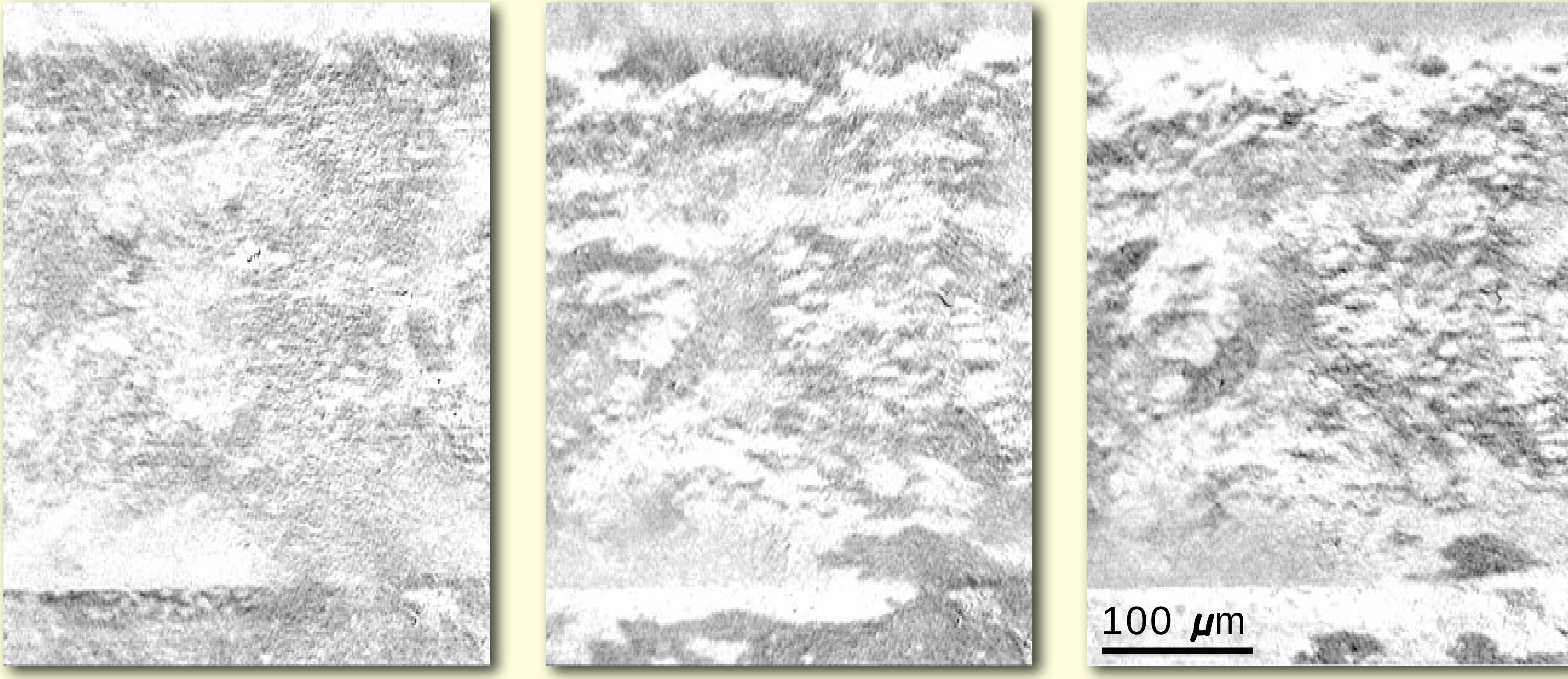

H = –0.15 kA/m | +0.11 kA/m | +0.14 kA/m

ribbon axis and field direction

sample: Pilar Marin, Madrid

Patches and ripple

Nanocrystalline $Fe_{84}Zr_{3.5}Nb_{3.5}B_8Cu_1$

20 μm thick

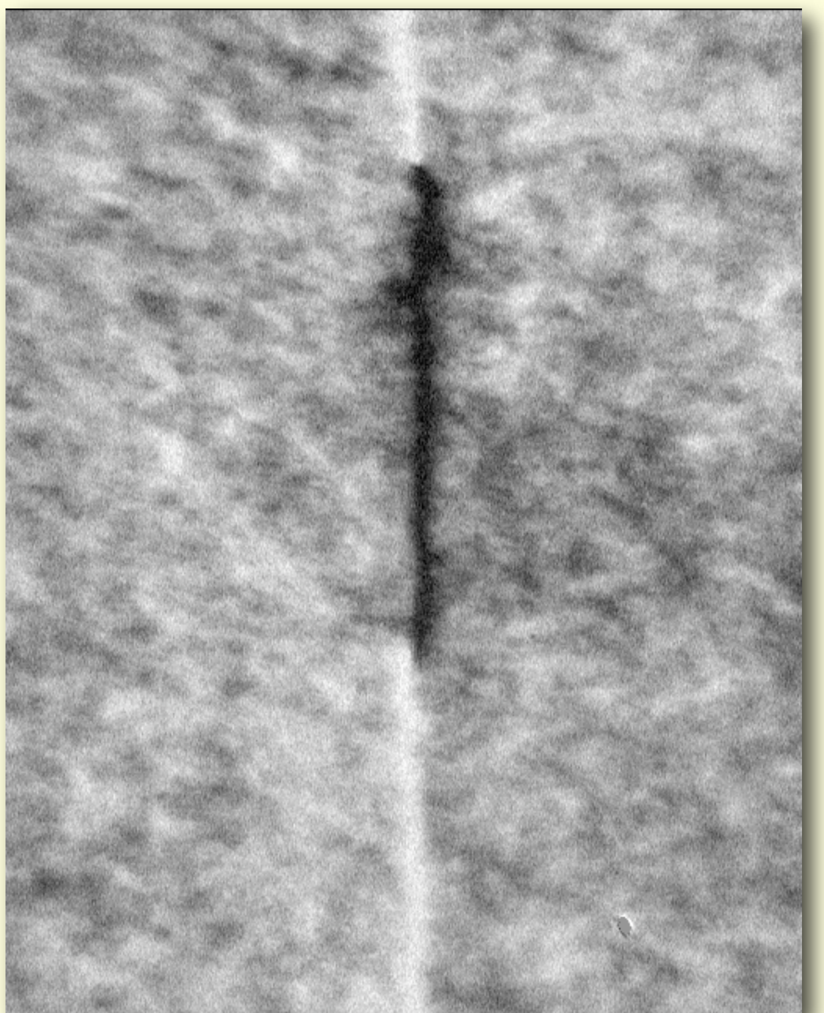

patches

thinned to μm

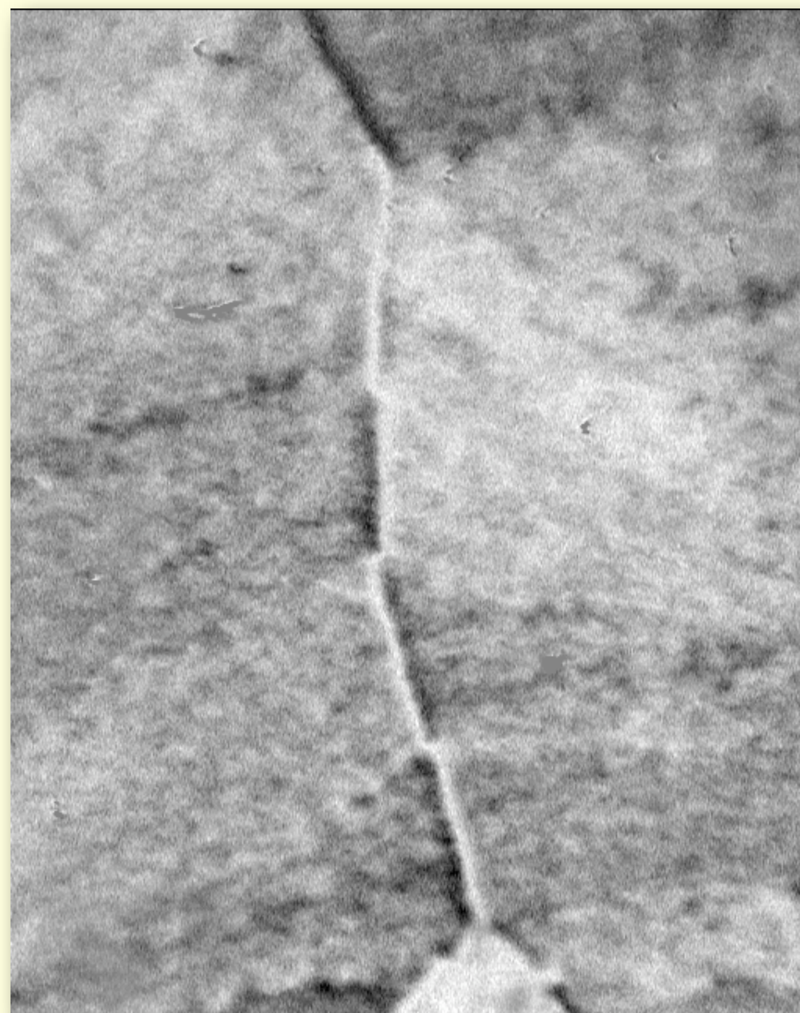

still thinner

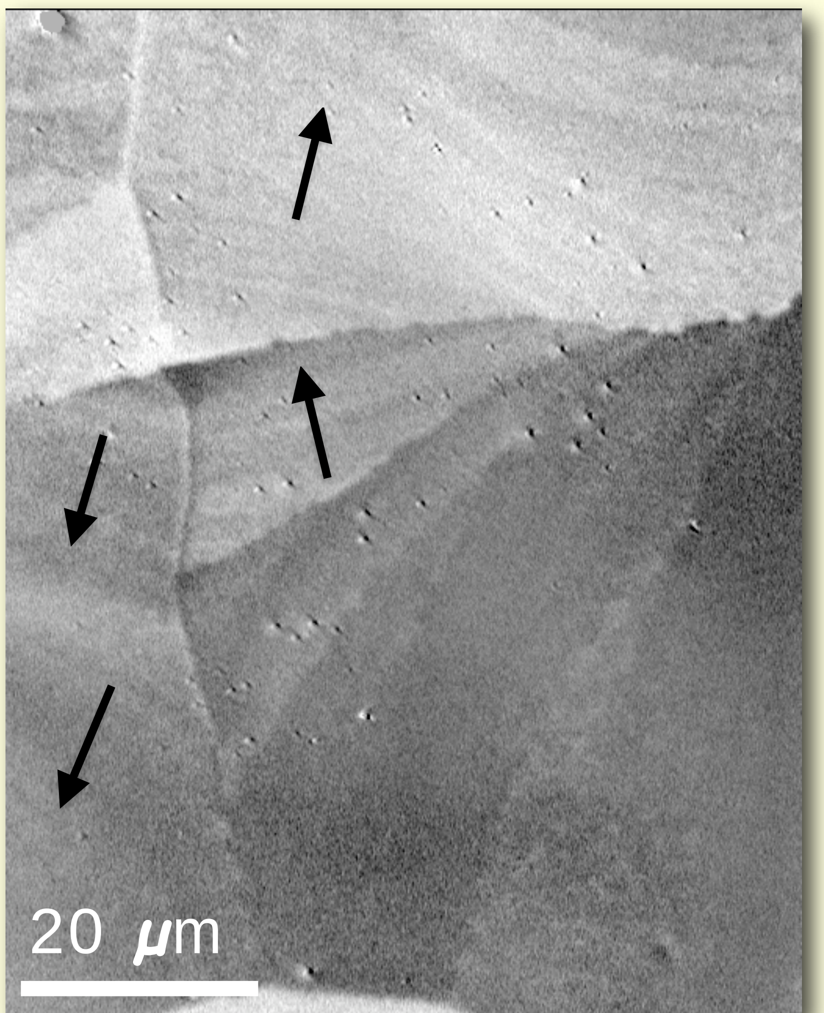

ripple

Excursion:

Ripple phenomenon

Ripple phenomenon: development

Cobalt (42 nm thick)

H = 0.5 H_k H = 0.15 H_k H = 0

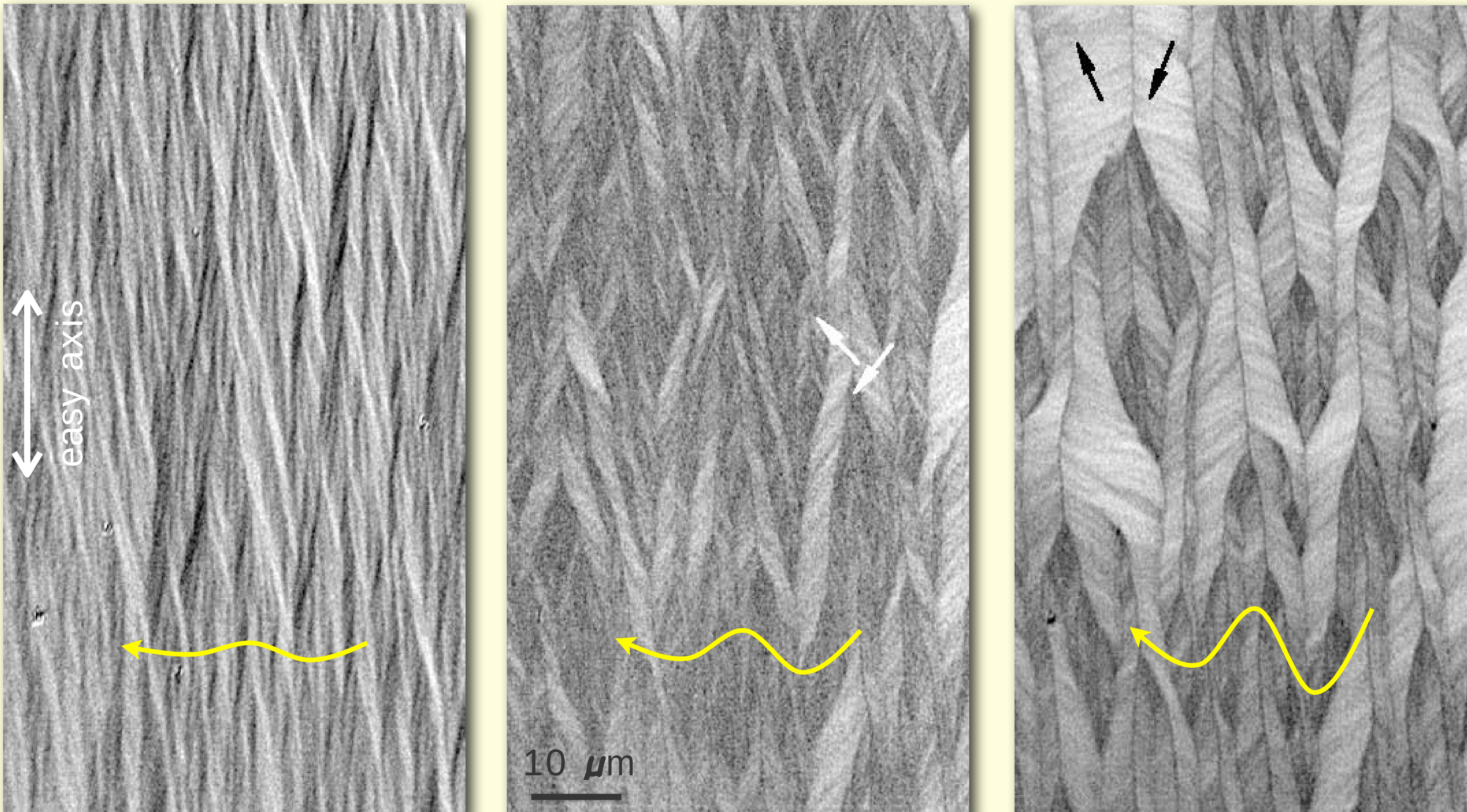

Ripple phenomenon: development

C thick)

$H = 0.5\ H_k$

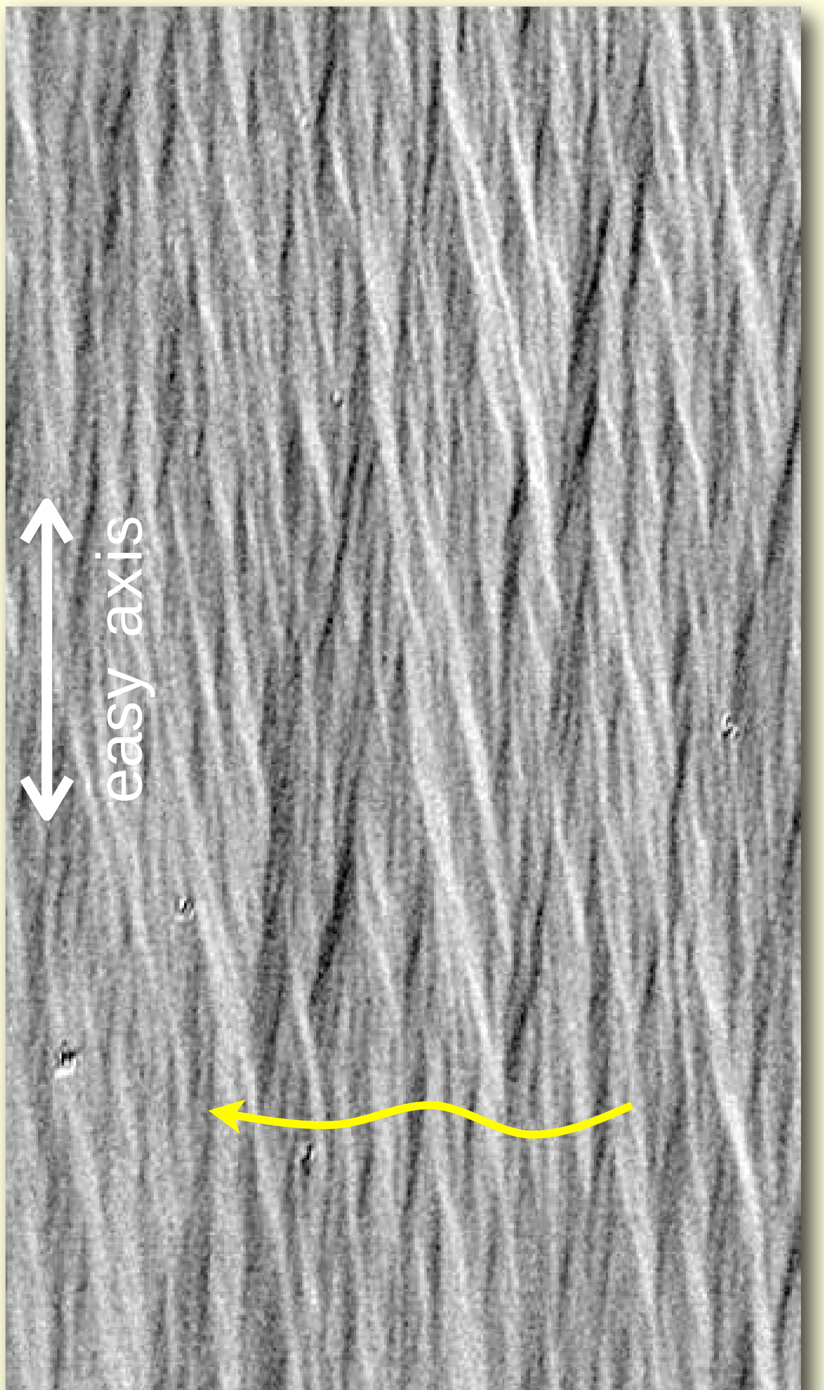

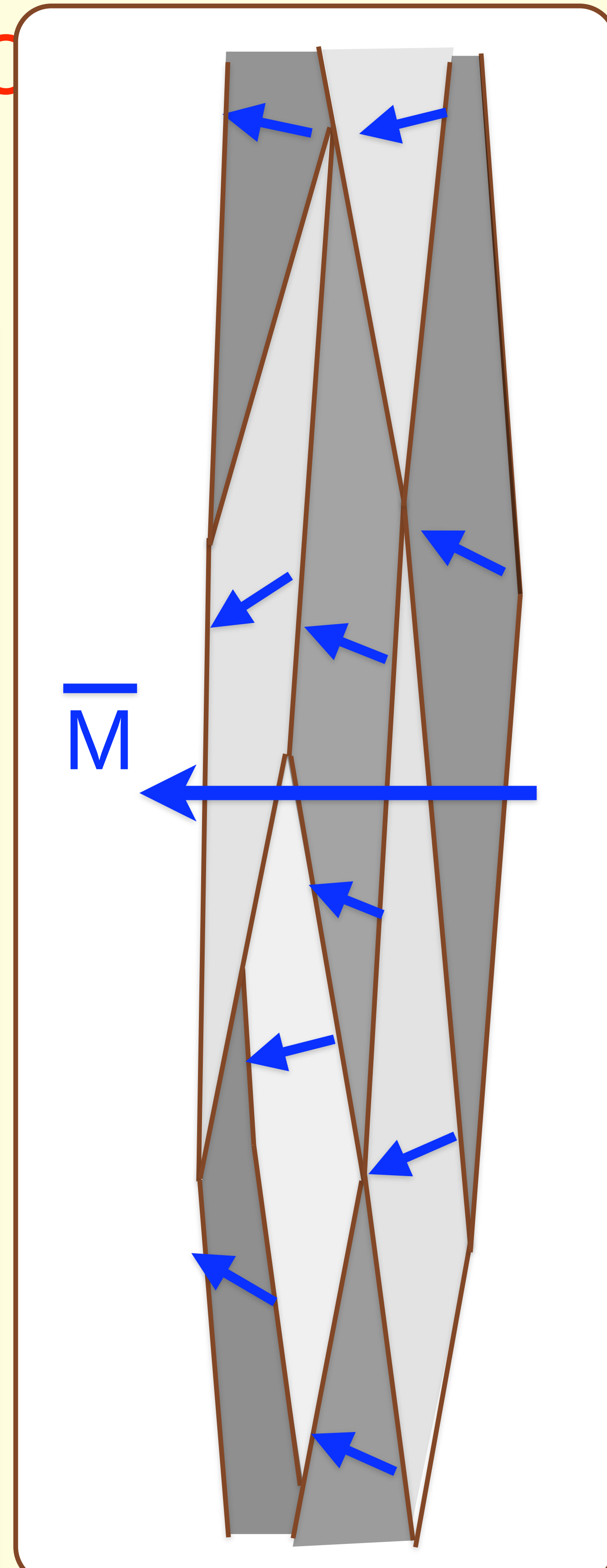

$H = 0$

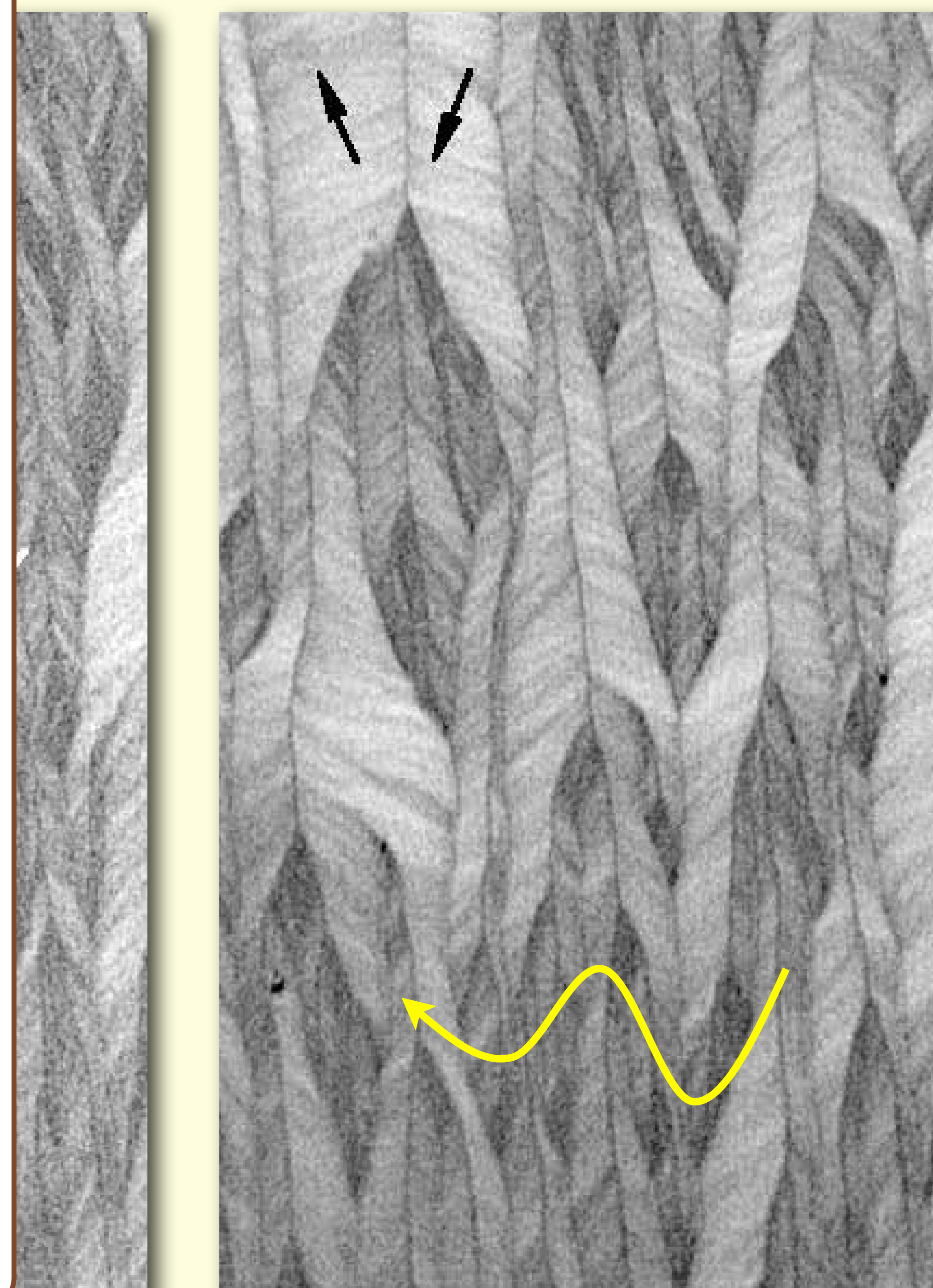

Ripple phenomenon: development

C thick)

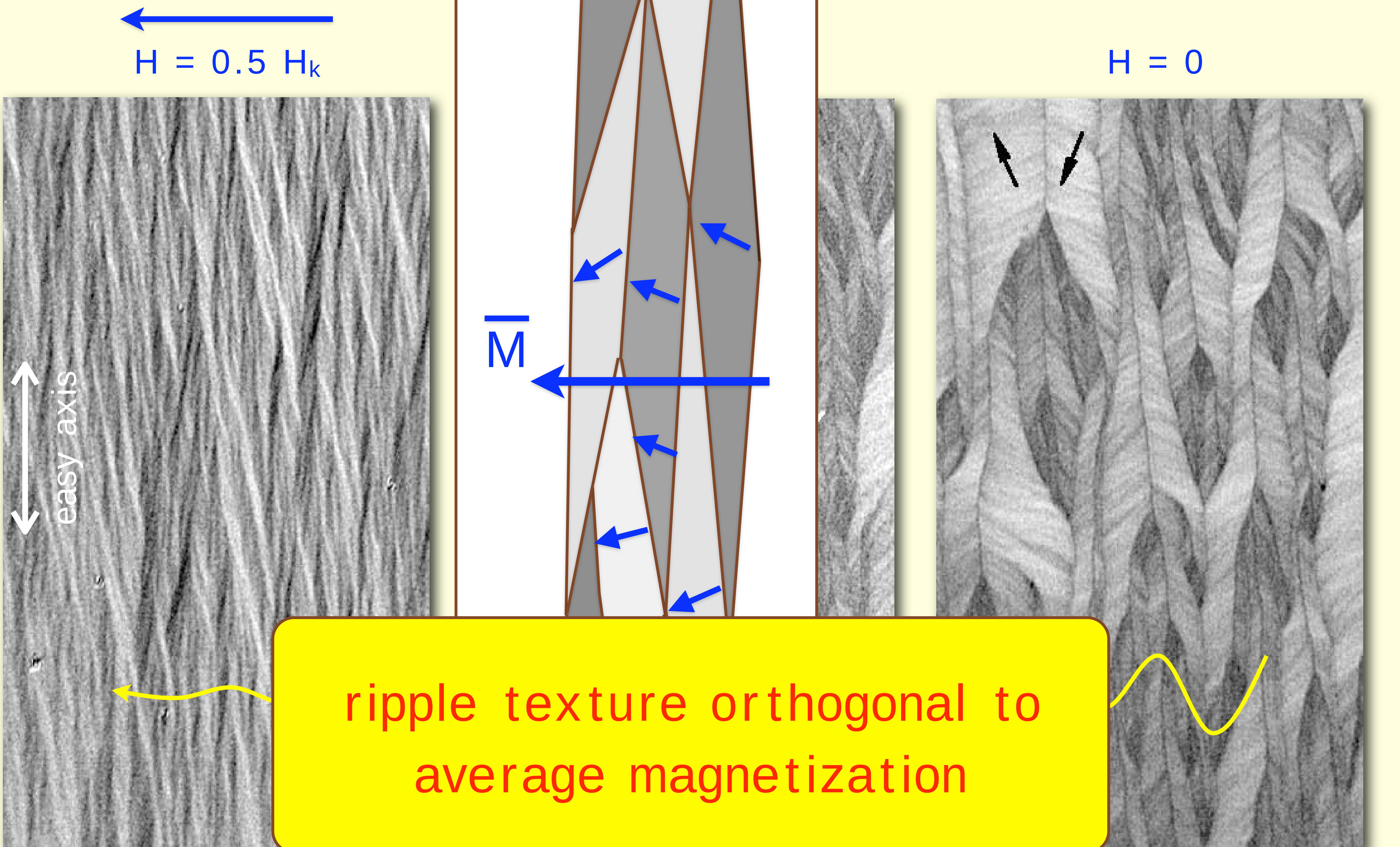

Ripple phenomenon: development

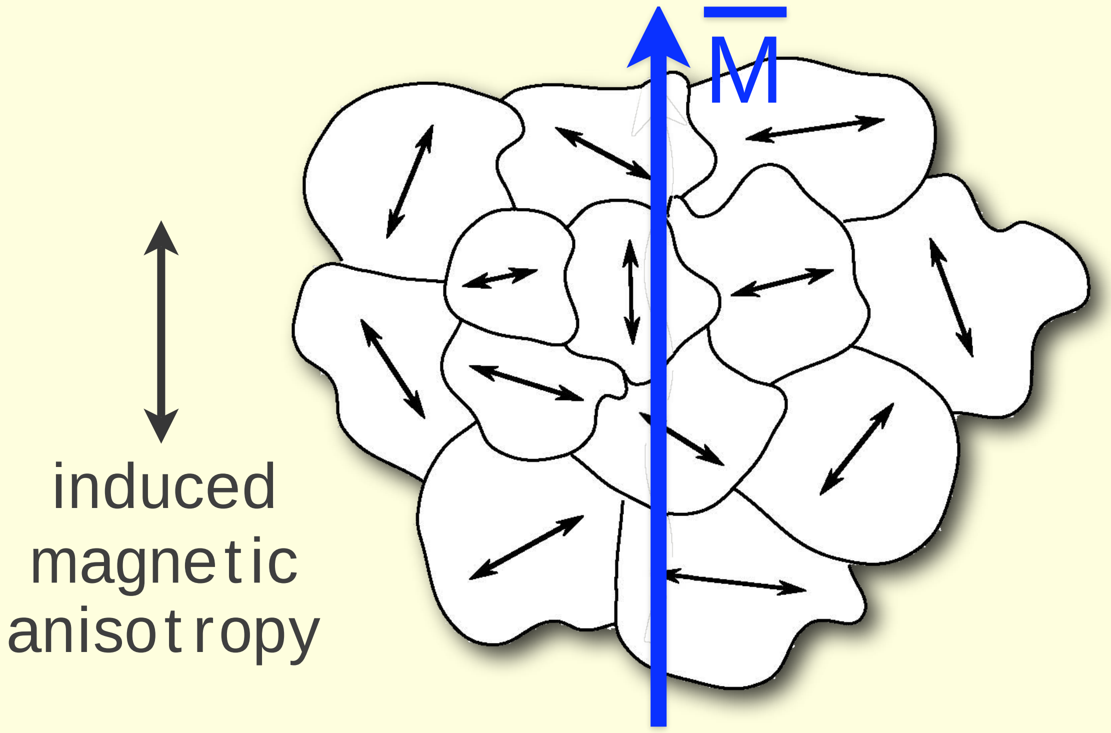

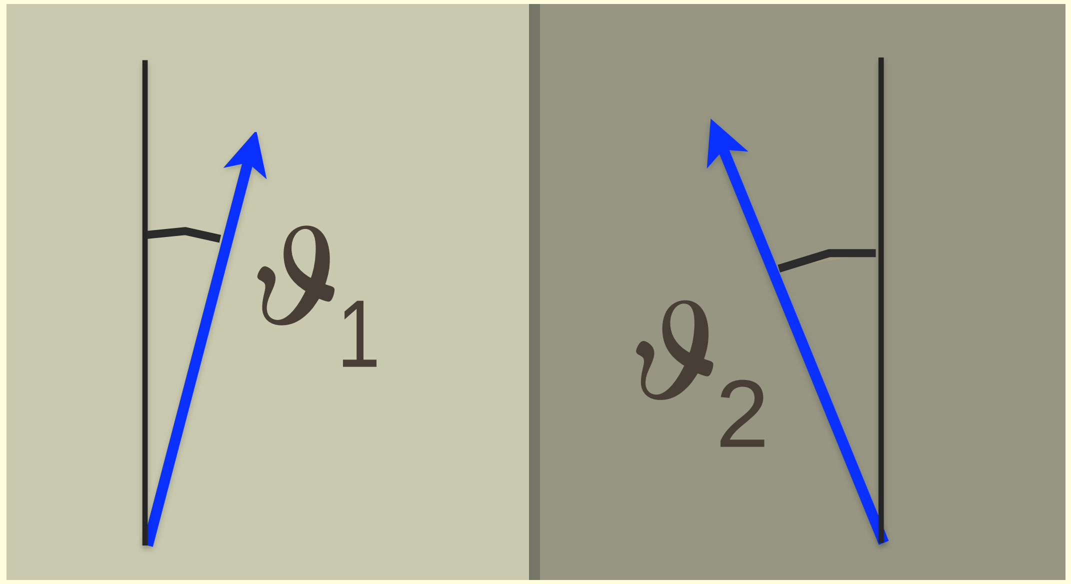

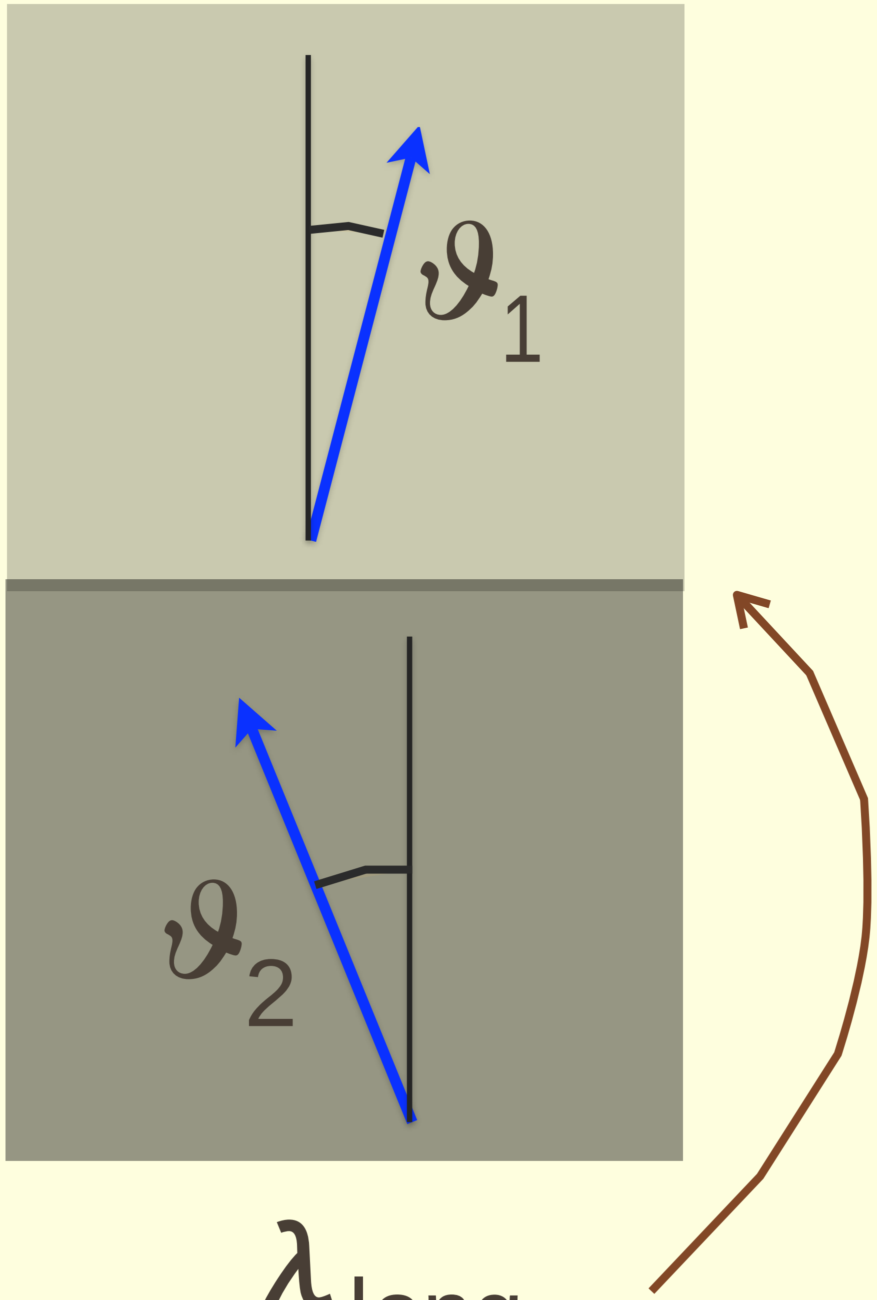

$$\lambda_{trans} = \sin\vartheta_1 - \sin\vartheta_2$$

$$\lambda_{long} = \cos\vartheta_1 - \cos\vartheta_2$$

Ripple phenomenon: development

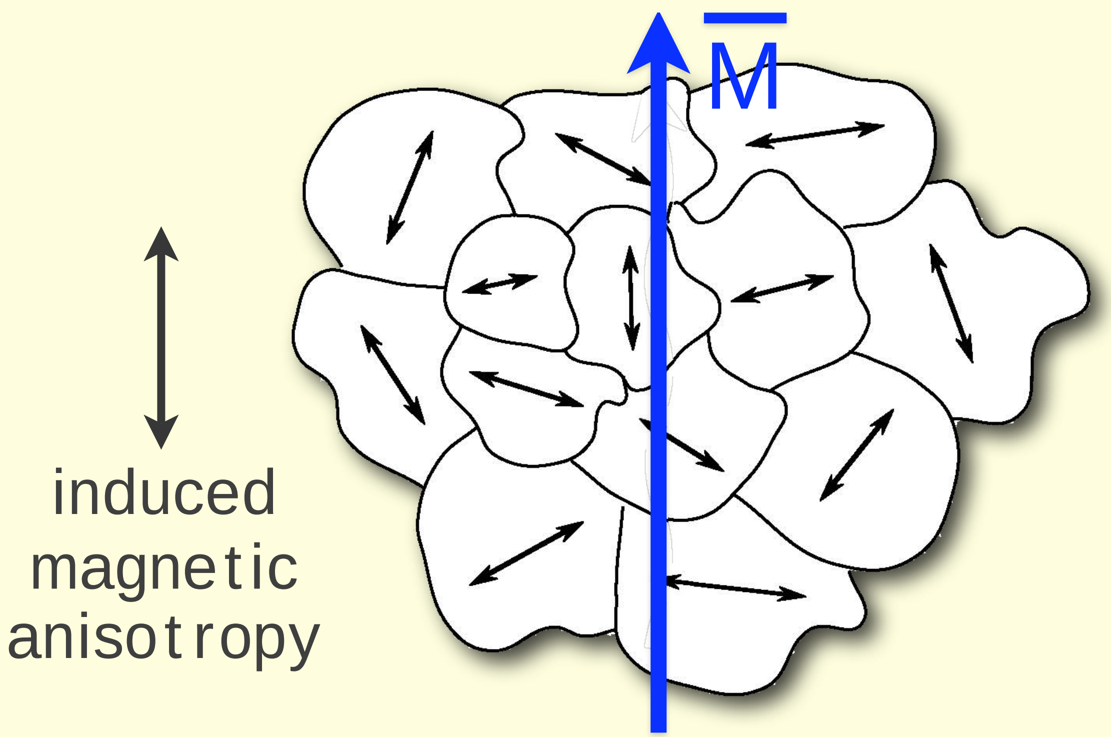

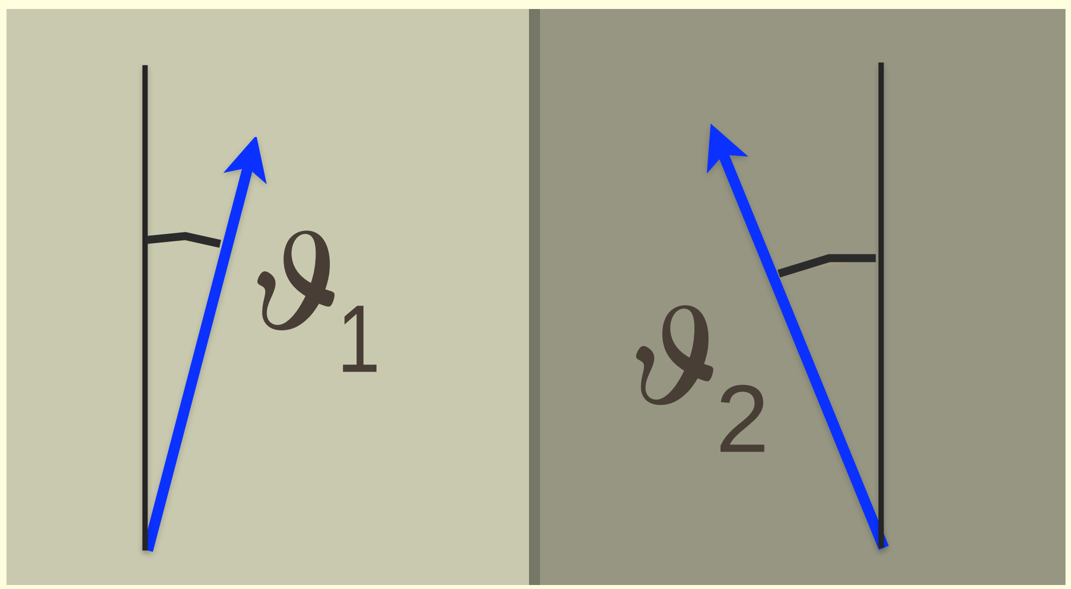

$$\lambda_{trans} = \sin\vartheta_1 - \sin\vartheta_2$$

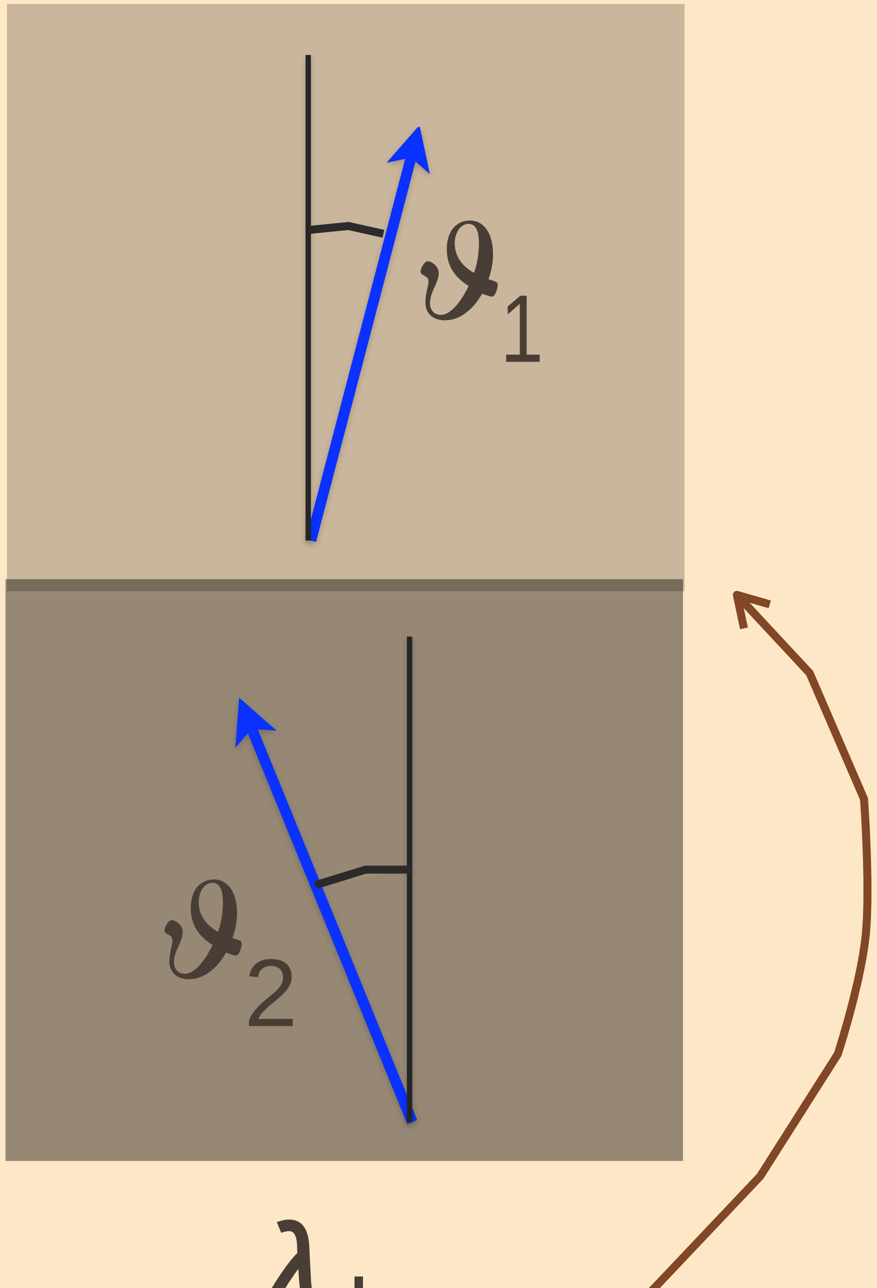

$$\lambda_{long} = \cos\vartheta_1 - \cos\vartheta_2$$

Ripple and patches

ripple in films

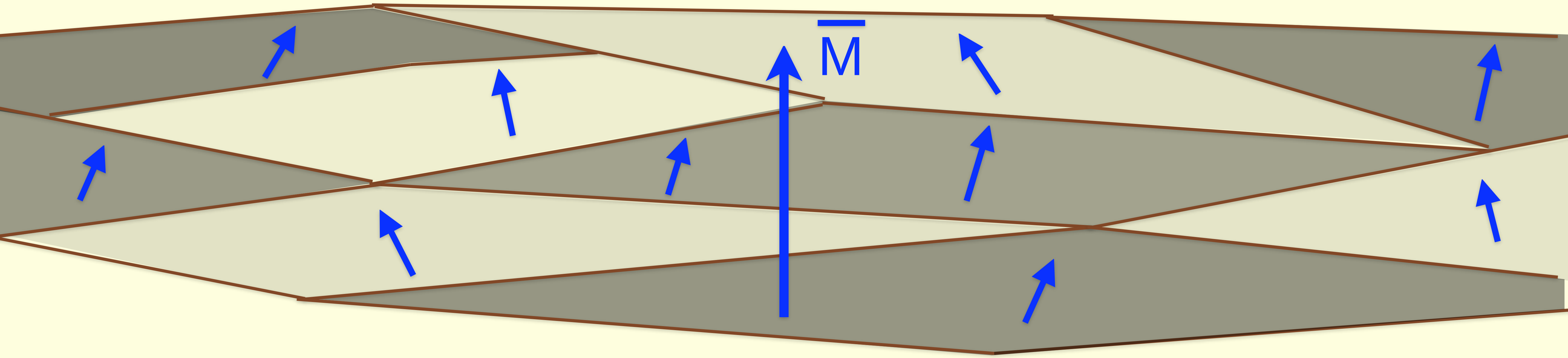

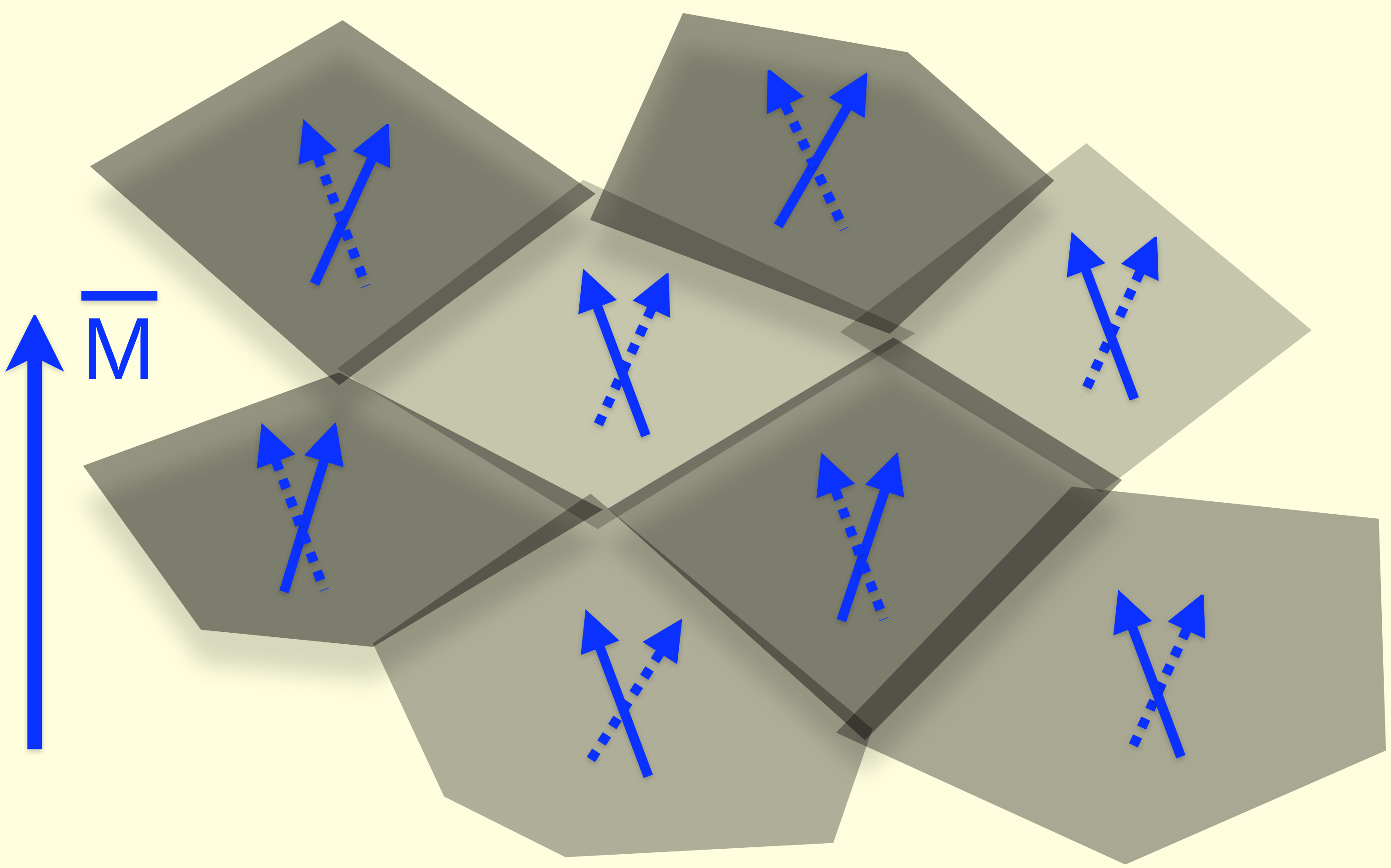

patches in
thick materials

Patches and ripple

20 μm thick

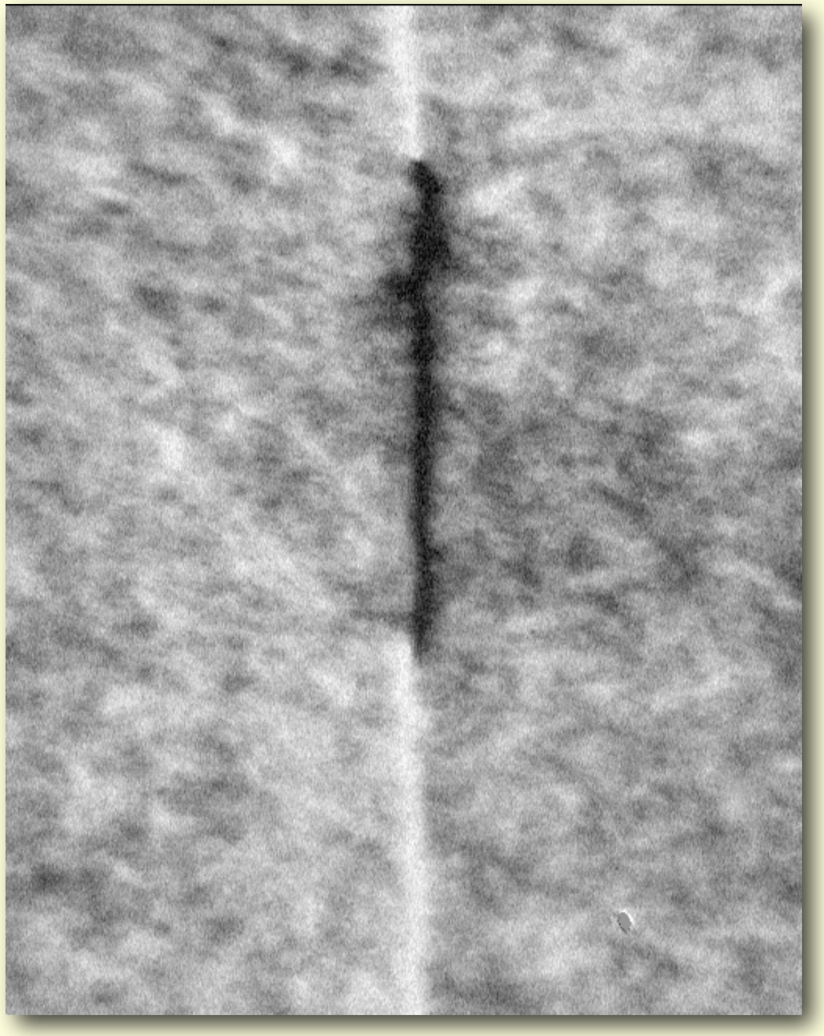

thinned to μm

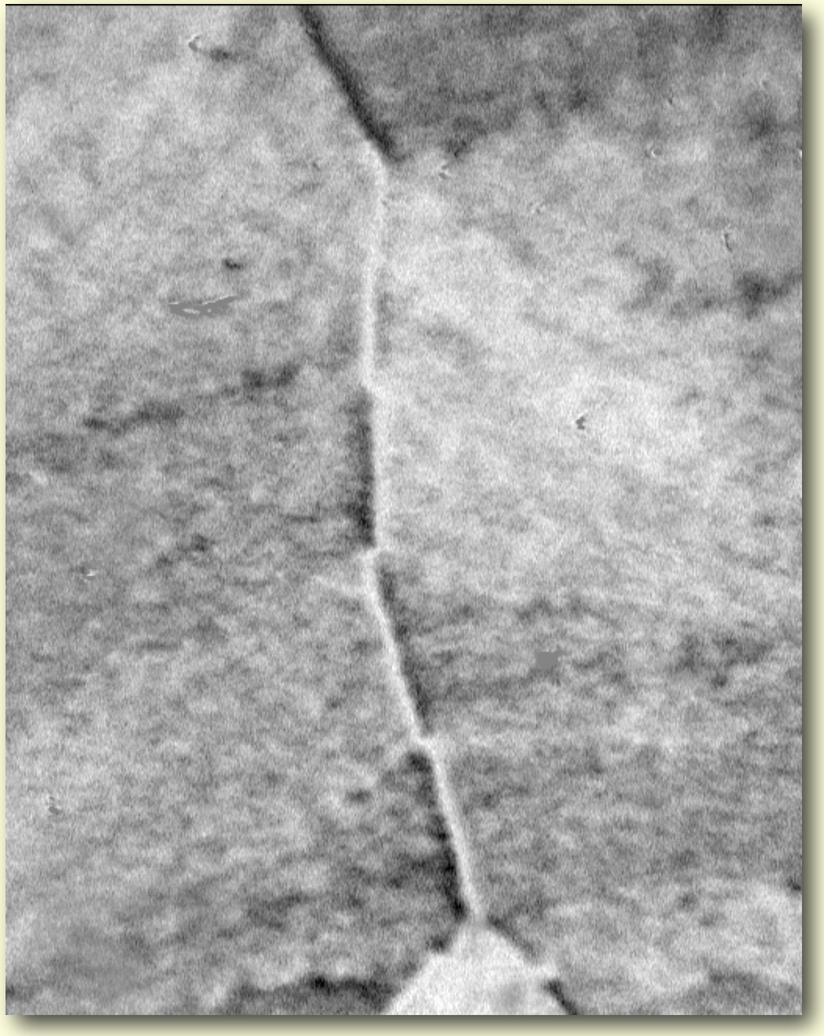

still thinner

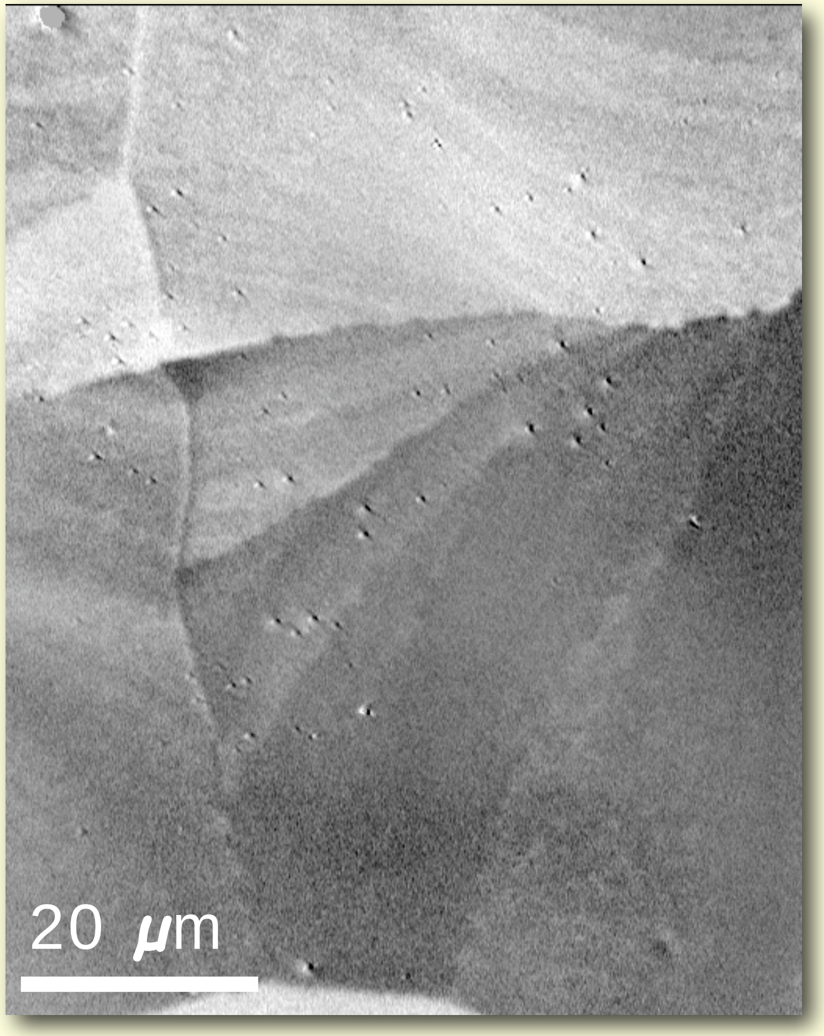

statistical perturbation by crystal anisotropy causes:

- patches in thick samples (ribbons)
- ripple in thin films

Ripple phenomenon: Comparison Ni/Co

Permalloy (10 nm thick)

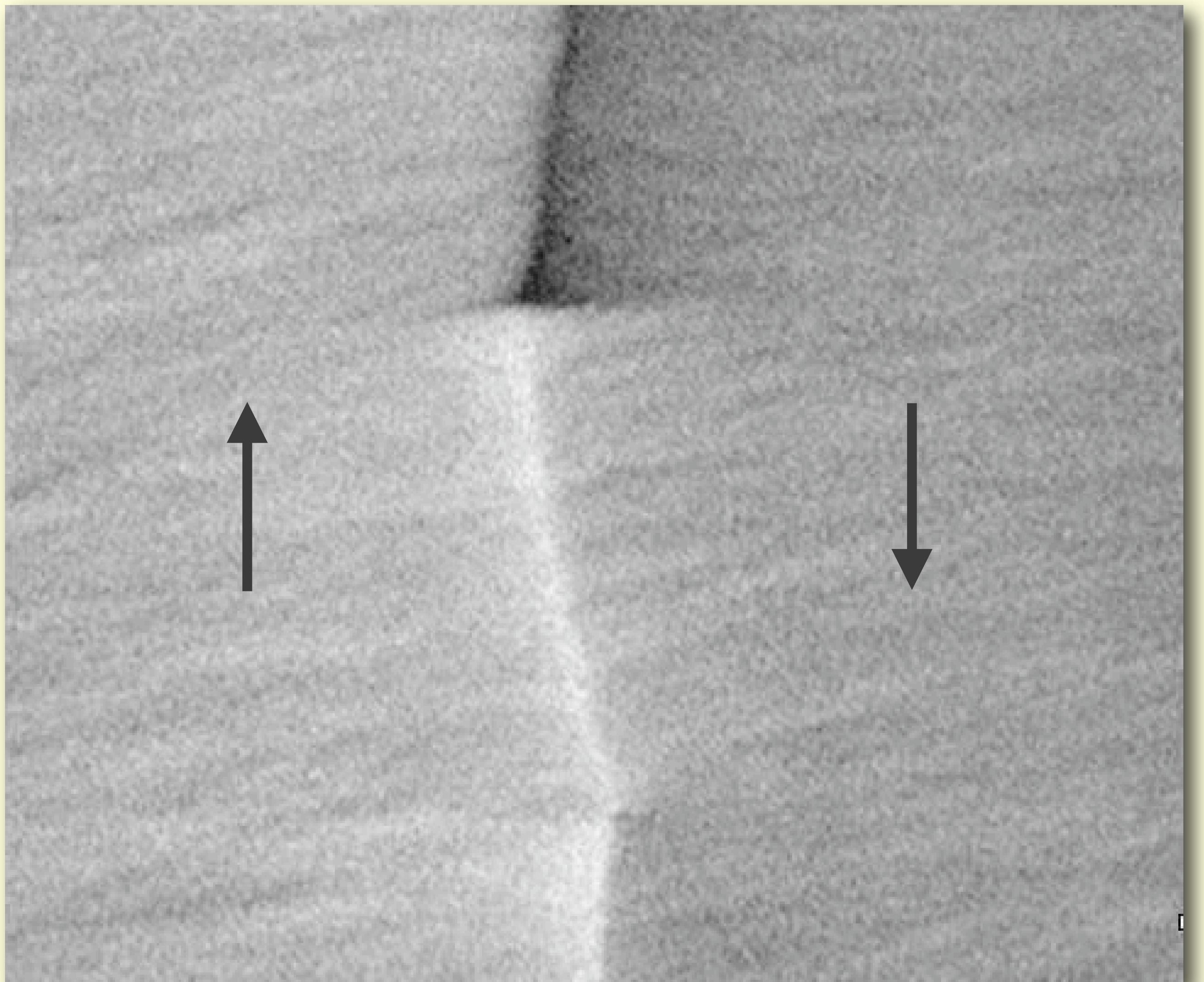

Co (6 nm thick)

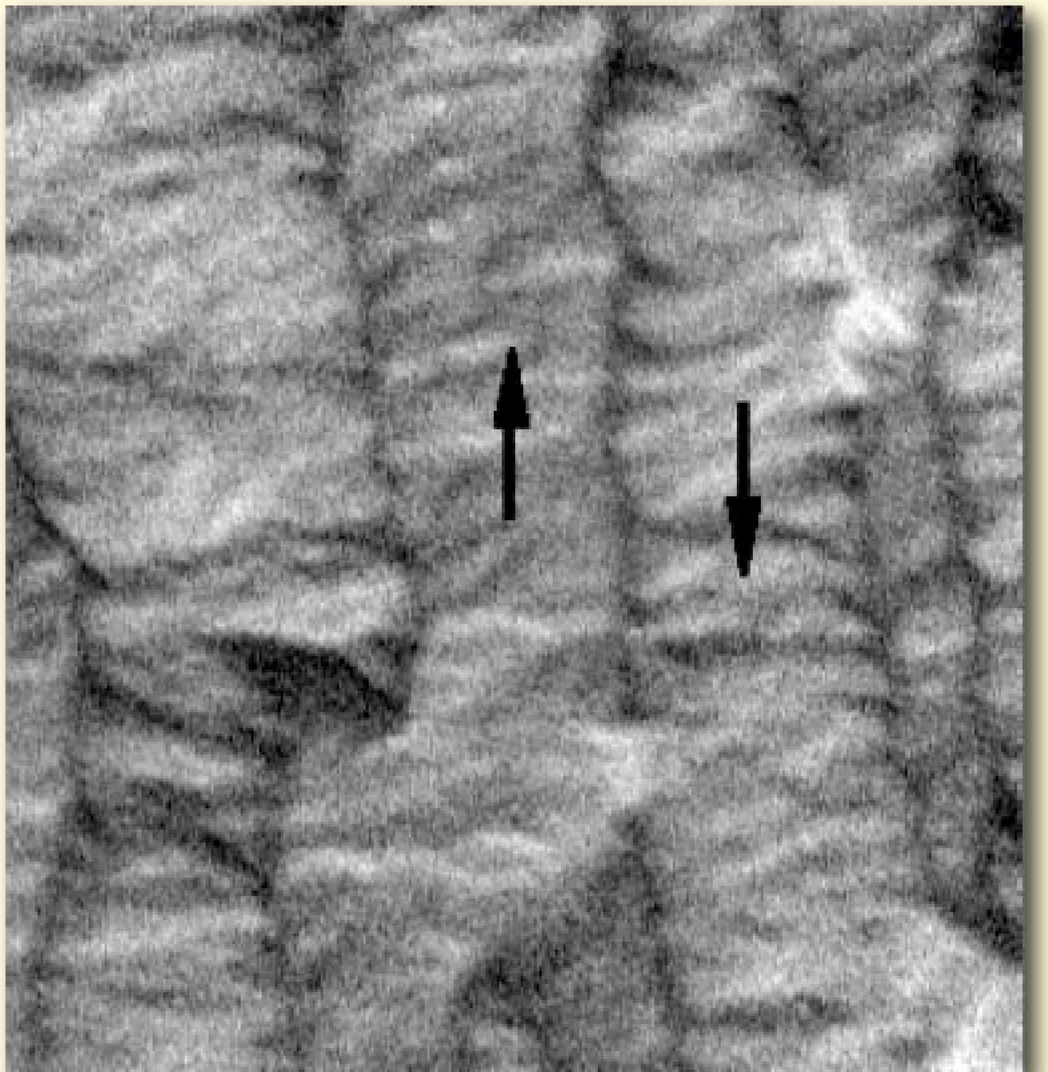

10 μm

Ripple phenomenon: Comparison Ni/Co

Cobalt film (6 nm thick)

nucleation and growth

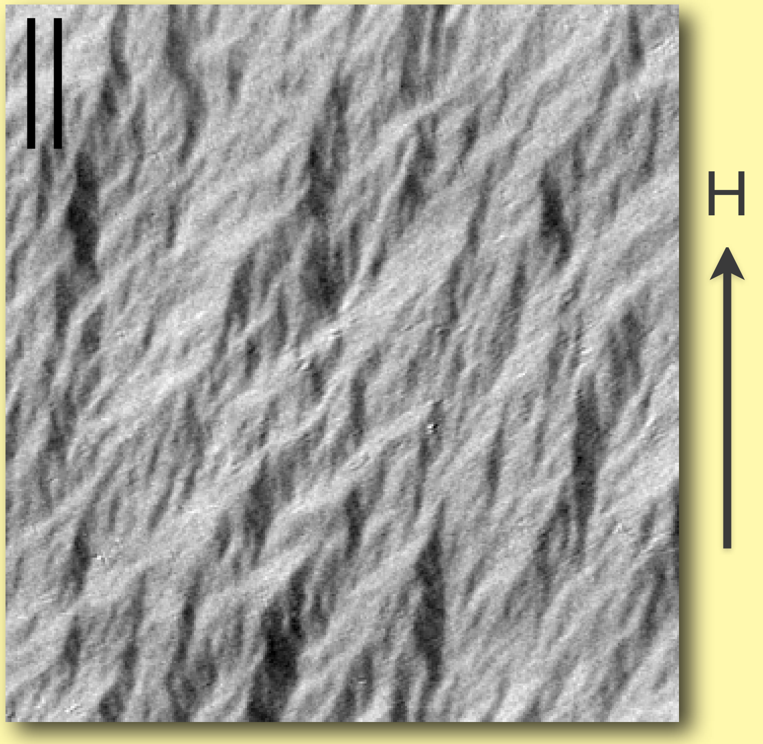

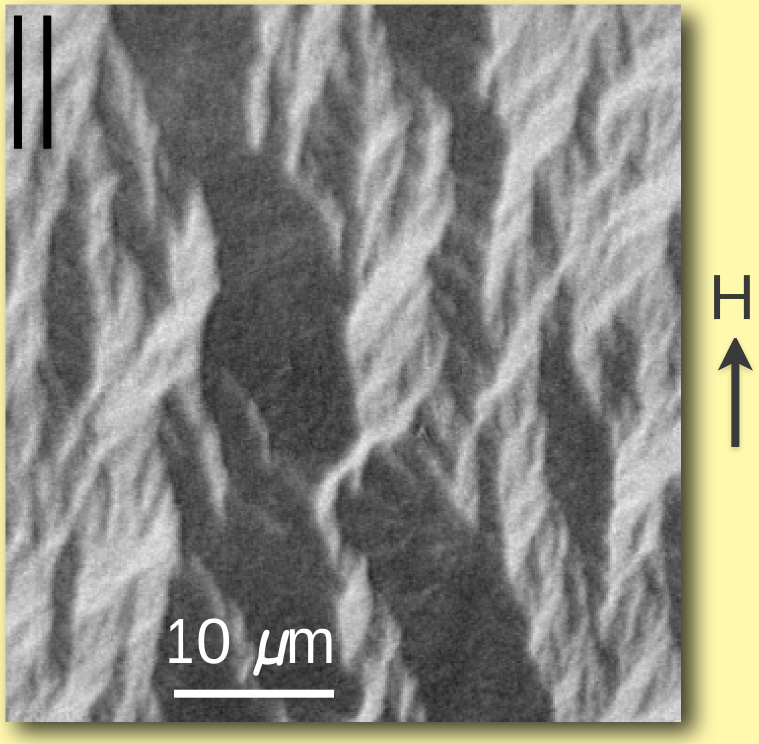

Co (6 nm thick)

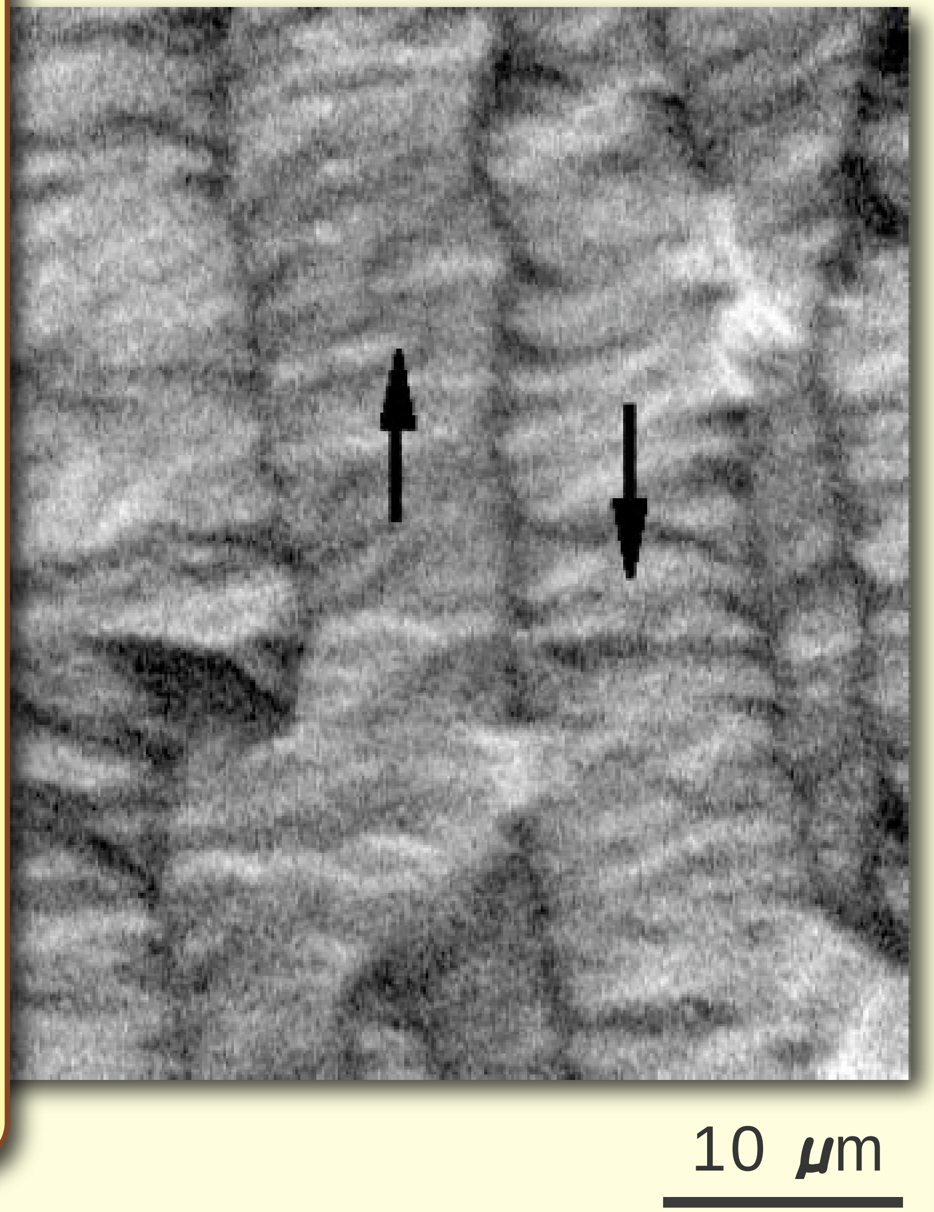

$Co_{45}Fe_{28.5}Si_{13.5}B_9Cu_1Nb_3$

$$\langle K_1 \rangle \sim \frac{K_1}{\sqrt{N}}$$

increases anisotropy of grains

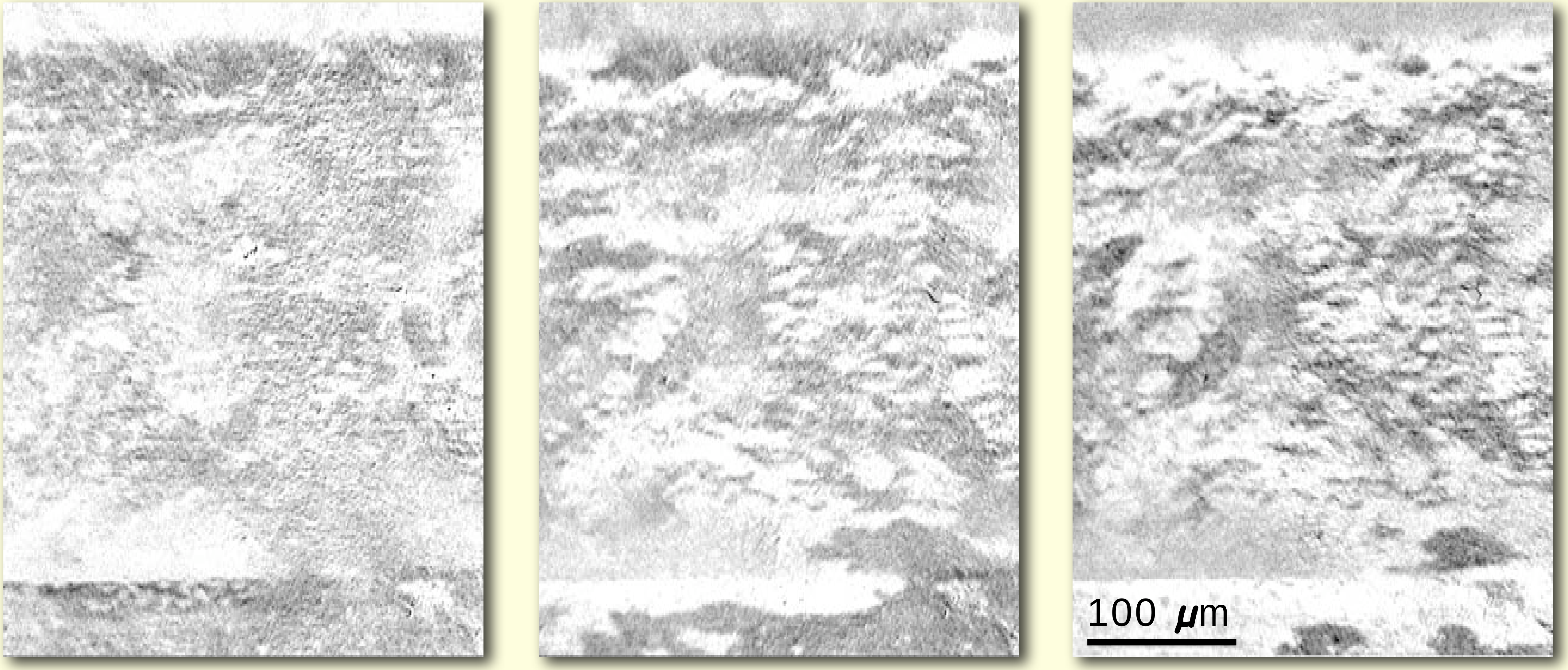

H = –0.15 kA/m | +0.11 kA/m | +0.14 kA/m

ribbon axis and field direction

sample: Pilar Marin, Madrid

Summary: Coercivity and domains

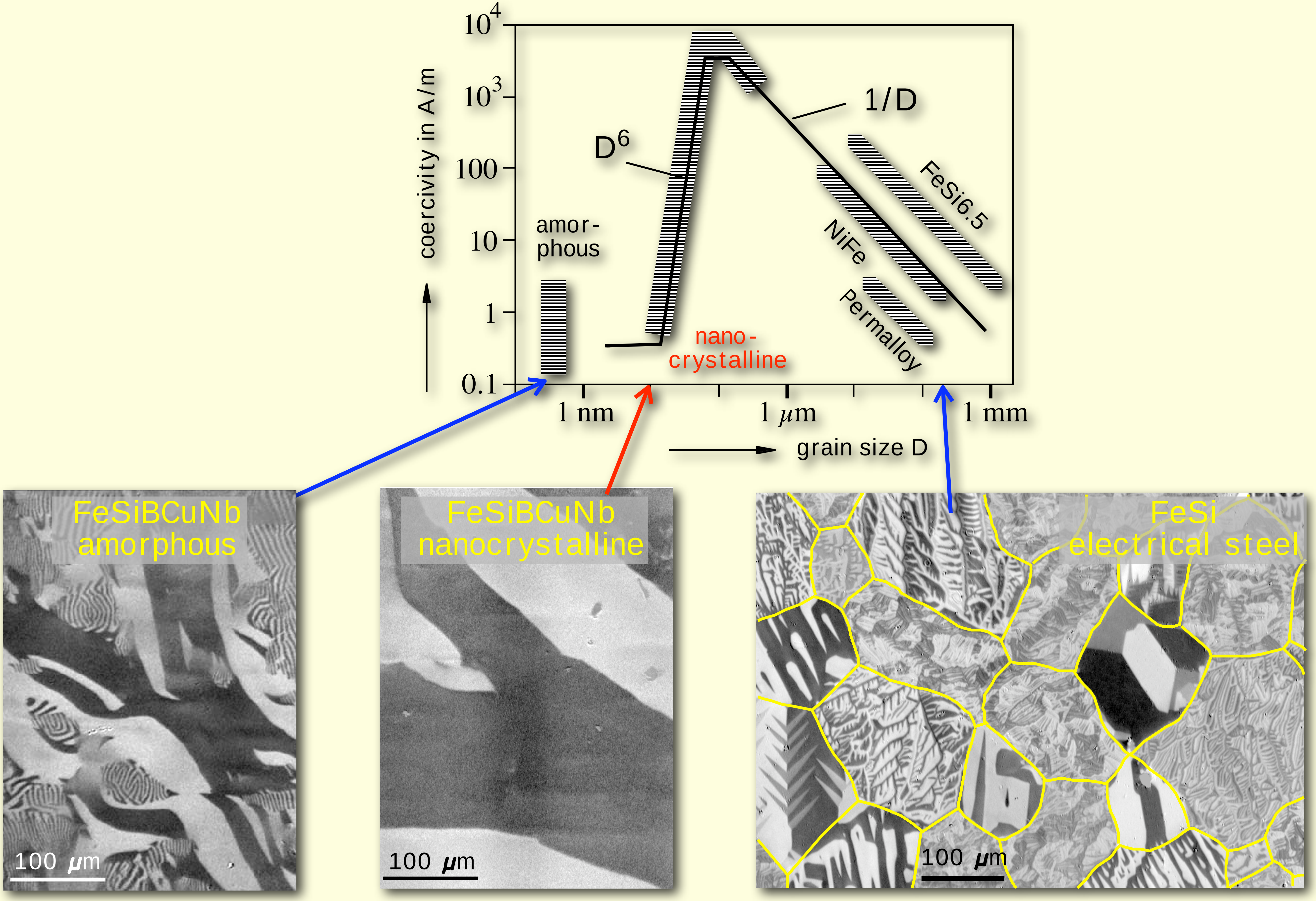

Summary: Coercivity and domains

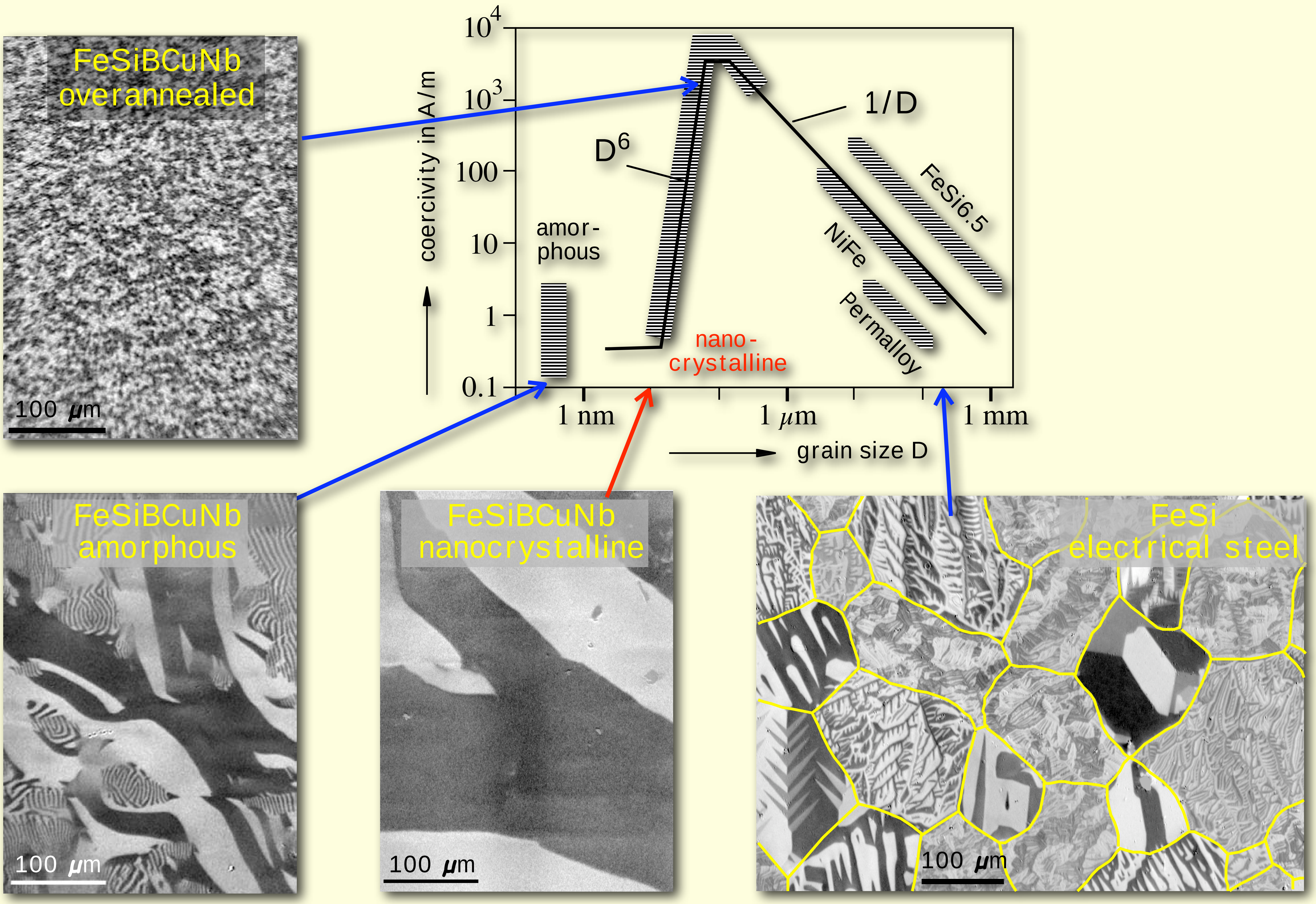

FeSiBCuNb: over-annealed

20°C

625°C

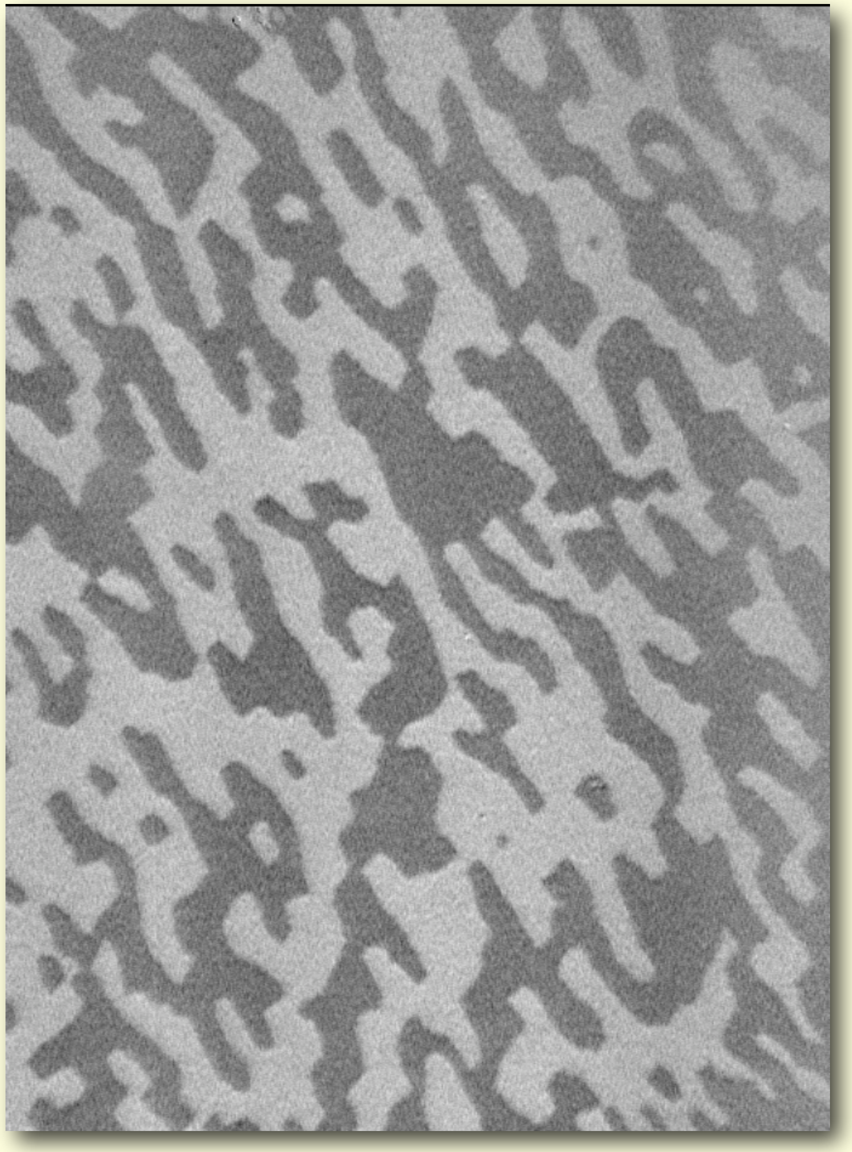

800°C

grain coarsening

precepitation of borides

Overview

1. Domains in coarse-grained material

2. Domains in amorphous material

3. Domains in nanocrystalline, soft magnetic ($Q<<1$) materials

4. Domains in fine- and nanostructured, permanent magnetic ($Q>1$) materials

Permanent magnets, basics

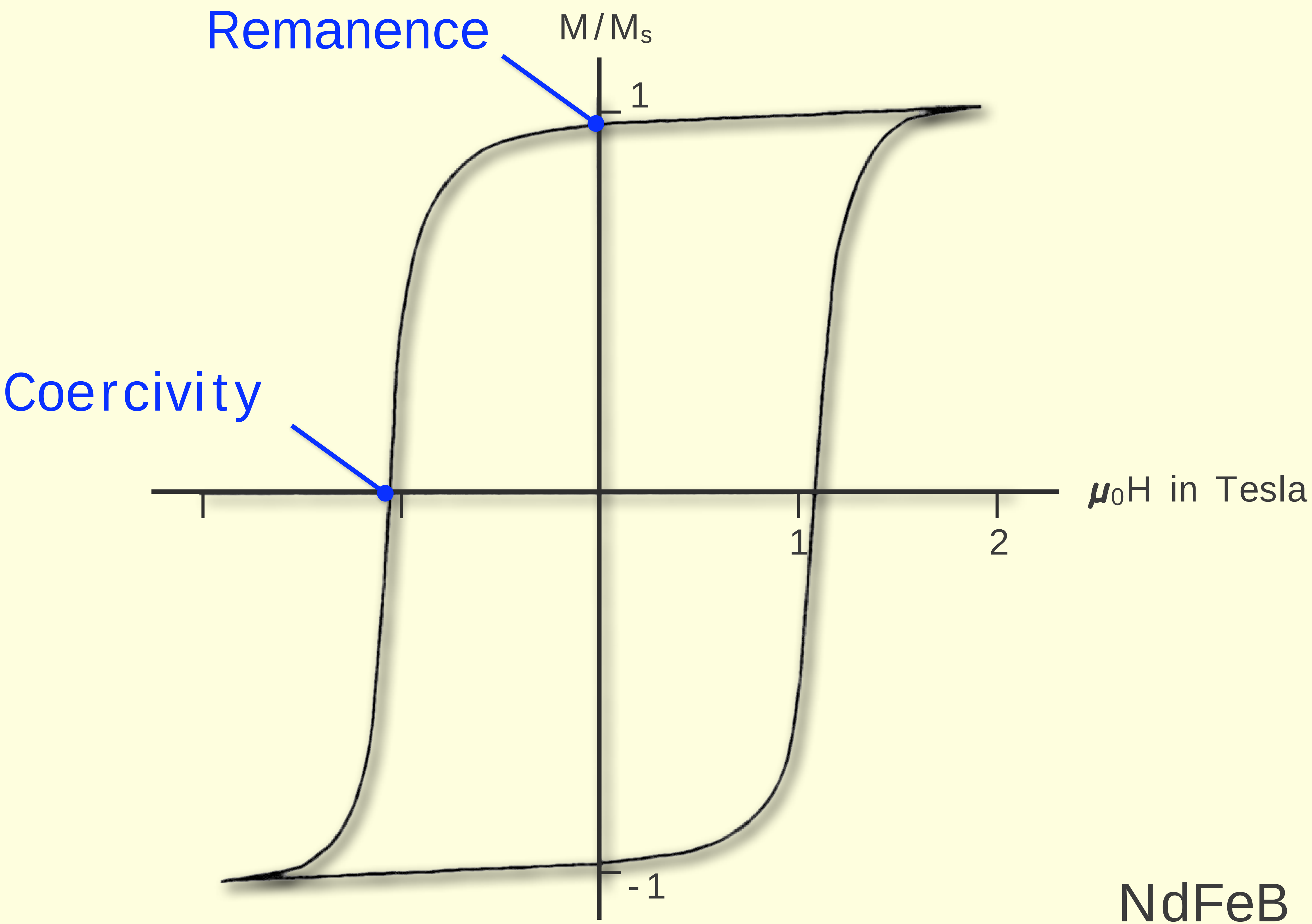

NdFeB

NdFeB permanent magnet

Thermally demagnetized

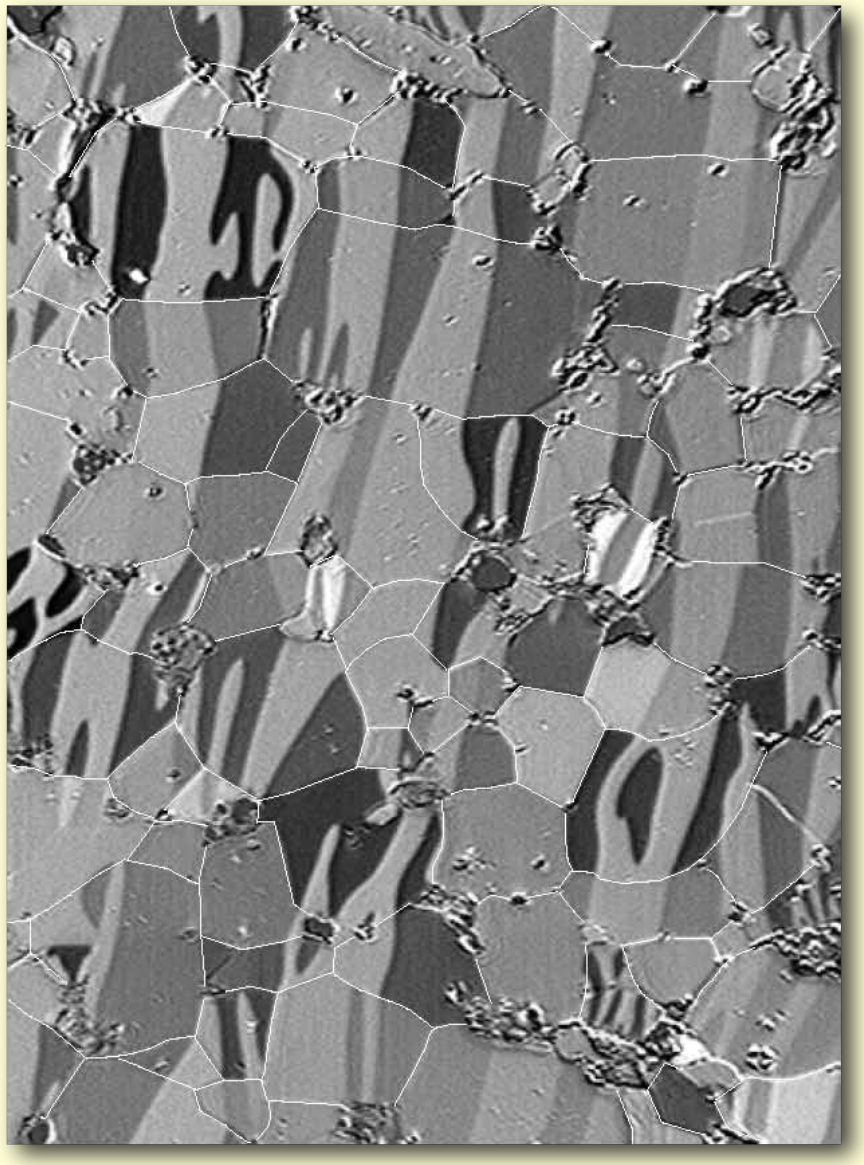

along texture axis

Thermally demagnetized

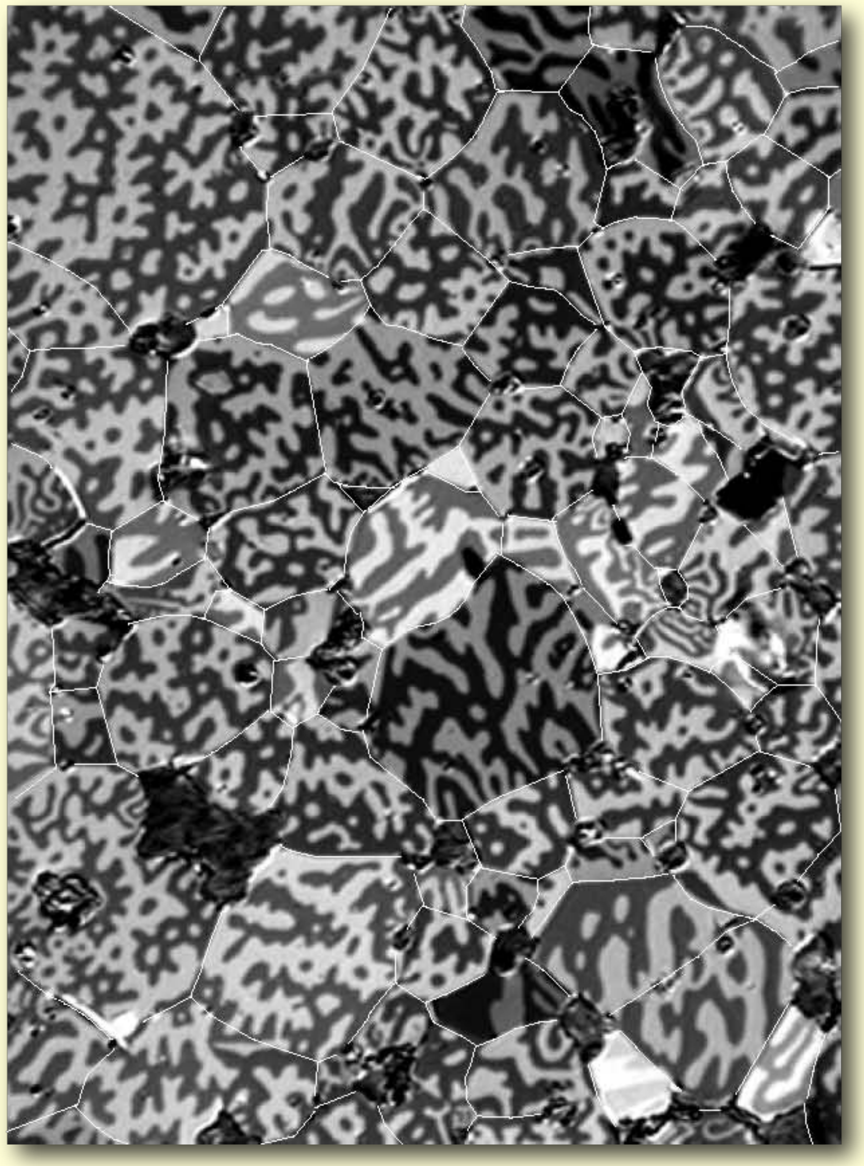

perpendicular texture axis

Magnetized

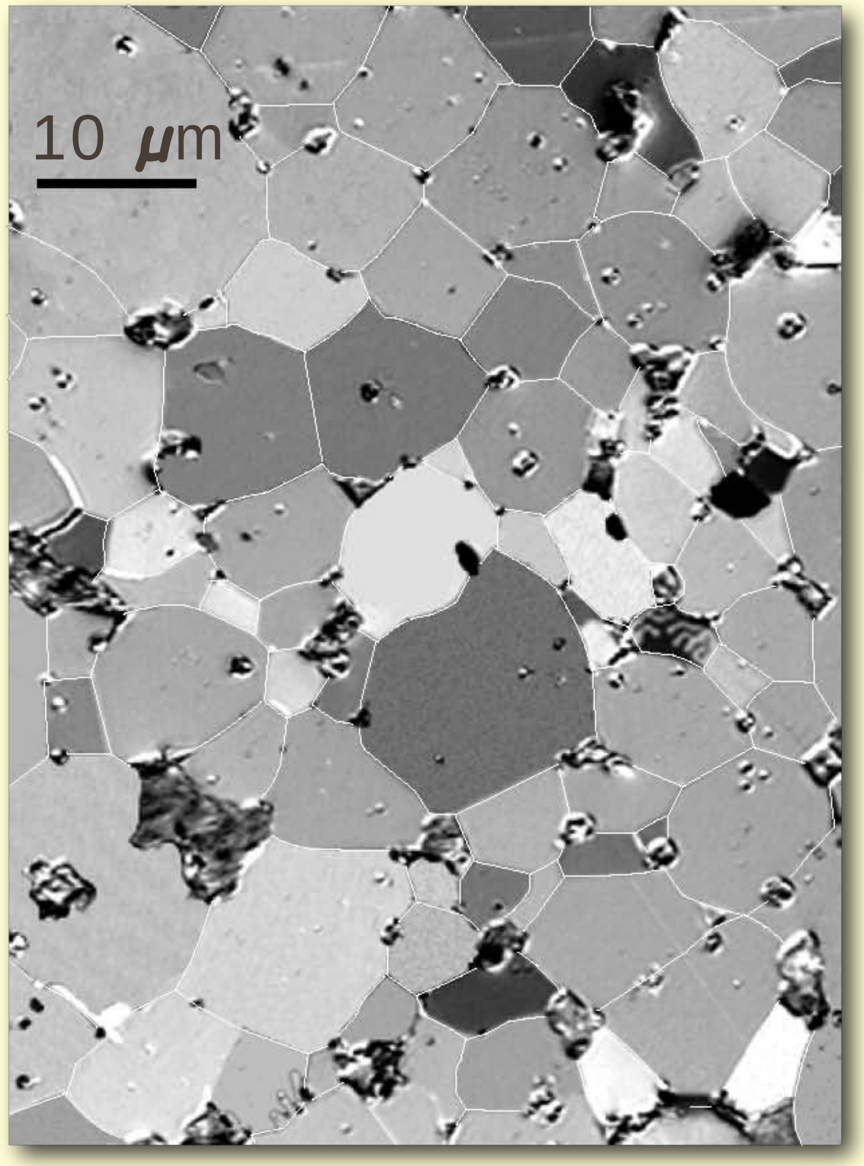

perpendicular texture axis

NdFeB permanent magnet

Thermally demagnetized

Thermally demagnetized

Magnetized

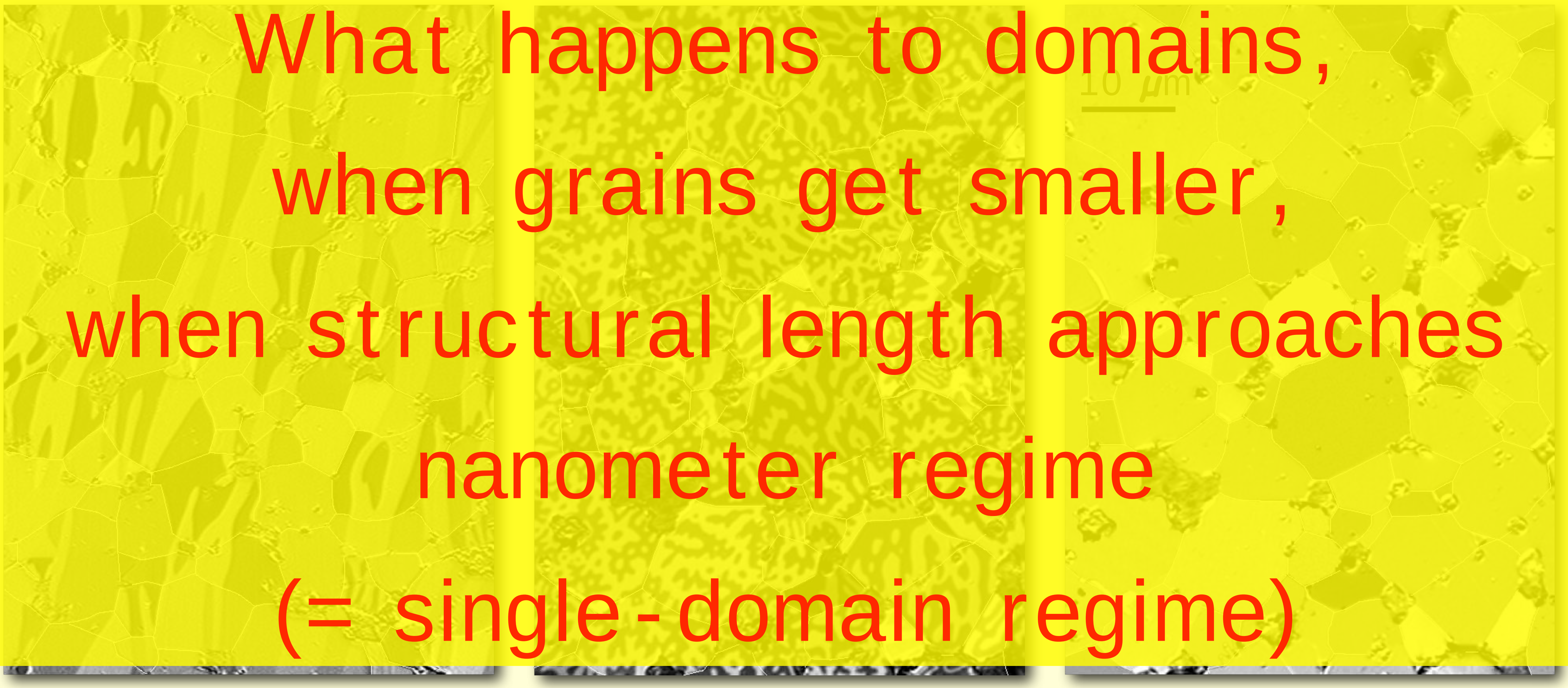

What happens to domains,

when grains get smaller,

when structural length approaches

nanometer regime

(= single-domain regime)

along texture axis

perpendicular texture axis

perpendicular texture axis

Nanostructured permanent magnet

Ensemble of single-domain grains (or particles)

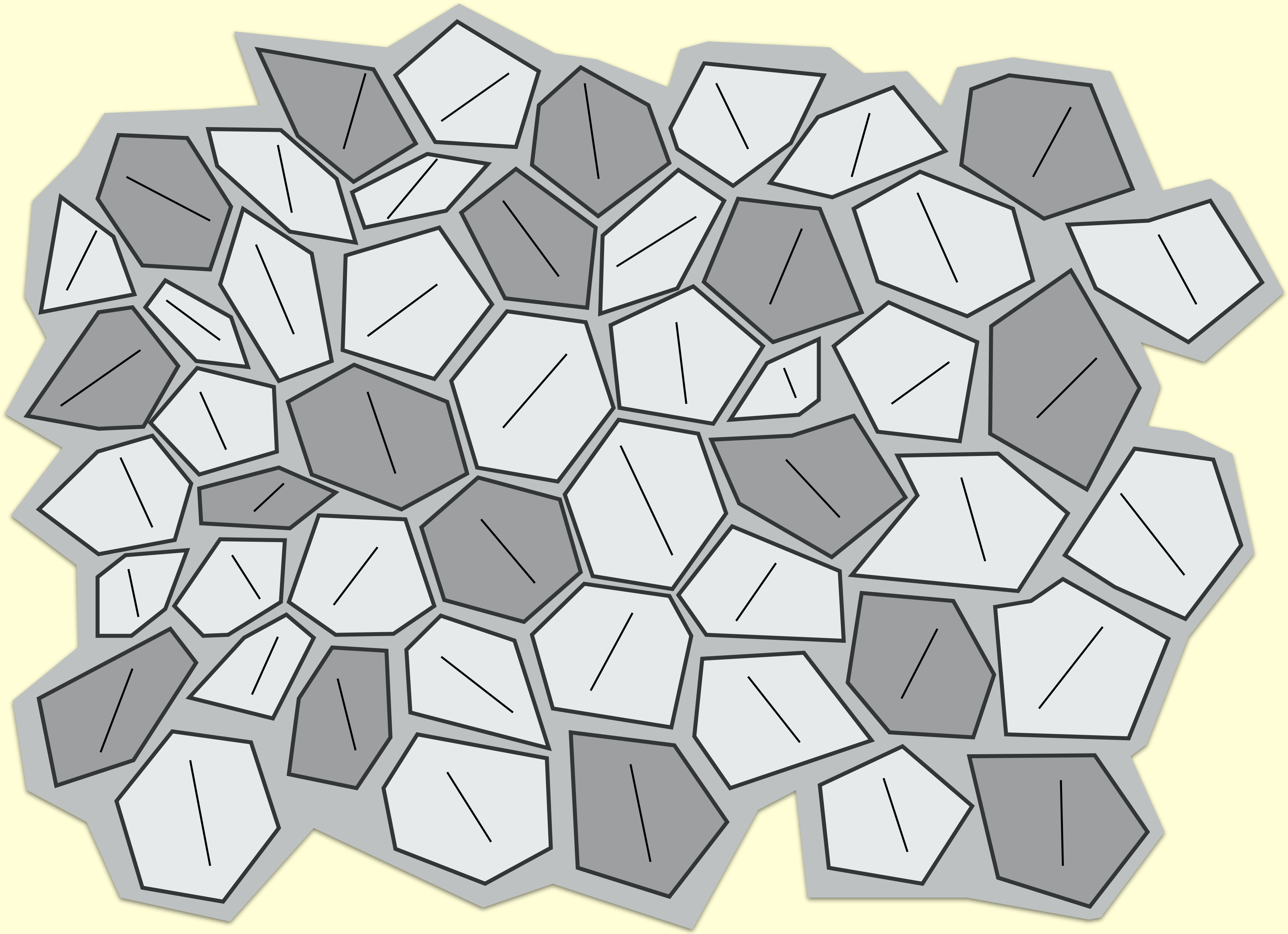

Nanostructured permanent magnet

Ensemble of single-domain grains (or particles)

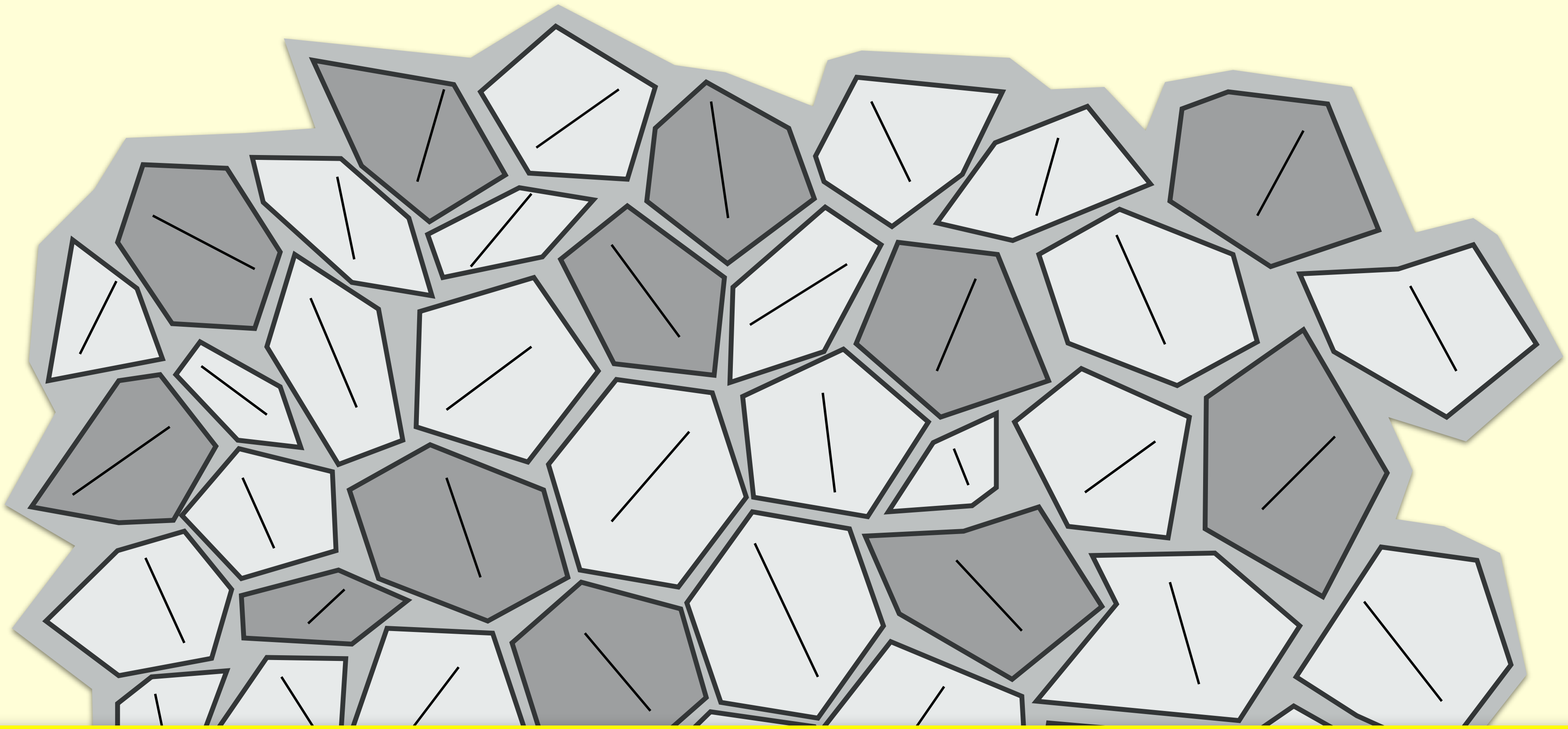

Expectation:

each grain (particle) magnetized

along its easy axis.

Nanostructured permanent magnet

Ensemble of single-domain grains (or particles)

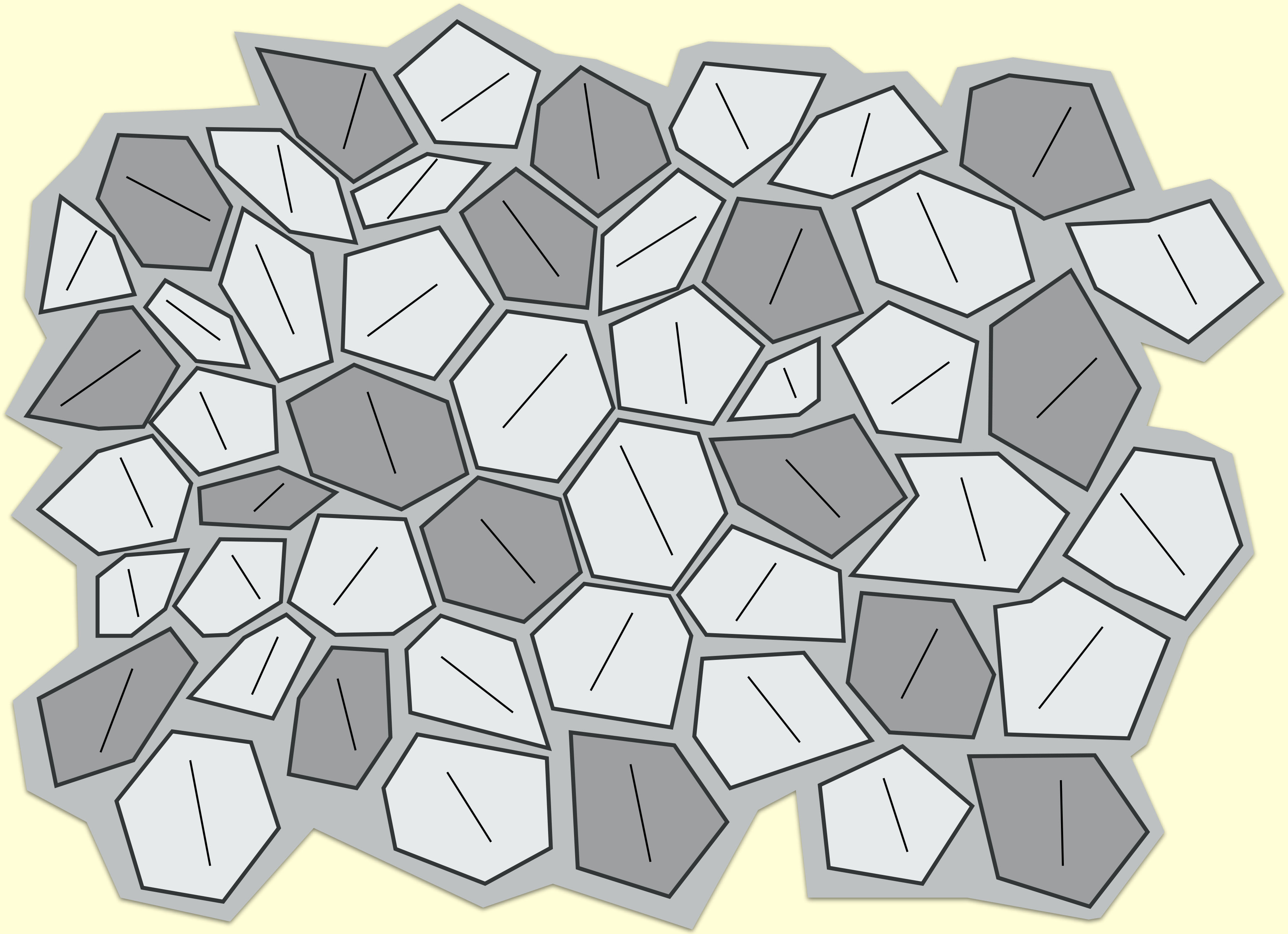

Nanostructured permanent magnet

Ensemble of single-domain grains (or particles)

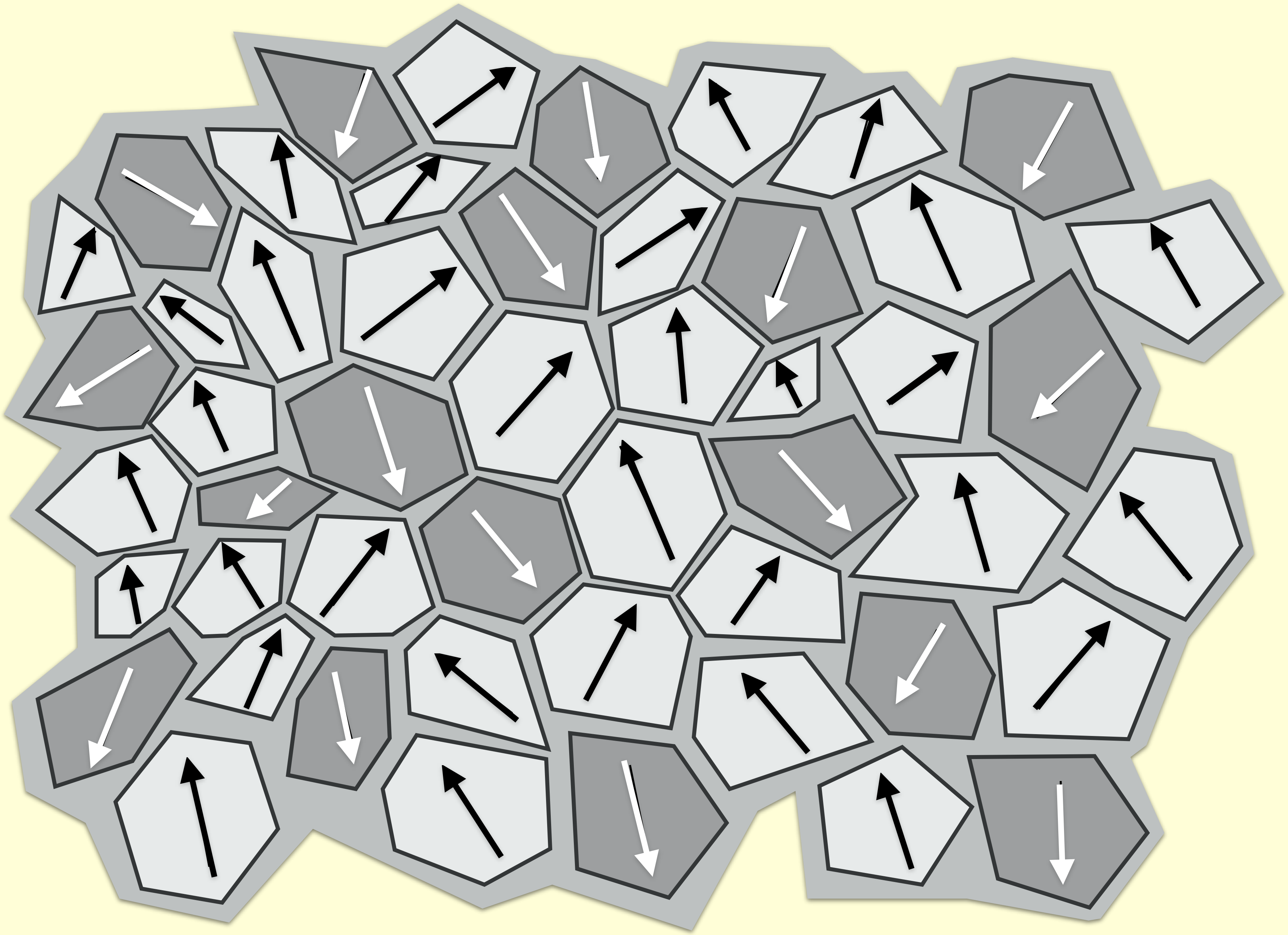

Nanostructured permanent magnet

Ensemble of single-domain grains (or particles)

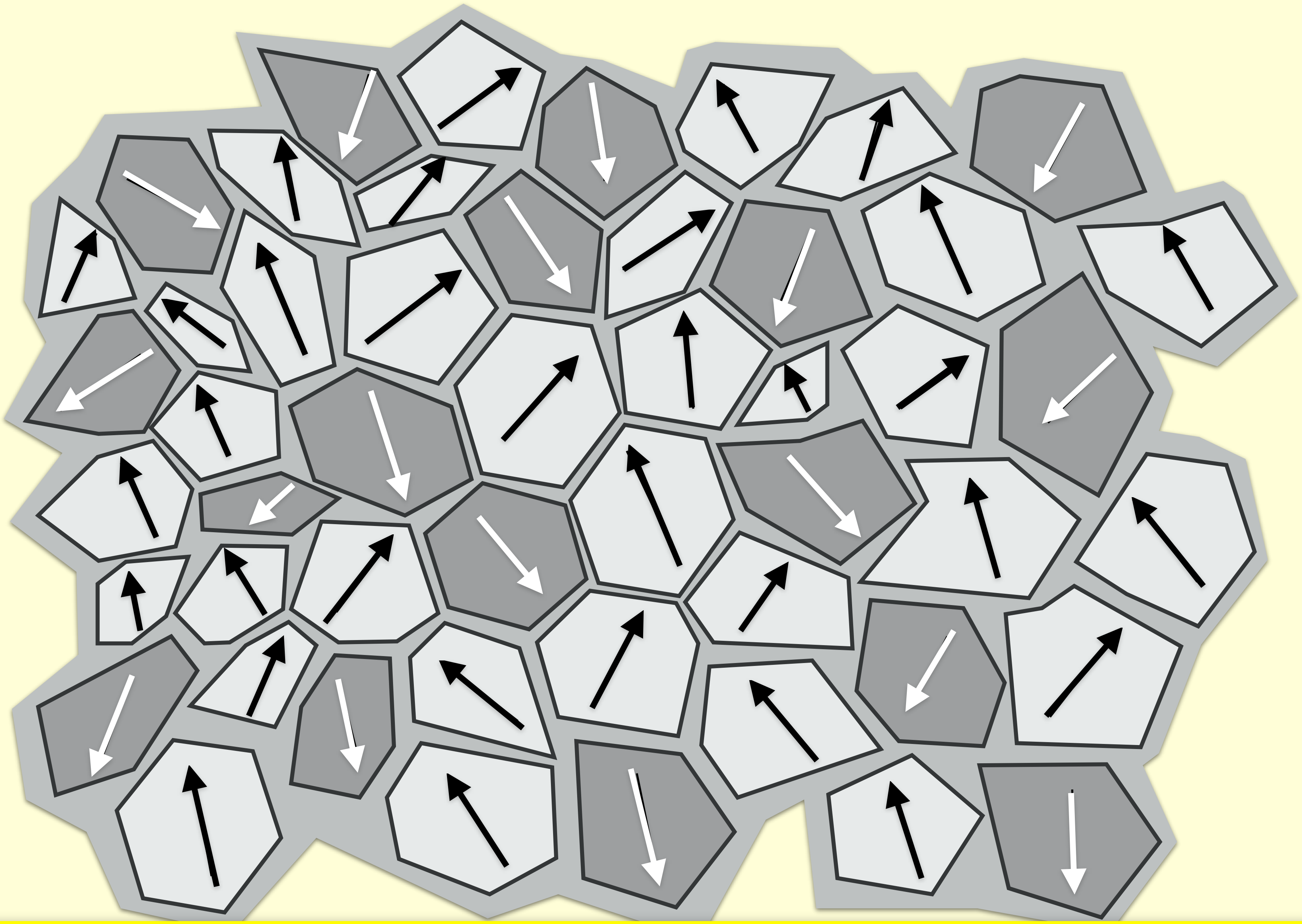

Details depend on grain interaction

Nanostructured NdFeB: remanence enhancement

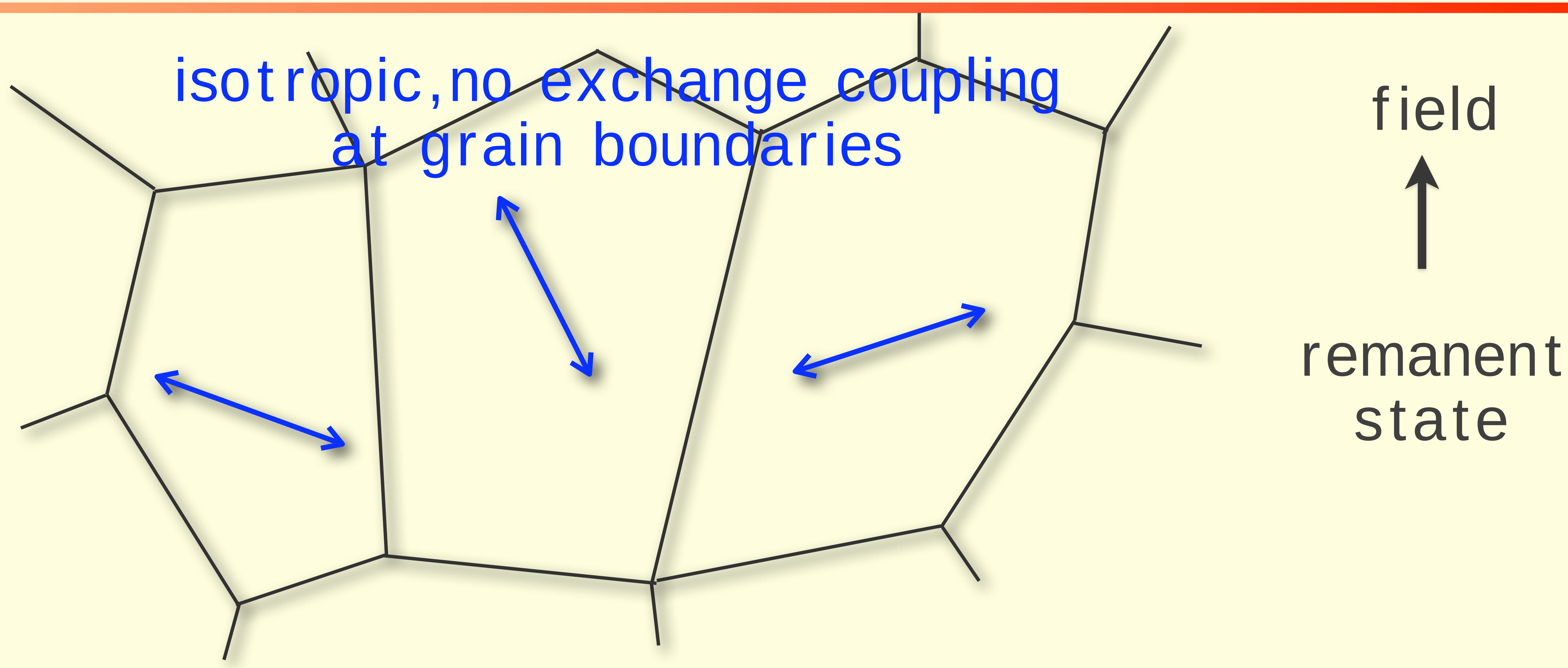

Nanostructured NdFeB: remanence enhancement

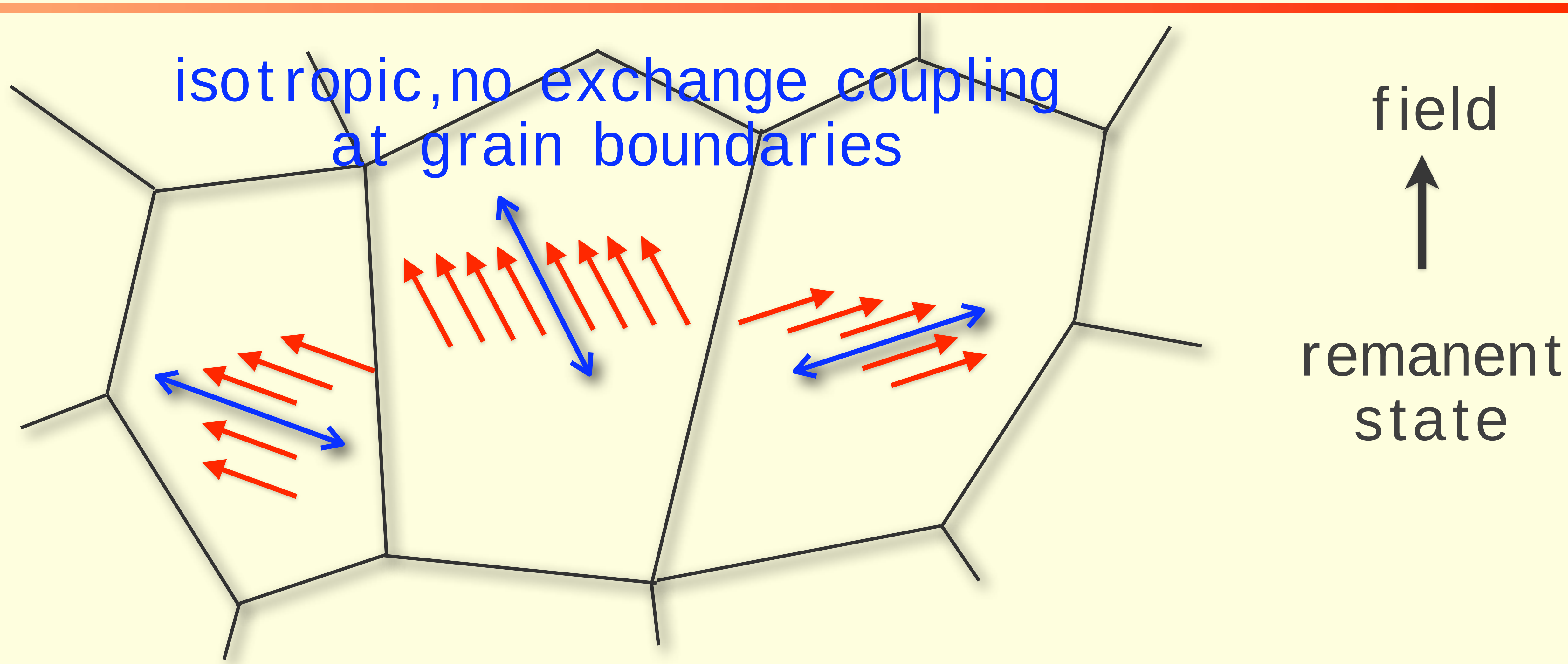

Nanostructured NdFeB: remanence enhancement

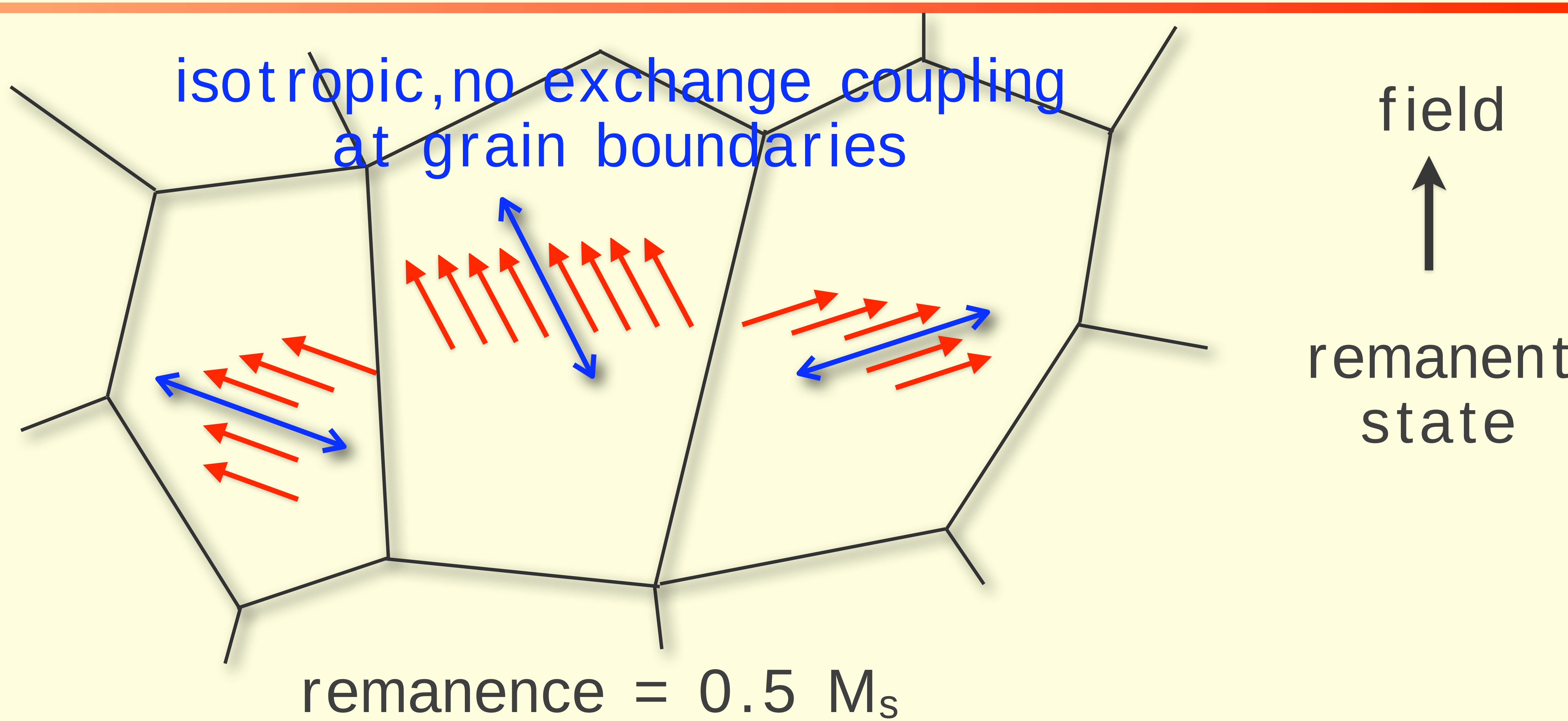

Nanostructured NdFeB: remanence enhancement

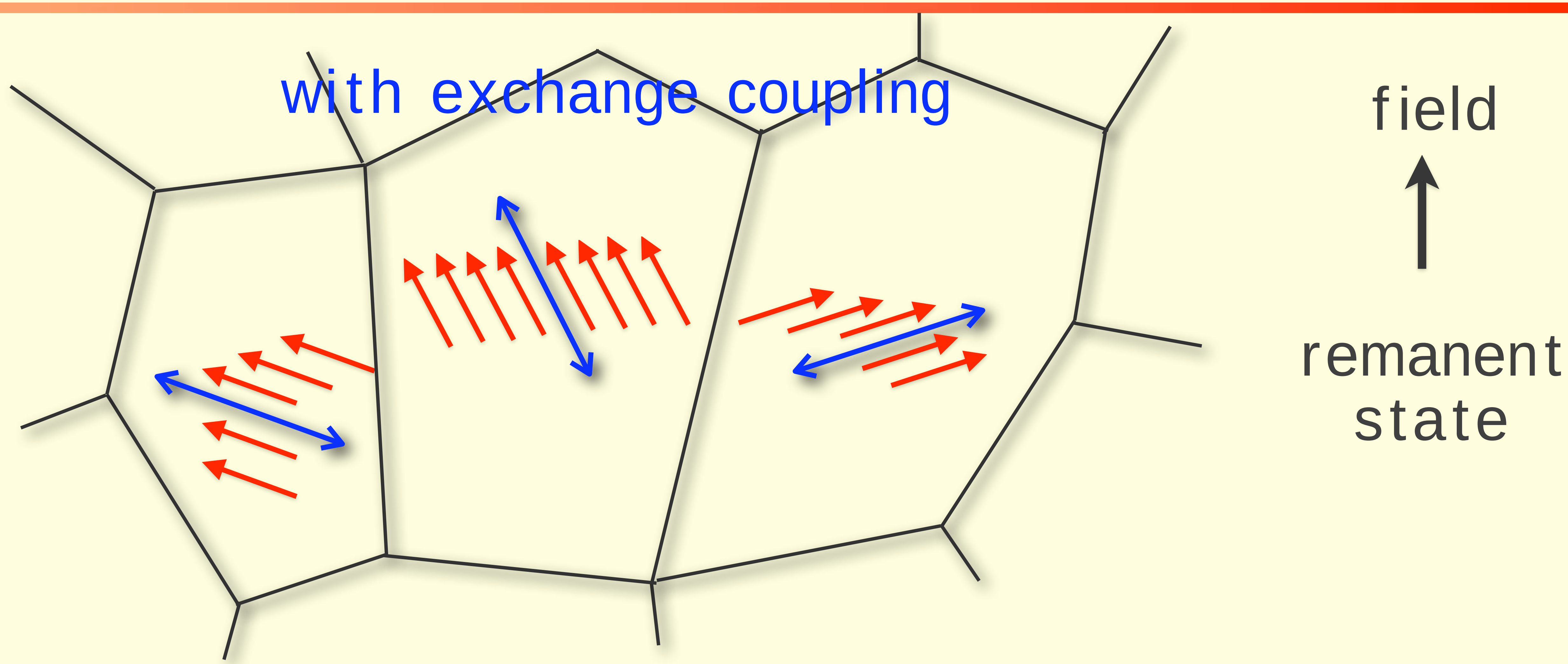

Nanostructured NdFeB: remanence enhancement

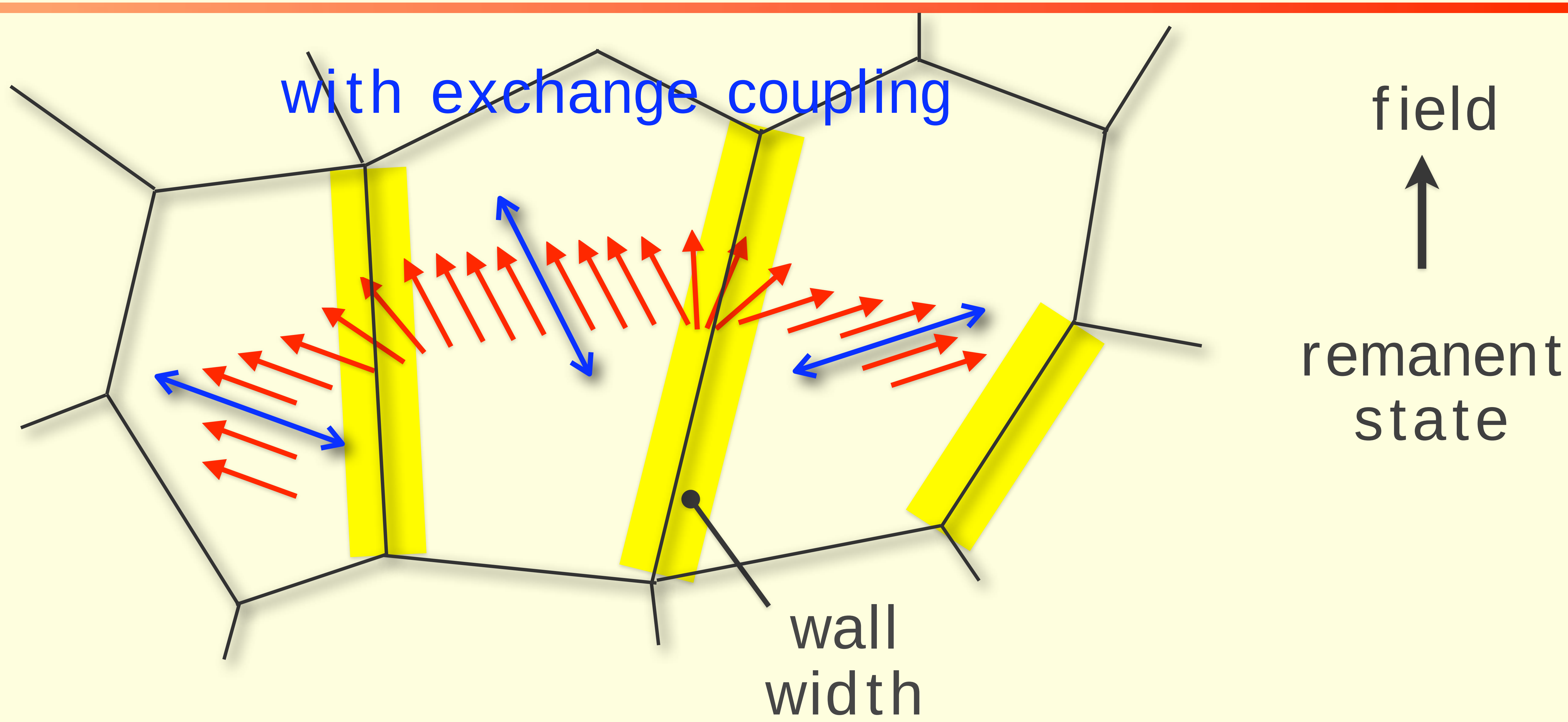

Nanostructured NdFeB: remanence enhancement

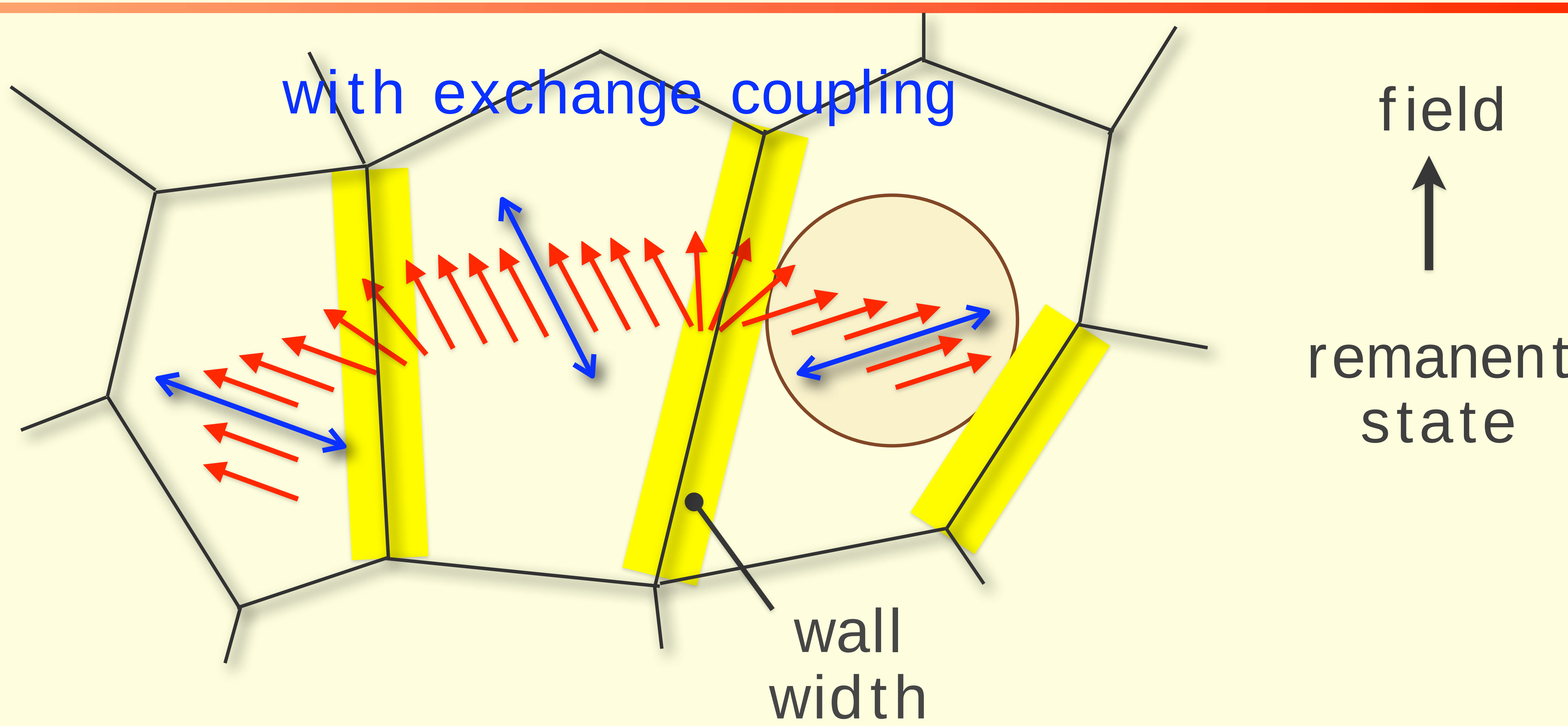

Nanostructured NdFeB: remanence enhancement

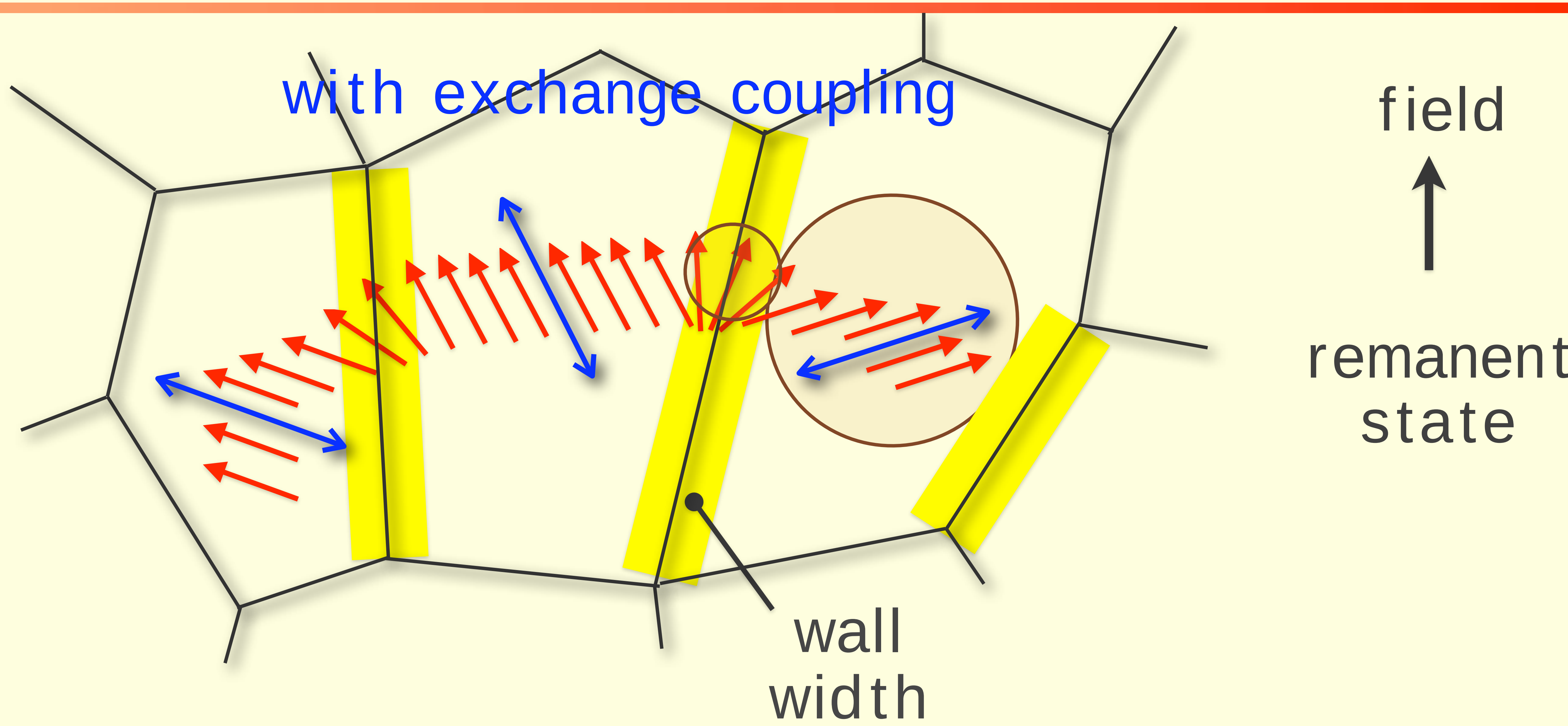

Nanostructured NdFeB: remanence enhancement

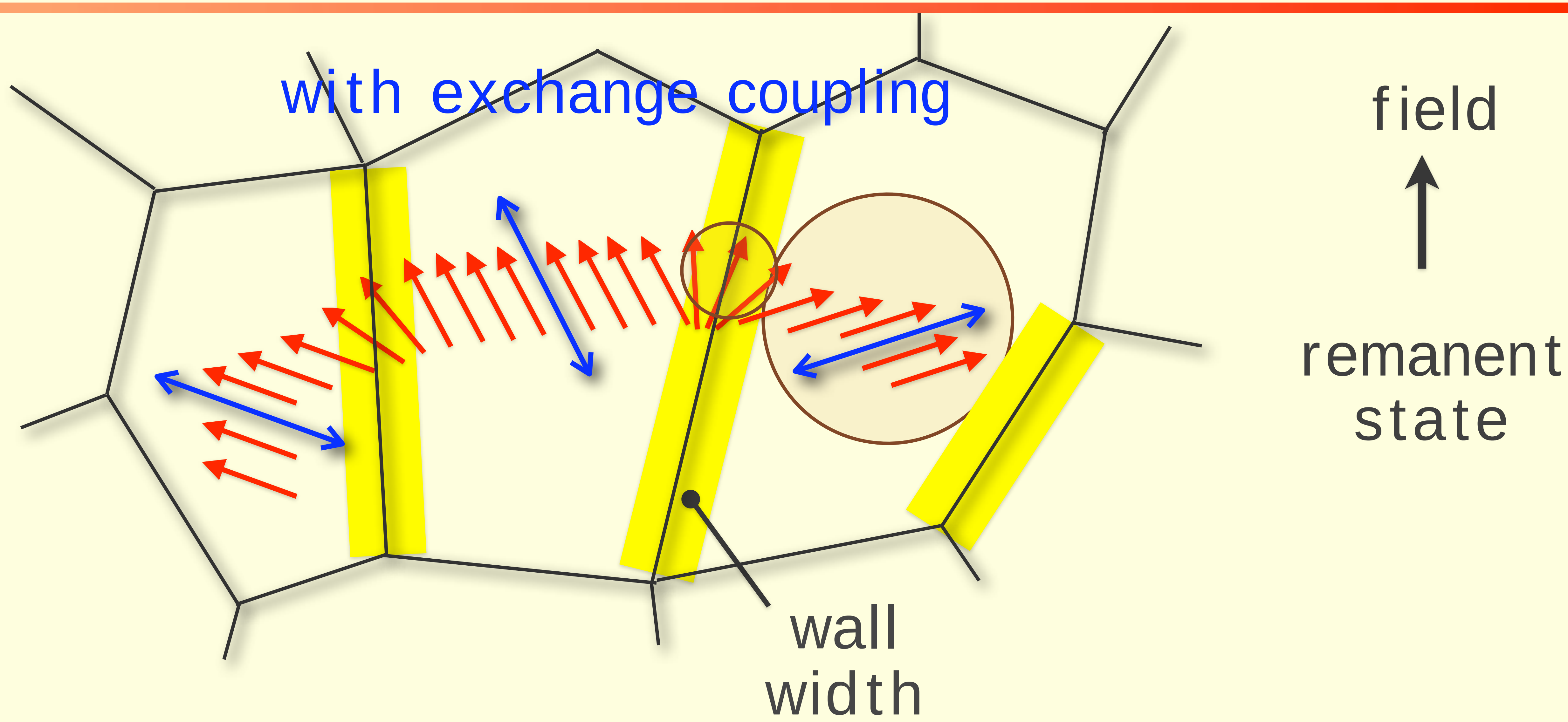

remanence > 0.5 M_s

Nanostructured NdFeB: remanence enhancement

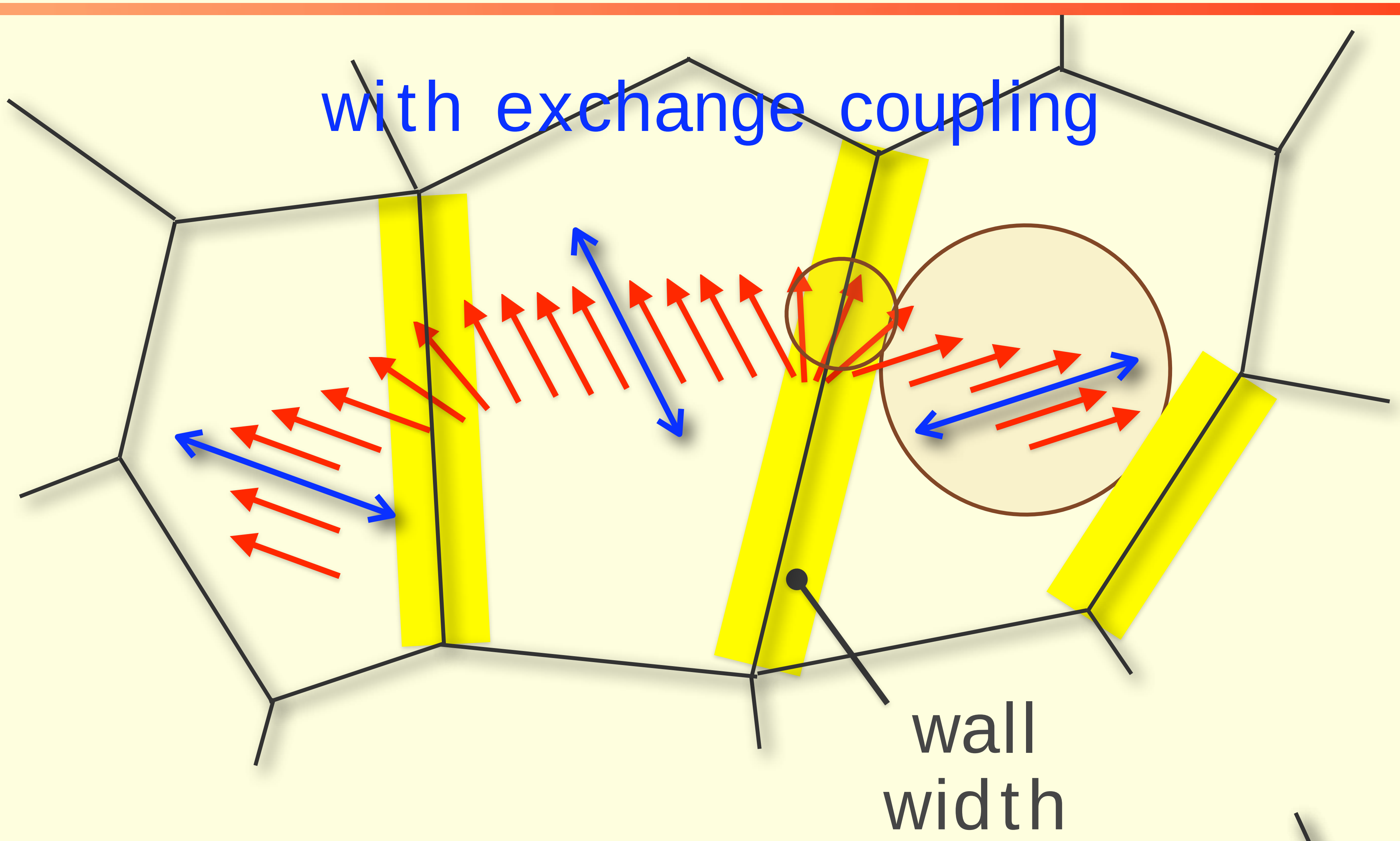

field

remanent state

remanence > 0.5 M_s

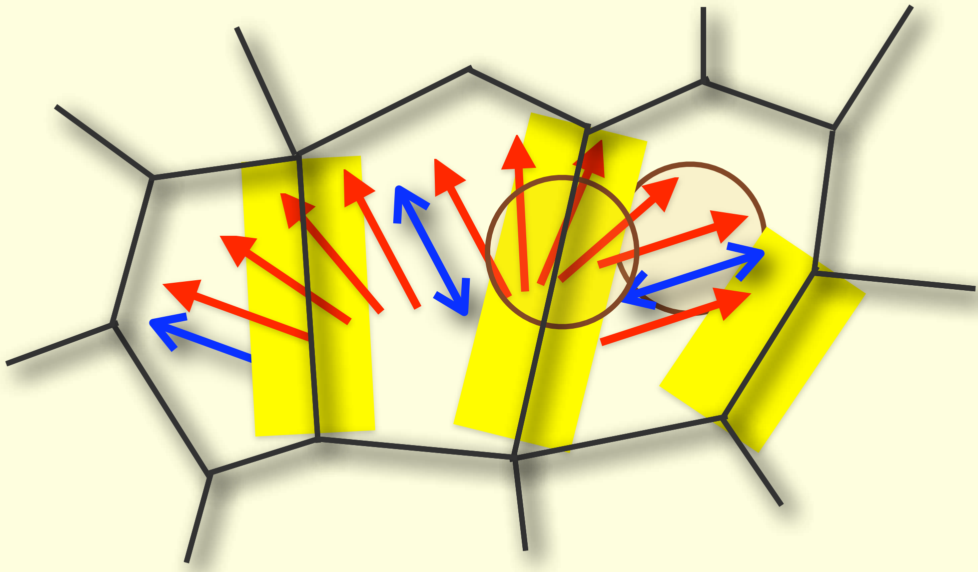

Nanostructured NdFeB: remanence enhancement

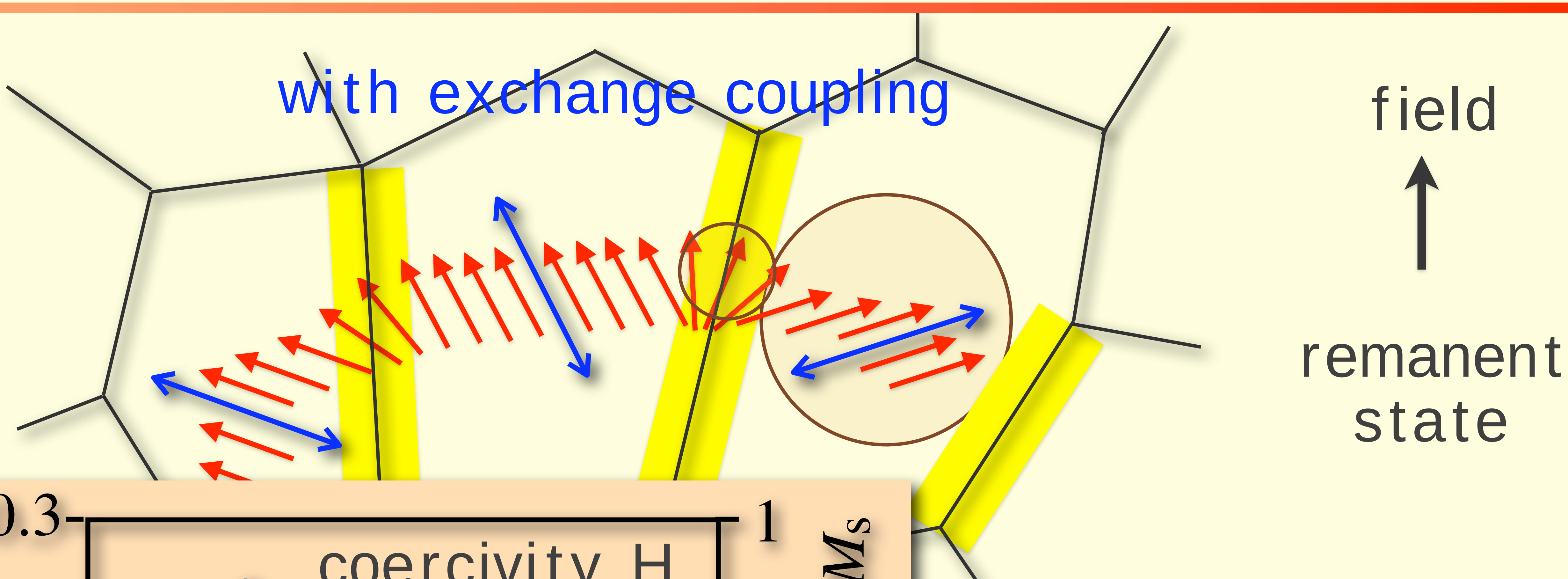

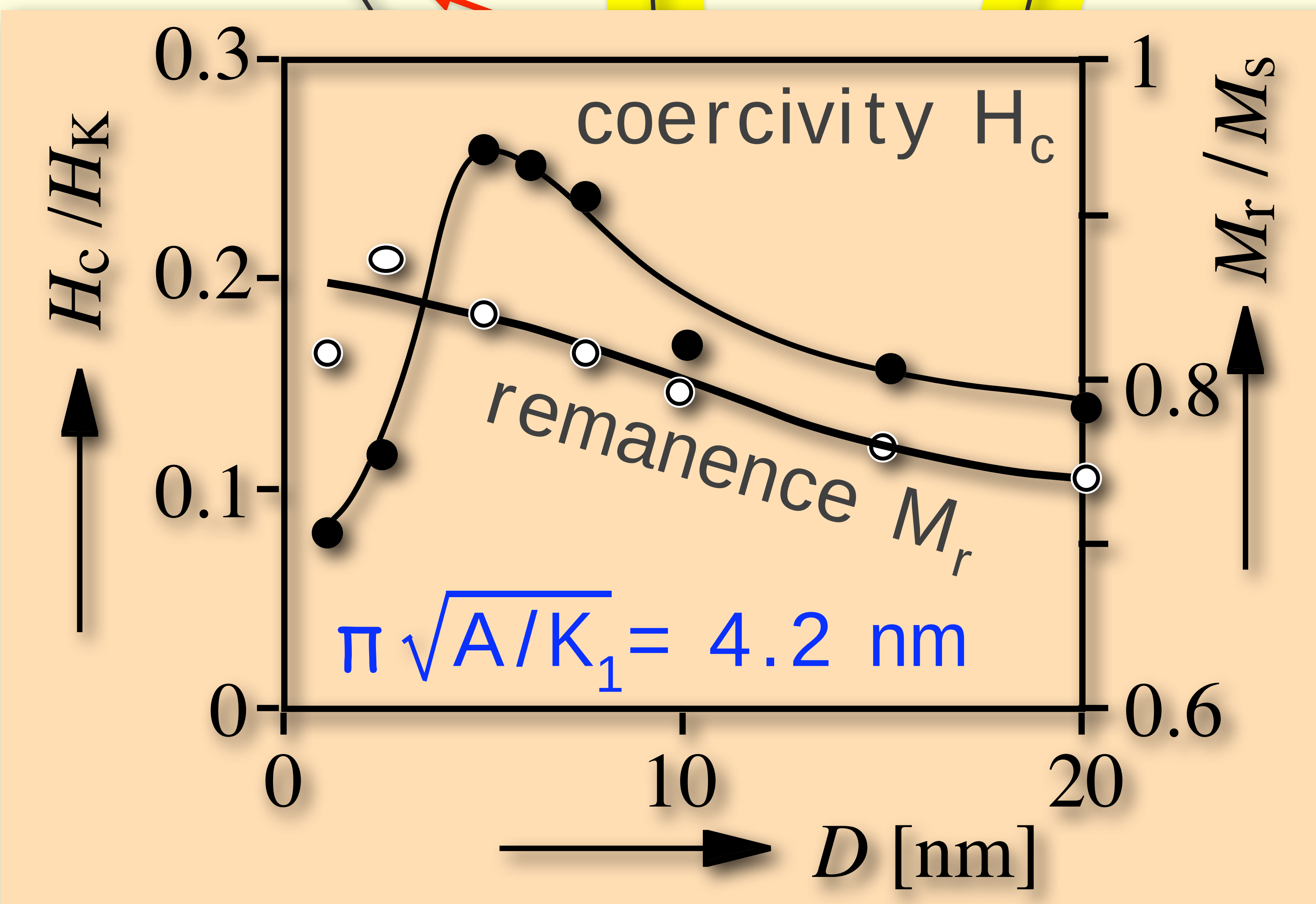

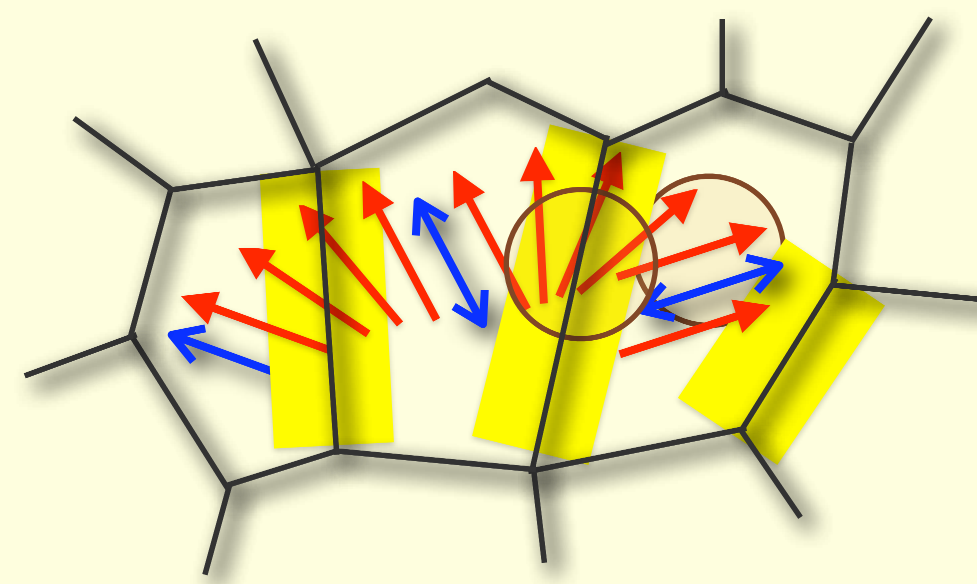

W.Rave & K.Ramstöck, JMMM 171 (1997)

Nanostructured NdFeB: remanence enhancement

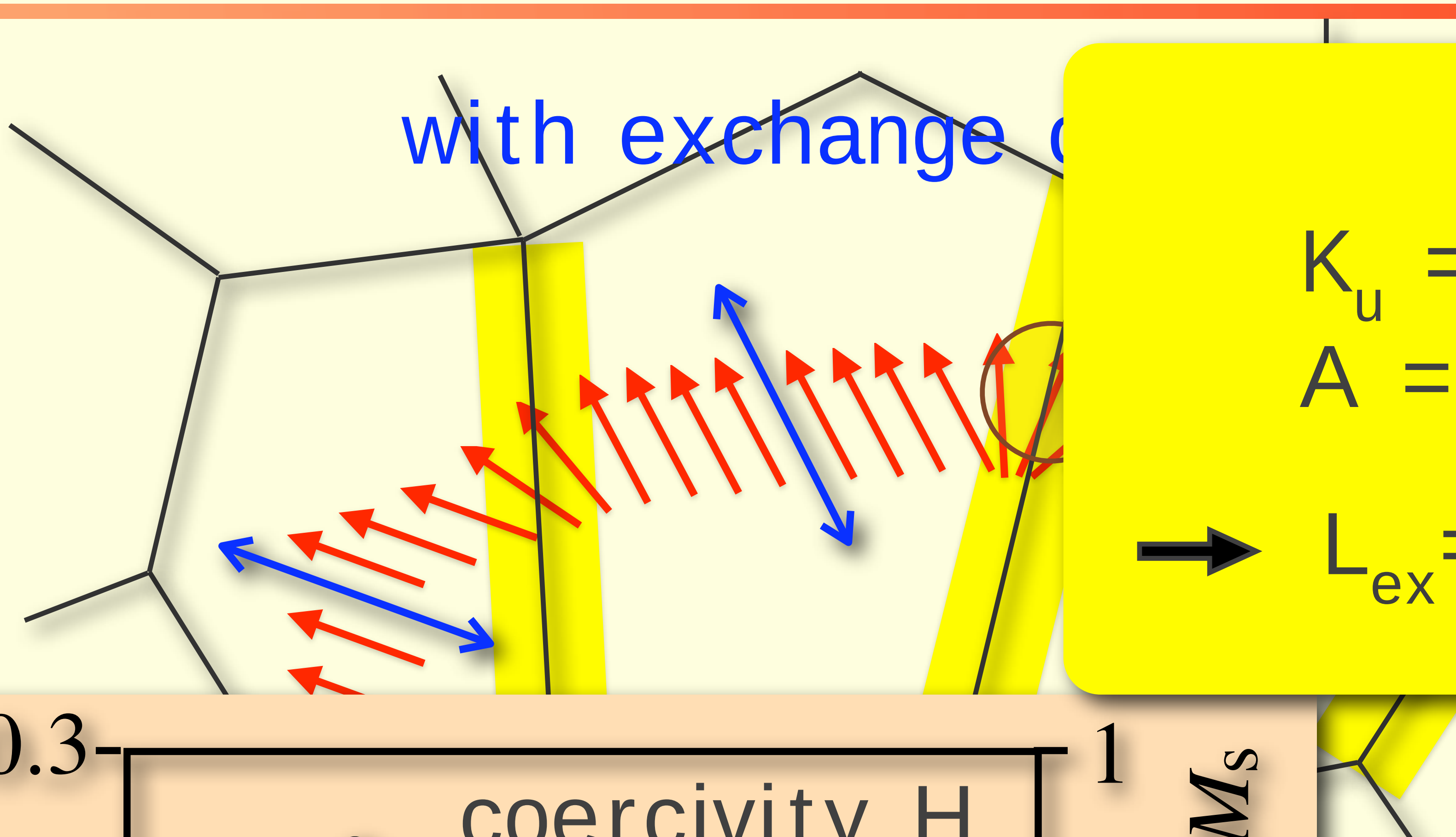

$Nd_2Fe_{14}B$:

$K_u = 4.3 \cdot 10^6\ kJ/m^3$

$A = 8 \cdot 10^{-12}\ J/m$

$\rightarrow\ L_{ex} = \sqrt{A/K_1} = 1.3\ nm$

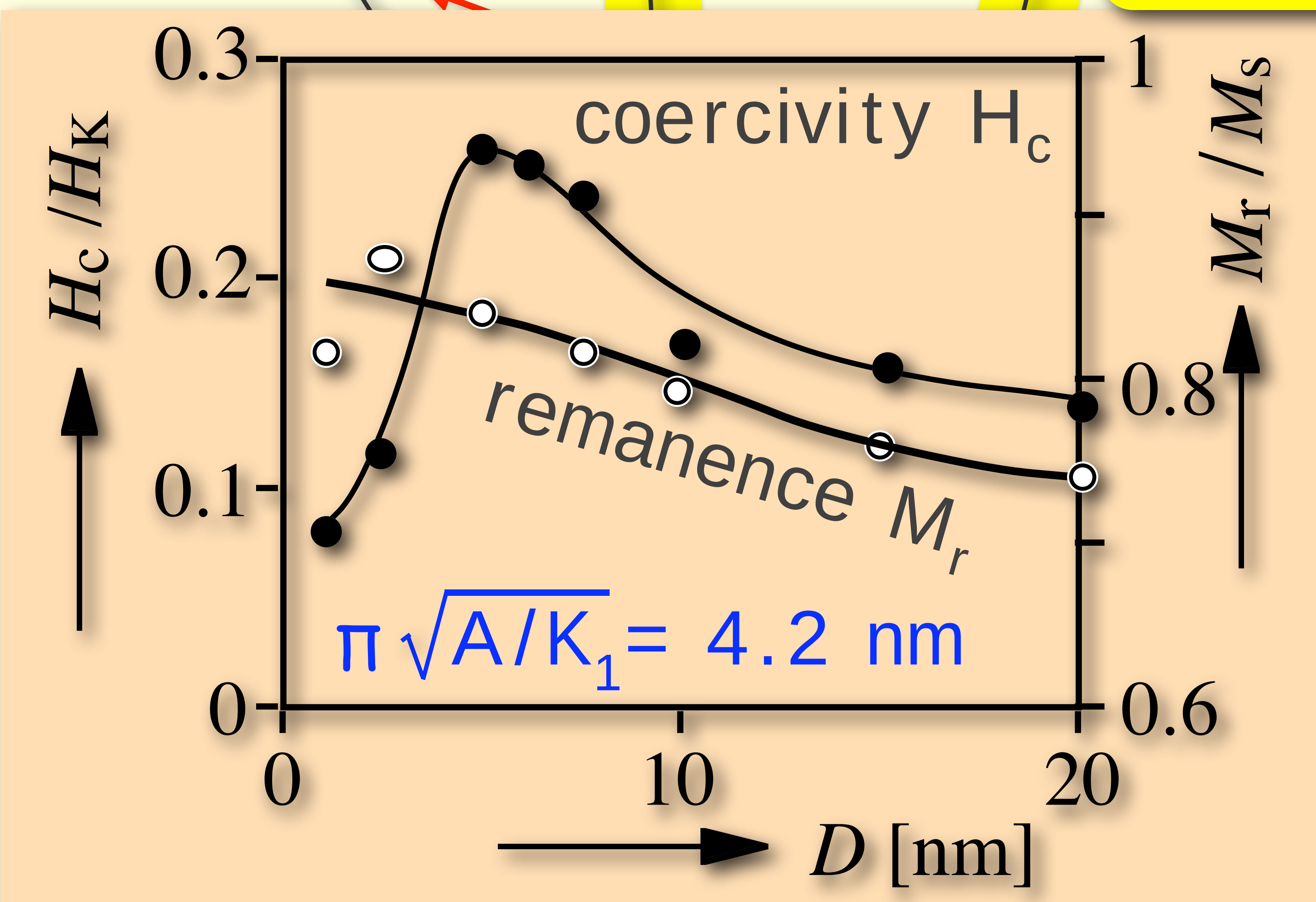

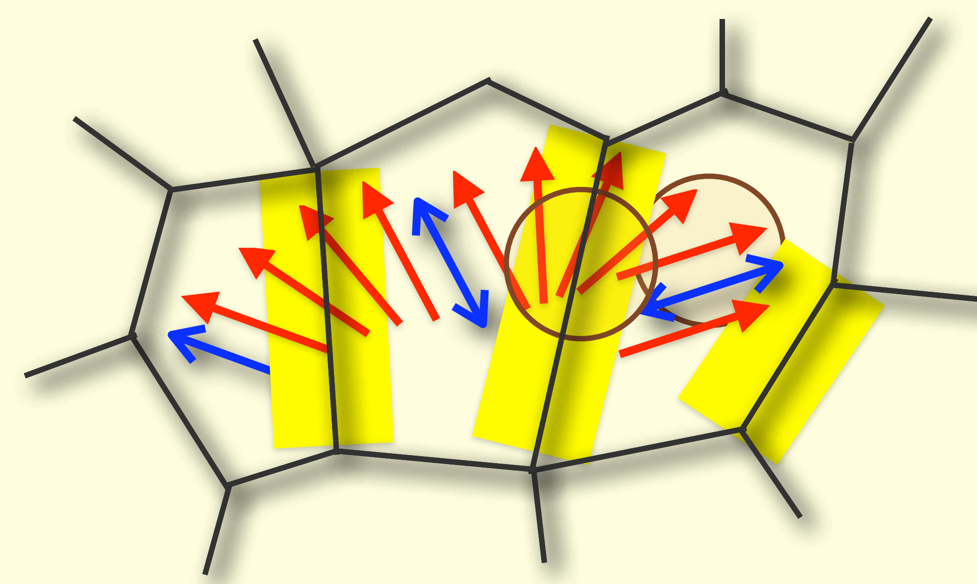

W.Rave & K.Ramstöck, JMMM 171 (1997)

Nanostructured NdFeB: remanence enhancement

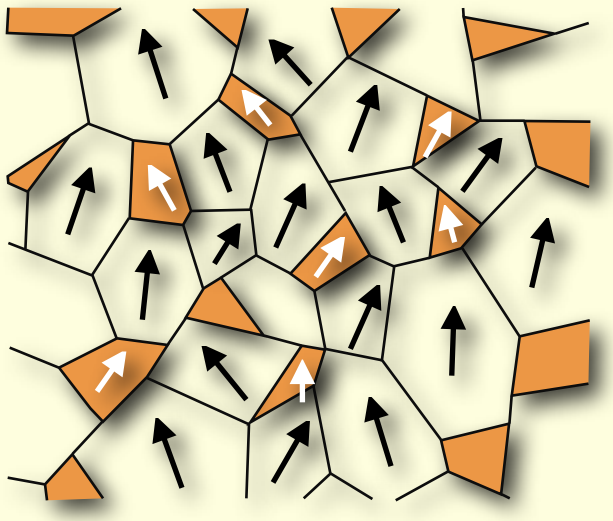

$Nd_2Fe_{14}B$ (J_s = 1.6 T)

α-Fe (J_s = 2.1 T)

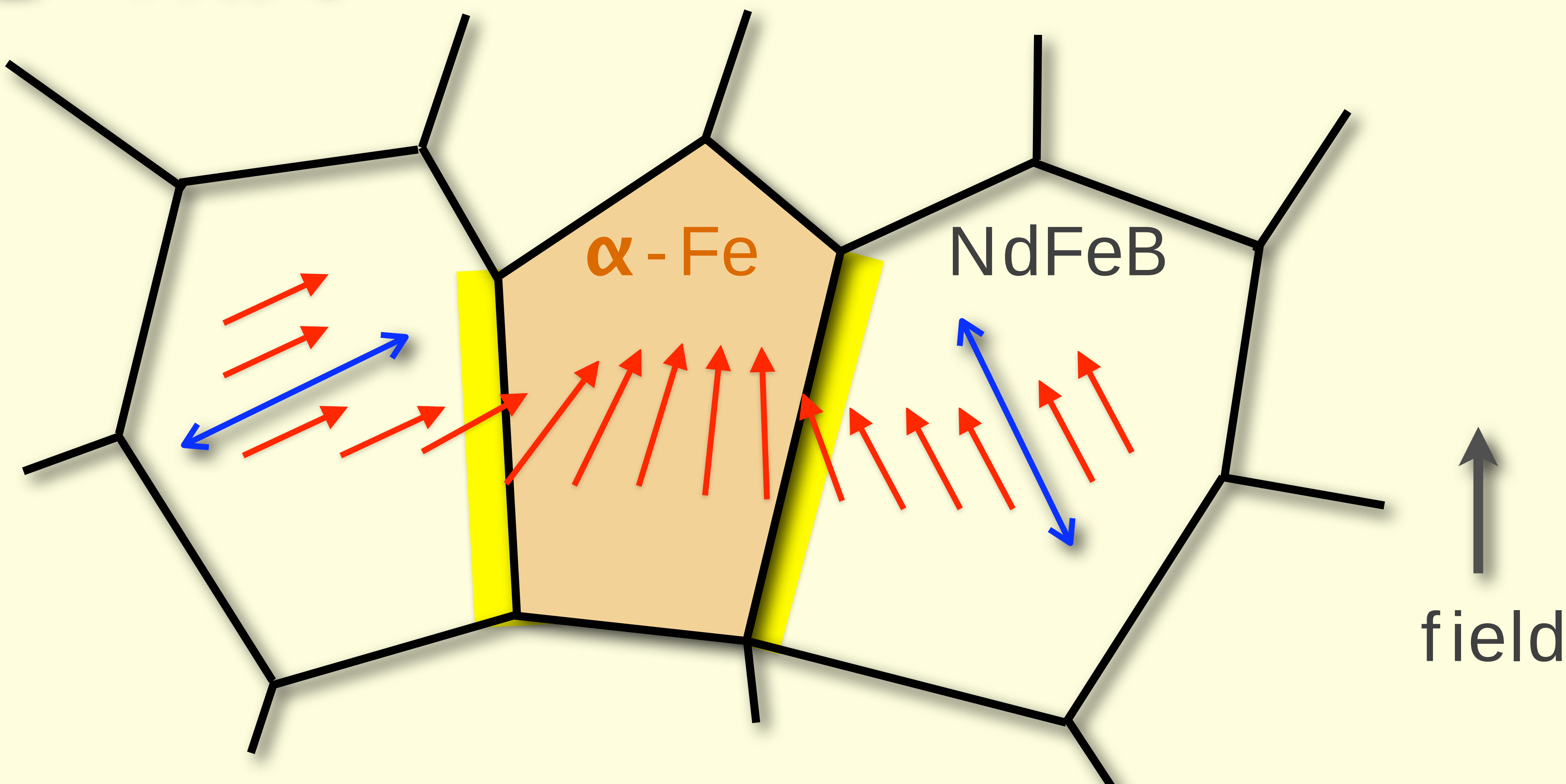

exchange-spring magnet

Nanostructured NdFeB: exchange-spring magnet

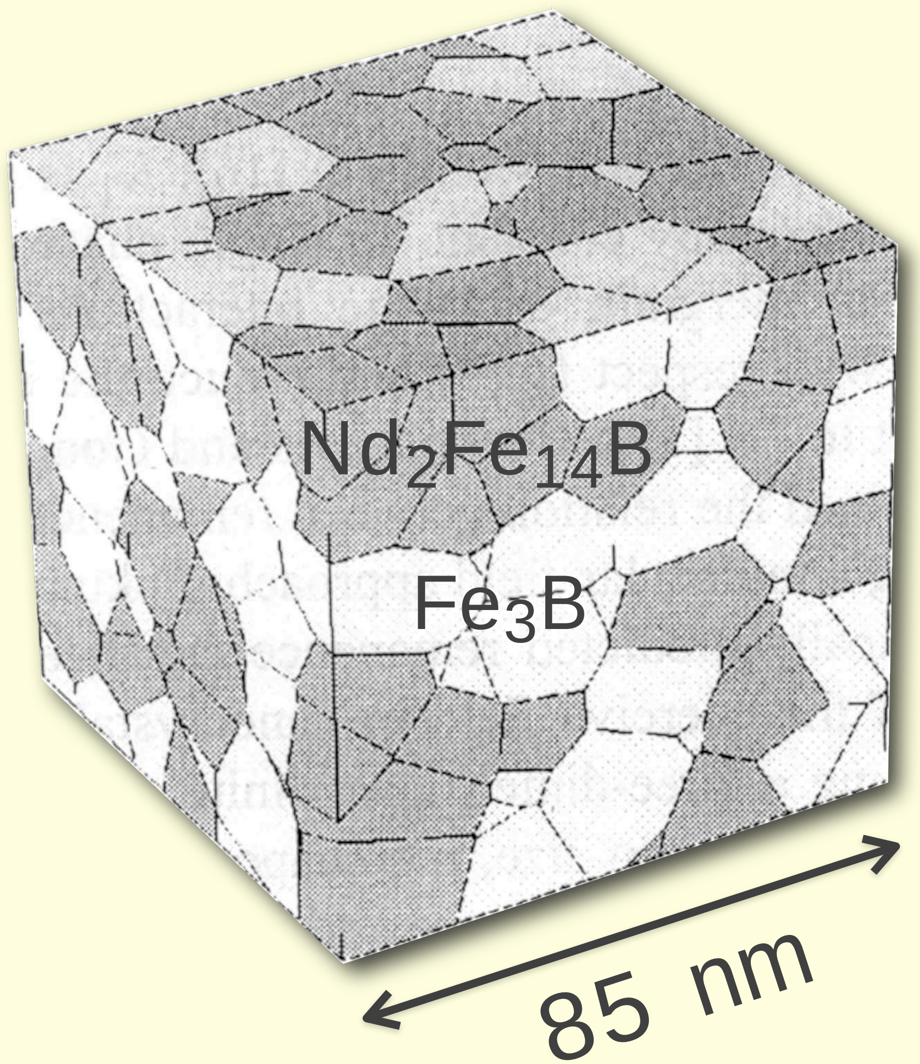

remanent state

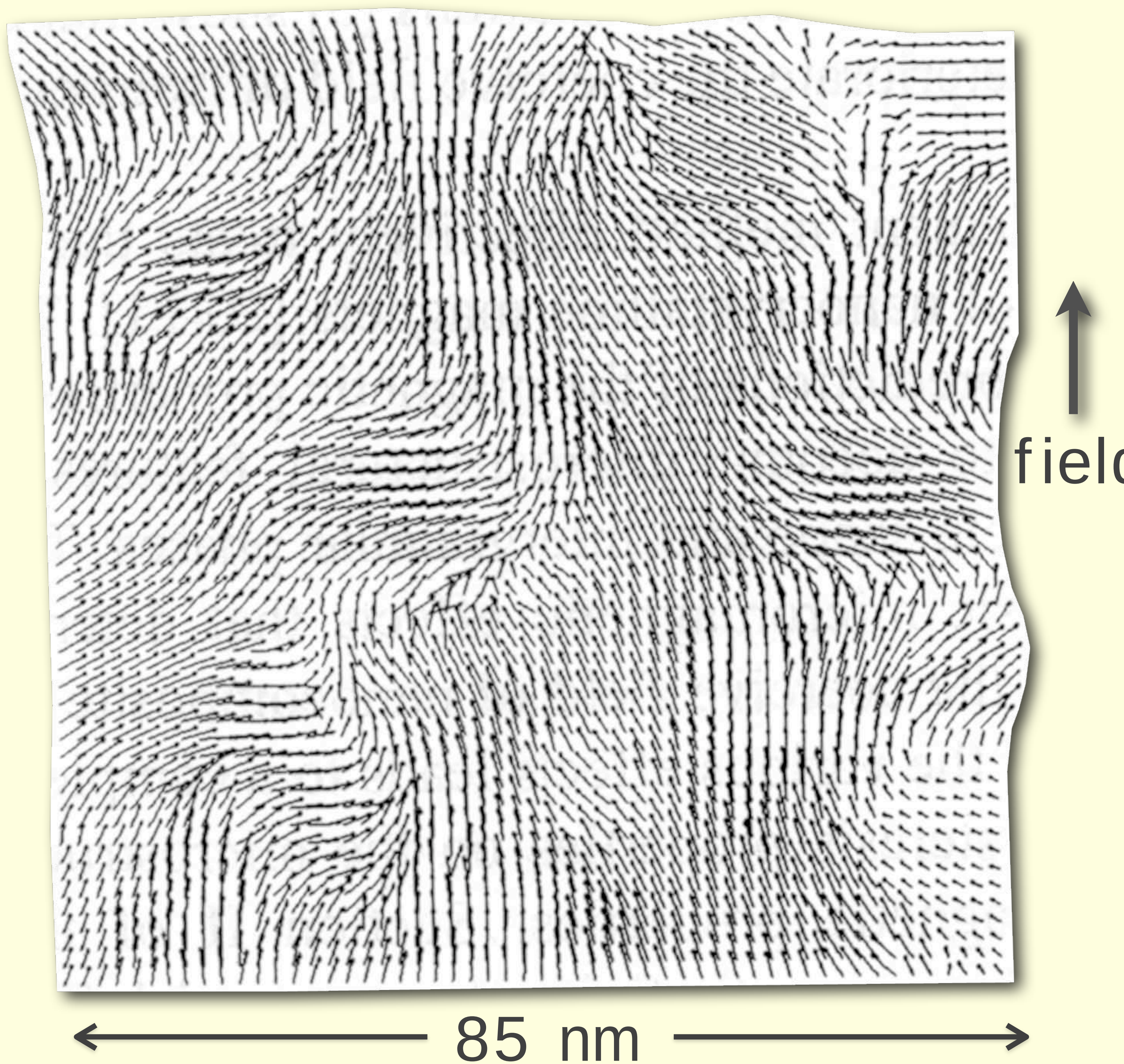

T. Schrefl and J. Fidler, IEEE Trans. Magn. 35, 3223 (1999)

Nanostructured NdFeB: exchange-spring magnet

Bright field
TEM image

Foucault
image

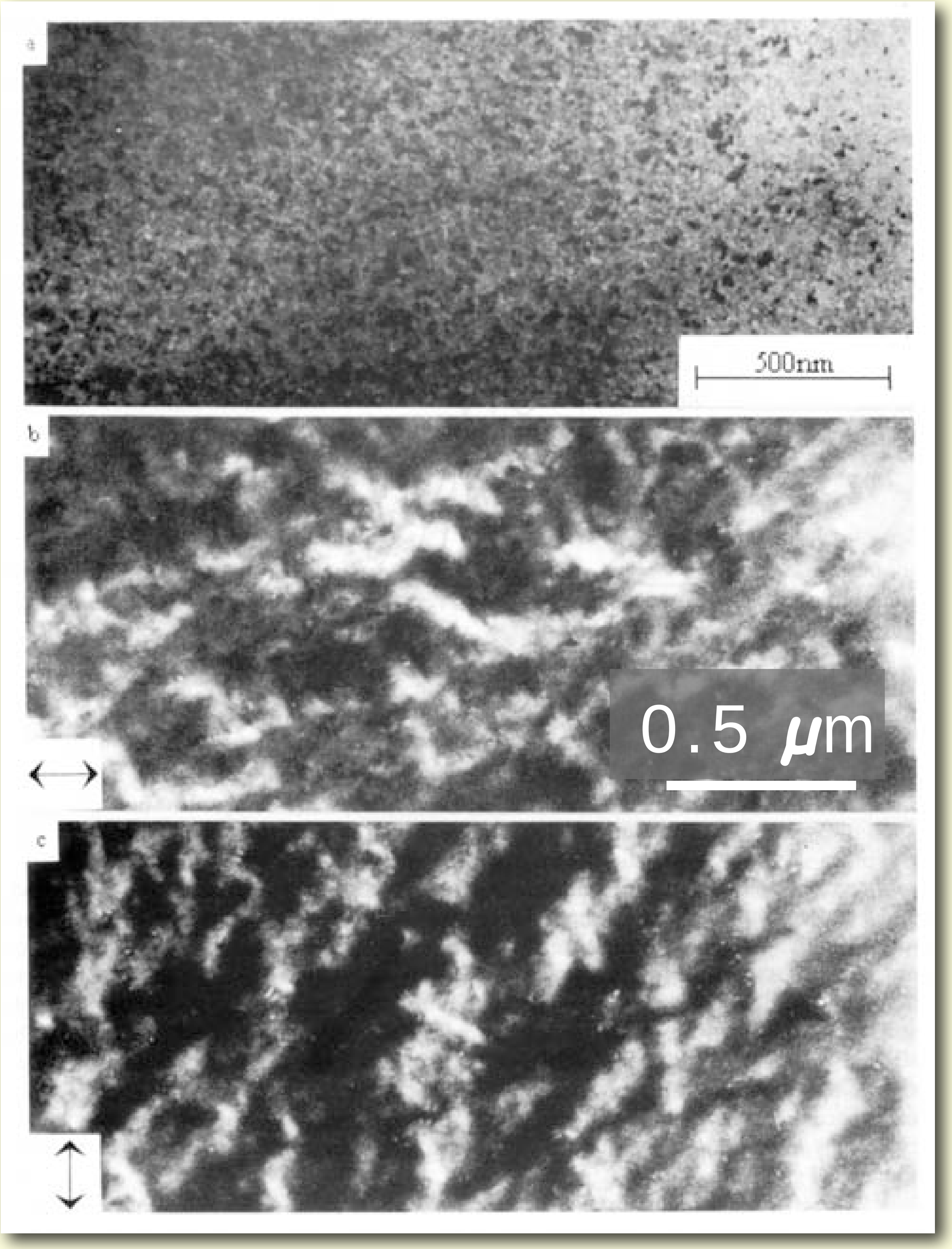

J. Chapman et al.,
13th Int. Workshop on
RE Magnets and their
Applications (1994)

Nanostructured NdFeB: exchange-spring magnet

FeSiBCuNb overannealed

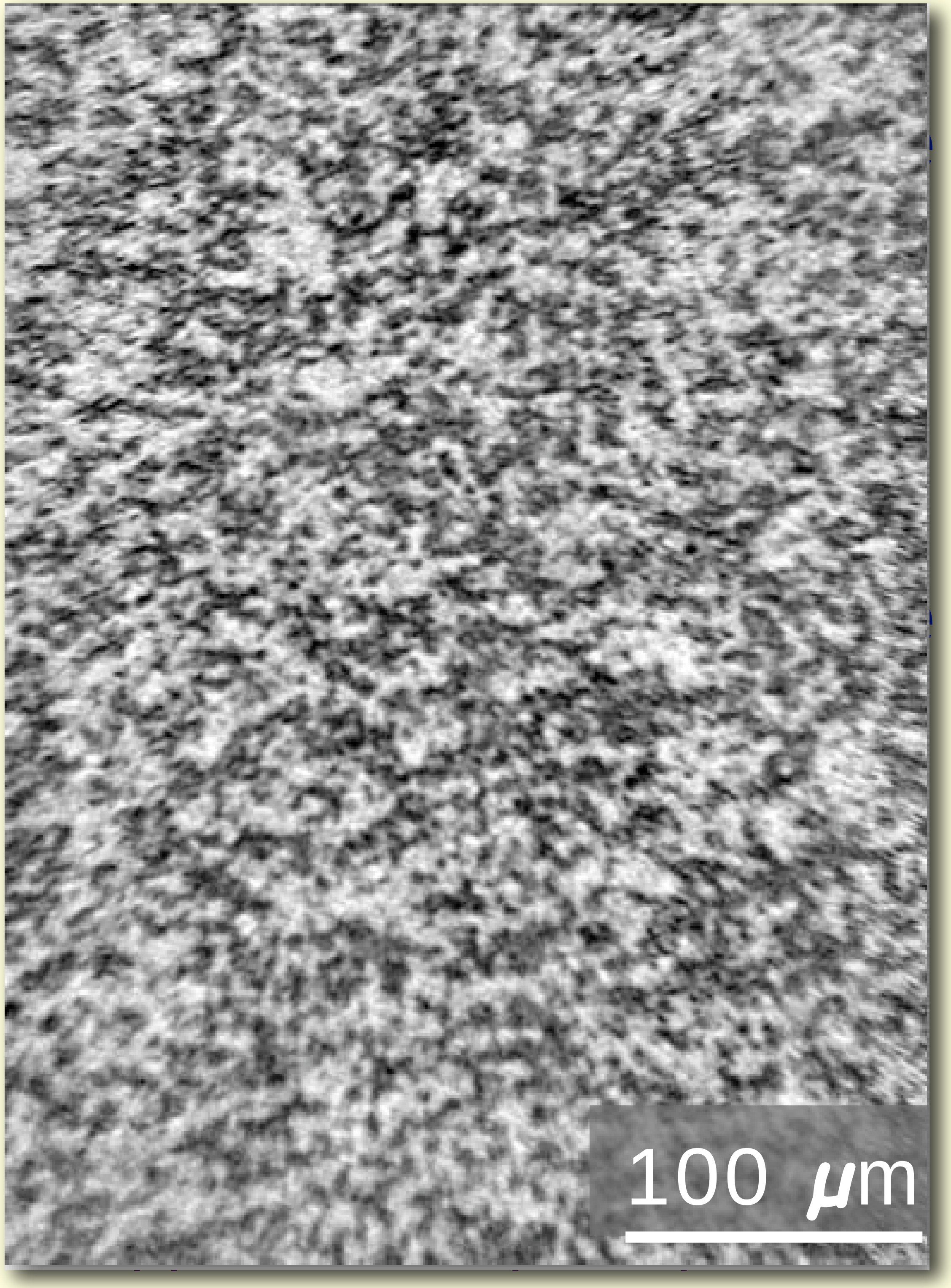

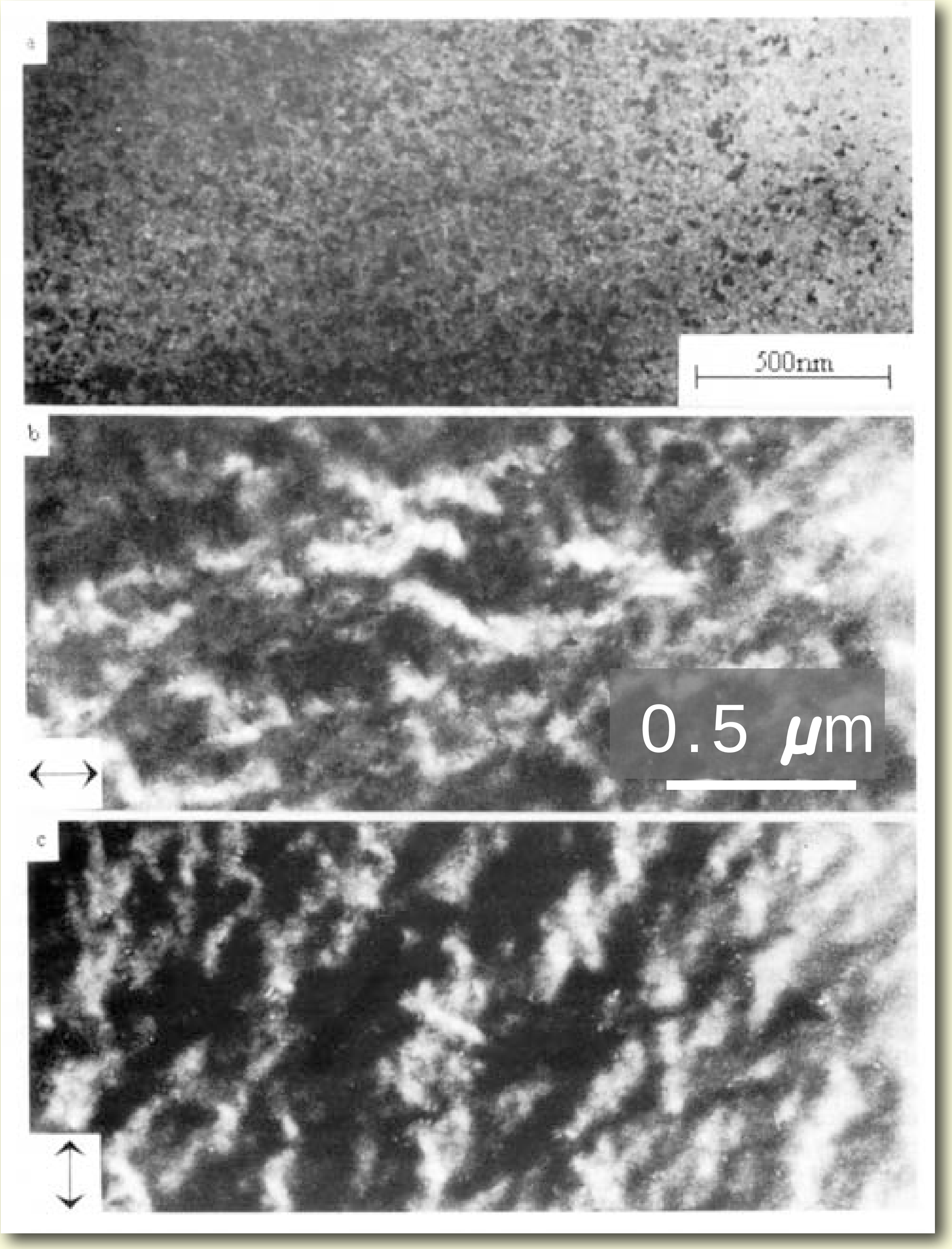

3 types of nanostructured NdFeB magnets

Isotropic magnets: Remanence ($M_r = M_s/2$)

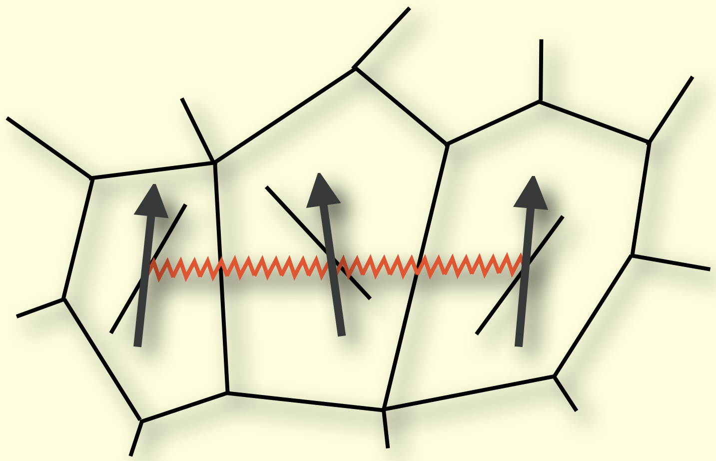

exchanged coupled grains based on stoichiometric $Nd_2Fe_{14}B$

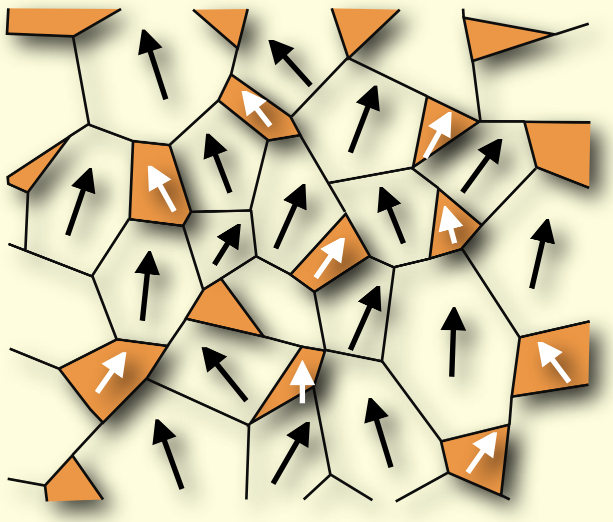

exchanged coupled grains based on nanocomposite $Nd_2Fe_{14}B$ / **α**-Fe

Remanence enhancement for isotropic magnets

3 types of nanostructured NdFeB magnets

Isotropic magnets: Remanence ($M_r = M_s/2$)

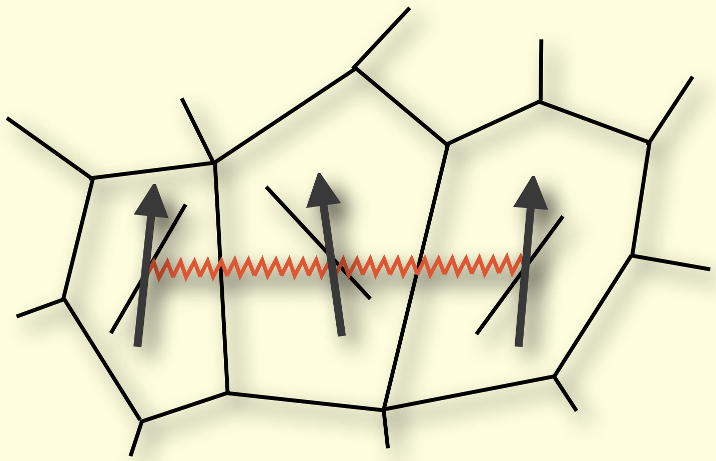

exchanged coupled grains based on stoichiometric $Nd_2Fe_{14}B$

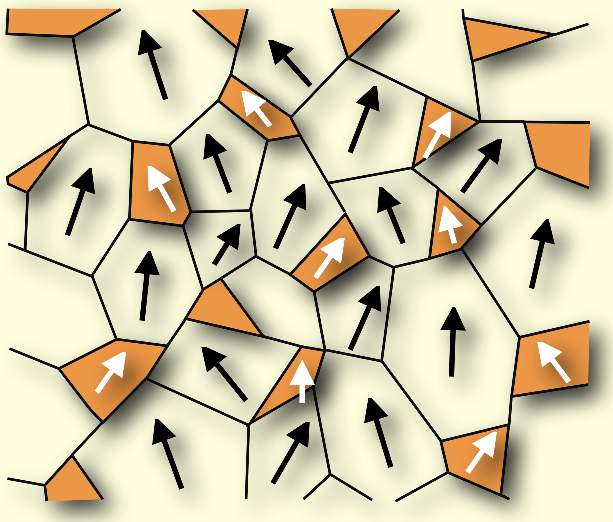

exchanged coupled grains based on nanocomposite $Nd_2Fe_{14}B$ / α-Fe

Remanence enhancement for isotropic magnets

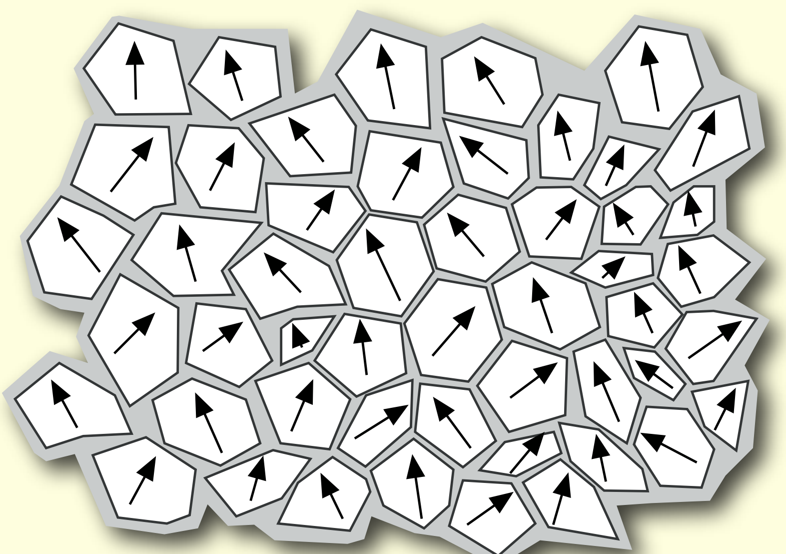

decoupled $Nd_2Fe_{14}B$ grains separated by thin paramagnetic layer

Remanence enhancement by texturing

Permanent magnets, basics

isotropic

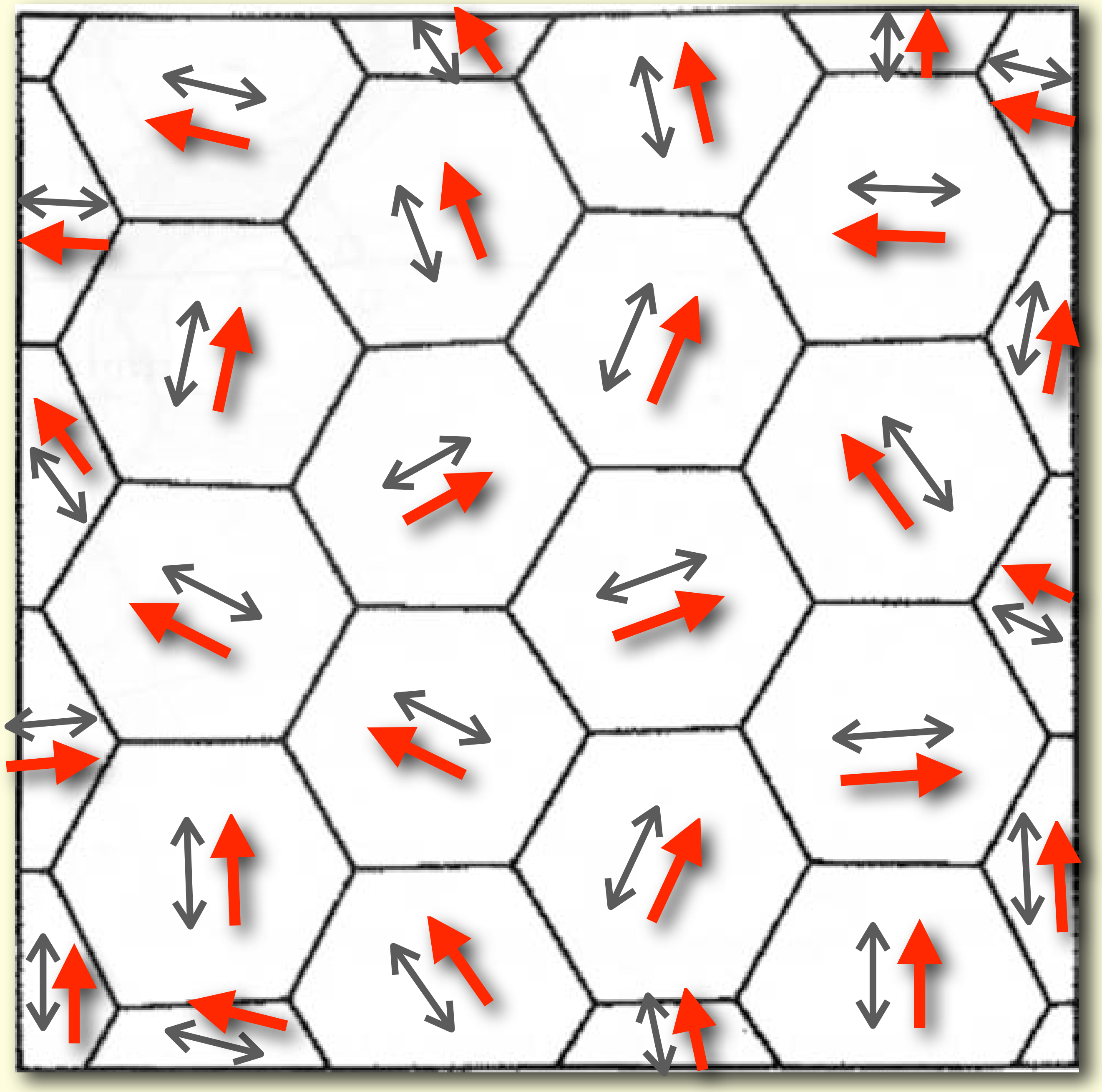

remanence = 0.5 M_s

anisotropic (textured)

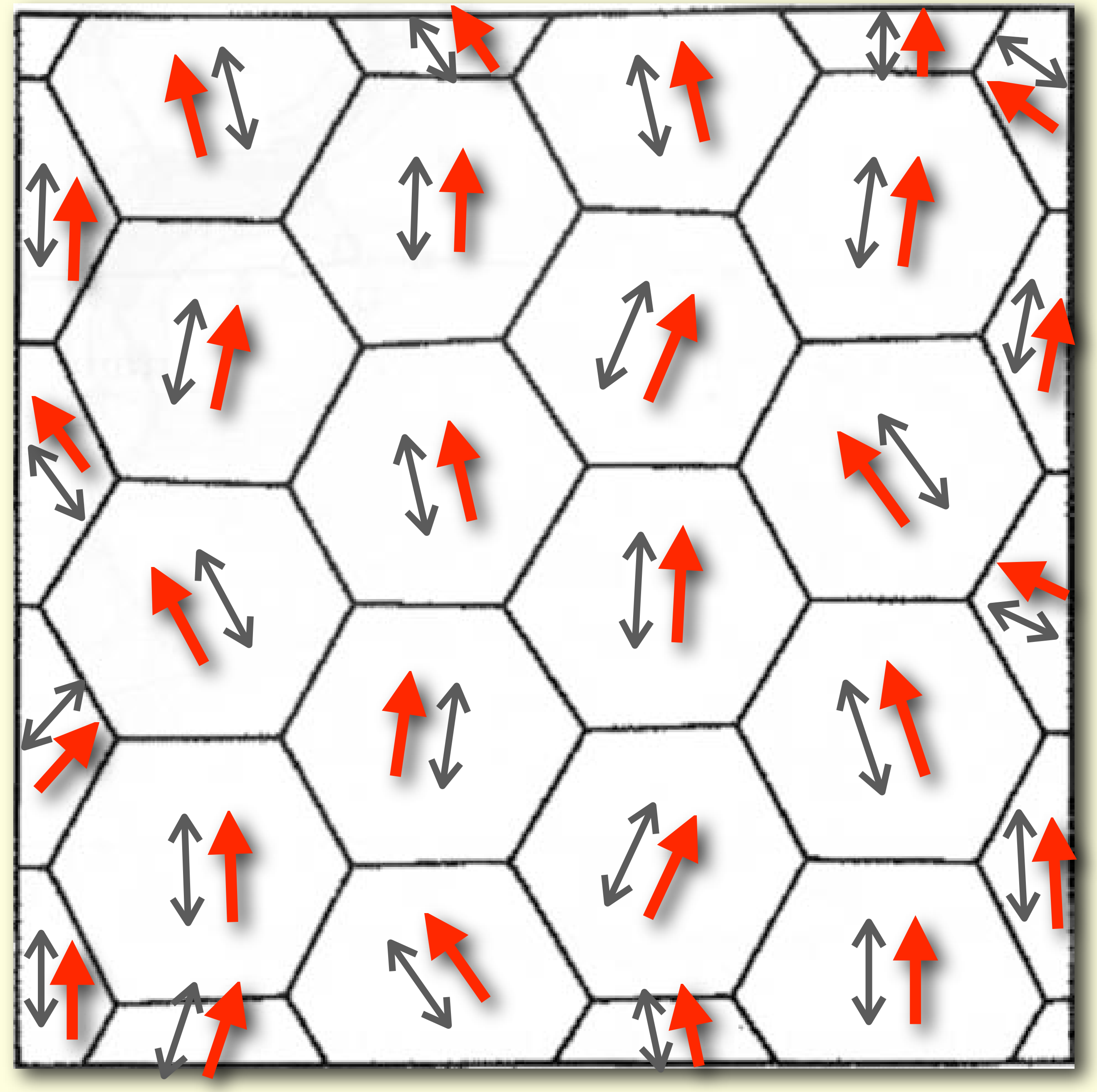

remanence > 0.5 M_s

field

Nanostructured NdFeB: decoupled grains

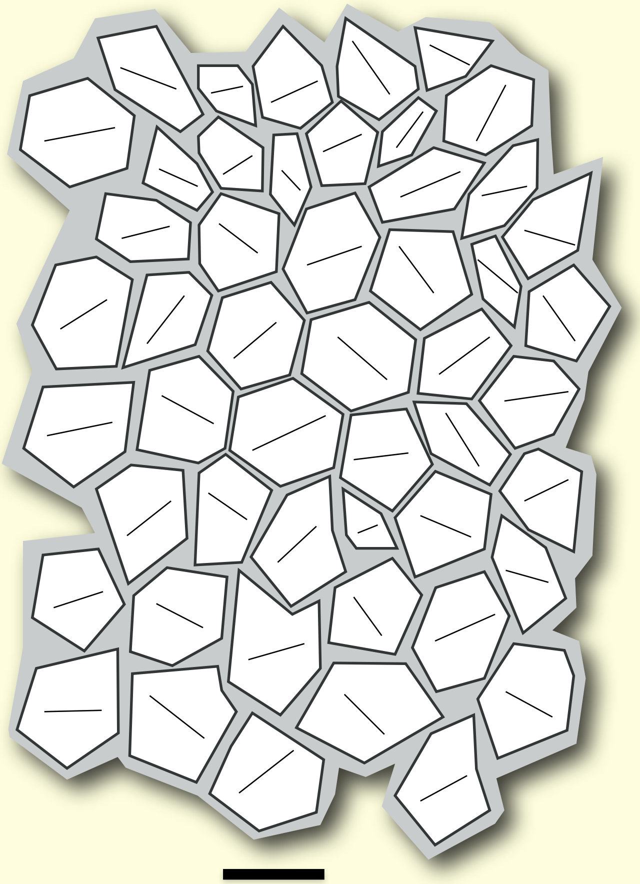

some 100 nm

Nanostructured NdFeB: decoupled grains

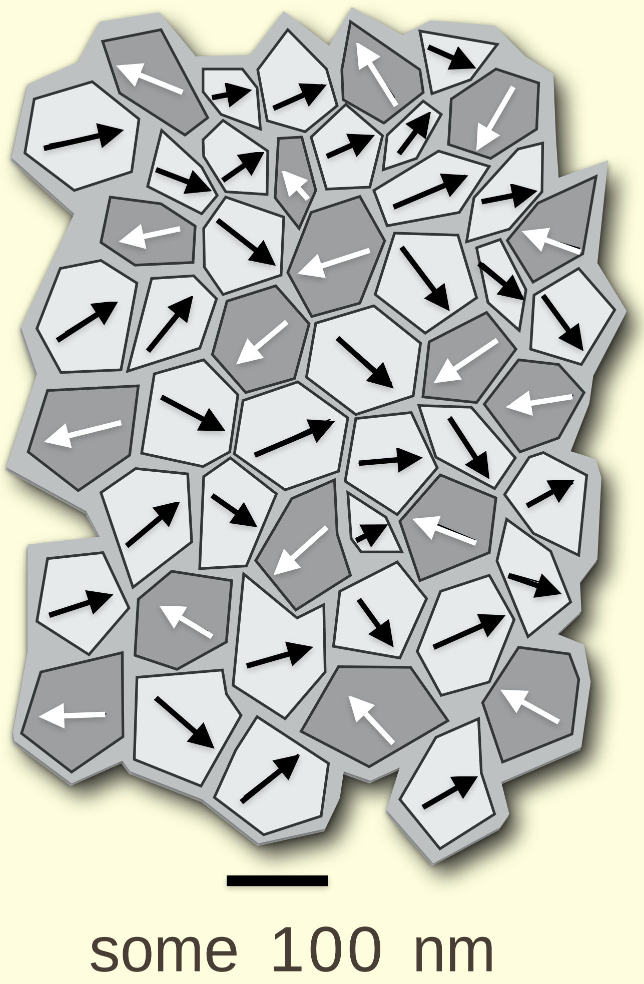

Nanostructured NdFeB: decoupled grains

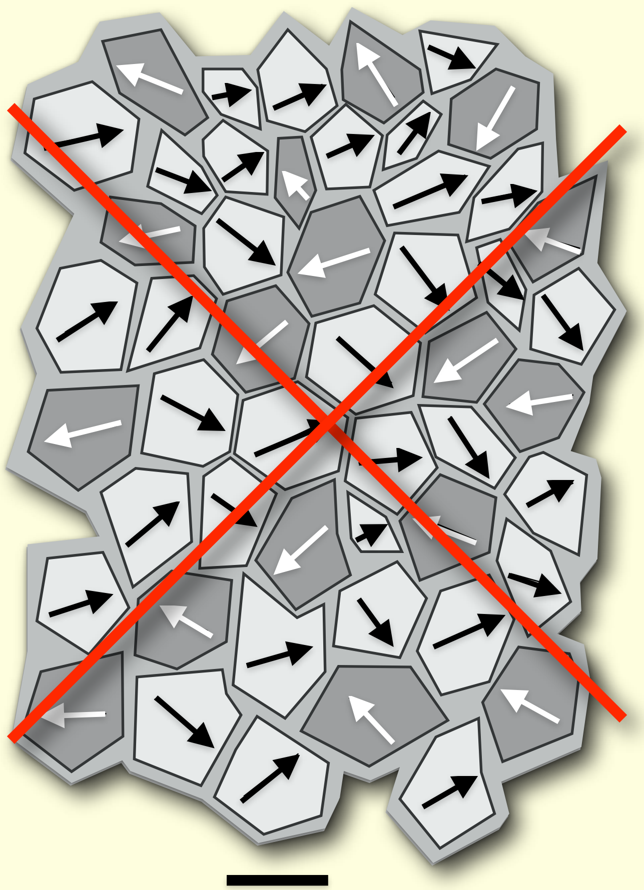

some 100 nm

Nanostructured NdFeB: decoupled grains

observation perpendicular to texture axis

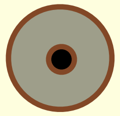

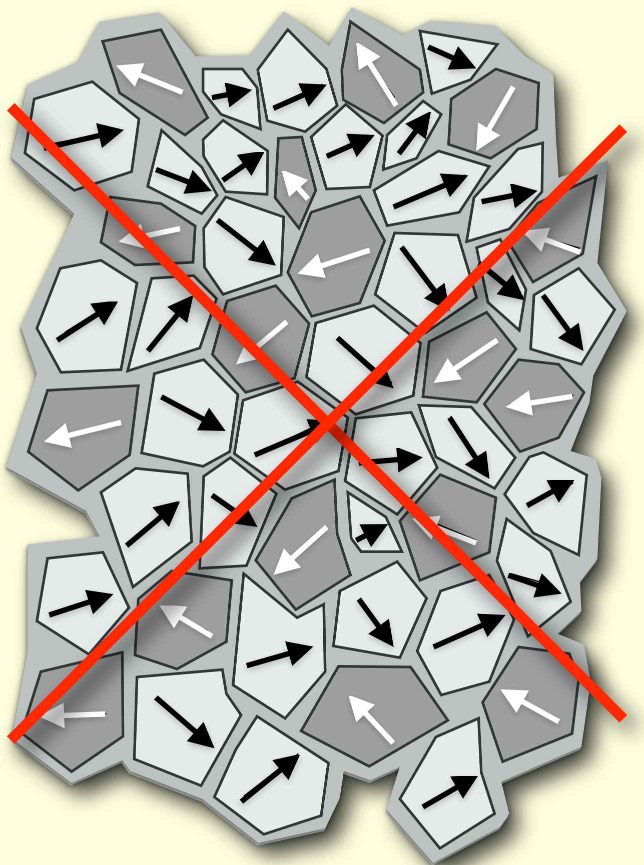

some 100 nm

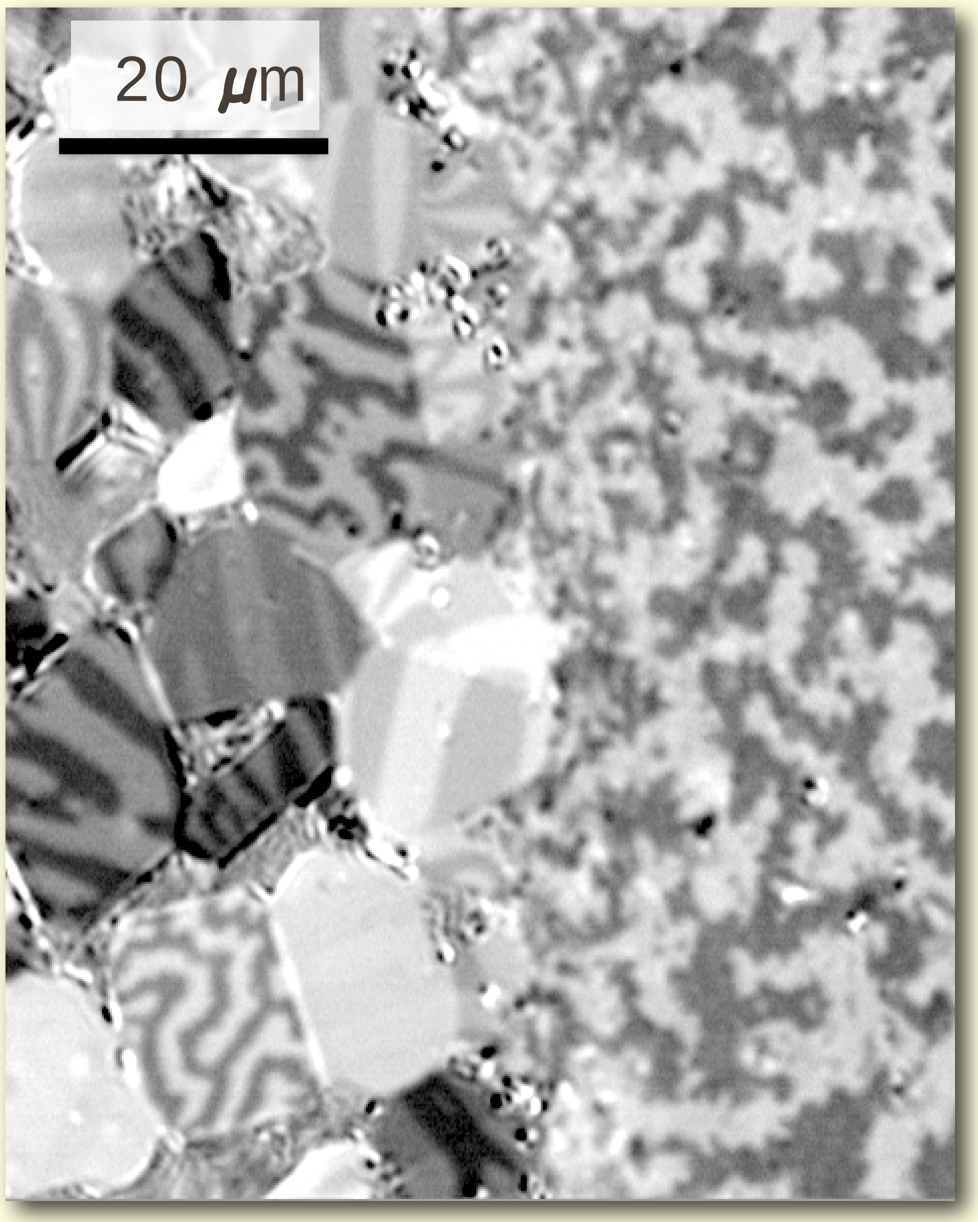

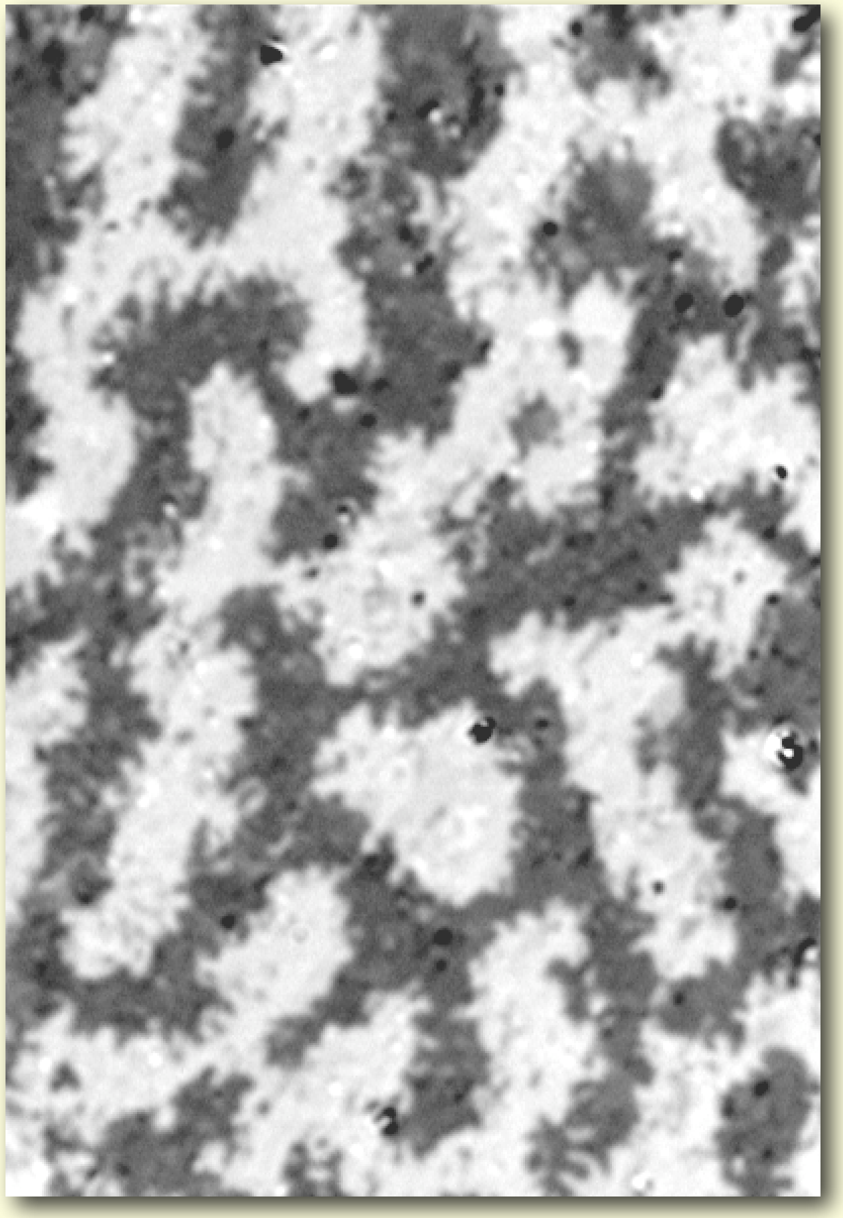

coarse grains | fine grains

Nanostructured NdFeB: decoupled grains

Hot deformed NdFeB magnet (thermally demagnetized)

(deformation degree ~ 76%, texture parameter $(B_r^{||} - B_r^{\perp})/B_r^{||} = 0.79$)

observed perpendicular to texture axis

grain structure

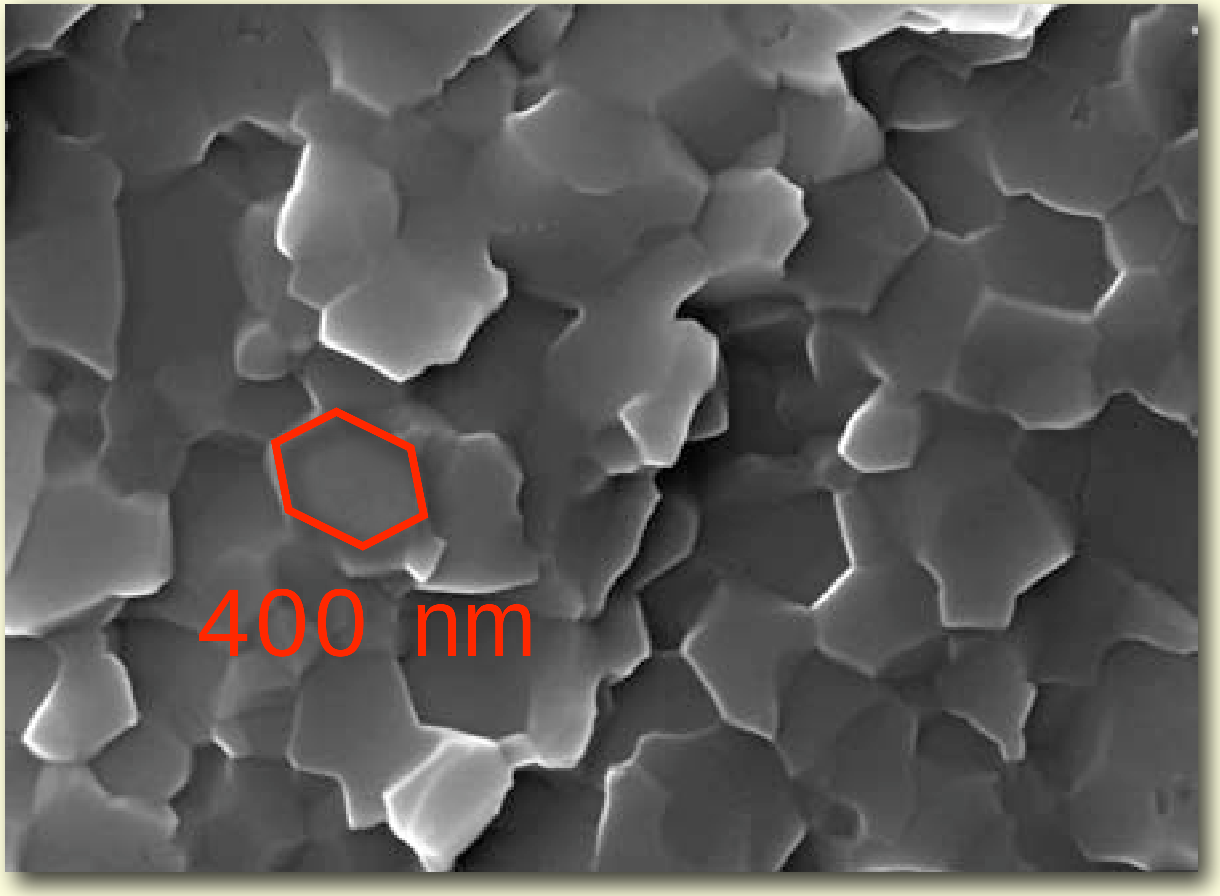

domains

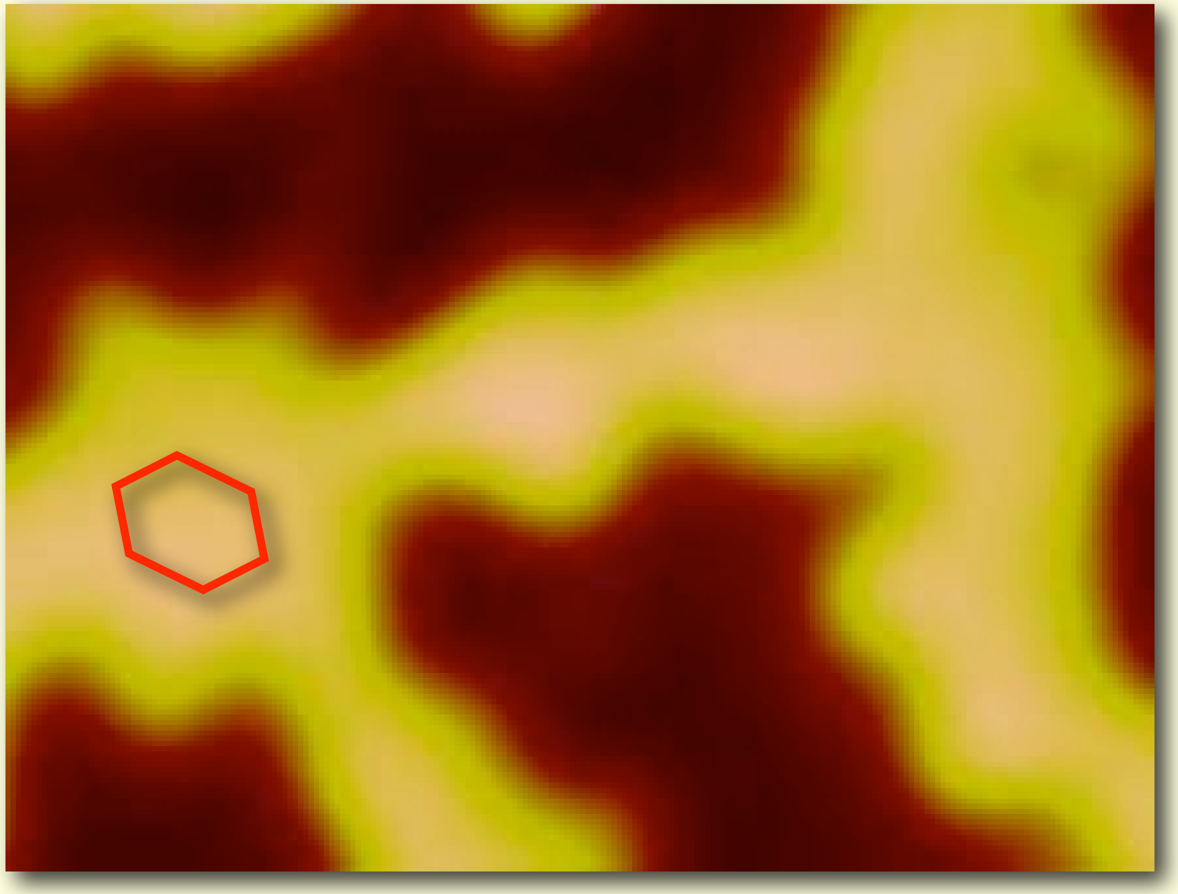

courtesy K. Khlopkov and O. Gutfleisch (IFW Dresden)

Nanostructured NdFeB: decoupled grains

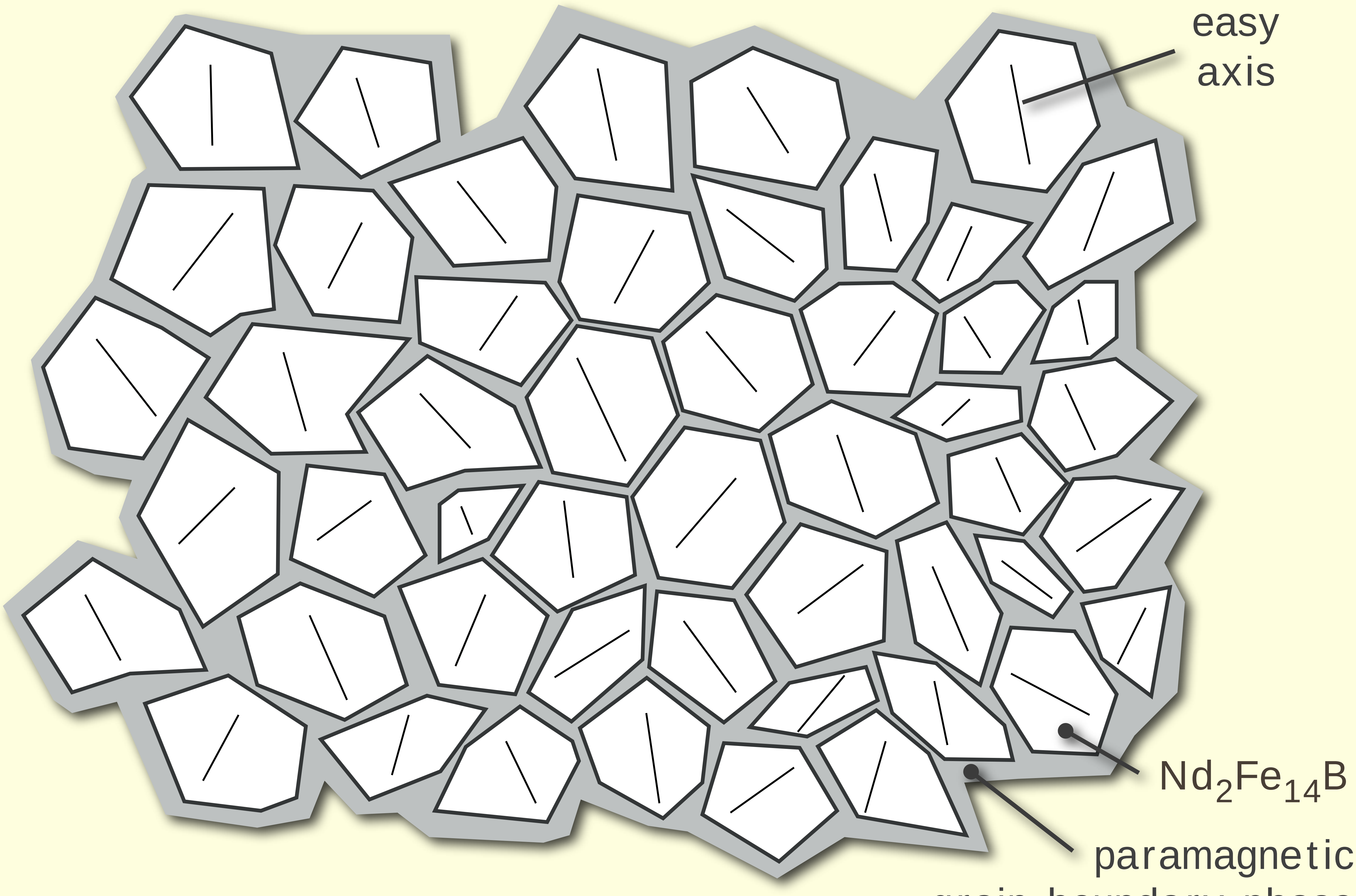

Nanostructured NdFeB: decoupled grains

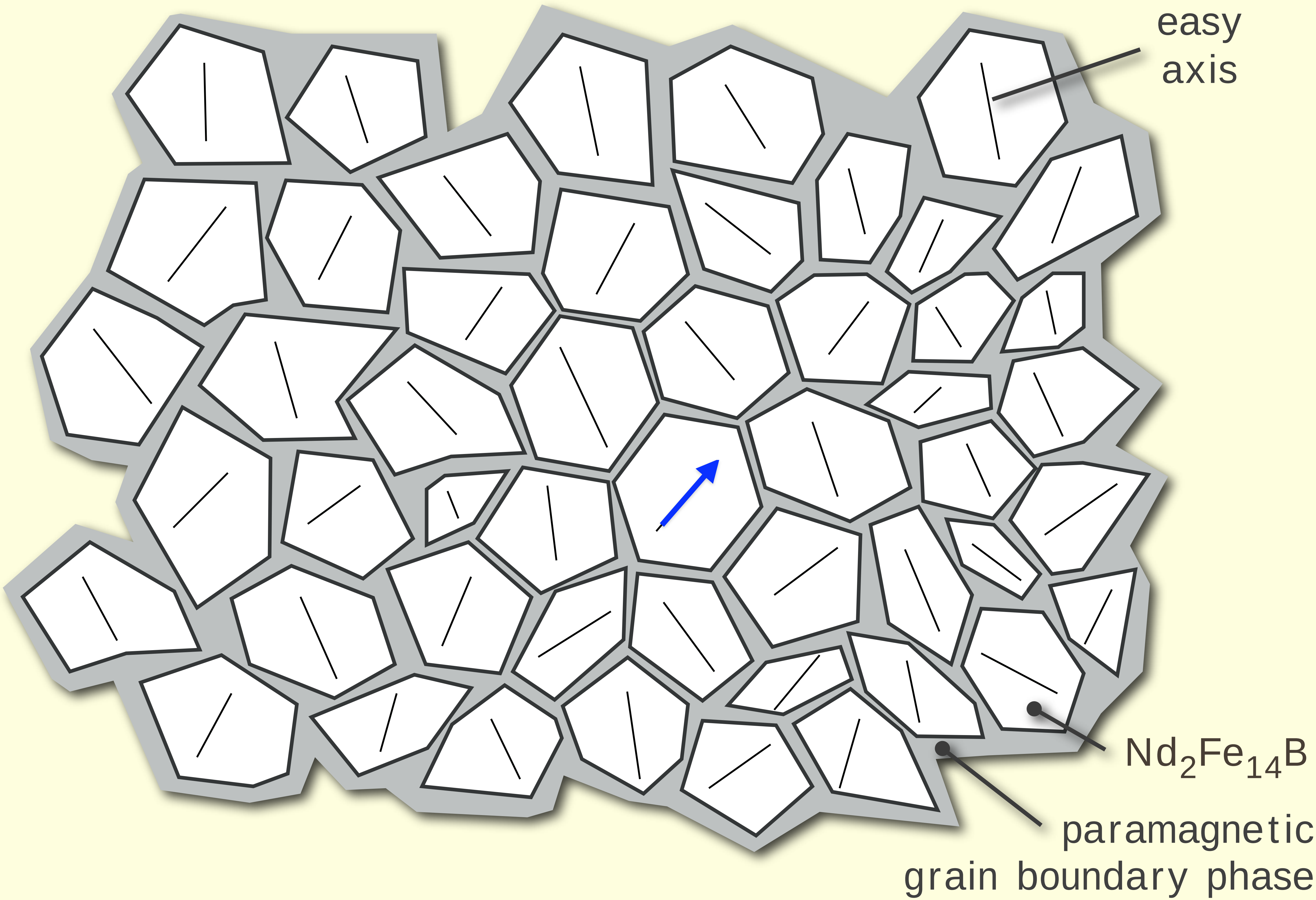

Nanostructured NdFeB: decoupled grains

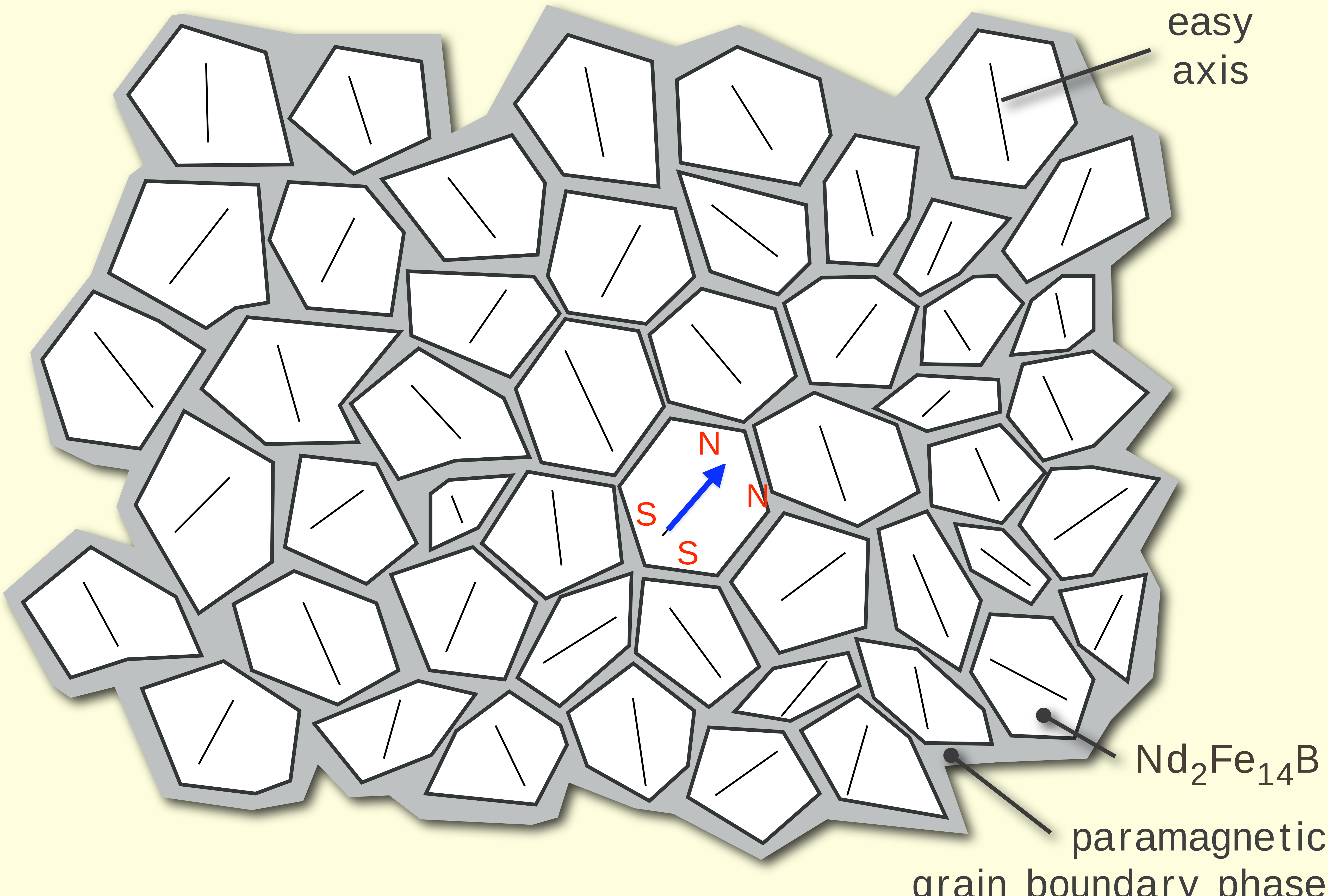

Nanostructured NdFeB: decoupled grains

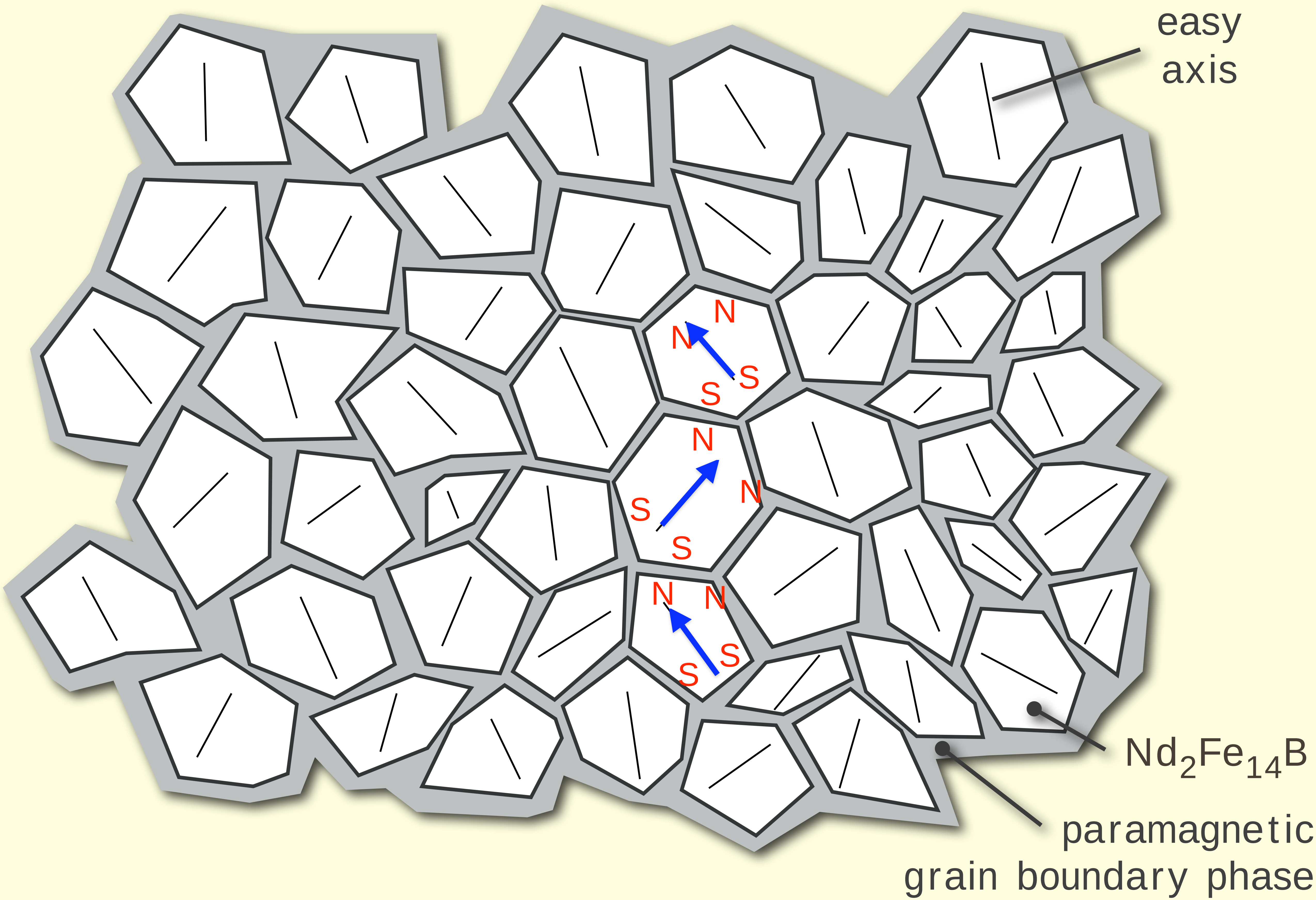

Nanostructured NdFeB: decoupled grains

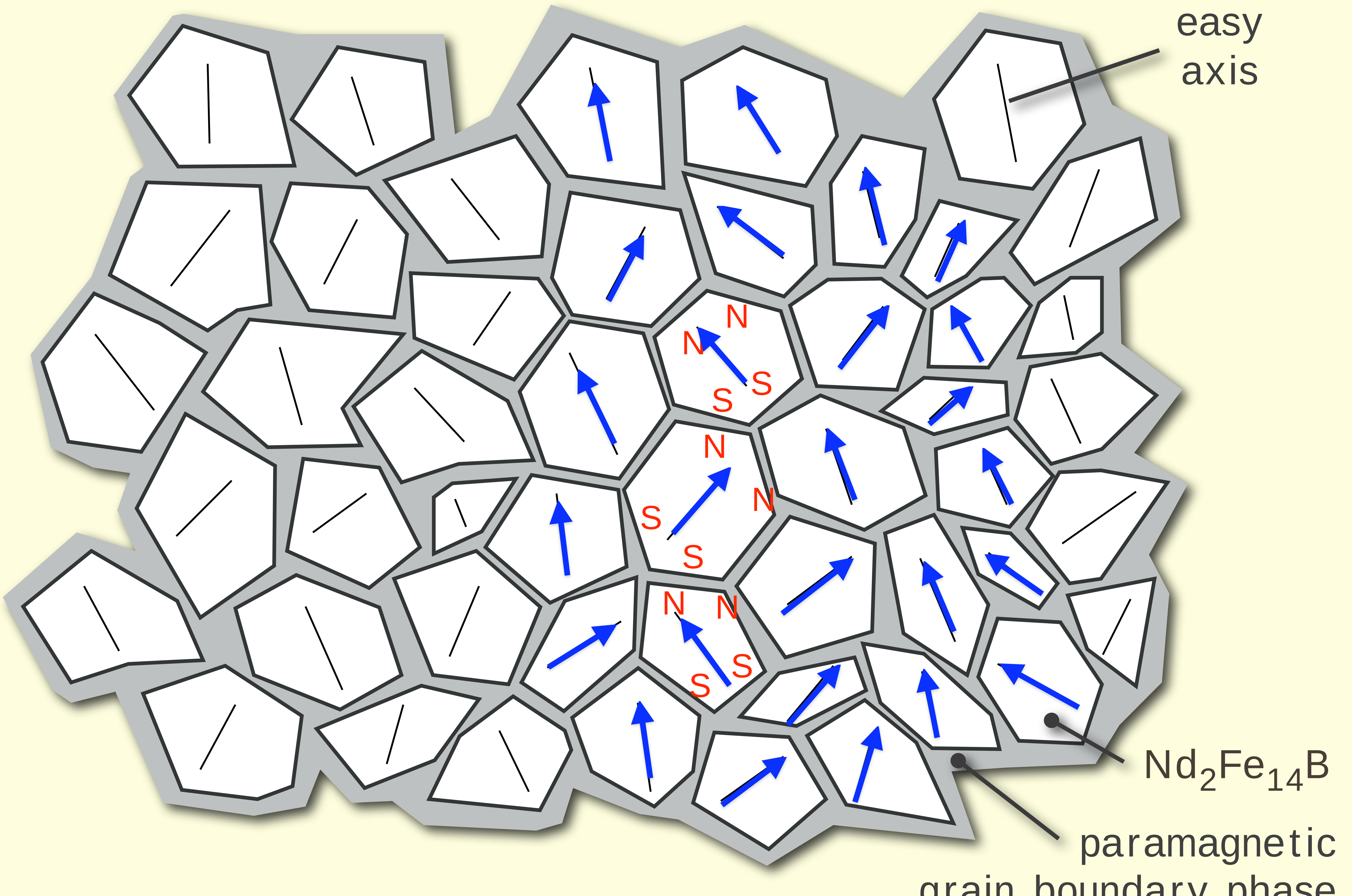

Nanostructured NdFeB: decoupled grains

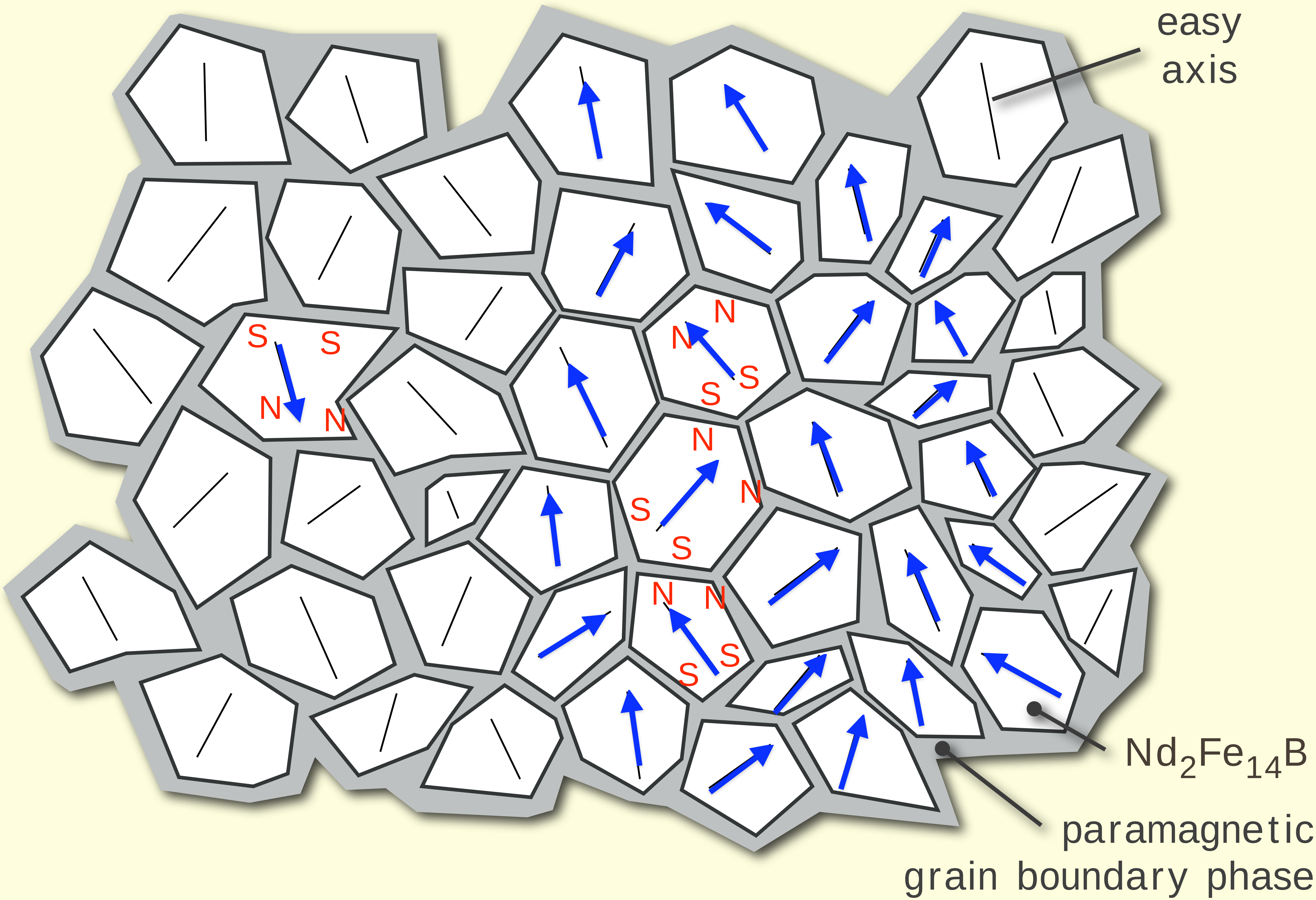

Nanostructured NdFeB: decoupled grains

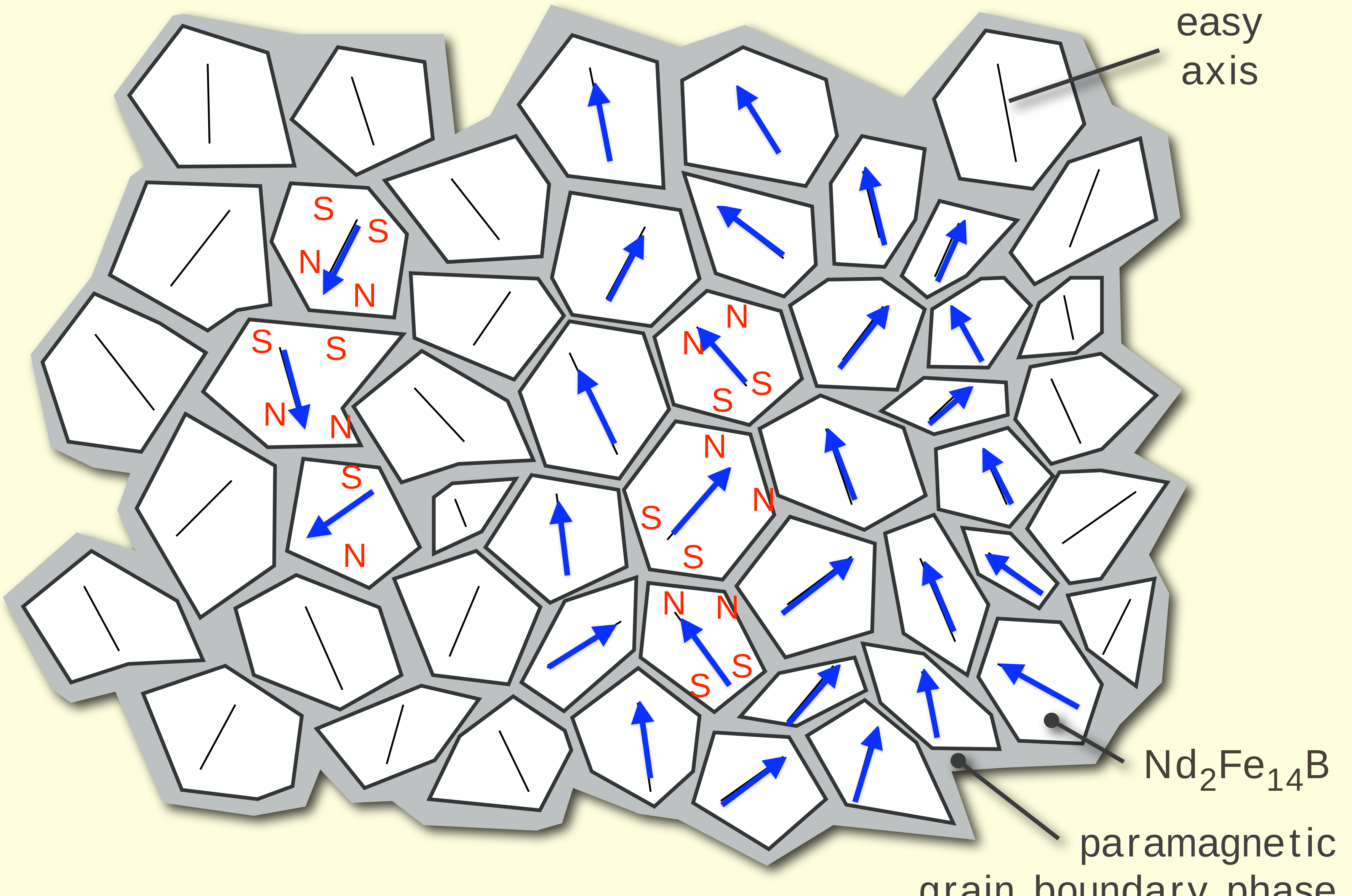

Nanostructured NdFeB: decoupled grains

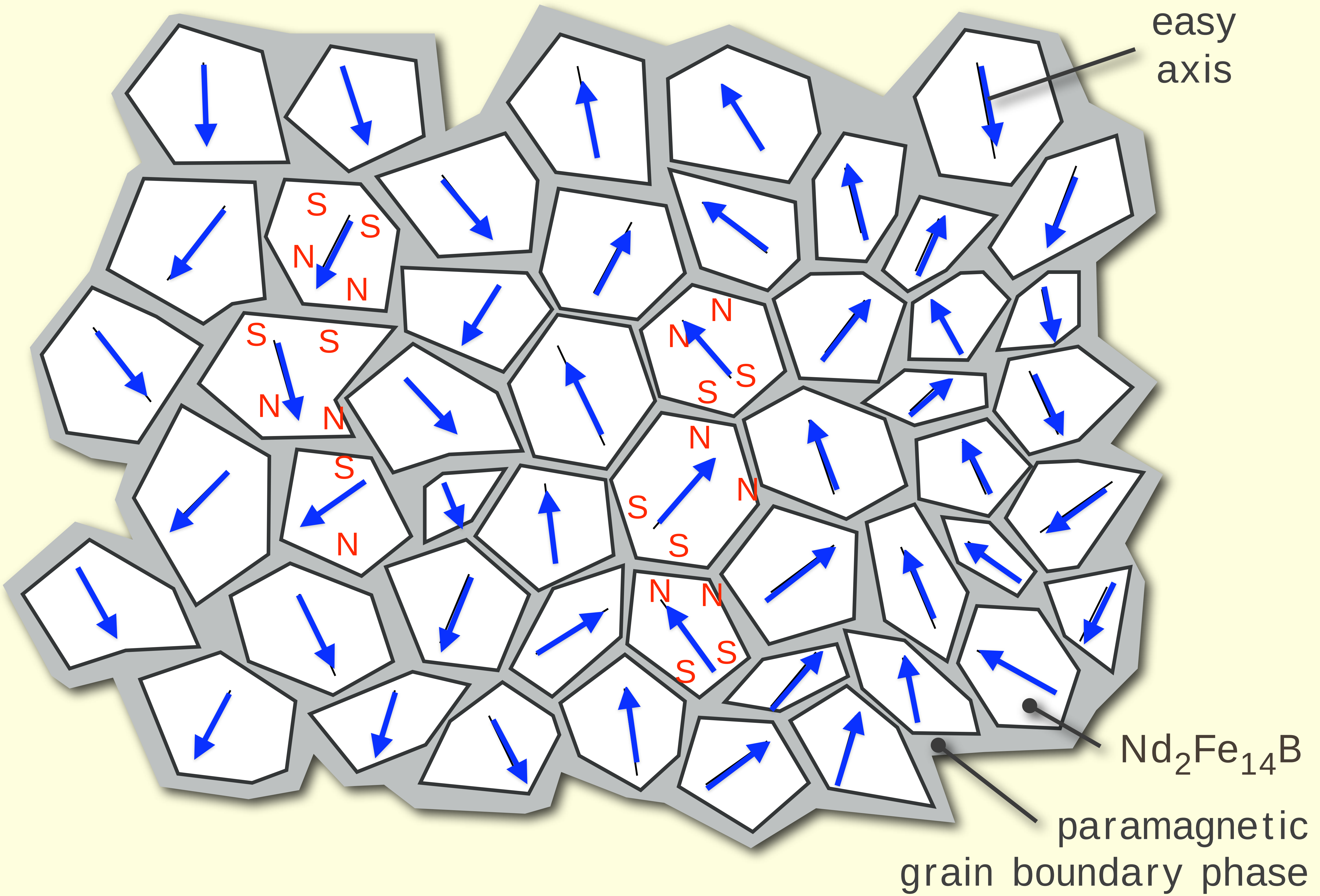

Nanostructured NdFeB: decoupled grains

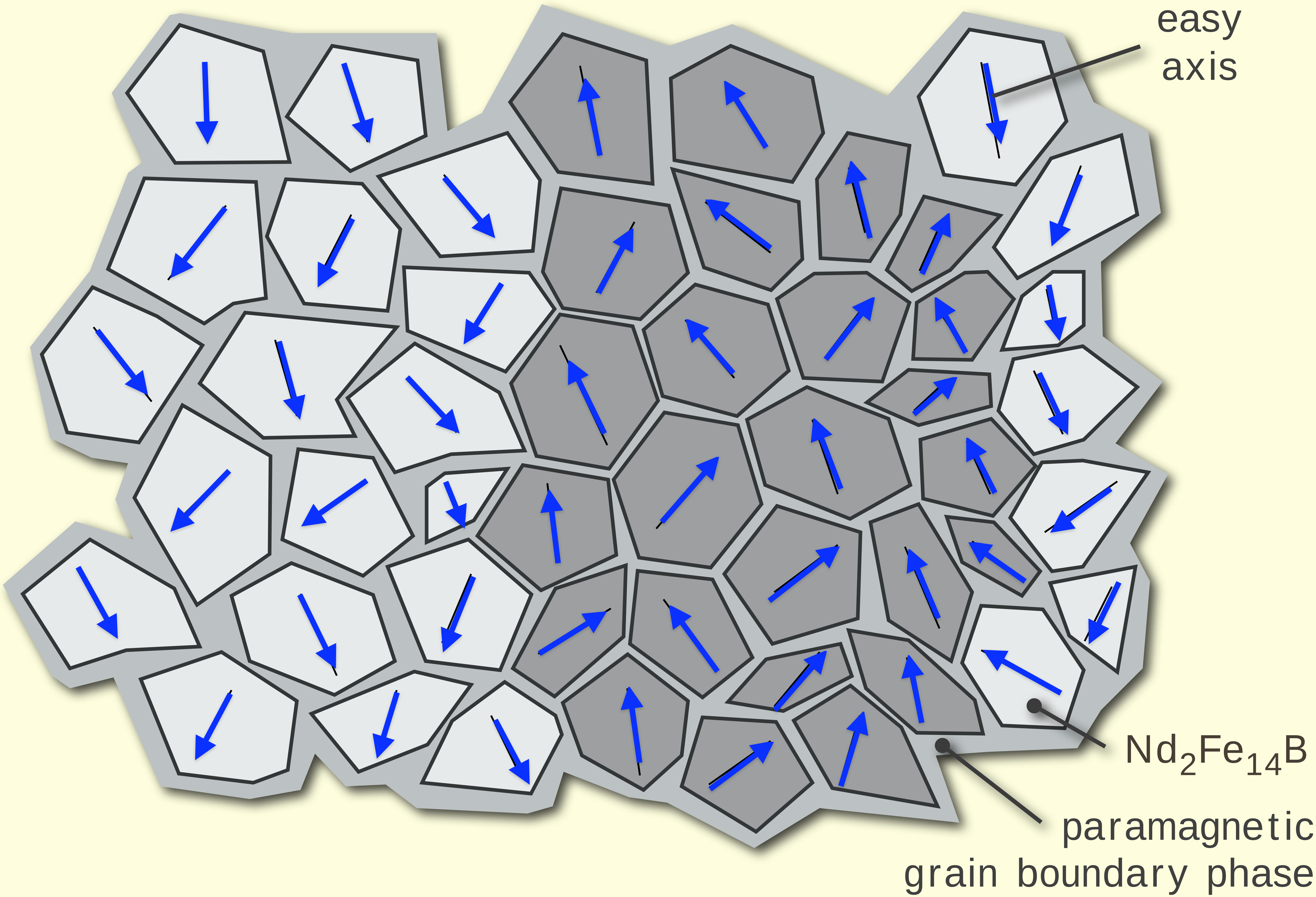

Nanostructured NdFeB: decoupled grains

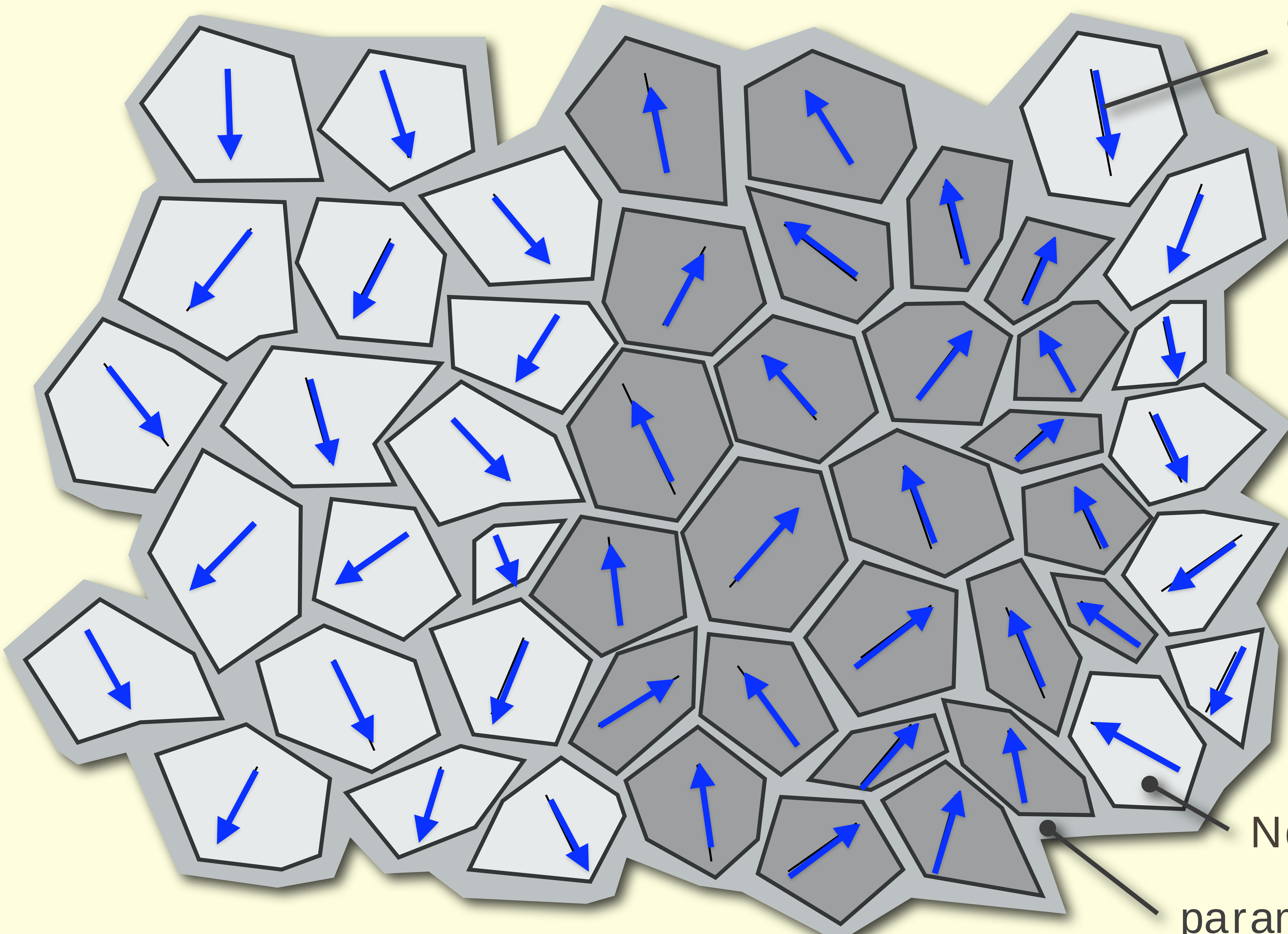

magnetostatic interaction domains

Nanostructured NdFeB: decoupled grains

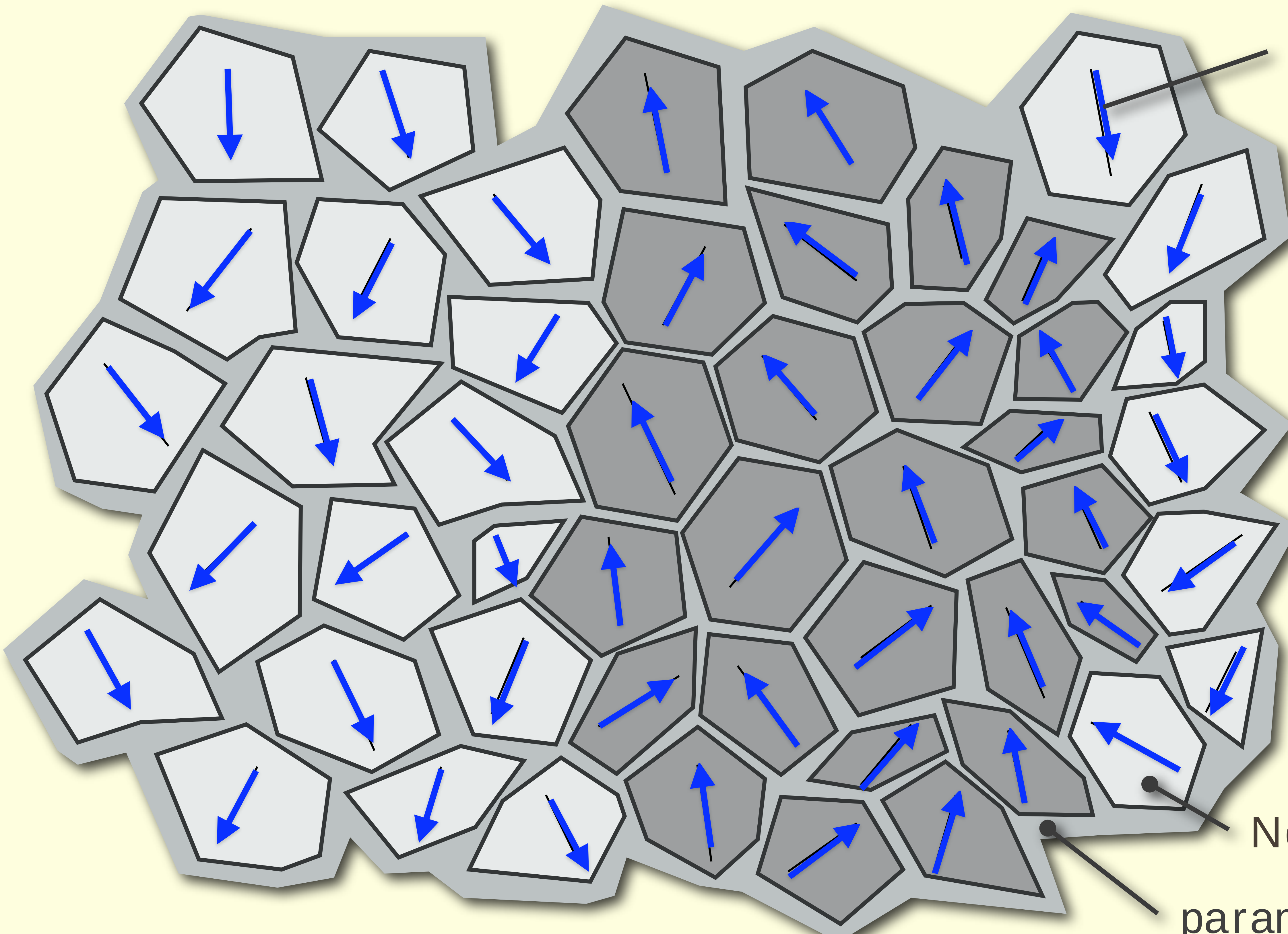

magnetostatic interaction domains

Nanostructured NdFeB: decoupled grains

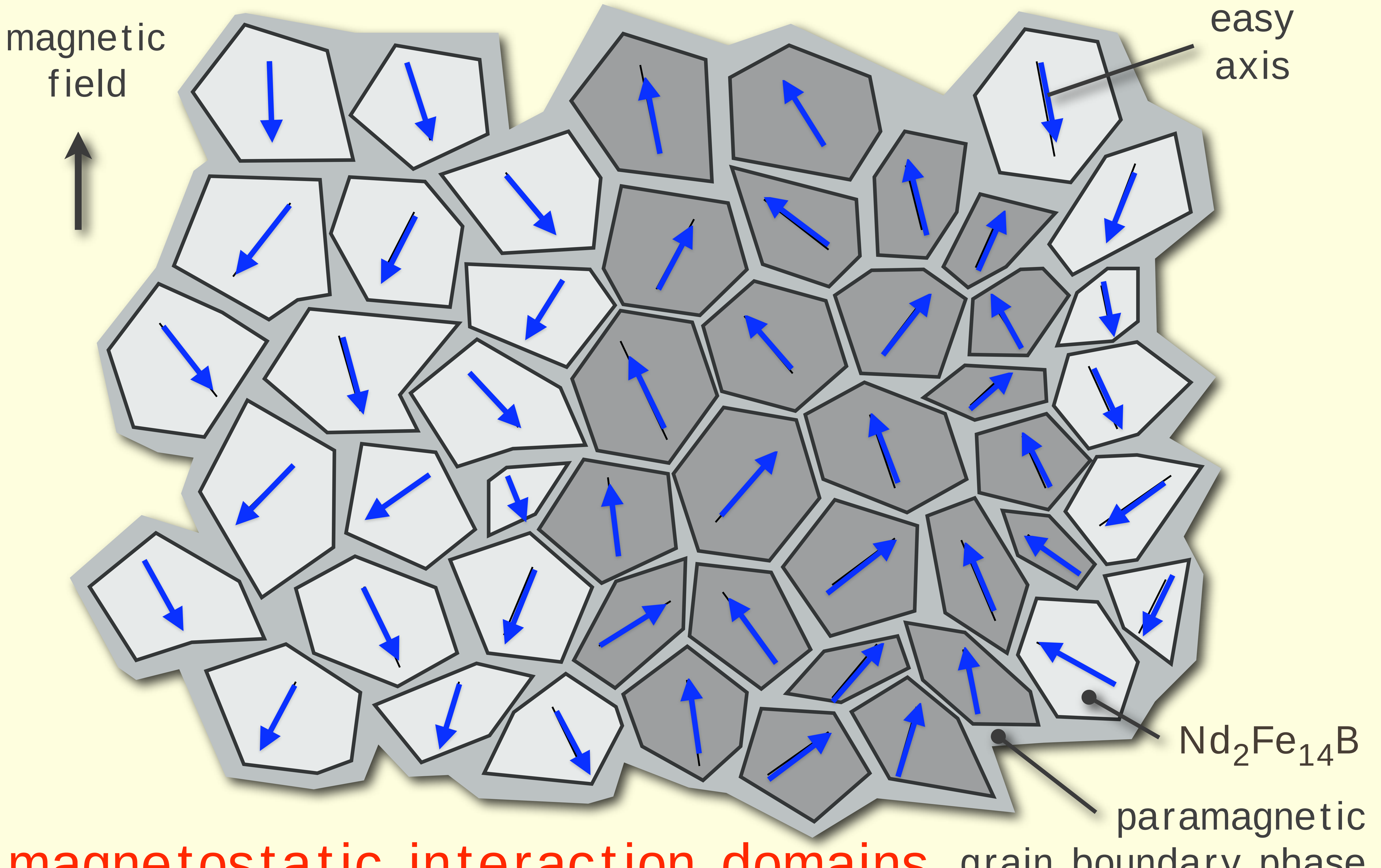

magnetostatic interaction domains

Nanostructured NdFeB: decoupled grains

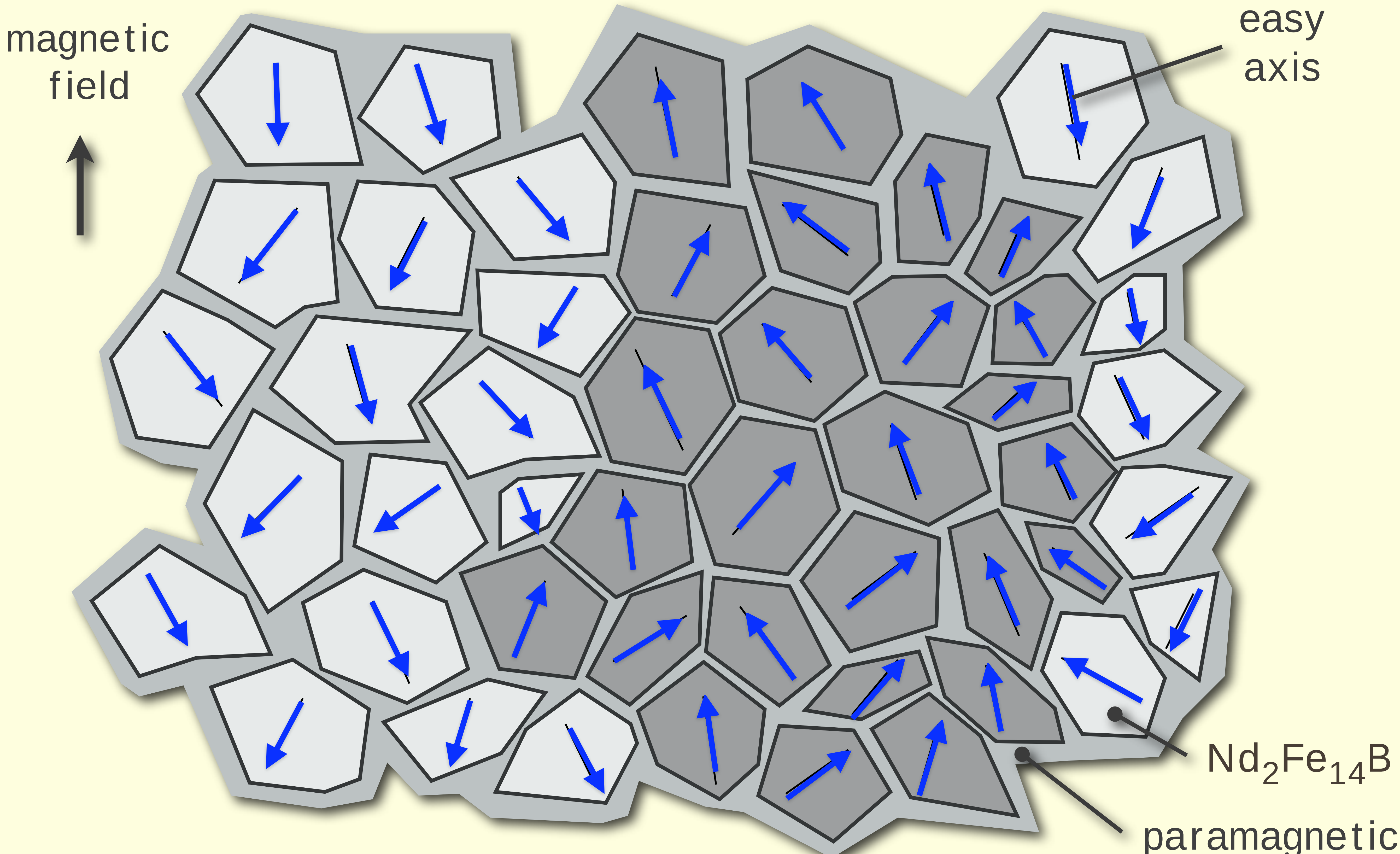

magnetostatic interaction domains

Nanostructured NdFeB: decoupled grains

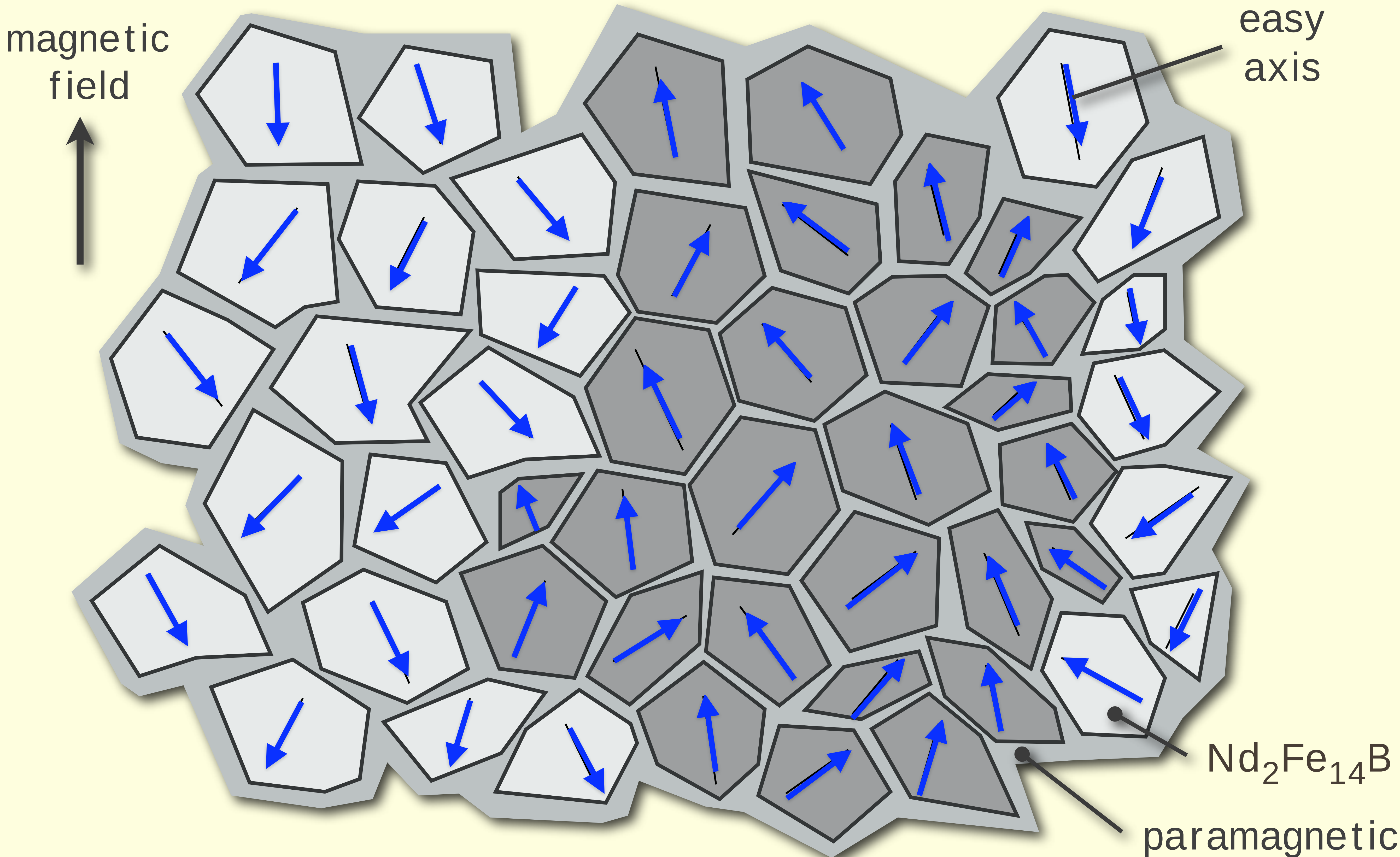

magnetostatic interaction domains

Nanostructured NdFeB: decoupled grains

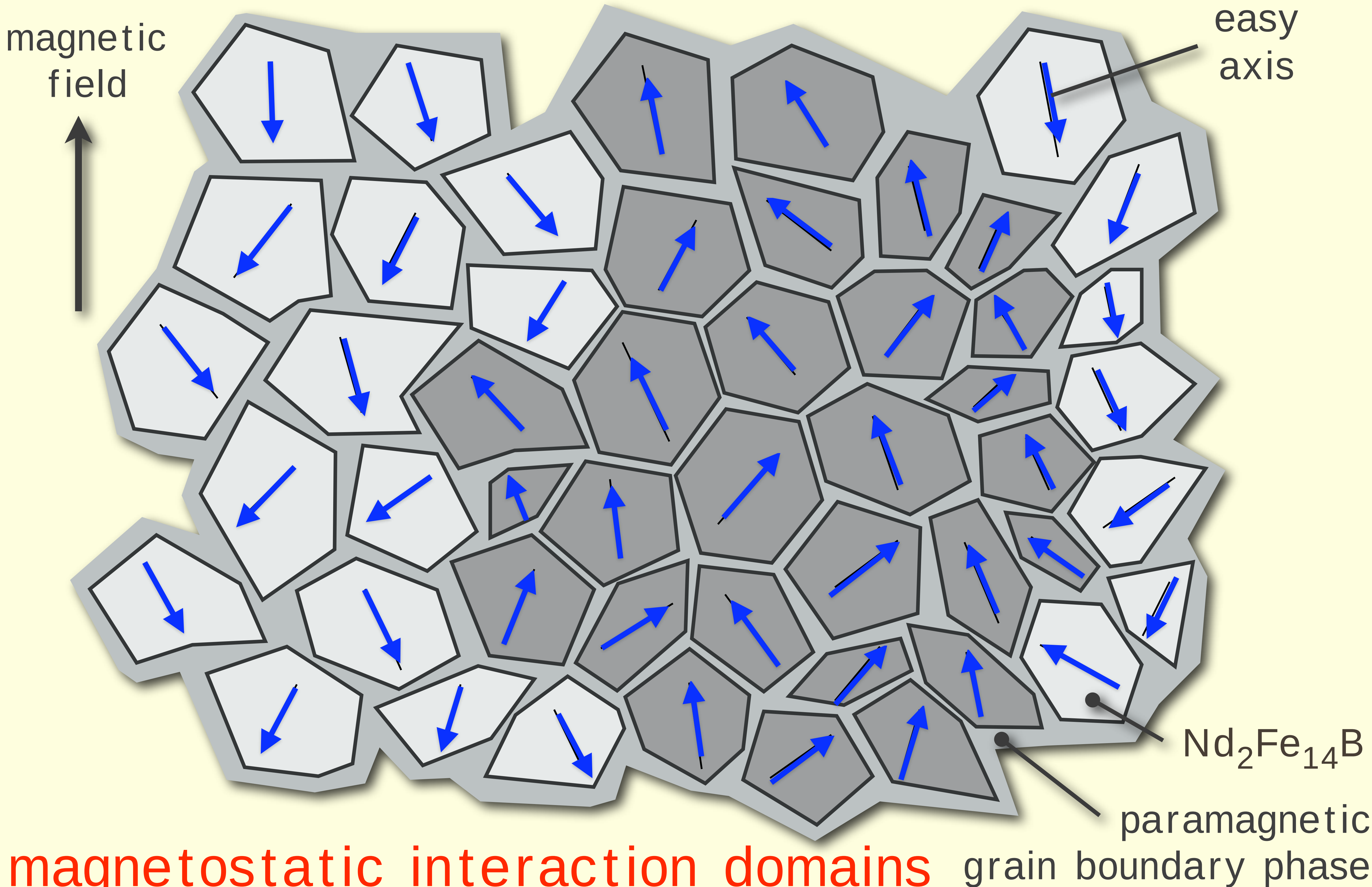

magnetostatic interaction domains

Nanostructured NdFeB: decoupled grains

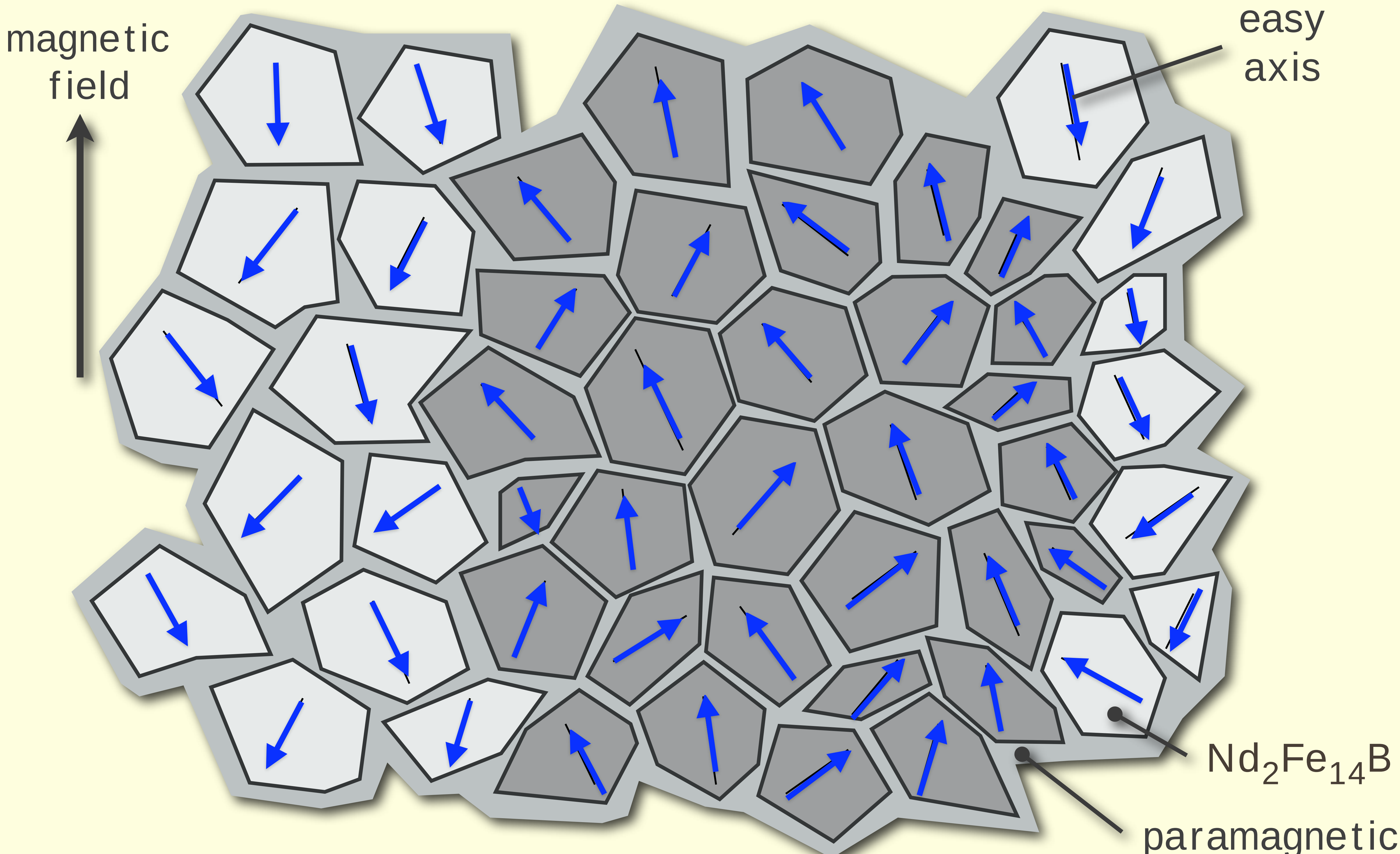

magnetostatic interaction domains

Nanostructured NdFeB: decoupled grains

magnetization process along preferred axis

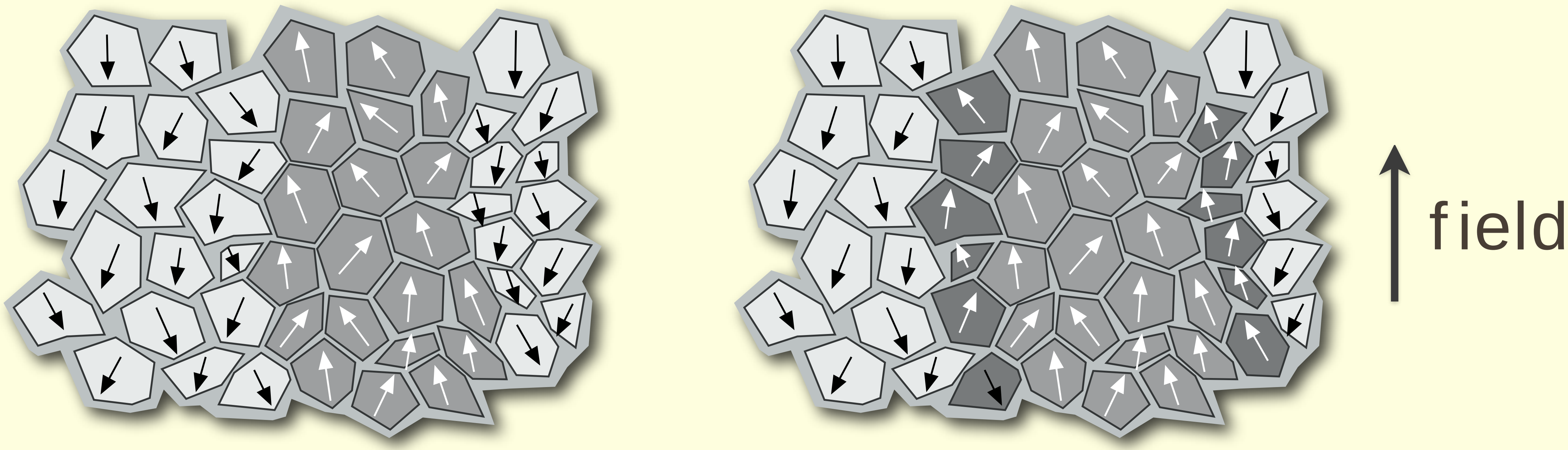

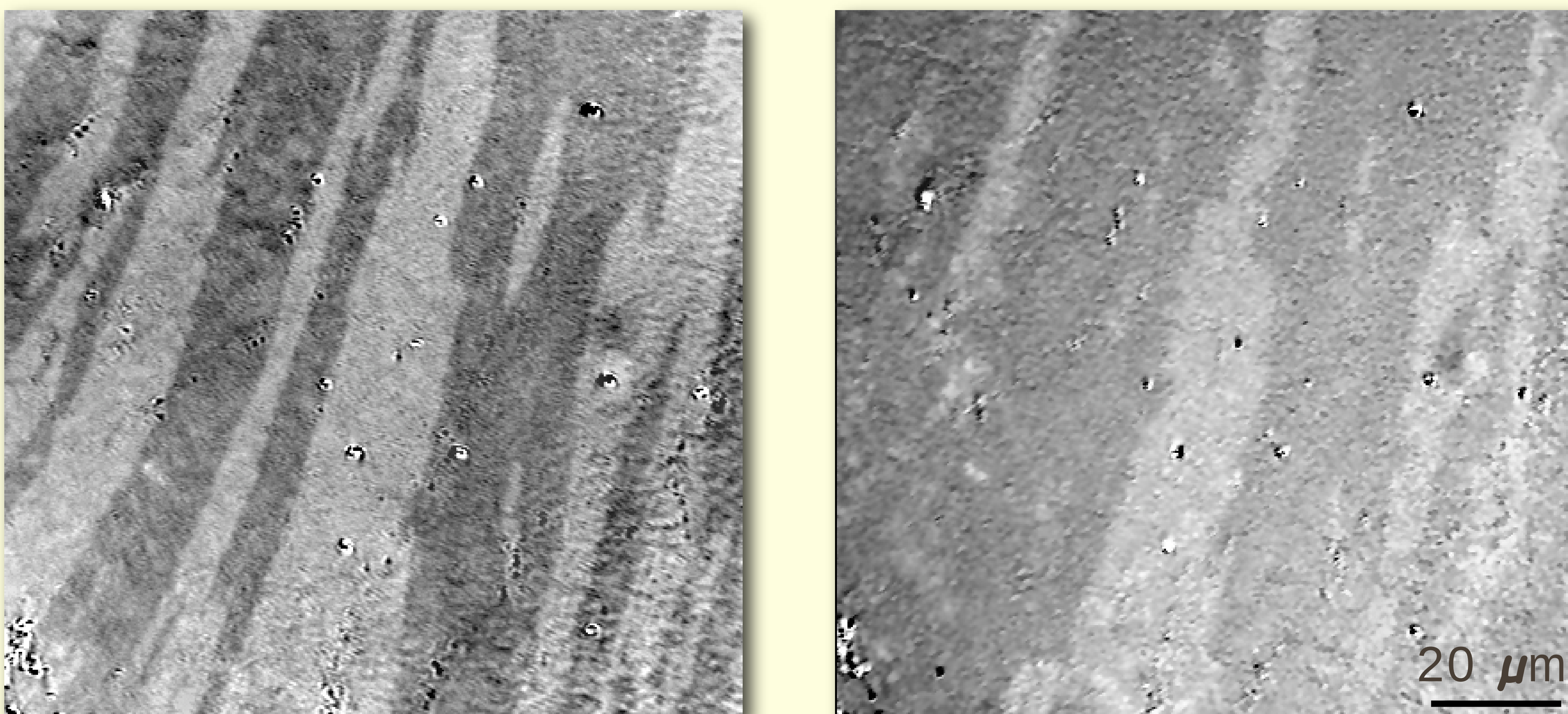

NdFeB
grain size
about 100 nm

Nanostructured NdFeB: decoupled grains

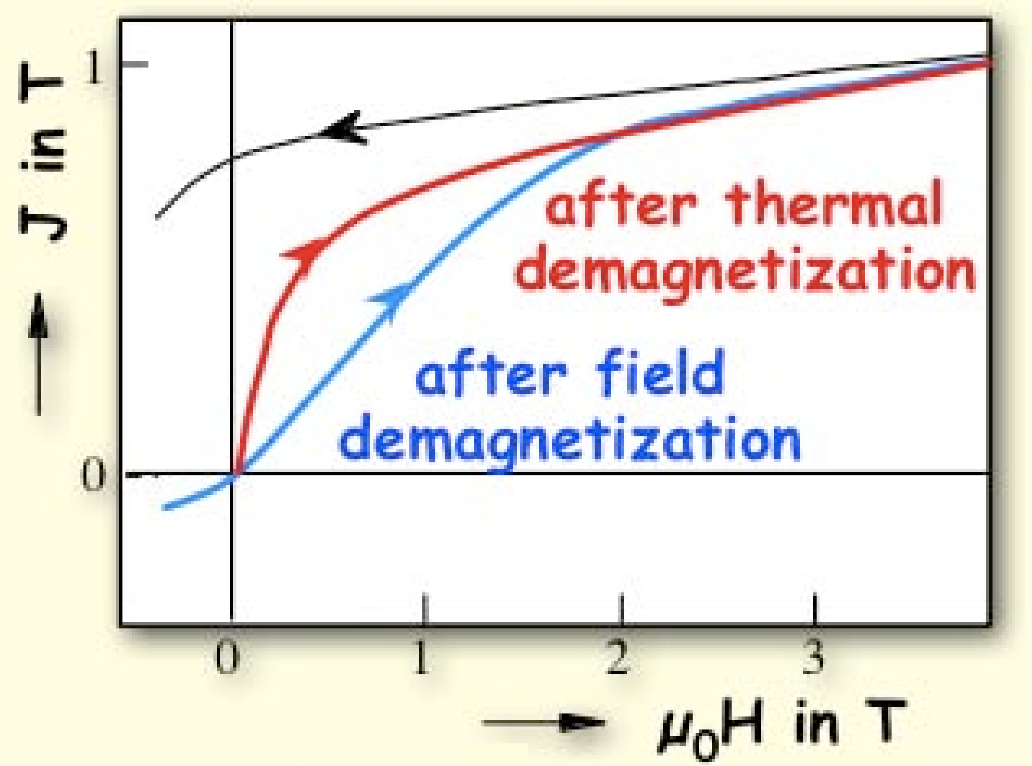

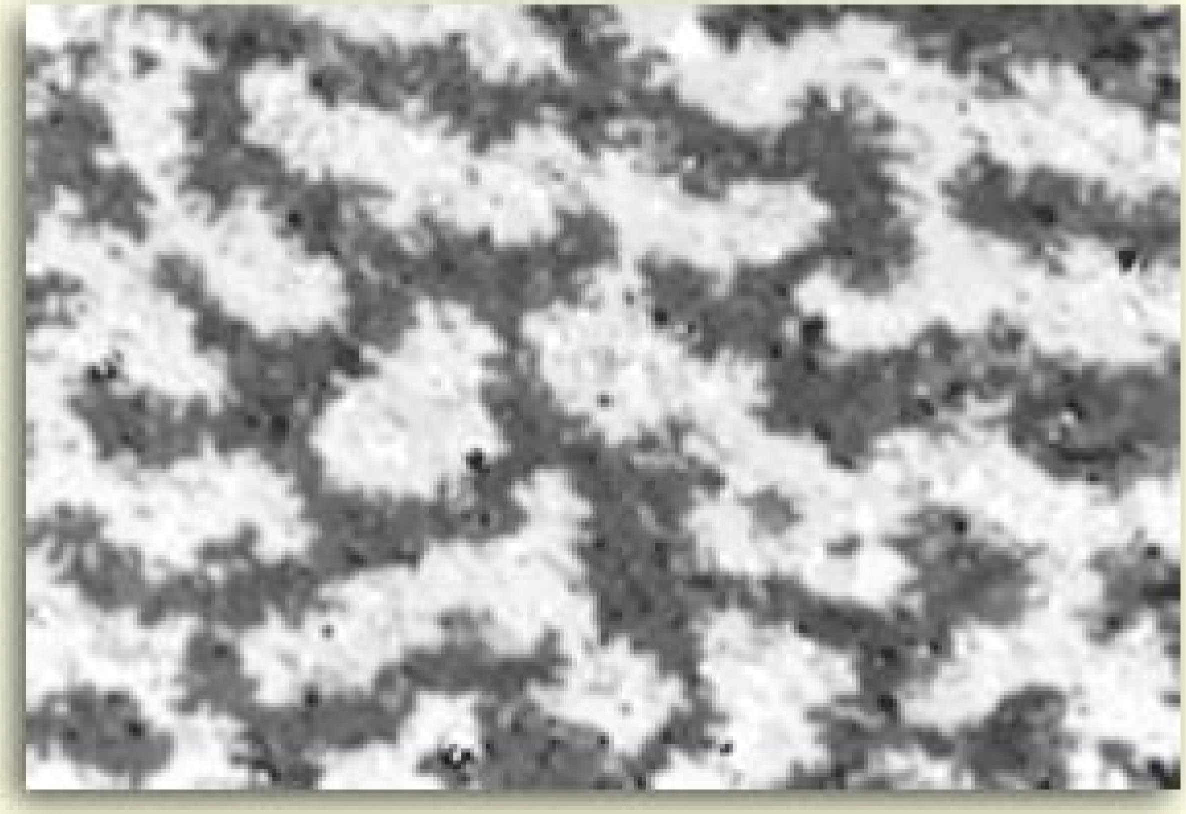

after thermal demagnetization

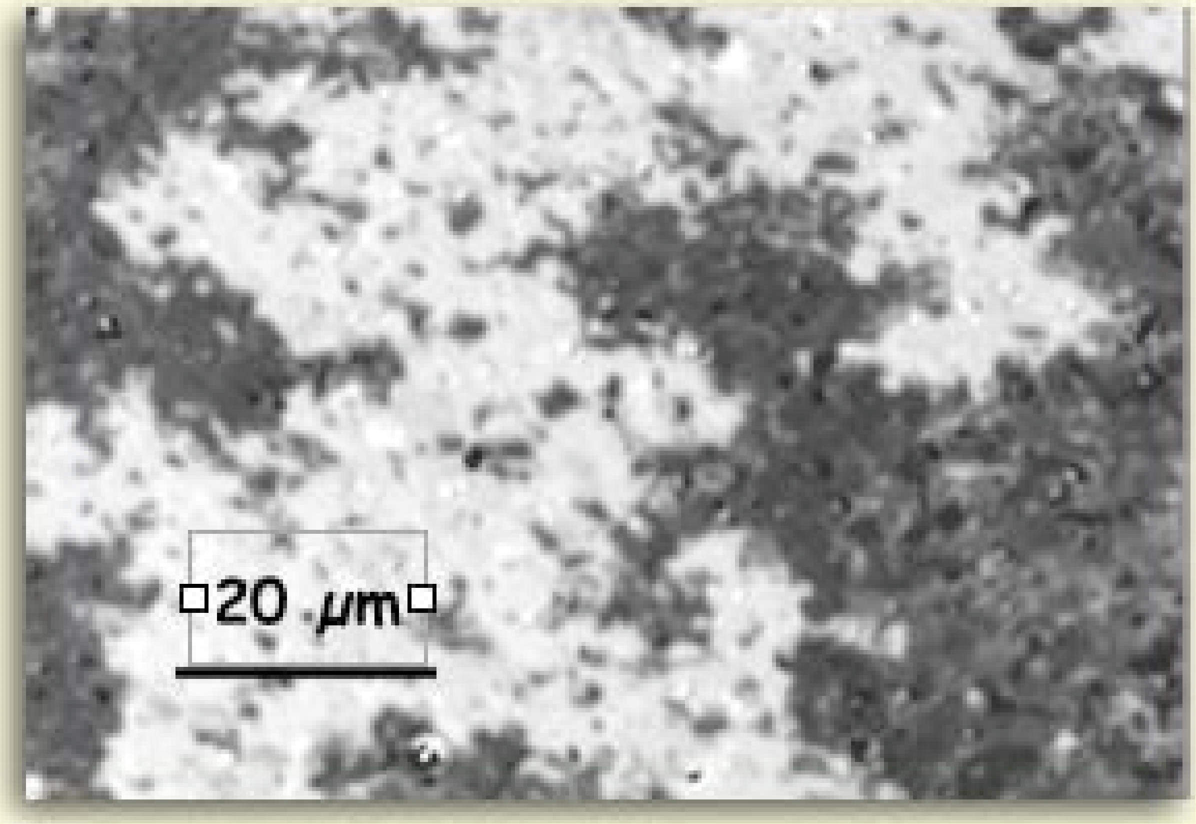

after field demagnetization

Nanostructured NdFeB: decoupled grains

Preparation: melt spinning, ball milling, hot-pressing, die-upsetting

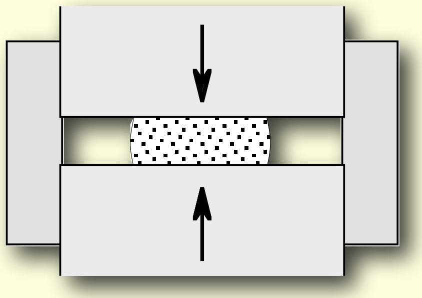

degree of deformation: $\ln \dfrac{\text{initial thickness}}{\text{final thickness}}$

decreasing degree of deformation and texture

1.44	0.97	0.74	0.56	isotropic

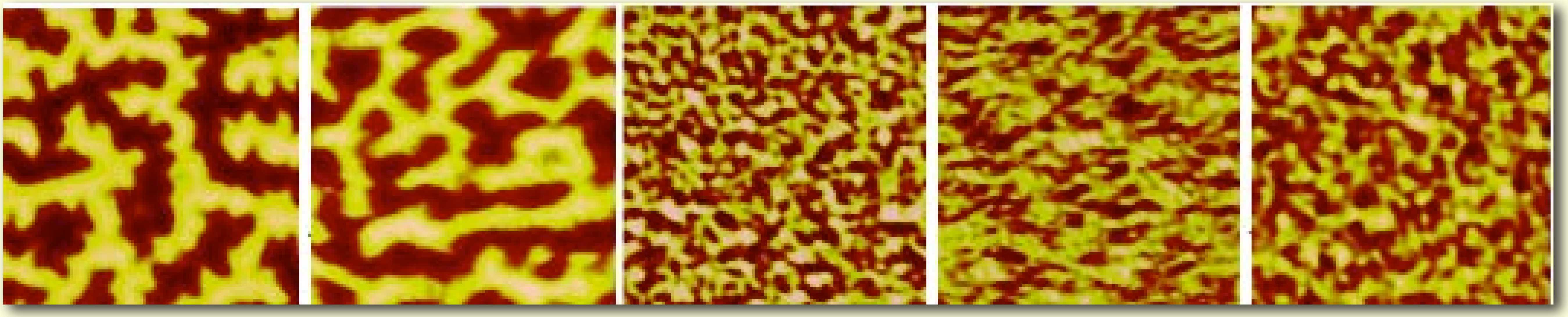

10 μm

MFM observation

courtesy K. Khlopkov and O. Gutfleisch (IFW Dresden)

Domains in Sm_2Co_{17} magnets

$Sm(Co_{0.784}Fe_{0.1}Cu_{0.088}Zr_{0.028})_{7.19}$

known as pinning magnet

c-axis parallel

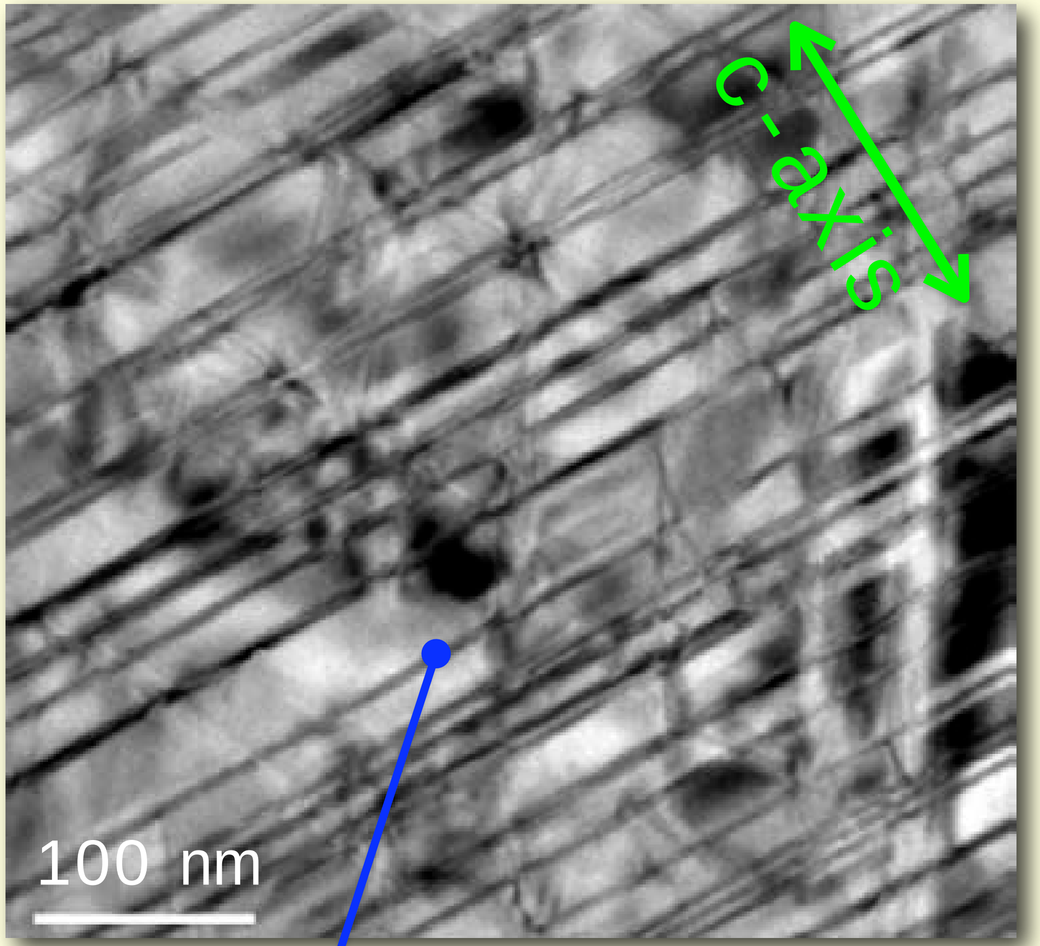

c-axis perpendicular

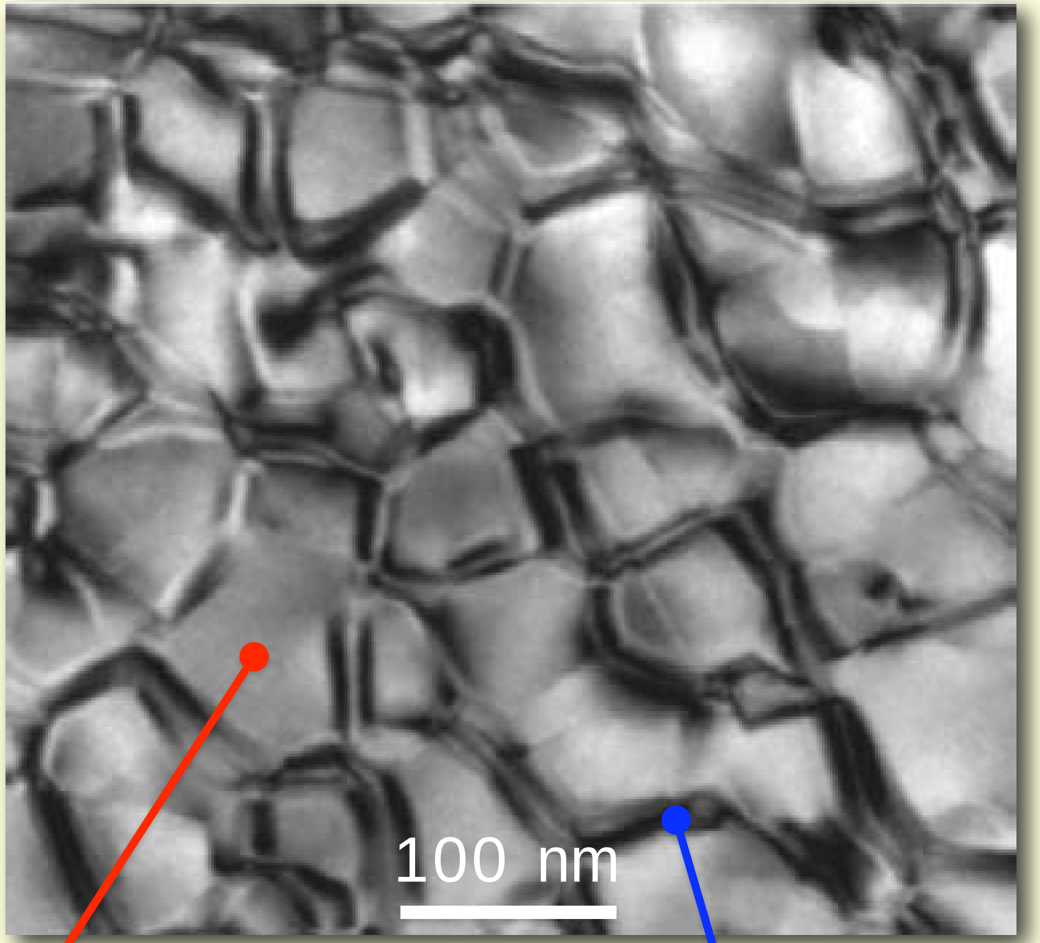

Zr-rich
precipitation phase

$Sm_2(CoFe)_{17}$
cells (100 nm)

Cu-rich
precip. phase

Domains in Sm_2Co_{17} magnets

$Sm(Co_{0.784}Fe_{0.1}Cu_{0.088}Zr_{0.028})_{7.19}$

magnetic microstructure (Lorentz-TEM):

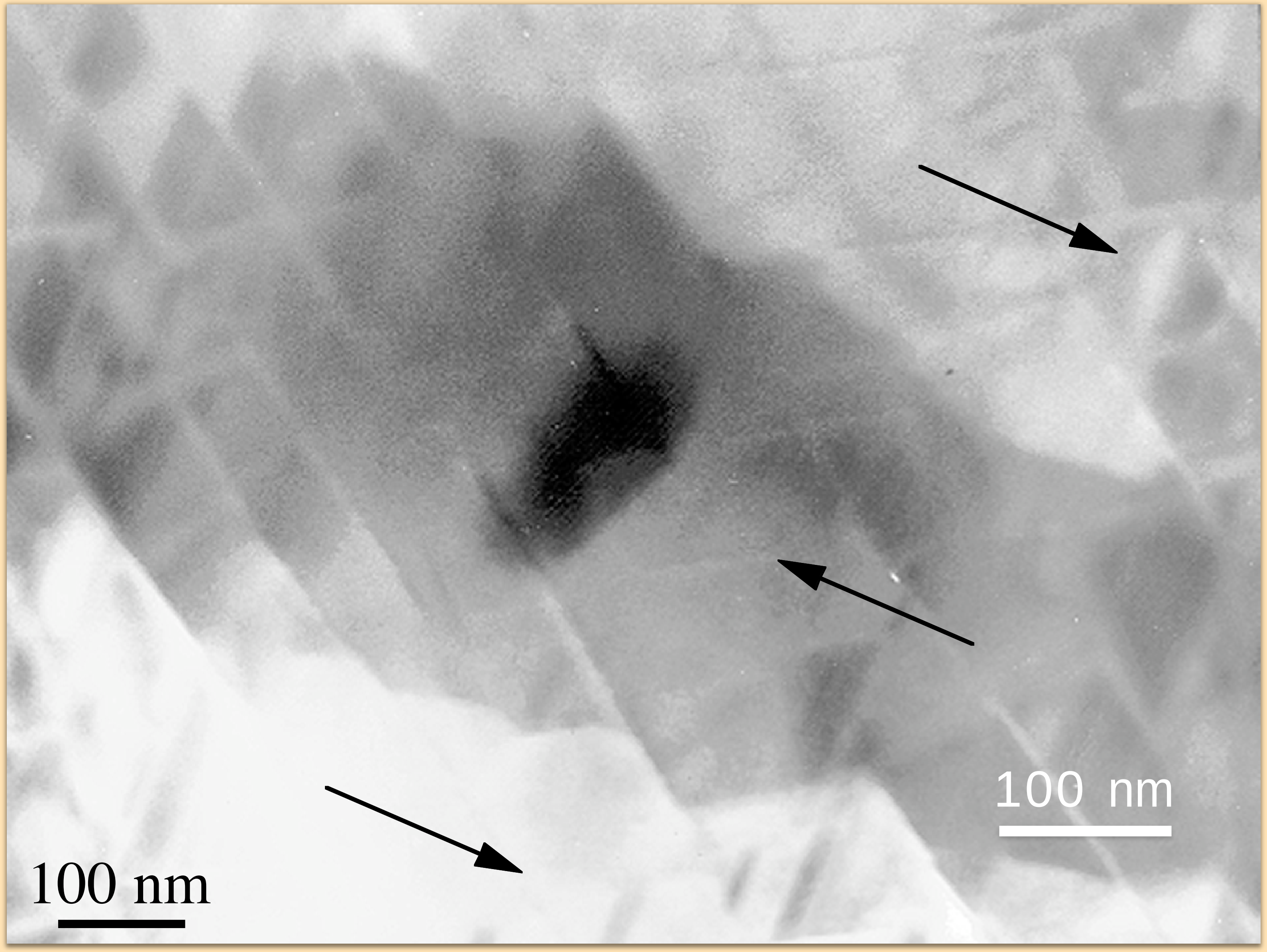

courtesy J. Fidler, Vienna

Domains in Sm_2Co_{17} magnets

quenched from 850°C
(low coercive state)

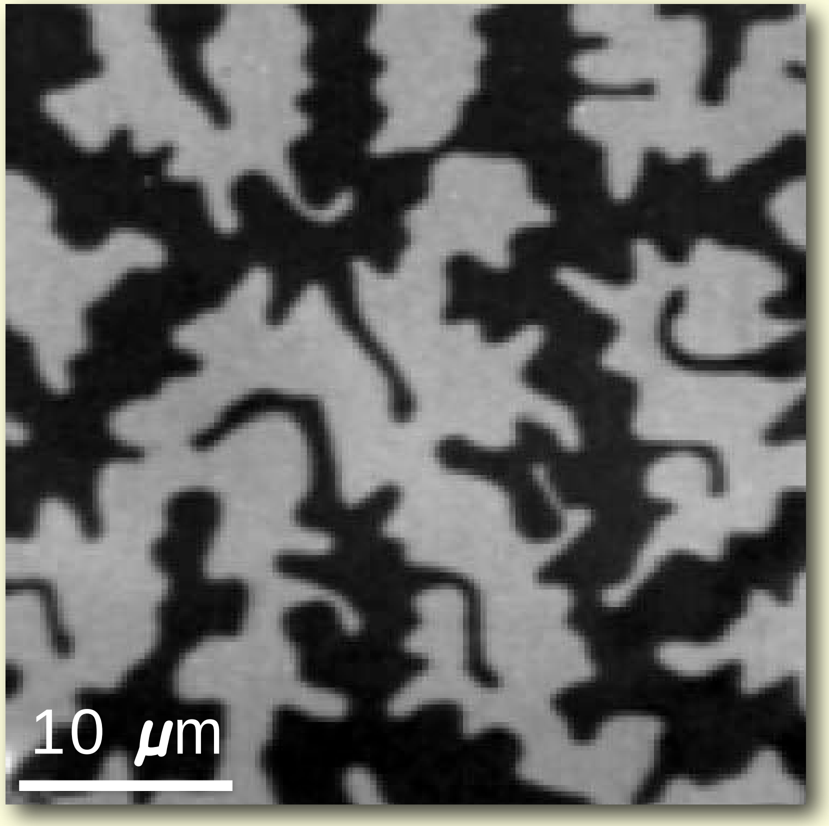

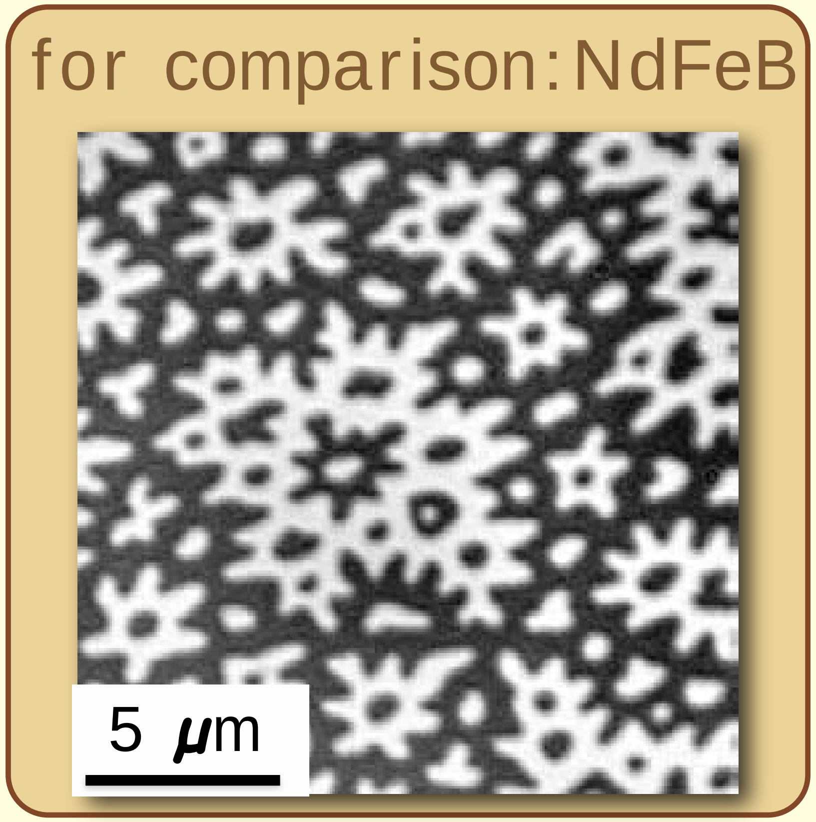

O. Gutfleisch et al.,
Acta Mater. 54 (2006)

slowly cooled to 400°C
(optimally processed,
high coercive state
$\mu_0 H_c \approx 3T$)

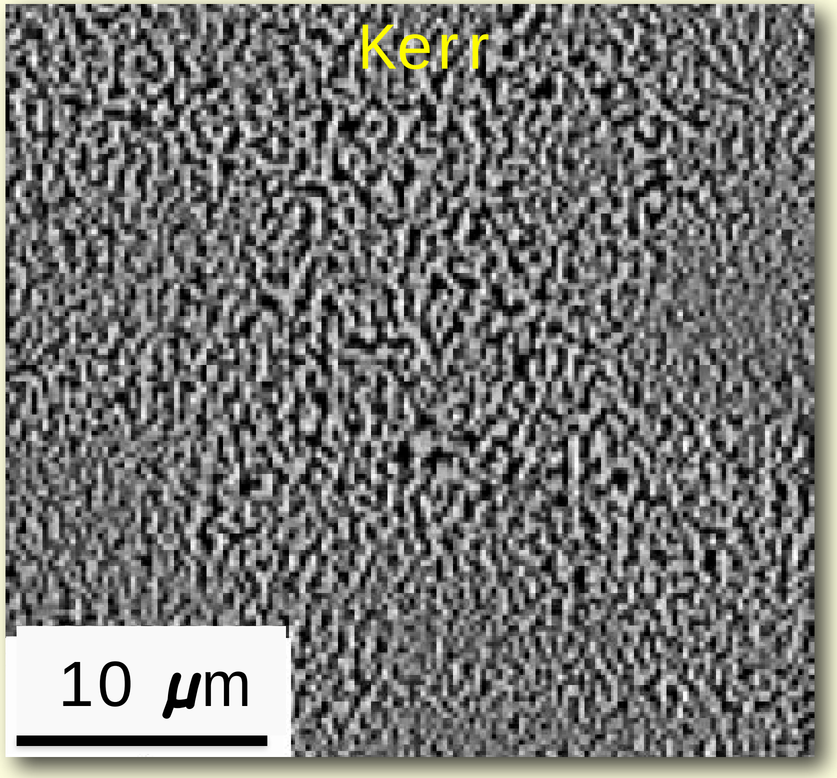

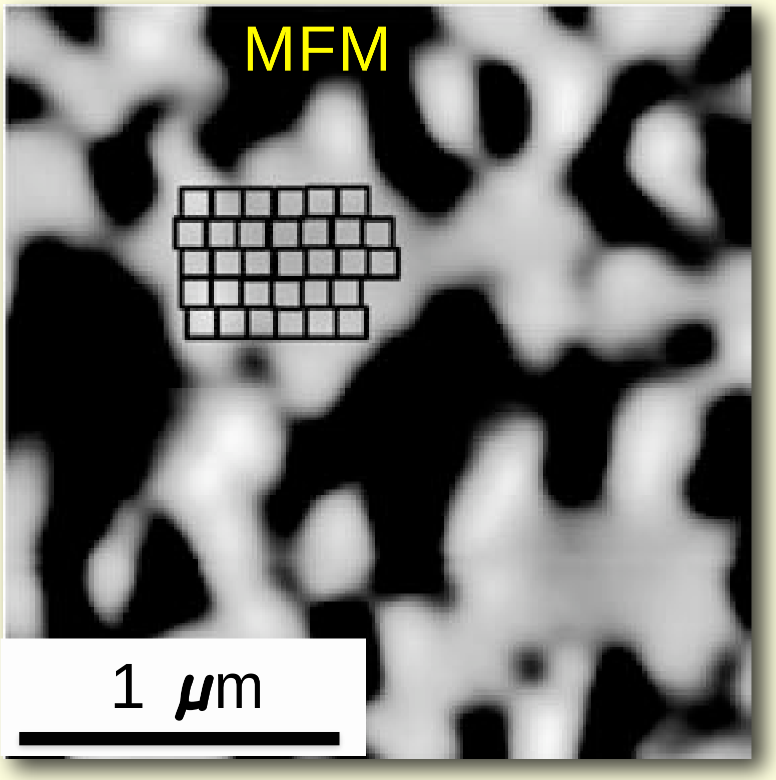

Summary

Domains in coarse-grained material

- wide volume domains
  fine surface domains

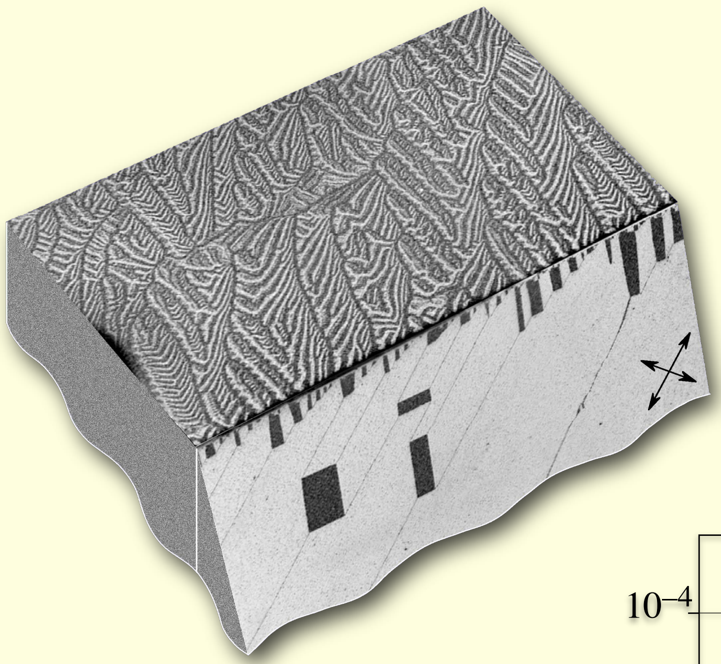

- domain width increases linearily
  with thickness (i.e. grain size)

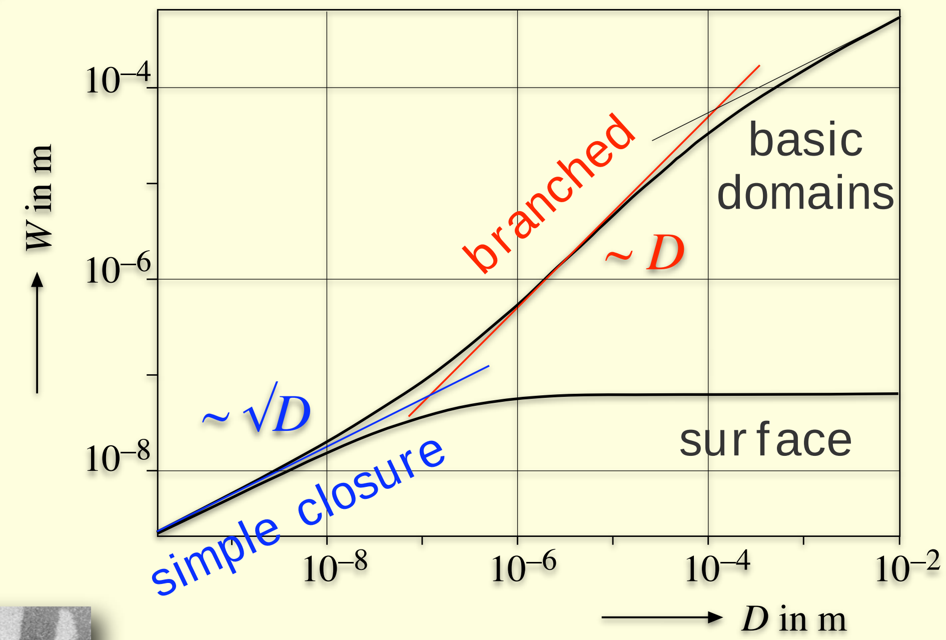

- coercivity due to
  grain boundary effects

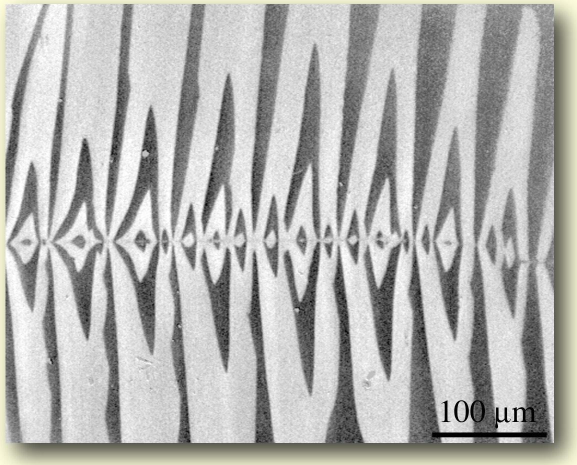

Summary

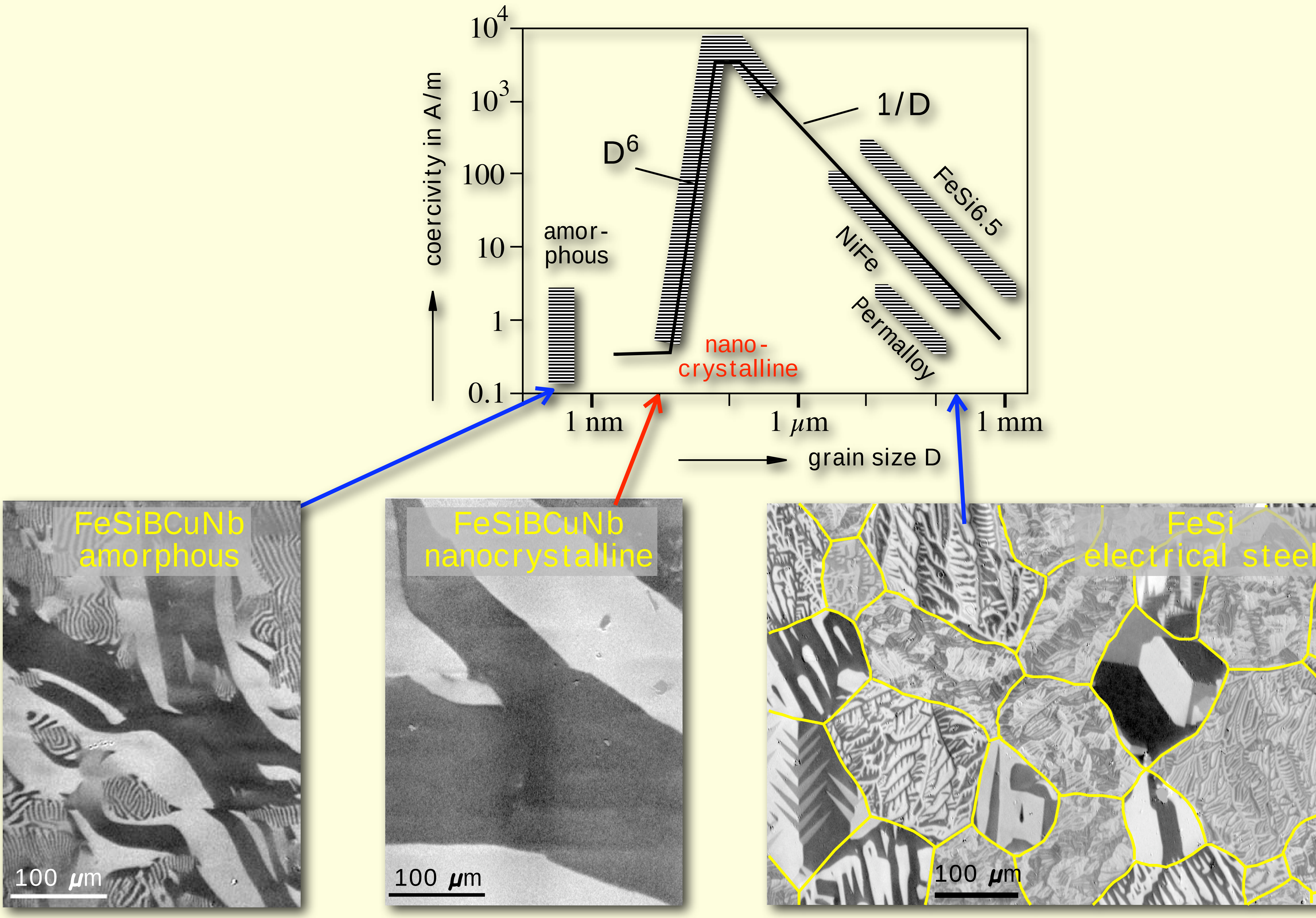

10^4
10^3
100
10
1
0.1
coercivity in A/m
1 nm
1 μm
1 mm
grain size D
amor-
phous
D^6
1/D
nano-
crystalline
FeSi6.5
NiFe
Permalloy
FeSiBCuNb
amorphous
100 μm
FeSiBCuNb
nanocrystalline
100 μm
FeSi
electrical steel
100 μm

Summary

Domains in nanocrystalline ribbons

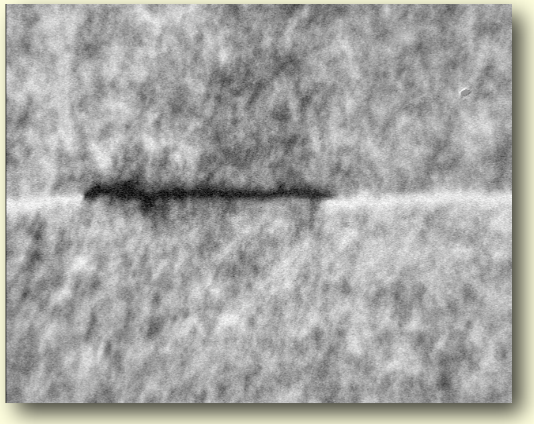

- patchy modulation (connection to ripple), depends on induced anisotropy

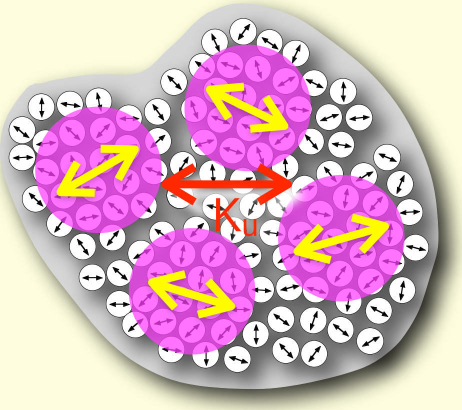

- counterplay uniform induced anisotropy/ averaged magnetocrystalline anisotropy

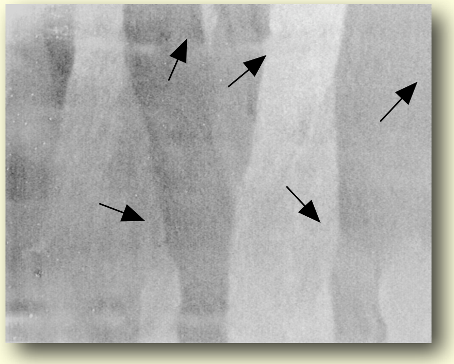

- counterplay also explains:
  - patch domains for T > $T_{c,\ amorph}$
  - irregularities in hard- and easy-axis magnetization process

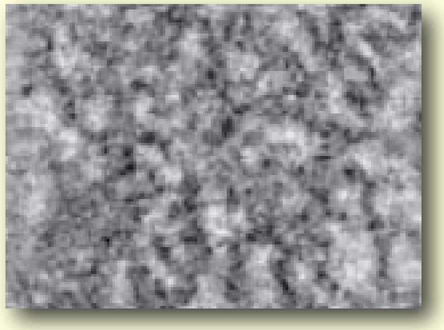

- nucleation-dominated domain refinement (patch domains) at high f

Summary

Domains in fine and nanostructured permanent magnets

- highly in
  for exch
- magneto
  for deco

typical grain sizes: 20 – 300 nm

$Nd_2Fe_{14}B$:

$K_u = 4.3 \cdot 10^6\ kJ/m^3$

$A = 8 \cdot 10^{-12}\ J/m$

→ $L_{ex} = \sqrt{A/K_1} = 1.3\ nm$

→ random anisotropy model irrelevant

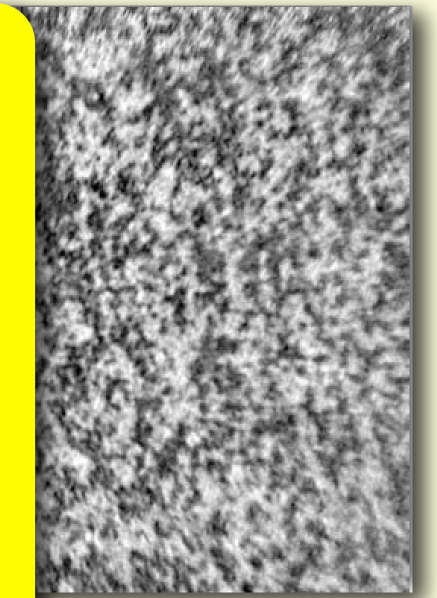

Summary

Domains in fine and nanostructured permanent magnets

- highly imobile patch domains
  for exchange coupled materials

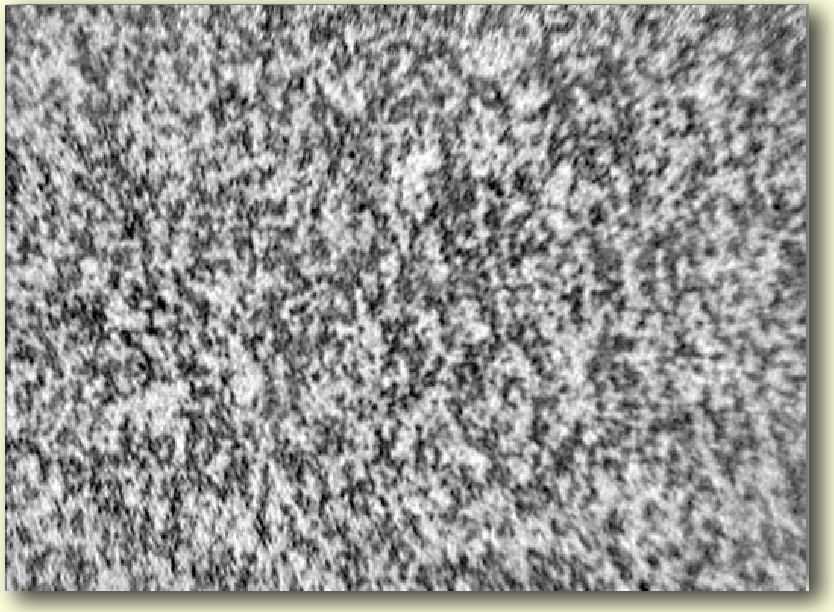

- magnetostatic interaction domains
  for decoupled grains

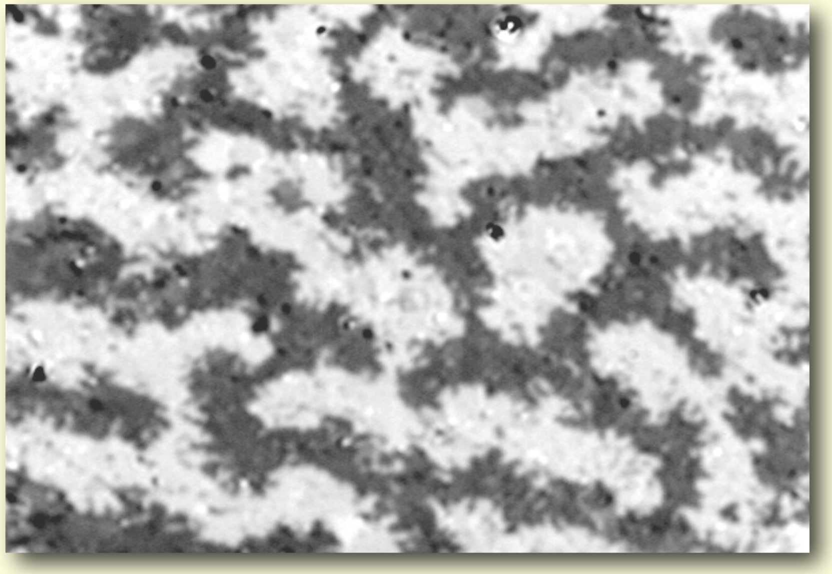

Hirarchy of descriptive levels of magnetic materials

5. Magnetic Hysteresis, or Magnetization Curve
Describing the *average magnetization* vector of a sample as a function of the external field (always applicable)

4. Phase, or Magnetic Texture Analysis
Collecting domains of equal magnetization direction in "phases". More generally, describing the distribution function (*texture*) of magnetization directions (> 0.1 mm)

3. Domain, or Magnetic Microstructure Analysis
Describing the *magnetic microstructure* of a sample, the shape and detailed spatial arrangement of domains and domain boundaries (1–1000 μm)

2. Micromagnetic Analysis
Describing the *internal structure of domain walls* and their substructures in terms of a continuum theory of a classical magnetization vector field (1–1000 nm)

1. Atomic Level Theory
Describing the origin, the interactions, the mutual arrangement and the statistical thermodynamics of elementary magnetic moments (< 1 nm)

Comparison of Domain Obervation Techniques

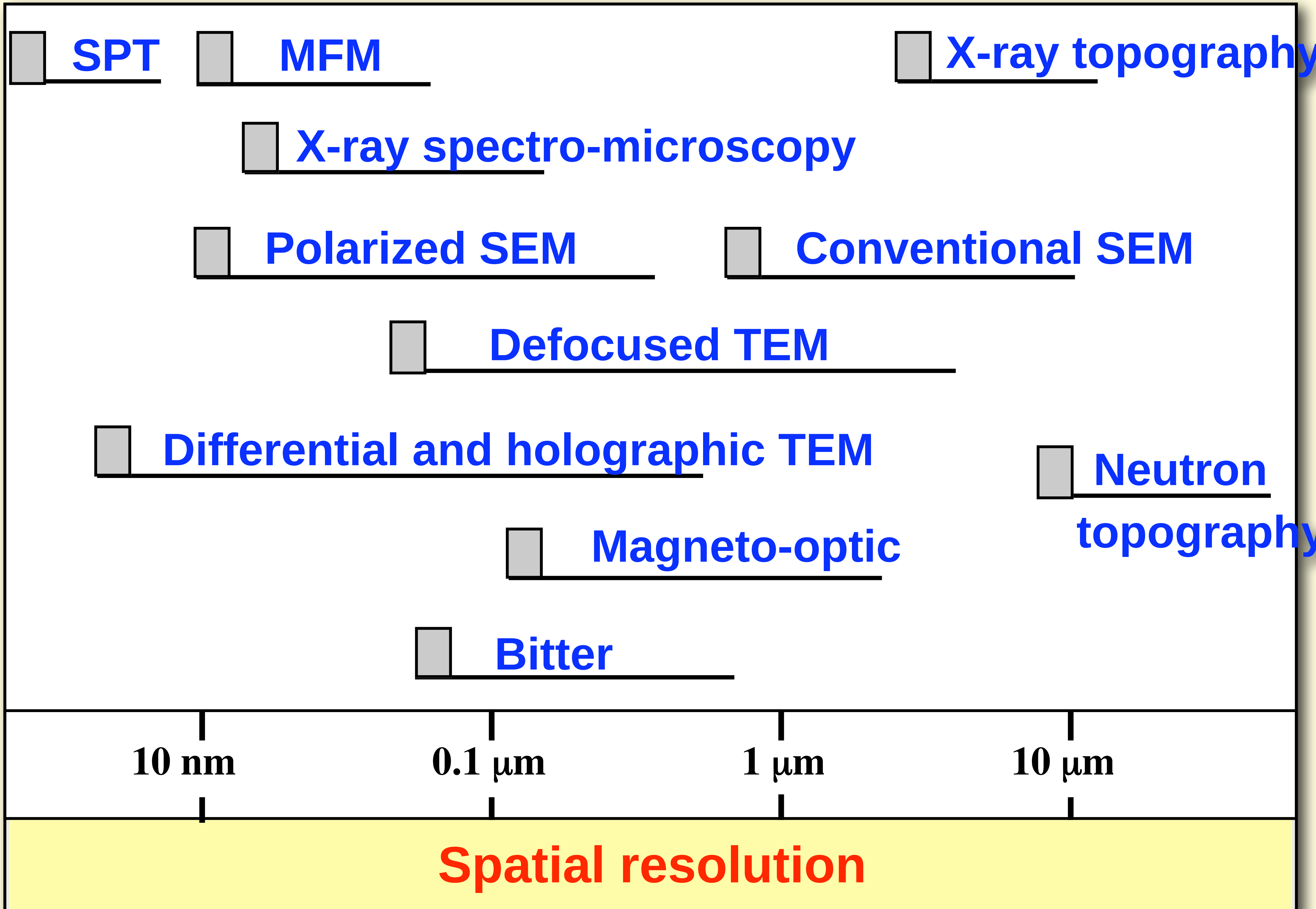

MFM: Magnetic Force Microscopy
SPT: Spin-Polarized Tunneling
MO: Magnetoptic Method

SEM: Scanning (reflection) Electron Microscopy
TEM: Transmission Electron Microscopy

Resolution of optical microscopy (E. Abbe 1840 - 1905)

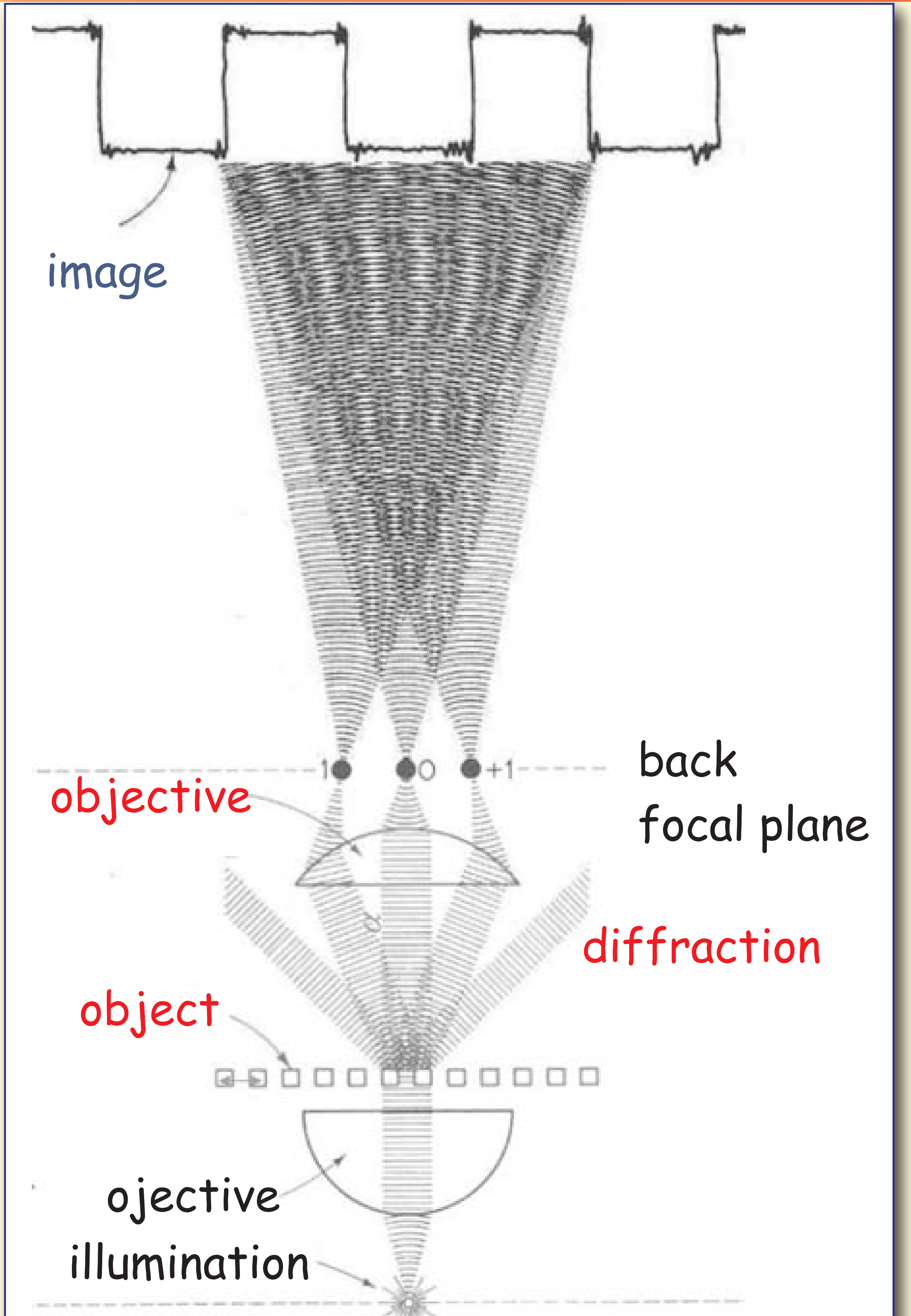

resolution determined by constructive interference

diffraction limited image formation

Rayleigh equation: $d = \dfrac{0.5\ \lambda}{NA}$

d = separation between particles, still allowing to see them

λ = wavelength

NA = numerical aperture of objective

$NA = n \sin\theta$

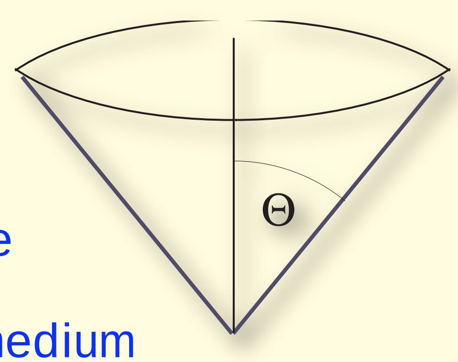

θ = half the cone angle of light accepted by objective

n = referaction index of medium between sample and objective

↓

best around 200 nm

Comparison of Domain Obervation Techniques

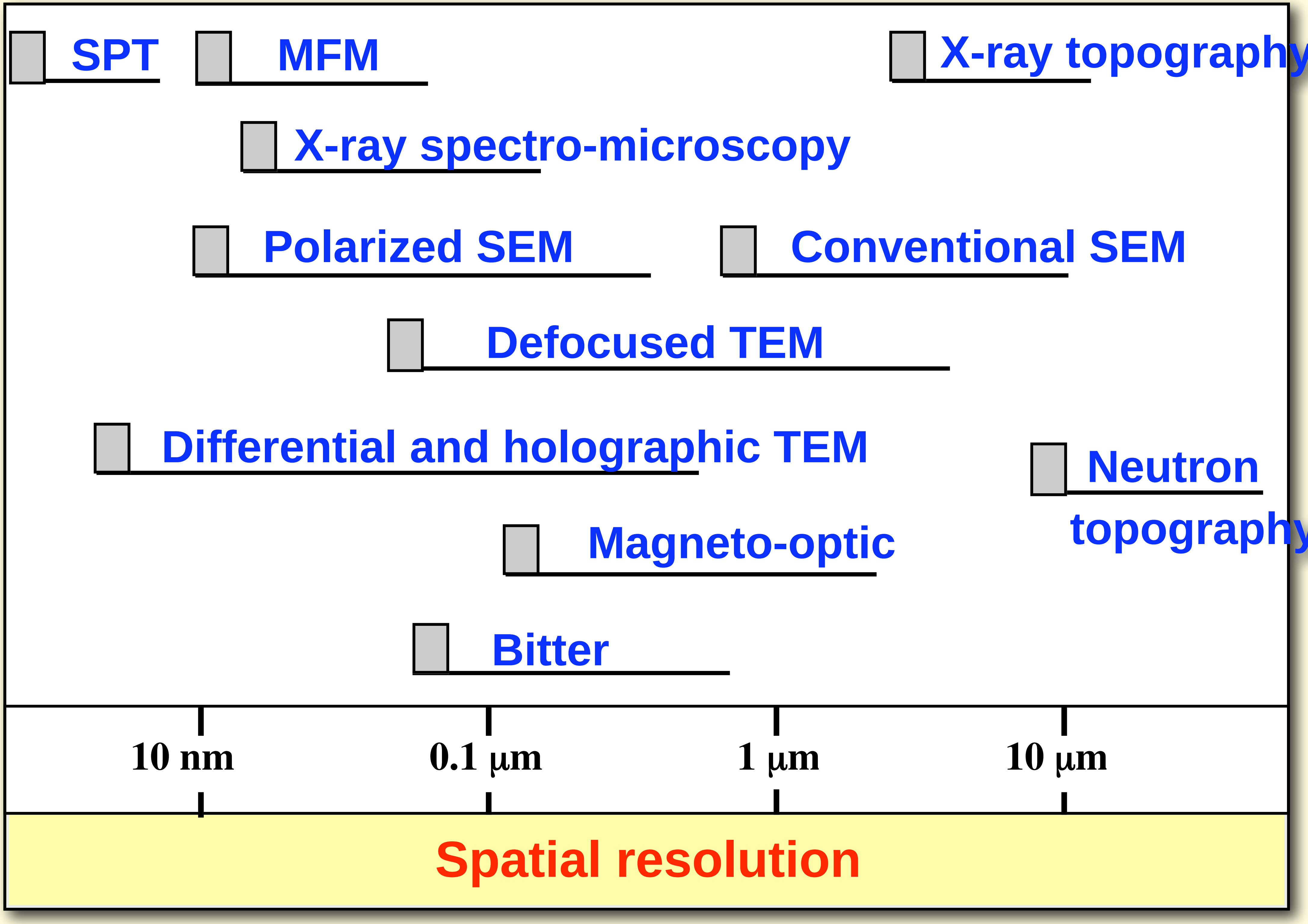

MFM: Magnetic Force Microscopy
SPT: Spin-Polarized Tunneling
MO: Magnetoptic Method

SEM: Scanning (reflection) Electron Microscopy
TEM: Transmission Electron Microscopy

Comparison of Domain Obervation Techniques

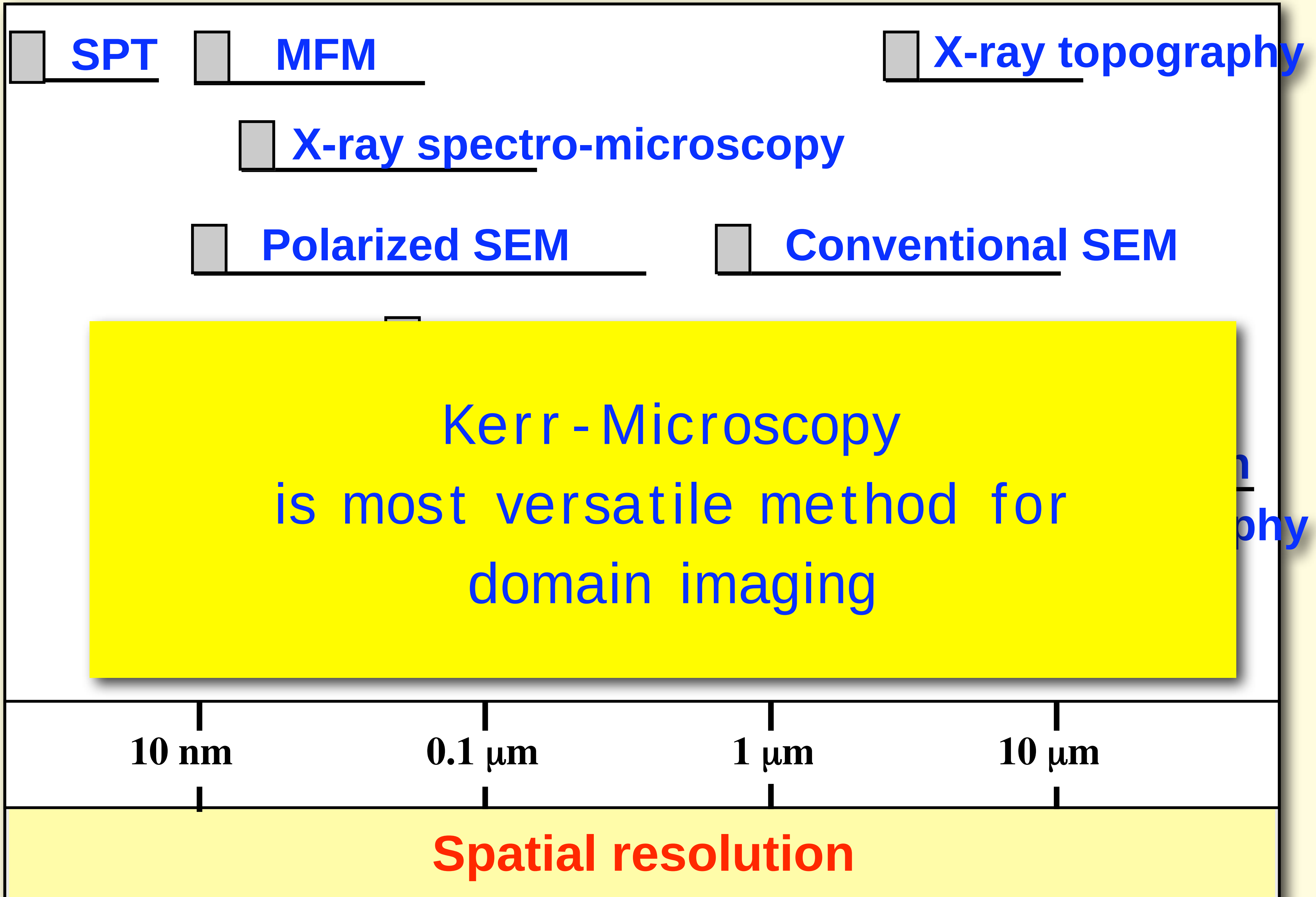

MFM: Magnetic Force Microscopy
SPT: Spin-Polarized Tunneling
MO: Magnetoptic Method

SEM: Scanning (reflection) Electron Microscopy
TEM: Transmission Electron Microscopy

Kerr microscopy

Kerr effect

Kerr-effect: rotation of polarized light

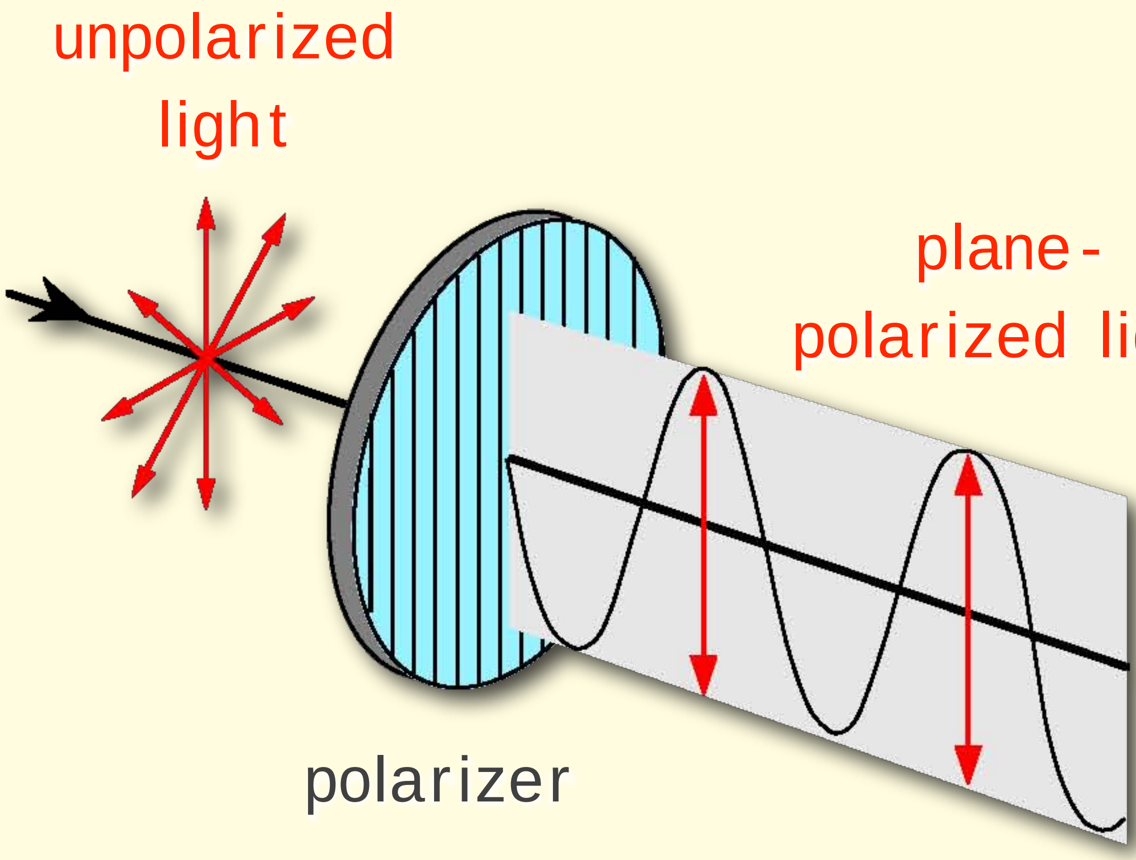

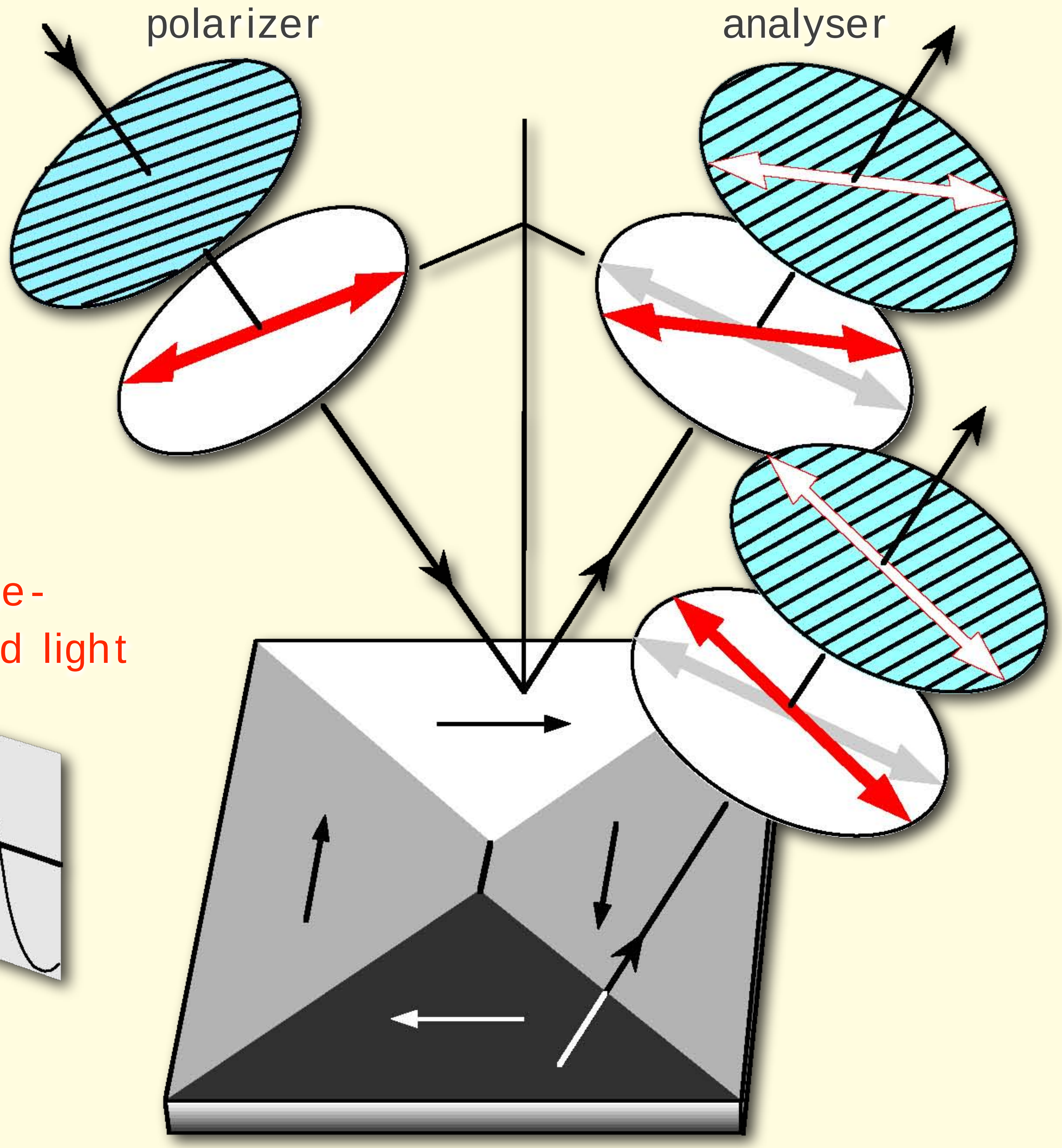

Wide-field Kerr microscope

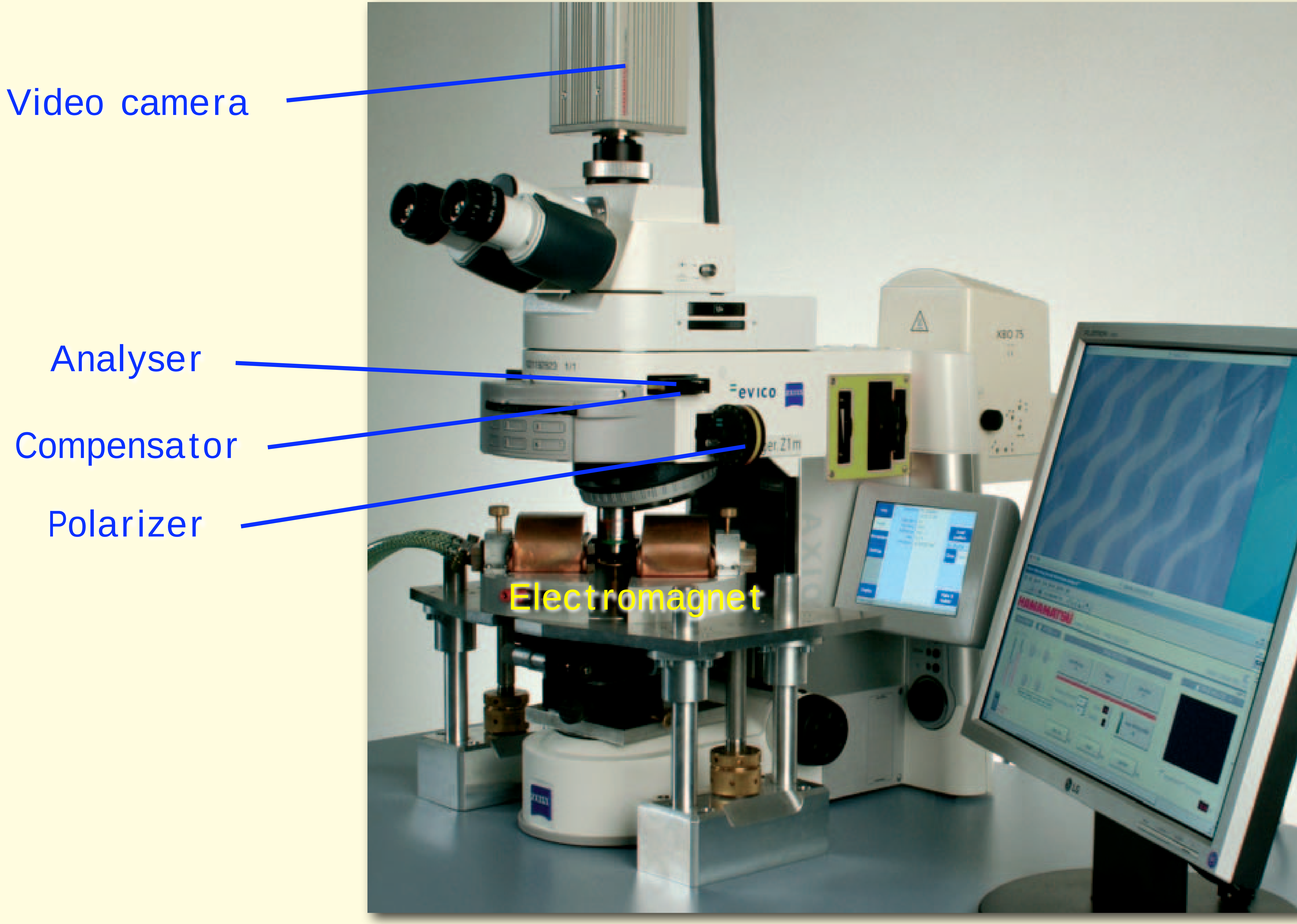

Kerr microscopy: advantages

Hysteresis curve

and

magnetization process

Asymmetric reversal in exchange biased CoFe/IrMn

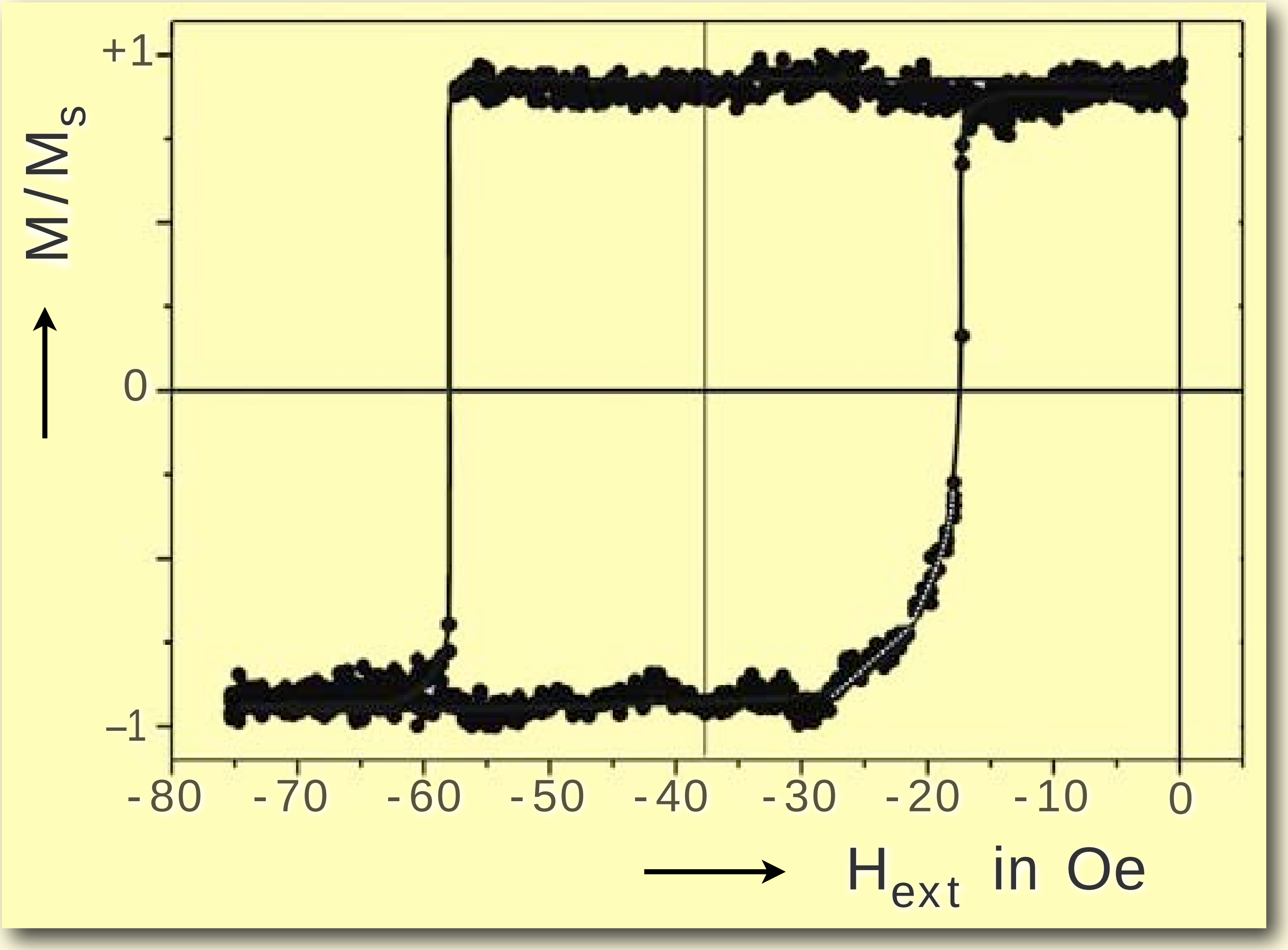

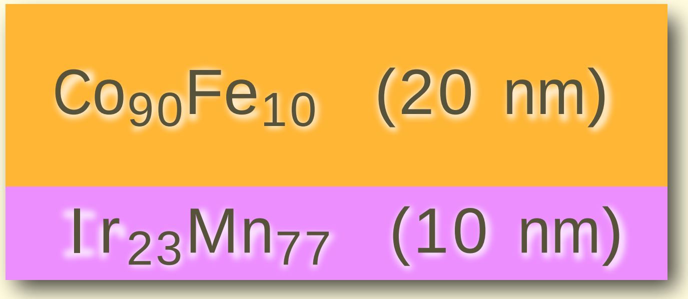

J. McCord, R.S., R. Mattheis, K.-U. Barholz, JAP 93, 5491 (2003)

Asymmetric reversal in exchange biased CoFe/IrMn

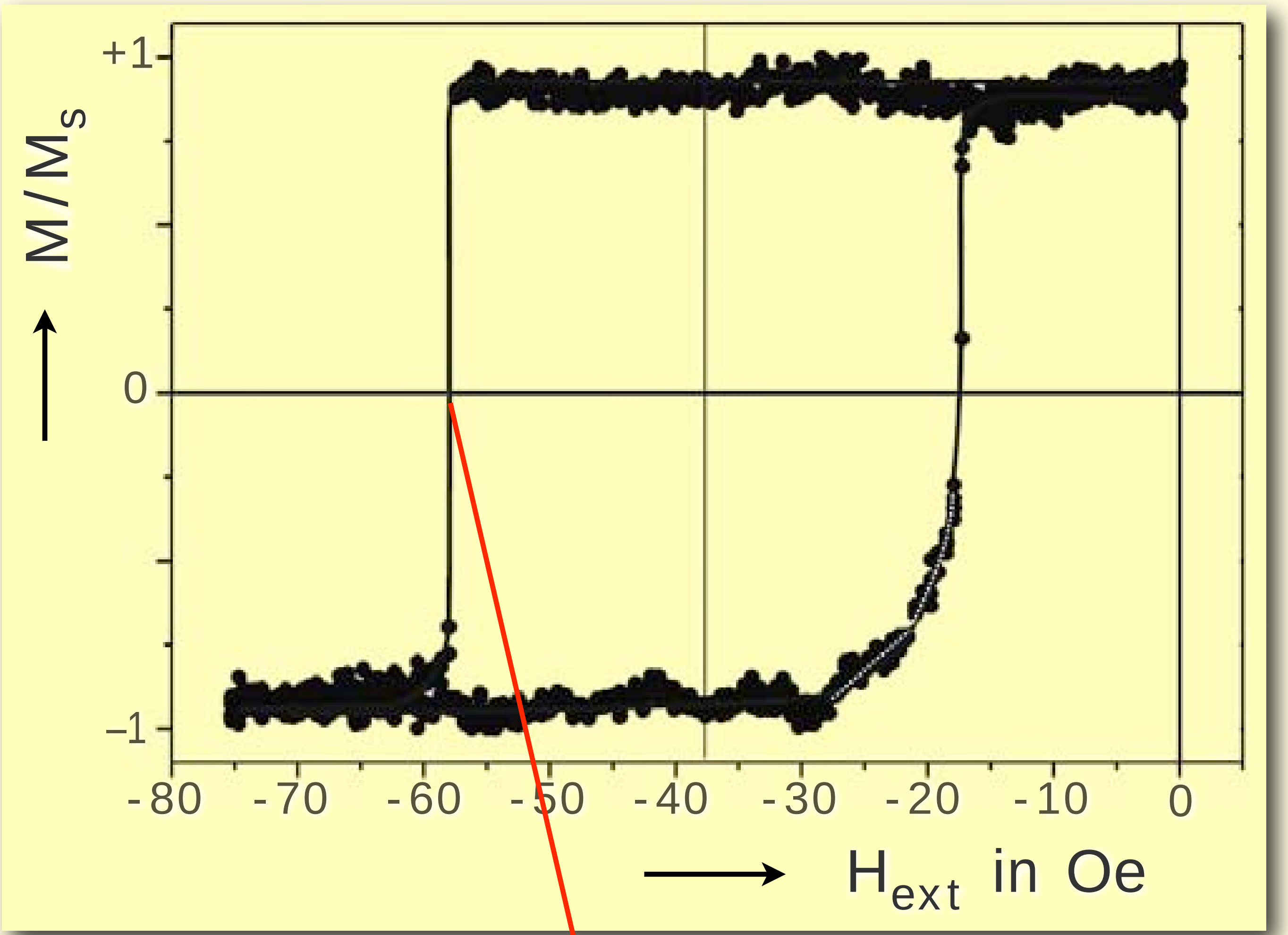

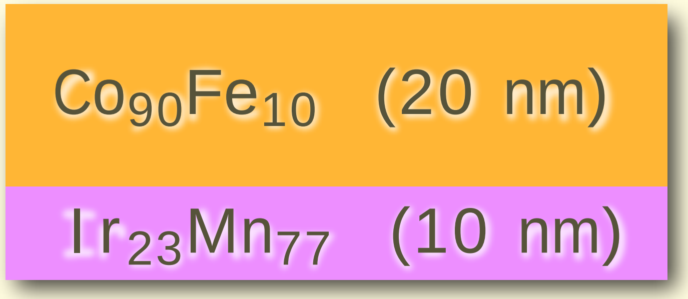

J. McCord, R.S., R. Mattheis, K.-U. Barholz, JAP 93, 5491 (2003)

Asymmetric reversal in exchange biased CoFe/IrMn

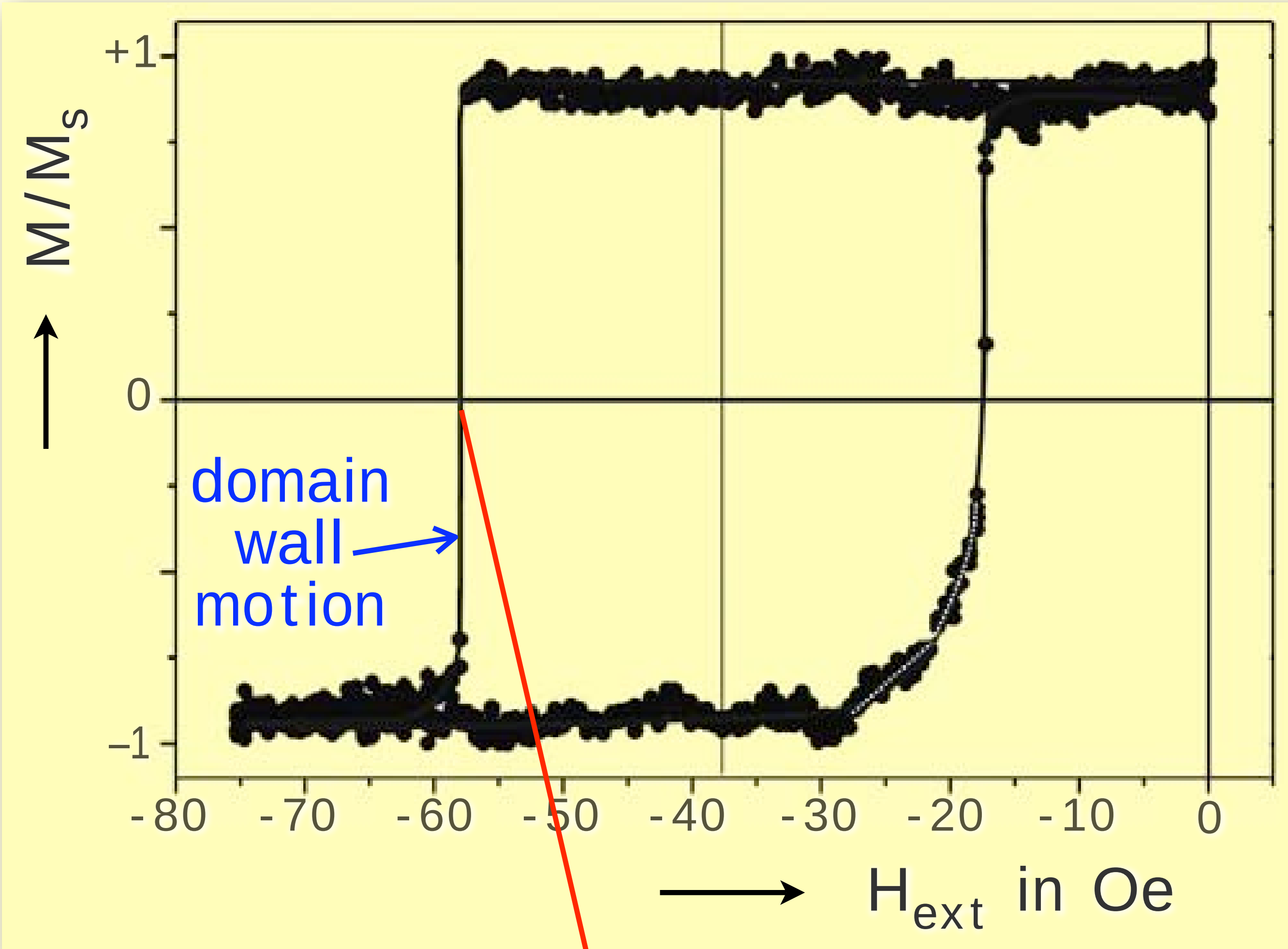

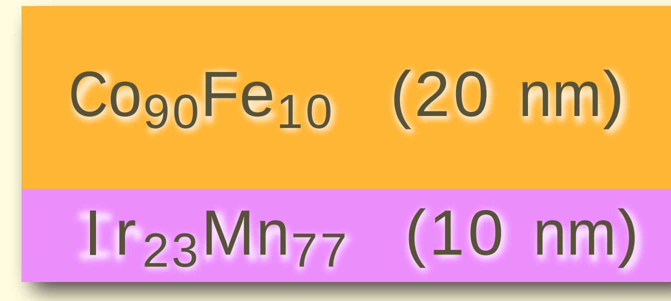

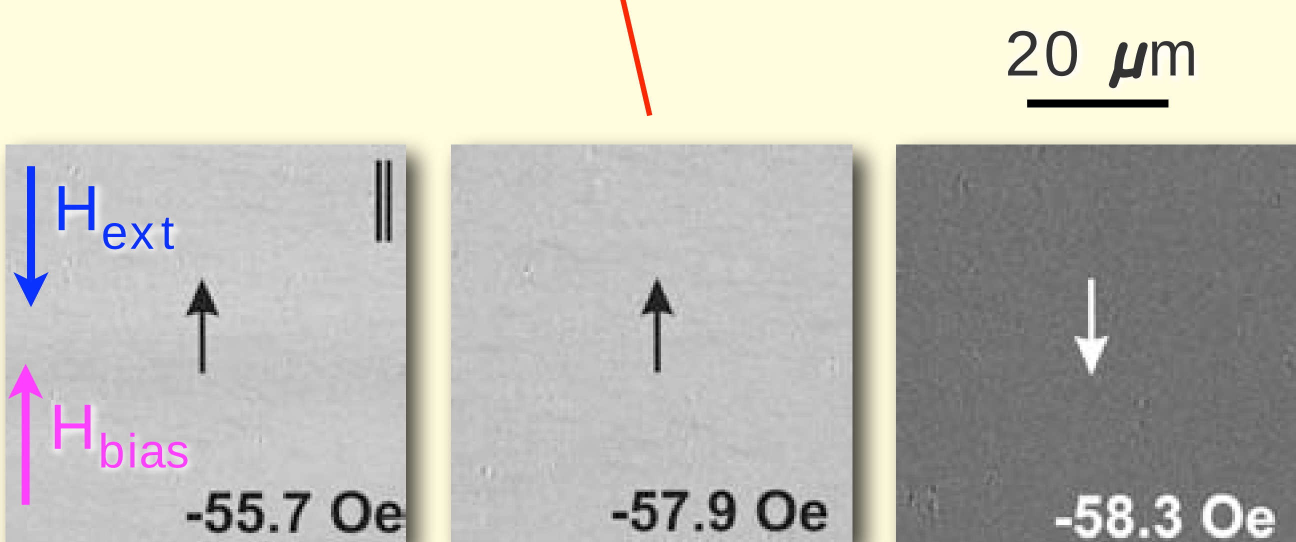

J. McCord, R.S., R. Mattheis, K.-U. Barholz, JAP 93, 5491 (2003)

Asymmetric reversal in exchange biased CoFe/IrMn

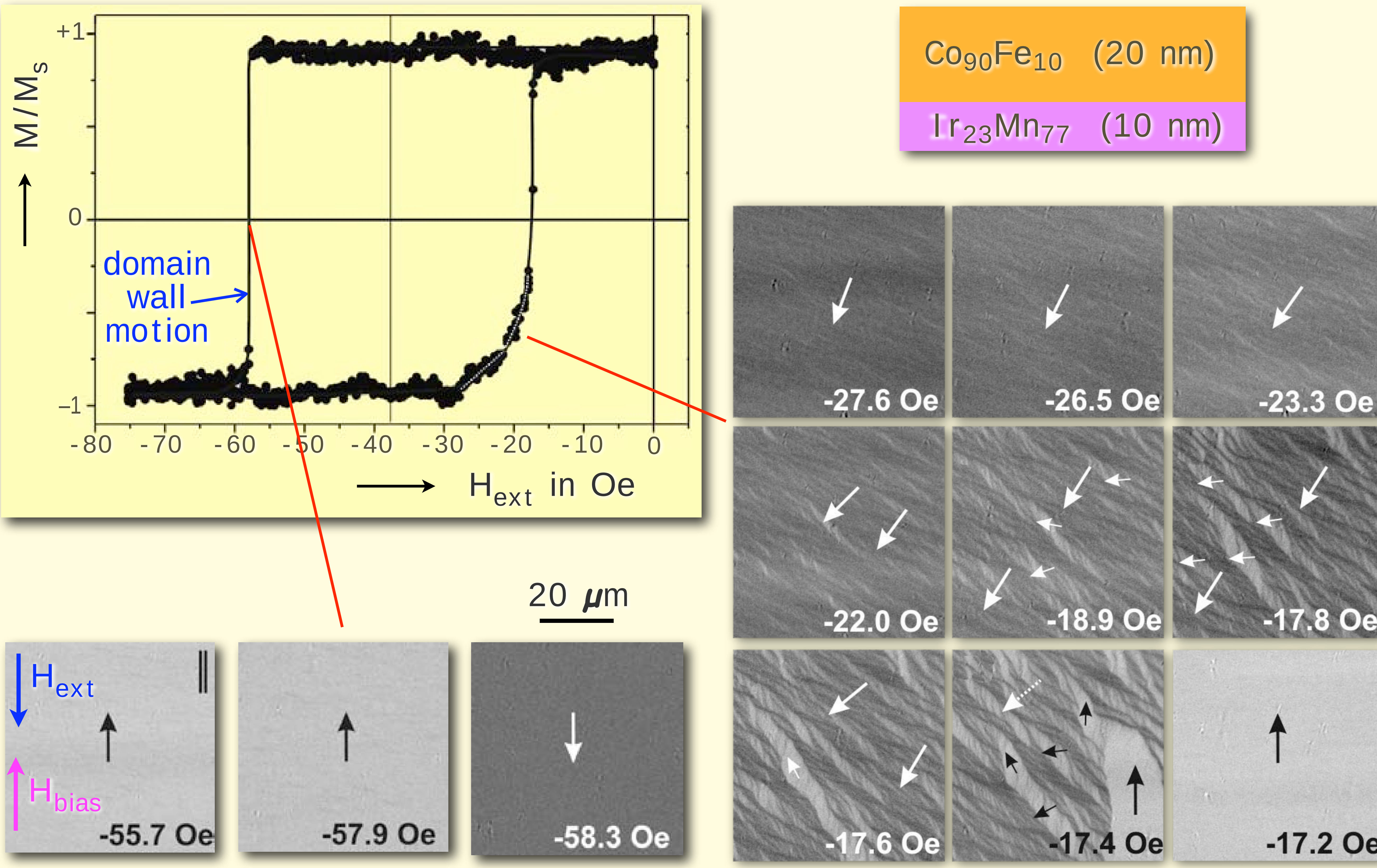

J. McCord, R.S., R. Mattheis, K.-U. Barholz, JAP 93, 5491 (2003)

Asymmetric reversal in exchange biased CoFe/IrMn

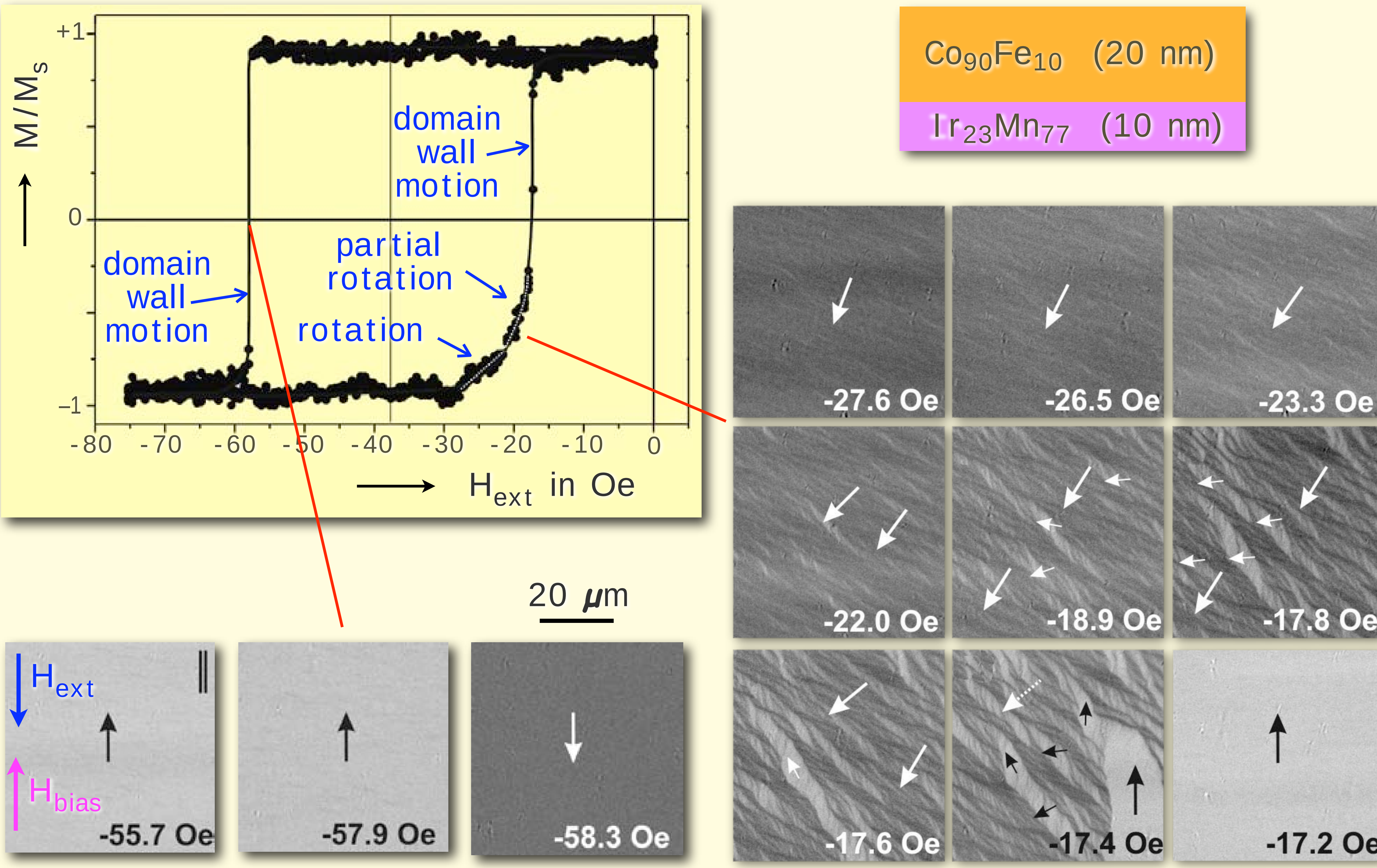

J. McCord, R.S., R. Mattheis, K.-U. Barholz, JAP 93, 5491 (2003)

Concertina decay and hysteresis

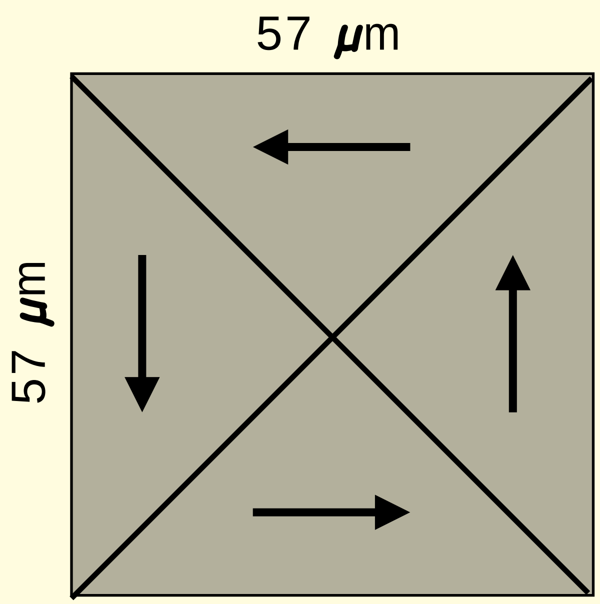

magnetic-
field

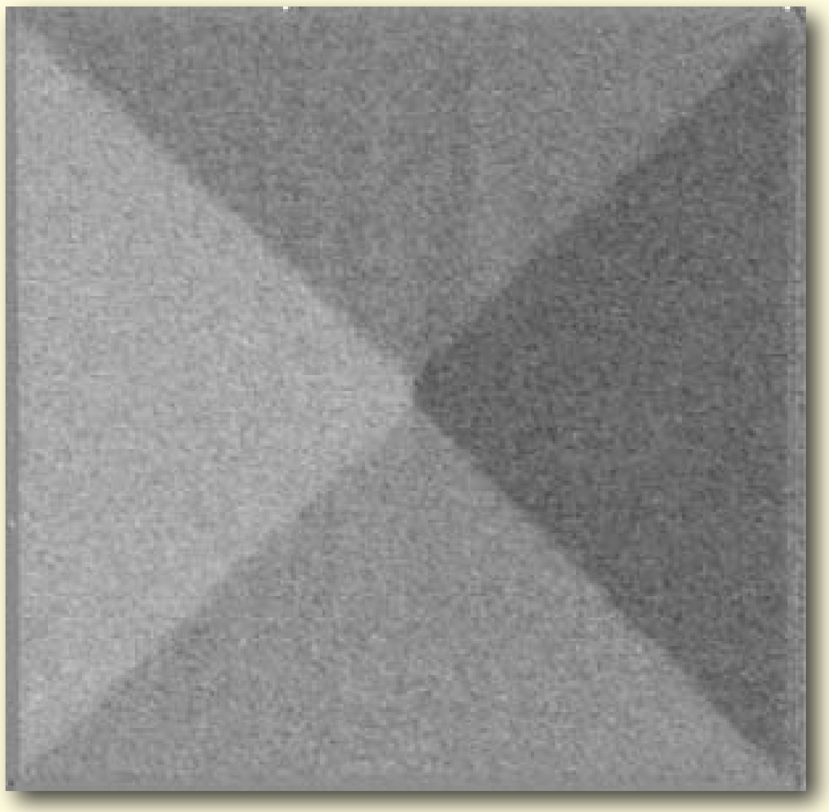

small field

large field

NiFe film
207 nm thick

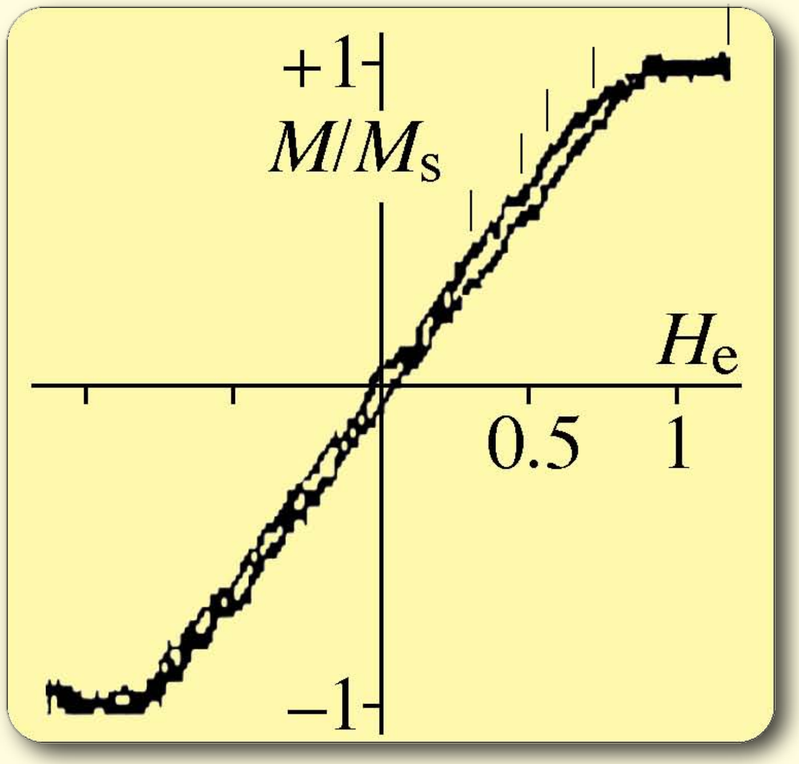

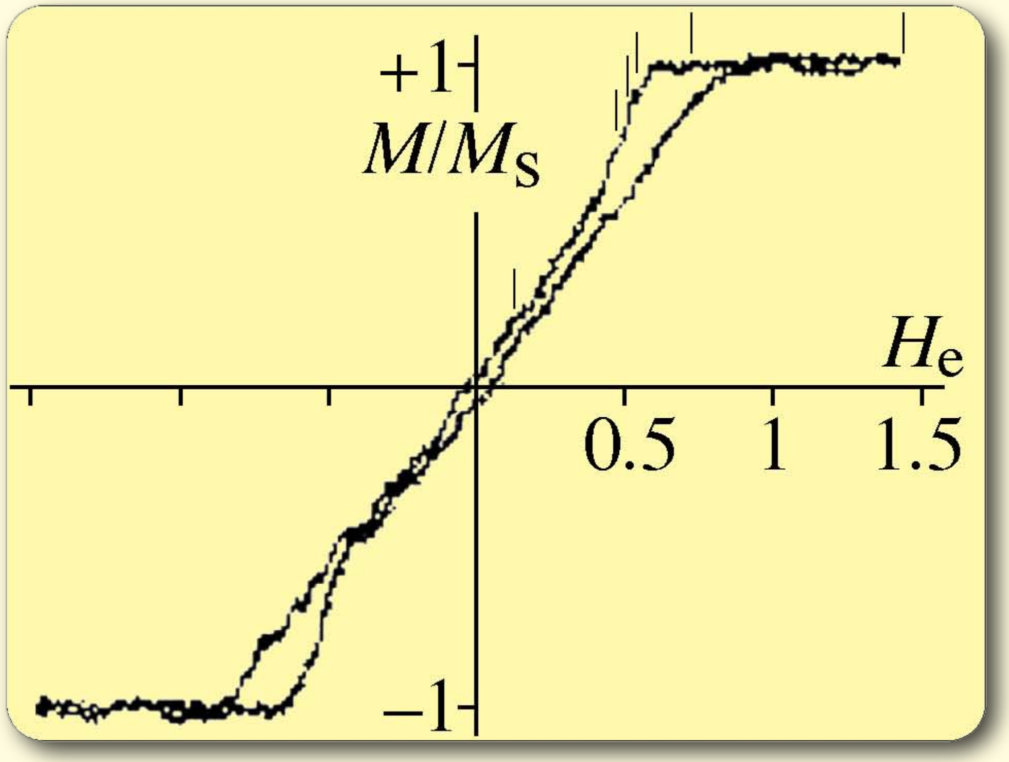

Concertina decay and hysteresis

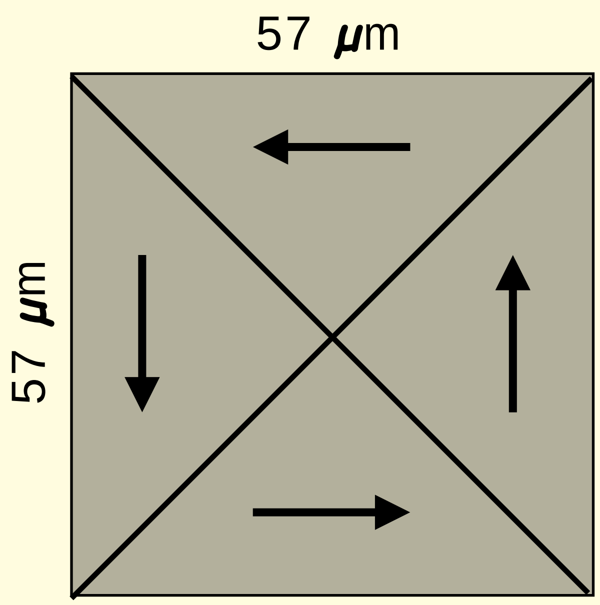

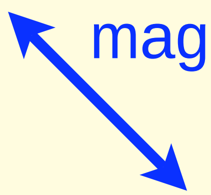

magnetic-
field

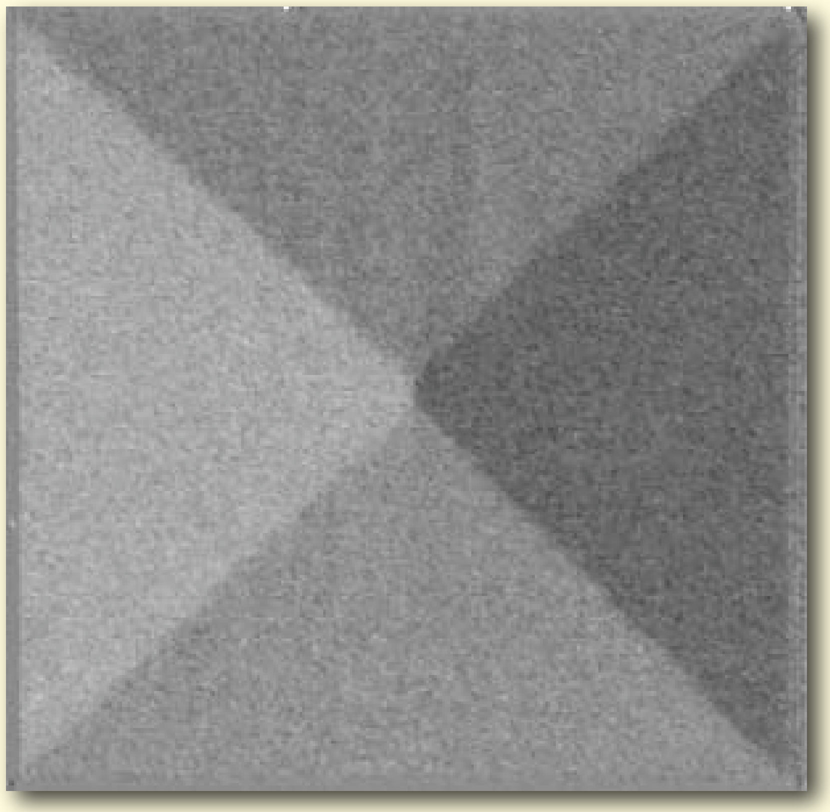

small field

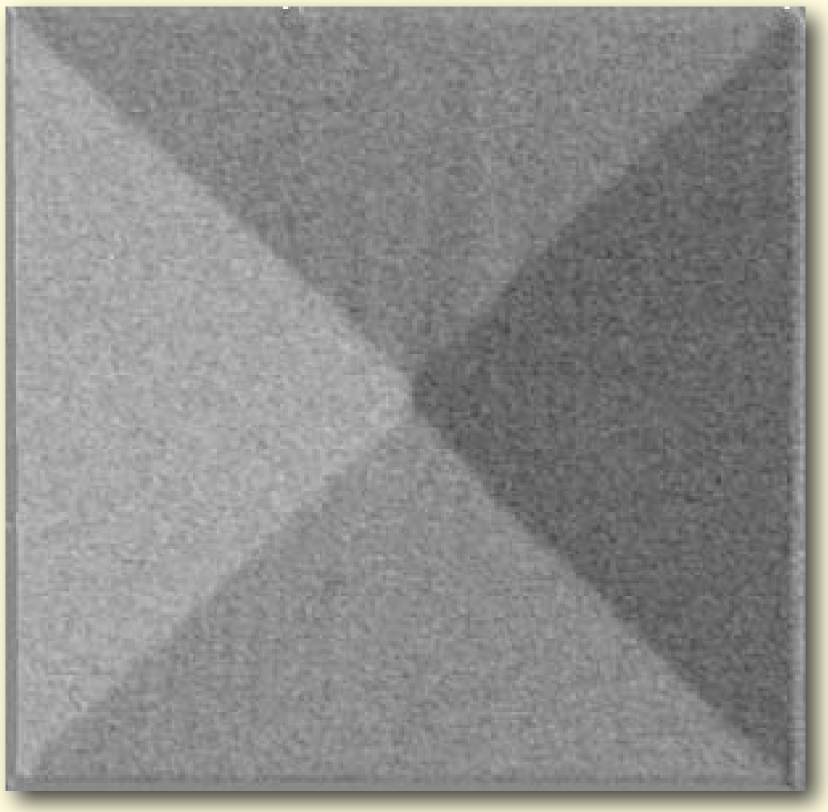

large field

NiFe film
207 nm thick

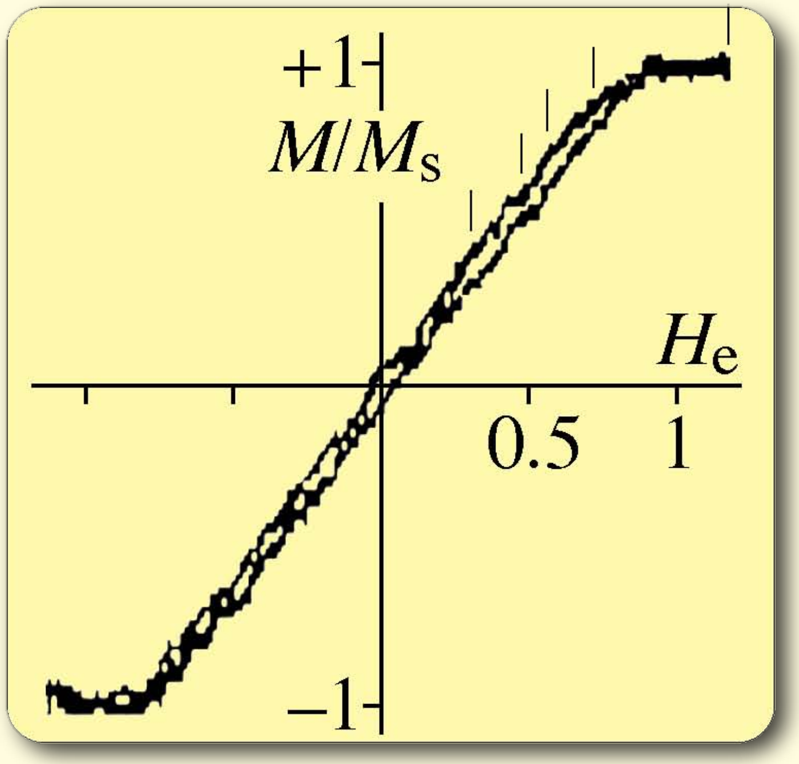

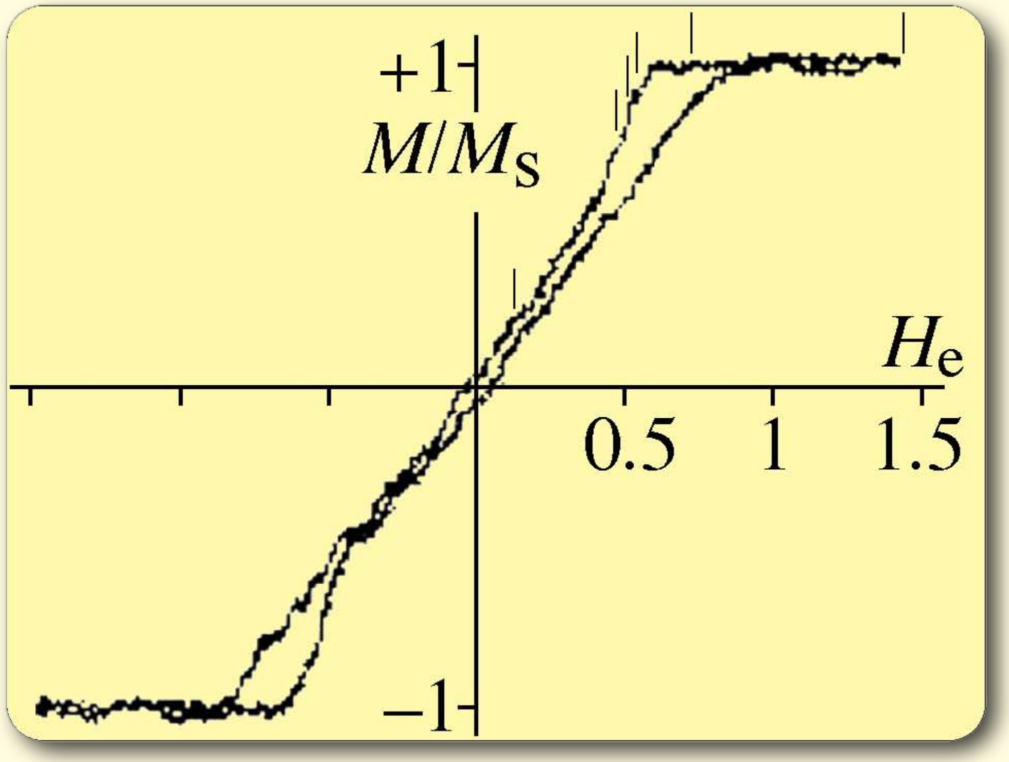

Kerr microscopy: advantages

Sample manipulation

Sample manipulation by mechanical stress

CoFeBSi amorphous film (500 nm thick)

$$e_K = K_u \sin^2\theta + K_\sigma \cos^2\theta$$

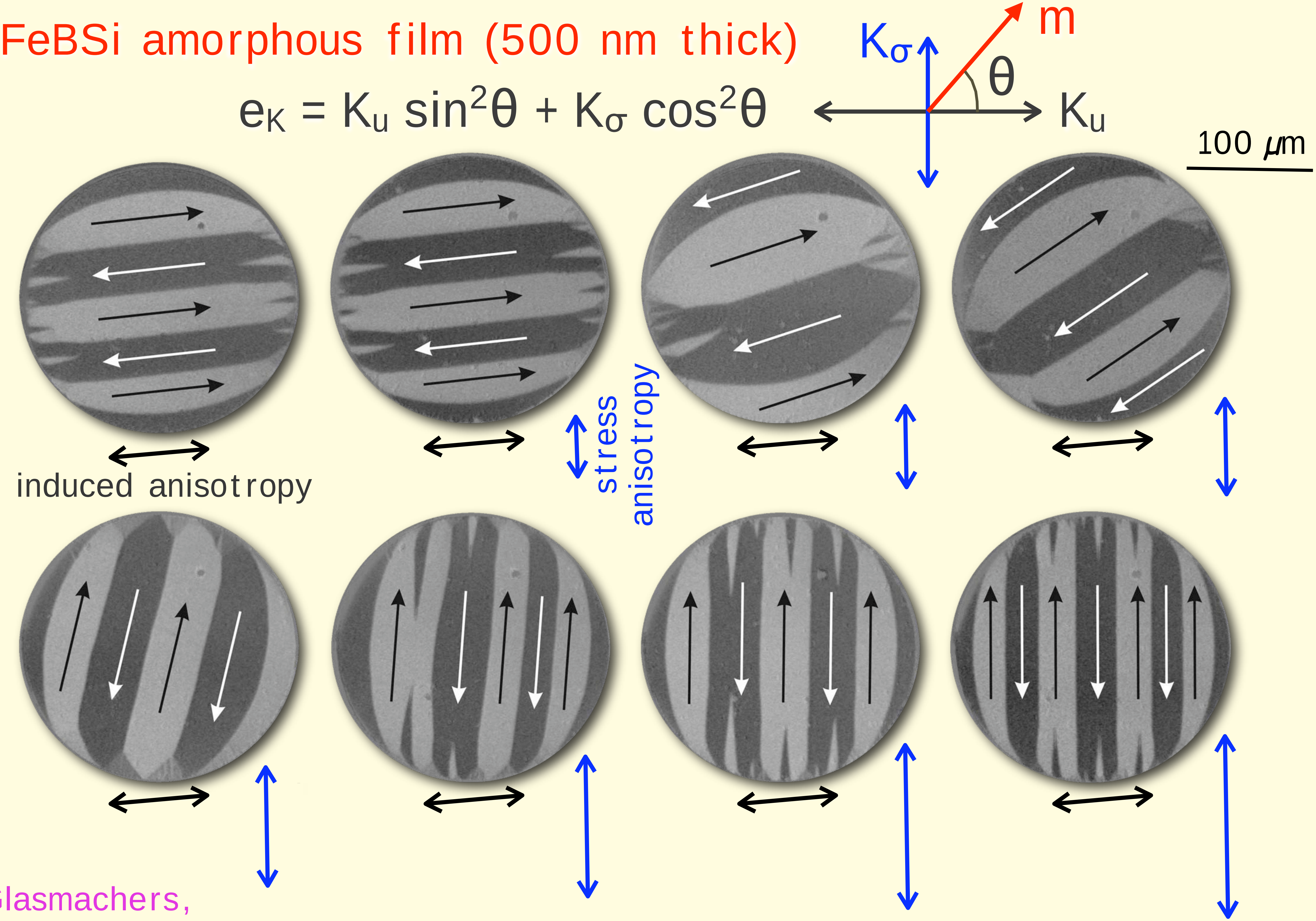

S. Glasmachers,
M. Frommberger, J. McCord, E. Quandt: phys. stat. sol. (a) 201, 3319 (2004)

Kerr microscopy: high/low temperature observation

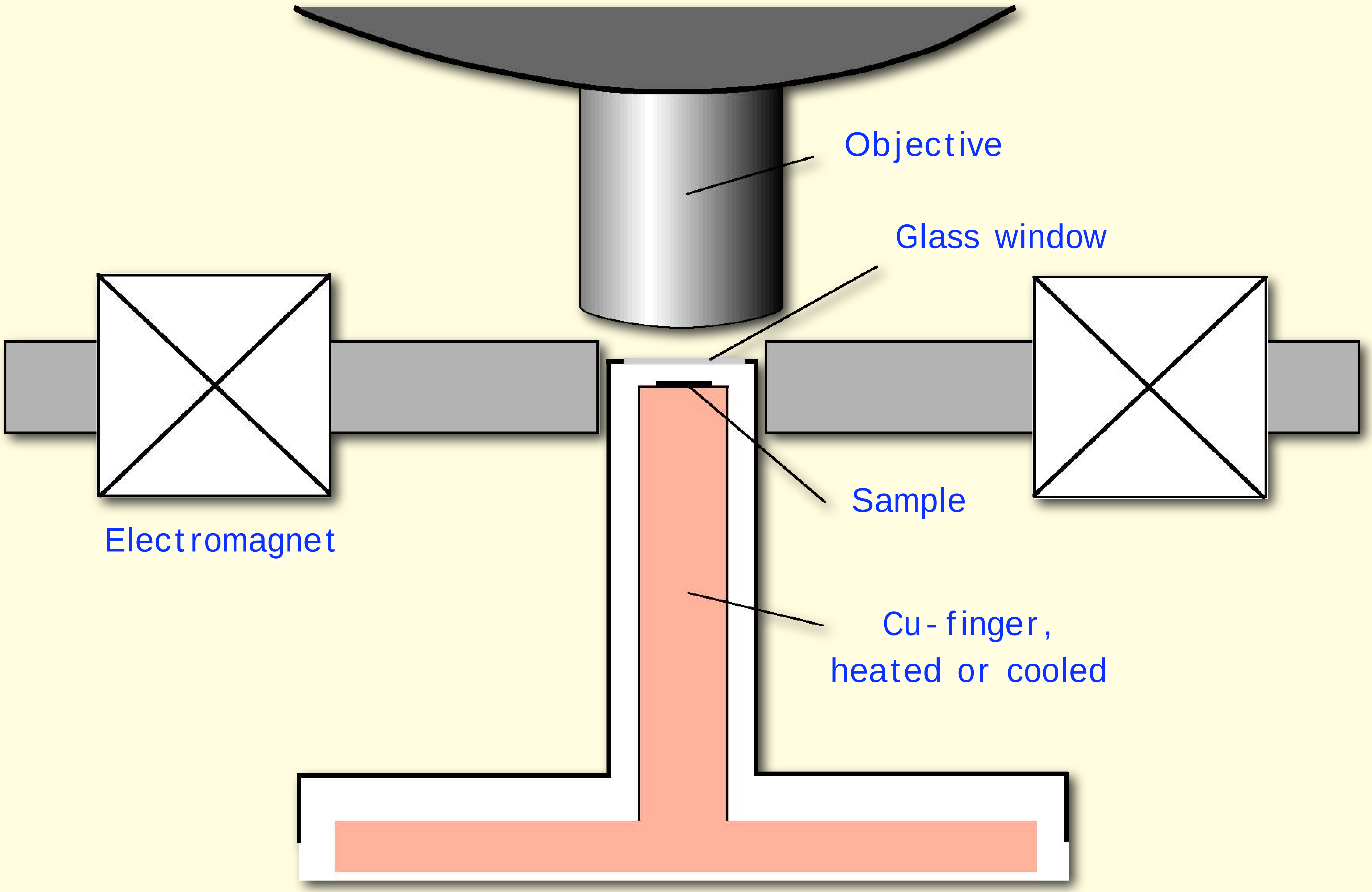

Heating above T_{Curie} of amorphous phase

$$\langle K_1 \rangle \sim \frac{K_1}{\sqrt{N}}$$

N: number of exchange-coupled grains within correlation volume

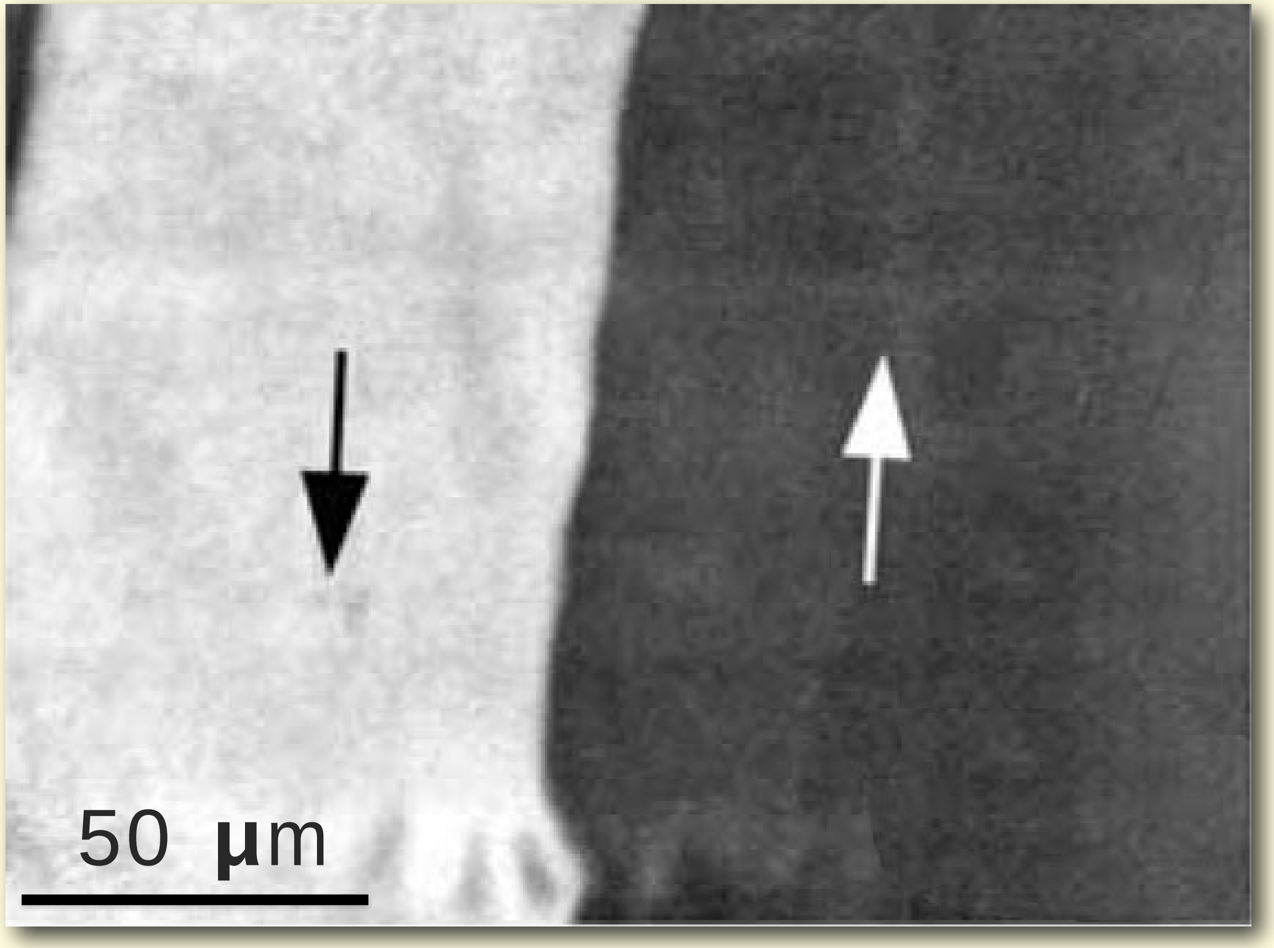

room temperature

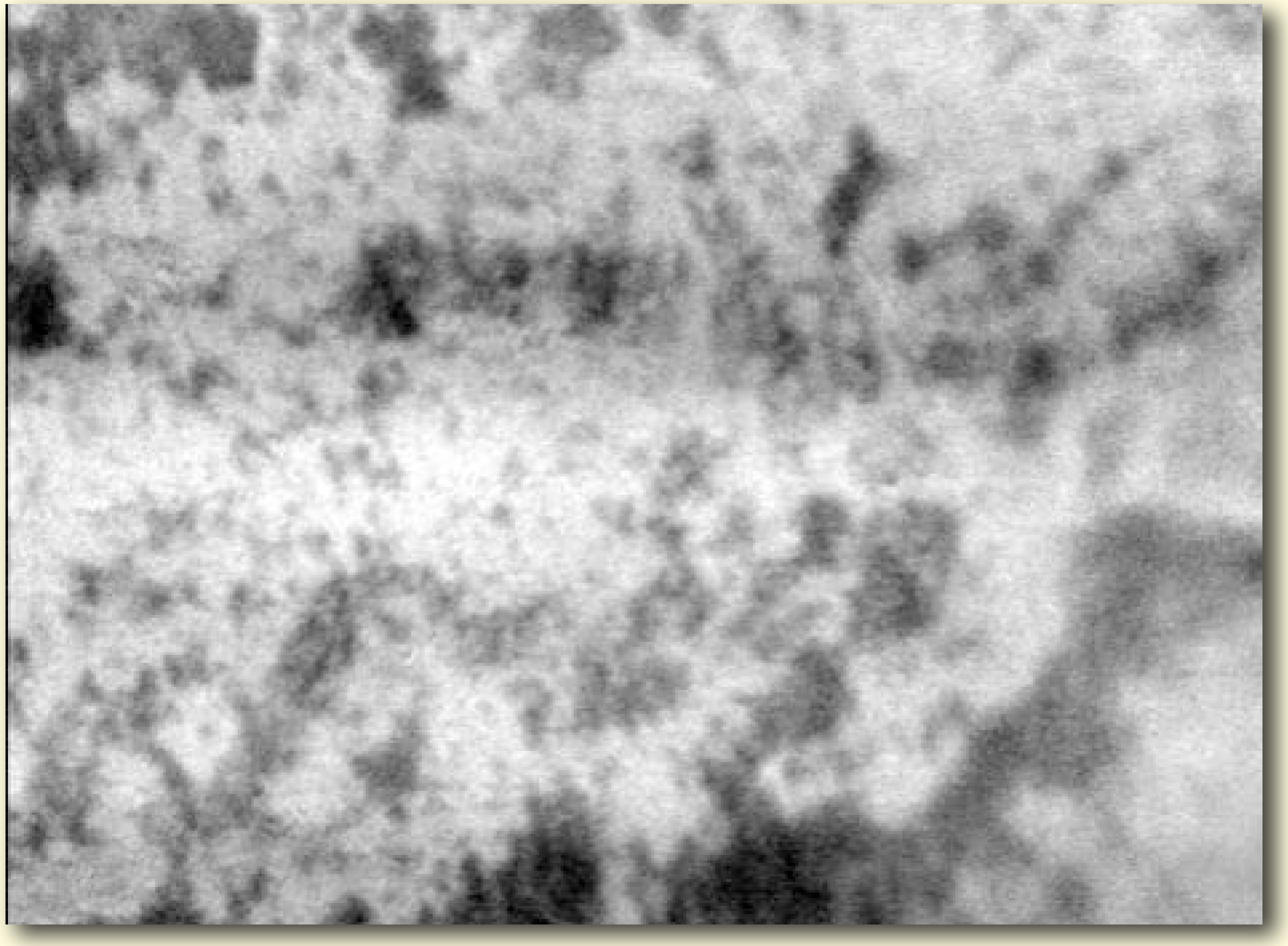

350°C

S. Flohrer, R.S., C. Polak, G. Herzer, Acta Mater. 53, 2937 (2005)

Kerr microscopy: advantages

Variable magnification

Stress effects in trafo steel

initial state

under tensile stress

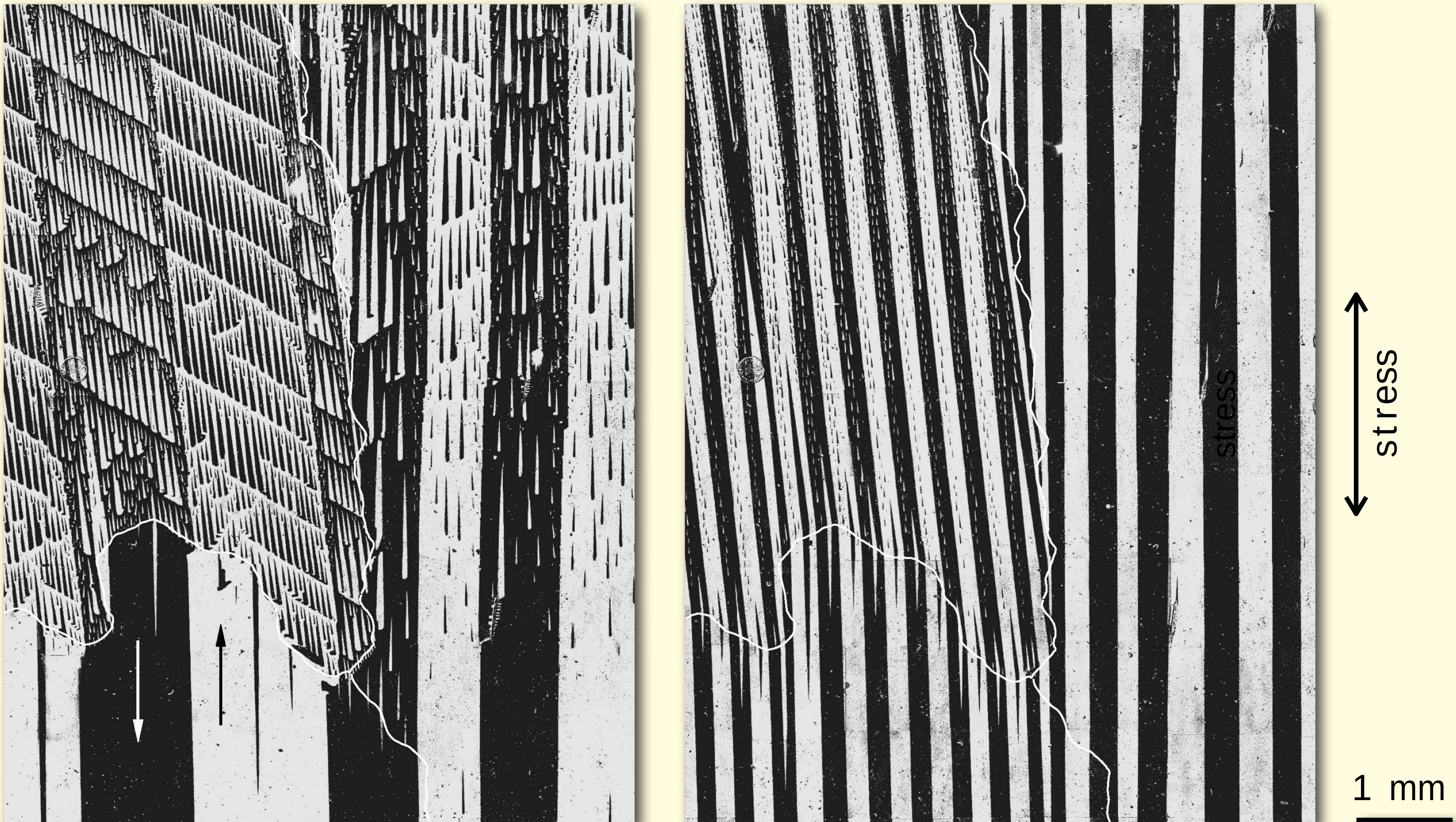

transformer steel

Change of magnification

Non-oriented electrical steel
(0.5 mm thick)

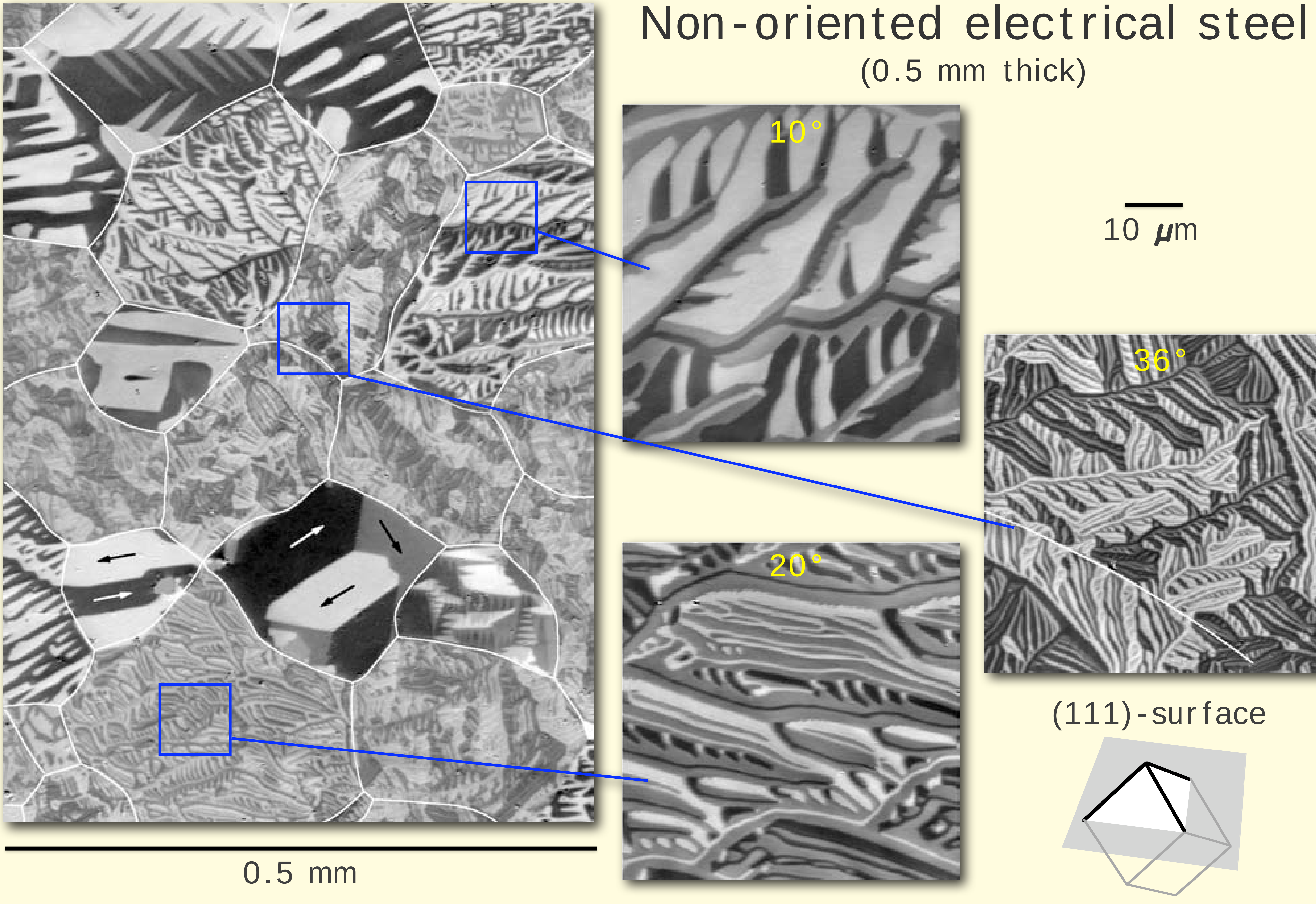

High-resolution observations

Co basal plane

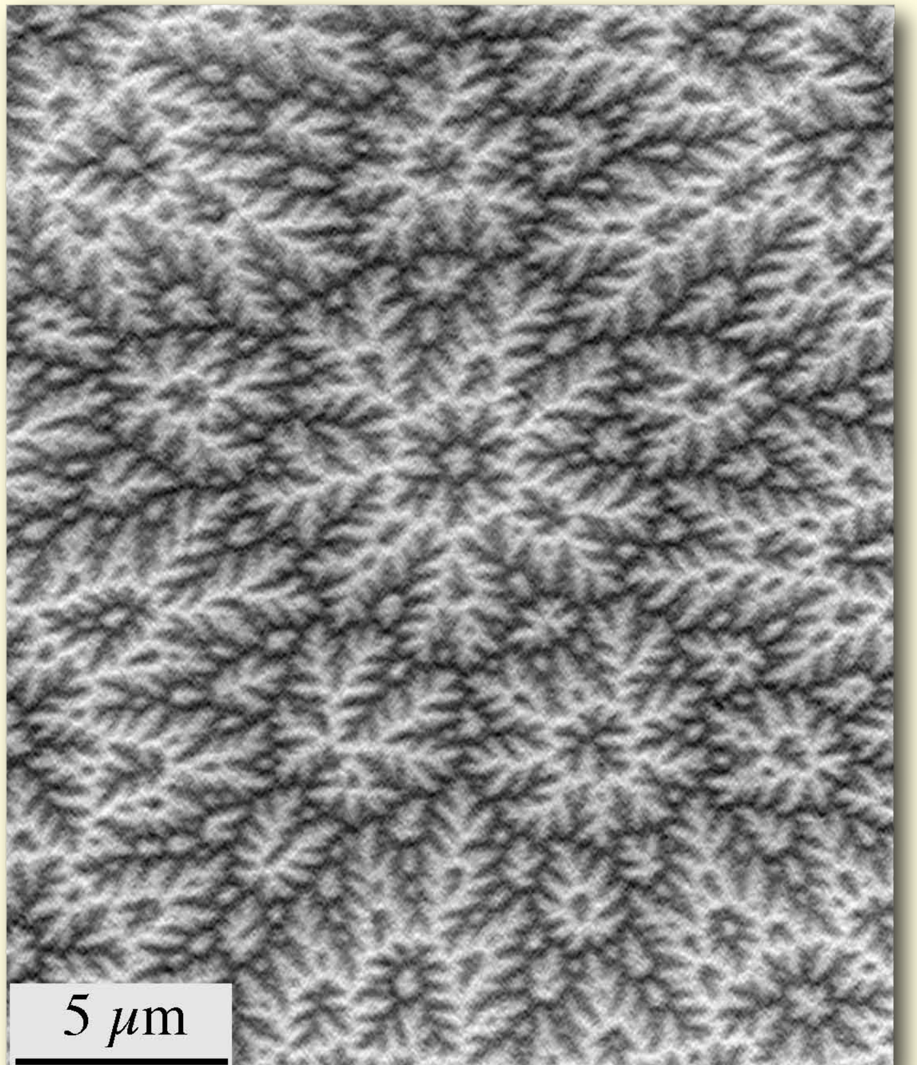

asymmetric Bloch wall (met. Glass)

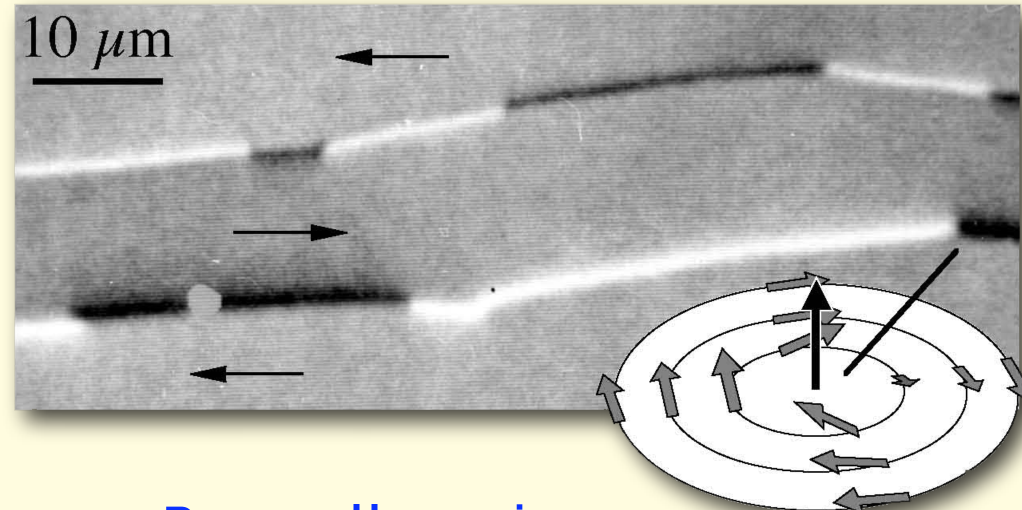

Surface swirl

Permalloy ring core

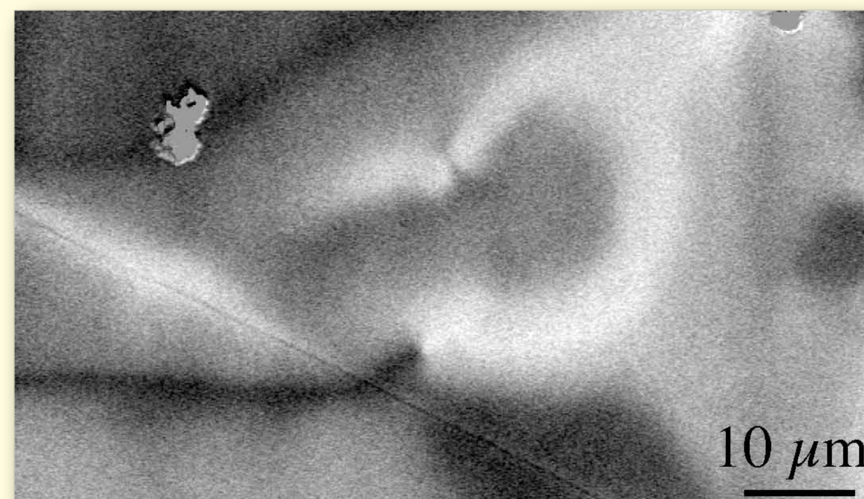

amorphous layer (1 μm thick)

Crosstie wall (Permalloy)

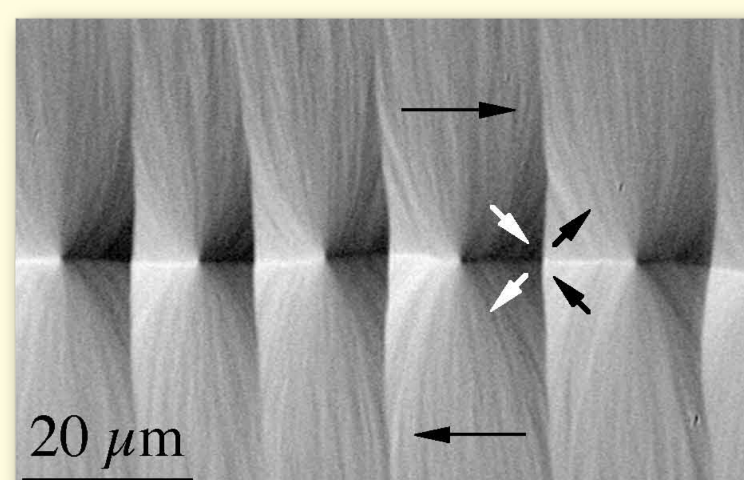

Kerr microscopy: advantages

Quantitative Kerr microscopy

Quantitative Kerr microscopy: principle

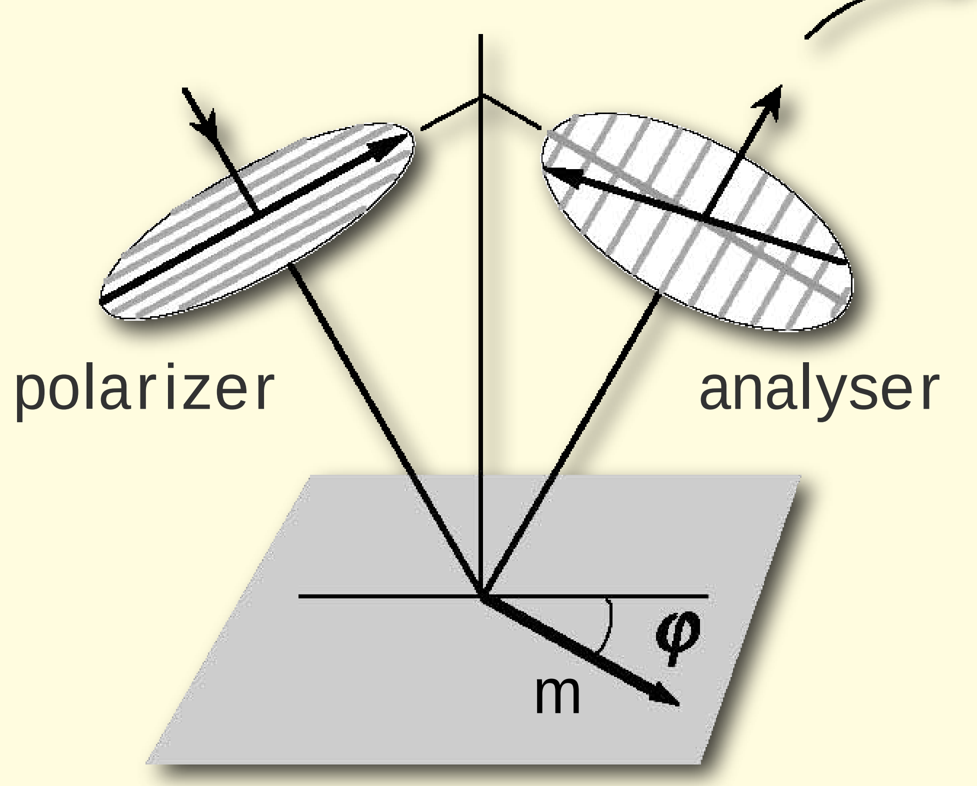

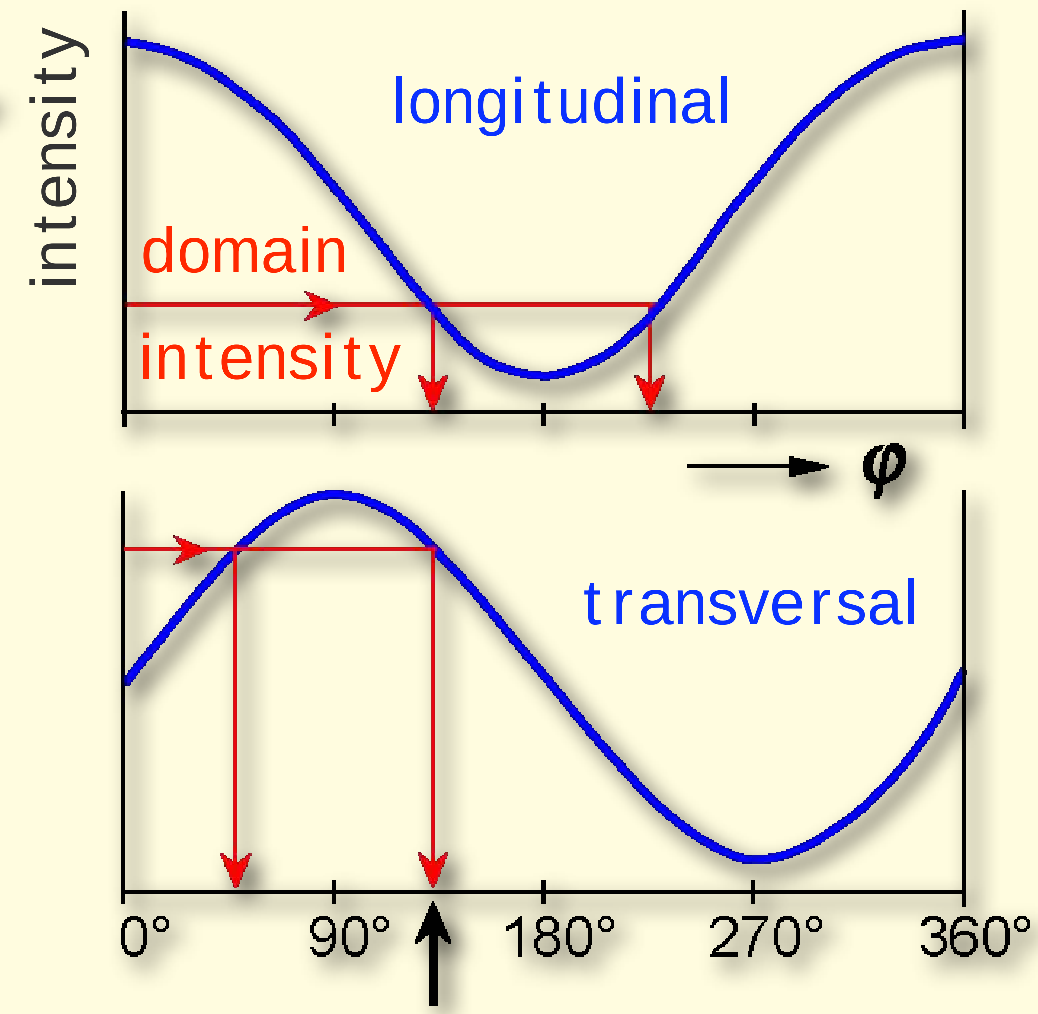

domains on
(100)-FeSi
sheet

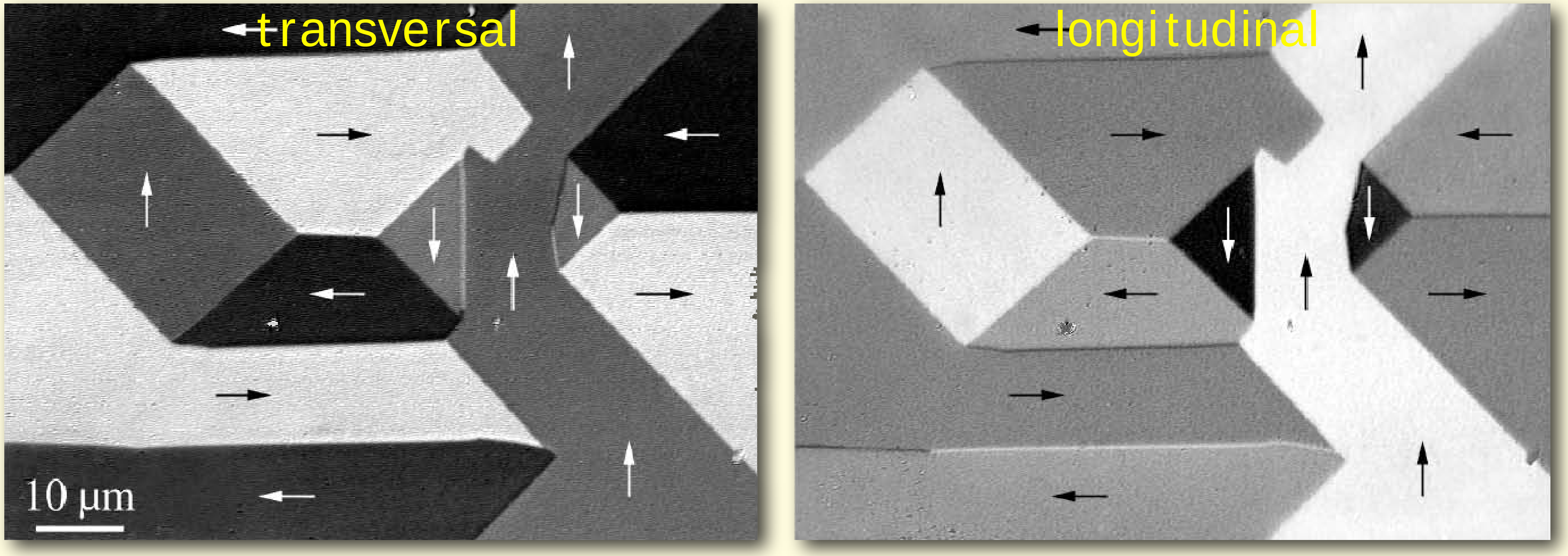

Quantitative Kerr microscopy: example

Domains in magnetostriction-free amorphous ribbon

as-quenched state

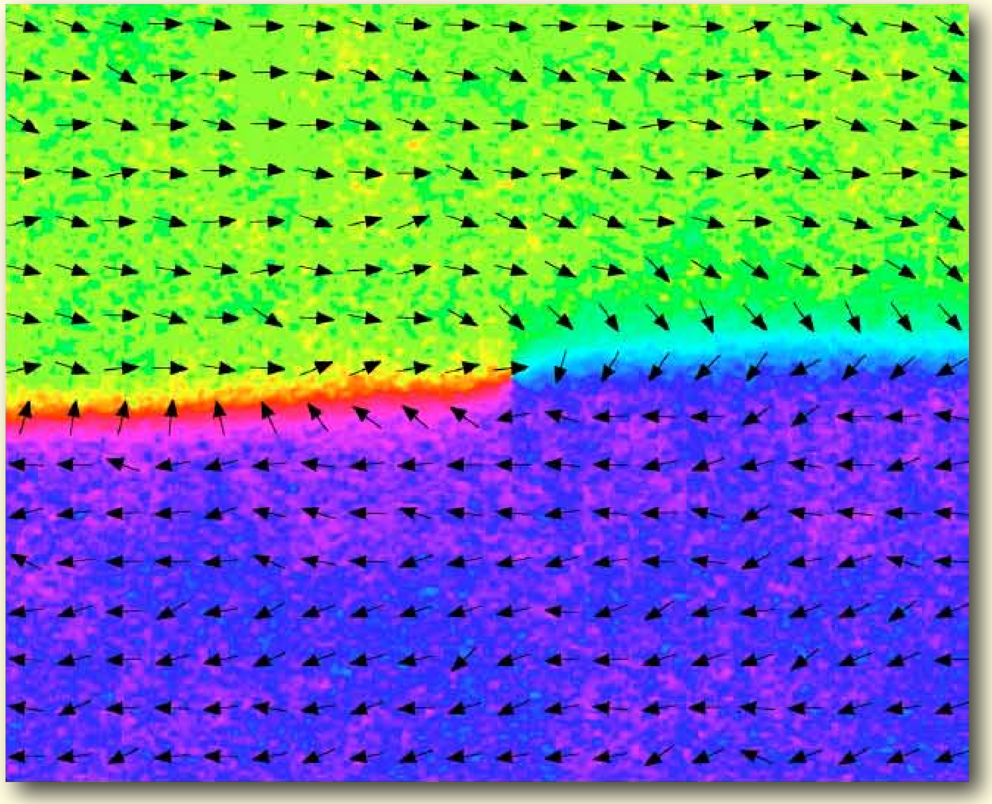

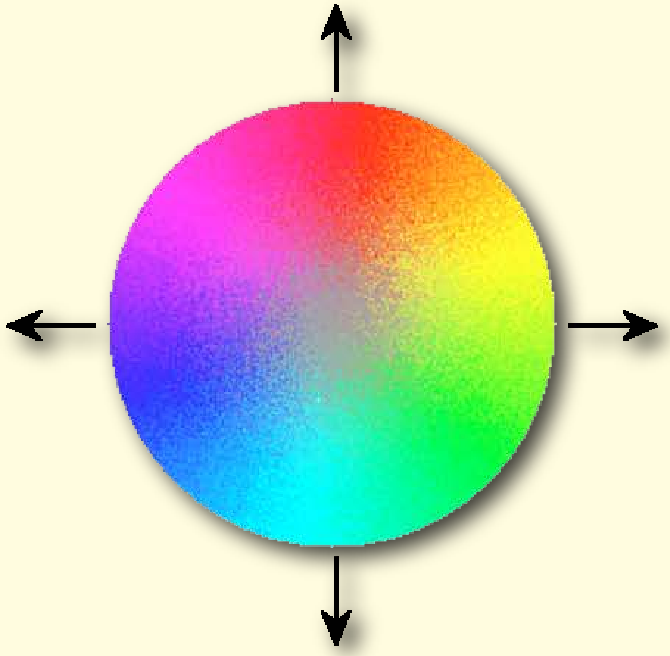

after annealing in rotating field

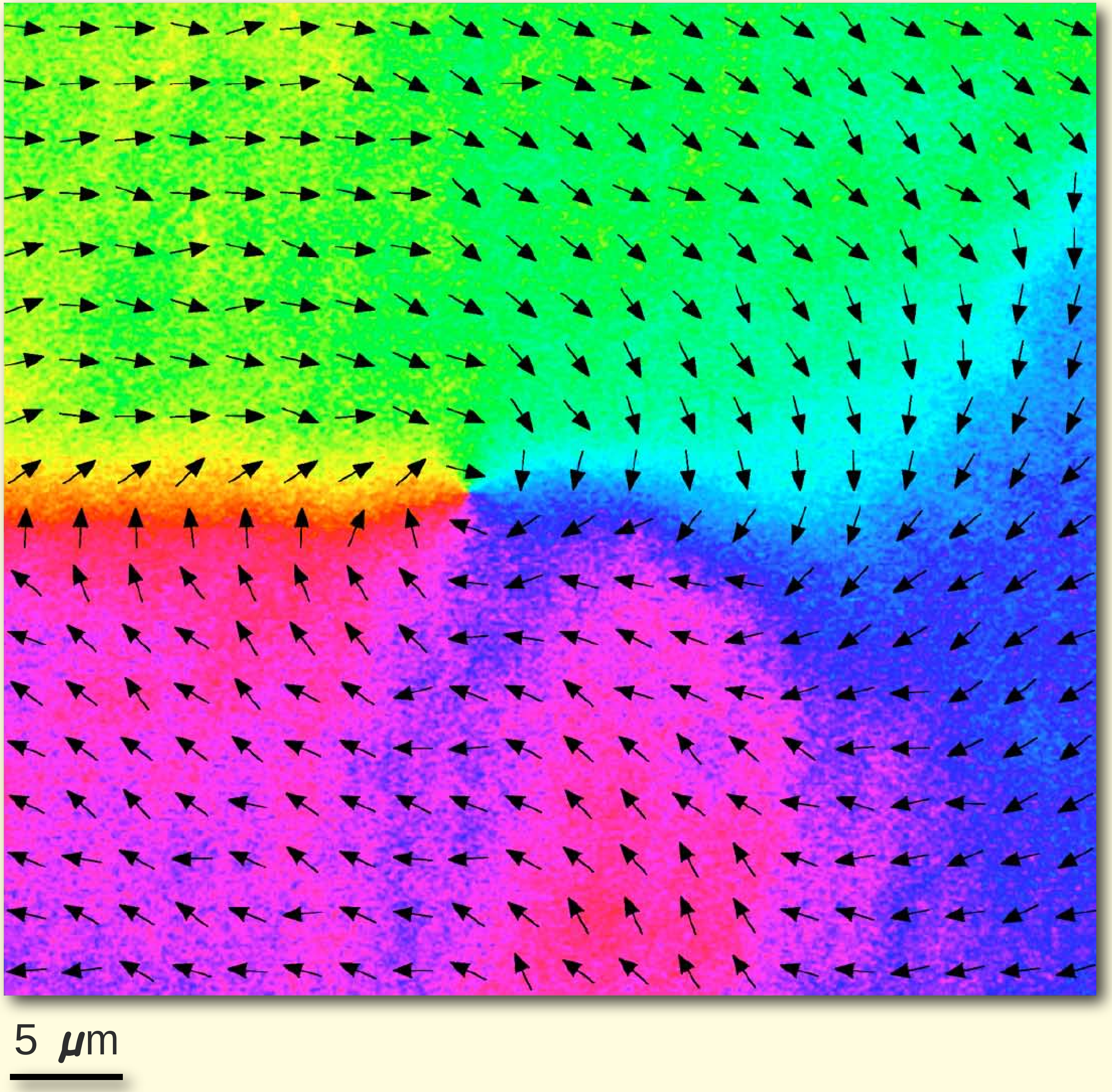

Kerr microscopy: advantages

Depth sensitivity

Depth sensitivity of Kerr microscopy

Spin-valve system

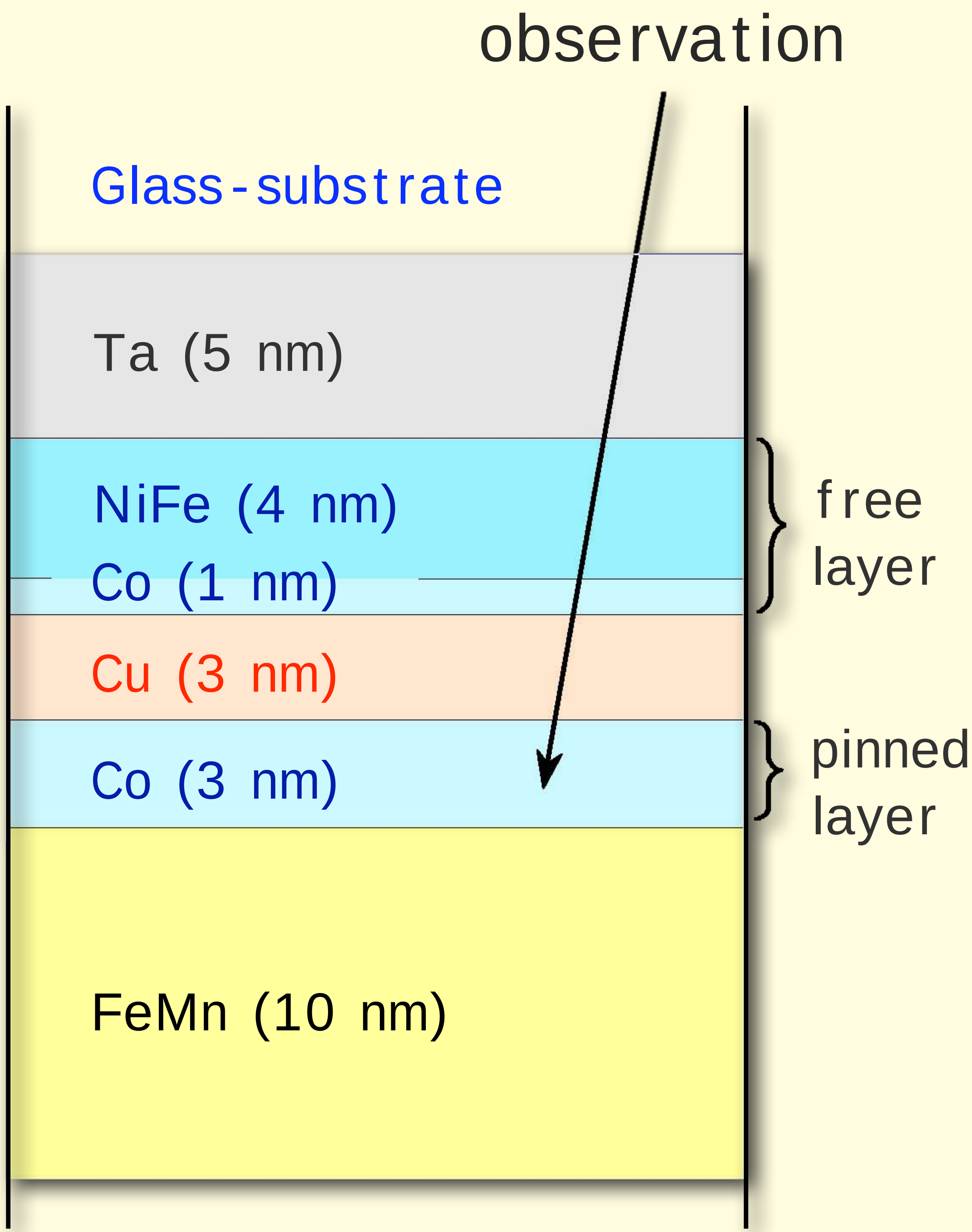

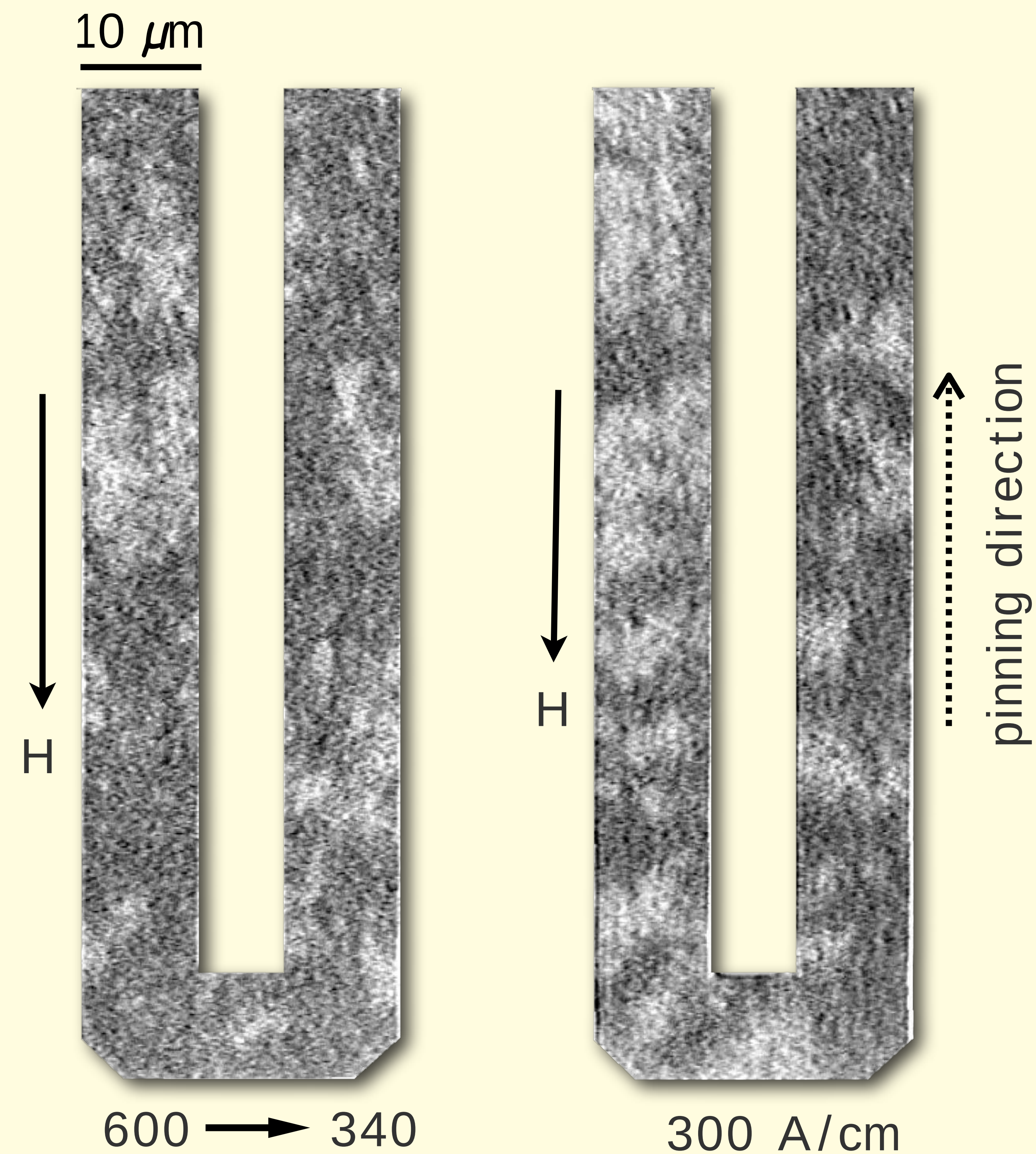

R.S., et al.,
IEEE Trans. Magn. 39, 2089 (2003)

together with
U. Barholz, R. Mattheis (IPHT Jena)

Depth sensitivity of Kerr microscopy

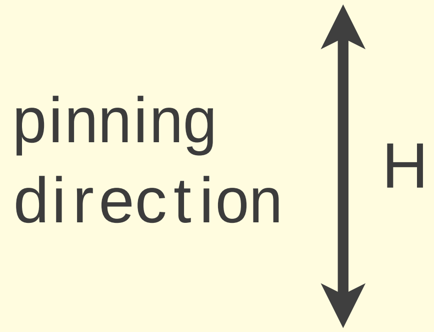

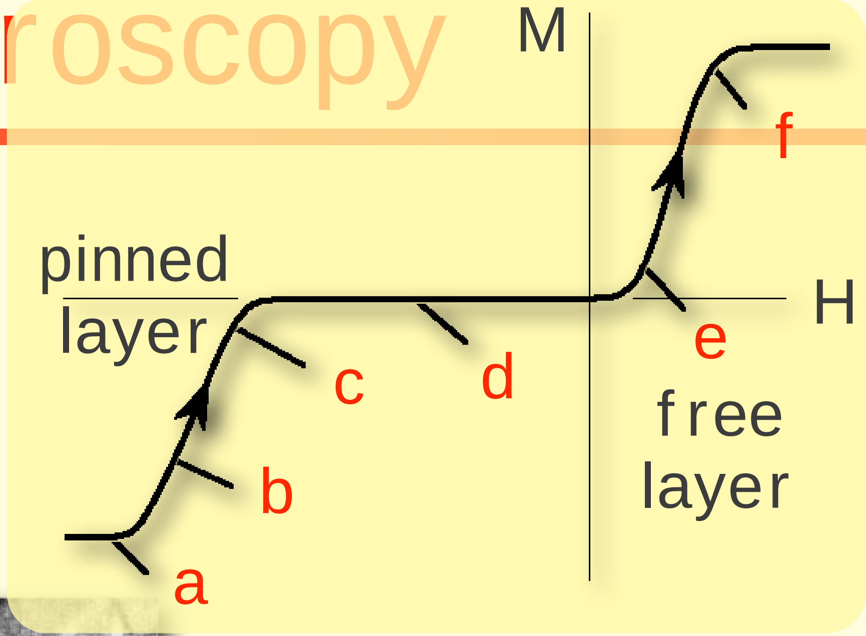

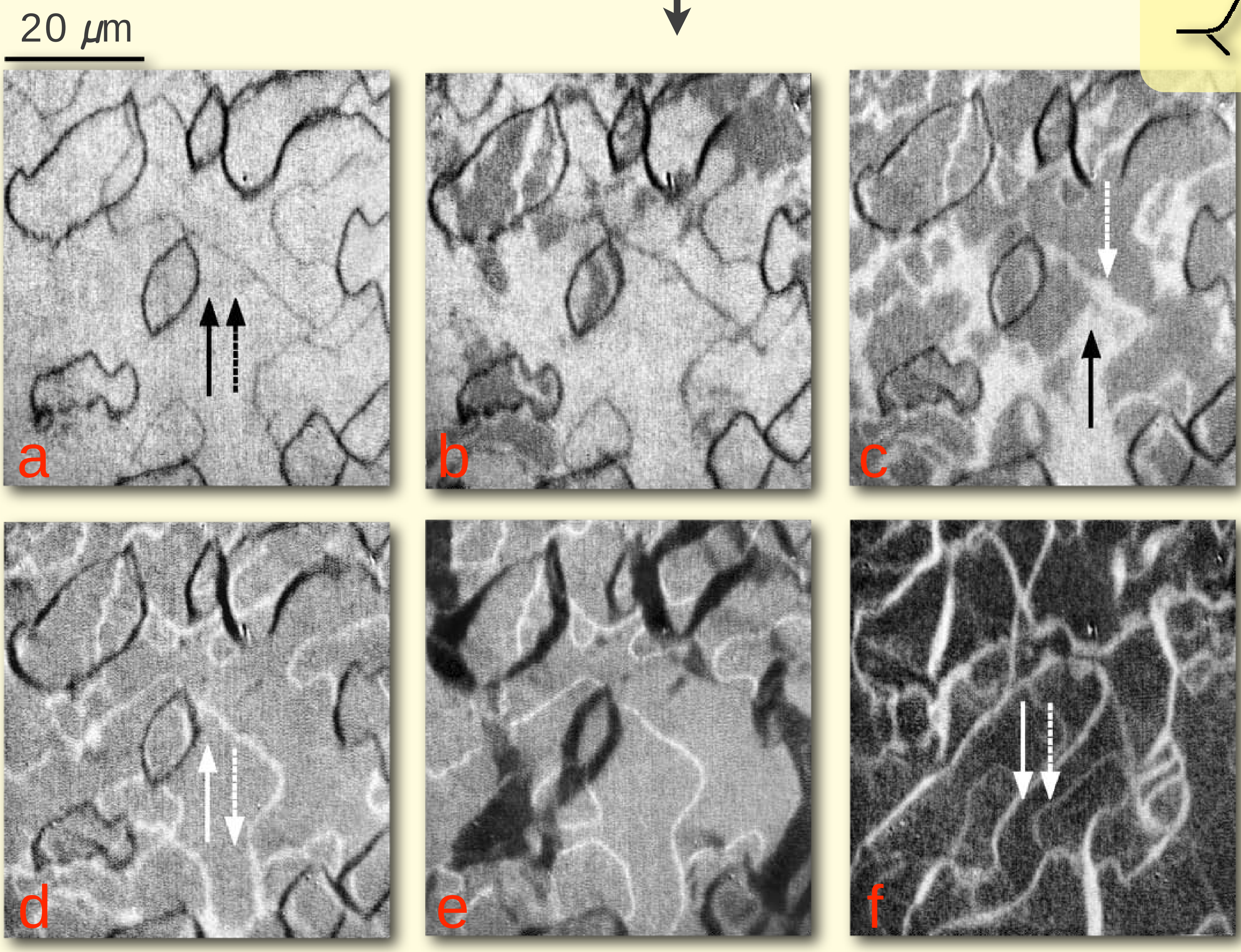

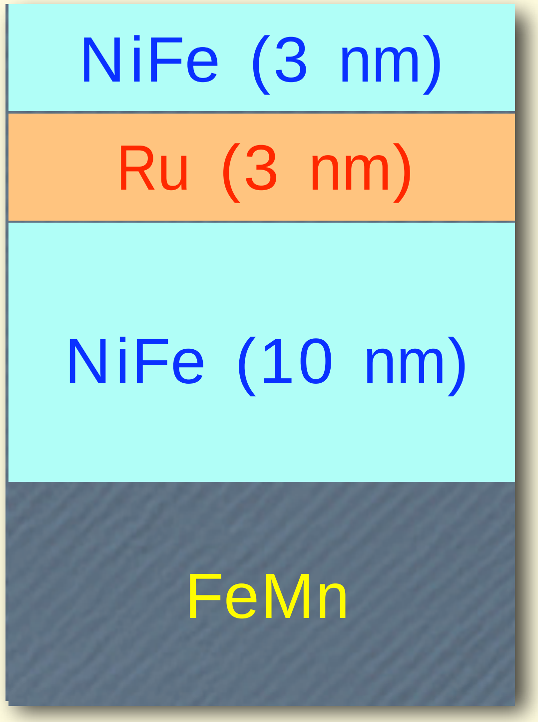

Sample:
S. Parkin, IBM

Kerr microscopy: advantages

Dynamic and time-resolved
Kerr microscopy

Dynamic observations

FeSiB amorphous ribbon,
as-quenched

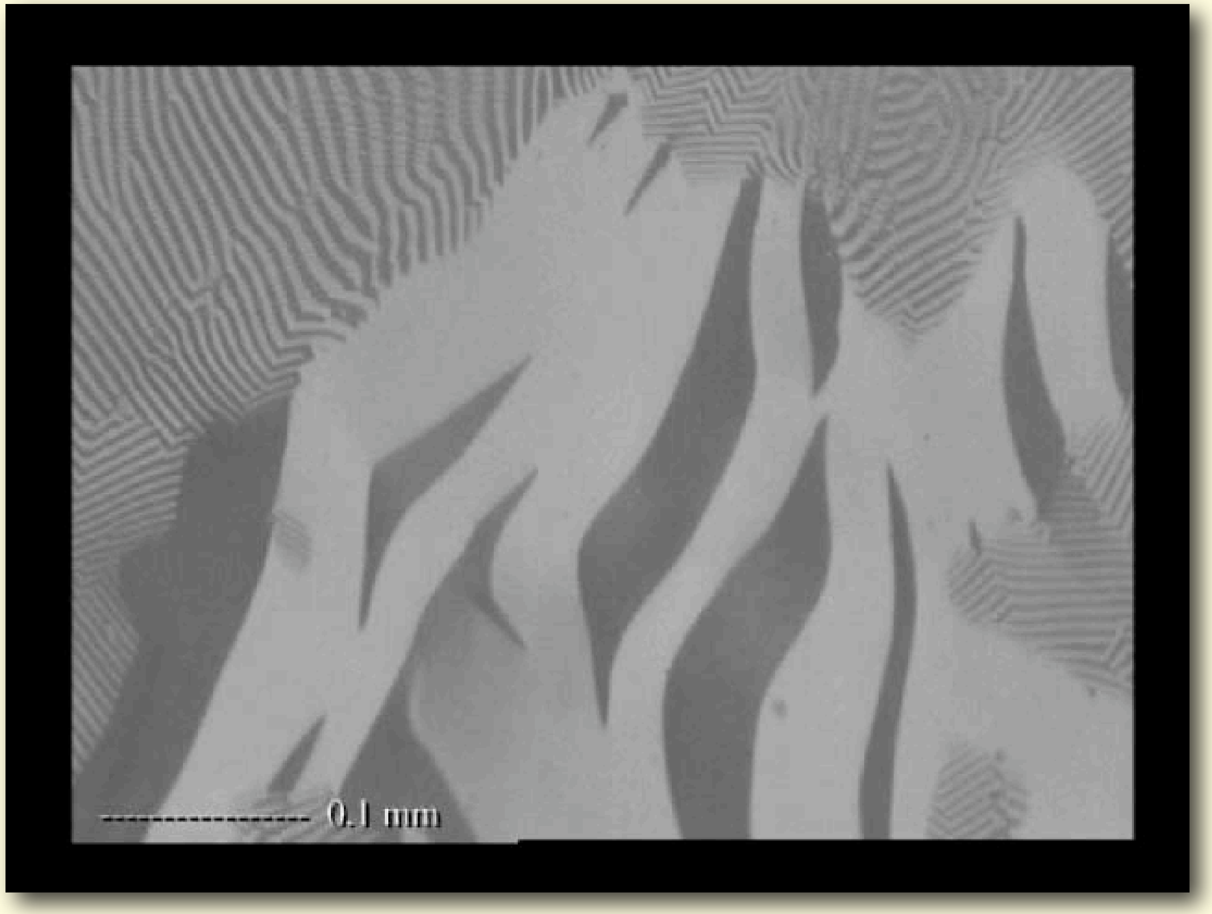

Slow dynamics

0.2 mm

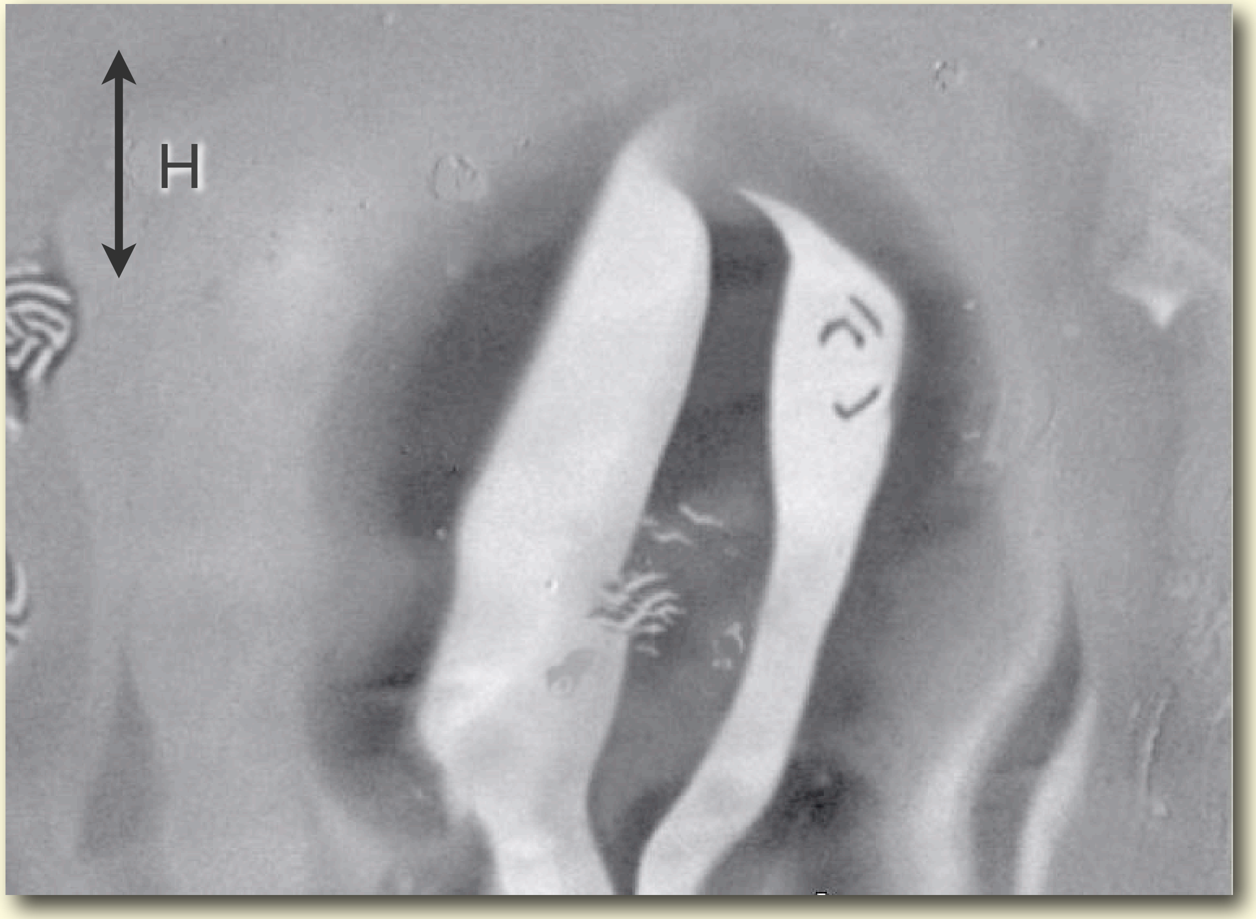

25 Hz sinusoidal field

Time-resolved imaging: Stroboscopic mode

illumination intensity and repetition rate are limited

→ no single-shot imaging possible

→ accumulation of large number of independent events necessary (at fixed time delay)

→ requires repetitive magnetization processes !!

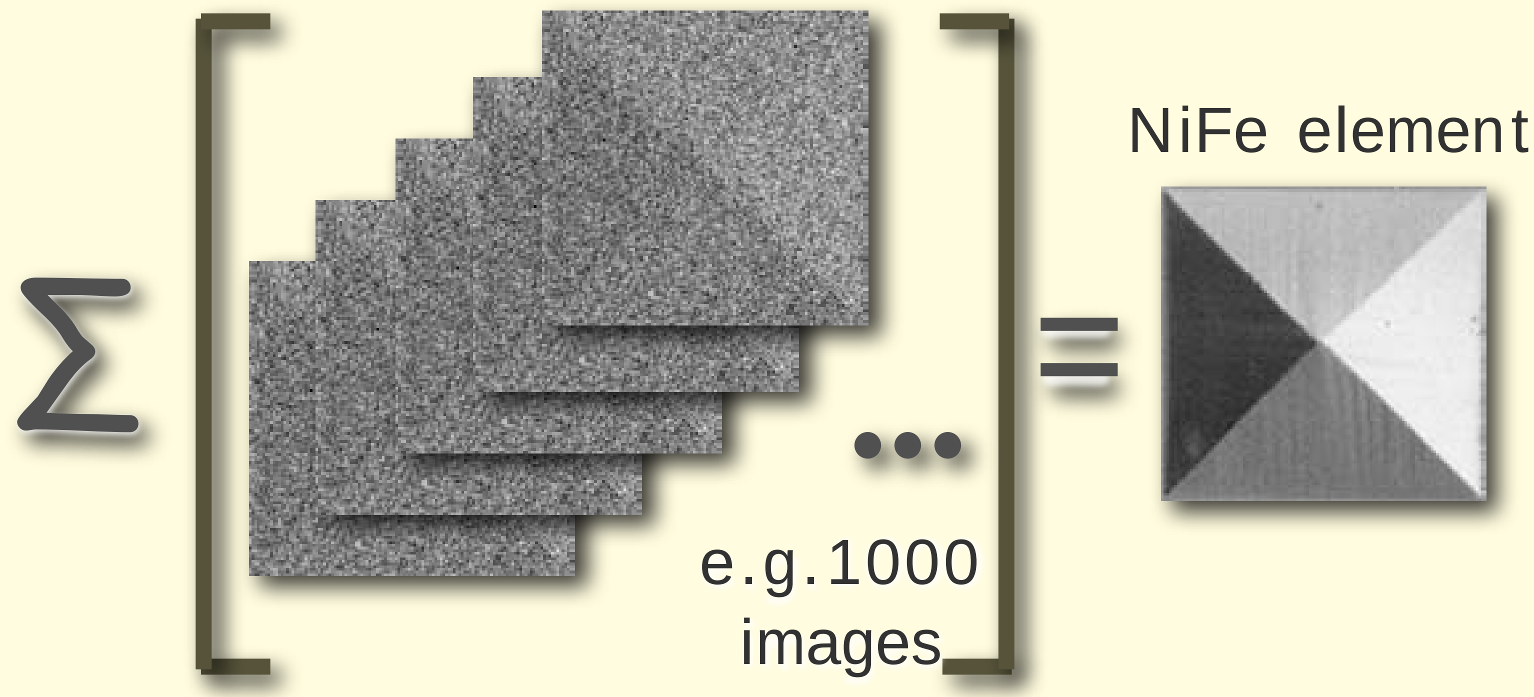

probing with defined time delay

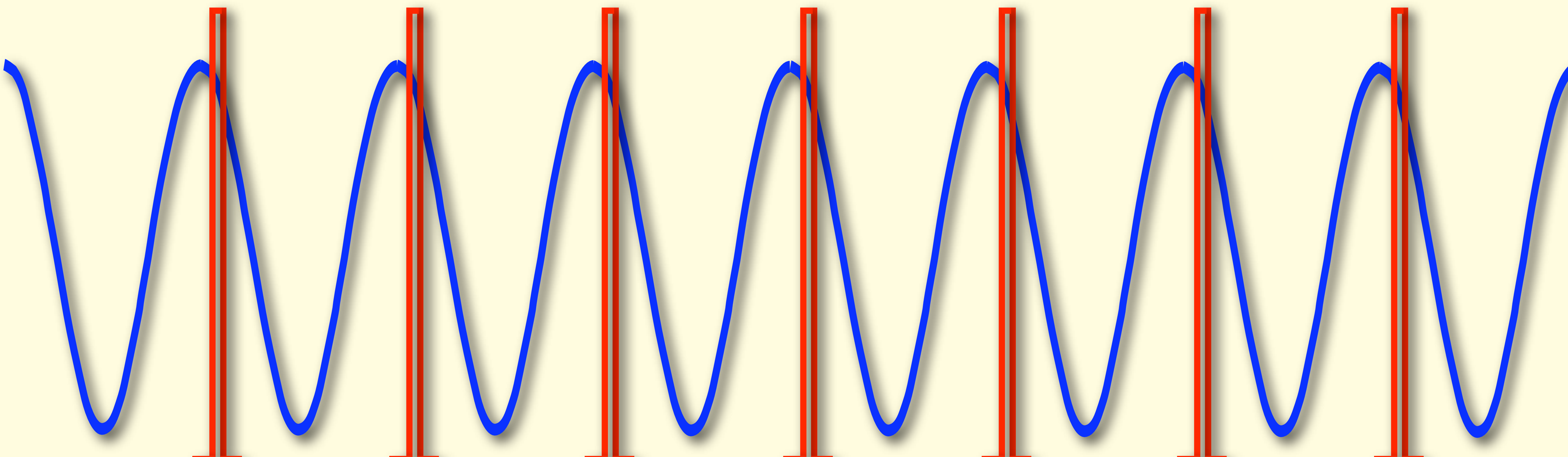

periodic magnetic field excitation

Time-resolved imaging: Stroboscopic mode

illumination intensity and repetition rate are limited

→ no single-shot imaging possible

→ accumulation of large number of independent events necessary (at fixed time delay)

→ requires repetitive magnetization processes !!

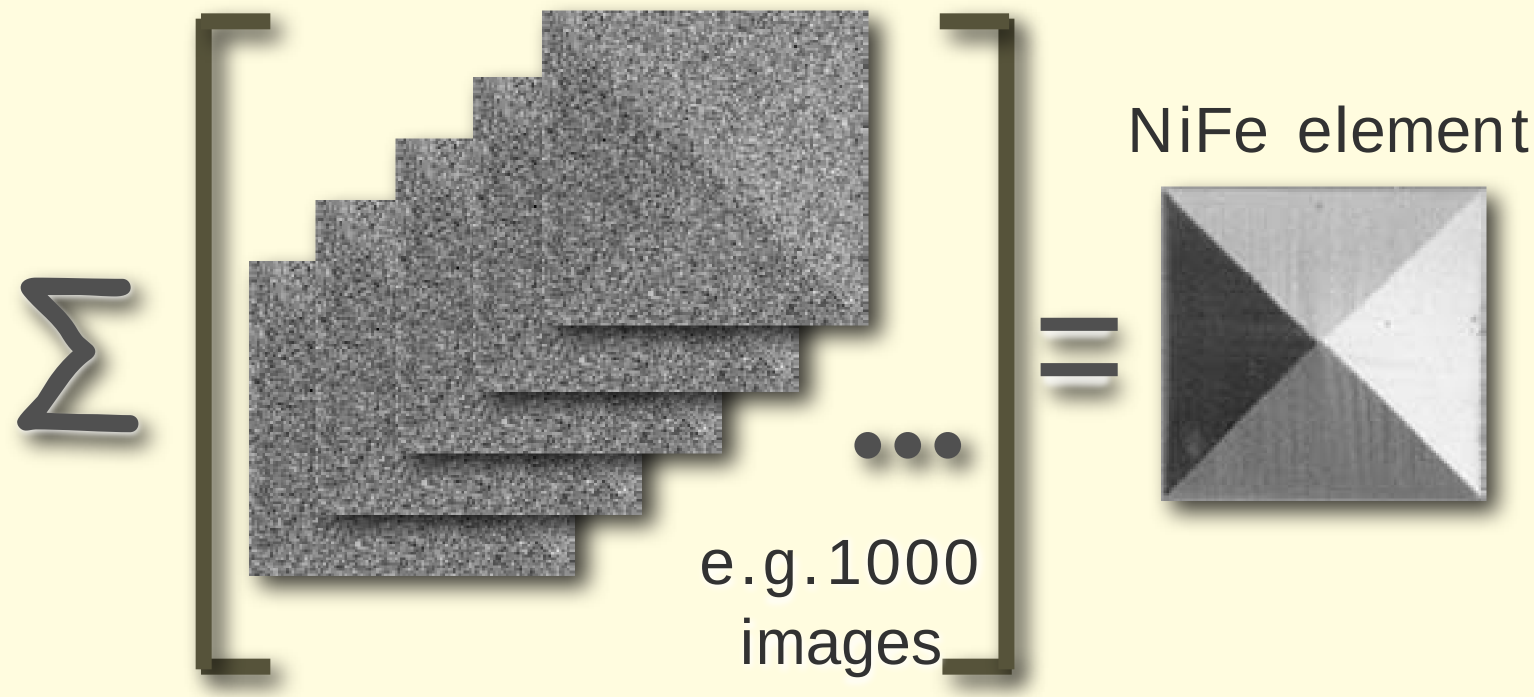

probing with defined time delay

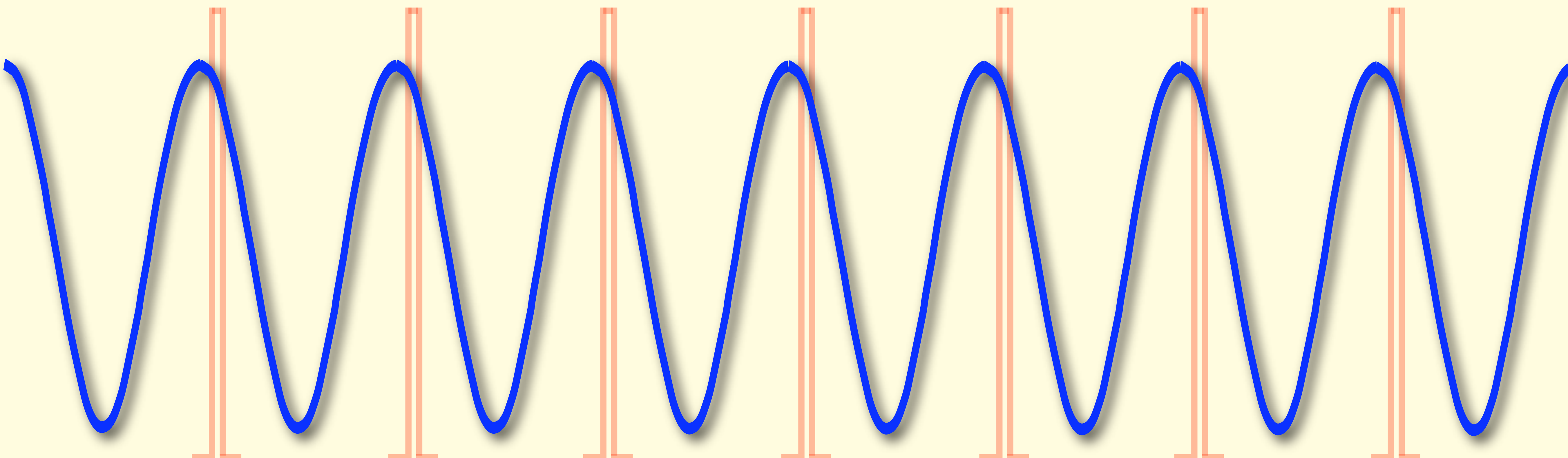

periodic magnetic field excitation

Time-resolved imaging: Stroboscopic mode

illumination intensity and repetition rate are limited

→ no single-shot imaging possible

→ accumulation of large number of independent events necessary (at fixed time delay)

→ requires repetitive magnetization processes !!

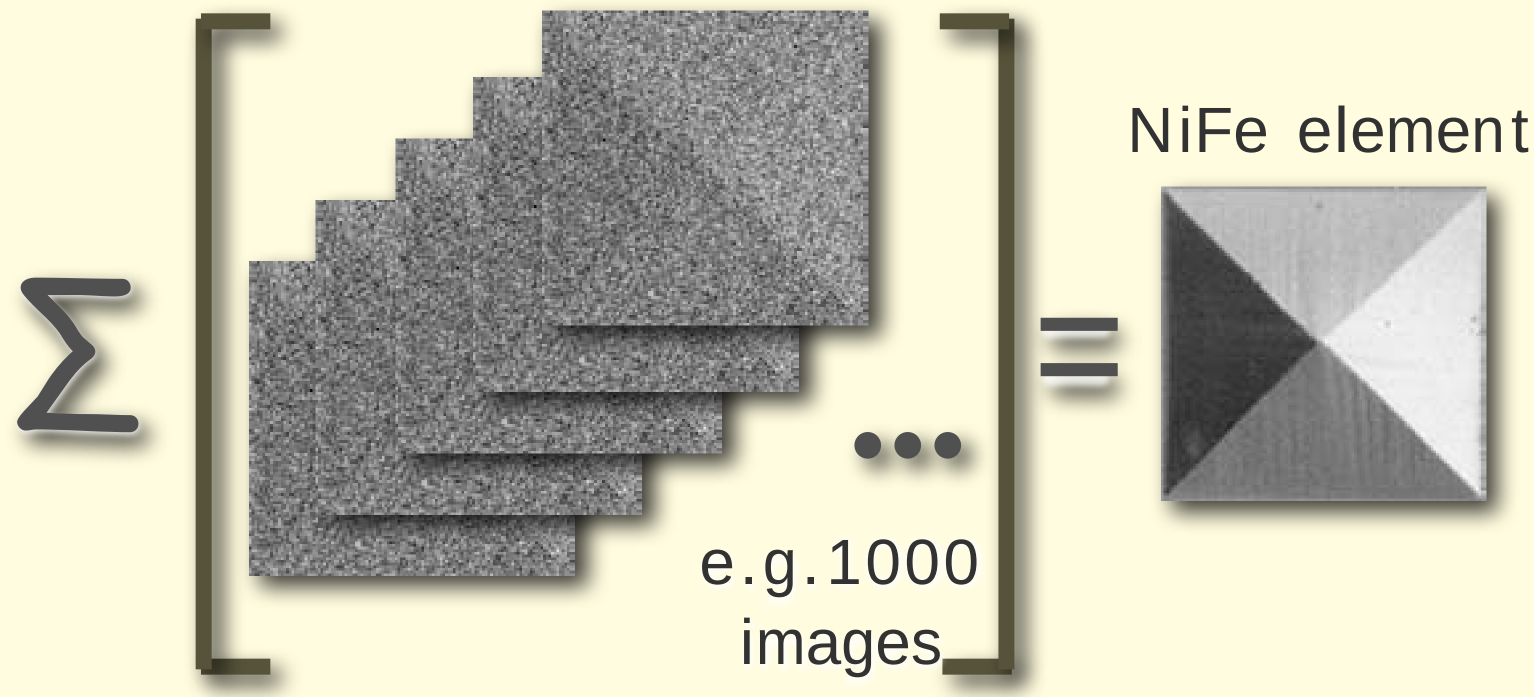

probing with defined time delay

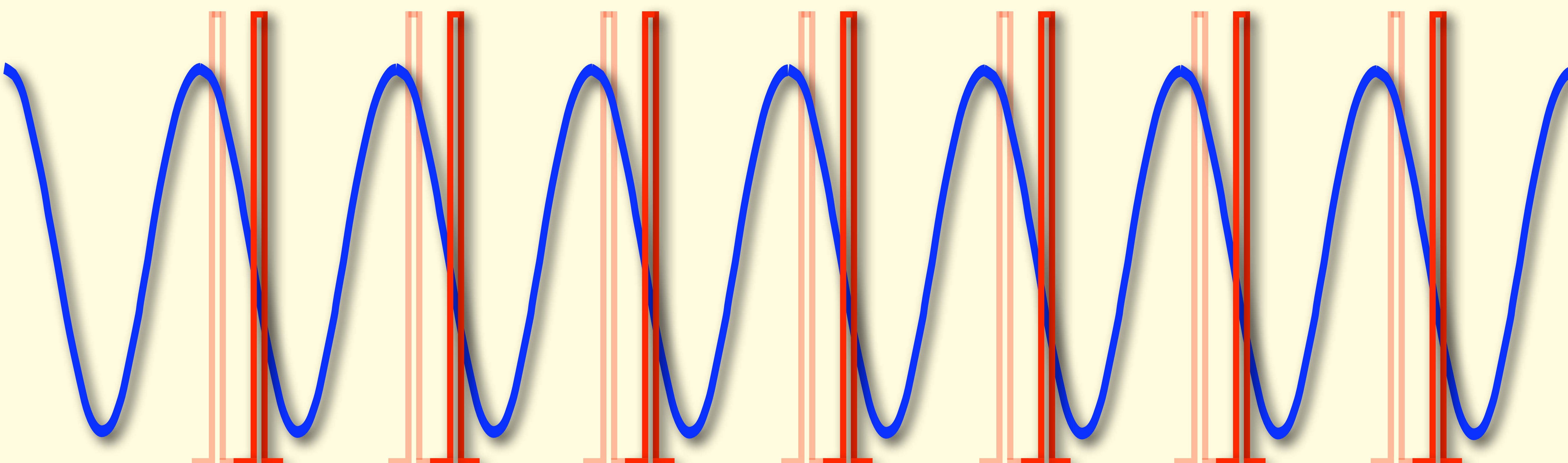

periodic magnetic field excitation

Low-frequency dynamics in amorphous ribbon

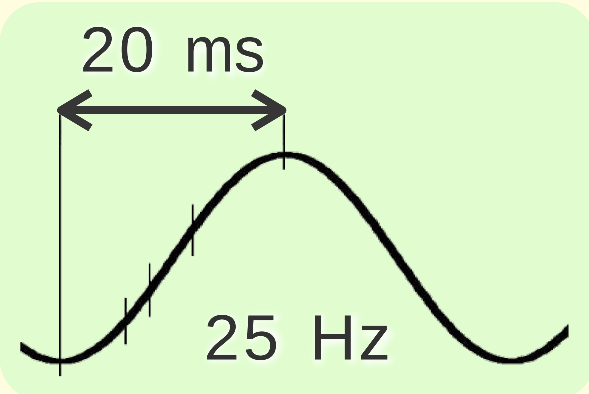

$Fe_{78}Si_9B_{13}$ amorphous ribbon, 20 μm thick

Stroboscopic images

$\Delta t = 0.4$ ms
800 images

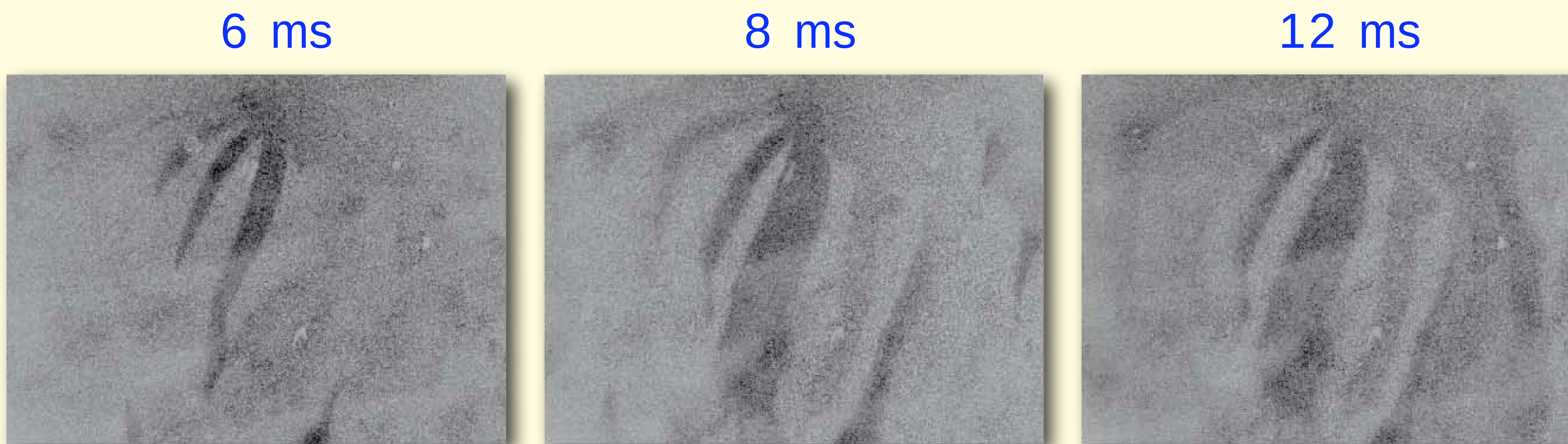

slowly changing field (< Hz)

H

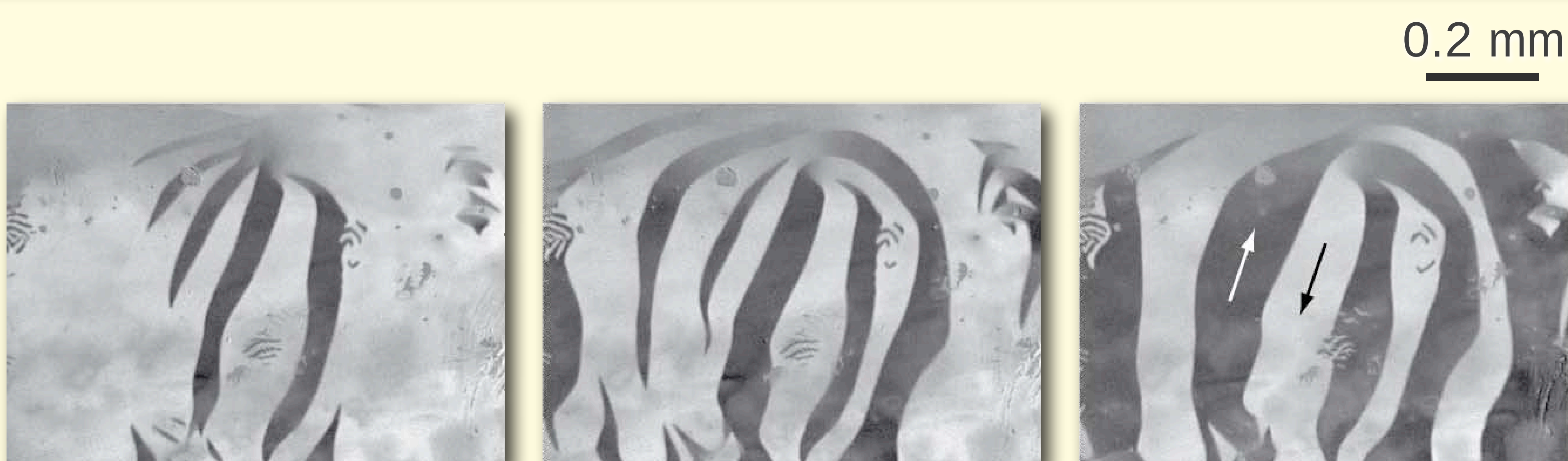

decreasing field

remanence

Stroboscopic wide-field microscopes

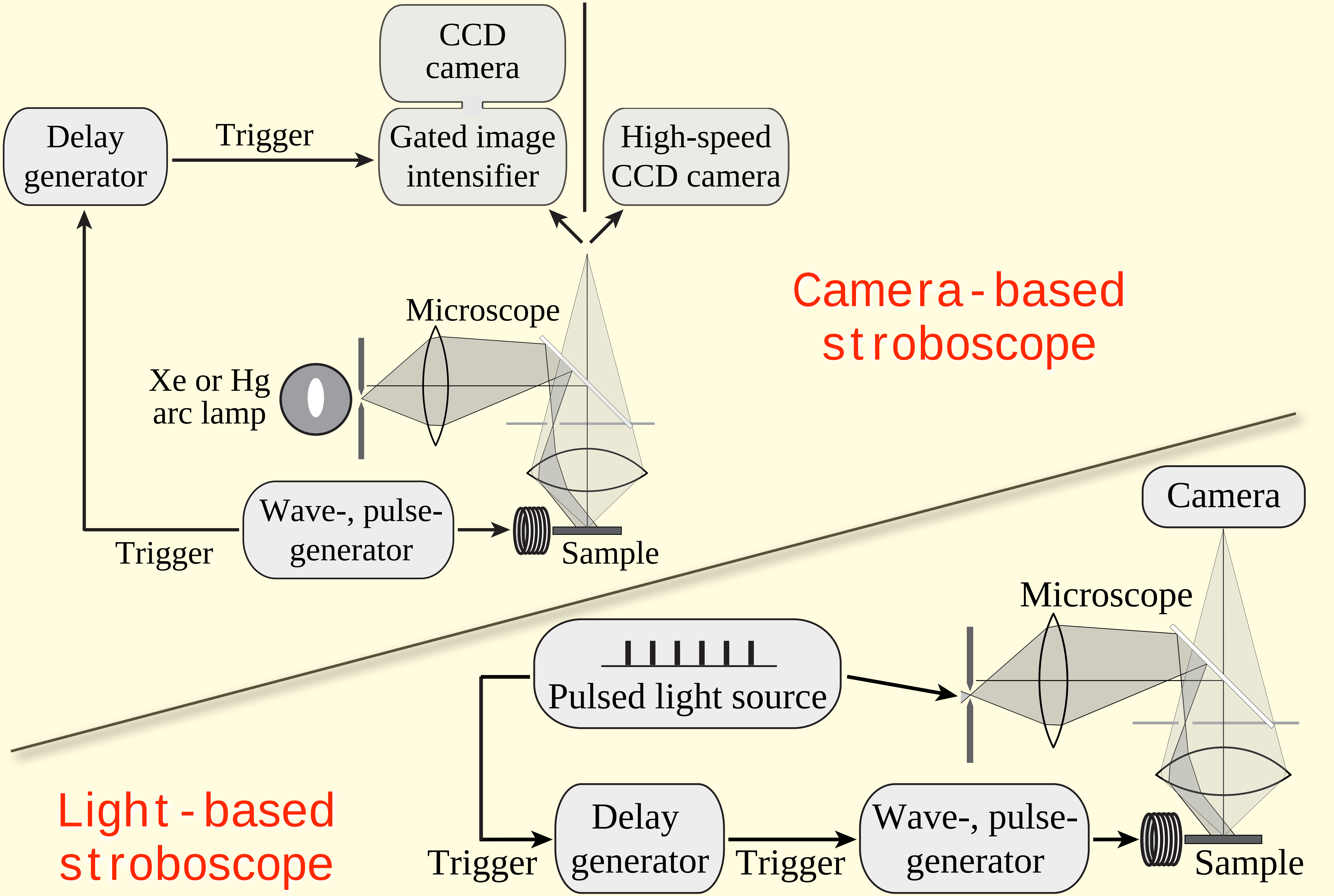

Nanocrystalline core with weak K_u

S. Flohrer et al., Acta Mat. (2006)

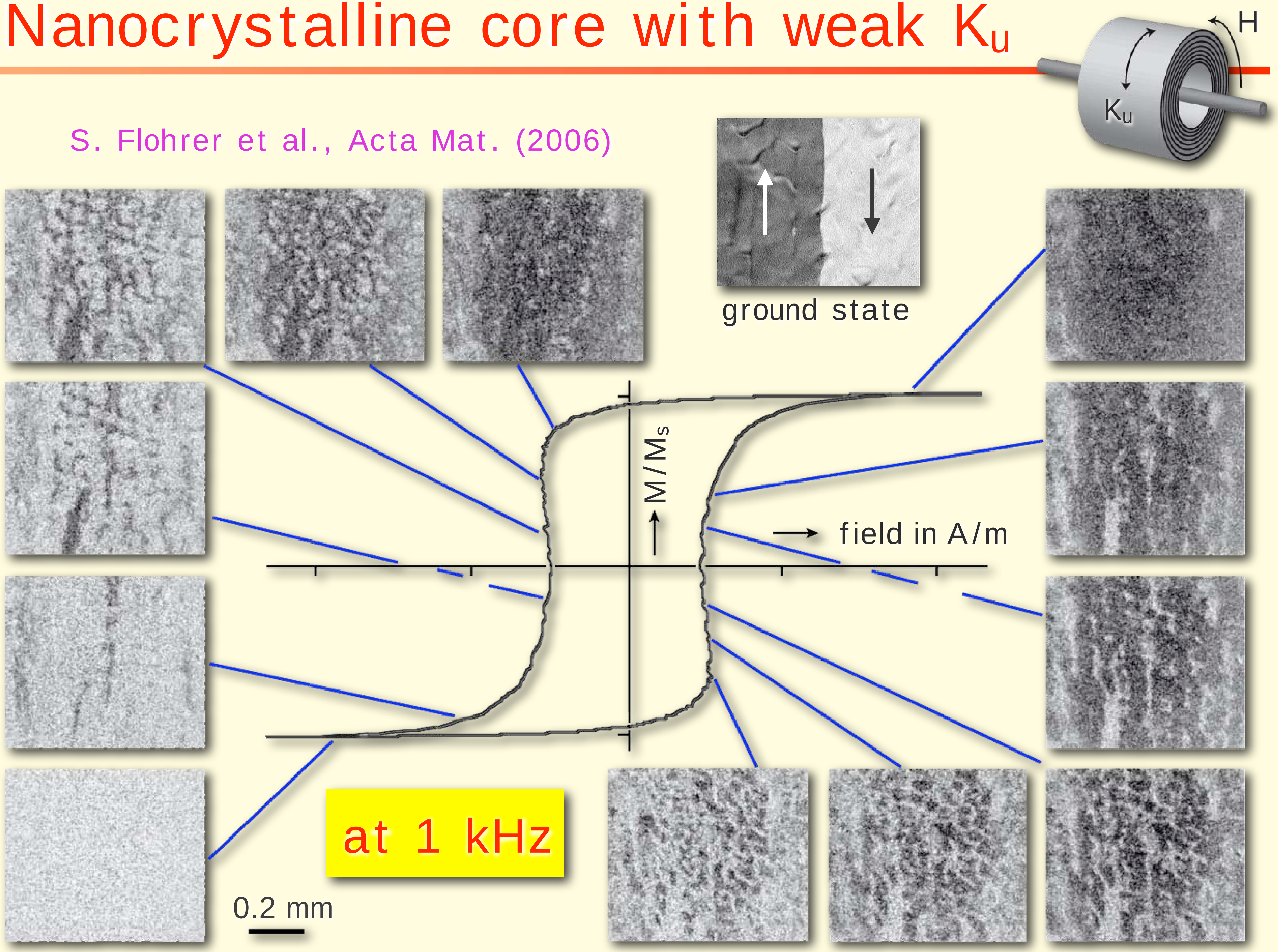

Summary: limitations of dynamics

Bulk metallic ferromagnets:
eddy current effects dominate

Thick metallic films (1 μm):
eddy currents dominate

Thin metallic films (<100 nm)
or non-conducting materials
eddy currents negligible

↓

spin precession
(for frequency in GHz regime)

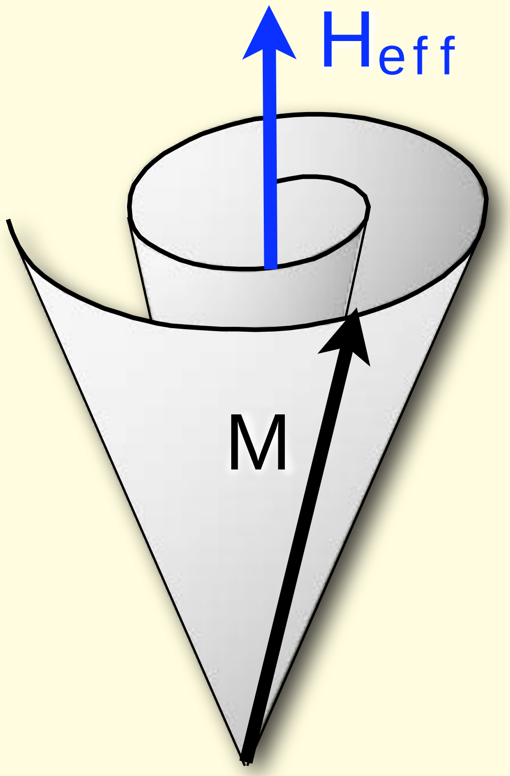

Landau-Lifshitz-Gilbert dynamics

$$\frac{dM}{dt} = \boxed{-\gamma_0 [M \times H_{eff}]} + \boxed{\frac{\alpha}{M_s} [M \times \frac{dM}{dt}]}$$

magnetic moment
↓
angular momentum
↓
gyrotropic reaction

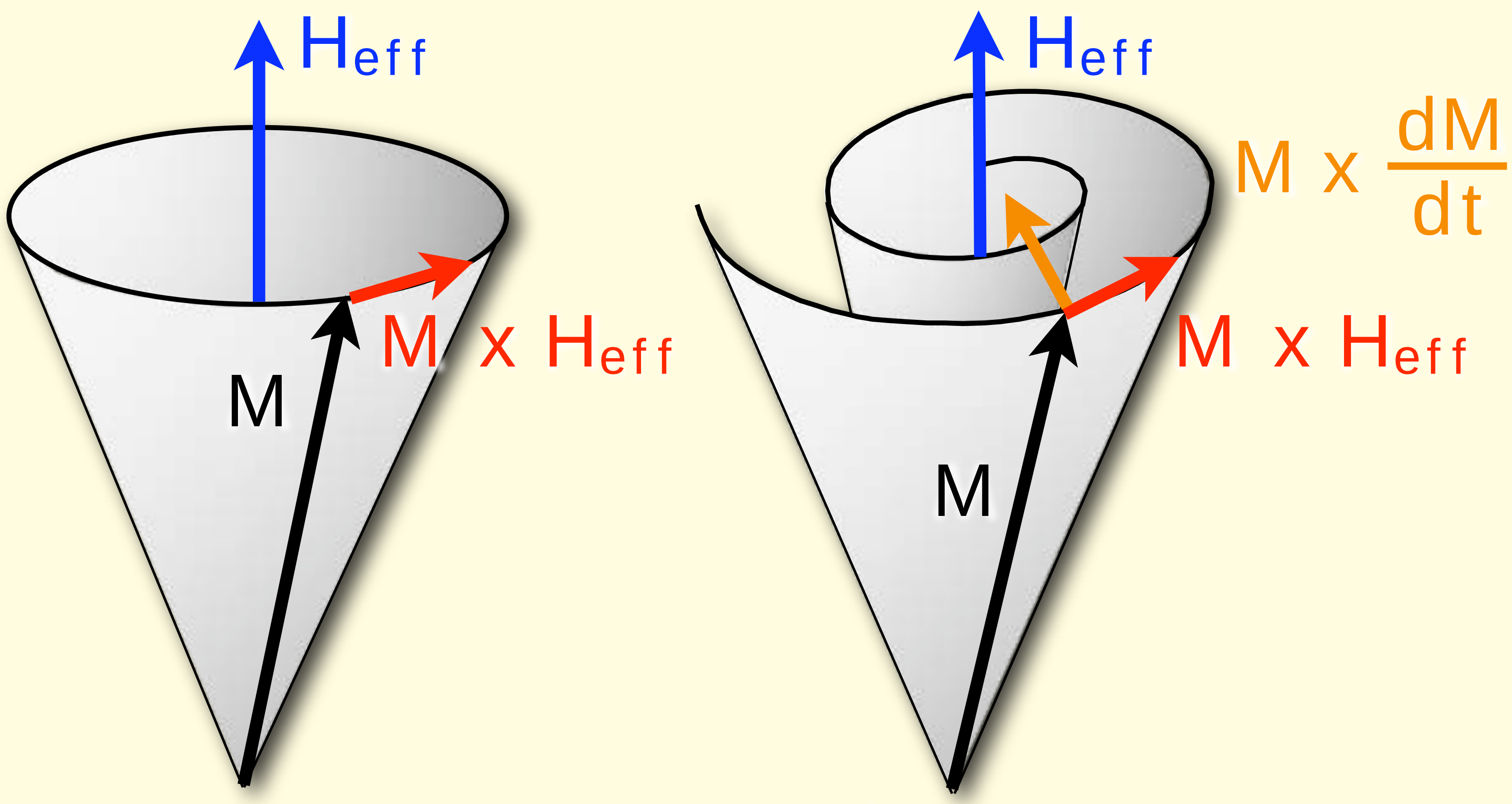

precession relaxation

H_{eff} : acting magnetic field (embedding pulse field)

α : damping parameter

γ_0 : gyromagnetic ratio

Permalloy element (40 x 40 μm^2, 50 nm thick)

static

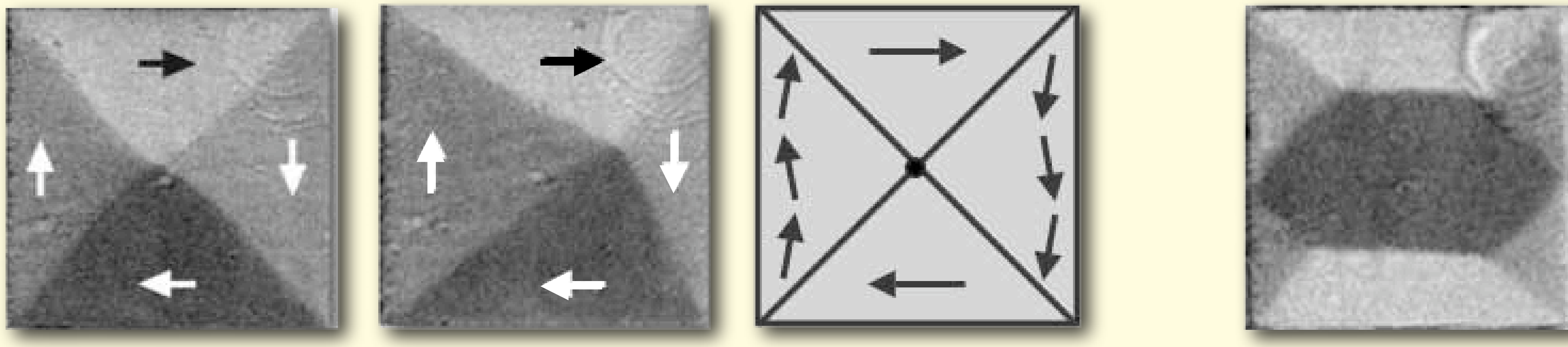

no field | ↑ field | ripple in hard-axis domains | ↔ anisotropy

dynamic

0 ns | 0.28 ns | 0.38 ns | 0.64 ns | 0.93 ns | 15.76 ns

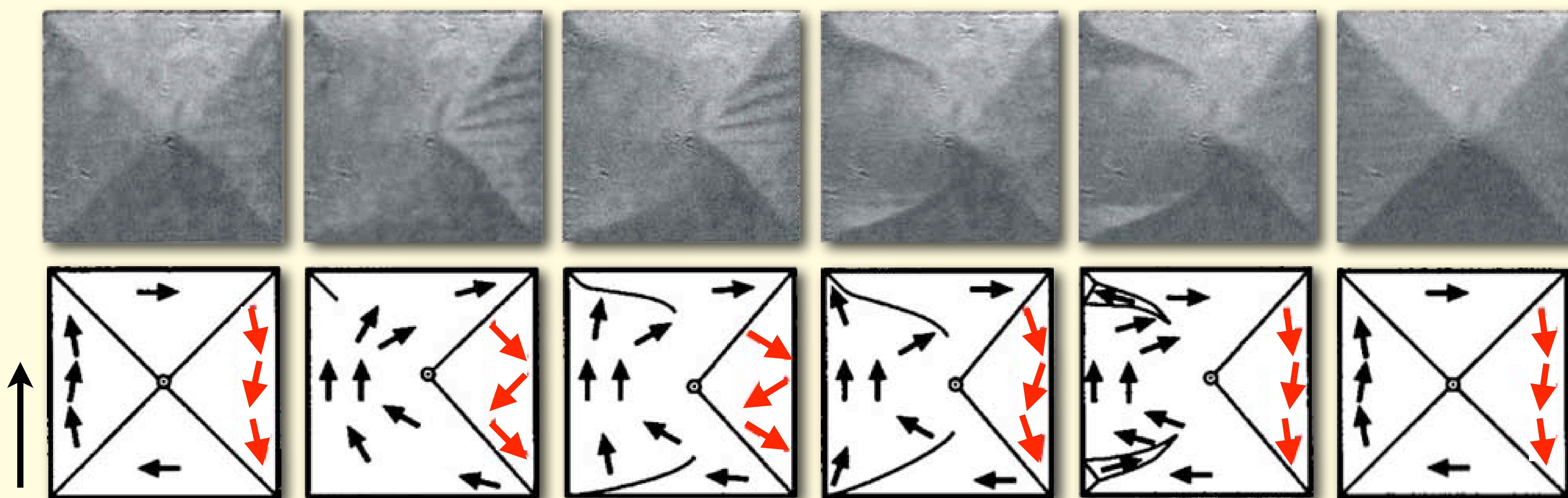

$\boldsymbol{H}_{\text{pulse}}$

A. Neudert et al., Phys. Rev. B 71, 134405 (2005)

Permalloy element (40 x 40 μm^2, 50 nm thick)

static

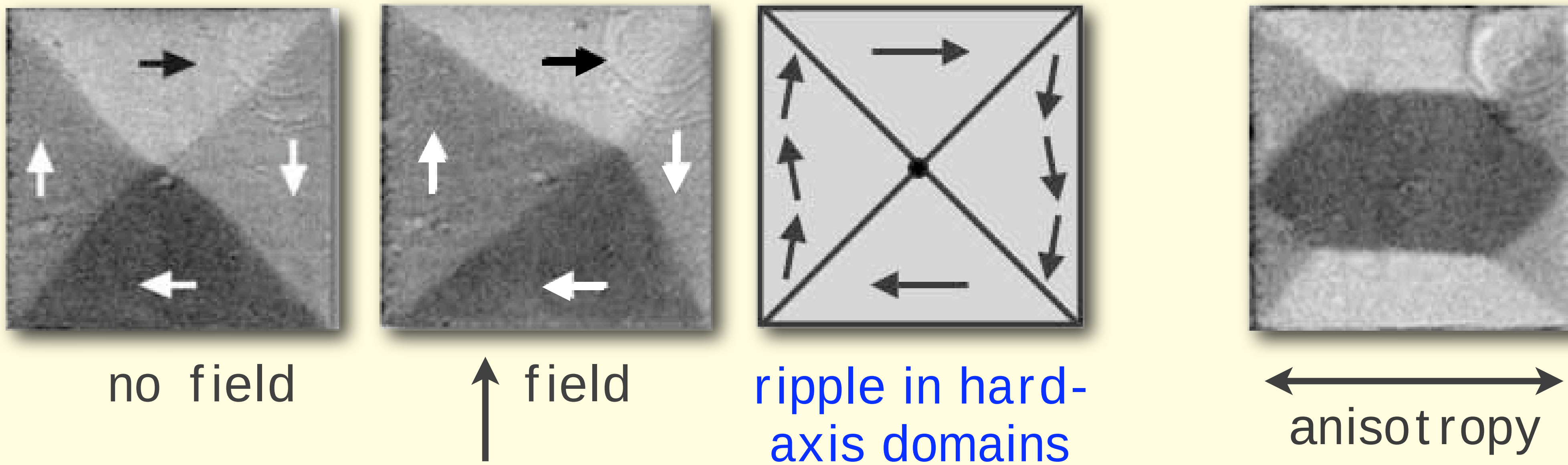

dynamic

0 ns

15.76 ns

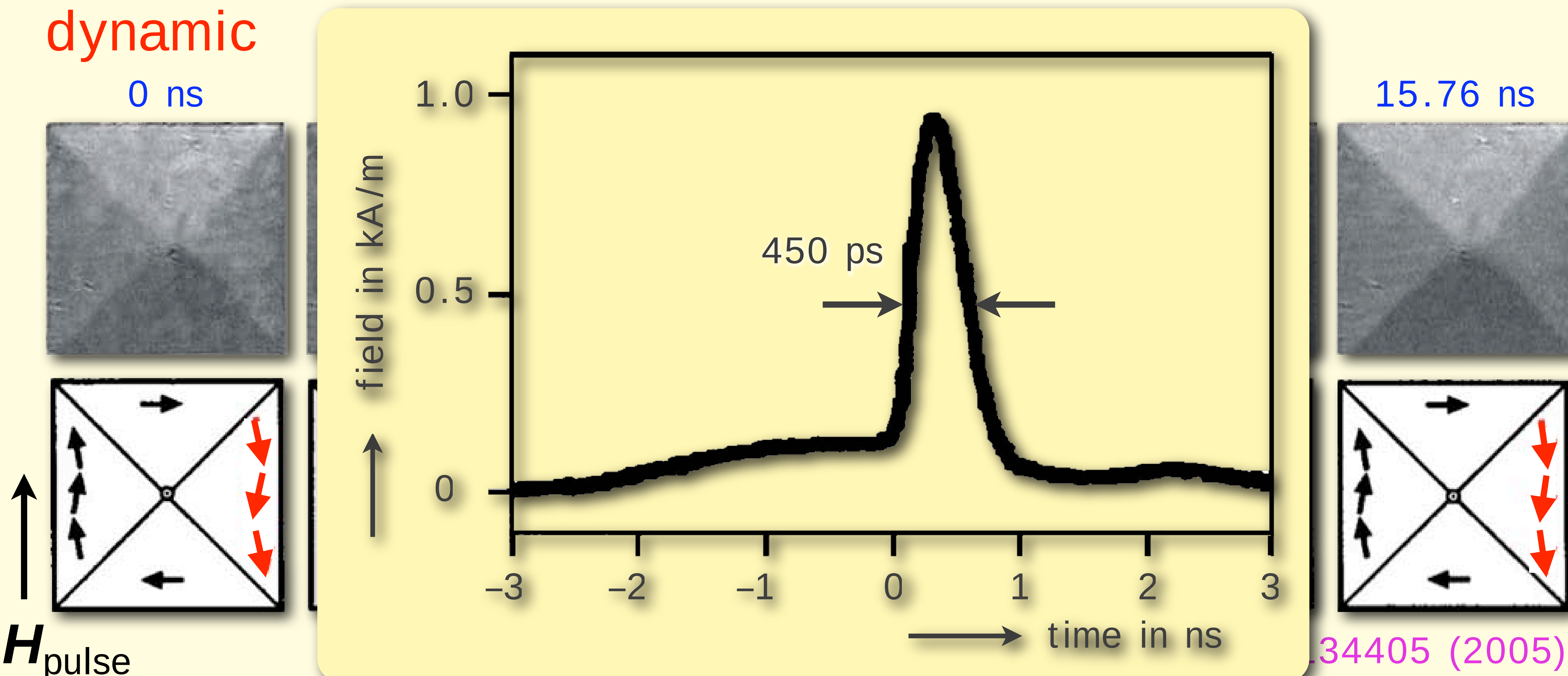

.34405 (2005)

Permalloy element (40 x 40 μm^2, 50 nm thick)

static

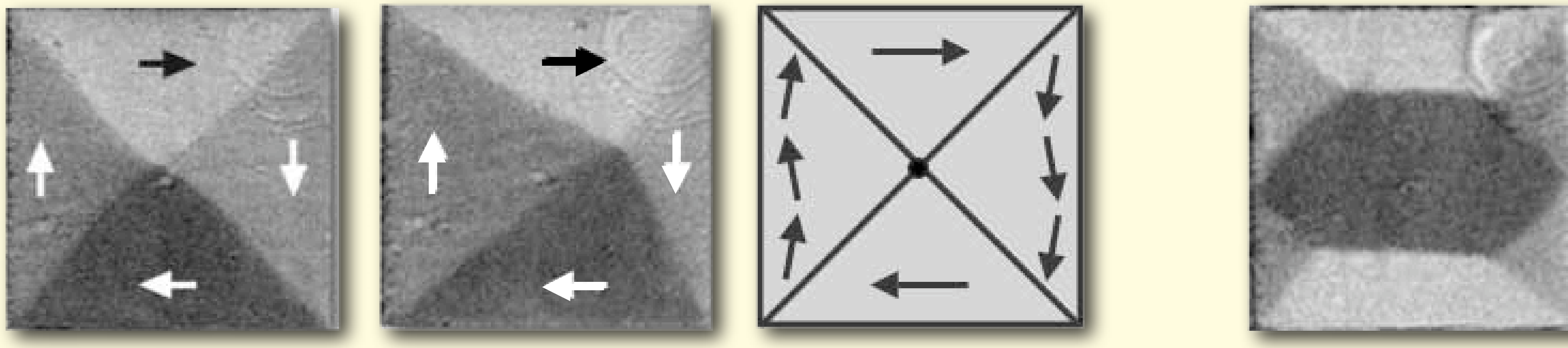

no field

field

ripple in hard-axis domains

anisotropy

dynamic

0 ns | 0.28 ns | 0.38 ns | 0.64 ns | 0.93 ns | 15.76 ns

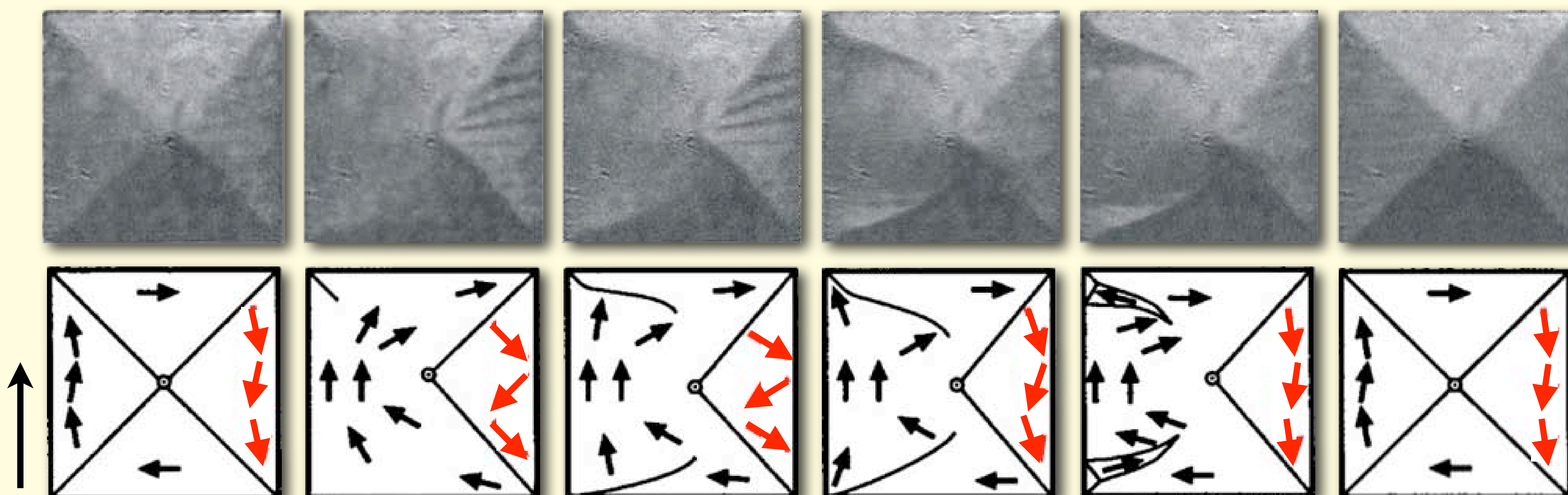

$\boldsymbol{H}_{pulse}$

A. Neudert et al., Phys. Rev. B 71, 134405 (2005)

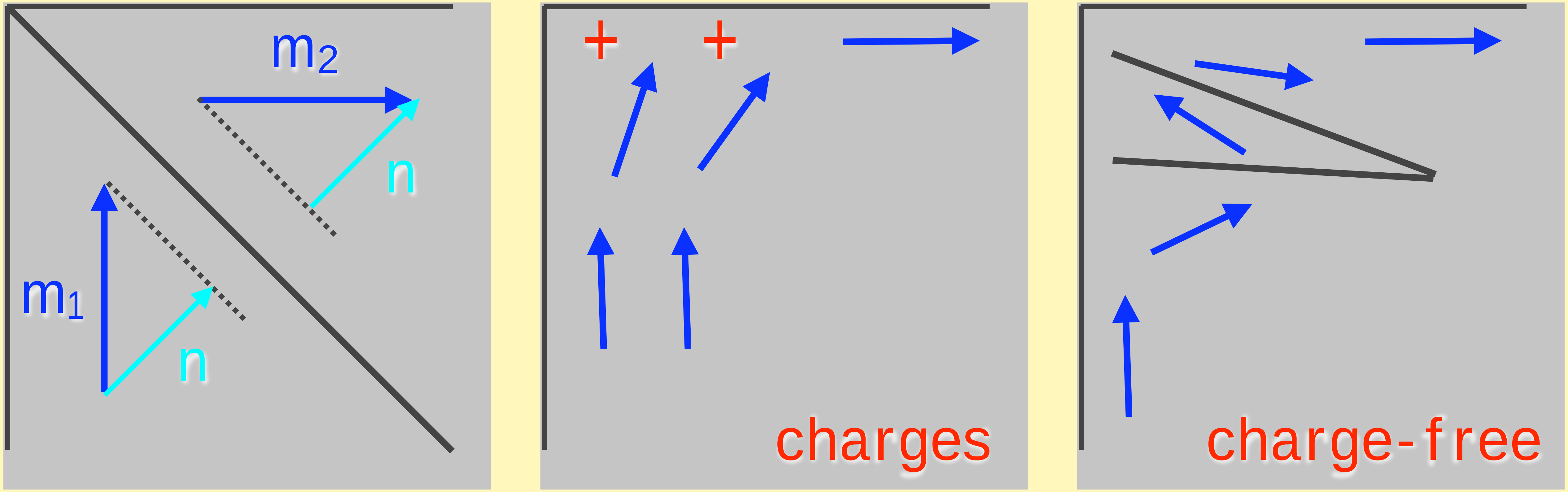

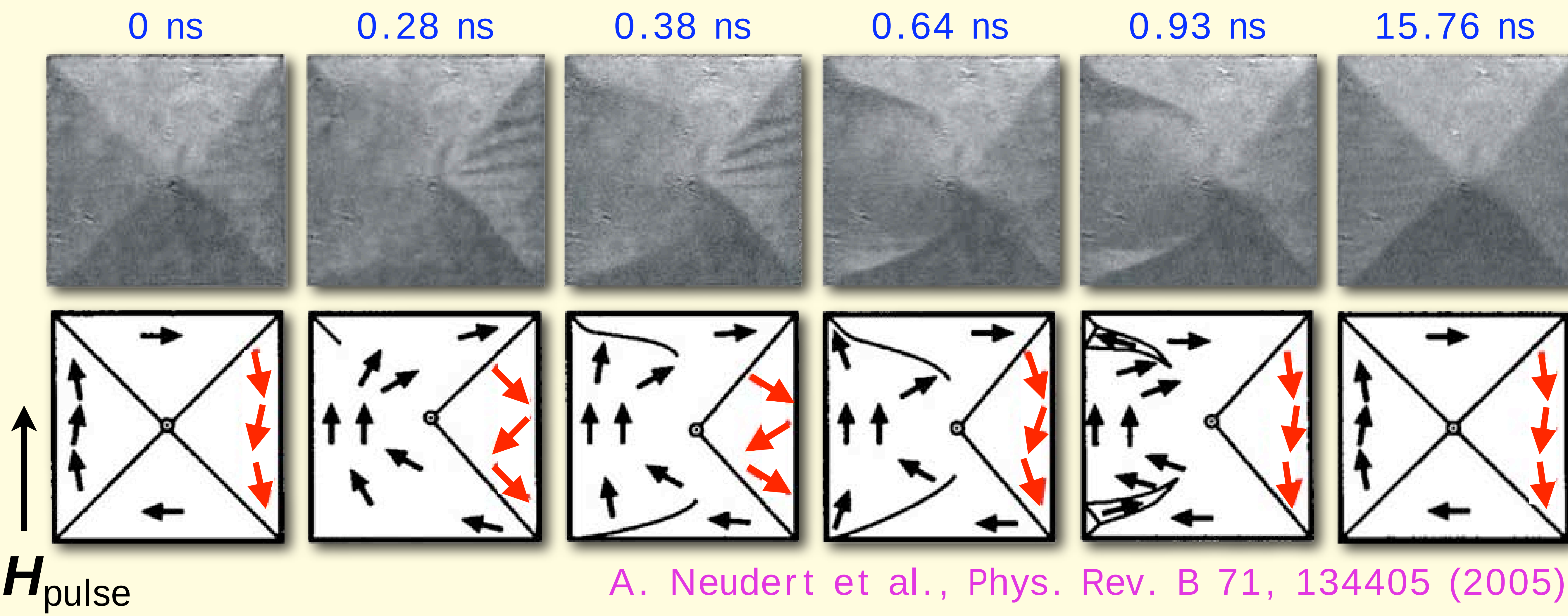

A. Neudert et al., Phys. Rev. B 71, 134405 (2005)

Permalloy element (40 x 40 μm^2, 50 nm thick)

static

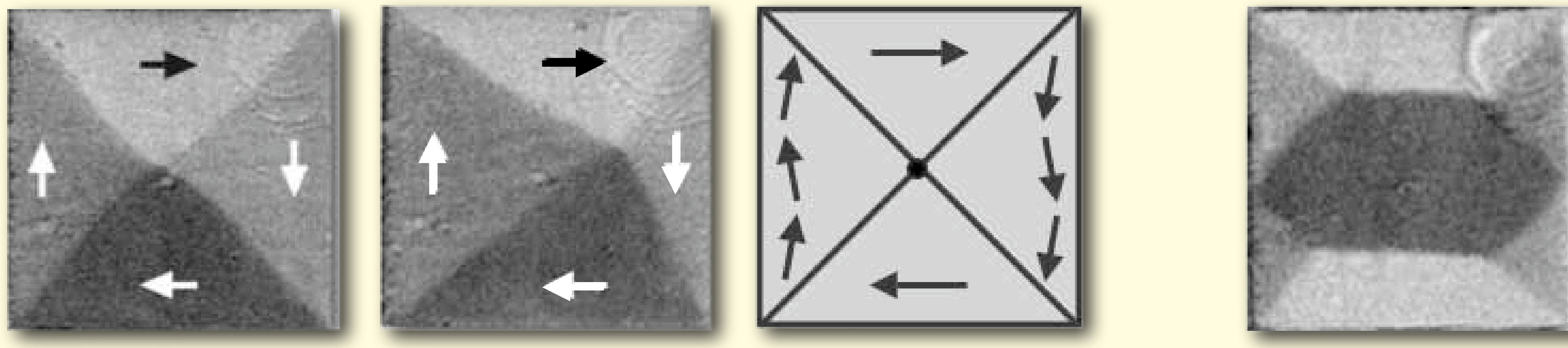

no field

field

ripple in hard-axis domains

anisotropy

dynamic

0 ns | 0.28 ns | 0.38 ns | 0.64 ns | 0.93 ns | 15.76 ns

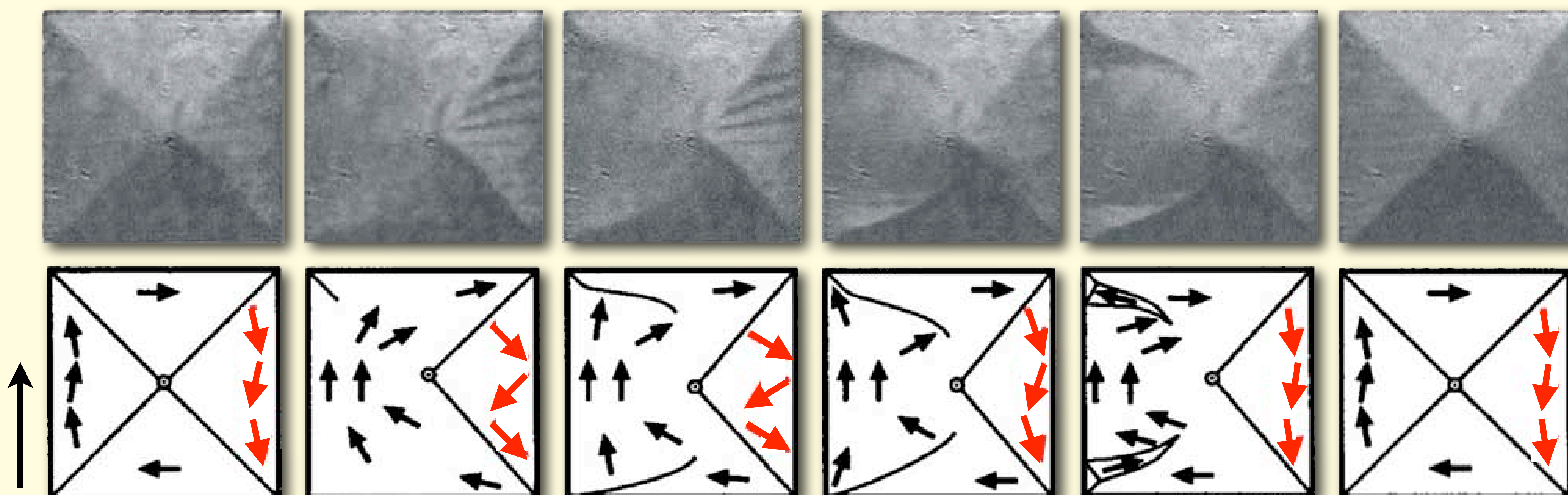

$\boldsymbol{H}_{\text{pulse}}$

A. Neudert et al., Phys. Rev. B 71, 134405 (2005)

Kerr microscopy: drawbacks

Small objects?

Resolution of optical microscopy (E. Abbe 1840 - 1905)

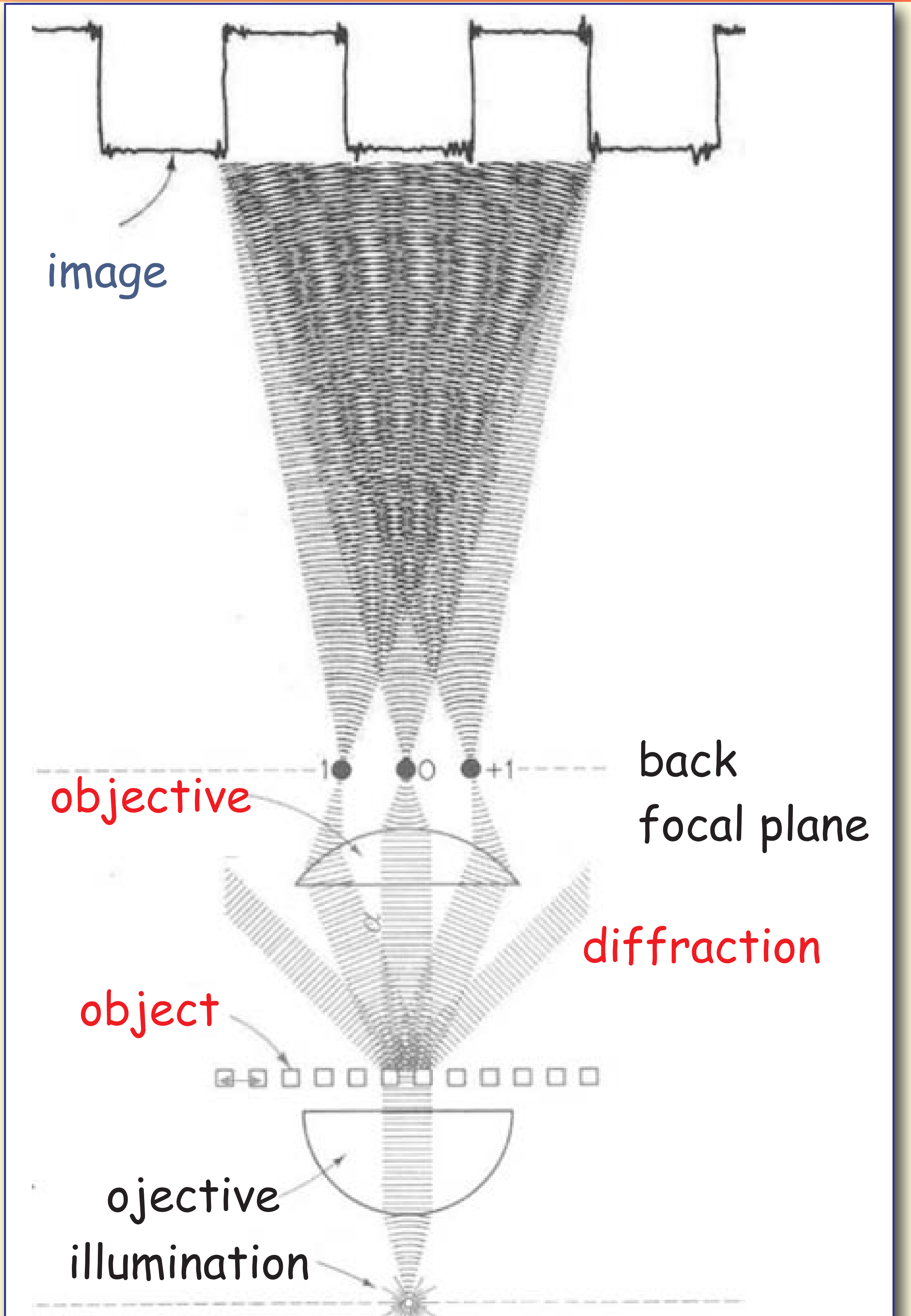

resolution determined by constructive interference

diffraction limited image formation

Rayleigh equation: $d = \dfrac{0.5\,\lambda}{NA}$

d = separation between particles, still allowing to see them

λ = wavelength

NA = numerical aperture of objective

$NA = n \sin\theta$

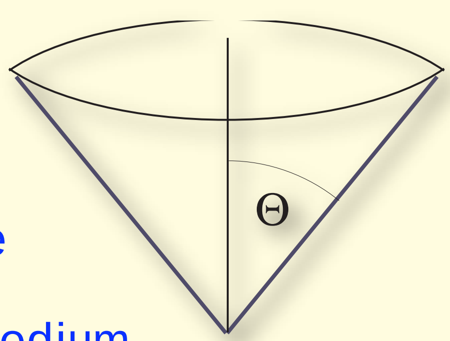

θ = half the cone angle of light accepted by objective

n = referaction index of medium between sample and objective

↓

best around 200 nm

About resolution

Co elements (sample: Axel Carl)

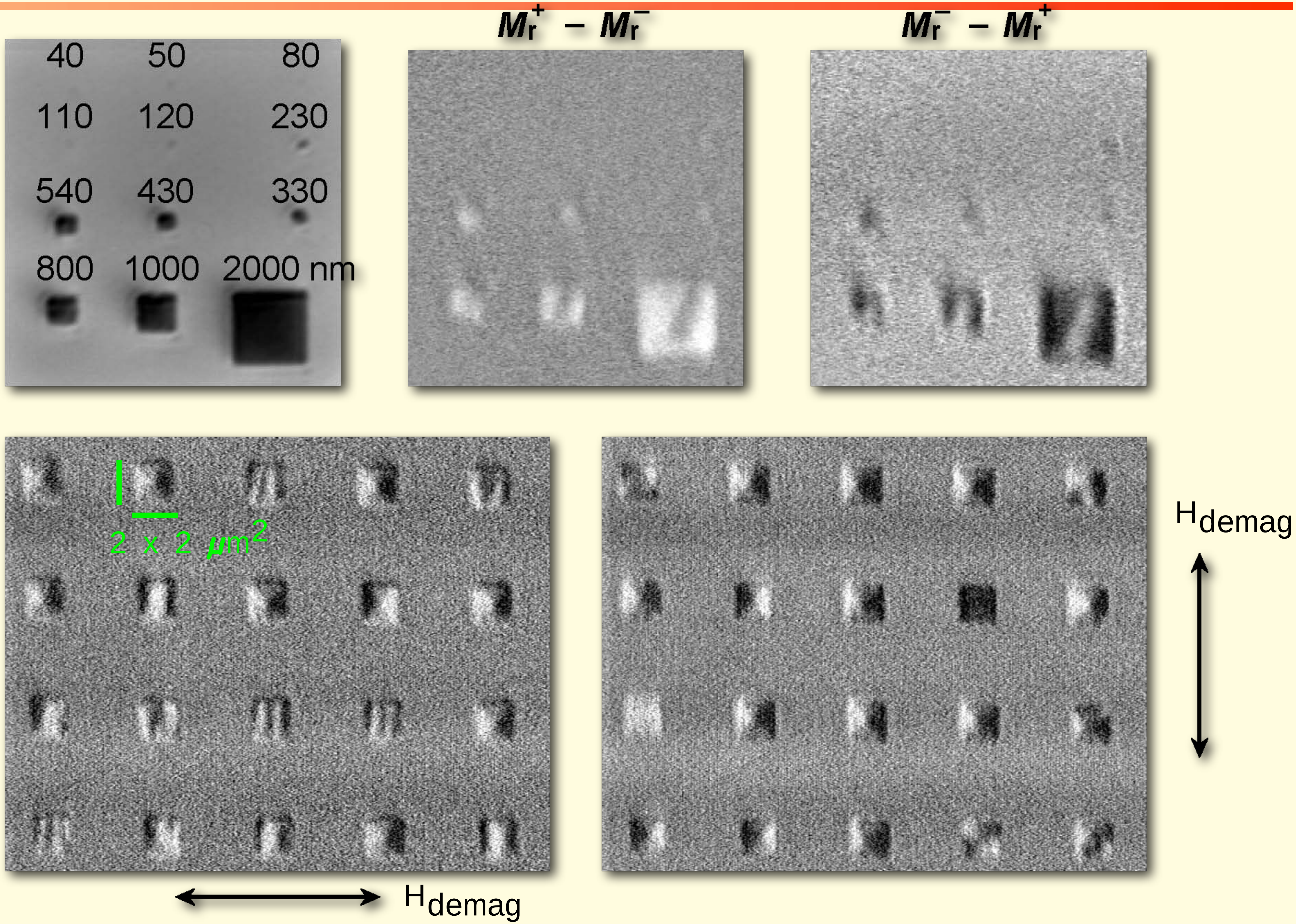

Magnetization reversal of Co-wires

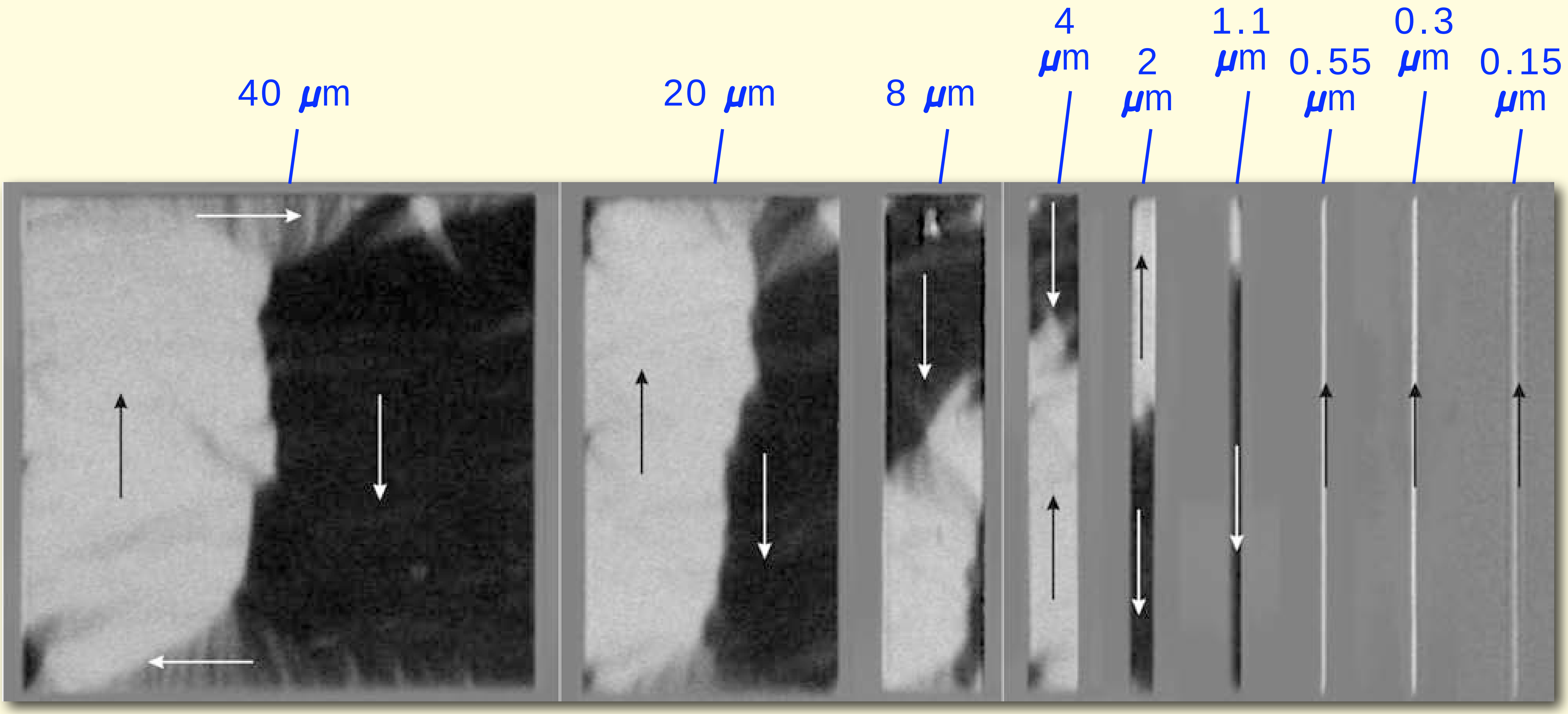

courtesy J.McCord (IFW Dresden),
sample: B. Hausmanns (Duisburg)

Magnetization reversal of Co-wires

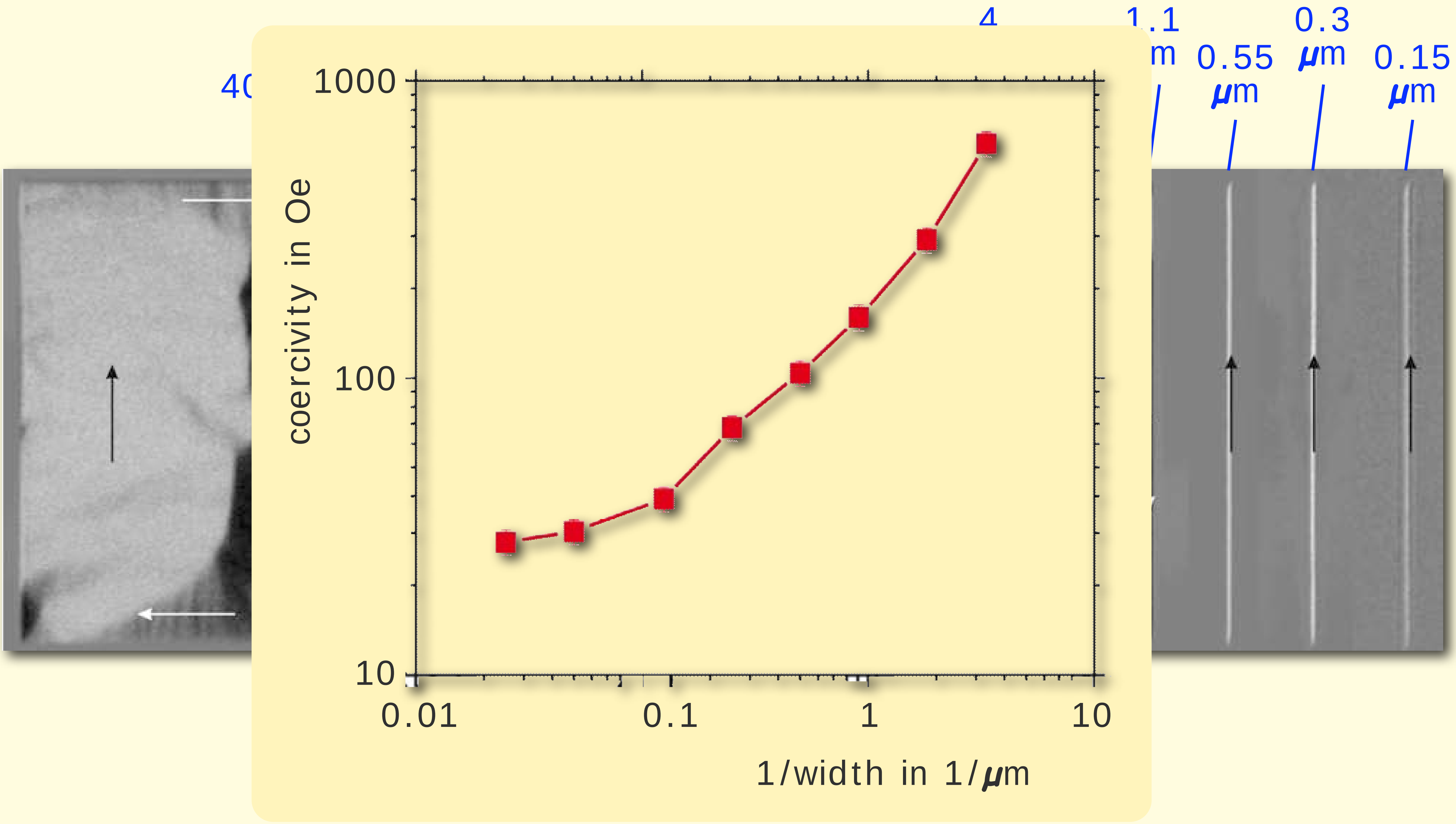

courtesy J.McCord (IFW Dresden),
sample: B. Hausmanns (Duisburg)

Sub-micrometer imaging

NiFe wires, 0.5 μm wide, 20 nm thick

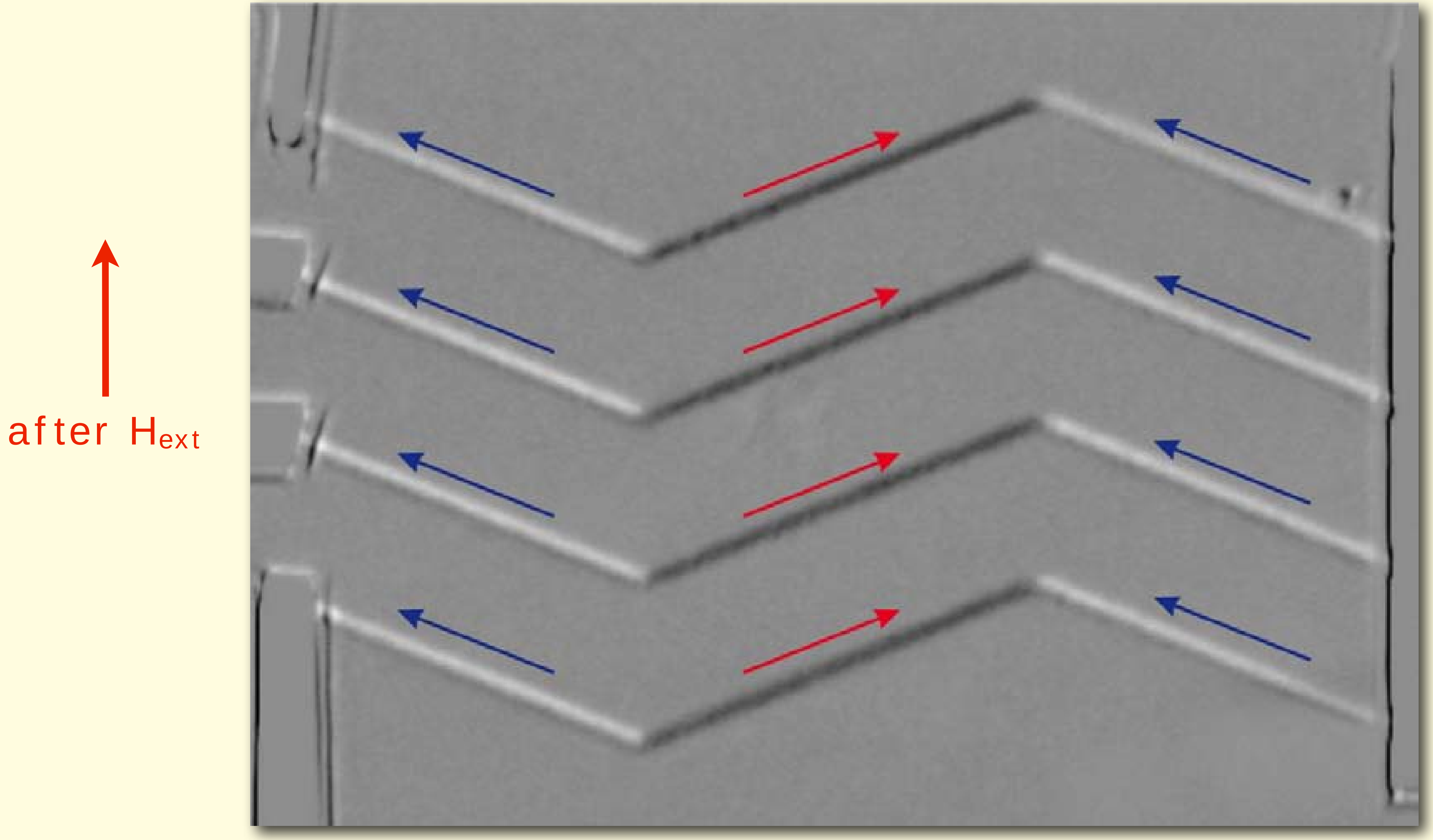

together with: M. Kläui, T.Moore, U. Rüdiger (Konstanz),
J.McCord (IFW Dresden),

Sub-micrometer imaging

NiFe wires, 0.5 μm wide, 20 nm thick

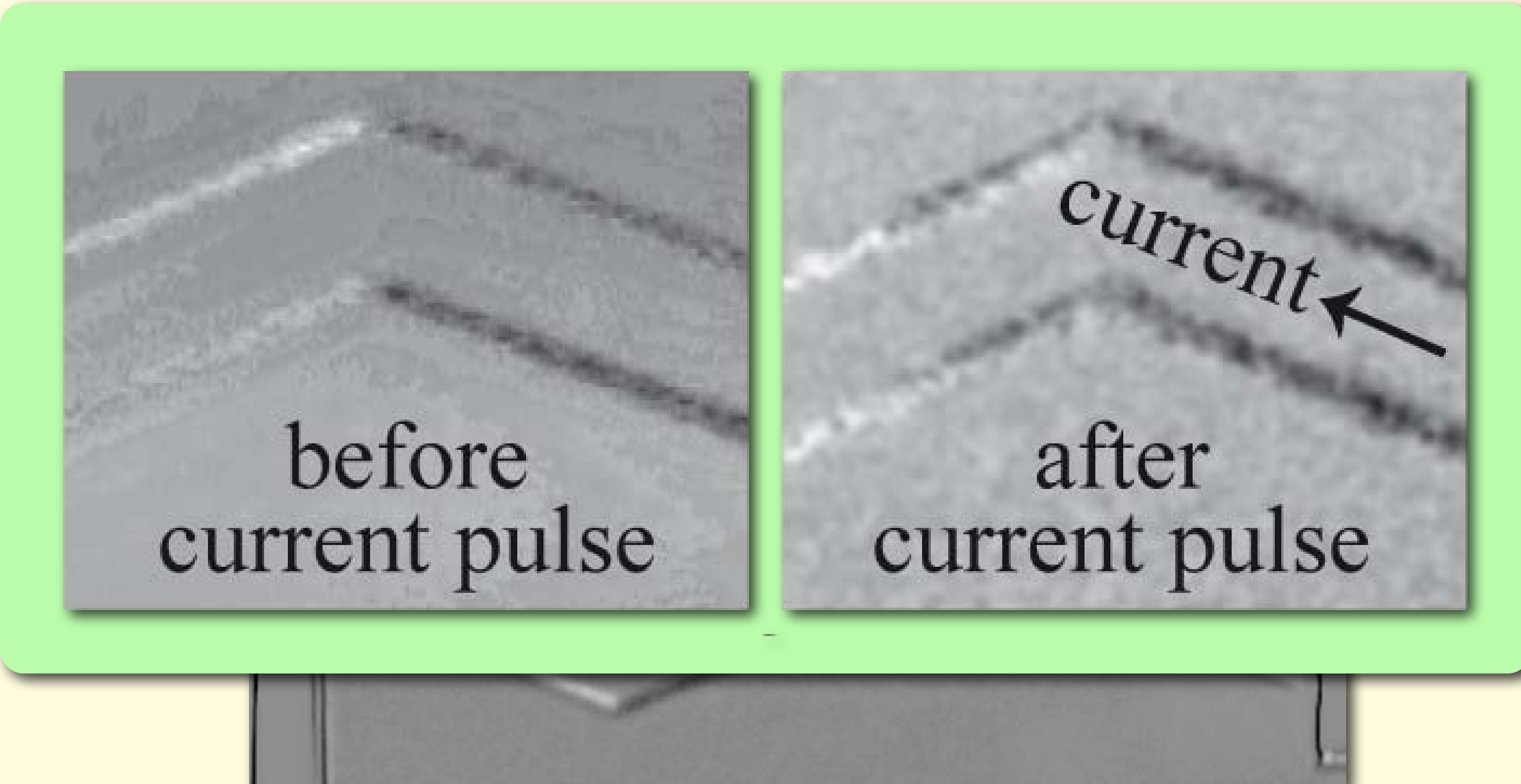

together with: M. Kläui, T.Moore, U. Rüdiger (Konstanz),
J.McCord (IFW Dresden),

Some

Magneto-optics

Kerr effect: dielectric law

$$\boldsymbol{D} = \boldsymbol{\varepsilon}\,\boldsymbol{E} = \varepsilon \begin{pmatrix} 1 & -\mathrm{i}\,Q\,m_3 & \mathrm{i}\,Q\,m_2 \\ \mathrm{i}\,Q\,m_3 & 1 & -\mathrm{i}\,Q\,m_1 \\ -\mathrm{i}\,Q\,m_2 & \mathrm{i}\,Q\,m_1 & 1 \end{pmatrix} \boldsymbol{E}$$

$$= \varepsilon\,\boldsymbol{E} + \mathrm{i}\,\varepsilon\,Q\,\boldsymbol{m} \times \boldsymbol{E}$$

E : electric vector of light wave

D : dielectric displacement vector
(= vector of light after reflection)

m_i: components of magnetization vector (cubic crystal)

$\boldsymbol{\varepsilon}$: dielectric tensor

Q : material constant ($\sim M_s$, complex, determines strength of rotation)

Kerr effect: dielectric law

$$\boldsymbol{D} = \boldsymbol{\varepsilon}\boldsymbol{E} = \varepsilon \begin{pmatrix} 1 & -\mathrm{i}\,Q\,m_3 & \mathrm{i}\,Q\,m_2 \\ \mathrm{i}\,Q\,m_3 & 1 & -\mathrm{i}\,Q\,m_1 \\ -\mathrm{i}\,Q\,m_2 & \mathrm{i}\,Q\,m_1 & 1 \end{pmatrix} \boldsymbol{E}$$

$$= \varepsilon\boldsymbol{E} + \mathrm{i}\,\varepsilon\,Q\,\boldsymbol{m}\times\boldsymbol{E} \longrightarrow \text{concept of Lorentz force}$$

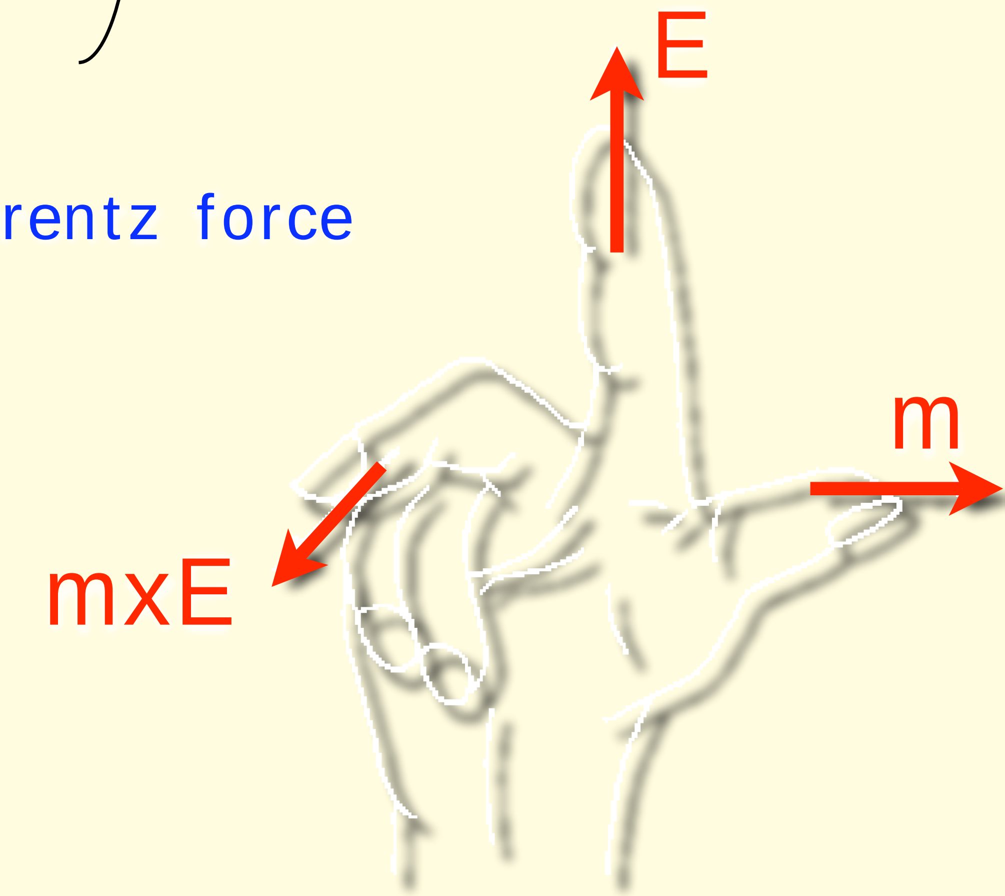

E : electric vector of light wave

D : dielectric displacement vector (= vector of light after reflection)

m_i: components of magnetization vector (cubic crystal)

$\boldsymbol{\varepsilon}$: dielectric tensor

Q : material constant (~M_s , complex, determines strength of rotation)

Kerr effect: Lorentz concept

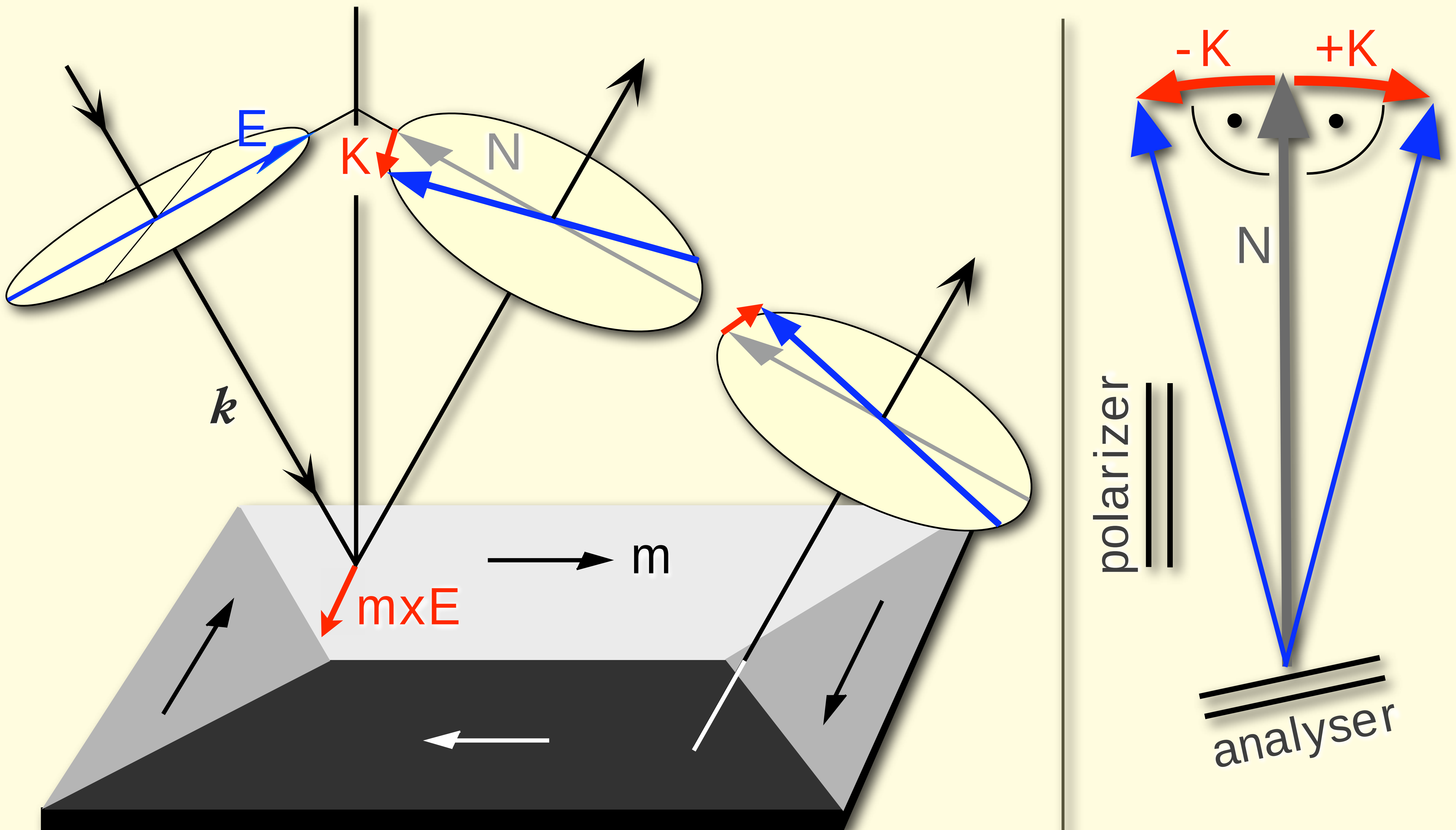

Kerr rotation = K/N

Compensator

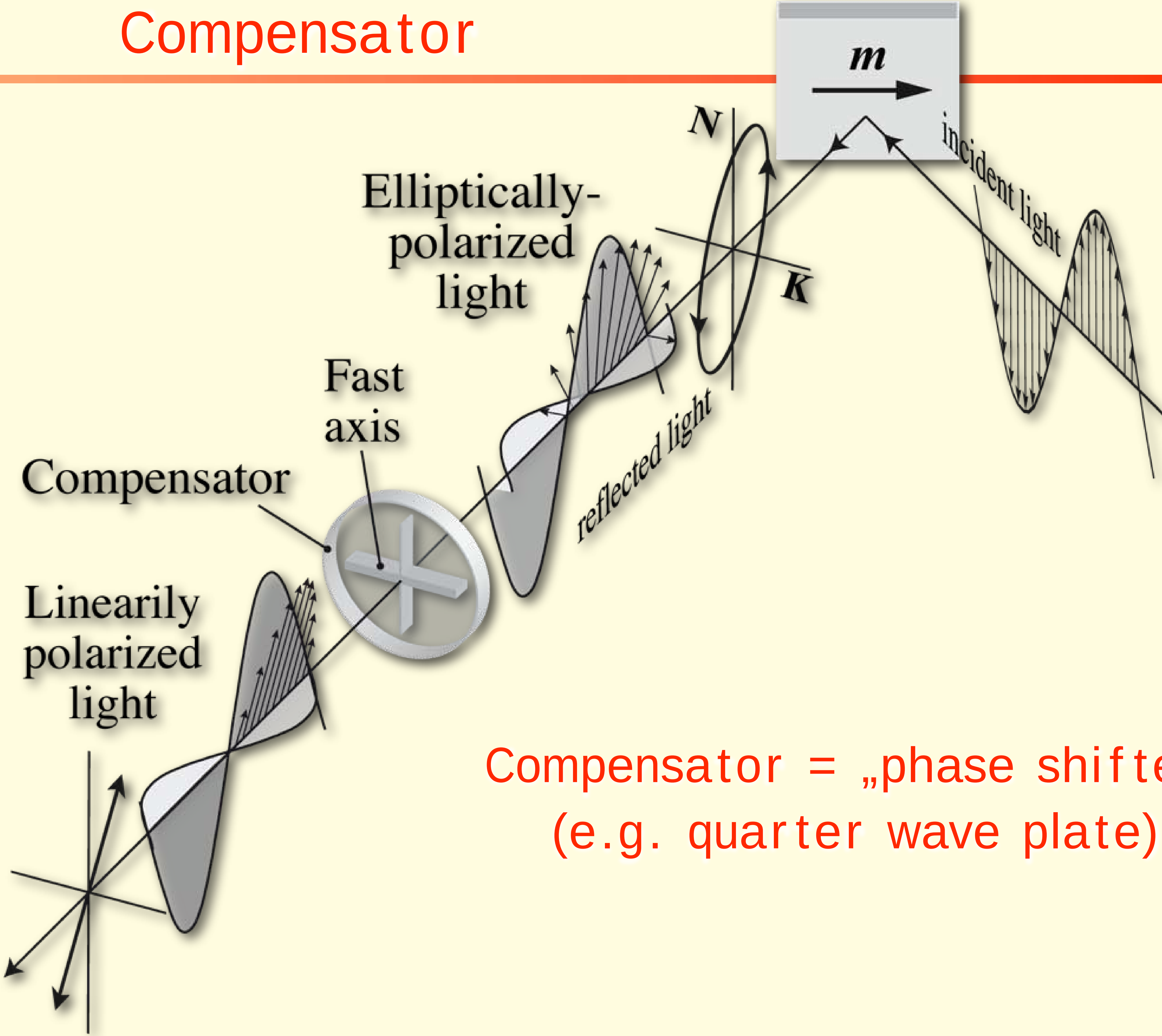

Compensator = „phase shifter“
(e.g. quarter wave plate)

Depth selective Kerr microscopy

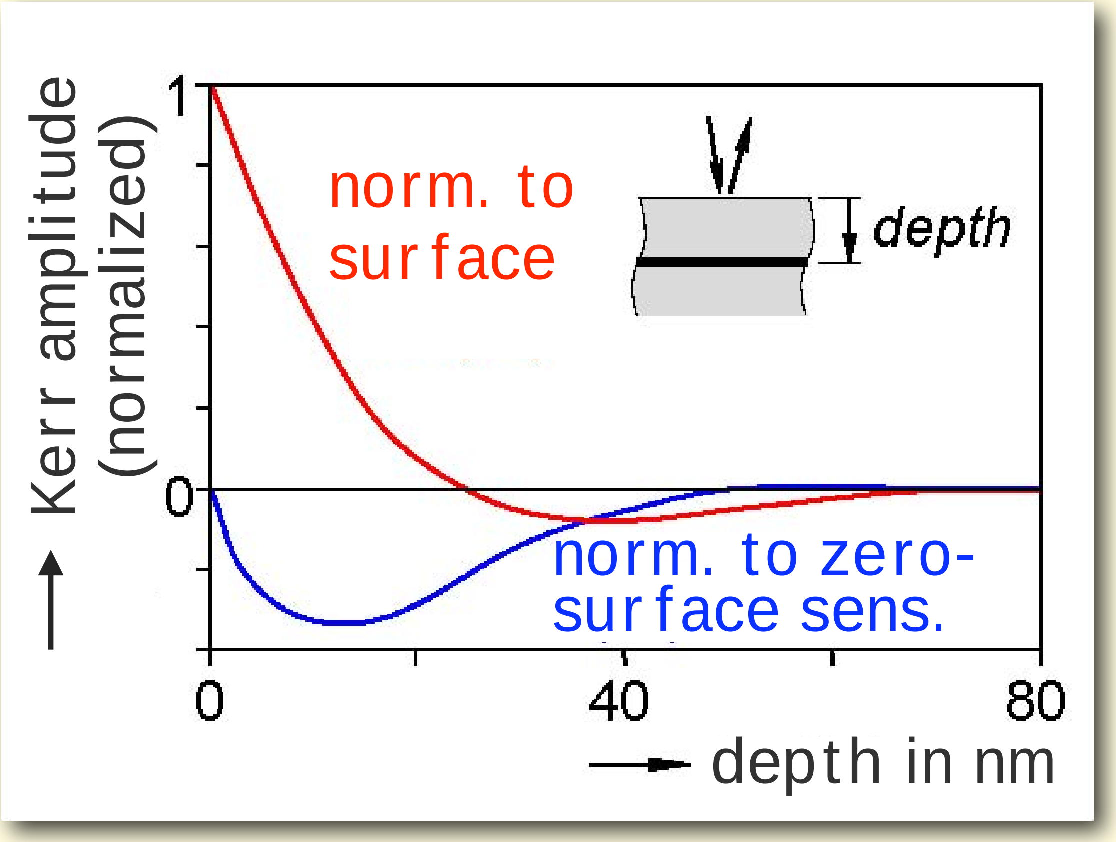

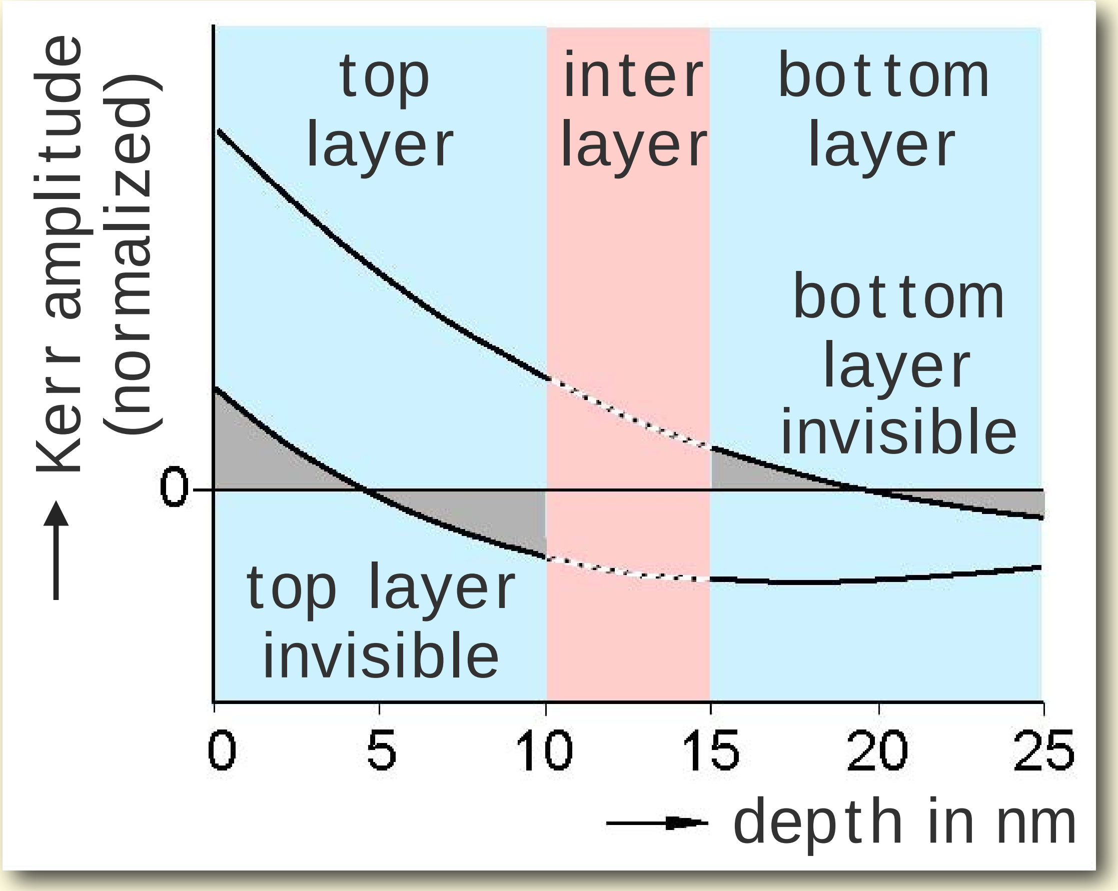

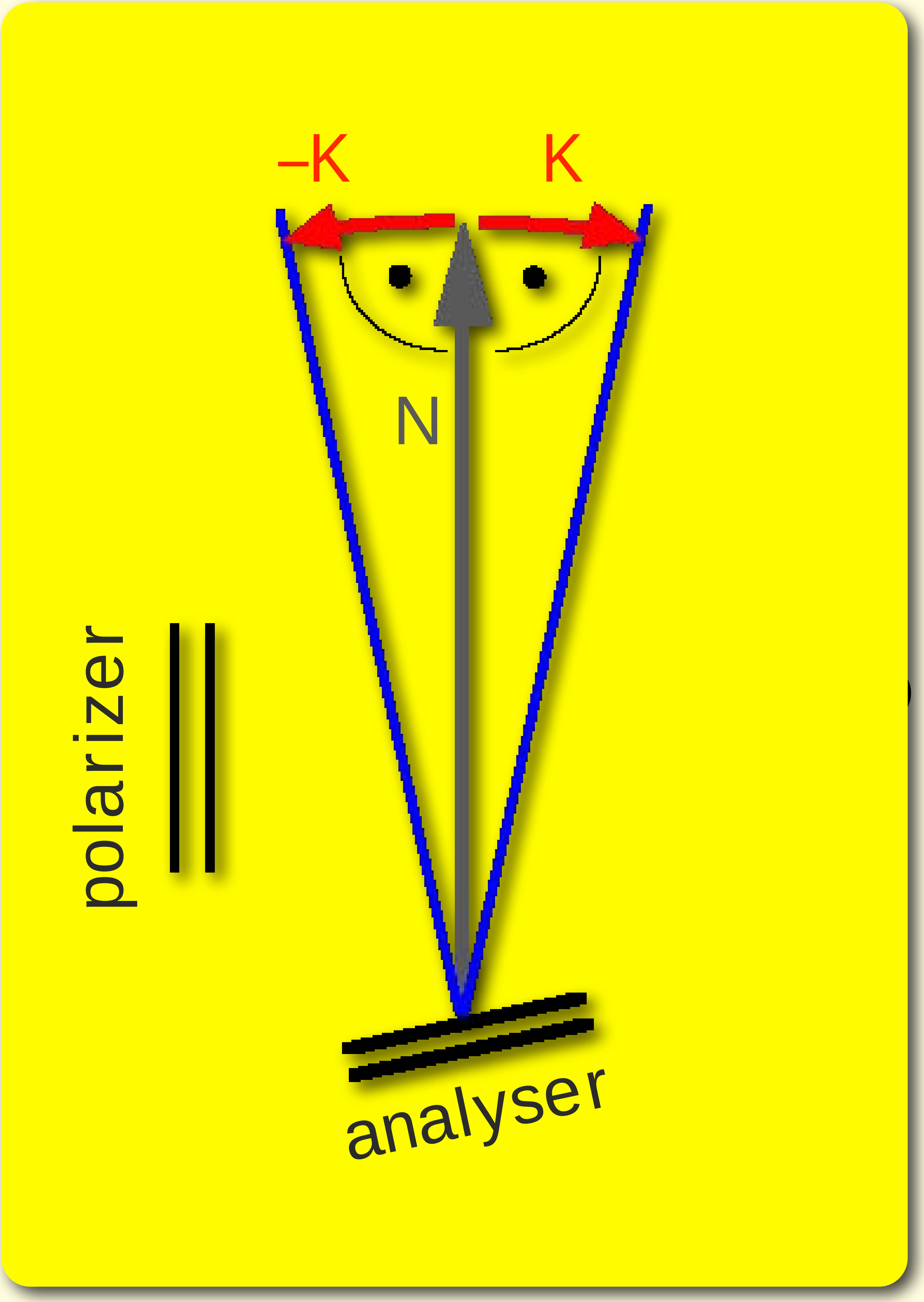

Depth selective Kerr microscopy

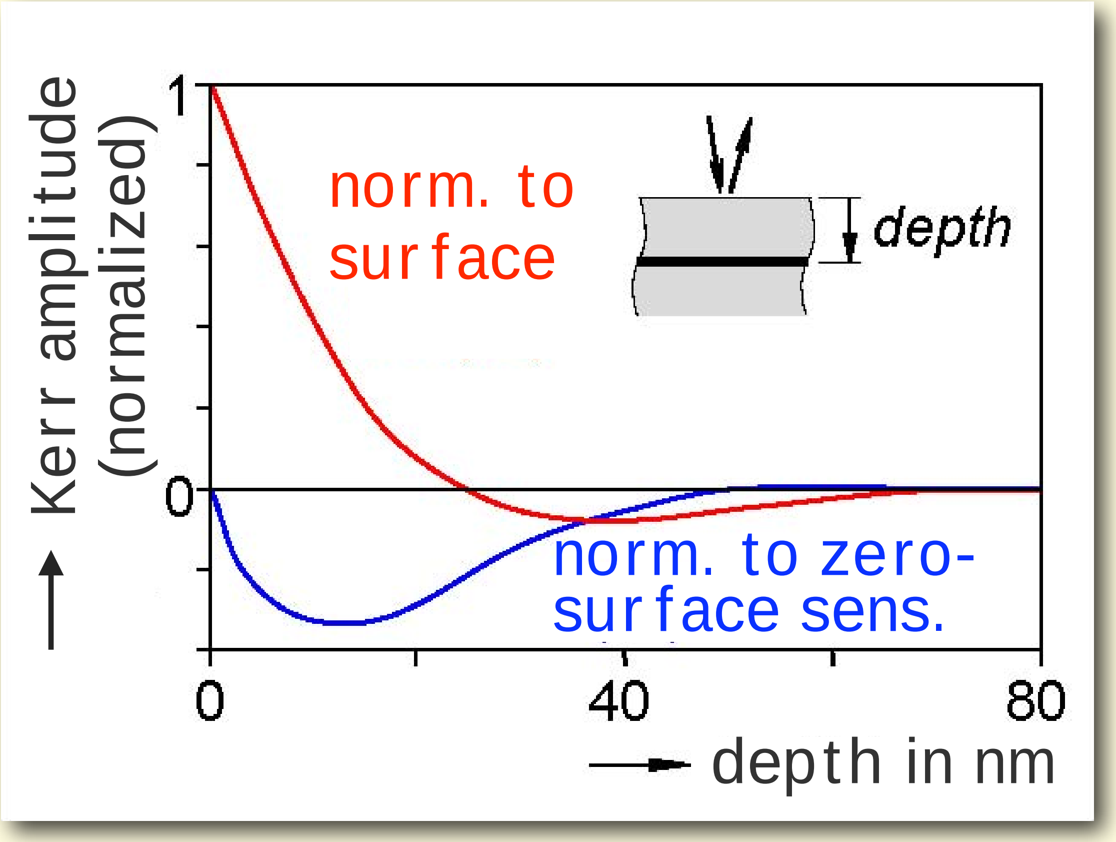

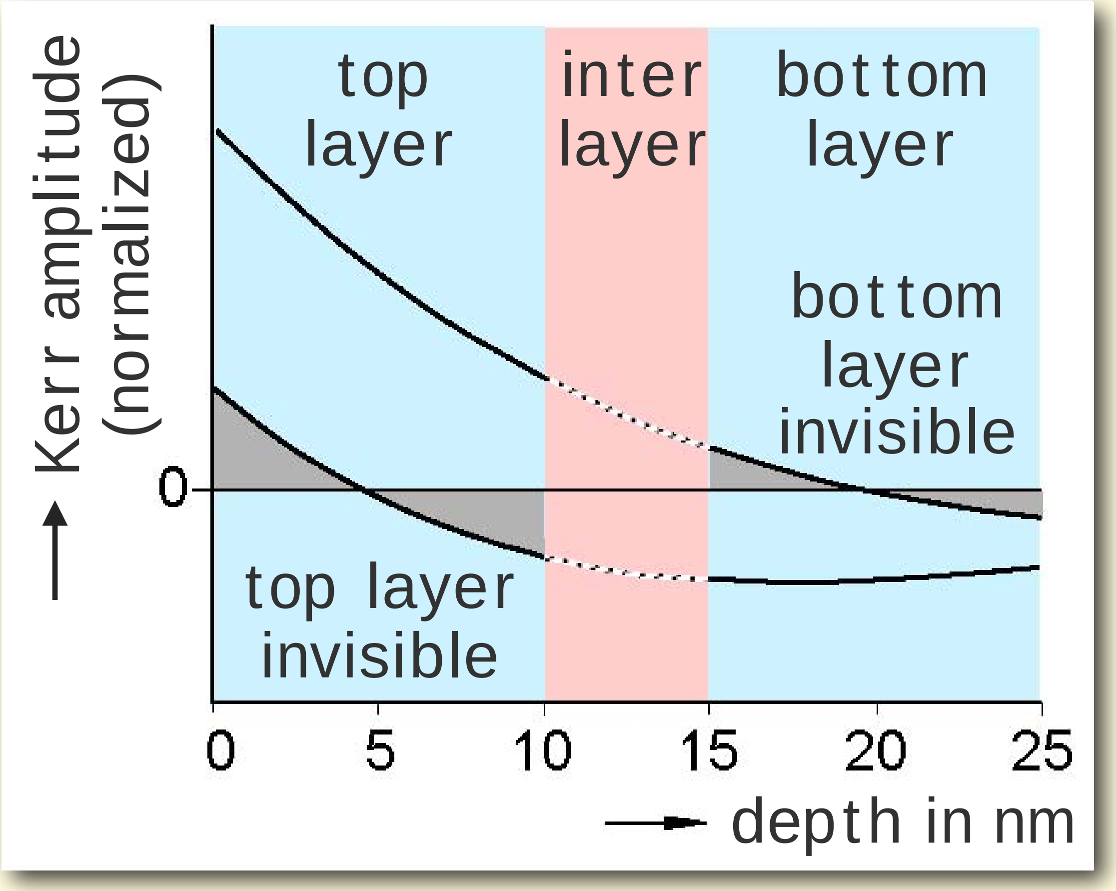

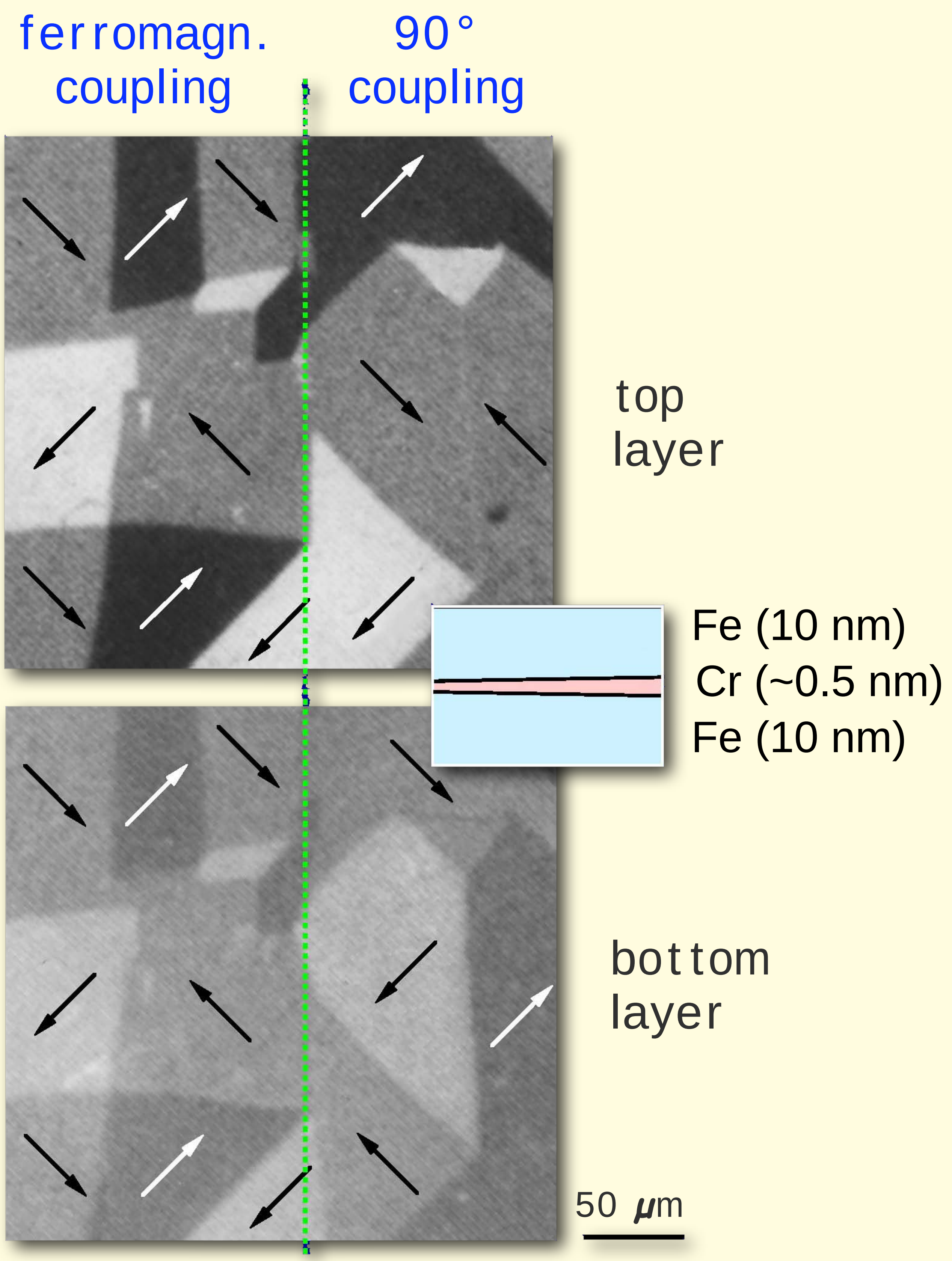

Magnetooptical microscopy: history

Michael Faraday
(1791-1867)

small change of polarization plane due to magnetooptic interaction in transmission, circular birefringence, ~ M

Fowler and Fryer, 1956

About polarized light

Plane-polarized light

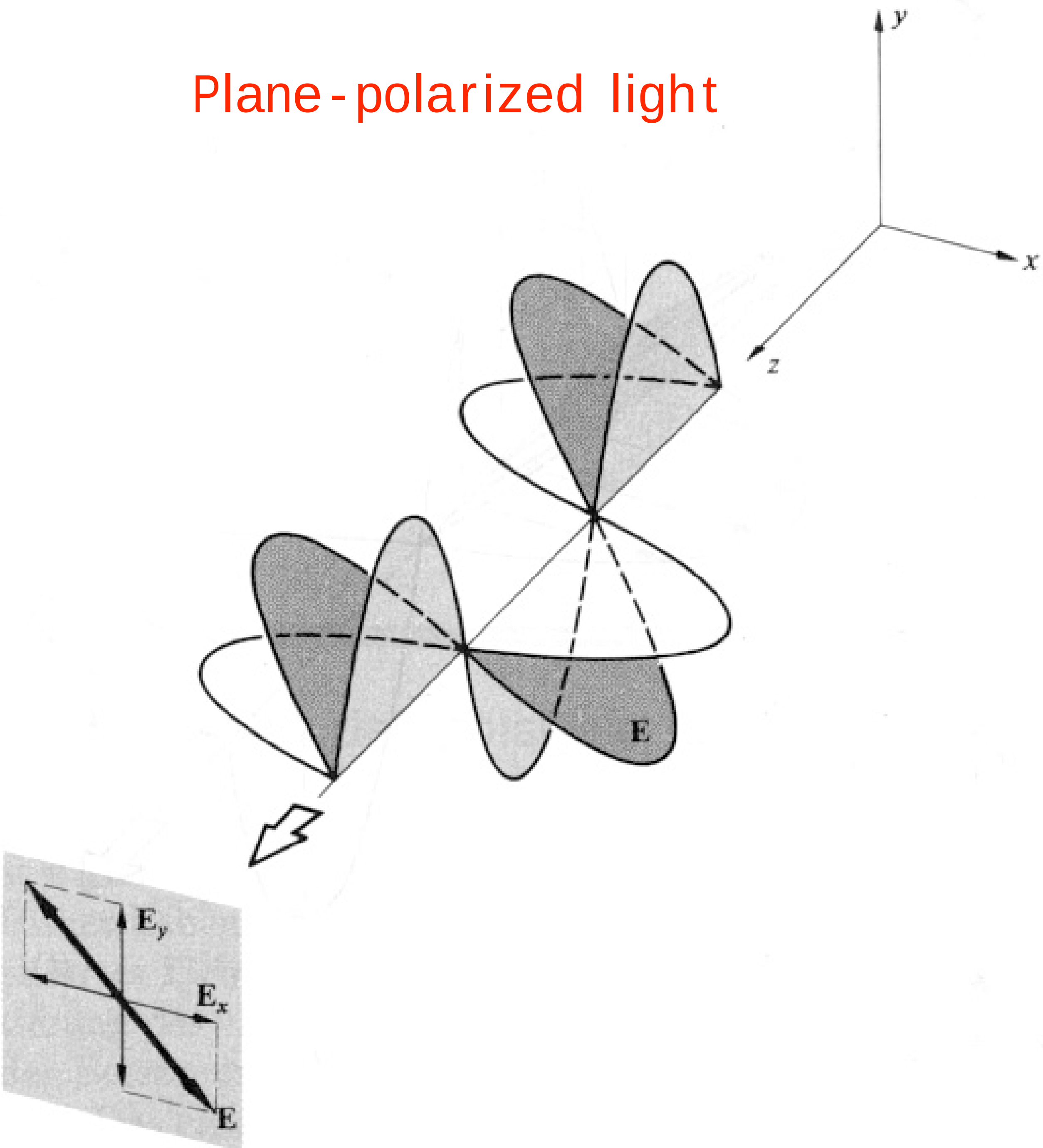

Elliptical light

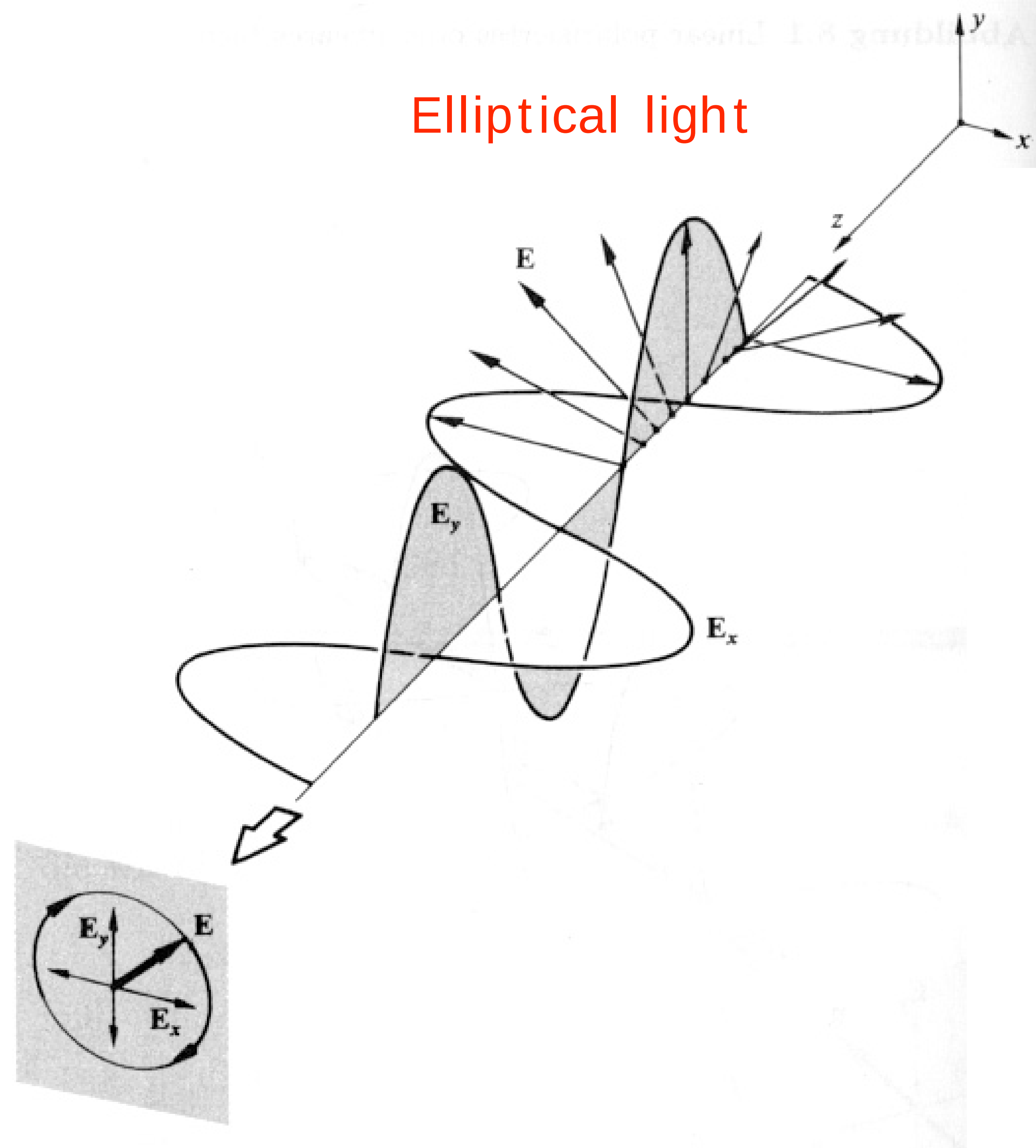

superposition of two orthogonal transverse waves of <u>equal</u> phase

superposition of two orthogonal transverse waves of <u>different</u> phase

About polarized light

Linearily polarized light =
superposition of two circular waves of opposite rotation sense
and equal frequency

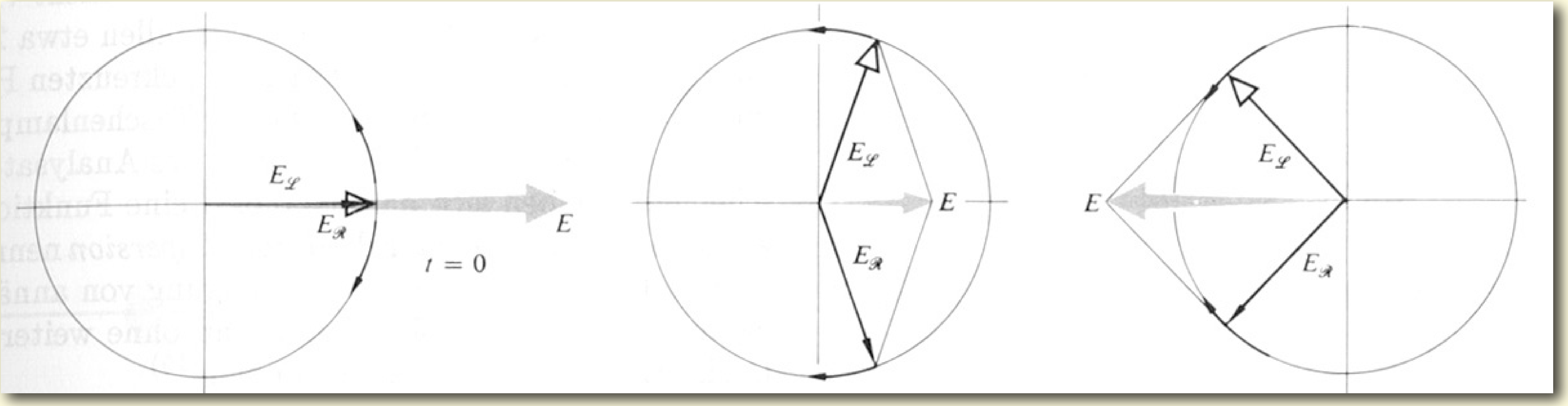

Circular birefringence

- if sample is illuminated parallel to the magnetization vector (k || m), the light wave can only propagate in two circularly polarized modes of opposite rotation sense

- due to the magnetization, both circular modes feel different refraction indices
  - → both modes propagate with different velocities
  - → modes are shifted in phase
  - → after leaving the sample they unify to plane-polarized wave again, which is rotated
  - → circular magnetic birefringence (Faraday rotation)

- if also absorption:
  - → both modes are damped differently
  - → elliptical wave
  - → circular magnetic dichroism (Faraday ellipticity)

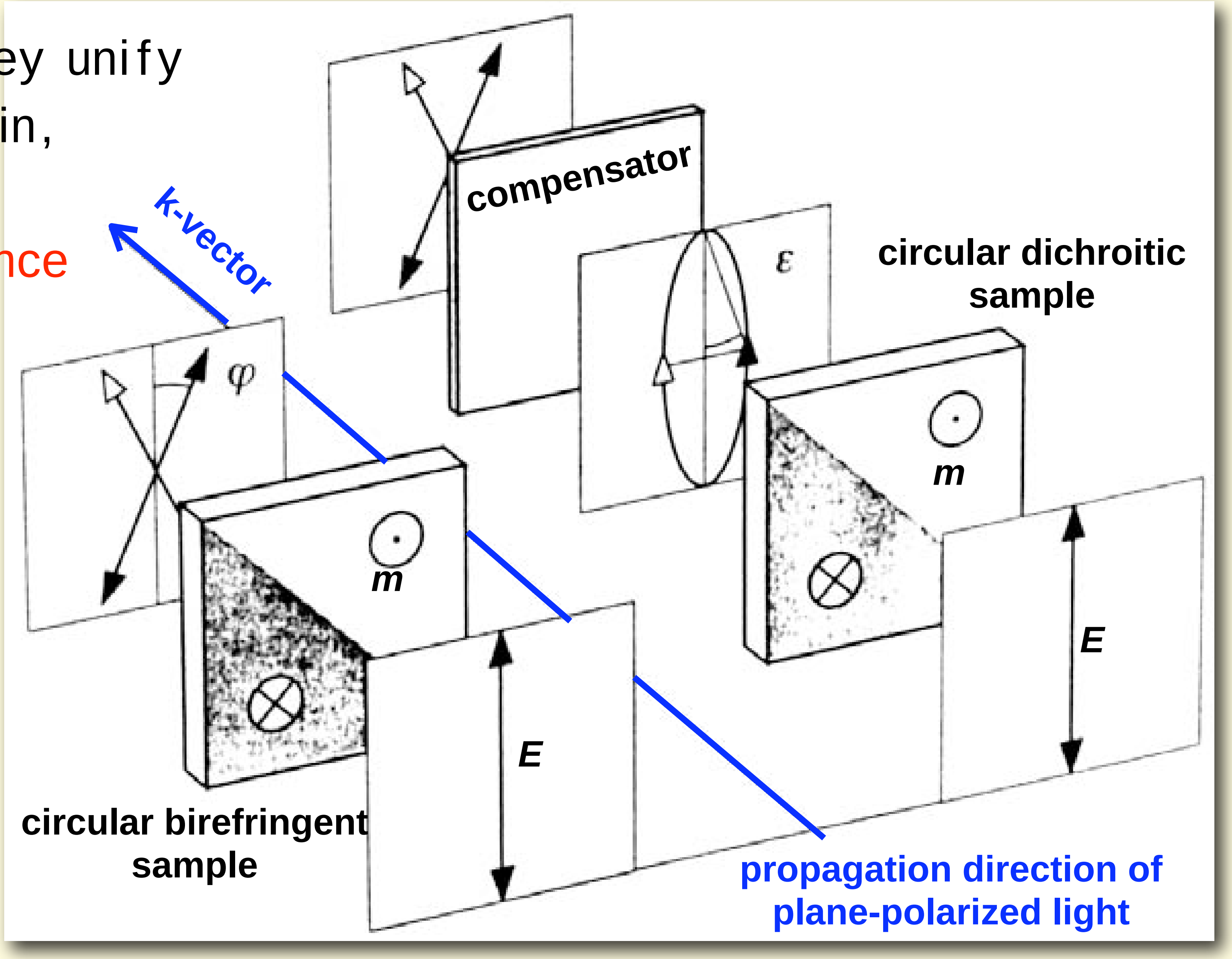

Faraday microscopy in transparent films

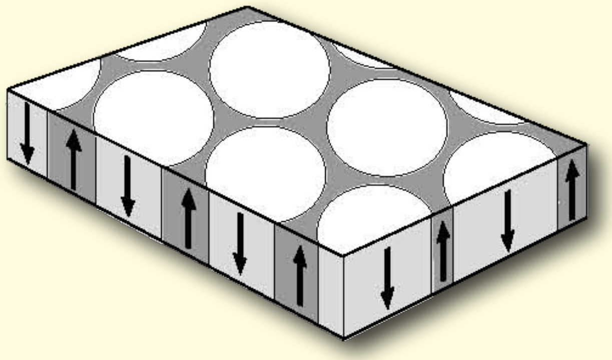

Yttrium iron garnet film
5 μm thick

50 μm

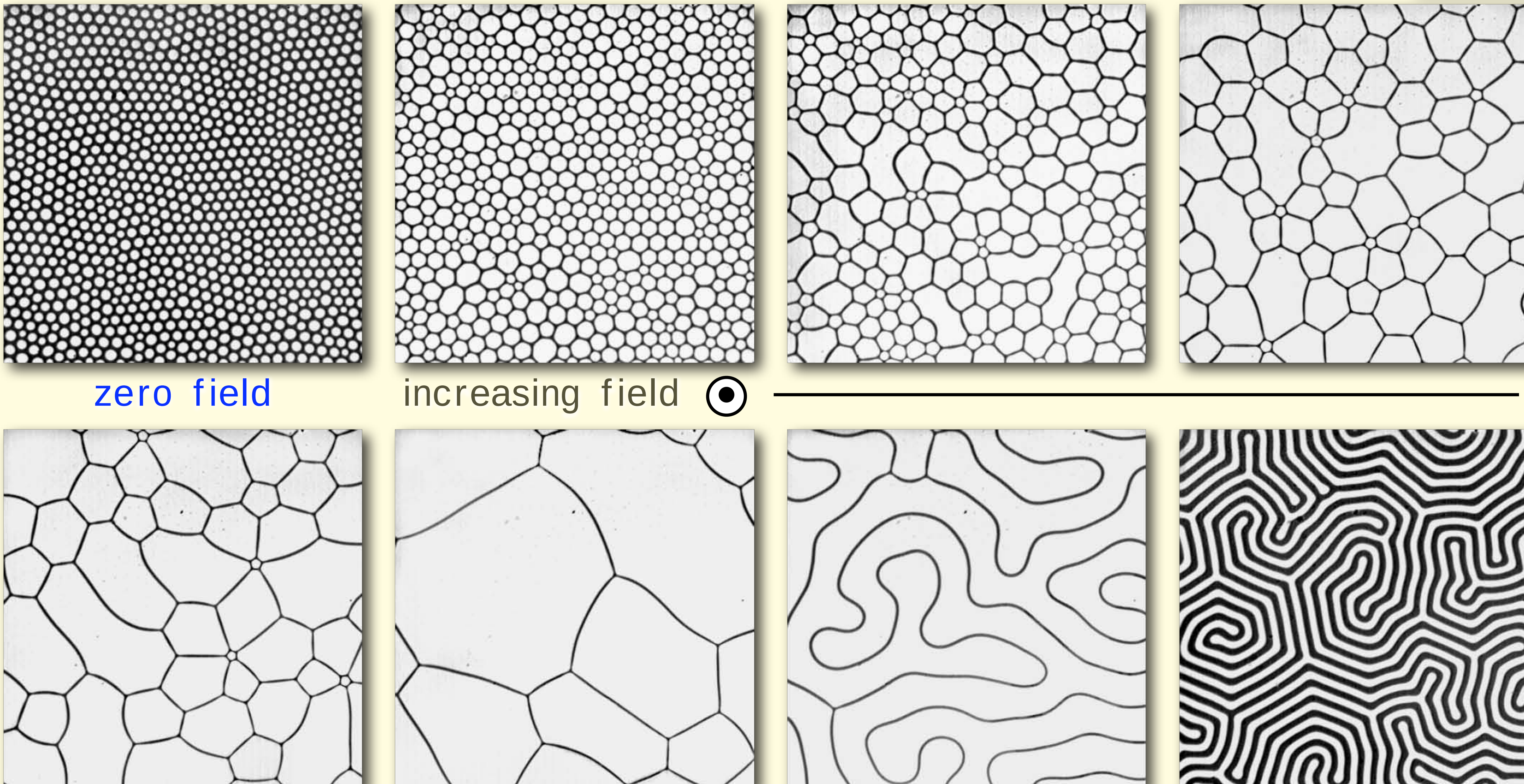

zero field

increasing field $\odot$

decreasing field

zero field

Magnetooptical microscopy: history

Michael Faraday
(1791-1867)

small change of polarization plane due to magnetooptic interaction in transmission, circular birefringence, ~ M

Fowler and Fryer, 1956

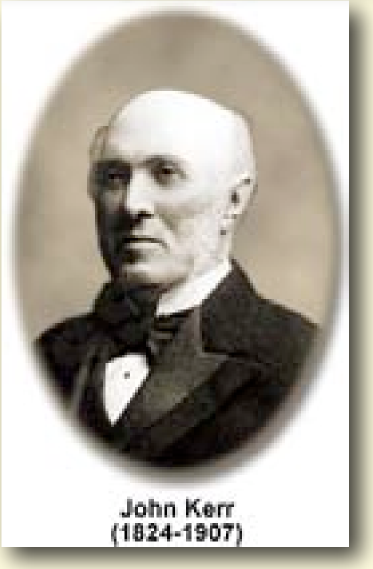

John Kerr
(1824-1907)

small change of polarization plane due to magnetooptic interaction in reflection, circular birefringence, ~ M

Williams et al., 1951;

Fowler and Fryer, 1952

W. Voigt
(1850-1919)

small change of polarization state due to magnetooptic interaction in reflection, linear birefringence, ~ M^2

Dillon, 1958

Schäfer and Hubert, 1990

Linear birefringence

- if sample is illuminated perpendicular to magnetization vector (k ⊥ m), the light wave can only propagate in two linearly polarized modes of orthogonal pol. direction
- one plane is along m, the other perpendicular to m
- due to the magnetization, both plane modes feel different refraction indices

  → both modes propagate with different velocities

  → modes are shifted in phase

  → after leaving the sample they unify to elliptical wave

  → linear magnetic birefringence (Voigt effect)

- requires compensator due to ellipticity

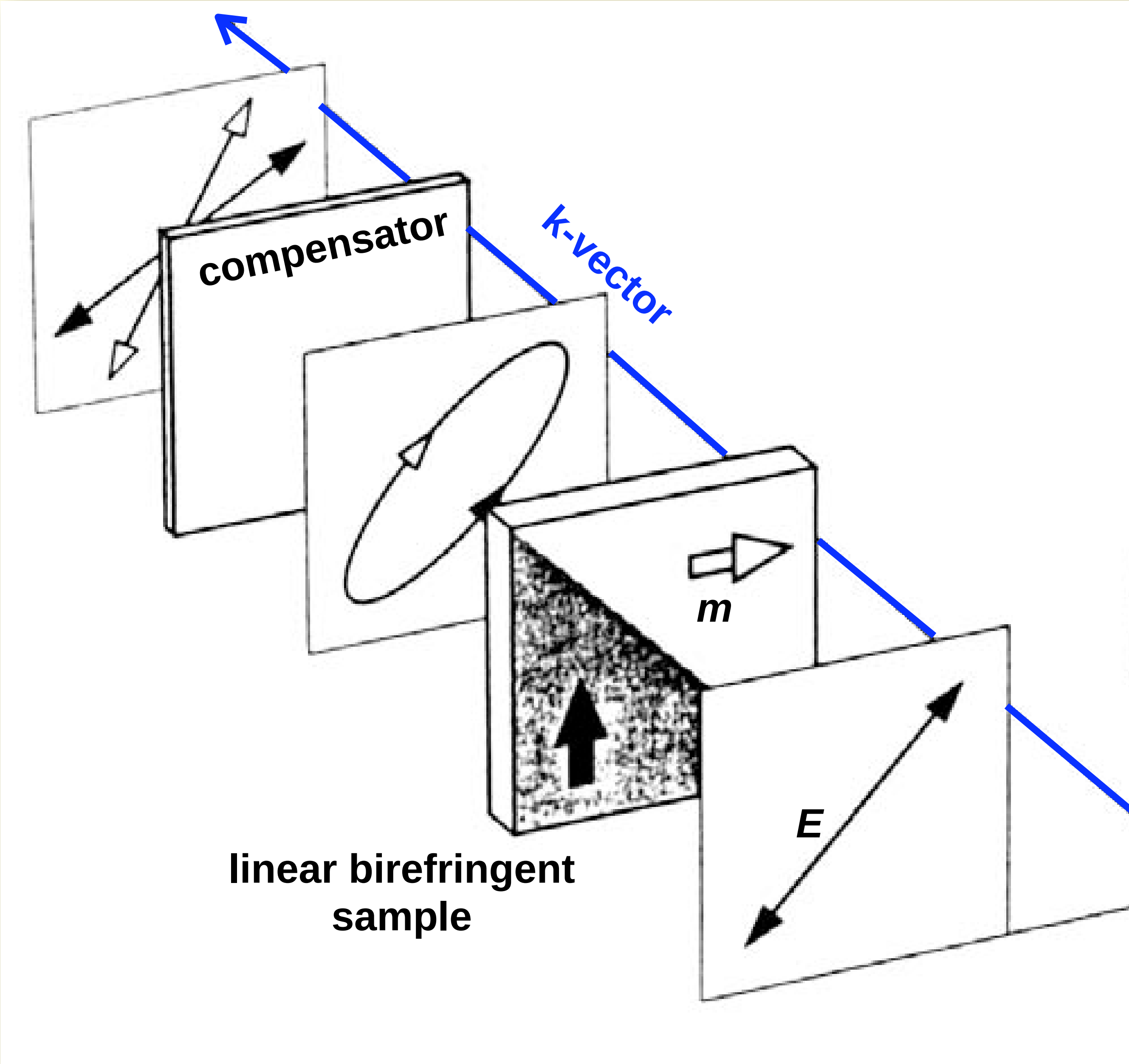

Kerr-, Voigt- und Gradient Effects

Kerr Effect

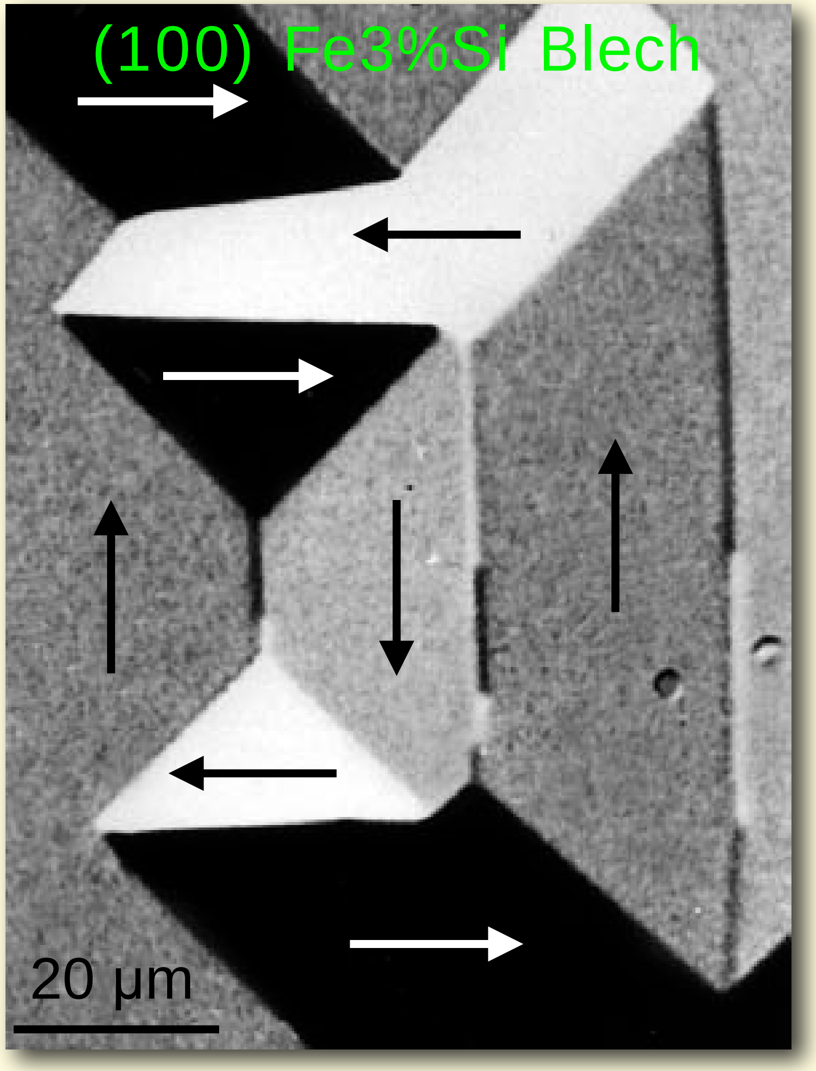

polarizer

oblique incidence

Voigt and Gradient Effect

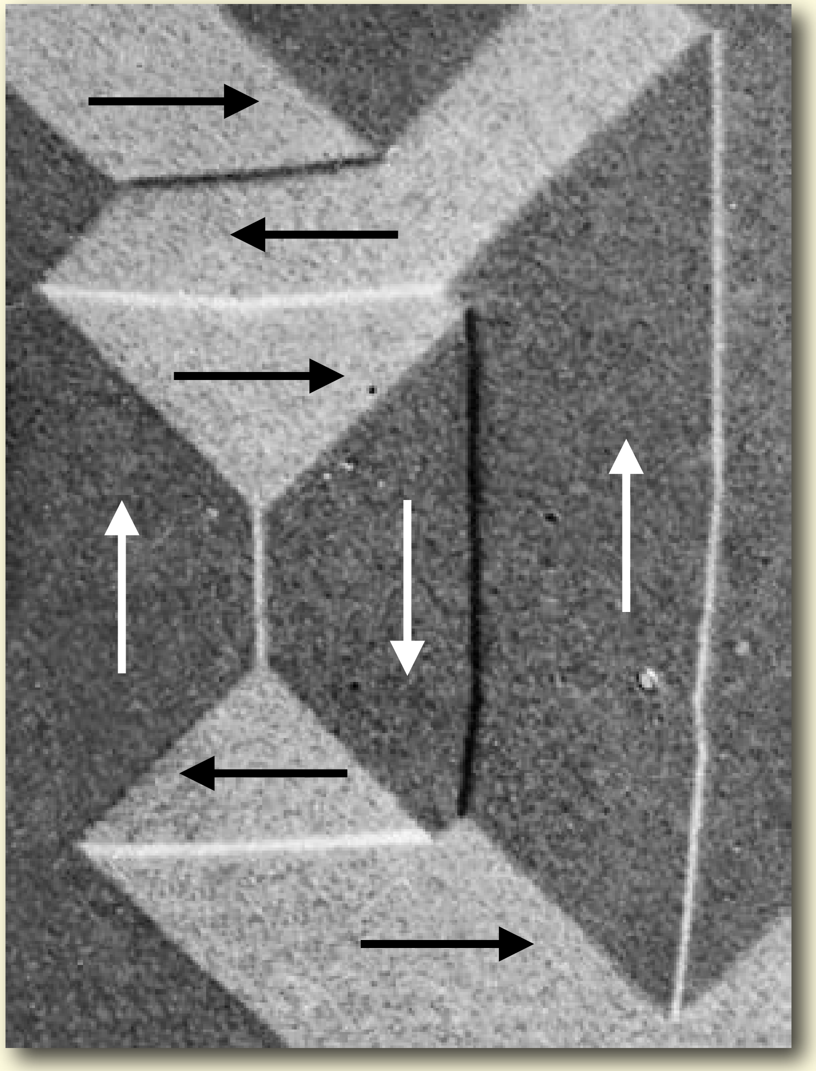

polarizer

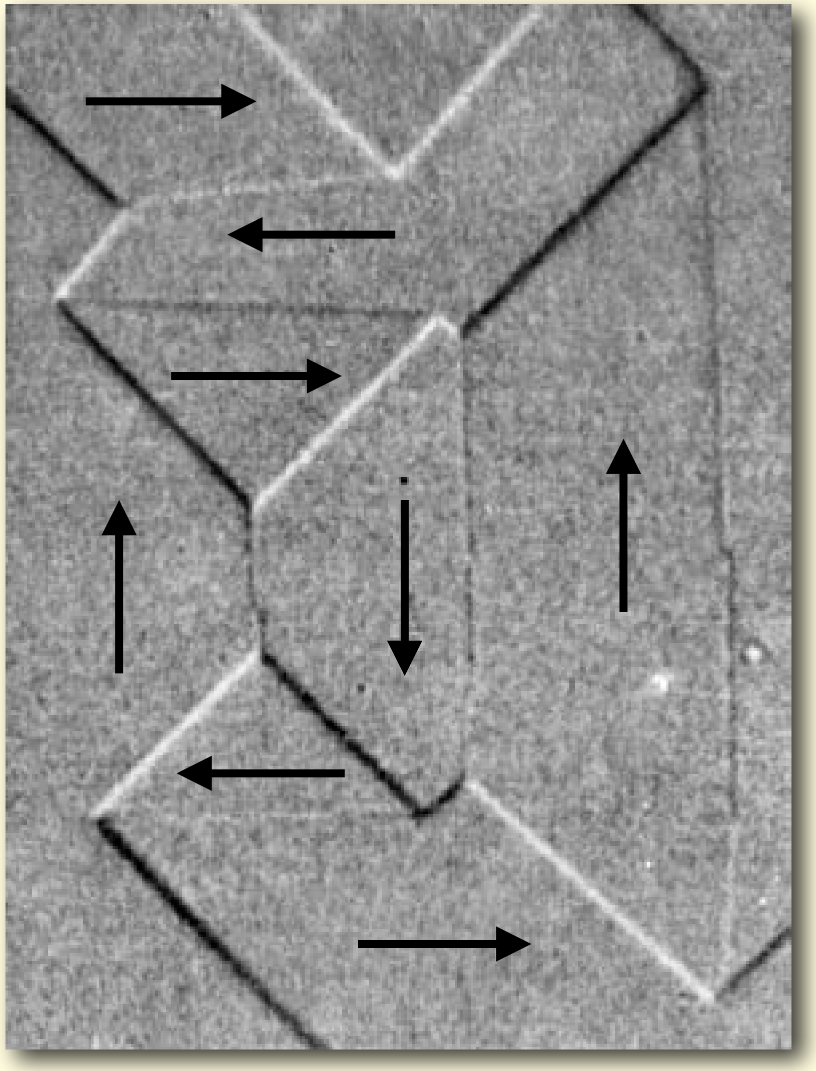

polarizer

perpendicular incidence,
compensator

Kerr-, Voigt- und Gradient Effects

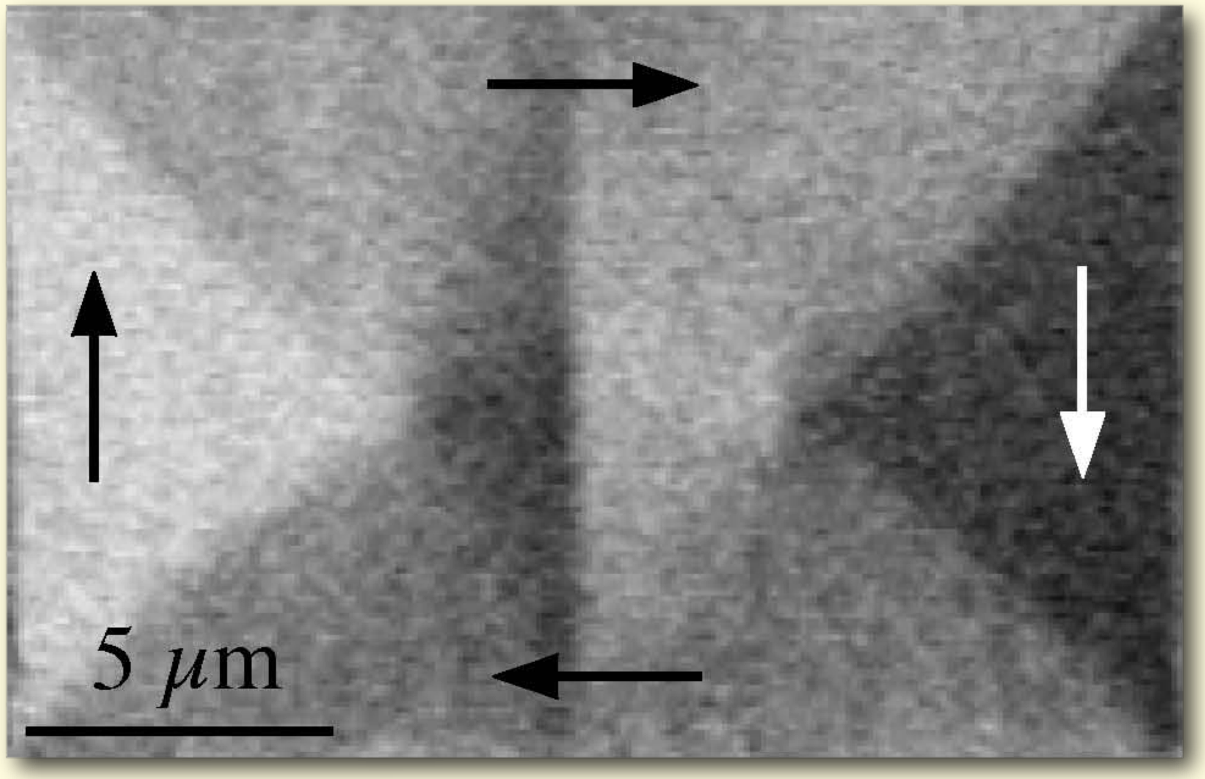

Kerr Effect

crosstie wall in
NiFe-film (50 nm thick)

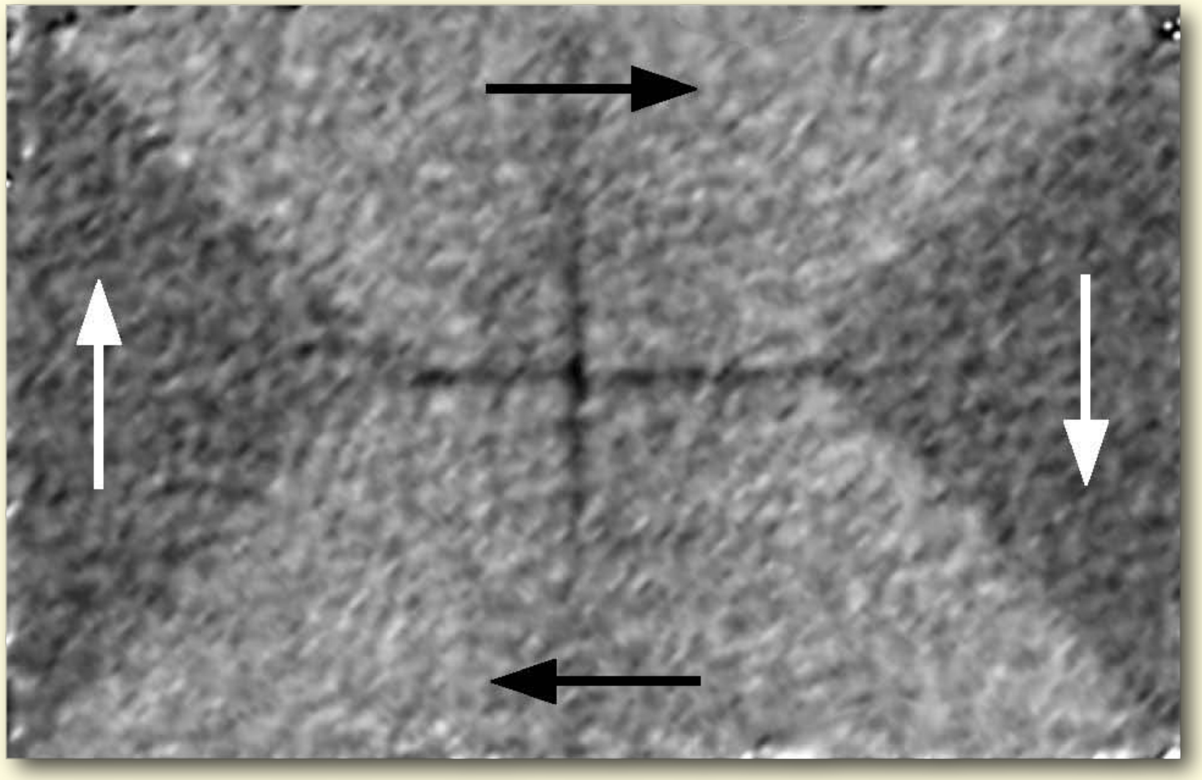

Voigt- and
Gradient-Effect

Application of Gradient effect

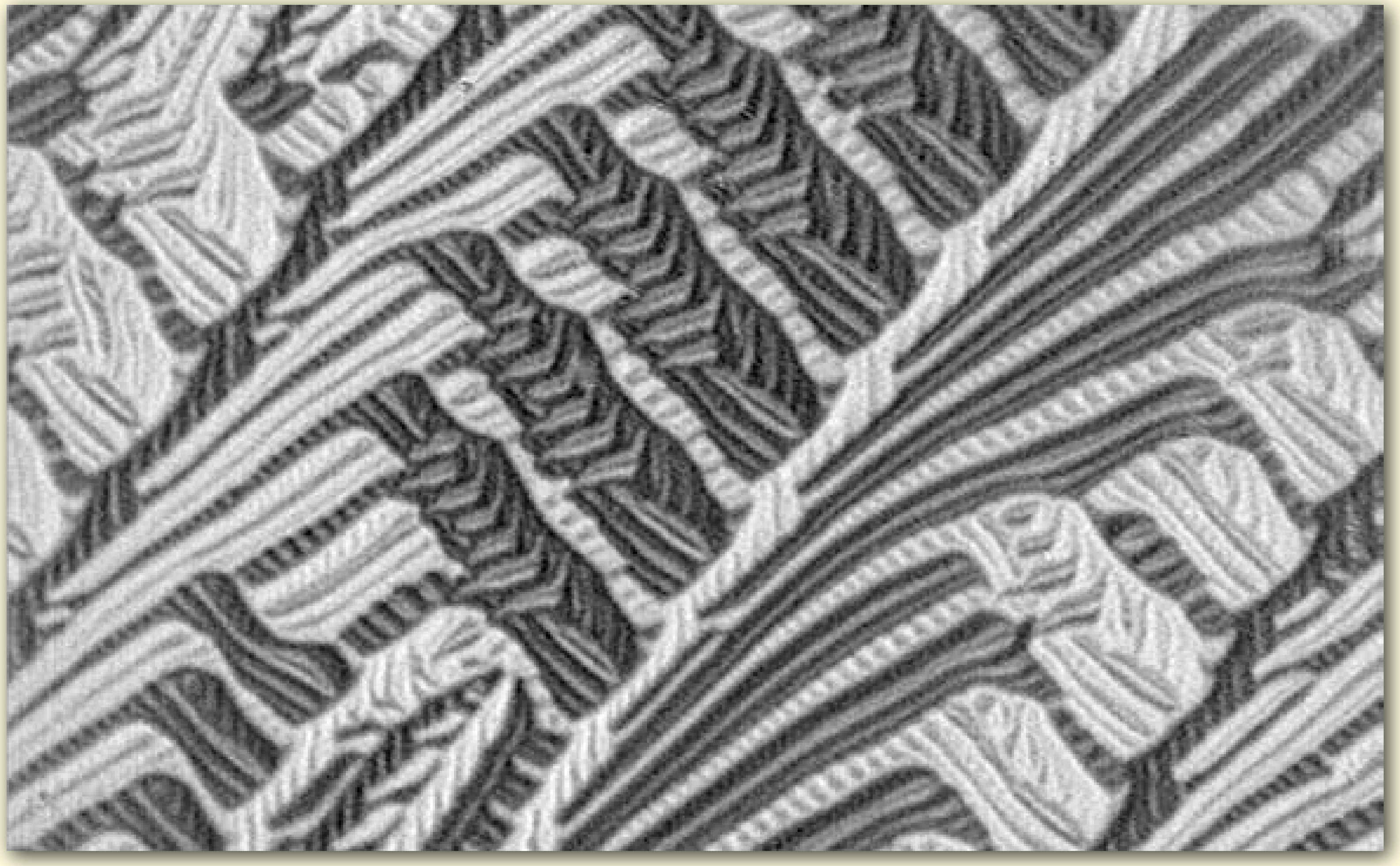

FeSi (111) surface

Kerr-contrast

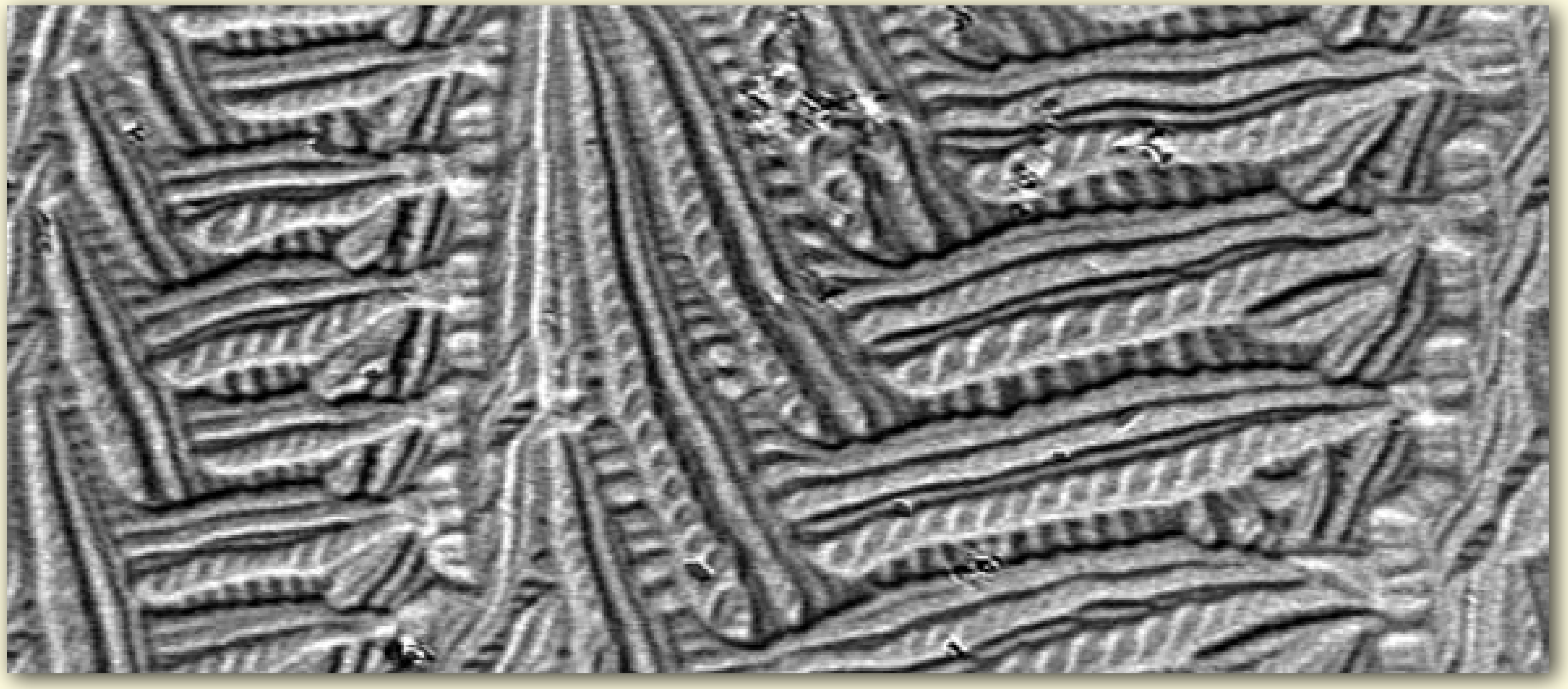

Gradient-Contrast

10 μm